frontiers | Research Topics

# Animal welfare, volume I: Animal welfare in aquaculture - physiological basis and recent findings

**Edited by**
Marce Herrera, Benjamin Costas and Enric Gisbert

**Published in**
Frontiers in Marine Science
Frontiers in Physiology

ISSN 1664-8714
ISBN 978-2-83251-010-0
DOI 10.3389/978-2-83251-010-0

## About Frontiers

Frontiers is more than just an open access publisher of scholarly articles: it is a pioneering approach to the world of academia, radically improving the way scholarly research is managed. The grand vision of Frontiers is a world where all people have an equal opportunity to seek, share and generate knowledge. Frontiers provides immediate and permanent online open access to all its publications, but this alone is not enough to realize our grand goals.

## Frontiers journal series

The Frontiers journal series is a multi-tier and interdisciplinary set of open-access, online journals, promising a paradigm shift from the current review, selection and dissemination processes in academic publishing. All Frontiers journals are driven by researchers for researchers; therefore, they constitute a service to the scholarly community. At the same time, the *Frontiers journal series* operates on a revolutionary invention, the tiered publishing system, initially addressing specific communities of scholars, and gradually climbing up to broader public understanding, thus serving the interests of the lay society, too.

## Dedication to quality

Each Frontiers article is a landmark of the highest quality, thanks to genuinely collaborative interactions between authors and review editors, who include some of the world's best academicians. Research must be certified by peers before entering a stream of knowledge that may eventually reach the public - and shape society; therefore, Frontiers only applies the most rigorous and unbiased reviews. Frontiers revolutionizes research publishing by freely delivering the most outstanding research, evaluated with no bias from both the academic and social point of view. By applying the most advanced information technologies, Frontiers is catapulting scholarly publishing into a new generation.

## What are Frontiers Research Topics?

Frontiers Research Topics are very popular trademarks of the *Frontiers journals series*: they are collections of at least ten articles, all centered on a particular subject. With their unique mix of varied contributions from Original Research to Review Articles, Frontiers Research Topics unify the most influential researchers, the latest key findings and historical advances in a hot research area.

Find out more on how to host your own Frontiers Research Topic or contribute to one as an author by contacting the Frontiers editorial office: frontiersin.org/about/contact

# Animal welfare, volume I: Animal welfare in aquaculture - physiological basis and recent findings

**Topic editors**

Marce Herrera — IFAPA Centro Agua del Pino, Spain

Benjamin Costas — University of Porto, Portugal

Enric Gisbert — Institute of Agrifood Research and Technology (IRTA), Spain

**Citation**

Herrera, M., Costas, B., Gisbert, E., eds. (2022). *Animal welfare, volume I: Animal welfare in aquaculture - physiological basis and recent findings*.

Lausanne: Frontiers Media SA. doi: 10.3389/978-2-83251-010-0

# Table of contents

frontiers | Frontiers in Physiology

TYPE Editorial
PUBLISHED 25 November 2022
DOI 10.3389/fphys.2022.1097913



OPEN ACCESS

EDITED AND REVIEWED BY
Pung Pung Hwang,
Academia Sinica, Taiwan

*CORRESPONDENCE
M. Herrera,
marcelino.herrera@juntadeandalucia.es

SPECIALTY SECTION
This article was submitted to Aquatic Physiology, a section of the journal Frontiers in Physiology

RECEIVED 14 November 2022
ACCEPTED 17 November 2022
PUBLISHED 25 November 2022

CITATION
Herrera M, Costas B and Gisbert E (2022), Editorial: Animal welfare, Volume I: Animal welfare in aquaculture - Physiological basis and recent findings.
*Front. Physiol.* 13:1097913.
doi: 10.3389/fphys.2022.1097913



# Editorial: Animal welfare, Volume I: Animal welfare in aquaculture - Physiological basis and recent findings

M. Herrera[1]*, B. Costas[2,3] and E. Gisbert[4]

[1]Department of Agroforestry Sciences, University of Huelva, Huelva, Spain, [2]Centro Interdisciplinar de Investigação Marinha e Ambiental, Universidade do Porto (CIIMAR), Matosinhos, Portugal, [3]Instituto de Ciências Biomédicas Abel Salazar (ICBAS), Universidade do Porto, Porto, Portugal, [4]Aquaculture Program, Institut de Recerca i Tecnología Agroalimentaries (IRTA), La Rápita, Spain

KEYWORDS

**aquaculture, stress, welfare, physiology, fish**

Editorial on the Research Topic
Animal welfare, Volume I: Animal welfare in aquaculture - Physiological basis and recent finding

Since animal welfare is a multidisciplinary scientific discipline, the papers published in this special issue are based on diverse subjects, such as feeding and nutrition, behavior, immunology, reproduction, pathology, endocrinology, and neuroendocrinology. The studies targeting fish species have been the most frequent, being salmonids the main group. Nevertheless, only one out of the thirteen published articles deals with an invertebrate species, the lobster (*Homarus americanus*), which highlights the recent interest for crustaceans' welfare. The results derived from these works state objectively the importance of animal welfare in both physiological and behavioral traits and responses, as well as in zootechnical parameters of interest for farmers.

The feeding and nutrition studies linked to fish welfare are an important group in the present topic. In particular, Salamanca et al. aimed to evaluate the effects of functional feeds supplemented with phenylalanine and tyrosine on the endocrine condition and physiological status of gilthead seabream (*Sparus aurata*) exposed to chronic stress. These authors reported that fish fed functional supplemented diets showed a reduction in various stress markers and physiological parameters. Additionally, they concluded that the stress condition favored a mobilization of amino acids towards the tissues, especially in supplemented diets, so this excess of amino acids could be used as an energy substrate to cope with stress, which is of special relevance for aquafeed manufacturers and fish farmers. The second study in this special issue dealing with nutrition was focused on probiotics. Amenyogbe et al. aimed to select potential probiotic bacteria from cobia (*Rachycentron canadum*) gut to be used as feed additive as a prophylactic nutritional strategy. Those authors isolated three indigenous bacteria with potential probiotic effects: *Bacillus* sp., *Pantoea agglomerans* and *B. cereus*. These bacteria demonstrated antagonistic

effects on the growth of pathogenic *Vibrio alginolyticus*, *V. harveyi*, *Streptococcus iniae*, and *S. agalactiae*, etiological agents of vibriosis and streptococcosis. Such effect against pathogenic bacteria was achieved by their capacity of producing antibiotic compounds, hence authors suggested that their inclusion in functional feeds could prevent or control disease outbreaks instead of using antibiotics or chemicals. Furthermore, Pelusio et al. and Sundell et al. have published a more classical nutritional study, based on fishmeal (FM) and oil (FO), and dietary fatty acids contents. In brief, Pelusio et al. focused on investigating the interaction between very low dietary levels of FM and FO and animal welfare in gilthead seabream (*Sparus aurata*) when exposed to a crowding stress challenge. For evaluating the effect of dietary regimes on fish condition, authors analyzed a wide range of parameters like stress and metabolic biomarkers in plasma, humoral immunity biomarkers in skin mucus and stress, and immune gene expression markers from the brain and the head-kidney. Overall, this study concluded that low FM (10%) and FO (3%) levels might compromise stress and immune responses, as well as growth performance in farmed fish. Sundell et al. carried on a more specific study, at intestinal level, on dietary omega-3 fatty acids in Atlantic salmon (*Salmo salar*) smolts. Specifically, those authors stated that low levels of omega-3 in the diet did not affect osmoregulation but decreased growth and changed the fatty acid composition of the proximal intestine. Additionally, those levels also reduced omega-3 content of the intestinal epithelial membranes as well as in impaired intestinal barrier function and decreased TEP (transepithelial potential difference) in the proximal intestine. Consequently, the authors concluded that low levels of omega-3 in the diet impaired the intestinal functions, which might reduce fish health and welfare.

The study of fish behavior in order to get a better understanding of fish welfare is increasingly gaining interest. In fact, it has been reported that the analysis of fish behavior coupled with personality studies is a good tool for proper understanding and improvement of fish welfare. In the present research topic, Li et al. evaluated the background color preference of the lined seahorse (*Hippocampus erectus*) and its relationship with personality (bold vs. shy) by assessing fish preference for different colored tank compartments (white, red, green, black, yellow, and blue backgrounds). Authors found that the lined seahorse showed a general preference for white and blue backgrounds, while they avoided black and red backgrounds. Therefore, this study recommended to use white and blue background colors for culturing this seahorse species, whereas they also proposed that it was able to assess the personality (bold-shy) of fish by means of their background color preference. A similar study was carried on by Yi et al., who researched on the effects of the light spectra on the GIFT tilapia (*Oreochromis niloticus*) welfare. Thanks to a transcriptomic analysis, the authors stated that different light spectra could regulate signaling pathway associated with the tilapia juveniles growth, stress, and behavior. Specifically, that work demonstrated that white and red lights affected positively the growth performance, meanwhile yellow light enhanced fish stress and aggressive behaviors. Following with the study of light as key factor in fish physiology, behavior and welfare, Frau et al. analyzed the ontogeny of six visual photopigments in Senegalese sole (*Solea senegalensis*) specimens at different ages. Such study using qPCR and *in situ* hybridization techniques was conducted in animals reared under different light conditions (light-dark cycles of white, blue, red, and continuous white lights) to understand how visual photoreceptors adapted to different light conditions. The authors concluded that visual opsin transcript levels changed during ontogeny depending on developmental stages and light regime and recommended using blue/green lights as an alternative to white lights in sole rearing protocols during early stages.

Probably, cortisol is the stress indicator which has been more used and studied in fish welfare studies. The works in the present topic do not suppose an exception and some works on cortisol dynamics and analysis have been published. It is known that the stress response in fish modulate the immune system due to systemic cortisol actions, including responses at mucosal tissues level. In this sense, Vallejos-Vidal et al. aimed to better understand whether cortisol can also play a modulatory role on the mucosal transcriptomic profile through its presence in the mucosal tissue surface of two important farmed species, the rainbow trout (*Oncorhynchus mykiss*) and the gilthead seabream. Therefore, an *ex-vivo* study was conducted to evaluate in a time-course fashion the effect of cortisol on selected immune- and stress-related genes. Those authors concluded that the quick modulation of the gene expression during the first 24 h after the exposure to a stressor challenge reported in previous studies, is probably coordinated and mediated through a systemic-dependent mechanism but not through a peripheral/local response on mucosal tissue surfaces. A more innovative approach to the analysis of cortisol was described by Höglund et al., who assessed stress resilience in Atlantic salmon after smolt transportation through waterborne cortisol. Those authors suggested that, together with behavioral responses to feed, water cortisol measurements are promising non-invasive indicators of adaptive processes associated with stress resilience in recirculating aquaculture systems (RAS). Additionally, that method was suggested to be used for evaluating the impact of potential stressors, such as compromised water quality, crowding and handling, on fish welfare. However, they also reported that water cortisol concentrations and cortisol release rate are sensitive to system (RAS) perturbations. Besides cortisol, the research on other hormones or neurotransmitters for evaluating stress response at endocrine and neuronal level is also enhancing. In this context, Staven et al. researched the responses of lumpfish (*Cyclopterus lumpus*) to the presence of Atlantic salmon or salmon sensory cues. They analyzed the catecholamine and cortisol levels in

plasma and tissues, and other parameters in lumpfish cohabiting with Atlantic salmons. Interaction with live salmon induced alterations in the brain of the lumpfish, which revealed reduced levels of brain catecholamines, namely norepinephrine and dopamine. However, health scores and skin coloration remained unaltered. Based on these results, authors concluded that lumpfish were not negatively impacted by cohabitation or exposure to salmon cues, which suggested that welfare disruption in commercial production is probably related to a combination of Atlantic salmon exposure with other stressors.

Recently, the importance of fish skin and associated mucus for fish health and welfare has been subject of interest in many works. In this sense, Doyle et al. looked into the transport and barrier functions in rainbow trout skin. They assessed the contribution of the different skin layers to barrier function, determined the effect of salinity, and tested for possible active transport mechanisms, stating that the epidermis was the diffusion barrier in the skin, with the scales and dermis playing a negligible role. The study also reported that environmental salinity affects significatively the epidermal barrier function, demonstrating that freshwater exposure derived in a high reduction of epithelial permeability. Nevertheless, regards active transport, they concluded that further research is required to determine if skin V-ATPase contributes significantly to overall ion homeostasis in rainbow trout, or whether it plays a more specialized role.

The only work on invertebrates published in this Research Topic deals with the involvement of crustacean hyperglycemic hormones (CHHs) in the reproductive cycle of the female lobster (Wang et al.). This basic research showed that HaCHH-A and HaCHH-B transcripts are derived from two different 4-exon CHH genes, and each gene can produce different but larger transcript variants (i.e., sHaCHH-A and sHaCHH-B) mainly in different non-eyestalk tissues of the females. Results showed that recombinant protein for sHaCHH-A and sHaCHH-B inhibited vitellogenin gene expression whereas dsRNA for sHaCHH-A and sHaCHH-B inhibited the expression of vitellogenin gene *in vitro*. The authors concluded their findings can provide insights for the development of techniques to induce gonad development without the use of the eyestalk ablation operation, improving the animal welfare.

The successful application of findings coming from research is the last and crucial step for an effective research activity. In this sense, a technical and general approach to the study of fish behavior and welfare was performed by Calduch-Giner et al., who revised the use of a new bio-logger (AEFishBIT) that allows the simultaneous monitoring of swimming activity and ventilation rates under steady and unsteady swimming conditions. The proof of concept of such technology was validated under different tools like video recording, exercise tests in swim tunnel respirometers, and differential operculum and body tail movements across fish species with differences in swimming capabilities. Authors concluded their review recommending the incorporation of behavioral variables in fish as a routine procedure of academia researchers as well as fish farmers, by the application of bio-loggers that accurately measure their swimming activity among other physiological variables.

To conclude, topic editors hope that above mentioned works can contribute to a deeper knowledge on animal welfare in aquaculture, and thank and congratulate authors for their excellent findings presented here. In this sense, topic editors encourage them to follow researching within this topic.

## Author contributions

All authors listed have made a substantial, direct, and intellectual contribution to the work and approved it for publication.

## Conflict of interest

The authors declare that the research was conducted in the absence of any commercial or financial relationships that could be construed as a potential conflict of interest.

## Publisher's note

frontiers in Marine Science

ORIGINAL RESEARCH
published: 17 May 2021
doi: 10.3389/fmars.2021.672213

# Probiotic Potential of Indigenous (*Bacillus* sp. RCS1, *Pantoea agglomerans* RCS2, and *Bacillus cereus strain* RCS3) Isolated From Cobia Fish (*Rachycentron canadum*) and Their Antagonistic Effects on the Growth of Pathogenic *Vibrio alginolyticus*, *Vibrio harveyi*, *Streptococcus iniae*, and *Streptococcus agalactiae*

*Eric Amenyogbe[1], Jian-sheng Huang[1,2,3]*, Gang Chen[1,2,3]* and Wei-zheng Wang[1]*

[1] Fishery College, Guangdong Ocean University, Zhanjiang, China, [2] Southern Marine Science and Engineering Guangdong Laboratory (Zhanjiang), Zhanjiang, China, [3] Guangdong Provincial Key Laboratory of Pathogenic Biology and Epidemiology for Aquatic Economic Animals, Zhanjiang, China

OPEN ACCESS

**Edited by:**
Enric Gisbert,
Institute of Agrifood Research and Technology (IRTA), Spain

**Reviewed by:**
Paola Navarrete,
University of Chile, Chile
Dariel Tovar-Ramírez,
Centro de Investigación Biológica del Noroeste (CIBNOR), Mexico

***Correspondence:**
Jian-sheng Huang
huangjs@gdou.edu.cn
Gang Chen
gdoucg@126.com

**Specialty section:**
This article was submitted to Aquatic Physiology, a section of the journal Frontiers in Marine Science

**Received:** 25 February 2021
**Accepted:** 23 April 2021
**Published:** 17 May 2021

**Citation:**
Amenyogbe E, Huang J-s, Chen G and Wang W-z (2021) Probiotic Potential of Indigenous (Bacillus sp. RCS1, Pantoea agglomerans RCS2, and Bacillus cereus strain RCS3) Isolated From Cobia Fish (Rachycentron canadum) and Their Antagonistic Effects on the Growth of Pathogenic Vibrio alginolyticus, Vibrio harveyi, Streptococcus iniae, and Streptococcus agalactiae. Front. Mar. Sci. 8:672213. doi: 10.3389/fmars.2021.672213

Large-scale fish farming faces many environmental stresses, which affect their immune systems, growth performance, and physiological homeostasis, resulting in increase in their susceptibility to infections. Some of the most common bacterial infections of cobia fish (*Rachycentron canadum*) include streptococcosis, vibriosis, furunculosis and mycobacteriosis, and pastelleurosis. Probiotics could be helpful in reducing or limiting the incidence of severe disease infections or outbreaks. Therefore, the present study aimed to isolate the indigenous bacterial species from healthy cobia fish and then selected 3 strains, including *Bacillus* sp. RCS1 (MW560712), *Pantoea agglomerans* RCS2 (MW560713), and *Bacillus cereus* RCS3 (MW560714) from the gut of juvenile's cobia having advantageous assets or positive characteristics. Their analysis indicated the presence of similar biochemical profiles and all could effectively utilize carbon sources. The biosafety assessment did not show any pathological symptoms after 10 days of injecting the fish with isolated bacteria. The results showed that all the isolated bacteria in the present study had low auto-aggregation capacity within the first 3 h of incubation. The isolated bacteria showed strong tolerance when exposed to a range of pH. Although asymmetrically, a slow rise in the growth of isolated bacteria was observed within the pH range of 1–8 for RC1, 1–7 for RC2, and 1–6 for RC3. The antagonistic effects of isolated bacterial strains on the development of pathogens, including *Vibrio alginolyticus*, *Vibrio harveyi*, *Streptococcus iniae*, and *Streptococcus*

*agalactiae*, were investigated using Luria-Bertani (LB) agar plates. All the isolated bacteria exhibited inhibitory effects against the pathogens, including *V. alginolyticus*, *V. harveyi*, *S. iniae*, and *S. agalactiae*. These isolated bacteria were characterized with a wide range of antagonistic activities, non-hemolytic activities, high survivability after heat-treatments and safety confidence, and antibiotic susceptibility. Generally, the characteristics displayed by these strains indicated that they could be used as potential probiotics in the aquaculture industry.

**Keywords: *Rachycentron canadum*, *Bacillus* spp. RCS1, *Pantoea agglomerans* strain RCS2, *Bacillus cereus* RCS3, antagonistic effects**

## INTRODUCTION

Aquaculture is a reliable production source for sustenance and nourishment of the global population's increasing demand for animal and fish proteins. Ensuring a suitable environment, healthy fish seeds and juveniles, and quality feed are necessary for successful aquaculture. Cobia (*Rachycentron canadum*) is appreciated for its characteristic features, which make it an important culture fish. It has a fast growth rate and inadequate availability in the wild, along with high market values due to its excellent flesh quality. These characteristics have inspired its production in aquaculture all over Asia, especially in China and other parts of the globe as well (Holt et al., 2007; Benetti et al., 2008, 2010; Zhang et al., 2013; Chen et al., 2016; Huang et al., 2020; Xie et al., 2021). Its production reached to approximately 40,000 tons worldwide in 2015 and 59538 tons in 2018 [Food and Agriculture Organization (FAO), 2015, 2020; Wang et al., 2021]. The cobia aquaculture faces challenges due the frequent incidences of disease infections in fish farming, high risk of disease infection and inadequate knowledge of its gut microbiota. Large-scale fish farming face many environmental stresses, which affect their immune systems, growth performance, and physiological homeostasis, resulting in their susceptibility to infections. Antibiotics have been used previously, and have effectively decreased the incidence of disease infection but the excessive use of many antibiotics has resulted in bacterial resistance (Montes et al., 2006; Dlamini et al., 2019). Some of the most common bacterial infections that affect cobia include streptococcosis, vibriosis, furunculosis, and mycobacteriosis. The opportunistic species from *Photobacterium* genus causes a disease pastelleurosis that has been identified as a significant emerging problem for the aquaculture of cobia throughout its production cycle (Lopez et al., 2002; Liu et al., 2003; Rajan et al., 2003; Liao et al., 2004; Chen and Hsu, 2005).

The indigenous gut microbiota of fish plays a significant role in the growth, development, and health of host (Vine et al., 2004) by safeguarding and protecting against pathogens in gut and assisting in host's digestive function by producing exogenous digestive enzymes and vitamins (Ray et al., 2012; Bhatnagar and Dhillon, 2019).

The utilization of valuable microbes and probiotics as a substitute approach to antimicrobial compounds for the control and prevention of diseases in aquaculture is increasing, which has become a hot-spot topic for research. Therefore, the probiotics can be utilized in aquatic farming, especially in fish farming, for the establishment of disease-free aquaculture (Bhatnagar and Dhillon, 2019). In order to fight diseases and promote growth, weight gain, and size, a range of valuable diet supplements and probiotics, which are advantageous to aquatic organisms, especially for fish, are being used in fish farming (Irianto and Austin, 2002; Amenyogbe et al., 2020), and encourage the host's immune response. Probiotics can improve host's health. Therefore, the Food and Agriculture Organization (FAO) has defined probiotics as foods or supplements, containing live microorganisms, which are intended to maintain or improve host's health [Food and Agriculture Organization (FAO), 2001]. Probiotics are useful in reducing or limiting the incidence of severe disease infections or outbreaks and enhance digestive function and non-specific immunity in aquaculture species (Carnevali et al., 2006; Knackstedt and Gatherwright, 2019; Ringo, 2019).

Many indigenous microbial species from fish gut, such as *Agarivorans* spp. (Liu et al., 2017), *Pseudomonas* spp. (Nayak and Mukherjee, 2011), *Lactobacillus* spp. (Balcázar et al., 2007), and *Bacillus* spp. (Bandyopadhyay and Patra, 2004; Bhatnagar et al., 2012; Bhatnagar and Raparia, 2014; Bhatnagar and Lamba, 2015, 2017; Yang et al., 2015; Kuebutornye et al., 2019; Li et al., 2019; Wang et al., 2019) and *Aeromonas* spp. (Hao et al., 2014) have been isolated and utilized as feed additives in order to study their effects on immunity, growth performance and development, and nutritional superiority. Among the probiotics utilized in feed additives and disease control, the species in *Bacillus* genus, including *B. subtilis,* B. *licheniformis,* and *B. cereus,* are the dominant species (Aleti et al., 2015; Wang et al., 2015; Chen et al., 2019; Park et al., 2020). Many of these indigenous species have been proven to be beneficial for fish species by improving immunity, performance of growth and development, and nutritional superiority.

*Pantoea,* a Gram-negative bacterial genus that belongs to *Enterobacteriaceae* family, currently includes 21 identified species (Walterson and Stavrinides, 2015; Nawrath et al., 2020). The strains of this genus, including *P. agglomerans* BSL 2, are commercially utilized as biological control agents (Smits et al., 2010; Nawrath et al., 2020). Many studies have discussed and reviewed the harmful and beneficial effects of *Pantoea* species (Dutkiewicz et al., 2015, 2016b,c). Nevertheless, *Pantoea* is a diverse and versatile bacterium genus that displays some mutual

traits associated with extraordinary biochemical actions and adaptation to a wild range of hosts and ecological conditions (Völksch et al., 2009; Nadarasah and Stavrinides, 2014; Walterson and Stavrinides, 2015; Dutkiewicz et al., 2016a). This makes an exclusive opportunity to utilize *P. agglomerans* as an effective candidate for the control of bio-remediation, and as drug, and bio-control agent. Interestingly, some of their potential traits include their capability of controlling several functions of animal-pathogen interactions, subject to their density of population, which is acknowledged as quorum sensing (Chalupowicz et al., 2008; Dutkiewicz et al., 2015, 2016b,c). These potential traits can be competently utilized for the treatment of human infections (Kohchi et al., 2006) and advancement of plant/animal growth (Jiang et al., 2015).

The most efficient approach to have probiotics is to isolate them from host's gut (O'Sullivan, 2001; Bhatnagar and Dhillon, 2019). Generally, the selection of probiotics depends on their growth and colonization in gastric mucus, adhesion, or *in vitro* antagonism (Vine et al., 2004). Therefore, the present study isolated indigenous bacteria (*Bacillus* sp. RCS1, *Pantoea agglomerans* RCS2, and *Bacillus cereus strain* RCS3) having advantageous assets or positive characteristics from the gut of juvenile's cobia. The antagonistic effects of these isolated indigenous bacteria on the growth of pathogenic *Vibrio alginolyticus*, *Vibrio harveyi*, *Streptococcus iniae*, and *Streptococcus agalactiae* were characterized and preliminary scrutinized.

## MATERIALS AND METHODS

### Collection of Samples

Eight (8) cobia, carnivorous marine fish (mix gender), from the wild with an average body weight of 202 ± 04 g (Mean ± SD) and average standard length of 28 ± 9 cm, having no symptoms of infection were obtained from Donghai Island. The live fish were transported in polythene bags containing oxygenated water with the DO level in the water (>6 mg/L), water temperature (26.3 ± 2.5°C) to Fish Seed Engineering and Healthy Farming laboratory, Fisheries College of Guangdong Ocean University, China, for immediate use.

### Isolation of Gut Microbiota

The fish were anesthetized using ethyl 3-aminobenzoate methanesulfonate, tricaine methanesulfonate (Sigma-Aldrich, 150 mg L-1MS-222), in order to minimize pain, which were then killed through a blow to their head. The fish were cleaned externally with cotton dipped into 75% ethanol to eliminate any external microbes on their bodies. Fish intestines were removed and cautiously stripped to eradicate all digestive content after the fish were dissected with sterile scissors. The intestine sections were washed with sterile phosphate buffer saline (PBS) three times. The intestinal sections were weighed and equal amounts of PBS by volume were added to them. The intestinal samples were homogenized using 15 mL borosilicate glass tissue homogenizer (Shanghai Lenggu Instrument Company, Shanghai, China) under sterile ice conditions. After homogenization, to a volume of 0.5 mL homogenized mixture, 4.5 mL of PBS solution was added to dilute the mixture. A volume of 0.1 mL of the diluted mixture was spread on Luria-Bertani (LB) agar plates. The LB plates were incubated for 24 h at 30°C. After 24 h of incubation, individual colonies were selected randomly and cultured into Luria-Bertani media to grow on a large scale under similar incubation conditions. Streaking of the isolated mixture was done repeatedly in order to obtain pure bacterial colonies. Based on their morphology, the potential probiotic strains were selected and identified using *16S rRNA* gene sequencing. For this, polymerase chain reaction (PCR) (Weisburg et al., 1991) was carried out using universal bacterial primers 1492R (5′-GGTTACCTTGTTACGACTT-3′) and 27F (5′-AGAGTTTGATCCTGGCTCAG-3′). The PCR reaction mixture included 2.5 μL of each isolate, 2.5 μL of each primer at 0.2 μ M concentration (27F and 1492R), 25 μL of rTaq buffers, and 17.5 μL of double-distilled water. *Streptococcus agalactiae,* acquired from Provincial Key Laboratory of Pathogenic Biology and Epidemiology for Aquatic Animals, College of Fisheries, Guangdong Ocean University, Huguang Yan East, Zhanjiang 524088, Guangdong, China, was used as positive control. Double distilled water was used as negative control (Kuebutornye et al., 2018). The PCR conditions were as follows: initial denaturation at 95°C for 5 min; followed by 35 cycles of denaturation at 95°C for 30 s, annealing at 55°C for 45 s, and extension at 72°C for 1 min 30 s; and final extension at 72°C for 10 min (Kuebutornye et al., 2019). The PCR products were analyzed using agarose (1% w/v) gel electrophoresis and later sent to Sangon Biotech Co., Ltd. (Guangzhou, China) for sequencing. The basic local alignment search tool (BLAST) from National Center for Biotechnology Information (NCBI) was used for comparing the sequences with available *16S rRNA* gene sequences in database and the isolated strains were identified. Mega 7 software was employed to construct a phylogenetic tree with other sequences obtained from NCBI for establishing evolutionary relationships among different isolates. The confidence of the resultant phylogenetic tree branch topology was set to bootstrap value of 10,000. The *16S rRNA* gene sequences of the isolated microorganisms were submitted to NCBI for accession numbers.

### Biochemical Characterization

For biochemical characterization (**Table 1**) and confirmation, the commercial kits from Huankai Microbial, Guangzhou, China, and *Bacillus cereus* (HBIG07-1) identification bar from Qingdao Hope Bio-Technology Co., Ltd., Qingdao, China were used, following the manufacturer's protocol.

### Bacterial Growth in Luria-Bertani Broth

From the LB agar plates, a distinct colony of the isolated probiotic bacteria was carefully chosen and incubated at 37°C overnight in 5.0 mL of LB broth. A 500-mL Erlenmeyer flask containing 100 mL sterile LB broth and 1 mL of the culture was incubated at 37°C with constant shaking at 150 rpm. Their growth was monitored by measuring the absorbance at 600 nm for 24 h at 2 h intervals (Xie et al., 2014).

## Biosafety Assay

In order to analyze the pathogenic effects of isolated microorganisms in cobia, 0.1 mL ($10^8$ CFU/mL) of each sample was injected intra-peritoneally into two groups, each containing 6 cobia fish with an average body weight of 150 g. The same volume of sterile PBS (pH 7.2) was injected into sixth fish as a control group. The conditions for fish culture were monitored as described previously (Abarike et al., 2018; Wang et al., 2021). Briefly, the fiberglass was a flowing water aquaculture system with continuous aeration for 24 h, and plastic tanks of 500 L capacity of filling with water. A dissolved oxygen meter (Hengxin, Taiwan, AZ8403) was used to monitor changes in dissolved oxygen. The experimental fish was fed with compound feed (Guangdong Yuequn Marine Biology Research and Development Co., Ltd., Jieyang, China) twice a day. The feed composed of about 430 $g.kg^{-1}$ crude protein and 80 $g.kg^{-1}$ crude lipid using the fish meal and soybean as protein sources, and fish oil and soybean oil as lipid sources (Geng et al., 2011). The feed was calculated as 10% of their body weights. Their feces were cleaned regularly by siphoning off with water. The fish were observed daily for clinical signs and mortality rate for 2 weeks (14 days).

## Antibiotic Susceptibility

The isolated bacteria were assessed for their antibiotic susceptibility against some antibiotics (**Table 3**), using the commercially available antibiotics discs obtained from Hangzhou Microbial Reagent Co., Ltd., Hangzhou, China. Using the disk diffusion susceptibility method (Murray et al., 2007; Clinical and Laboratory Standards Institute, 2009), the isolated bacteria (100 μL) were spread on LB agar plates with the commercial antibiotics discs carefully placed on them and incubated for 24 h at 37°C. Their antibiotic susceptibility was calculated by measuring (mm) their inhibition zone as previously described (Patel et al., 2009; Kuebutornye et al., 2019).

## Bile Salts Resistance

The resistance of isolated bacteria to bile salts was analyzed using the modified methods, as described by Argyri et al. (2013); Kuebutornye et al. (2019). In brief, the bacteria were cultured in LB broth overnight, harvested the following morning (9,000 g, 5 min, 4°C), washed with PBS buffer (pH 7.2) twice and then kept in PBS solution (pH 7.4), containing 0.5% (w/v) bile salts (BBI Life Sciences, Shanghai, China). Their resistance to bile salts was assessed by counting the colonies at 1 h interval during the incubation at 37°C for 4 h (counting viable colonies at 1, 2, 3, and 4 h of incubation).

## High-Temperature Resistance

The resistance of isolated microorganisms to different temperatures was evaluated using the previously described procedures with slight modifications (Guo et al., 2016; Kuebutornye et al., 2019). Since the fish feed processing at times demands high temperatures. After culturing the isolated bacteria in LB broth overnight at 37°C and 150 rpm, the isolates were harvested by centrifuging at 9,000g for 5 min, followed by washing with PBS (pH 7.4) twice. The isolates were then exposed to 80, 90, and 100°C temperature for 2, 5, and 10 min, respectively. After exposure, sterile LB broth of equal volume was added to the temperature-exposed isolated bacteria in order to evaluate their growth capacity after heat treatments. The bacterial growth was observed by measuring the absorbance at 600 nm after 12 h of incubation at 37°C with constant shaking at the speed of 150 rpm.

## Compatibility Test

According to literature, the mono-probiotics species are used in food products. Hence, the compatibility test was carried out for the utilization of multispecies probiotics (Saarela et al., 2000; Rajyalakshmi et al., 2016; Kuebutornye et al., 2019). The compatibility test was performed as described previously by Rajyalakshmi et al. (2016); Kuebutornye et al. (2019). Briefly, the isolated bacteria were streaked vertically and perpendicularly on LB agar plates at a distance of 5 and 10 mm from each other. After 24 h of incubation at 37°C, their compatibility was determined by observing and measuring the inhibition zone of isolated bacteria.

## Antimicrobial Activity

The pathogenic bacterial strains, including *V. alginolyticus*, *V. harveyi*, *S. iniae*, and *S. agalactiae,* were obtained from Provincial Key Laboratory of Pathogenic Biology and Epidemiology for Aquatic Animals, College of Fisheries, Guangdong Ocean University, Huguang Yan East, Zhanjiang 524088, Guangdong, China, for laboratory use. These pathogenic bacterial strains were tested against the isolated bacteria using the agar well diffusion method and cross-streak methods (Lertcanawanichakul and Sawangnop, 2008).

## Auto-Aggregation

The auto-aggregation of the isolated bacteria was evaluated using the previously described method by Lee et al. (2017); Kuebutornye et al. (2019) with slight modifications. After centrifugation at 9,400 g for 5 min, the cells of isolated bacteria were harvested. The harvested cells were washed twice with PBS, kept back into the supernatant, and then mixed using vortex for 30 s. The absorbance was measured at 600 nm using a spectrophotometer (Shanghai Inesa Analytical Instrument Company, shanghai, China), at 0, 1, 2, 3, and 24 h of harvesting. The auto-aggregation was measured using Eq. (1).

$$\text{Auto} - \text{aggregation}(\%) = (1 - -\mathrm{A_t}/\mathrm{A_0}) \times 100 \quad (1)$$

where $A_0$ = Absorbance at 0 h at 600 nm and $A_t$ = Absorbance at 1, 2, 3, and 24 h at 600 nm.

## Cell Hydrophobicity

The cell hydrophobicity is the most generally used method to determine the microbial cell surface adhesion. Since the assay is based on adhesion, its efficacy to determine the cell surface hydrophobicity is questionable. The cell hydrophobicity of isolated bacteria was analyzed using the previously described methods by Lee et al. (2017) with slight modifications. In brief,

the isolates were cultured for 24 h and then centrifuged at 9,000 g for 5 min to harvest the bacterial cells. The harvested cells were washed with 2 mL of PBS (PBS, pH 7.4) twice. The absorbance was measured at 600 nm wavelength using a spectrophotometer in order to evaluate the percentage hydrophobicity and recorded as A0. Then, the harvested cells were mixed with ethyl acetate (a basic solvent), xylene (a non-polar solvent) and chloroform (an acidic solvent) using vortex for 5 min. The solution was kept for 30 min to allow it to separate into two phases. The absorbance was measured and recorded as A1. Hydrophobicity (%) could be calculated as given in Eq. (2).

$$\text{Hydrophobicity}(\%) = 1 - \mathrm{A}_1/\mathrm{A}_0 \times 100 \quad (2)$$

where *A0* = absorbance before mixing with solvent at 600 nm and *A1* = absorbance after mixing with solvent at 600 nm.

## Hemolytic Activity

The isolated bacteria were exposed to a hemolytic assay by streaking onto agar plates supplemented with 7% sheep blood. The agar plates were incubated at 37°C for 48 h followed by the observation and measurement of hemolytic zones. Subsequently, the isolated microbes were classified as β, α, or γ-hemolysis. The isolated bacteria with clear zone were denoted as β-hemolysis, those with green zone were denoted as α-hemolysis, and those without any zone were denoted as without hemolysis (Engel et al., 1972; Lee et al., 2017; Kuebutornye et al., 2019).

## Optimal Growth and pH Determination

The determination of optimal growth and pH was carried out following the method described by Kavitha et al. (2018) with slight modifications. Briefly, the isolates were cultured for 24 h at 37°C in LB broth with adjustable pH (1–10). HCl and NaOH were used to adjust pH. The growth was measured by measuring the OD (optical density) using spectrophotometer (Shanghai Inesa Analytical Instrument Company, shanghai, China) at 600 nm. The LB broth without any bacteria was used as control.

## Biofilm Formation and Detection (Congo Red Agar Method)

In order to measure the production of biofilm, the methods described by Kavitha et al. (2018) were followed with slight modifications. Briefly, the isolates were cultured at 37°C for 24 h. The cultured bacteria were streaked and incubated at 37°C for 48 h on Mueller Hinton agar medium, containing 0.8 g/l of Congo red dye. The red colonies were identified as non-biofilm-producing strains, while the black colonies with consistent dry crystalline structures were identified as biofilm-producing strains.

## Statistical Analysis

In this study, the data were analyzed with one-way analysis of variance (ANOVA) using SPSS (IBM SPSS STATISTICS, 16.0 package, IBM Corporation, New York, United States) for Windows version 7.0 (SPSS, Chicago, United States). The data were previously tested for normal distribution and equal variances between treatments and homogeneity before ANOVA analysis and expressed in percentages. Data expressed as percentage were angularly transformed before being statistically assessed. The data were expressed as mean ± standard error (SE). The differences in mean values were identified using Tukey's HSD tests ($P < 0.05$). Different letters were used to indicate the statistical significant differences.

# RESULTS

## Identification of Gut Bacteria

Following biochemical and morphological characterization, three prospective probiotic bacteria were isolated and identified, namely, *Bacillus* sp. RCS1, *Pantoea agglomerans* RCS2, and *Bacillus cereus* RCS3, which were selected as microorganisms to be investigated in this study (**Table 1**). The gene sequencing analysis of *16S rRNA* gene indicated that the isolated bacteria were *Bacillus* sp., *Bacillus cereus strain,* and *Pantoea agglomerans strain*. The *Bacillus* sp. RCS1, and *Bacillus cereus strain* RCS3 exhibited neighboring sequence homology (99. 52%) with *Bacillus cereus strains* while *Pantoea agglomerans* RCS2 exhibited neighboring sequence homology (98. 39%) with the *Pantoea agglomerans strains.* The analysis of the constructed phylogenetic tree (**Figure 1**) indicated that the isolates *Bacillus* sp. RCS1, and *Bacillus cereus* RCS3 had the highest similarity to *Bacillus cereus strain* NBRC 15305 (NR_112630.1) while the *Pantoea agglomerans* RCS2 had the highest similarity to *Pantoea agglomerans strain* CZ-BHG003, *Pantoea agglomerans strain* TPD7001 and *Pantoea agglomerans strain* NSH. The *16S rRNA* gene sequences of the isolated strains were submitted to the NCBI for GenBank accession numbers as follows; *Bacillus* sp. RCS1 (MW560712), *Bacillus cereus* RCS3 (MW560714), and *Pantoea agglomerans* RCS2 (MW560713), respectively.

The biochemical characteristics of the isolated bacteria are listed in **Table 1**. Their analysis showed that they had comparable biochemical characteristics and hence can all virtually utilize carbon sources. The three isolated microbes were tested negative for gelatin liquefaction, inositol, urea, lysozyme broth, and hippuric acid, while tested positive for mannitol; hence they were halophiles. Nonetheless, they had different morphological features.

Generally, microbes reproduce via binary fission, which include the establishment two equal-sized progeny cells and hence amplifying their number with each division. A process of cell division of this kind, is known as exponential phase. The unit of bacterial growth is "generation time." In order to identify the exponential growth phase of isolates in the present study, the growth of potential probiotics were determined. The exponential growth phase for all the three isolated bacteria started at roughly 2 h subsequently incubation at 37°C with uninterrupted shaking (150 rpm) (**Figure 2**).

The biosafety assessment showed that after 10 days of injecting the fish with isolated bacteria, they showed no pathological symptoms (such as mucus, lesions, edema, loss of scale and hemorrhage) as witnessed in both the control and experimental groups. There were no mortalities recorded during the biosafety

**TABLE 1 |** Biochemical characterization of isolated bacterial strains.

| Test | Biochemical characterization | | |
|---|---|---|---|
| | ***Bacillus* sp. RCS1** | ***Pantoea agglomerans* RCS2** | ***Bacillus cereus* RCS3** |
| Catalase | + | + | + |
| Simon citrate | + | + | + |
| Adonitol | – | – | – |
| Rhamnose | + | + | + |
| V-P Test | + | + | + |
| Inositol | – | – | – |
| Gelatin | – | – | – |
| Sorbitol | + | + | + |
| Urea | – | – | – |
| Glucose | + | + | |
| Manitol | + | + | + |
| Hippurate hydrolysis | – | – | – |
| Nitrate broth | – | + | – |
| Lysozyme broth | – | – | – |
| Power culture medium | – | – | – |
| Starch hydrolysis | + | + | + |
| Arginine dihydrolase | + | + | + |
| Biofilm production | – | – | – |
| Haemolysis | γ | α | α |
| Spore formation | + | + | + |
| Gram staining | + | – | + |

+, *positive*, - *negative.*

assay, which actually confirmed that these isolated bacteria were not pathogenic.

The outcomes of the antibiotic susceptibility tests for isolated bacteria are listed in **Table 2**. Out of the 22 antibiotics tested, the isolates *Bacillus* sp. RCS1, *Pantoea agglomerans* RCS2, and *Bacillus cereus* RCS3 were susceptible to 15, 16, and 11 of the antibiotics, respectively. They showed intermediate susceptibility to 3, 3, and 5 antibiotics, respectively and resistance to 4, 3, and 6 antibiotics, respectively.

In order to analyze the bile resistance, the isolated microbes were subjected to 0.5% bile salt stress and resistance assay. The resistance was observed by counting the unit colonies formed subsequently after 4 h of exposure and calculated as a percentage. After 3 h of exposure, the result indicated that 76.16% of the *Pantoea agglomerans* RCS3 survived, while 54.06 and 65.38% of *Bacillus* sp. RCS1 and *Bacillus cereus* RCS2 survived, respectively. Nonetheless, the percentage of survivability of all the isolated bacteria dropped subsequently after 4 h of exposure to bile salt but still remained above 50% (**Figure 3**).

The isolated bacteria showed promising results after exposing them to different temperatures of 100, 90, and 80°C for different duration of 10, 5, and 2 min, respectively. Though the multiplying capacity of the strains declined differentially with accumulative temperature, they could still proliferate at 80, 90, and 100°C, demonstrating that these strains could tolerate temperature up to 100°C. In comparison with controls, an increase in the growth (OD) of all the three microbes was observed at all the three temperature exposures (**Figure 4**). The compatibility tests showed that there was no convincing sign of dominance of one isolated bacterium over another, suggesting their compatible nature.

Both isolated bacteria were assessed for their antimicrobial activities against four fish pathogens namely; *Vibrio alginolyticus*, *Vibrio haeveyi*, *Streptococcus iniae*, and *Streptococcus agalactiae* in this study. The isolates were observed to inhibit all the pathogenic bacteria tested in this study (**Table 3**) and in the agar well diffusion method (**Supplementary Figure 1**).

The results showed that all the isolated bacteria in the present study had low auto-aggregation capacity within the first 3 h of incubation. Nonetheless, their auto-aggregation capacity increased after 24 h–79 ± 0.44, 80.1 ± 0.25, and 80.6 ± 0.13%, respectively (**Figure 5**).

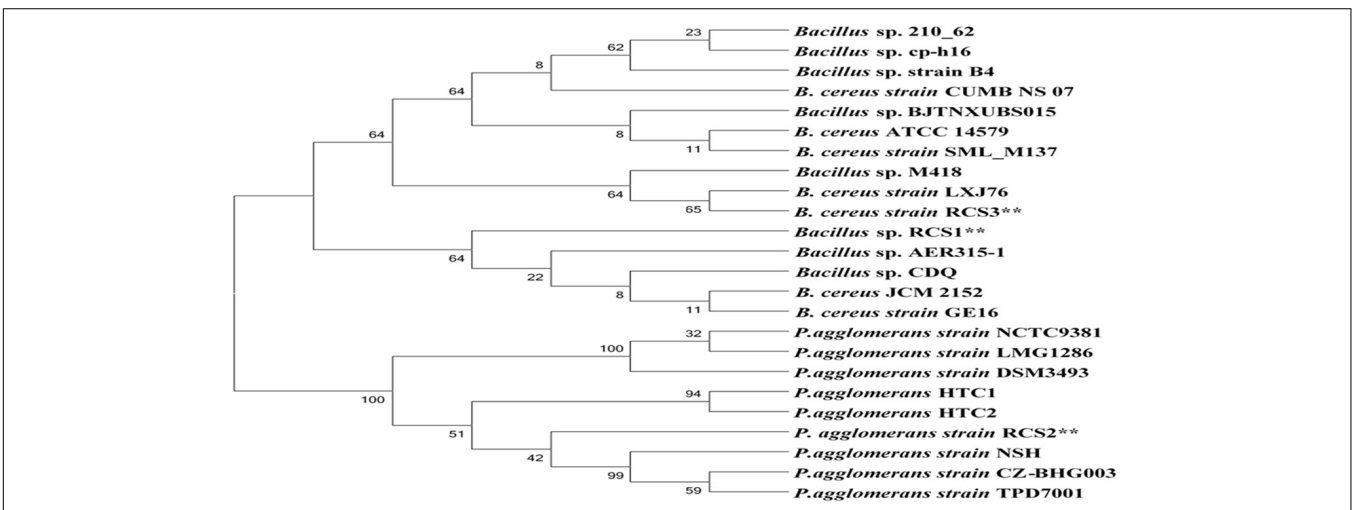


**FIGURE 1 |** A neighbor joining method was used to construct phylogenetic tree using the sequences of isolated bacterial strains and others from NCBI database in order to identify genetic relatedness.

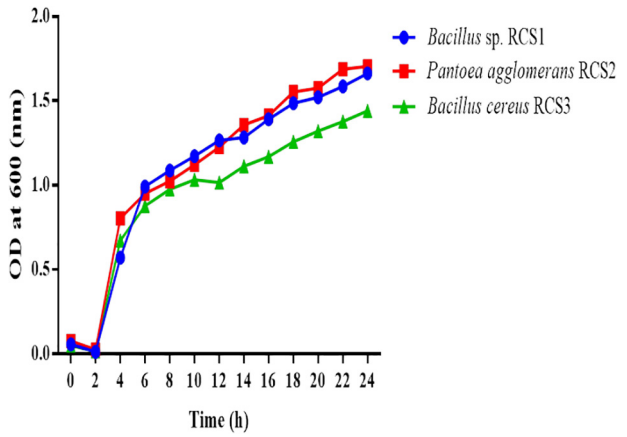


**FIGURE 2 |** Growth curves of isolated microorganisms. The growth curves were observed to determine the growth of these bacteria. The curves of the microbial growth were measured at 600 nm.

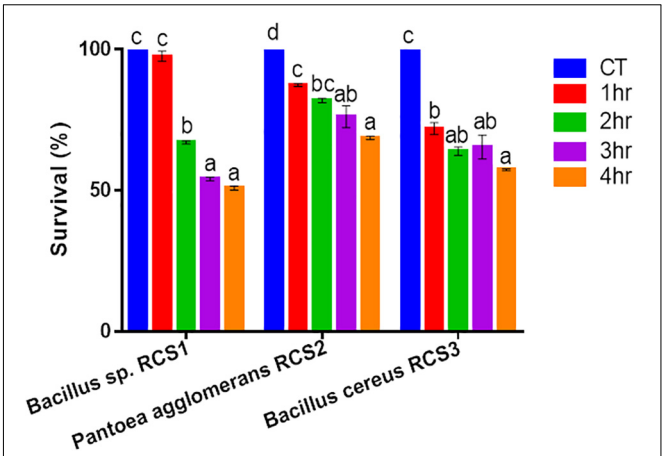


**FIGURE 3 |** Bile endurance of bacteria after 4 h at 37°C. Values are presented as mean ± SE. Different letters show significant differences ($P < 0.05$).

**TABLE 2 |** Antibiotics susceptibility of isolated bacterial strains.

| | Antibiotics susceptibility | | |
|---|---|---|---|
| | ***Bacillus* sp. RCS1** | ***Pantoea agglomerans* RCS2** | ***Bacillus cereus* RCS3** |
| Gentamicin (10 μg) | S | S | S |
| Ampicillin (10 μg) | R | I | I |
| Kanamycin (30 μg) | S | S | S |
| Penicillin (10 μg) | R | S | S |
| Polymyxin (300 IU) | I | S | S |
| Chloramphenicol (30 μg) | S | S | S |
| Erythromycin (15 μg) | I | I | R |
| Neomycin (30 μg) | S | S | S |
| Amikacin (30 μg) | S | S | S |
| Minocycline (30 μg) | R | S | I |
| Cefoperazone (75 μg) | S | S | I |
| Furazolidone (300 μg) | S | R | R |
| Doxycycline (30 μg) | S | I | R |
| Piperacillin (100 μg) | S | S | R |
| Midecamycinum (30 μg) | S | R | S |
| Ofloxacin (5 μg) | S | S | S |
| Vancomycin (30 μg) | I | S | R |
| Carbenicillin (100 μg) | R | S | I |
| Ceftriaxone (30 μg) | S | S | R |
| Clindamycin (2 μg) | S | R | S |
| Noefloxacin (10 μg) | S | S | I |
| Ciprofloxaxin (5 μg) | S | S | S |

*I, intermediate; R, resistant; S, susceptible.*

The adhesion of bacterial isolates to the ethyl acetate (a basic solvent), chloroform (an acidic solvent), and xylene (a non-polar solvent) was assessed, and the percentages of their cell surface hydrophobicity competence were consequently calculated. All the three isolated bacterial strains showed excellent adherence to ethyl acetate, chloroform, and xylene. The adhesion of the isolated bacteria to xylene, chloroform and ethyl acetate were investigated in the present study to determine their adhesion competence to cell surfaces. The results indicated that all the three isolated bacteria showed good cell surface hydrophobicity to the three solvents tested as mentioned above, thereby qualifying the adhesion effectiveness (**Figure 6**).

The results of hemolytic activities showed that *Pantoea agglomerans* RCS2 and *Bacillus cereus* RCS3 displayed α-hemolysis, while *Bacillus* sp. RCS1 demonstrated γ-hemolysis (**Table 1**).

The isolated bacteria showed strong tolerance when exposed to a range of pH. Although asymmetrically, a slow rise in the growth of isolated microbes was observed within the pH range of 1–8 for RC1, 1–7 for RC2, and 1–6 for RC3. The bacterial growth was observed to be declined at pH of 10.0. This indicated that the isolated microbes could endure both the alkaline as well as highly acidic conditions. At some points in different pH conditions, the three isolated bacteria exhibited significant differences ($P < 0.05$) (**Figure 7**).

After 24 h of incubation at 37°C, the morphology of bacterial colonies changed to different colors, which indicated the absence or presence of biofilm production. The screening and analysis of the biofilm-producing capability of the isolated bacteria were investigated using Congo red agar method. The results showed that none of the isolated microorganisms formed black colonies, suggesting that they all were non-biofilm producing strains.

## DISCUSSION

In an endeavor to curtail the incidence of fish infections in aquaculture, the isolation of probiotics from host's tract and then utilization as probiotics is a promising alternative to antibiotics, which have extensively utilized but have adversarial effects as well (Magnadottir, 2010; Resende et al., 2012). The isolation of probiotics from host's tract is also use for promoting the condition and health of the host as well. In the present

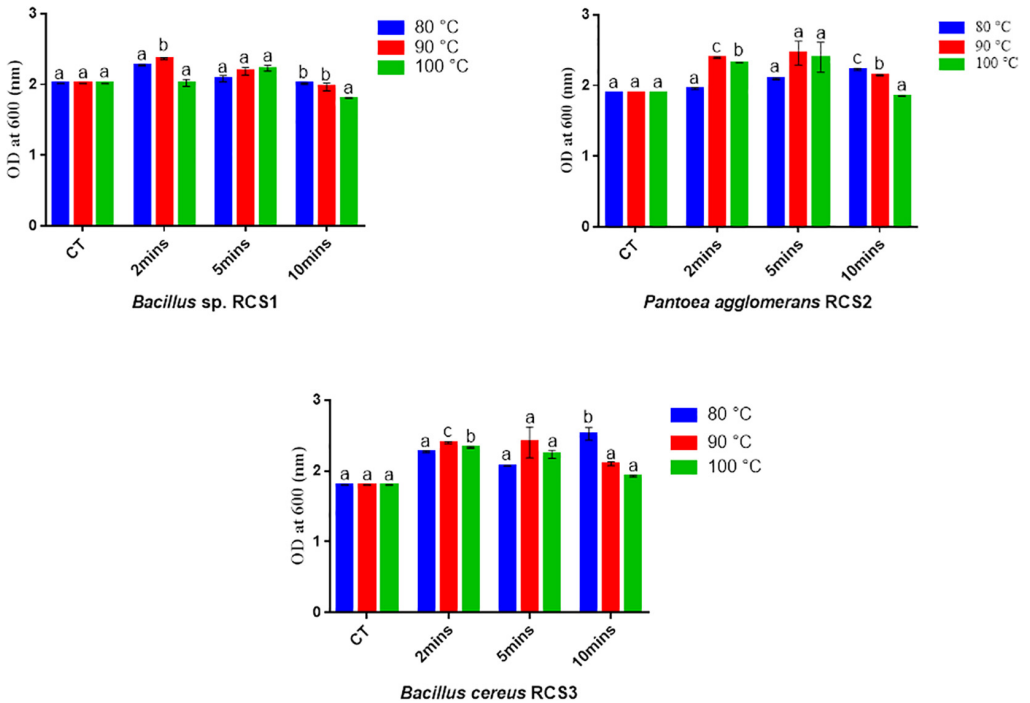


**FIGURE 4 |** Bacterial endurance to high temperatures. Values are presented as mean ± SE. Different letters show significant differences ($P < 0.05$). CT indicates control.

**TABLE 3 |** Antagonistic activity of isolated bacterial strains against selected fish pathogens.

| Pathogenic bacteria | Antagonistic activities | | |
|---|---|---|---|
| | Isolated bacterial | | |
| | ***Bacillus* sp. RCS1** | ***Pantoea agglomerans* RCS2** | ***Bacillus cereus* RCS3** |
| *Streptococcus agalactiae* (SA) | ++ | +++ | +++ |
| *Vibrio harveyi* (VH) | +++ | +++ | +++ |
| *Vibriio alginolyticus* (VA) | ++++ | ++++ | +++ |
| *Streptococcus iniae* (SI) | ++++ | + ++ | ++ |

*Values were calculated as inhibition zone diameter minus paper diameter (mm). The inhibition zones of 2–4 mm are indicated by ++, inhibition zone of 5–6 mm are indicated by +++, and inhibition zone of 7–8 mm are indicated by ++++.*

study, the indigenous *Bacillus* sp. RCS1, *Pantoea agglomerans* RCS2, and *Bacillus cereus strain* RCS3 were isolated from the intestines of cobia fish through culture and *in vitro* approaches, and their probiotic potentials were evaluated. These isolated indigenous potential probiotics bacteria were assessed using different biochemical and morphological tests and identified using *16S rRNA* gene sequencing. For the identification of different microbial species, their specific reactions or biochemical responses are very important. The biochemical tests depend on some enzymes, such as gelatinase, urease and catalase, which are produced by these microbes. Different kinds of bacteria produce different spectra of enzymes. For instance, certain enzymes are essential for the metabolism of individual bacteria, while others expedite the bacterium's capacity to compete with other microorganisms or launch an infection. Traditionally, the living organisms have been classified, according to similarities and differences in their phenotypic characteristics. However, the objective of taxonomic classification by these methods can be difficult because of variations in their phenotypic characteristics. Nowadays, the *16S rRNA* gene sequencing has been widely used for the bacterial identification (Woese et al., 1990).

Several strains from *Bacillus* genus have been previously reported to effectively protect cultured aquaculture species from pathogens (Mishra, 2011; Silva et al., 2012; Laranja et al., 2017; Mukherjee et al., 2019; Hu et al., 2021). Besides, other studies have demonstrated that the dietary species of *Bacillus* species, including *B. cereus, B. subtilis*, and *B. subtilis* T13 (Wu et al., 2014), have improved the sea cucumber's growth and quality of water against pathogens (Galagarza et al., 2018). *Bacillus* sp. JL47 (Silva et al., 2012), *B. subtilis* AQAHBS001 (Zhang et al., 2010), and *B. cereus* BC-1 (Yang et al., 2015) have been reported to fight against pathogens and regulate microbiota to improve the growth performance of cultured species. Nevertheless, the inhibitory effects of *B. cereus* are still not wholly studied in many species, including cobia.

In the present study, the growth of *V. alginolyticus*, *V. haeveyi*, *S. iniae*, and *S. agalactiae* was inhibited by *Bacillus* sp. RCS1, *Pantoea agglomerans* RCS2, and *Bacillus cereus strain* RCS3. The potential probiotics bacteria display antagonism against pathogenic microorganisms by producing

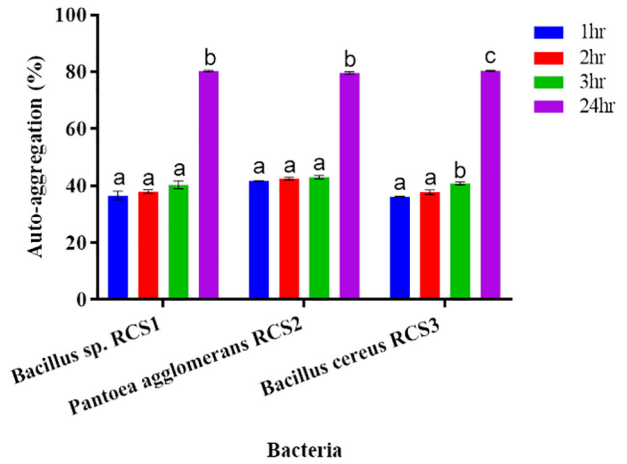


**FIGURE 5 |** Auto-aggregation of bacteria after 24 h. Values are presented as mean ± SE. Different letters show significant differences ($P < 0.05$).

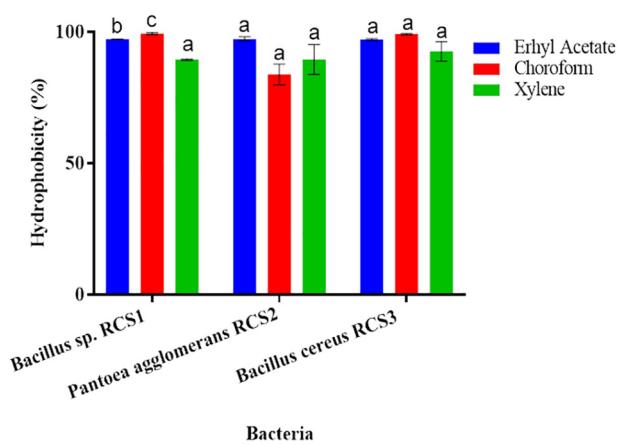


**FIGURE 6 |** Cell surface hydrophobicity of bacterial strains to various solvents (such as Ethyl acetate, Chloroform and Xylene). Values are presented as mean ± SE. Different letters (a, b, and c) indicate significant differences ($P < 0.05$).

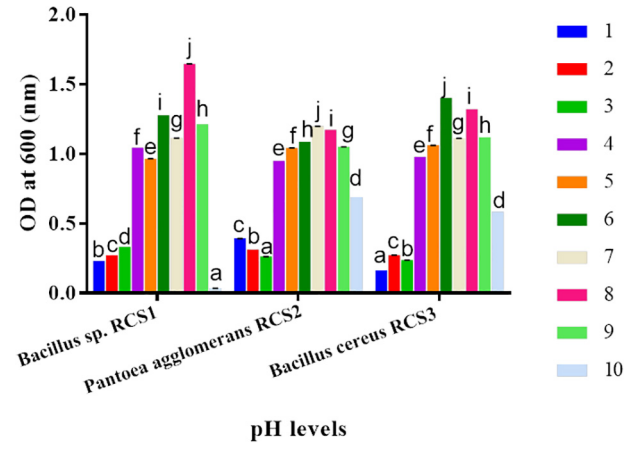


**FIGURE 7 |** Bacteria growths at different pH (1.0–10.0) levels. Values are shown as mean ± SE. Different letters (a, b, c, d, e, f, g, h, i, and j) indicate significant differences ($P < 0.05$).

antibiotics, which affect the colon microbiota. The production of "antibacterial compounds" is a key property of probiotics, which distinguish them from the other bacteria. The ability to produce "antibacterial compounds" is an actual or fundamental property for the competitive inhibition of bacterial pathogens and is a vital characteristic of potential probiotic bacterial strains.

The antagonistic activities of *Bacillus* sp. RCS1 and *Bacillus cereus strain* RCS3 have inhibition zones within the region of 2.0 cm. The antagonistic elements could impede the reproduction and growth of pathogens of cultured species in aquaculture and efficiently inhibited and regulated the incidence of infections in culture fish species (Marianeto et al., 2012; Sumi et al., 2015). The isolated bacteria *Bacillus* sp. RCS1 and *Bacillus cereus strain* RCS3 in the present study exploited a wide range of carbon sources, including starch, adonitol, sorbitol, rhamnose, glucose, mannitol, citrate, and inositol, as well as amino acid arginine, which indicated that these isolates might be useful in the assimilation of carbohydrates and hydrolysis of amino acids (arginine) (Ramesh et al., 2015; Lee et al., 2017; Kavitha et al., 2018). *Bacillus* species are characterized with heat tolerance (Nicholson et al., 2000; Guo et al., 2016) and resistance to low pH and a high proportion of bile concentration (Spinosa et al., 2000; Barbosa et al., 2005). They are also capable of evolving and enduring in the intestines of fish (Hoa et al., 2000; Barbosa et al., 2005; Hong et al., 2009). The probiotics need to tolerate the intestinal (high bile concentration) and gastric (low pH) environments to colonize there and endure intestine and yield valuable traits for host (Guglielmotti et al., 2007; Cartman et al., 2008). A probiotic bacterial strain should be capable of surviving gastric acidic environment, which makes the acid tolerance as an essential selection standard for a bacterial strain to be probiotic. In order to reach colon, the probiotic microbes are more resilient to stomach acidity than other microbes. They are generally exposed to intestinal acids with pH ranges from 2.5 to 3.5. Similarly, the heat-treatment is an indispensable procedure in the course of feed preparation to kill pathogens and increase palatability (Guo et al., 2016). The isolated potential probiotics in the present study demonstrated that they were capable of enduring low pH, higher temperatures (100, 90, and 80°C) and 0.5% bile concentration. Therefore, it can be suggested that the high temperatures triggered the microbe's strains, which resulted in increase in their growth. The greater capability of the isolated strains to withstand heat treatments strongly indicated that the isolates can be utilized as feed supplements.

*Pantoea agglomerans* have revealed exceptional metabolic competences (Smith et al., 2013). They can be utilized against human, plant, and animal pathogens (Dutkiewicz et al., 2016a). In the present study, *Pantoea agglomerans* RCS2 was isolated from the intestines of cobia fish through culture and *in vitro* approaches, their probiotic potentials were evaluated. This isolated indigenous probiotic microbe was assessed using different biochemical and morphological tests and identified

using *16S rRNA* gene sequencing. It also exploited a wide range of carbon sources, including starch, adonitol, sorbitol, rhamnose, glucose, mannitol, citrate, and inositol, as well as amino acid arginine, which indicated that the isolate might be useful in the assimilation of carbohydrates and hydrolysis of amino acids (Ramesh et al., 2015; Lee et al., 2017; Kavitha et al., 2018). The growth of *V. alginolyticus*, *V. haeveyi*, *S. iniae*, and *S. agalactiae* was inhibited by *Pantoea agglomerans* RCS2, having the inhibition zones within the region of 2.0 cm.

Researchers in Japan have demonstrated an exceptionally wide spectrum of curative properties of *P. agglomerans* LPS (IP-PA1), mostly owing to its macrophage-triggering ability, which plays a significant role in the maintenance of homeostasis in all multi-cellular animals and averts several categories of stresses, such as chronic psychological stress (Kohchi et al., 2006; Dutkiewicz et al., 2016a). Skalli et al. (2013) also reported that the LPS derived from the cell walls of Gram-negative bacteria *Pantoea agglomerans* stimulated the growth and immune status of rainbow trout (*Oncorhynchus mykiss*) juveniles. An additional valuable asset of IP-PA1 is its efficacy in the treatment of wide range of diseases (Inagawa et al., 1992a,b, 2011; Nishizawa et al., 1992; Hebishima et al., 2010a,b). Hebishima et al. (2010b) showed that IP-PA1 is an effective edible immuno-modulator that can be utilized to treat and prevent a wide range of infections, either triggered or aggravated by stress-induced immunosuppression in humans and several other animals. According to Nakata et al. (2011), a major reason of the development of infection is the destruction of macrophage's function that plays a crucial role in the maintenance of homeostasis and innate immunity. Although the above-mentioned functions of *P. agglomerans* LPS (IP-PA1) were observed in human, we presumed that the same functions could be performed in fish. The *Pantoea agglomerans* RCS2 showed promising characteristics, which were comparable to the one mentioned above.

The physiological concentration of bile salts ranges between 0.3 and 0.5% in intestinal tract (Begley et al., 2005). The ability of probiotics bacteria to withstand the bile salts is related to the action of bile salt hydrolases, which alleviate the inhibitory effect of bile by hydrolyzing the conjugated bile salts (Oh et al., 2000; Mourad and Nour-Eddine, 2006). After 3 h of exposure, the results indicated that these potential probiotics bacteria could endure bile salts up to 0.5%.

Hydrophobicity could be beneficial for the strains that compete with other microorganisms in digestive system (Todorova et al., 2007; Yerlikaya, 2018). The adhesion to and colonization of mucosal surfaces and epithelial cells (Conventional enterocytes "colonocytes in colon," of prominence are goblet cells) are the essential features of potential probiotics, as it ensure their ability to resist the vacillation of gastric contents, as well as besides inhibits the adhesion of pathogenic microbes and inflammatory reactions (Kos et al., 2003; Guo et al., 2010; Sim et al., 2015). The adhesion capability of probiotics can be indirectly evaluated by finding their hydrophobicity and auto-aggregation (Collado et al., 2008; Meidong et al., 2017; Kuebutornye et al., 2019). Per Wasko et al. (2014) reported bacterial hydrophobicity as vital for adhesion, while others found no connection between the microorganisms' adhesive properties and hydrophobicity (Iturralde et al., 1993). Microorganisms "favor a substrate for adhesion resembling their surface charge" (An and Friedman, 1998). In the present study, all the isolates (*Bacillus* sp. RCS1, *Pantoea agglomerans* RCS2, and *Bacillus cereus* RCS3), exhibited considerable high hydrophobicity: 97.2, 97.3, and 97.1%, respectively, in ethyl acetate; 99.1, 83.8, and 99.1%, respectively, in chloroform; and 89.4, 89.5, and 92.5%, respectively, in xylene. This demonstrated their adhesion potential to hydrocarbons. There is no standard requirement for hydrophobicity value in bacteria but high hydrophobicity is favored for probiotic properties (Yerlikaya, 2018).

The results of hydrophobicity in the present study were similar to those reported by Kuebutornye et al. (2019) with respect to *Bacillus* species, but were comparatively higher as reported by Lee et al. (2017); Manhar et al. (2015). This indicated higher affinity for electron acceptance (ethyl acetate) and electron donation (chloroform) of the current isolates, thereby suggesting their higher epithelial cells adhesion potential and qualifying their adhesion effectiveness. The *in vitro* assessment of auto-aggregation could be utilized for the initial selection and screening of the most refined probiotic strains. There is also a solid connection between the adhesion and auto-aggregation of probiotics to the gastrointestinal tract, as a precondition for potential probiotics (Kuebutornye et al., 2019). All the isolates (*Bacillus* sp. RCS1, and *Pantoea agglomerans* RCS2, *Bacillus cereus* RCS3) showed high auto-aggregation (80.2, 79, and 80.4%, respectively) after 24 h of incubation. The *in vitro* assessment of auto-aggregation could be utilized for the initial selection and screening of the finest probiotics strain. The results of the *in vitro* assessment of auto-aggregation showed the competence of isolated potential probiotics to self-aggregate efficiently.

The important preconditions for the selection of probiotic strains are their lack of antibiotic resistance and hemolytic activity (Argyri et al., 2013). The hemolysis is well-known virulent factor, which triggers infections by entering into trivial lesions in skin and mucous membranes of host (Ramesh et al., 2015; Nandi et al., 2017). The safe hemolysis includes α-hemolysis, γ-hemolysis, and no hemolysis, whilst the β-hemolysis is thought to be dangerous (Prescott, 2005; Shin et al., 2012; Pelczar, 2017)[1]. *Pantoea agglomerans* RCS2 and *Bacillus cereus* RCS3 exhibited α-hemolysis while *Bacillus* sp. RCS1 exhibited γ- hemolysis in the present study. Comparable observations were reported by Lee et al. (2017) and Kavitha et al. (2018) for *Bacillus strains*. In this study, 22 antibiotics were tested, among which, *Bacillus* sp. RCS1 was susceptible to 15, intermediate susceptible to 3 and resistant to 4 (**Table 3**), *Pantoea agglomerans* RCS2 was susceptible to 16, intermediate susceptible to 3 and resistant to 3, while *Bacillus cereus* RCS3 was susceptible to 11, intermediate susceptible to 5 and resistant to 6. These results indicated that these isolates are susceptible to a sufficient number of antibiotics tested (**Table 2**), which were similar to the results reported for *Bacillus* species by Kuebutornye et al. (2019).

[1]https://www.advancedwriters.com/custom-research-paper.html

Biofilm producing microbes cause nosocomial and recurring infections. The formation of biofilm starts with the adhesion of microorganisms to abiotic surfaces, such as a host cell. After attachment, the aggregation of microbes is initiated by cell-cell adhesion. Congo red agar method is a qualitative assay for the detection of biofilm producing microbes, indicated by the differences in the colors of colonies on Congo red agar medium (Kırmusaoğlu, 2019). A study has shown that the infections could be accompanied by the formation of microbial biofilm (Schönborn and Krömker, 2016). Donlan (2002) described biofilm as the grouping of microbes permanently enclosed in a matrix and attached to a surface. A number of studies relate biofilms with the failure of antibiotic therapy and persistent infections. The biofilm can escape hosts' immune system (An and Friedman, 1998) and decrease the influence of valuable antibiotics (Anderl et al., 2000; Zahller and Stewart, 2002). Biofilms possess a great importance for public wellbeing. For instance, the biofilm-producing microbes show reduced susceptibility to antagonistic agents (Donlan, 2001), despite the benefits related to biofilm formation (O'Toole et al., 2000; Morikawa, 2006). Meanwhile, the antibiotics-resistant species are thought to be dangerous for being used as probiotics. Frola et al. (2012) reported that the formation of biofilm can be beneficial due to the colonization of the internal surfaces of udder, thereby building a fence against pathogenic microbes, an imperative factor of the potential probiotics strains. All the three isolated microorganisms in this study tested negative for biofilm formation, as reported by Kavitha et al. (2018).

Some of the well-known fish diseases, reported in aquaculture, are caused by *Vibrio* (Bluford et al., 2017), *Aeromonas* (Amal et al., 2018), and *Streptococcus* (Shoemaker et al., 2001) species. Particularly, in cobia fish, streptococcosis, vibriosis, furunculosis, and mycobacteriosis, and pasteurellosis, are considered as emerging fish diseases in aquaculture (Lopez et al., 2002; Liu et al., 2003; Rajan et al., 2003; Liao et al., 2004; Chen and Hsu, 2005). Several studies have reported that a number of *Bacillus* species exhibit antagonistic effects against a number of Gram-negative and Gram-positive pathogenic bacteria. All the isolated microbes in this study, including *Bacillus* sp. RCS1, *Pantoea agglomerans* RCS2, and *Bacillus cereus* RCS3 were all effective against *V. alginolyticus*, *V. harveyi*, *S. iniae*, and *S. agalactiae*. These results indicated that these isolated bacterial strains are potential probiotics and can be utilized to combat fish diseases in aquaculture.

## CONCLUSION

In conclusion, the bacterial strains, including *Bacillus* sp. RCS1, *Pantoea agglomerans* RCS2, and *Bacillus cereus* RCS3 were isolated from the intestine of a healthy juvenile cobia fish (*Rachycentron canadum*). All the isolated microorganisms exhibited inhibitory effects against the pathogens, including *V. alginolyticus*, *V. harveyi*, *S. iniae*, and *S. agalactiae*. These microbes are characterized with a wide range of antagonistic activities, non-hemolytic activities, high survivability after heat-treatments and safety confidence as well antibiotic susceptibility. Generally, the characteristics displayed by these microorganisms indicated that they could be potentially used as probiotics in aquaculture industry.

## DATA AVAILABILITY STATEMENT

The datasets presented in this study can be found in online repositories. The names of the repository/repositories and accession number(s) can be found below: https://www.ncbi.nlm.nih.gov/, (MW560712, MW560713, and MW560714).

## ETHICS STATEMENT

This animal study was reviewed and approved by the Guangdong Ocean University Research Council (approval number: GDOU-LAE-2020-013).

## AUTHOR CONTRIBUTIONS

EA participated in data curation, data analysis, writing, reviewing, and editing of the original article. W-ZW participated in data collection. GC and J-SH planned and designed the experiments, supervised the experiments, and acquired funding. All authors contributed to the article and approved the submitted version.

## FUNDING

This work was supported by the grants from Southern Marine Science and Engineering Guangdong Laboratory (Zhanjiang) (ZJW-2019-06) and China Agriculture Research System (CARS-47).

## SUPPLEMENTARY MATERIAL

The Supplementary Material for this article can be found online at: https://www.frontiersin.org/articles/10.3389/fmars.2021.672213/full#supplementary-material

**Supplementary Figure 1 |** Graphical representation of the morphological and antagonistic activities of the three isolated bacterial strains. Lane 1: morphology of RCS1, RCS2, RCS3. Lane 2: antagonistic activities of RCS1, RCS2, and RCS3 against *Vibrio haeveyi.* Lane 3: antagonistic activities of RCS1, RCS2, and RCS3 against *Vibrio alginolyticus.* Lane 4: antagonistic activities of RCS1, RCS2, and RCS3 against *Streptococcus iniae.* Lane 5: antagonistic activities of RCS1, RCS2, and RCS3 against *Streptococcus agalactiae*. Note: A represents *Bacillus spp.*RCS1; C represents *Pantoea agglomerans strain* RCS2 and F represents *Bacillus Cereus strain* RCS3; VH indicates *Vibrio haeveyi;* VA indicates *Vibrio alginolyticus;* SI indicates *Streptococcus iniae,* and SA indicates *Streptococcus agalactiae*.

## REFERENCES


Abarike, E. D., Jian, J., Tang, J., Cai, J., Yu, H., Lihua, C., et al. (2018). Influence of traditional Chinese medicine and *Bacillus* species (TCMBS) on growth, immune response and disease resistance in Nile tilapia, *Oreochromis niloticus*. *Aquac. Res.* 49, 2366–2375. doi: 10.1111/are.13691

Aleti, G., Sessitsch, A., and Brader, G. (2015). Genome mining: prediction of lipopeptides and polyketides from *Bacillus* and related firmicutes. *Comput. Struct. Biotechnol. J.* 15, 192–203. doi: 10.1016/j.csbj.2015.03.003

Resende, A. J. L., Silva, V., Oliveira Fontes, C., Alves Souza-Filho, J., Rocha de Oliveira, T. L., et al. (2012). Multidrug-resistance and toxic metal tolerance of medically important bacteria isolated from an aquaculture system. *Microb. Environ.* 27, 449–455. doi: 10.1264/jsme2.me12049

Amal, M. N. A., Koh, C. B., Nurliyana, M., Suhaiba, M., Nor-Amalina, Z., Santha, S., et al. (2018). A case of natural co-infection of Tilapia Lake virus and *Aeromonas veronii* in a Malaysian red hybrid tilapia (*Oreochromis niloticus*×*O. mossambicus*) farm experiencing high mortality. *Aquaculture* 485, 12–16. doi: 10.1016/j.aquaculture.2017.11.019

Amenyogbe, E., Chen, G., Wang, Z., Huang, J.-S., Huang, B., and Li, H.-J. (2020). The exploitation of probiotics, prebiotics and synbiotics in aquaculture: present study, limitations and future directions: a review. *Aquacult Int.* 28, 1017–1041. doi: 10.1007/s10499-020-00509-0

An, Y. H., and Friedman, R. J. (1998). Concise review of mechanisms of bacterial adhesion to biomaterial surfaces. *J. Biomed. Mater. Res.* 43, 338–348. doi: 10.1002/(sici)1097-4636(199823)43:3<338::aid-jbm16>3.0.co;2-b

Anderl, J. N., Franklin, M. J., and Stewart, P. S. (2000). Role of antibiotic penetration limitation in *Klebsiella pneumoniae* biofilm resistance to ampicillin and ciprofloxacin. *Antimicrob. Agents Ch.* 44, 1818–1824. doi: 10.1128/aac.44.7.1818-1824.2000

Argyri, A. A., Zoumpopoulou, G., Karatzas, K. A. G., Tsakalidou, E., Nychas, G. J. E., Panagou, E. Z., et al. (2013). Selection of potential probiotic lactic acid bacteria from fermented olives by in vitro tests. *Food Microbiol.* 33, 282–291. doi: 10.1016/j.fm.2012.10.005

Balcázar, J. L., Vendrell, D., de Blas, I., Ruiz-Zarzuela, I., Gironés, O., and José Luis Múzquiz, J. L. (2007). *In vitro* competitive adhesion and production of antagonistic compounds by lactic acid bacteria against fish pathogens. *Vet. Microbiol.* 122, 373–380. doi: 10.1016/j.vetmic.2007.01.023

Bandyopadhyay, P., and Patra, B. C. (2004). *Probiotics for Sustainable Aquaculture and its Utilization Trial: Course Manual of the Summer School on Development of Sustainable Aquaculture Technology for Fresh and Saline Waters, Department of Zoology*. India: CCS Haryana Agricultural University, 61–66.

Barbosa, T. M., Serra, C. R., La Ragione, R. M., Woodward, M. J., and Henriques, A. O. (2005). Screening for *Bacillus* isolates in the broiler gastrointestinal tract. *Appl. Environ. Microbiol.* 71, 968–978. doi: 10.1128/AEM.71.2.968-978.2005

Begley, M., Gahan, C. G., and Hill, C. (2005). The interaction between bacteria and bile. *FEMS Microbiol. Rev.* 29, 625–651. doi: 10.1016/j.femsre.2004.09.003

Benetti, D. D., O'Hanlon, B., Rivera, J. A., Welch, A. W., Maxey, C., and Orhun, M. R. (2010). Growth rates of cobia (*Rachycentron canadum*) cultured in open ocean submerged cages in the Caribbean. *Aquaculture* 302, 195–201. doi: 10.1016/j.aquaculture.2010.02.021

Benetti, D. D., Orhun, M. R., Sardenberg, B., O'Hanlon, B., Welch, A. W., Hoenig, R., et al. (2008). Advances in hatchery and grow-out technology of cobia *Rachycentron canadum* (Linnaeus). *Aquacult. Res.* 39, 701–711. doi: 10.1111/j.1365-2109.2008.01922.x

Bhatnagar, A., and Dhillon, O. (2019). Characterization, screening and application of bacteria with probiotic adequacy isolated from the gut of *Labeo calbasu* (Hamilton, 1822). *Fisher. Aquat. Life* 27, 178–189. doi: 10.2478/aopf-2019-0020

Bhatnagar, A., and Lamba, R. (2015). Antimicrobial ability and growth promoting effects of feed supplemented probiotic bacterium isolated from gut microflora of *Cirrhinus mrigala*. *J. Integrat. Agricult.* 14, 583–592. doi: 10.1016/s2095-3119(14)60836-4

Bhatnagar, A., and Lamba, R. (2017). Molecular characterization and dosage application of autochthonous potential probiotic bacteria in *Cirrhinus mrigala*. *J. Fisher. Sci. Com* 11, 46–56.

Bhatnagar, A., and Raparia, S. (2014). Optimum dietary inclusion level of *Bacillus coagulans* for growth and digestibility improvement for Catla catla (Hamilton). *Int. J. Curr. Res. Rev.* 6, 1–10.

Bhatnagar, A., Raparia, S., and Kumari, S. (2012). Influence of isolated *Bacillus coagulans* on growth performance and digestive enzyme activities of *Catla catla*. *J. Nat. Sci. Sustain. Technol.* 6, 225–235.

Bluford, J., Gauthier, D., Colasanto, M., Rhodes, M., Vogelbein, W., and Haines, A. (2017). Identification of virulence genes in Vibrio spp. isolates from the 2009 Bermuda reef fish mortality event. *J. Fish Dis.* 40, 597–600. doi: 10.1111/jfd.12532

Carnevali, O., de Vivo, L., Sulpizio, R., Gioacchini, G., Olivotto, I., Silvi, S., et al. (2006). Growth improvement by probiotic in European sea brass juveniles (*Dicentrachus labrax*, L.), with particular attention to IGF-1, myostatin and cortiosol gene expression. *Aquaculture* 258, 430–438. doi: 10.1016/j.aquaculture.2006.04.025

Cartman, S. T., La Ragione, R. M., and Woodward, M. J. (2008). *Bacillus subtilis* spores germinate in the chicken gastrointestinal tract. *Appl. Environ. Microbiol.* 74, 5254–5258. doi: 10.1128/AEM.00580-08

Chalupowicz, L., Manulis-Sasson, S., Itkin, M., Sacher, A., Sessa, G., and Barash, I. (2008). Quorum-sensing system affects gall development incited by *Pantoea agglomerans* pv. *gypsophilae*. *Mol. Plant Microbe. Interact.* 21, 1094–1105. doi: 10.1094/mpmi-21-8-1094

Chen, B., Peng, M., Tong, W., Zhang, Q., and Song, Z. (2019). The quorum quenching bacterium *Bacillus licheniformis* T-1 protects zebrafish against *Aeromonas hydrophila* infection. *Probiot. Antimicrob. Proteins* 12, 160–171. doi: 10.1007/s12602-018-9495-7

Chen, Q., Liu, H., Tan, B. P., Dong, X. H., Chi, S. Y., Yang, Q. H., et al. (2016). Effects of dietary cholesterol level on growth performance, blood biochemical parameters and lipid metabolism of juvenile cobia (*Rachycentron canadu*). *J. Guangd. Ocean Univ.* 36, 35–43.

Chen, S. C., and Hsu, C. (2005). Studies on the pathogenicity and pathology of photobacterium damselae subsp. piscicida on *Rachycentron canadum*. *J. Fish. Soc. Taiwan* 32:4.

Clinical and Laboratory Standards Institute (2009). *Clinical and Laboratory Standards Institute, Performance Standards for Antimicrobial Disk Susceptibility Tests. Approved Standard M2-A10*. Wayne, PA: Clinical and Laboratory Standards Institute.

Collado, M. C., Meriluoto, J., and Salminen, S. (2008). Adhesion and aggregation properties of probiotic and pathogen strains. *Eur. Food Res. Technol.* 226, 1065–1073. doi: 10.1007/s00217-007-0632-x

Dlamini, M. T., Lessells, R. J., Iketleng, T., and Oliveira, T. (2019). Whole genome sequencing for drug-resistant tuberculosis management in South Africa: what gaps would this address and what are the challenges to implementation. *J. Clin. Tubercul. Other Mycobacter. Dis.* 16:100115. doi: 10.1016/j.jctube.2019.100115

Donlan, R. M. (2001). Biofilm formation: a clinically relevant microbiological process. *Clin. Infect. Dis.* 33, 1387–1392. doi: 10.1086/322972

Donlan, R. M. (2002). Biofilms: microbial life on surfaces. *Emerg. Infect. Dis.* 8, 881–890. doi: 10.3201/eid0809.020063

Dutkiewicz, J., Mackiewicz, B., Lemieszek, M. K., Golec, M., and Milanowski, J. (2016a). *Pantoea agglomerans*: a mysterious bacterium of evil and good. Part IV. Beneficial effects. *Ann. Agric. Environ. Med.* 23, 206–222. doi: 10.5604/12321966.1203879

Dutkiewicz, J., Mackiewicz, B., Lemieszek, M. K., Golec, M., and Milanowski, J. (2015). *Pantoea agglomerans*: a mysterious bacterium of evil and good. Part I. Deleterious effects: dust-borne endotoxins and allergens – focus on cotton dust. *Ann. Agric. Environ. Med.* 22, 576–588. doi: 10.5604/12321966.1185757

Dutkiewicz, J., Mackiewicz, B., Lemieszek, M. K., Golec, M., and Milanowski, J. (2016b). *Pantoea agglomerans*: a mysterious bacterium of evil and good. Part III. Deleterious effects: Infections of humans, animals and plants. *Ann. Agric. Environ. Med.* 23, 197–205. doi: 10.5604/12321966.1203878

Dutkiewicz, J., Mackiewicz, B., Lemieszek, M. K., Golec, M., Skórska, C., Góra-Florek, A., et al. (2016c). *Pantoea agglomerans*: a mysterious bacterium of evil and good. Part II. Deleterious effects: Dust-borne endotoxins and allergens – focus on grain dust, other agricultural dusts and wood dust. *Ann. Agric. Environ. Med.* 23, 110–133.

Engel, R. R., Matsen, J. M., Chapman, S. S., and Schwartz, S. (1972). Carbon monoxide production from heme compounds by bacteria. *J. Bacteriol.* 112, 1310–1315. doi: 10.1128/jb.112.3.1310-1315.1972

Food and Agriculture Organization (FAO) (2001). *Food and Agricultural Organization 815 of the United Nations and World Health Organization. Health*

*and Nutritional Properties of Probiotics in Food Including Powder Milk With Live Lactic Acid Bacteria*. Rome: RAO.

Food and Agriculture Organization (FAO) (2015). *Global Aquaculture Production 1950-2013*. Available online at: http://www.fao.org/fishery/statistics/global-aquaculture-production/query/en (accessed November 15, 2015).

Food and Agriculture Organization (FAO) (2020). "Fishery and aquaculture statistics. Global production by production source 1950-2018 (FishstatJ)," in *FAO Fisheries and Aquaculture Department [online]*, Rome. Available online at: www.fao.org/fishery/statistics/software/fishstatj/en

Frola, I. D., Pellegrino, M. S., Espeche, M. C., Giraudo, J. A., Nader-Macias, M. E., and Bogni, C. I. (2012). Effects of intramammary inoculation of *Lactobacillus perolens* CRL1724 in lactating cows' udders. *J. Dairy Res.* 79, 84–92. doi: 10.1017/S0022029911000835

Galagarza, O. A., Smith, S. A., Drahos, D. J., Eifert, J. D., Williams, R. C., and Kuhn, D. D. (2018). Modulation of innate immunity in nile tilapia (*Oreochromis niloticus*) by dietary supplementation of *Bacillus subtilis* endospores. *Fish Shellf. Immunol.* 83, 171–179. doi: 10.1016/j.fsi.2018.08.062

Geng, X., Dong, X.-H., Tan, B.-P., Yang, Q.-H., Chi, S.-Y., Liu, H.-Y., et al. (2011). Effects of dietary probiotic on the growth performance, non-specific immunity and disease resistance of cobia, *Rachycentron canadum*. *Aquacult. Nutri.* 18, 46–55. doi: 10.1111/j.1365-2095.2011.00875.x

Guglielmotti, D. M., Marcó, M. B., Golowczyc, M., Reinheimer, J. A., and Quiberoni, A. L. (2007). Probiotic potential of *Lactobacillus delbrueckii* strains and their phage resistant mutants. *Int. Dairy J.* 17, 916–925. doi: 10.1016/j.idairyj.2006.11.004

Guo, X. H., Kim, J. M., Nam, H. M., Park, S. Y., and Kim, J. M. (2010). Screening lactic acid bacteria from swine origins for multistrain probiotics based on in vitro functional properties. *Anaerobe* 16, 321–326. doi: 10.1016/j.anaerobe.2010.03.006

Guo, X., Chen, D. D., Peng, K. S., Cui, Z. W., Zhang, X. J., Li, S., et al. (2016). Identification and characterization of *Bacillus subtilis* from grass carp (*Ctenopharynodon idellus*) for use as probiotic additives in aquatic feed. *Fish Shellf. Immunol.* 52, 74–84. doi: 10.1016/j.fsi.2016.03.017

Hao, K., Liu, J., Ling, F., Liu, X., Lu, L., Xia, L., et al. (2014). Effects of dietary administration of *Shewanella haliotis* D4, *Bacillus cereus* D7 and *Aeromonas bivalvium* D15, single or combined, on the growth, innate immunity and disease resistance of shrimp, *Litopenaeus vannamei*. *Aquaculture* 428, 141–149. doi: 10.1016/j.aquaculture.2014.03.016

Hebishima, T., Matsumoto, Y., Watanabe, G., Soma, G., Kohchi, C., Taya, K., et al. (2010a). Protective effects of the immunopotentiator from *Pantoea agglomerans* 1 on chemotherapeutic agent-induced macrophage growth inhibition. *Anticancer Res.* 30, 2033–2040.

Hebishima, T., Matsumoto, Y., Watanabe, G., Soma, G., Kohchi, C., Taya, K., et al. (2010b). Recovery from immunosuppression-related disorders in humans and animals by IP-PA1, an edible lipopolysaccharide. *Anticancer Res.* 30, 3113–3118.

Hoa, N. T., Baccigalupi, L., Huxham, A., Smertenko, A., van, P. H., Ammendola, S., et al. (2000). Characterization of *Bacillus* species used for oral bacteriotherapy and bacterioprophylaxis of gastrointestinal disorders. *Appl. Environ. Microbiol.* 66, 5241–5247. doi: 10.1128/AEM.66.12.5241-5247.2000

Holt, G. J., Faulk, C. K., and Schwarz, M. H. (2007). A review of the larviculture of cobia *Rachycentron canadum,* a warm water marine fish. *Aquaculture* 268, 181–187. doi: 10.1016/j.aquaculture.2007.04.039

Hong, H. A., To, E., Fakhry, S., Baccigalupi, L., Ricca, E., and Cutting, S. M. (2009). Defining the natural habitat of *Bacillus* spore-formers. *Res. Microbiol.* 160, 375–379. doi: 10.1016/j.resmic.2009.06.006

Hu, Z., Zhang, W., Liang, W., Zhang, Z., Guo, M., and Li, C. (2021). Bacillus cereus LS2 from *Apostichopus japonicus* antagonizes *Vibrio splendidus* growth. *Aquaculture* 531:735983. doi: 10.1016/j.aquaculture.2020.735983

Huang, J.-S., Amenyogbe, E., Chen, G., and Wang, W.-Z. (2020). Biochemical composition and activities of digestive and antioxidant enzymes during the egg and yolk-sac larval development of the cobia (*Rachycentron canadum*). *Aquacult. Res.* 20, 1–14. doi: 10.1111/are.15017

Inagawa, H., Kohchi, C., and Soma, G. (2011). Oral administration of lipopolysaccharides for the prevention of various diseases: benefit and usefulness. *Anticancer Res.* 31, 2431–2436.

Inagawa, H., Nishizawa, T., Tsukioka, D., Suda, T., Chiba, Y., Okutomi, T., et al. (1992a). Homeostasis as regulated by activated macrophage. II. LPS of plant origin other than wheat flour and their concomitant bacteria. *Chem. Pharm. Bull. (Tokyo)* 40, 994–997. doi: 10.1248/cpb.40.994

Inagawa, H., Saitoh, F., Iguchi, M., Nishizawa, T., Okutomi, T., Morikawa, A., et al. (1992b). Homeostasis as regulated by activated macrophage. III. Protective effect of LPSw (lipopolysaccharide (LPS) of wheat flour) on gastric ulcer in mice as compared with those of other LPS from various sources. *Chem. Pharm. Bull. (Tokyo)* 40, 998–1000. doi: 10.1248/cpb.40.998

Irianto, A., and Austin, B. (2002). Probiotics in aquaculture. *J. Fish Dis.* 25, 633–642.

Iturralde, M., Aguilar, B., Baselga, R., and Amorena, B. (1993). Adherence of ruminant mastitis *Staphylococcus aureus* strains to epithelial cells from ovine mammry gland primary cultures and from a rat intestinal cell line. *Vet. Microbiol.* 38, 115–127. doi: 10.1016/0378-1135(93)90079-m

Jiang, J., Wu, S., Wang, J., and Feng, Y. (2015). AHL-type quorum sensing and its regulation on symplasmata formation in *Pantoea agglomerans* YS19. *J. Basic Microbiol.* 55, 607–616. doi: 10.1002/jobm.201400472

Kavitha, M., Raja, M., and Perumal, P. (2018). Evaluation of probiotic potential of *Bacillus* spp. isolated from the digestive tract of freshwater fish *Labeo calbasu* (Hamilton, 1822). *Aquac. Rep.* 11, 59–69. doi: 10.1016/j.aqrep.2018.07.001

Kırmusaoğlu, S. (2019). *The Methods for Detection of Biofilm and Screening Antibiofilm Activity of Agents. Antimicrobials, Antibiotic Resistance, Antibiofilm Strategies and Activity Methods*. London: IntechOpen. doi: 10.5772/intechopen.84411

Knackstedt, R., and Gatherwright, J. (2019). The role of thermal injury on intestinal bacterial translocation and the mitigating role of probiotics: a review of animal and human studies. *Burns* 46, 1005–1012. doi: 10.1016/j.burns.2019.07.007

Kohchi, C., Inagawa, H., Nishizawa, T., Yamaguchi, T., Nagai, S., and Soma, G. (2006). Applications of lipopolysaccharide derived from *Pantoea agglomerans* (IP-PA1) for health care based on macrophage network theory. *J. Biosci. Bioeng.* 102, 485–496. doi: 10.1263/jbb.102.485

Kos, B., Šušković, J., Vuković, S., Šimpraga, M., Frece, J., and Matošić, S. (2003). Adhesion and aggregation ability of probiotic strain *Lactobacillus acidophilus* M92. *J. Appl. Microbiol.* 94, 981–987. doi: 10.1046/j.1365-2672.2003.01915.x

Kuebutornye, F. K. A., Liao, J., Pang, H., Lu, Y., Ayiku, S., and Sakyi, M. E. (2018). Molecular cloning and bioinformatics analysis of T3SS inner membrane ring HrpQ from Vibrio harveyi. *Genom. Appl. Biol.* 9, 40–47. doi: 10.5376/gab.2018.09.0007

Kuebutornye, F. K. A., Lu, Y., Abarike, E. D., Wang, Z., Li, Y., and Sakyi, M. E. (2019). In vitro Assessment of the probiotic characteristics of three *Bacillus* species from the gut of nile tilapia, *Oreochromis niloticus*. *Probiot. Antimicrob. Prot.* 12, 412–424. doi: 10.1007/s12602-019-09562-5

Laranja, J. L. Q., Amar, E. C., Ludevese-Pascual, G. L., Niu, Y. F., Geaga, M. J., De Schryver, P., et al. (2017). A probiotic *Bacillus* strain containing amorphous poly-betahydroxybutyrate (PHB) stimulates the innate immune response of *Penaeus monodon* postlarvae. *Fish Shellf. Immunol.* 68, 202–210. doi: 10.1016/j.fsi.2017.07.023

Lee, S., Lee, J., Jin, Y. I., Jeong, J. C., Chang, Y. H., Lee, Y., et al. (2017). Probiotic characteristics of *Bacillus* strains isolated from Korean traditional soy sauce. *LWT Food Sci. Technol.* 79, 518–524. doi: 10.1016/j.lwt.2016.08.040

Lertcanawanichakul, M., and Sawangnop, S. (2008). A comparison of two methods used for measuring the antagonistic activity of *Bacillus* species. *Walailak J. Sci. Technol.* 5, 161–171. doi: 10.2004/wjst.v5i2.86

Li, A., Wang, Y., Pei, L., Mehmood, K., Li, K., Qamar, H., et al. (2019). Influence of dietary supplementation with *Bacillus velezensis* on intestinal microbial diversity of mice. *Microb. Pathog.* 136:103671. doi: 10.1016/j.micpath.2019.103671

Liao, I. C., Huang, T. S., Tsai, W. S., Hseueh, C. M., Chang, S. L., and Leano, E. M. (2004). Cobia culture in Taiwan: current status and problems. *Aquaculture* 237, 155–165. doi: 10.1016/j.aquaculture.2004.03.007

Liu, N., Zhang, S., Zhang, W., and Li, C. (2017). *Vibrio* sp. 33 a potential bacterial antagonist of *Vibrio splendidus* pathogenic to sea cucumber (*Apostichopus japonicus*). *Aquaculture* 470, 68–73. doi: 10.1016/j.aquaculture.2016.12.028

Liu, P. C., Liu, J. Y., and Lee, K. K. (2003). Virulence of *Photobacterium damselae* subsp piscicida in cultured cobia *Rachycentron canadum*. *J. Basic Microbiol.* 43, 499–507.

Lopez, C., Rajan, P. R., Lin, J. H., Kuo, T., and Yang, H. (2002). Disease outbreak in seafarmed cobia (*Rachycentron canadum*) associated with Vibrio spp., *Photobacterium damselae* ssp. piscicida, mongenean and myxosporean parasites. *Bull. Eur. Assoc. Fish Pathol.* 22, 206–211.

Magnadottir, B. (2010). Immunological control of fish diseases. *Mar. Biotechnol.* 12, 361–379. doi: 10.1007/s10126-010-9279-X

Manhar, A. K., Saikia, D., Bashir, Y., Mech, R. K., Nath, D., Konwar, B. K., et al. (2015). In vitro evaluation of celluloytic *Bacillus amyloliquefaciens* AMS1 isolated from traditional fermented soybean (Churpi) as an animal probiotic. *Res. Vet. Sci.* 99, 149–156. doi: 10.1016/j.rvsc.2015.01.008

Marianeto, S., Candido, E. D., Rodrigues, D. R., Sousa, D. A., Silva, E. M., Moraes, L. M., et al. (2012). Deciphering the magainin resistance process of *Escherichia coli* strains in light of the cytosolic proteome. *Antimicrob. Agents Chemother.* 56, 1714–1724. doi: 10.1128/aac.05558-11

Meidong, R., Doolgindachbaporn, S., Jamjan, W., Sakai, K., Tashiro, Y., Okugawa, Y., et al. (2017). A novel probiotic *Bacillus siamensis* B44v isolated from Thai pickled vegetables (Phakdong) for potential use as a feed supplement in aquaculture. *J. Gen. Appl. Microbiol.* 63, 246–253. doi: 10.2323/jgam.2016.12.002

Mishra, G. P. (2011). Treatment of drug-resistant tuberculosis. *Lancet Infect. Dis.* 4, 129–135. doi: 10.2147/idr.s10332

Montes, M., Farto, R., Maria, J. P., Armada, S. P., and Nieto, T. P. (2006). Genotypic diversity of *Vibrio* isolates associated with turbot (*Scophthalmus maximus*) culture. *Res. Microbiol.* 157, 495.

Morikawa, M. (2006). Beneficial biofilm formation by industrial bacteria *Bacillus subtilis* and related species. *J. Biosci. Bioeng.* 101, 1–8. doi: 10.1263/jbb.101.1

Mourad, K., and Nour-Eddine, K. (2006). Microbiological study of naturally fermented Algerian green olives: Isolation and identification of lactic acid bacteria and yeasts along with the effects of brine solutions obtained at the end of olive fermentation on *Lactobacillus plantarum*. *Grasas Aceites* 57, 292–300.

Mukherjee, A., Chandra, G., and Ghosh, K. (2019). Single or conjoint application of autochthonous *Bacillus* strains as potential probiotics: effects on growth, feed utilization, immunity and disease resistance in Rohu *Labeo rohita* (Hamilton). *Aquaculture* 512:734302. doi: 10.1016/j.aquaculture.2019.734302

Murray, P. R., Baron, E. J., Jorgensen, J. H., Landry, M. L., and Pfaller, M. A. (2007). *Antibacterial Susceptibility Tests: Dilution and Disk Diffusion Methods, Manual of Clinical Microbiolog*, 9th Edn. Washington, DC: American Society for Microbiology, 1152–1172.

Nadarasah, G., and Stavrinides, J. (2014). Quantitative evaluation of the host-colonizing capabilities of the enteric bacterium *Pantoea* using plant and insect hosts. *Microbiology.* 160, 602–615. doi: 10.1099/mic.0.073452-0

Nakata, K., Inagawa, H., and Soma, G. (2011). Lipopolysaccharide IP-PA1 from *Pantoea agglomerans* prevents suppression of macrophage function in stress-induced diseases. *Anticancer Res.* 31, 2437–2440.

Nandi, A., Dan, S. K., Banerjee, G., Ghosh, P., Ghosh, K., Ringø, E., et al. (2017). Probiotic potential of autochthonous bacteria isolated from the gastrointestinal tract of four freshwater teleosts. *Probiot. Antim. Prot.* 9, 12–21. doi: 10.1007/s12602-016-9228-8

Nawrath, M. M., Ottenheim, C., Wu, J. C., and Zimmermann, W. (2020). *Pantoea sp. P37* as a novel nonpathogenic host for the heterologous production of rhamnolipids. *Microbiol. Open* 9:e1019. doi: 10.1002/mbo3.1019

Nayak, S. K., and Mukherjee, S. C. (2011). Screening of gastrointestinal bacteria of Indian major carps. *Aquacult. Res.* 42, 1034–1041. doi: 10.1111/j.1365-2109.2010.02686.x

Nicholson, W. L., Munakata, N., Horneck, G., Melosh, H. J., and Setlow, P. (2000). Resistance of *Bacillus* endospores to extreme terrestrial and extraterrestrial environments. *Microbiol. Mol. Biol. Rev.* 64, 548–572. doi: 10.1128/MMBR.64.3.548-572.2000

Nishizawa, T., Inagawa, H., Oshima, H., Okutomi, T., Tsukioka, D., Iguchi, M., et al. (1992). Homeostasis as regulated by activated macrophage. I. Lipopolysaccharide (LPS) from wheat flour: isolation, purification and some biological activities. *Chem. Pharm. Bull. (Tokyo)* 40, 479–483. doi: 10.1248/cpb.40.479

O'Sullivan, D. J. (2001). Screening of intestinal microflora for effective probiotic bacteria. *J. Agric. Food Chem.* 49, 1751–1760. doi: 10.1021/jf0012244

O'Toole, G., Kaplan, H. B., and Kolter, R. (2000). Biofilm formation as microbial development. *Annu. Rev. Microbiol.* 54, 49–79. doi: 10.1146/annurev.micro.54.1.49

Oh, S., Kim, S. H., and Worobo, R. W. (2000). Characterization and purification of a bacteriocin produced by a potential probiotic culture, *Lactobacillus acidophilus* 30SC. *J. Dairy Sci.* 83, 2747–2752. doi: 10.3168/jds.s0022-0302(00)75169-1

Park, Y., Kim, H., Won, S., Hamidoghli, A., Hasan, T., Kong, I., et al. (2020). Effects of two dietary probiotics (*Bacillus subtilis* or *licheniformis*) with two prebiotics (mannan or fructo oligosaccharide) in Japanese eel, *Anguilla japonica*. *Aquac. Nutr.* 26, 316–327. doi: 10.1111/anu.12993

Patel, A. K., Ahire, J. J., Pawar, S. P., Chaudhari, B. L., and Chincholkar, S. B. (2009). Comparative accounts of probiotic characteristics of *Bacillus spp*. isolated from food wastes. *Food Res. Int.* 42, 505–510. doi: 10.1016/j.foodres.2009.01.013

Pelczar, M. J. (2017). *Microbiology*, 5 Edn. New York, NY: Mc-Graw Hill Education.

Prescott, M. L. (2005). *Microbiology*, 6 Edn. New York, NY: Mc-Graw Hill publication, G1–G30.

Rajan, P. R., Lin, J. H., Ho, M. S., and Yang, H. L. (2003). Simple and rapid detection of *Photobacterium damselae* ssp. piscicida by a PCR technique and plating method. *J. Appl. Microbiol.* 95, 1375–1380. doi: 10.1046/j.1365-2672.2003.02119.x

Rajyalakshmi, K., Roopa, B., Saikat, D. M., Priyanka, D., Vadlamudi, S., and Subramaniam, G. (2016). Characterization of potential probiotic bacteria isolated from sorghum and pearl millet of the semi-arid tropics. *Afr. J. Biotechnol.* 15, 613–621. doi: 10.5897/AJB2016.15212

Ramesh, D., Vinothkanna, A., Rai, A. K., and Vignesh, V. S. (2015). Isolation of potential probiotic *Bacillus* spp. and assessment of their subcellular components to induce immune responses in *Labeo rohita* against *Aeromonas hydrophila*. *Fish Shellf. Immunol.* 45, 268–276. doi: 10.1016/j.fsi.2015.04.018

Ray, A. K., Ghosh, K., and Ringo, E. (2012). Enzyme-producing bacteria isolated from fish gut, A review. *Aquac. Nutr.* 18, 465–492. doi: 10.1111/j.1365-2095.2012.00943.x

Ringo, E. (2019). Probiotics in shellfish aquaculture. *Aquacult. Fish.* 5, 1–27. doi: 10.1016/j.aaf.2019.12.001

Saarela, M., Mogensen, G., Fondén, R., Mättö, J., and Mattila-Sandholm, T. (2000). Probiotic bacteria: safety, functional and technological properties. *J. Biotechnol.* 84, 197–205. doi: 10.1016/S0168-1656(00)00375-8

Schönborn, S., and Krömker, V. (2016). Detection of the biofilm component polysaccharide intercellular adhesin in *Staphylococcus aureus* infected cow udders. *Vet. Microbiol.* 196, 126–128. doi: 10.1016/j.vetmic.2016.10.023

Shin, H. J., Choi, H., and Kim, D. W. (2012). Probiotic potential of *Pediococcus pentosaceus* BCNU 9070. *J. Life Sci.* 22, 1194–1200. doi: 10.5352/JLS.2012.22.9.1194

Shoemaker, C. A., Klesius, P. H., and Evans, J. J. (2001). Prevalence of *Streptococcus iniae* in tilapia, hybrid striped bass, and channel catfish on commercial fish farms in the United States. *Am. J. Vet. Res.* 62, 174–177. doi: 10.2460/ajvr.2001.62.174

Silva, E. F., Soares, M. A., Calazans, N. F., Vogeley, J. L., do Valle, B. C., Soares, R., et al. (2012). Effect of probiotic (*Bacillus* spp.) addition during larvae and postlarvae culture of the white shrimp *Litopenaeus vannamei*. *Aquac. Res.* 44, 13–21. doi: 10.1111/j.1365-2109.2011.03001.x

Sim, I., Koh, J. H., Kim, D. J., Gu, S. H., Park, A., and Lim, Y. H. (2015). In vitro assessment of the gastrointestinal tolerance and immunomodulatory function of *Bacillus methylotrophicus* isolated from a traditional Korean fermented soybean food. *J. Appl. Microbiol.* 118, 718–726. doi: 10.1111/jam.12719

Skalli, A., Castillo, M., Andree, K. B., Tort, L., Furones, D., and Gilbert, E. (2013). The LPS derived from the cell walls of the Gram-negative bacteria *Pantoea agglomerans* stimulates growth and immune status of rainbow trout (*Oncorhynchus mykiss*) juveniles. *Aquaculture* 416-417, 272–279. doi: 10.1016/j.aquaculture.2013.09.037

Smith, D. D., Kirzinger, M. W., and Stavrinides, J. (2013). Draft genome sequence of the antibiotic-producing cystic fibrosis isolate *Pantoea agglomerans* Tx10. *Genome Announc.* 1, e904–e913.

Smits, T. H. M., Rezzonico, F., Kamber, T., Goesmann, A., Ishimaru, C. A., Stockwell, V. O., et al. (2010). Genome sequence of the biocontrol agent *Pantoea vagans* strain C9–1. *J. Bacteriol.* 192, 6486–6487. doi: 10.1128/JB.01122-10

Spinosa, M. R., Braccini, T., Ricca, E., de Felice, M., Morelli, L., Pozzi, G., et al. (2000). On the fate of ingested *Bacillus* spores. *Res. Microbiol.* 151, 361–368. doi: 10.1016/S0923-2508(00)00159-5

Sumi, C. D., Yang, B. W., Yeo, I. C., and Hahm, Y. T. (2015). Antimicrobial peptides of the genus *Bacillus*: a new era for antibiotics. *Can. J. Microbiol.* 61, 93–103. doi: 10.1139/cjm-2014-0613

Todorova, S. D., Nyati, H., Meincken, M., and Dicks, L. M. T. (2007). Partial characterization of bacteriocin AMA-K, produced by *Lactobacillus plantarum* AMA-K isolated from naturally fermented milk from Zimbabwe. *Food Control* 18, 656–664. doi: 10.1016/j.foodcont.2006.03.003

Vine, N. G., Leukes, W. D., Kaiser, H., Daya, S., Baxter, J., and Hecht, T. (2004). Competition for attachment of aquaculture candidate probiotic and pathogenic bacteria on fish intestinal mucus. *J. Fish. Dis.* 27, 319–326. doi: 10.1111/j.1365-2761.2004.00542.x

Völksch, B., Thon, S., Jacobsen, I. D., and Gube, M. (2009). Polyphasic study of plant- and clinic-associated *Pantoea agglomerans* strains reveals indistinguishable virulence potential. *Infect. Genet. Evol.* 9, 1381–1391. doi: 10.1016/j.meegid.2009.09.016

Walterson, A. M., and Stavrinides, J. (2015). Pantoea: insights into a highly versatile and diverse genus within the *Enterobacteriaceae*. *FEMS Microbiol. Rev.* 39, 968–984. doi: 10.1093/femsre/fuv027

Wang, C., Liu, Z., Huang, Y., Zhang, Y., Wang, X., and Hu, Z. (2019). Cadmium-resistant rhizobacterium *Bacillus cereus* M4 promotes the growth and reduces cadmium accumulation in rice (*Oryza sativa* L). *Environ. Toxicol. Pharmacol.* 72:103265. doi: 10.1016/j.etap.2019.103265

Wang, T., Liang, Y., Wu, M., Chen, Z., Lin, J., and Yang, L. (2015). Natural products from *Bacillus subtilis* with antimicrobial properties. *Chin. J. Chem. Eng.* 23, 744–754. doi: 10.1016/j.cjche.2014.05.020

Wang, W.-Z., Huang, J.-S., Zhang, J.-D., Wang, Z.-L., Li, H.-J., Amenyogbe, E., et al. (2021). Effects of hypoxia stress on the intestinal microflora of juvenile of cobia (*Rachycentron canadum*). *Aquaculture* 536:736419. doi: 10.1016/j.aquaculture.2021.736419

Wasko, A., Polak-Berecka, M., Paduch, R., and Jóźwiak, K. (2014). The effect of moonlighting proteins on the adhesion and aggregation ability of *Lactobacillus helveticus*. *Anaerobe* 30, 161–168. doi: 10.1016/j.anaerobe.2014.10.002

Weisburg, W. G., Barns, S. M., Pelletier, D. A., and Lane, D. J. (1991). 16S ribosomal DNA amplification for phylogenetic study. *J. Bacteriol.* 173, 697–703. doi: 10.1128/jb.173.2.697-703.1991

Woese, C. R., Kandler, O., and Wheelis, M. L. (1990). Towards a natural system of organisms: proposal for the domains Archaea, Bacteria, and Eucarya. *Proc. Natl. Acad. Sci. U.S.A.* 87, 4576–4579. doi: 10.1073/pnas.87.12.4576

Wu, H., Sun, L., Li, C., Li, Z., Zhang, Z., Wen, X., et al. (2014). Enhancement of the immune response and protection against *Vibrio parahaemolyticus* by indigenous probiotic *Bacillus* strains in mud crab (*Scylla paramamosain*). *Fish Shellf. Immunol.* 41, 156–162. doi: 10.1016/j.fsi.2014.08.027

Xie, F., Quan, S., Liu, D., Ma, H., Li, F., and Zhou, F. (2014). Purification and characterization of a novel α-amylase from a newly isolated *Bacillus methylotrophicus* strain P11-2. *Process Biochem.* 49, 47–53. doi: 10.1016/j.procbio.2013.09.025

Xie, R. t., Amenyogbe, E., Wang, W. z., Guo, Z.-X., Chen, G., and Huang, J.-S. (2021). Cloning and expression analysis of hypoxia-related gene HO in cobia. *Aquacult. Int.* 1, 75–89. doi: 10.1007/s10499-020-00611-3

Yang, G., Tian, X., Dong, S., Peng, M., and Wang, D. (2015). Effects of dietary *Bacillus cereus* G19, *B. cereus* BC-01, and *Paracoccus marcusii* DB11 supplementation on the growth, immune response, and expression of immune-related genes in coelomocytes and intestine of the sea cucumber (*Apostichopus japonicus* Selenka). *Fish Shellf. Immunol.* 45, 800–807. doi: 10.1016/j.fsi.2015.05.032

Yerlikaya, O. (2018). Probiotic potential and biochemical and technological properties of *Lactococcus lactis ssp*. lactis strains isolated from raw milk and kefir grains. *J. Dairy Sci.* 102, 124–134. doi: 10.3168/jds.2018-14983

Zahller, J., and Stewart, P. S. (2002). Transmission electron microscopic study of antibiotic action on *Klebsiella pneumoniae* biofilm. *Antimicrob Agents Ch.* 46, 2679–2683. doi: 10.1128/aac.46.8.2679-2683.2002

Zhang, Q., Ma, H., Mai, K., Zhang, W., Liufu, Z., and Xu, W. (2010). Interaction of dietary *Bacillus subtilis* and fructooligosaccharide on the growth performance, non-specific immunity of sea cucumber, *Apostichopus japonicus*. *Fish Shellf. Immunol.* 29:211.

Zhang, Z., Zhou, H., Shi, G., and Chen, G. (2013). Effects of diet soybean protein concentration on carbon and nitrogen isotope fractionation of juvenile cobia (*Rachycentron canadum* L.). *J. Guang. Ocean Univ.* 33, 30–36.

**Conflict of Interest:** The authors declare that the research was conducted in the absence of any commercial or financial relationships that could be construed as a potential conflict of interest.

frontiers in Marine Science

ORIGINAL RESEARCH
published: 04 January 2022
doi: 10.3389/fmars.2021.779053

# Different Fish Meal and Fish Oil Dietary Levels in European Sea Bass: Welfare Implications After Acute Confinement Stress

*Nicole Francesca Pelusio[1], Alessio Bonaldo[1], Enric Gisbert[2], Karl B. Andree[2], Maria Angeles Esteban[3], Francesco Dondi[1], Maria Chiara Sabetti[1], Pier Paolo Gatta[1] and Luca Parma[1]**

*[1] Department of Veterinary Medical Sciences, University of Bologna, Bologna, Italy, [2] Aquaculture Program, Institut de Recerca i Tecnologia Agroalimentàries, Centre de Sant Carles de la Ràpita, Sant Carles de la Ràpita, Spain, [3] Department of Cell Biology and Histology, University of Murcia, Murcia, Spain*

OPEN ACCESS

**Edited by:**
*Aires Oliva-Teles, University of Porto, Portugal*

**Reviewed by:**
*Manuel Gesto, Technical University of Denmark, Denmark*
*Patricia Diaz-Rosales, Centro de Investigación en Sanidad Animal (CISA), Instituto Nacional de Investigaciones Agrarias-Consejo Superior de Investigaciones Científicas (INIA-CSIC), Spain*

***Correspondence:**
*Luca Parma*
*luca.parma@unibo.it*

**Specialty section:**
*This article was submitted to Aquatic Physiology, a section of the journal Frontiers in Marine Science*

**Received:** *17 September 2021*
**Accepted:** *13 December 2021*
**Published:** *04 January 2022*

**Citation:**
*Pelusio NF, Bonaldo A, Gisbert E, Andree KB, Esteban MA, Dondi F, Sabetti MC, Gatta PP and Parma L (2022) Different Fish Meal and Fish Oil Dietary Levels in European Sea Bass: Welfare Implications After Acute Confinement Stress. Front. Mar. Sci. 8:779053. doi: 10.3389/fmars.2021.779053*

To provide practical feeding management guidelines preceding a stressful episode during farming practices, European sea bass juveniles (initial weight: 72.3 g) were fed for 60-days different fish meal (FM) and fish oil (FO) dietary levels [high (30% FM, 15% FO, FM30/FO15), intermediate (20% FM, 7% FO, FM20/FO7), and low (10% FM, 3% FO, FM10/FO3)] in triplicate conditions. Fish were then fasted for 36 h and exposed to a 2-h acute crowding (80 kg $m^{-3}$ biomass). Plasma biochemistry, skin mucus parameters and gene expression of stress and immune-related genes were performed before, at 2 and 24 h after crowding. At the end of the trial, the FM10/FO3 group showed lower final body weight, weight gain, and specific growth rate compared to the other treatments. Most of the plasma parameters were mainly affected by crowding condition rather than diet; however, after stress, lactate was higher in the FM30/FO15 group compared to the other treatments. Similarly, protease, antiprotease, peroxidase and lysozyme in skin mucus were mostly affected by crowding conditions, while fish fed FM10/FO3 displayed higher skin mucosal IgM and bactericidal activity against *Vibrio anguillarum* and *V. harveyi*. Most of the stress-related genes considered (*hsp70* and *gr-1* in the brain; *hsp70*, *gr-1* and *gr-2* in the head kidney), showed an overall expression pattern that increased over time after stress, in addition, *hsp70* in the head kidney was also up-regulated in fish fed FM30/FO15 after stress. Higher plasmatic lactate together with the up-regulation of some stress-related transcripts suggest a higher reactivity to acute crowding of the stress-response mechanism in fish fed high FM and FO dietary levels. Otherwise, the higher skin mucosal IgM and bactericidal activity observed in fish fed FM10/FO3 dietary levels seems to indicate that acute crowding was able to activate a higher pro-inflammatory response in this treatment. Overall, the results of the present study seem to indicate that 10% FM and 3% FO dietary levels might affect stress and immune responses.

**Keywords: aquaculture, feeding strategy, dietary fishmeal and fishoil, crowding stress, growth, skin mucus, plasma biochemistry, gene expression**

## INTRODUCTION

Nowadays, fish farmers are urged to apply feeding management practices that implement feed formulations which address both optimal growth and fish welfare issues, especially for coping with exposures to various types of stress (Boyd et al., 2020; Reverter et al., 2021). Certainly, under current aquaculture intensive rearing conditions, fish are continuously exposed to many stressors both biotic and abiotic; among them, husbandry-related stressors such as handling, crowding, transportation, or confinement are the most important (Tort and Teles, 2012). When experienced, these stressors are well-known to cause a wide range of physiological alterations, thus, worsening overall fish performance (Barton et al., 2005; Bagni et al., 2007; Castro et al., 2018; Balasch and Tort, 2019). In recent years, for several fish species including Mediterranean carnivorous ones, significant amounts of dietary fishmeal (FM) and fish oil (FO) have been successfully replaced with alternative ingredients mainly derived from commodity agricultural crops (Kaushik et al., 2004; Sitjà-Bobadilla et al., 2005; Médale and Kaushik, 2009; Hardy, 2010; Sales and Glencross, 2011; Nasopoulou and Zabetakis, 2012; Bonvini et al., 2018c; Sutili et al., 2018; Parma et al., 2019; Kwasek et al., 2020). Among Mediterranean fish species, European sea bass (*Dicentrarchus labrax*) feed formulation has been evolving constantly, successfully reaching very low contents of FM and FO while providing for optimal rearing conditions; thus, demonstrating their potential for commercial use (Torrecillas et al., 2017a; Bonvini et al., 2018a; Parma et al., 2019). However, at the commercial farm scale this species is highly susceptible to stressful rearing-related problems such as netting, handling, sorting, transportation, and crowding giving rise to a wide range of negative physiological responses affecting their rearing performance and welfare (Gornati et al., 2004; Poltronieri et al., 2007; Fanouraki et al., 2011; Maricchiolo et al., 2011; Ellis et al., 2012; Tsalafouta et al., 2015; Samaras et al., 2017; Serradell et al., 2020). To counteract the negative impact of these stressors in fish, several feeding strategies have been developed to boost animal welfare, most of them including the utilization of functional feed additives (Volpatti et al., 2013; Gisbert et al., 2018; Serradell et al., 2020). However, only limited studies have investigated the interaction between very low dietary levels of FM and FO and animal welfare under suboptimal rearing conditions (Gisbert et al., 2018; Machado et al., 2019; Serradell et al., 2020). The effects of chronic stress on the immune system of fish are known to be clearly immunosuppressive; however, acute stress-induced immunomodulation is still poorly understood (Guo and Dixon, 2021). For instance, a recent study in European sea bass juveniles exposed to acute stress (netting and 1 min air exposure) and fed high levels of vegetable oils (VO) and carbohydrates resulted in depression of the immune response in both undisturbed and stressed fish (Machado et al., 2019). In order to find practical feeding management guidelines for fish farmers, the aim of this study was to evaluate the effect of different FM and FO dietary levels on growth performance, feed efficiency and, stress and immune-related biomarkers in European sea bass exposed to acute crowding. Fish responses to acute confinement were evaluated by analysis of different humoral immune biomarkers from skin mucus, plasma biochemistry, and gene expression of stress and immune-related genes in order to provide insight into the overall effects of experimental diets on fish welfare.

## MATERIALS AND METHODS

### Experimental Diets

Three isonitrogenous (46% protein) and isolipidic (18% lipid) extruded diets (pellet size = 4.0 mm) were formulated to contain high, medium and low dietary levels of FM and FO (30% FM, 15% FO, FM30/FO15; 20% FM and 7% FO, FM20/FO7 and 10% FM and 3% FO, FM10/FO3, respectively). Diets were formulated with both, FM and a mixture of vegetable ingredients currently used for European sea bass aquafeeds (Parma et al., 2019), and were produced by SPAROS Lda (Portugal). Ingredients, proximate composition and fatty acid profile of the experimental diets are presented in **Tables 1**, **2**.

**TABLE 1 |** Ingredients and proximate composition of the experimental diets.

| Ingredients, % of the diet | FM30/FO15 | FM20/FO7 | FM10/FO3 |
|---|---|---|---|
| Fishmeal LT70 | 30.0 | 20.0 | 10.0 |
| Soy protein concentrate | 10.0 | 12.0 | 20.0 |
| Wheat gluten | 5.0 | 10.0 | 11.0 |
| Corn gluten | 10.0 | 11.7 | 13.5 |
| Soybean meal 48 | 9.0 | 9.0 | 8.1 |
| Rapeseed meal | 5.0 | 5.0 | 4.5 |
| Sunflower meal | 5.0 | 5.0 | 4.5 |
| Wheat meal | 9.5 | 9.0 | 7.9 |
| Fish oil | 15.0 | 7.0 | 3.0 |
| Rapeseed oil | | 8.5 | 13.0 |
| *Vitamin and mineral premix | 1.0 | 1.0 | 1.0 |
| Lutavit C35 | 0.1 | 0.1 | 0.1 |
| Betaine HCl | 0.1 | 0.1 | 0.1 |
| Antioxidant | 0.2 | 0.2 | 0.2 |
| Sodium propionate | 0.1 | 0.1 | 0.1 |
| MCP | – | 0.8 | 1.8 |
| L-Lysine | – | 0.4 | 0.6 |
| L-Threonine | – | – | 0.2 |
| L-Tryptophan | – | – | 0.1 |
| D,L-Methionine | – | 0.10 | 0.3 |
| **Proximate composition, % on a wet basis** | | | |
| Moisture | 7.92 | 6.85 | 6.26 |
| Protein | 44.84 | 45.75 | 45.25 |
| Lipid | 17.90 | 18.48 | 18.10 |
| Ash | 8.05 | 7.12 | 6.26 |
| Gross energy (Cal $g^{-1}$) | 21.2 | 21.2 | 21.1 |

**Vitamins and mineral premix (IU or mg $kg^{-1}$ diet; in vivo NSA: Portugal); DL alpha tocopherol acetate, 200 mg; sodium menadione bisulfate, 10 mg; retinyl acetate, 16,650 IU; D,L-cholecalciferol, 2,000 IU; thiamine, 25 mg; riboflavin, 25 mg; pyridoxine, 25 mg; cyanocobalamin, 0.1 mg; niacin, 150 mg; folic acid, 15 mg; l-ascorbic acid monophosphate, 750 mg; inositol, 500 mg; biotin, 0.75 mg; calcium pantothenate, 100 mg; choline chloride, 1,000 mg, betaine, 500 mg; copper sulfate heptahydrate, 25 mg; ferric sulfate monohydrate, 100 mg; potassium iodide, 2 mg; manganese sulfate monohydrate, 100 mg; sodium selenite, 0.05 mg; zinc sulfate monohydrate, 200 mg; yttrium oxide, 100 mg.*

**TABLE 2 |** Fatty acids composition of the experimental diets.

| Fatty acids composition (g/100 g) | FM30/FO15 | FM20/FO7 | FM10/FO3 |
|---|---|---|---|
| Lauric acid (12:0) | | 0.01 ± 0.00 | 0.02 ± 0.00 |
| Myristic acid (14:0) | 1.23 ± 0.15 | 0.40 ± 0.06 | 0.18 ± 0.04 |
| Pentadecanoic acid (15:0) | 0.08 ± 0.02 | 0.03 ± 0.01 | 0.02 ± 0.00 |
| Palmitic acid (16:0) | 3.15 ± 3.32 | 1.54 ± 0.18 | 1.10 ± 0.14 |
| Isoheptadecanoic acid (17:0 iso) | 0.07 ± 0.01 | 0.02 ± 0.00 | 0.01 ± 0.00 |
| Hexadecenoic acid (16:1) | 1.49 ± 0.45 | 0.50 ± 0.42 | 0.24 ± 0.07 |
| 14-methylhexadecanoic acid (17:0 anteiso) | 0.05 ± 0.01 | 0.02 ± 0.00 | 0.01 ± 0.00 |
| Margaric acid (17:0) | 0.07 ± 0.01 | 0.03 ± 0.01 | 0.02 ± 0.00 |
| Heptadecenoic acid (17:1) | 0.05 ± 0.01 | 0.03 ± 0.00 | 0.02 ± 0.00 |
| Stearic acid (18:0) | 0.58 ± 0.08 | 0.35 ± 0.05 | 0.30 ± 0.05 |
| Octadecenoic acid (18:1) | 3.05 ± 0.27 | 4.80 ± 0.41 | 5.72 ± 0.49 |
| Octadecadienoic acid (18:2) | 1.34 ± 0.15 | 2.56 ± 0.27 | 3.12 ± 0.31 |
| Arachidic acid (20:0) | 0.03 ± 0.01 | 0.05 ± 0.01 | 0.05 ± 0.01 |
| Octadecatrienoic acid (18:3) | 0.43 ± 0.06 | 0.56 ± 0.07 | 0.67 ± 0.08 |
| Eicosenoic acid (21:0) | 0.35 ± 0.05 | 0.24 ± 0.04 | 0.18 ± 0.04 |
| Stearidonic acid (18:4 n-3) | 0.39 ± 0.06 | 0.13 ± 0.03 | 0.05 ± 0.00 |
| Behenic acid (22:0) | 0.01 ± 0.00 | 0.03 ± 0.00 | 0.04 ± 0.01 |
| Docosanoic acid (22:1) | 0.45 ± 0.06 | 0.24 ± 0.04 | 0.12 ± 0.02 |
| Lignoceric acid (24:0) | 0.01 ± 0.00 | 0.02 ± 0.00 | 0.01 ± 0.00 |
| Polyunsaturated fatty acids (> C20) | 2.19 ± 0.21 | 0.76 ± 0.08 | 0.30 ± 0.04 |
| Polyunsaturated fatty acids | 5.38 ± 0.37 | 2.53 ± 0.20 | 1.76 ± 0.16 |
| Monounsaturated fatty acids | 5.50 ± 0.53 | 5.87 ± 0.59 | 6.30 ± 0.65 |
| Saturated fatty acids | 7.84 ± 0.42 | 5.12 ± 0.32 | 4.59 ± 0.33 |
| **Fatty acids' ratios** | | | |
| Polyunsaturated fatty acids/monounsaturated fatty acids | 1.43 ± 0.16 | 0.87 ± 0.11 | 0.73 ± 0.09 |
| Polyunsaturated fats/saturated fatty acids | 1.46 ± 0.13 | 2.02 ± 0.21 | 2.61 ± 0.30 |

*FM30/FO15 = 300 g kg$^{-1}$ fishmeal (FM), 150 g kg$^{-1}$ fish oil (FO); FM20/FO7 = 200 g kg$^{-1}$ fishmeal (FM), 70 g kg$^{-1}$ fish oil (FO); FM10/FO3 = 100 g kg$^{-1}$ fishmeal (FM), 30 g kg$^{-1}$ fish oil (FO).*
*SD, standard deviation.*

## Fish and Rearing Conditions

The experiment was carried out at the Laboratory of Aquaculture, Department of Veterinary Medical Sciences of the University of Bologna (Cesenatico, Italy). European sea bass (*Dicentrarchus labrax*) specimens were obtained from an Italian fish farm (Orbetello, GR) and adapted to the laboratory facilities for 1 week before the beginning of the trial. Afterward, 50 fish tank$^{-1}$ (initial weight: 72.2 ± 1.3 g, mean ± standard deviation, SD) were randomly distributed in nine 800 L volume tanks. Each diet was randomly assigned and administered to triplicate tanks over 60 days. Tanks were provided with natural seawater and connected to a closed recirculation system (overall water volume: 13 m$^3$). The rearing system consisted of a mechanical sand filter (PTK 1200, Astralpool, Barcelona, Spain), ultraviolet lights (SH-88, BLUGEO S.r.l., Parma, Italy) and a biofilter (PTK 1200, Astralpool, Barcelona, Spain). The water exchange rate within each tank was 100% every hour, while the overall water renewal amount in the system was 5% daily. During the trial, the temperature was kept at 23.0 ± 0.5°C and an artificial photoperiod of 12 h light and 12 h dark. The oxygen level was kept constant (8.0 ± 1.0 mg L$^{-1}$) through a liquid oxygen system regulated by a software program (B&G Sinergia snc, Chioggia, Italy). Ammonia (total ammonia nitrogen ≤ 0.1 mg L$^{-1}$) and nitrite (≤0.2 mg L$^{-1}$) were daily monitored spectrophotometrically (Spectroquant Nova 60, Merck, Lab business, Darmstadt, Germany), while salinity (30 g L$^{-1}$) was measured by a salt refractometer (106 ATC, Giorgio Bormac S.r.l., Carpi, Italy). Sodium bicarbonate was added on a daily basis to keep pH at 7.8–8.2. Fish were fed twice a day (8:30 and 16:30 h) for 6 days a week by automatic feeders to provide 10% overfeeding as reported by Bonvini et al. (2018a). Each meal lasted 1 h, after which the uneaten pellets of each tank were collected, dried overnight at 105°C, and weighed for further calculations of feed intake.

## Sampling

At the beginning and at the end of the experiment, all the fish in each tank were anesthetized by MS222 at 100 mg L$^{-1}$ and individually weighed (BW, g). Proximate composition of carcasses was determined at the beginning of the trial on a pooled sample of 10 fish and on a pooled sample of five fish per tank at the end of the trial. Furthermore, wet weight of body, viscera, liver, perivisceral fat and total length were individually recorded for five fish per tank to determine viscerosomatic (VSI), hepatosomatic (HSI) and mesenteric fat (MFI) indices, and condition factor (CF).

At the end of the 60-day period of feeding, animals were fasted for 36 h. Subsequently, a crowding stress challenge (80 kg m$^{-3}$ biomass) was conducted by lowering the water level in tanks for 2 h. At the end of this time frame, the water level was brought back to the initial level, allowing the animals to recover from the stressful event for 24 h. Before (time 0, T0), at the end of the 2-h exposure (time 1, T1) and 24 h after confinement at high density (time 2, T2), eight fish per tank were euthanized with an overdose of MS222 (300 mg L$^{-1}$) and sampled at each considered time point (T0, T1, and T2) in order to explore the capacity of the different diets to provide any advantage or disadvantage in front of the challenge test.

Skin mucus samples were collected from eight fish per tank according to Parma et al. (2020). Briefly, skin mucus was collected by gently scraping the dorsolateral surface of specimens using a cell scraper, taking care to avoid contamination with urinogenital and intestinal excretions. Collected mucus samples (3 mL each) were then stored at −80°C until analysis.

For the assessment of plasma biochemistry, blood from five fish per tank ($n$ = 15 fish per diet treatment, same fish used for skin mucus samples) was collected from the caudal vein and placed in 4 mL heparin tubes (Vacutest Kima, Arzergrande, Italy). Samples were then centrifuged (3,000 × $g$, 10 min, 4°C) and plasma aliquots were stored at −80°C until analysis (Bonvini et al., 2018b).

Similarly, two fish per tank ($n$ = 6 fish per diet treatment at T0, T1, and T2) were randomly sampled, euthanized with an overdose anesthetic as previously described, then head kidney

(both sides) and brain (whole) were dissected to gain 100 mg of tissue in order to evaluate the impact of dietary treatments on genetic markers of stress-response in fish that had been submitted to crowding stress. The brain and head kidney samples were kept at 4°C overnight into RNA Later (Sigma-Aldrich), and then stored at −80°C until further analysis.

All experimental procedures were evaluated and approved by the Ethical-Scientific Committee for Animal Experimentation of the University of Bologna (protocol ID 942/2019) in accordance with European directive 2010/63/UE on the protection of animals used for scientific purposes.

## Growth Performance, Feed Efficiency, and Body Condition Indices

In order to evaluate the effect of experimental diets, the following formulae were employed to calculate growth performance, somatic and nutritional index values:

Weight gain (WG, g) = BWf- BWi (where BWf and BWi represent the final and the initial body weight).

Specific growth rate (SGR,% $day^{-1}$) = 100 * (ln BWf- ln BWi)/days

Feed intake (FI, g kg $\Delta BW^{-1}$ $day^{-1}$) = ((1000*total feed ingestion)/($\Delta$BW))/days.

Feed conversion ratio (FCR) = FI/WG.

Condition factor (CF) = 100 * (BWf/total body $length^3$).

Viscerosomatic index (VSI,%) = 100 * (viscera weight/BWf).

Hepatosomatic index (HSI,%) = 100 * (liver weight/BWf).

Mesenteric fat index (MFI,%) = 100 * (mesenteric fat weight/BWf).

Protein efficiency rate (PER) = (BWf – BWi)/total protein intake.

Gross protein efficiency (GPE,%) = 100 * [(% final body protein content * BWf) – (% initial body protein * BWi)]/total protein intake fish.

Lipid efficiency rate (LER) = (BWf – BWi)/total lipid intake.

Gross lipid efficiency (GLE,%) = 100 * [(% final body lipid content * BWi) – (% initial body lipid * BWi)]/total lipid intake fish.

## Proximate Composition Analyses

Diets and whole bodies of fish were analyzed for proximate composition. Moisture content was obtained by weight loss after drying samples in a stove at 105°C overnight. Crude protein was determined as total nitrogen (N*6.25) using the Kjeldahl's method according to the AOAC International (AOAC, 2010). Total lipids were determined according to Bligh and Dyer's (1959) extraction method. Ash content was estimated by incineration in a muffle oven at 450°C overnight. Gross energy was determined by a calorimetric bomb (Adiabatic Calorimetric Bomb Parr 1261; PARR Instrument, IL, United States). Fatty acid analyses composition of diets was performed according to ISO16958:2015.

## Stress and Metabolic Biomarkers in Plasma

Plasma samples (500 μL) were analyzed by automated analyzer (AU 480; 220 Olympus/Beckman Coulter, Brea, CA, United States) using specific methods (Olympus system 221 reagent, OSR) detecting the levels of glucose (GLU), triglycerides (TRIG), lactate, total protein, aspartate aminotransferase (AST), alanine transaminase (ALT), alkaline phosphatase (ALP), creatine kinase (CK), lactate dehydrogenase (LDH), calcium ($Ca^{+2}$), inorganic phosphorus (P), potassium ($K^+$) sodium ($Na^+$), magnesium (Mg) according to Pelusio et al. (2021). In addition, plasma cortisol (CORT) concentration was determined using a chemiluminescence immunoassay (Immulite cortisol, Diagnostic Product Corporation, Los Angeles, CA, United States) using an automated analyzer (Immulite XP2000, Siemens) (Pelusio et al., 2021).

## Humoral Immunity Markers in Skin Mucus

The peroxidase activity was measured by oxidation of 3,3′,5,5′-Tetramethylbenzidine (TMB) according to Quade and Roth (1997). Aliquots of 10 μL of mucus solution were diluted with Hanks' buffer (HBSS) to a final volume of 50 μL in a flat-bottomed 96-well plate. As substrate, $H_2O_2$ was added, and the color change reaction was halted by adding 50 μL 2 M $H_2SO_4$. The optical density (OD) was read at λ = 450 nm in a plate reader (FLUOstar Omega, BMG Labtech, Germany). Samples without mucus solution were used as blanks. One unit was defined as the amount producing an absorbance change of 1, and the activity was expressed as U mg $protein^{-1}$.

Protease activity was quantified using the azocasein hydrolysis assay according to the method described by Ross et al. (2000). Briefly, 100 μL of skin mucus were incubated with 100 μL of ammonium bicarbonate buffer and 125 μL of 0.7% azocasein (Sigma, United States) in sterile Eppendorf vials. The reaction was then halted by adding 250 μL of 4.6% trichloroacetic acid (TCA, Sigma, United States) and the OD was read at λ = 450 nm using a plate reader. Skin mucus was replaced by trypsin (5 mg $mL^{-1}$, Sigma) for the positive controls or by ammonium bicarbonate buffer for the negative one. The activity for each sample was expressed as % protease activity in relation to the controls.

Antiprotease activity was determined by the capacity of skin mucus to inhibit trypsin activity (Hanif et al., 2004). Briefly, 100 μL of skin mucus were incubated (10 min, RT) with 10 μL of trypsin solution (5 mg $mL^{-1}$, Sigma, United States). Subsequently, 100 μL of ammonium bicarbonate buffer and 125 μL of 0.7% azocasein (Sigma, United States) were added and mixtures incubated for 2 h at RT. Afterward, 250 μL of 4.6% trichloroacetic acid (TCA; Sigma, United States) were added and samples incubated for an additional 30 min. Later 100 μL of 0.5 N NaOH were added and the OD was read at λ = 450 nm using a plate reader. Buffer without sample or trypsin was used as positive controls and a combination of buffer and trypsin solution was used for the negative controls. The activity for each sample was expressed as% trypsin inhibition in relation to the controls.

Lysozyme activity was measured according to the turbidimetric method described by Parry et al. (1965). Volumes of 10 μL of skin mucus diluted 1:2 with 10 mM PBS, pH 6.2, were placed in a flat-bottomed 96-well plate. To each well, 200 μL

of freeze-dried *Micrococcus lysodeikticus* in the above buffer (0.3 mg $mL^{-1}$, Sigma) were added as lysozyme substrate. The reduction in absorbance at $\lambda$ = 450 nm was measured. One unit of lysozyme activity was defined as a reduction in absorbance of 0.001 units $min^{-1}$. The units of lysozyme present in skin mucus were obtained from a standard curve made with hen's egg-white lysozyme (HEWL, Sigma), and the results were expressed as U mg $protein^{-1}$.

Alkaline phosphatase activity was measured by incubating 100 μL of skin mucus with an equal volume of 4 mM *p*-nitrophenyl liquid phosphate (Sigma, United Kingdom) in 100 mM ammonium bicarbonate buffer containing 1 mM $MgCl_2$ (pH 7.8, 30°C) (Ross et al., 2000). The OD was continuously measured at 1 min intervals over 3 h at 405 nm in a plate reader and one unit of activity was defined as the amount of enzyme required to release 1 mmol of *p*-nitrophenol product in 1 min. The activity was expressed as U mg $protein^{-1}$.

Esterase activity was measured by incubating aliquots of 100 μL of skin mucus with an equal volume of 0.4 mM *p*-nitrophenylmyristate substrate (Sigma, United Kingdom) in 100 mM ammonium bicarbonate buffer containing 0.5% Triton X-100 (Sigma, United Kingdom) (pH 7.8, 30°C) in a flat-bottomed 96-well plate, as described by Ross et al. (2000). The OD and activity were determined and expressed as previously described for the alkaline phosphatase.

Total skin mucus immunoglobulin M (IgM) levels were analyzed by ELISA method as described by Hanif et al. (2004). Samples of 100 μL per well of skin mucus diluted 1:5 with 50 mM carbonate-bicarbonate buffer (35 mM $NaHCO_3$ and 15 mM $Na_2CO_3$, pH 9.6), the proteins were adsorbed during an overnight incubation at 4°C and blocked for 2 h at room temperature with 200 μL blocking buffer containing 3% BSA in PBS-T, followed by three new rinses with PBS-T. Plates were then incubated (1 h with 100 μL per well) with mouse anti-European sea bass IgM monoclonal antibody (Aquatic Diagnostics Ltd., 1/100 in blocking buffer) and with 100 μL per well of secondary antibody anti-mouse IgG-HRP (1/1000 in blocking buffer, Sigma-Aldrich). After exhaustive rinsing with PBS-T the plates were developed using 100 μL of a 0.42 mM solution of 3,3,5,5-tetramethyl benzidine hydrochloride (TMB, Sigma-Aldrich). The reaction was allowed to proceed for 10 min and halted by the addition of 50 μL 2 M $H_2SO_4$ and the plates were then read at $\lambda$ = 450 nm. Negative controls consisted of samples without skin mucus or without primary antibody, whose OD values were subtracted from each sample value.

Two bacteria, pathogenic for marine fish species (*Vibrio harveyi* and *Vibrio anguillarum*), were used in the bactericidal assays. Bacteria were cultured for 48 h at 25°C in Tryptic Soy Agar (TSA, Difco Laboratories), and then single colonies were inoculated in Tryptic Soy Broth (TSB, Difco Laboratories), both supplemented with NaCl to a final concentration of 1% (w/v), and grown with continuous shaking (100 rpm) for 24 h. Bactericidal activity was determined according to the method of Stevens et al. (1991). For this, aliquots of 100 μL of bacteria were added to wells of a flat-bottomed 96-well plate and incubated with the same volume of skin mucus. The absorbance of the dissolved formazan was measured at $\lambda$ = 570 nm. Bactericidal activity was expressed as a percentage of non-viable bacteria (the difference between the absorbance of surviving bacteria in test samples compared with the absorbance of bacteria from positive controls).

Soluble total protein concentration in mucus samples was determined by the Bradford dye binding method, using bovine serum albumin (BSA, Sigma-Aldrich) as a standard (Bradford, 1976).

## Gene Expression in Brain and Head-Kidney

RNA from tissues (50 mg per sample) was extracted using the RNeasy Mini Kit (Qiagen, Spain) following the instructions of the manufacturer. RNA concentration and quality were determined by spectrophotometry ($\lambda$ = 260/280) (Nanodrop-2000® spectrophotometer; Thermo Scientific, United States) and denaturing electrophoresis in TAE agarose gel (1.5%) (Masek et al., 2005). For each tissue sample, *ca.* l μg of RNA was reverse transcribed into cDNA using Super-Script™ First-Strand Synthesis System for RT-PCR (Invitrogen™, Life Technologies, Warrington, United Kingdom) primed with oligo $(dT)_{12-18}$ and random hexamers. Primers for quantitative PCR analyses were obtained for most genes by searching the literature for previously reported gene expression studies in this species (**Table 3**). When genes of interest were not previously published, an alignment of marine teleost homologs for the gene of interest obtained from GenBank, was made using BioEdit Sequence Alignment Editor ver 7.0.5.2 (Hall, 1999). Consensus primers designed from conserved regions identified in these alignments were used for *D. labrax*-specific qPCR assays (**Table 2**). Quantitative real-time polymerase chain reaction (qPCR) was performed using a C1000 Touch Thermal Cycler (BioRad, Spain). Beta actin (β-*actin*) was used as the reference gene. All cDNA samples were diluted 1:20 in molecular biology grade water. An aliquot of 5 μL from each diluted sample was pooled to provide a "calibrator sample" that was included as a calibrator reaction (β-*actin*) sample on each plate to correct for variation among experimental plates. A standard curve was prepared by amplification of a dilution series of this pooled cDNA for calculation of the efficiency (%E) for each assay to ensure that efficiency was close to 100%.

Quantitative PCR analyses for each gene were performed in triplicate in a total volume of 20 μL containing 2 μL cDNA, 20 μmol of each primer, 10 μL SYBR™ Green (Life Technologies, Warrington, United Kingdom) and 7 μL of sterile water. A negative control was included (NTC = no template control) for each set of reactions on each 96-well plate. All reactions were performed using the following conditions: 1 cycle at 95°C for 10 min; 40 cycles at 95°C for 15 s, Ta°C (primer-specific annealing temperature) for 30 s. A final melt curve stage completed the program, enabling confirmation of the amplification of a single product in each reaction. The final relative mRNA levels were then calculated following Pflaff's method (Pfaffl, 2004).

## Statistical Analysis

All data are presented as mean ± SD. A tank was used as the experimental unit for analyzing growth performance, whereas

**TABLE 3 |** Primer sequences used for gene expression analyses.

| Gene | Abbreviation | GenBankID | Primer sequence (5′-3′) | Amplicon (bp) | References | Annealing T° |
|---|---|---|---|---|---|---|
| β-actin | *β-act* | AJ537421.1 | Fw: 5′-ATGTGGATCAGCAAGCAGG-3′<br>Rv: 5′-AGAAATGTGTGGTGTGGTCG-3′ | 144 | El Aamri et al., 2015 | 5860 |
| Glucocorticoid receptor-1 | *gr-1* | AY549305 | Fw: 5′-GAGATTTGGCAAGACCTTGACC-3′<br>Rv: 5′-ACCACACCAGGCGTACTGA-3′ | 401 | Reyes-López et al., 2018 | 6660 |
| Glucocorticoid receptor-2 | *gr-2* | AY619996 | Fw: 5′-GACGCAGACCTCCACTACATTC-3′<br>Rv: 5′-GCCGTTCATACTCTCAACCAC-3′ | 403 | Reyes-López et al., 2018 | 6864 |
| Melanocortin receptor | *mr* | JF824641.1 | Fw: 5′-CCTGTCTCCTCTATGAATGG-3′<br>Rv: 5′-AATCTGGTAATGGAATGAATGTC-3′ | 173 | Samaras et al., 2018 | 6062 |
| Caspase 3 | *csp3* | DQ345774.1 | Fw: 5′-ACGAAGCAGGTCAATCATCC-3′<br>Rv: 5′-GCAGTTTAAGGGTATCCAGAGC-3′ | 98 | El Aamri et al., 2015 | 6066 |
| Heat shock protein 70 | *hsp70* | AY423555 | Fw: 5′-CAACCTCCTGGGAAAGTTTG-3′<br>Rv: 5′-AGAATCTTCTGCTTGTCGTCG-3′ | 353 | Serradell et al., 2020 | 56.356.3 |
| Transforming growth factor | *tgf* | AM421619.1 | Fw: 5′-ACGGGCTACCATGCCAACTAC-3′<br>Rv: 5′-AGAGGCTCCTGGGTTGTGATG-3′ | 110 | Designed | 6670 |
| Tumor necrosis factor α | *tnf-α* | DQ200910 | Fw: 5′-ACAGCGGATATGGACGGTG-3′<br>Rv: 5′-GCCAAGCAAACAGCAGGAC-3′ | 76 | El Aamri et al., 2015 | 6060 |
| Interleukin 10 | *il10* | AM268529 | Fw: 5′-ACCCCGTTCGCTTGCCA-3′<br>Rv: 5′-CATCTGGTGACATCACTC-3′ | 163 | El Aamri et al., 2015 | 5654 |
| Dicentrarcin | *dcn* | AY303949.1 | Fw: 5′-GTTCACGTCGGCAAGTCCATCC-3′<br>Rv: 5′-GATGAACCGCCATAGATTCACTC-3′ | 175 | Designed | 7068 |
| Cyclooxygenase 2 | *cox2* | AJ630649 | Fw: 5′-AGCACTTCACCCACCAGTTC-3′<br>Rv: 5′-AAGCTTGCCATCCTTGAAGA-3′ | 148 | Cordero et al., 2016 | 6258 |
| Lysozyme | *lys* | KJ433681.1 | Fw: 5′-TGATGCAGGTTGTTGATGTTAATC-3′<br>Rv: 5′-TCCATCCCCCATATTGTAGGC-3′ | 194 | Reyes-López et al., 2018 | 6664 |

a pool of five sampled fish was considered the experimental unit for analyzing carcass composition and somatic indices. Individual fish were used for analyzing plasma biochemistry, skin mucus parameters and relative expression of stress and immune-related transcripts. At the end of the feeding trial with diets differing in the FM and FO levels (60 days), data of growth performance, nutritional indices and somatic indices were analyzed by a one-way analysis of variance (ANOVA) and in case of significance ($P \leq 0.05$) Tukey's *post hoc* test was performed. In order to provide the effect of diets on the basal status of skin mucus parameters, plasma and gene expression before the stress episode; results were analyzed by a two-tier statistical approach analyzing first the data at T0 by one way ANOVA and followed by a two-way ANOVA considering sampling points and diets as factors. When statistically significant differences were found among groups ($P \leq 0.05$), Tukey's *post hoc* test was performed to determine differences among experimental groups. Prior to ANOVA analyses, all data were checked for normality and homogeneity of variance by means of the Shapiro Wilk and Levene tests, respectively. All the statistical analyses were conducted using GraphPad Prism and Statistical Package for Social Science (SPSS) for Windows version 20.0.

# RESULTS

## Key Performance Indicators and Body Proximate Composition

Results on growth performance and feeding efficiency parameters are summarized in **Table 4**. Significant differences were found in terms of BWf, WG, and SGR, while the lowest values were found in animals fed the FM10/FO7 diet. In particular, European sea bass fed FM30/FO15 and FM20/FO7 diets were 11.2 and 9.2% heavier than those from the FM10/FO3 dietary treatment.However, FCR, FI, and survival values displayed no significant differences among experimental groups.

Results on proximate body composition and, nutritional and somatic indices are reported in **Table 5**. No significant differences were found on any of the analyzed parameters.

## Plasma Biochemistry

Plasma biochemistry results are summarized in **Supplementary Table 1** and **Table 6**. At the end of the growth trial (T0) dietary treatments did not affect all the parameters analyzed except cortisol which was higher in FM30/FO15 than the other treatments (One-way ANOVA – **Supplementary Table 1**).

**TABLE 4 |** Growth performance of European seabass fed experimental diets over 60 days before crowding stress exposure.

| | FM30/FO15 | FM20/FO7 | FM10/F03 | *P*-value |
|---|---|---|---|---|
| BWi | 72.40 ± 1.66 | 71.75 ± 1.02 | 72.42 ± 1.73 | 0.832 |
| BWf | 210.72 ± 3.00$^{b}$ | 203.65 ± 6.33$^{b}$ | 187.00 ± 5.00$^{a}$ | **0.003** |
| WG | 138.32 ± 4.20$^{b}$ | 131.90 ± 5.33$^{b}$ | 114.58 ± 4.32$^{a}$ | **0.002** |
| SGR | 1.78 ± 0.07$^{b}$ | 1.74 ± 0.04$^{b}$ | 1.58 ± 0.05$^{a}$ | **0.003** |
| FCR | 1.25 ± 0.01 | 1.29 ± 0.06 | 1.37 ± 0.08 | 0.098 |
| FI | 20.41 ± 0.53 | 20.56 ± 0.67 | 20.16 ± 0.84 | 0.782 |
| Survival | 100.00 ± 0.00 | 99.30 ± 1.20 | 99.30 ± 1.20 | 0.630 |

*Data are given as the tanks mean (n = 3) ± SD. In each line, different superscript letters indicate significant differences among treatments ($P \leq 0.05$). FM30/FO15 = 300 g kg$^{-1}$ fishmeal (FM), 150 g kg$^{-1}$ fish oil (FO); FM20/FO7 = 200 g kg$^{-1}$ fishmeal (FM), 70 g kg$^{-1}$ fish oil (FO); FM10/FO3 = 100 g kg$^{-1}$ fishmeal (FM), 30 g kg$^{-1}$ fish oil (FO).*

**TABLE 5 |** Body composition and, nutritional and somatic indices of European seabass fed experimental diets over 60 days before crowding stress exposure.

| | FM30/FO15 | FM20/FO7 | FM10/F03 | *P*-value |
|---|---|---|---|---|
| **Whole body composition, %** | | | | |
| Protein | 16.71 ± 0.68 | 17.02 ± 0.11 | 17.02 ± 0.61 | 0.722 |
| Lipid | 17.50 ± 0.33 | 17.31 ± 0.75 | 17.26 ± 1.42 | 0.949 |
| Ash | 5.85 ± 0.08 | 3.76 ± 0.15 | 3.75 ± 0.08 | 0.994 |
| Moisture | 61.66 ± 0.12 | 61.57 ± 0.47 | 61.60 ± 1.00 | 0.984 |
| **Nutritional indices** | | | | |
| PER | 1.78 ± 0.02 | 1.70 ± 0.08 | 1.62 ± 0.09 | 0.080 |
| GPE | 29.96 ± 1.93 | 29.45 ± 1.64 | 28.11 ± 2.61 | 0.573 |
| LER | 4.46 ± 0.04 | 4.20 ± 0.20 | 4.04 ± 0.24 | 0.079 |
| GLE | 104.31 ± 3.75 | 98.13 ± 6.36 | 97.80 ± 9.44 | 0.475 |
| **Somatic indices** | | | | |
| HSI | 1.38 ± 0.06 | 1.35 ± 0.05 | 1.40 ± 0.10 | 0.363 |
| MFI | 7.52 ± 0.54 | 7.78 ± 0.44 | 7.29 ± 0.72 | 0.942 |
| VSI | 12.00 ± 0.84 | 12.24 ± 0.30 | 11.63 ± 0.50 | 0.980 |
| CF | 1.28 ± 0.06 | 1.29 ± 0.06 | 1.24 ± 0.04 | 0.447 |

*Data are given as the mean (n = 15 per diet for proximate composition and nutritional indices; n = 12 per diet for somatic indices) ± SD. FM30/FO15 = 300 g kg$^{-1}$ fishmeal (FM), 150 g kg$^{-1}$ fish oil (FO); FM20/FO7 = 200 g kg$^{-1}$ fishmeal (FM), 70 g kg$^{-1}$ fish oil (FO); FM10/FO3 = 100 g kg$^{-1}$ fishmeal (FM), 30 g kg$^{-1}$ fish oil (FO).*

*PER = Protein efficiency ratio = ((FBW-IBW)/protein intake); Gross protein efficiency (GPE,%) = 100*[(% final body protein*FBW) – (%initial body protein*IBW)]/total protein intake fish; Gross lipid efficiency (GLE,%) = 100*[(% final body lipid*FBW) – (%initial body lipid*IBW)]/total lipid intake fish; Lipid efficiency ratio (LER) = ((FBW-IBW)/lipid intake); Hepatosomatic index (HIS,%) = 100*(liver weight/FBW); Mesenteric Fat Index (MFI,%) = 100*(mesenteric fat weight/FBW); Viscerosomatic index (VSI,%) = 100*(viscera weight/FBW); Condition factor (CF) = 100*(FBW/length$^3$).*

*SD, standard deviation.*

**Table 6** reports plasma results in relation to dietary treatments and time after stress (Two-way ANOVA). Glucose was affected by diet and time after stress where FM30/FO15 showed higher values than FM20/FO7 and values were higher at T1 compared to T0 and T2. Triglyceride were affected by time where T0 groups displayed higher values than those of T1 and T2. Similarly, plasma protein was affected by time with higher values found at T1 and T2 compared to T0. Concerning AST and ALP, no significant diet- nor time-dependant effects were found among experimental groups while a significant time effect was found in ALT, with higher values found in T0 than T2 groups. CK and LDH were affected by time with lower values found in T2 compared to T0. $Ca^{2+}$ was affected by time where T1 and T2 showed higher values than T0. Both significant diet and time effects were found in P where FM30/FO15 and T0 displayed higher values than the other diets and time groups, respectively. $K^+$ was affected by time with higher values at T0 compared to the other sampling times. Concerning $Na^+$, significant diet, time and interaction effects were found and the combined effect of diet and time resulted in an increasing pattern from T0 to T1 only in FM10/F03 diets. In addition, at T1, FM10/FO3 displayed higher values than the other dietary treatments. Plasma $Mg^{2+}$ levels were influenced by time; specifically, values were lower at T2 in comparison to T0 and T1. Cortisol level was affected by time; specifically, values were higher at T1 in comparison to T0 and T2. A significant diet and interaction effect were observed in lactate, in particular the lactate levels recorded at T1 were higher in the FM30/FO15 group in comparison to those observed in FM20/FO7 and FM10/FO3 at the same time point. In addition, at T0 FM30/FO15 displayed higher lactate values at T1 than the other time points, while in FM20/FO7 values were higher at T0 than T1. In FM10/FO3 no significant difference within time points were observed.

## Humoral Immune Biomarkers in Skin Mucus

Results concerning humoral immune biomarkers in skin mucus are presented in **Supplementary Figures 1A–I** and in **Figures 1A–I**. At the end of the growth trial (T0) dietary treatments did not affect all the parameters analyzed except esterase which was lower in FM20/FO7 compared to the other treatments (One-way ANOVA – **Supplementary Figure 1**). In addition, bactericidal activities against *V. anguillarum* and *V. harveyi* were higher in FM10/FO3. **Figure 1** reports humoral immune biomarkers results in relation to dietary treatments and time after stress (Two-way ANOVA). Protease activity was affected by time after stress displaying higher values in T0 than T1 and T2 (**Figure 1A**). Antiprotease activity was affected by time with significant diet × time effect which resulted to increasing values at T1 and T2 in FM10/FO3. In addition, at T0, FM20/FO7 was higher than FM10/FO3 (**Figure 1B**). Peroxidase activity was significantly affected by time and diet, showing higher values at T2 compared to T0 and T1 (**Figure 1C**). In addition, peroxidase activity was also lower in fish fed FM10/FO3 than FM30/FO15. Esterase activity was affected by time with higher values at T2 than T1 and T0 (**Figure 1D**). Alkaline phosphatase activity showed a diet, time and interaction effect with higher values at T2 in the FM30/FO15 and FM10/FO3 compared to the same dietary groups recorded at T0 and T1. In addition at T2, FM20/FO7 was lower than the other diets while FM10/FO3 was lower than FM30/FO15 (**Figure 1E**). Lysozyme was affected by time with general increasing values at T1 even if not specific differences were detected in the *post hoc* test (**Figure 1F**). IgM levels showed a diet, time and interaction effect; specifically, values increased in animals fed the FM10/FO3 diet and sampled at T1 and T2 compared to those sampled at T0 within the same treatment. In contrast, fish from the FM20/FO7 group were characterized by lower IgM values at T2 compared to T0, while those from the FM30/FO15 group showed lower values at T1 compared to T0 and T2 sampling points (**Figure 1G**). In addition, at T1 FM30/FO15 displayed lower values than FM20/FO7 and FM10/FO3, while at T2, FM10/FO3 showed higher values than the other diets and FM30/FO15 was higher than FM20/FO7.

Bactericidal activity against *V. anguillarum* was affected by time, diet and interaction; specifically, in fish fed the FM10/FO3 values were higher at T2 than T0 within the same dietary group, while in fish fed FM20/FO7 values were higher at T1 compared to T0. At each considered time point, FM10/FO3 showed higher values than the other dietary treatments.

Similarly, bactericidal activity against *V. harveyi* was also affected by time and diet with higher values at T1 and T2 than

**TABLE 6 |** Plasma biochemistry values for European seabass fed the experimental diets and exposed to crowding stress and recovery after small fasting period.

| Analyte | Time | FM30/FO15 | FM20/FO7 | FM10/F03 | *P*-value | | |
|---|---|---|---|---|---|---|---|
| | | | | | Diet | Time | Inter |
| Glucose (mg $dL^{-1}$) | T0 | 188.25 ± 66.73 | 166.07 ± 40.07 | 170.14 ± 43.81 | **<0.001(B/A/AB)** | **<0.001(A/B/A)** | 0.382 |
| | T1 | 293.30 ± 110.62 | 213.12 ± 48.48 | 252.24 ± 65.27 | | | |
| | T2 | 223.15 ± 69.39 | 181.04 ± 44.81 | 188.14 ± 38.49 | | | |
| TRIG (mg $dL^{-1}$) | T0 | 730.39 ± 284.73 | 851.80 ± 347.61 | 773.87 ± 240.28 | 0.170 | **<0.001(B/A/A)** | 0.625 |
| | T1 | 436.07 ± 92.14 | 471.81 ± 115.19 | 389.09 ± 43.56 | | | |
| | T2 | 451.37 ± 123.85 | 442.58 ± 84.36 | 387.00 ± 69.65 | | | |
| TP (mg $dL^{-1}$) | T0 | 4.38 ± 0.45 | 4.31 ± 0.42 | 4.12 ± 0.38 | 0.051 | **<0.001(A/B/B)** | 0.910 |
| | T1 | 4.97 ± 0.54 | 4.90 ± 0.44 | 4.85 ± 0.34 | | | |
| | T2 | 4.78 ± 0.28 | 4.79 ± 0.55 | 4.52 ± 0.37 | | | |
| AST (U $L^{-1}$) | T0 | 273.61 ± 275.40 | 196.80 ± 157.33 | 153.07 ± 104.89 | 0.065 | 0.293 | 0.545 |
| | T1 | 137.00 ± 79.34 | 132.80 ± 105.08 | 139.64 ± 73.54 | | | |
| | T2 | 283.26 ± 443.76 | 142.58 ± 94.39 | 105.50 ± 82.14 | | | |
| ALT (U $L^{-1}$) | T0 | 8.61 ± 15.94 | 6.40 ± 7.84 | 4.07 ± 3.86 | 0.323 | **0.008(B/AB/A)** | 0.730 |
| | T1 | 3.00 ± 2.25 | 4.25 ± 5.00 | 2.36 ± 1.29 | | | |
| | T2 | 2.47 ± 2.25 | 2.70 ± 2.66 | 1.69 ± 1.01 | | | |
| ALP (U $L^{-1}$) | T0 | 79.00 ± 82.14 | 51.87 ± 17.24 | 52.20 ± 15.32 | 0.173 | 0.146 | 0.323 |
| | T1 | 53.93 ± 10.65 | 52.88 ± 10.05 | 53.00 ± 5.04 | | | |
| | T2 | 50.95 ± 13.20 | 50.32 ± 13.46 | 44.88 ± 7.76 | | | |
| CK (U $L^{-1}$) | T0 | 3530.93 ± 2783.44 | 4206.50 ± 4362.01 | 3190.43 ± 3469.04 | 0.274 | **0.003(B/AB/A)** | 0.460 |
| | T1 | 3940.69 ± 3519.65 | 2364.88 ± 2969.64 | 2049.73 ± 830.50 | | | |
| | T2 | 1544.67 ± 1106.93 | 2282.00 ± 1608.62 | 1169.62 ± 748.82 | | | |
| LDH (U $L^{-1}$) | T0 | 232.78 ± 252.62 | 167.80 ± 113.83 | 174.33 ± 169.45 | 0.481 | **0.024(B/AB/A)** | 0.770 |
| | T1 | 154.93 ± 107.26 | 126.27 ± 108.60 | 143.45 ± 62.59 | | | |
| | T2 | 120.95 ± 84.84 | 134.74 ± 109.52 | 95.75 ± 88.39 | | | |
| $Ca^{2+}$ (mg $dL^{-1}$) | T0 | 12.96 ± 3.17 | 13.69 ± 0.89 | 13.35 ± 0.73 | 0.912 | **<0.001(A/B/B)** | 0.217 |
| | T1 | 15.18 ± 1.65 | 14.47 ± 0.94 | 15.09 ± 1.30 | | | |
| | T2 | 14.62 ± 1.04 | 14.28 ± 0.89 | 13.99 ± 0.71 | | | |
| P (mg $dL^{-1}$) | T0 | 12.47 ± 4.44 | 11.75 ± 1.25 | 10.86 ± 1.29 | **0.004(B/A/A)** | **<0.001(B/A/A)** | 0.317 |
| | T1 | 11.54 ± 2.03 | 9.53 ± 0.91 | 10.28 ± 1.05 | | | |
| | T2 | 9.90 ± 1.14 | 9.39 ± 1.12 | 9.26 ± 0.97 | | | |
| $K^+$ (mEq $L^{-1}$) | T0 | 6.17 ± 2.67 | 6.01 ± 2.48 | 6.29 ± 1.83 | 0.512 | **<0.001(B/A/A)** | 0.869 |
| | T1 | 1.73 ± 0.64 | 2.32 ± 1.33 | 2.20 ± 1.16 | | | |
| | T2 | 2.59 ± 1.35 | 2.66 ± 1.46 | 3.18 ± 1.56 | | | |
| $Na^+$ (mEq $L^{-1}$) | T0 | 188.40 ± 4.03$^{a}$ | 188.13 ± 4.00$^{a}$ | 187.71 ± 3.60$^{a}$ | **0.041** | **<0.001(A/A/B)** | **0.009** |
| | T1 | 187.56 ± 2.34$^{a\#}$ | 185.16 ± 12.5$^{a\#}$ | 194.56 ± 6.63$^{b\dagger}$ | | | |
| | T2 | 193.84 ± 3.73$^{b}$ | 195.65 ± 3.27$^{b}$ | 195.63 ± 9.93$^{b}$ | | | |
| Mg (mg $dL^{-1}$) | T0 | 4.50 ± 0.82 | 4.23 ± 0.73 | 4.48 ± 1.17 | 0.103 | **< 0.001(B/B/A)** | 0.171 |
| | T1 | 4.63 ± 0.94 | 4.44 ± 0.70 | 5.10 ± 1.00 | | | |
| | T2 | 3.94 ± 0.61 | 3.52 ± 0.36 | 3.46 ± 0.55 | | | |
| Cortisol (μg $dL^{-1}$) | T0 | 35.61 ± 12.33 | 26.16 ± 5.86 | 25.56 ± 12.42 | 0.055 | **<0.001 (A/B/A)** | 0.123 |
| | T1 | 41.34 ± 12.30 | 43.19 ± 5.96 | 40.86 ± 8.43 | | | |
| | T2 | 34.98 ± 9.19 | 34.26 ± 10.26 | 31.59 ± 8.42 | | | |
| Lactate (mmol $L^{-1}$) | T0 | 53.37 ± 18.29$^{a}$ | 49.13 ± 17.46$^{b}$ | 48.98 ± 11.56 | **<0.001(B/A/A)** | 0.420 | **0.001** |
| | T1 | 68.90 ± 39.29$^{b\dagger}$ | 33.60 ± 7.07$^{a\#}$ | 45.87 ± 13.55$^{\#}$ | | | |
| | T2 | 48.79 ± 8.28$^{a}$ | 43.19 ± 7.21$^{ab}$ | 46.77 ± 9.84 | | | |

*Data are given as the mean (n = 15 diet$^{-1}$) each time (T) sampling ± SD. The uppercase letters in the parenthesis after P-values of two-way ANOVA represent significant differences in two-way ANOVA. The three sets of letters in a parenthesis correspond to the three time (T0/T1/T2) or diet (FM30/FO15/FM20/FO7/FM10/FO3) groups, respectively, and data value corresponding to "A" are lower than those corresponding to "B." Different symbols stand for significant differences among dietary treatments for the same time while lowercase letters stand for significant differences between times for the same diet. FM30/FO15 = 300 g kg$^{-1}$ fishmeal (FM), 150 g kg$^{-1}$ fish oil (FO); FM20/FO7 = 200 g kg$^{-1}$ fishmeal (FM), 70 g kg$^{-1}$ fish oil (FO); FM10/FO3 ( 100 g kg-1 fishmeal (FM), 30 g kg-1 fish oil (FO). Pre-stress time point after 36 h fating (T0); post-stress time point after 2 h confinement stress exposure (T1); recovery time point 24 h after the end of confinement stress exposure (T2).*

*TP, total protein; TRIG, triglycerides, AST, aspartate aminotransferase; ALT, alanine transaminase; ALP, alkaline phosphatase; CK creatine kinase (U $L^{-1}$); LDH, lactate dehydrogenase; $Ca^{+2}$ calcium; P, inorganic phosphorus; $K^{+}$, potassium; $Na^+$, sodium; Mg, magnesium; SD, standard deviation.*

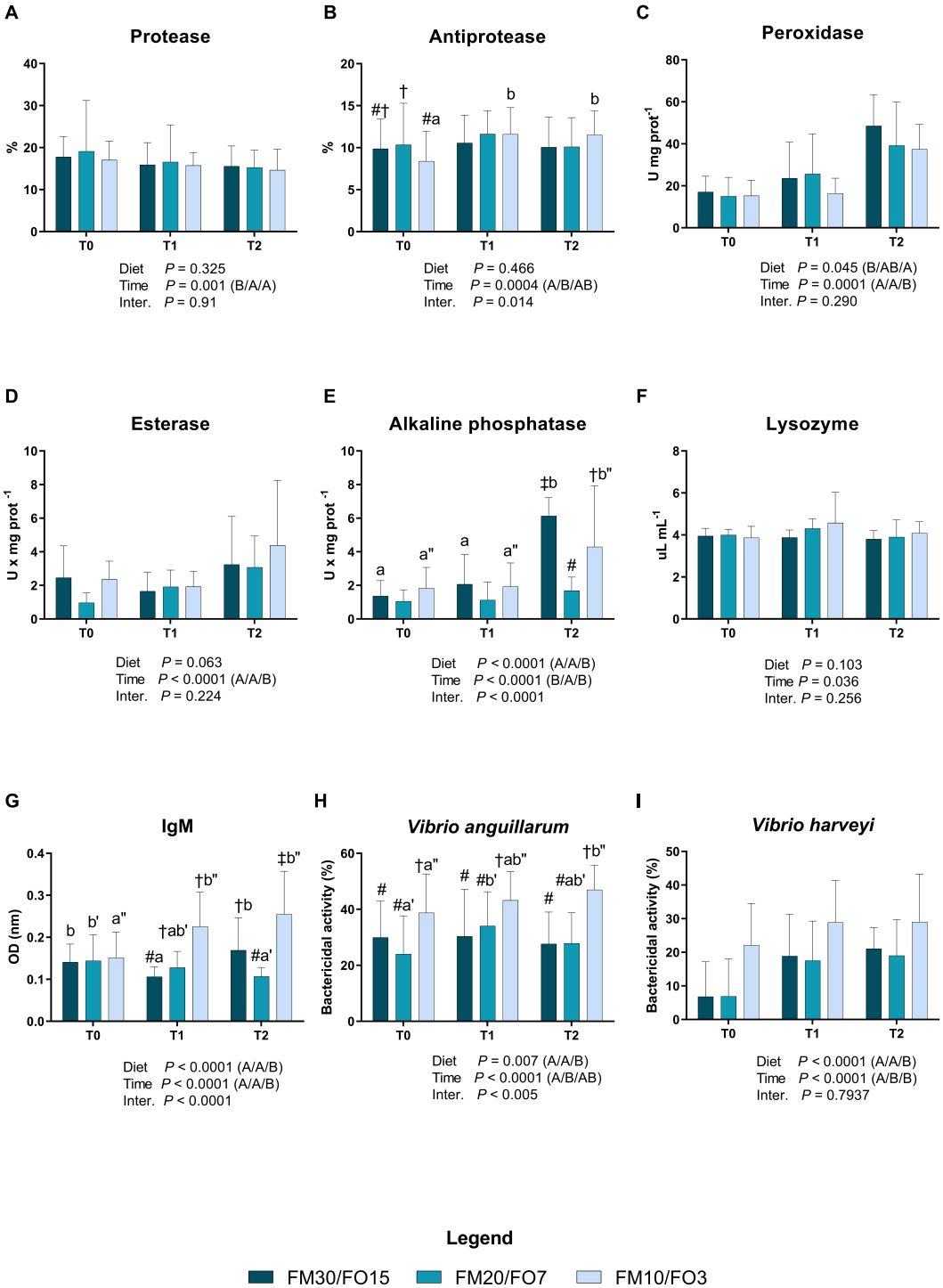


**FIGURE 1 |** Humoral immune biomarkers in skin mucus of European sea bass fed the experimental diets and exposed to crowding stress (2 h T1) and recovery (24 h T2) after fasting period (36 h, T0). FM30/FO15 = 300 g $kg^{-1}$ fishmeal (FM), 150 g $kg^{-1}$ fish oil; (FO); FM20/FO7 = 200 g $kg^{-1}$ FM; 70 g $kg^{-1}$ FO; FM10/FO3 = 100 g $kg^{-1}$ FM; 30 g $kg^{-1}$ FO. Data represent the mean ± S.D. (*N* = 24). The uppercase letters in the parenthesis after *P*-values of two-way ANOVA represent significant differences in two-way ANOVA ($P < 0.05$). The three sets of letters in a parenthesis correspond to the three times (T0/T1/T2) or diets (FM30/FO15/FM20/FO7/FM10/FO3) groups, respectively, and data value corresponding to "A" are lower than those corresponding to "B." Different symbols stand for significant differences among dietary treatments for the same time while lowercase letters (a b c, FM30/FO15; a'b'c' FM20/FO7; a"b"c" FM10/FO3) stand for significant differences between times for the same diet. **(A)** Protease activity (%); **(B)** antiprotease activity (%); **(C)** peroxidase activity (U* mg $prot^{-1}$); **(D)** esterase activity (U* mg $prot^{-1}$); **(E)** alkaline phosphatase activity (U* mg $prot^{-1}$); **(F)** lysozyme activity (μL* mg $prot^{-1}$); **(G)** IgM (OD nm); **(H)** bactericidal activity (%) against *Vibrio anguillarum*; **(I)** bactericidal activity (%) against *Vibrio harveyi*.

T0 and higher values reported in FM10/FO3 compared to the other treatments.

## Gene Expression of Stress and Immune-Related Genes in Brain and Head-Kidney

**Supplementary Figure 2** and **Figure 2** show the relative expression values of the four target genes involved in the stress response measured in the brain and the head kidney.

At the end of the growth trial (T0) brain *gr-1 and gr-2* relative expression decreased at decreasing FMFO level, while in the head kidney *hsp70* was lower in FM20/FO7 than FM30/FO15 and *mr* was lower in FM20/FO7 and FM10/FO3 compared to FM30/FO15 (One-way ANOVA – **Supplementary Figure 2**).

**Figure 2** reports the same stress target genes in relation to dietary treatments and time after stress (Two-way ANOVA).

In the brain, *hsp70* were affected by time displaying lower values at T0 than T1 and T2 while brain *gr-1* was lower in T0 than T2. Brain *gr-2* was affected by diet supported mainly by the higher values observed in FM30/FO15 than FM10/FO3. No significant time nor diet effects were reported for the relative expression of *mr* in the brain.

In the head kidney, *hsp70* was up-regulated at T2 in fish fed the FM30/FO15 diet with higher values compared to the other time points within dietary treatment and in comparison to the other diets at T2. In addition, head kidney *gr*-1 and *gr-2* were affected by time; specifically, *gr-1* showed higher values at T2 than T1 and T0 while *gr-2* showed higher values at T0 and T2 compared to T1. In the same tissue, *mr* was affected by time, diet and interaction; specifically, in FM30/FO15 transcripts decreased from T0 to T1, increasing again at T2 while in FM20/FO7 and FM10/FO3 values were higher at T0 than T1. At T0, FM30/FO15 displayed higher values than the other diets.

Concerning *gr-1/mr* a significant interaction effect was observed for brain where FM20/FO7 displayed higher values at T1 than T0. The *gr-1/mr* in the head kidney showed a time effect with values higher at T2 compared to the other time points.

The expression of the selected genes involved in the immune response for the brain and head kidney are depicted in **Supplementary Figure 3** and **Figure 3**. At the end of the growth trial (T0) brain *tgf* was lower in FM20/FO7 compared to FM10/FO3 while brain *tnf*-α was lower in FM10/FO3 than FM30/FO15 and FM20/FO7. At the same time brain *cox2* was lower in FM10/FO3 compared to FM30/FO15, while brain *csp3* was lower in FM10/FO3 than FM20/FO7 (One-way ANOVA – **Supplementary Figure 3**). Concerning head kidney, at the end of the growth trial (T0) FM20/FO7 and FM10/FO3 showed *tnf*-α, *cox2* and *csp3* values lower than FM30/FO15, while *lys* and *il10* values of FM20/FO7 were lower than FM30FO15 (One-way ANOVA – **Supplementary Figure 3**).

**Figure 3** reports the same immune response genes in relation to dietary treatments and time after stress (Two-way ANOVA).

In the brain, *tgf* was affected by time and interaction; specifically, values were up-regulated at T2 only in fish fed FM10/FO3. A similar trend occurred for *dcn,* where the relative expression in fish fed FM10/FO3 was higher than FM20/FO7

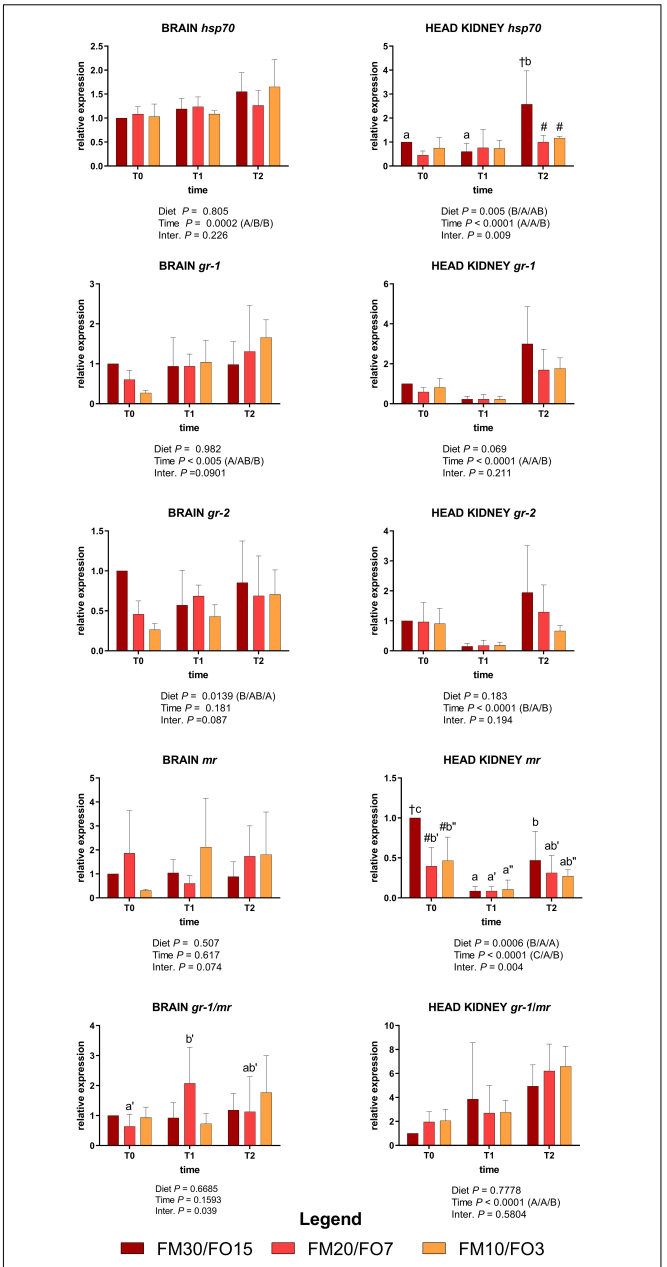


**FIGURE 2 |** Relative expression of stress-related genes in brain and head kidney of European sea bass fed the experimental diets and exposed to crowding stress (2 h T1) and recovery (24 h T2) after fasting period (36 h, T0). FM30/FO15 = 300 g $kg^{-1}$ fishmeal (FM), 150 g $kg^{-1}$ fish oil; (FO); FM20/FO7 = 200 g $kg^{-1}$ FM; 70 g $kg^{-1}$ FO; FM10/FO3 = 100 g $kg^{-1}$ FM; 30 g $kg^{-1}$ FO. Data represent the mean ± S.D. ($N$ = 6). The uppercase letters in the parenthesis after $P$-values of two-way ANOVA represent significant differences in two-way ANOVA ($P < 0.05$). The three sets of letters in a parenthesis correspond to the three times (T0/T1/T2) or diets (FM30/FO15/FM20/FO7/FM10/FO3) groups, respectively, and data value corresponding to "A" are lower than those corresponding to "B." Different symbols stand for significant differences among dietary treatments for the same time while lowercase letters (a b c, FM30/FO15; a'b'c' FM20/FO7; a"b"c" FM10/FO3) stand for significant differences between times for the same diet. Genes are reported as follows: *gr-1*, glucocorticoid receptor-1; *gr-2* glucocorticoid receptor-2; *mr,* melanocortin receptor; *hsp70*, heat shock protein 70.

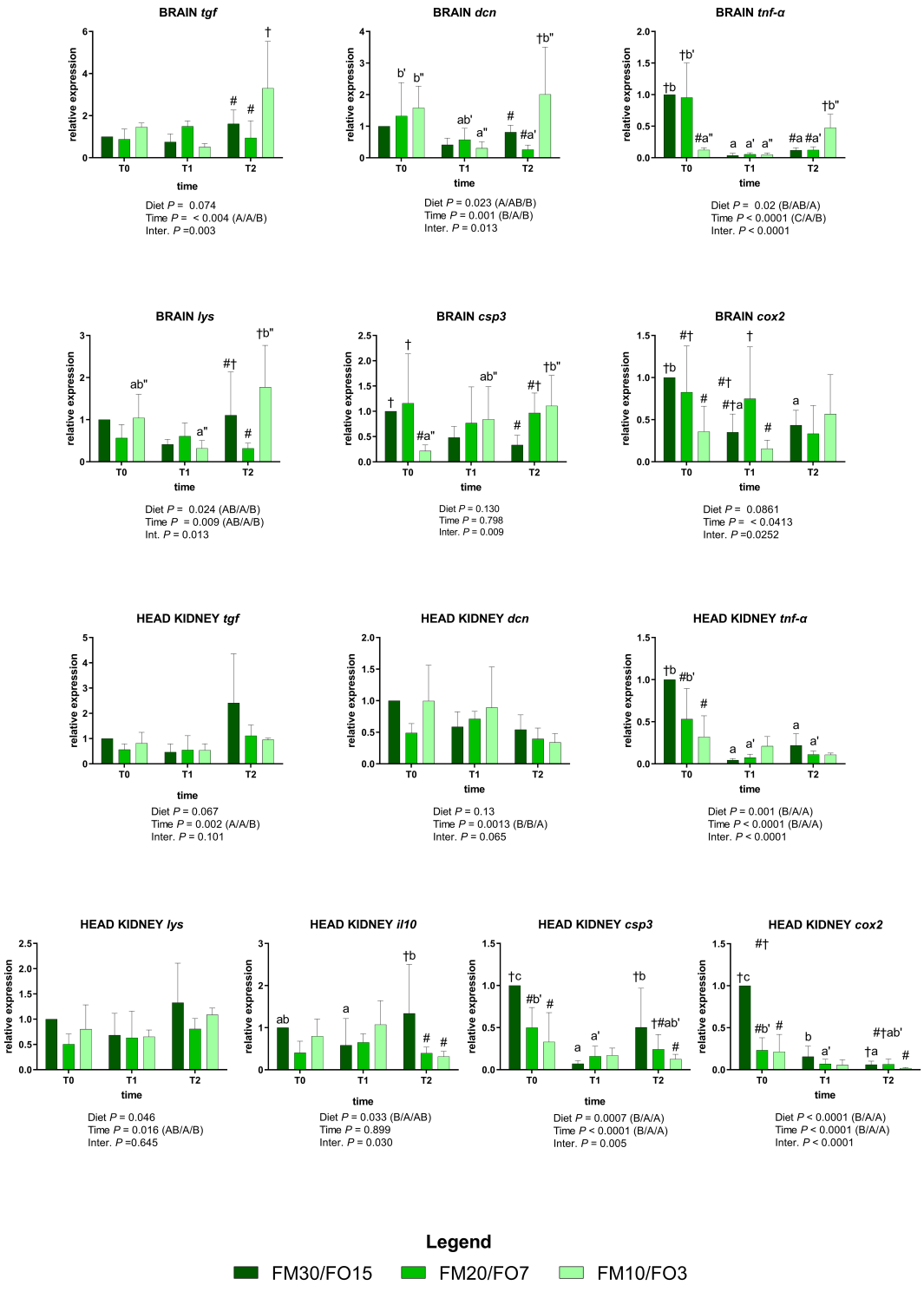


**FIGURE 3 |** Relative expression of immune-related genes in brain and head kidney of European sea bass fed the experimental diets and exposed to crowding stress (2 h T1) and recovery (24 h T2) after fasting period (36 h, T0). FM30/FO15 = 300 g $kg^{-1}$ fishmeal (FM), 150 g $kg^{-1}$ fish oil; (FO); FM20/FO7 = 200 g $kg^{-1}$ FM; 70 g $kg^{-1}$ FO; FM10/FO3 = 100 g $kg^{-1}$ FM; 30 g $kg^{-1}$ FO. Data represent the mean ± S.D. ($N = 6$). The uppercase letters in the parenthesis after *P*-values of two-way ANOVA represent significant differences in two-way ANOVA ($P < 0.05$). The three sets of letters in a parenthesis correspond to the three times (T0/T1/T2) or diets (FM30/FO15/FM20/FO7/FM10/FO3) groups, respectively, and data value corresponding to "A" are lower than those corresponding to "B." Different symbols stand for significant differences among dietary treatments for the same time while lowercase letters (a b c, FM30/FO15; a'b'c' FM20/FO7; a"b"c" FM10/FO3) stand for significant differences between times for the same diet. Genes are reported as follows: csp3, caspase 3; *hsp70*, heat shock protein 70; *tgf*, transforming growth factor; *tnf*-α, tumor necrosis factor α; *il10*, interleukin 10; *dcn*, dicentrarcin, *cox2*, cyclooxygenase 2, *lys*, lysozyme.

and FM30/FO15 at T2 and higher in comparison to the same dietary treatment at T1. In addition, values in FM20/FO7 were lower at T2 compared to the values from the same treatment recorded in T1. The relative expression of *tnf*-α was affected by time, diet and interaction; specifically, values decreased at T1 and T2 only in FM30/FO15 and FM20/FO7, while values increased at T2 compared to T1 in FM10/FO3. In addition, at T0 values were lower in FM10/FO3 than the other dietary treatments while the same diet displayed higher values at T2 than the other dietary treatments.

The expression of *lys* was affected by diet, time and interaction; specifically, values were higher in FM10/FO3 at T2 compared to fish fed the FM20/FO7 diet and compared to the same dietary treatment at T1.

The relative expression of *csp3* displayed a significant diet x time interaction where fish from the FM10/FO3 group displayed an increasing trend from T0 to T2 sampling points. In addition, at T0 values were lower in FM10/FO3 than the other diets while at T2 the same diet displayed higher values than FM30/FO15. Brain *cox2* reported significant time and interaction effects; specifically, values within FM30/FO15 were higher at T0 compared to T1 and T2. Data at T0 reported values in FM30/FO15 higher than FM10/FO3 while at T1 FM20/FO7 values were higher than FM10/FO3.

Regarding the assessment of gene expression patterns in the head kidney, *tgf* was affected by time with higher values at T2, than T1 and T0 while *dcn* displayed lower values in T2 than T0 and T1. The relative expression of *tnf*-α showed significant diet, time and interaction effect; specifically, values in FM30FO15 and FM20/FO7 were higher at T0 than T1 and T2, while at T0 FM30/FO15 values were higher the other diets.

Head kidney *lys* gene expression showed higher values at T2 than T1. The pro-inflammatory cytokine *il10* displayed significant diet x time interaction effect with higher values in fish fed FM30/FO15 diet at T2 compared to the same diet at T1, while at T2 FM30/FO15 values were higher compared to the other dietary treatments. Caspase 3 displayed a significant diet, time and interaction effects. In particular FM30/FO15 displayed higher values at T0 compared to the same diet at T1 and T2, while the same diet was higher at T2 than T1. In addition, *csp3* values at T0 were higher in FM30/FO15 than the other diets, while at T2 FM30/FO15 values were higher than FM10/FO3. The relative expression of *cox2* was higher in FM30/FO15 group at T0 compared to the same treatment at T1 and T2, while FM20/FO7 at T0 was higher than T1 and T2. At T0 *cox2* values were higher in FM30/FO15 than the other treatments, while at T2 FM30/FO15 values were higher than FM10/FO3.

# DISCUSSION

## Key Performance Indicators and Body Proximate Composition

Recently, several studies have explored the feasibility of using very low FM and FO diets in European sea bass, as their effects on fish performance, gut morphology and microbiome, plasma biochemistry and filet quality have been described (Torrecillas et al., 2017b; Bonvini et al., 2018c; Parma et al., 2019; Henry et al., 2020). Although it has been shown that the FM and FO reduction may affect stress resistance, cellular immunity and oxidative status in different marine fish species (Sitjà-Bobadilla et al., 2005; Montero and Izquierdo, 2010; Geay et al., 2011; Gisbert et al., 2018), this topic still deserves further attention especially regarding this species, as it is highly susceptible to common stressors under intensive farming conditions.

In the present study, despite the absence of significant differences on feed intake and FCR values among diets, fish from the FM10/FO3 group showed a tendency for higher FCR; thus, leading to a negative outcome on BWf and SGR, values that were 11.3% lower than the FM30/FO15 group individuals. These findings are in contrast with those previously reported by Parma et al. (2019), where juveniles (22.8–68.2 g in BW) fed 10% FM as their sole animal protein source showed equal growth, feed and protein utilization in comparison to a control containing 20% FM. These differences could be related to the different feed formulation (i.e., lower FO inclusion) in the present trial. Similar results were reported also by Coutinho et al. (2017) where juveniles (7–28 g in BW) fed diets containing 15% FO and 8 and 2% (on dry weight basis) of FM and soluble fish protein concentrate, respectively. On the other hand, Bonvini et al. (2018a) reported a trend toward lower growth performance and protein efficiency at higher FM replacement levels in 70–200 g European sea bass when fed a diet containing 10% FM compared to their congeners fed diets containing 20 and 30% FM.

In FM10/FO3 the reduced level of marine ingredients with a consequence reduction of LC-PUFA could have affected growth performance as previously described in this species where the supplementation of n-3 and n-6 LC-PUFA in fish fed free FM and FO diet led to increased growth (Torrecillas et al., 2017a, 2018).

Concerning body composition and nutritional uptake, all treatments were found to be comparable under the present experimental conditions, results which agreed with those previously reported by Bonvini et al. (2018a) and Parma et al. (2019).

## Plasma Biochemistry

Studying a farmed fish species blood biochemistry profile can be a valuable tool to assess nutritional and health status (Peres et al., 2014; Bonvini et al., 2015). Overall, the present results at T0 were within the range of normal values reported for this species under proper nutritional and non-stressing conditions (Bonvini et al., 2018b). Furthermore, different FM/FO dietary levels did not affect the basal status before stress even if cortisol level in FM30/FO15 was higher than the other treatments.

Data on plasma cortisol coupled with glucose levels is one of the first and main metabolites being released into the blood stream as a marker to acute stress response (Barton, 2002). European sea bass has been well characterized to have high basal and post-stress plasma cortisol concentrations (Fanouraki et al., 2011; Maricchiolo et al., 2011; Ellis et al., 2012) after even the minimum ordinary handling that occurs in fish farms (Tsalafouta et al., 2015; Samaras et al., 2017). In accordance with Di Marco et al. (2008), in our study the cortisol level peaked after stress

exposure with a tendency to return to values similar to those reported in the pre-stress condition.

Plasma lactate values reflect metabolic and hormonal responses and can be considered an indicator of secondary stress responses (Saccol et al., 2018). The observed higher plasma lactate after stress exposure only in fish fed the FM30/FO15 diet may indicate a stronger response to crowding by increasing anaerobic muscle activity, as also reported in other fish species exposed to stressors such as chasing, netting, and air exposure (Ruane et al., 2002; Fanouraki et al., 2007).

Under current experimental conditions, confinement stress induced a significant increase of plasma glucose, which tended to return to initial basal values after a recovery time of 24 h. Notably, glucose was found to be slightly higher in groups fed FM30/FO15 at 2 h (T1) after confinement stress. Similar trends in plasmatic glucose levels and recovery time have also been reported in European sea bass exposed to 100 kg/m$^3$ for 15 min (Di Marco et al., 2008). Basal TRIG levels before stress are within the range of values reported by Peres et al. (2014) on this species; however, they were lower than those reported by Bonvini et al. (2018a,b). The different basal levels among these studies might be attributed to different dietary formulations regarding lipid sources as well as to different post-prandial time at which analyses were conducted. In this work, TRIG levels decreased after 2 h post-stress exposure in all the treatments. A similar decrease was reported in European sea bass after 48–72 h post-stress challenge and in animals exposed to starvation (Pérez-Jiménez et al., 2007; Di Marco et al., 2008; Peres et al., 2014). The authors suggested that this decrease is probably due to its use as an energetic substrate and to the reduction in lipogenesis, which may have contributed to the maintenance of plasma glucose levels after an acute stress event (Pérez-Jiménez et al., 2007). Total protein level is a good potential indicator to predict the nutritional status of fish, since it is usually very stable in well-nourished animals. Under present experimental conditions, total protein increased after stress in all treatments. In contrast to our results, previous studies evidenced a plasma protein decline under fasting or stress conditions as a consequence of amino acid oxidation or peripheral proteolysis (Mommsen et al., 1999; Di Marco et al., 2008; Coeurdacier et al., 2011; Peres et al., 2014). However, Montero et al. (1999), described an increase of cortisol, glucose, and plasma protein in gilthead sea bream held at high stocking density as a strategy for increasing oxygen-carrying capacity of blood during periods of high energy demand. Such differences between studies may be related to the duration and intensity of the stressor, which would affect host metabolism and plasmatic protein levels.

Non-specific enzymes ALT, ALP, LDH, and CK are plasma indicators that may provide important information on fish health status, whose elevated levels in blood may indicate tissue damage in many organs including liver, muscle, spleen and kidney (Peres et al., 2013; Guardiola et al., 2018; Parma et al., 2020). Under current experimental conditions, ALT levels dropped after stress exposure and also continued to decrease after recovery time in all the treatments. An increasing level of plasma ALT may imply liver damage and less efficient absorption and transportation of lipids and carbohydrates from the intestine as described by other authors (Peres et al., 2014; Bonvini et al., 2018b), while ALT reduction may also be associated with changes in amino acid metabolism, since ALT degrades alanine for cellular energetic purposes.

The enzyme CK is particularly active in heart and skeletal muscle, while LDH converts lactate to pyruvate in cells; and their activity was described as being lowered by 30 and 50% respectively after 1 week fasting in European sea bass (Peres et al., 2014). Accordingly, CK and LDH concentration were found to be reduced at 24 h post-stress in a similar manner for all the treatments under current experimental conditions. Furthermore, plasma electrolytes are indicators of the secondary phase of stress response in fish, providing an indirect indication of altered plasma cortisol levels (Peres et al., 2014). Although fish may absorb some inorganic nutrients from the aquatic environment, when starvation or elevated stocking density occurs, a significant reduction in plasma phosphorus and calcium levels take place, confirming their importance as a general indicator of stress in fish (Lall, 2002; Hrubec and Smith, 2010; Guardiola et al., 2018). In this study, plasmatic calcium levels tended to increase after confinement stress and return to basal values at 24 h after stress in all dietary groups. Contrariwise, phosphorus concentration continued to decrease at T2, with generally lower values in animals fed FM20/FO7 and FM10/FO3 diets. This is consistent with a calcium and phosphorus drop and eventual resilience after starvation or stress described for this species (d'Orbcastel et al., 2010; Peres et al., 2014). Other plasma electrolytes such as potassium, sodium and magnesium alterations may be linked to acid-base balance and ions-transport disturbance (Roque et al., 2010; Bonvini et al., 2018b), which in the present study were found to tend to return to the initial values after the recovery period. However, at 2 h after stress only fish fed FM10/FO3 were characterized by an increase in the level of plasma sodium, finding which may be related to the reduced dietary LC-PUFA such as arachidonic acid which was able to attenuate the stressor-induced increase in plasma osmolality induced by acute crowding in gilthead sea bream (Van Anholt et al., 2004).

## Humoral Immune Biomarkers in Skin Mucus

The study of the innate immune parameters of skin mucus (lysozyme, proteases, anti-proteases, peroxidase, esterase, alkaline phosphatase, and bactericidal activities) is of great importance in the evaluation of mucosal immunity of fish as this is the first line of the host's defense. Their evaluation has been studied in relation to pathogens, environmental stress, feeding conditions, contaminants, crowding or handling in several fish species. However, data concerning the specific response of mucosal components to different dietary formulations and stressors such as crowding or handling in European sea bass are still scarce (Guardiola et al., 2014b, 2016; Sanahuja et al., 2019).

In the present study, acute crowding slightly reduced protease activity in the skin mucus with a similar response for all the dietary treatments. In contrast, a different response of skin mucus protease activity to acute crowding was observed in gilthead sea bream, which was characterized by a decrease and increase after

2 and 24 h stress exposure, respectively. In addition, protease activity in gilthead sea bream was reduced when fish were fed low fish meal content (10% FM and 3% FO vs. 30 FM%, 15% FO), while chronic high density rearing conditions did not affect its activity (Parma et al., 2020). Antiprotease activity was significantly affected by crowding condition in fish fed the FM10/FO3 diet, which resulted in increasing values at 2 and 24 h after stress. In contrast, antiprotease activity was not affected by acute crowding in gilthead sea bream and, in agreement with our findings, antiprotease and protease were negatively correlated as a physiological response to compensate for the variations in protease activity (Guardiola et al., 2016). Peroxidase activity peaked at 24 h after stress for all the treatments. No data on skin mucus peroxidase are available for European sea bass exposed to acute crowding; however, in gilthead sea bream a similar response to crowding was observed with increasing values obtained at 48 h after stress. These differences between species could be attributed to species-specific factors, fish health status or exposure time to stress (Guardiola et al., 2014a; Sanahuja et al., 2019). In addition, in the present study a lower response of peroxidase activity was observed in fish fed the FM10/FO3 diet in comparison to those animals from the FM30/FO15 group, data that may indicate that these low FM/FO levels may reduce the specific action of this skin mucus component. Esterase activity in fish skin mucus has been previously studied mostly in terms of defensive activity against pathogens or in response to environmental chemical compounds, although their role is still not fully understood (Guardiola et al., 2014a; Sanahuja et al., 2019). No data are reported on esterase activity in fish skin mucus in response to acute crowding; however, our results indicated a positive response to stress of this mucus component in all dietary groups. Interestingly, in olive flounder (*Paralichthys olivaceus*) esterase activity of skin mucus was negatively correlated with protease activity. A similar trend occurred in the present trial, supporting the hypothesis that these enzymes may have a direct or indirect role in immune function either by acting alone or in association with other biologically active substances present in the skin mucus (Jung et al., 2012). Alkaline phosphatase is an antibacterial agent in mucus due to its hydrolytic activity, and increases in fish after physical or chemical stress, including skin regeneration (Sheikhzadeh et al., 2012a,b). In our study, ALP peaked at 24 h post-stress with a similar time-related effect as that observed for peroxidase and esterase, indicating possible synergistic effects of these three parameters in response to stress (Jung et al., 2012). Increased activity of ALP was also demonstrated in tiger barb (*Puntius tetrazona*) mucus during crowding stress as response to the increase in mucus secretion or improved mucosal immune responses (Hoseinifar et al., 2014; Roosta and Hoseinifar, 2016). Lysozyme activity was marginally affected by crowding conditions with an increasing level at 2 h post stress. Recent findings showed that acute crowding conditions in Atlantic salmon (*Salmo salar*) induced an increase in lysozyme activity of skin mucus only at 1 h post-stress, while it returned to basal values at 3 h after stress (Djordjevic et al., 2021). Conversely, high rearing density during 98 and 120 days in gilthead sea bream and turbot (*Scophthalmus maximus*), respectively, reduced skin mucus lysozyme activity as a possible immunodepressive effect due to chronic stress caused by high stocking density (Jia et al., 2016).

In addition, the bactericidal activity of IgM production in skin mucus reached a relevant post-stress peak mainly in fish fed the FM10/FO3 diet, which displayed higher values in comparison to other treatments. Our values were higher than those reported for skin mucus IgM in gilthead sea bream after crowding stress (transfer from 10 to 50 kg $m^{-3}$ over 48 h) (Guardiola et al., 2016). The crowding stress employed in the present study seemed sufficient to activate a further excretion of IgM in fish fed the FM10/FO3 diet. Such a response may be interpreted as a mechanism to avoid possible invasion by pathogens when animals are highly challenged, subject to frequent surface abrasion, or vulnerable to infections. A further reinforcement for the idea of there being an enhanced humoral response in low FM/FO diet was the more elevated *in vitro* bactericidal activity against *V. anguillarum* and *V. harveyi* observed in fish fed the FM10/FO3 diet. These results may be the consequence of the sum of many intrinsic antimicrobial factors such as skin antimicrobial peptides and other innate immune components to fight pathogens. In particular, recent findings have shown the importance of LC-PUFA fractions in the composition of the skin mucus of gilthead seabream in relation to different FMFO dietary level, highlighting the needs for further studies to better understand the role of feed composition on skin mucus protective functions (Torrecillas et al., 2019).

## Gene Expression of Stress and Immune-Related Genes in Brain and Head-Kidney

Glucocorticoid (*gr-1, gr-2*) and mineral corticoid receptors (*mr*) are receptors for cortisol found in many tissues including brain and immune cells, which are related to the regulatory role of cortisol in immune defense such as the secretion of pro- and anti-inflammatory cytokines (Reyes-López et al., 2018). In addition, *hsp70* is responsible for repairing and preventing cellular damage from stress-induced protein denaturation and is considered an important indicator for stress in many species including European sea bass (Islam et al., 2021). In the present study, most of the stress-related genes considered, specifically *hsp70* and *gr-1*, in the brain, and *hsp70, gr-1,* and *gr-2* in head kidney, showed an overall time-dependent increasing pattern in expression after stress, findings which are in line with a positive response of the marker genes under consideration to crowding and handling stress in European sea bass and other fish species (Eissa and Wang, 2016).

Additionally, concerning *gr-1* and *gr-2*, it was previously explained that different expression patterns among *gr-1* and *mr* function as differential feed-forward and feed-back mechanisms, respectively, of cortisol on these receptor targets (Samaras et al., 2018). The *gr1*/*mr* ratio has been considered an appropriate indicator of stress load in fish species including European sea bass, as also reported in mammalian vertebrates (De Kloet et al., 2005, 2008; Samaras et al., 2018). In the present study, the *gr1*/*mr* ratio observed in the kidney increased after stress as result of the increasing, decreasing patterns of expression for *gr-1* and *mr*,

respectively. Interestingly, these genes were similarly expressed in the brain of European sea bass exposed to a combination of stresses including confinement, chasing and air exposure (Samaras et al., 2018).

Although not all the transcripts analyzed in the brain and head kidney showed a clear dietary effect, data reported for *hsp70, gr1, gr2* in the head kidney seemed to indicate a more acute response to crowding stress for fish fed the FM30/FO15 diet compared to lower FM/FO levels. In general, these results are in agreement with previous findings in European sea bass fed high levels of VOs, since dietary lipids can alter the ability of fish to cope with different types of stressors (Montero et al., 2003; Machado et al., 2019). At the biochemical level, these data are consistent with the higher glucose and lactate plasma level found in FM30/FO15, while no evident relation with plasma cortisol level was found. The absence of a direct relation between cortisol plasma level and the gene expression of glucocorticoid receptors was also previously observed in this species (Pavlidis et al., 2011; Reyes-López et al., 2018). In addition, the effect of the diet on the expression of stress-related genes was less evident in the brain than in the head kidney, possibly indicating a difference in the degree to which there is involvement of the diet in different target tissues.

While fish fed the high FM/FO (FM30/FO15) diet showed a higher response to stress, a low FM diet (FM10/FO3) resulted in a higher up-regulation of several immune-related genes at 24 h post stress, including *dcn*, and *lys* in the brain. These data were in agreement with the higher level of IgM and bactericidal activity against *V. anguillarum* and *V. harveyi* observed in skin mucus from animals fed the FM10/FO3 diet at 24-h post-stress; collectively these data all indicate a stronger activation of the immune response in fish fed this diet. Several antimicrobial molecules including lysozyme and dicentracin are known to play a key role in the innate immune response as they possess powerful microbiocidal activity against a wide range of pathogens. In European sea bass particularly, it has been suggested that dicentracin is involved in the antimicrobial function against bacteria such as *V. anguillarum* and *Photobacterium damselae* and its expression was up-regulated in head kidney at 5h post-infection with nodavirus (Mosca et al., 2014; Meloni et al., 2015; Valero et al., 2015, 2020). The higher pro-inflammatory activity observed at mucosal immune effectors (IgM and bactericidal activity) and gene expression levels (lysozyme and dicentracin) in fish from the FM10/FO3 group could also be related to the lower stress response observed after crowding, as evidenced by the lower lactate, glucose and gene expression of stress-related genes (*hsp70, gr-1, gr-2*) obtained in fish from this treatment. It is well documented that stress and immune response are closely connected due to the existing crosstalk between these two systems, since a stressor induces alterations in immune response. For instance, in fish species the inhibition of the pro-inflammatory response related to high cortisol production is well known (Castillo et al., 2009; Reyes-López et al., 2018). However, in the head kidney a different pattern of expression of immune-related genes compared to the brain was observed: in particular *tgf* and *il10* were up-regulated in fish fed the FM30/FO15 diet compared to the other treatments. Both of these cytokines have been shown to have significant autocrine activities for normal kidney function in mammals (Sinuani et al., 2013). Some types of nephropathy in mammals have been shown to benefit from increased expression of *il10*. Therefore, the up-regulation of anti-inflammatory cytokines such as *il10* and *tgf* may support the beneficial dietary effect of high FM/FO levels enhancing anti-inflammatory response after exposure to stress (Busti et al., 2020).

## CONCLUSION

In conclusion, 10% FM, 3% FO dietary inclusion levels showed a moderate reduction in growth performance, an effect that seemed to be related to the higher FCR reported in fish fed this diet. Although most of the plasma and skin mucus parameters analyzed were not affected by dietary treatments before stress, acute crowding induced different dietary-mediated responses. Specifically, a higher level of plasma lactate together with the up-regulation of some stress-related transcripts (*hsp70, gr-2*) suggests a higher reactivity to acute crowding of the stress-response mechanism, but a lower inflammatory response, as evidenced by higher expression of the anti-inflammatory *tnf*-α and *il10* genes in fish fed high FM and FO dietary levels (FM30/FO15). Otherwise, the higher IgM levels and bactericidal activity observed in skin mucus of fish fed the FM10/FO3 diet seems to indicate that acute crowding was able to activate a higher pro-inflammatory response in this treatment. The results of the present study seem to indicate that the low FM/FO dietary level employed could affect stress and immune response. Repeated or chronic exposure to stressors would be needed in order to further evaluate the dietary effects on fish welfare.

## DATA AVAILABILITY STATEMENT

The original contributions presented in the study are included in the article/**Supplementary Material**, further inquiries can be directed to the corresponding author/s.

## ETHICS STATEMENT

The animal study was reviewed and approved by Ethical-Scientific Committee for Animal Experimentation of the University of Bologna (protocol ID 942/2019) in accordance with European directive 2010/63/UE on the protection of animals used for scientific purposes.

## AUTHOR CONTRIBUTIONS

AB, NFP, LP, and PPG conceived and designed the experiment. NFP, AB, and LP wrote the first draft of the manuscript. NFP and LP carried out fish maintenance and sample collection. EG and KBA carried out the gene expression analysis and data processing. MAE carried out the skin mucus analysis and data

processing. FD and MCS carried out plasma biochemistry analysis. All authors reviewed, improved the writing and approved the final manuscript.

## FUNDING

This research was undertaken under the MedAID (Mediterranean Aquaculture Integrated Development) project, which has received funding from the European Union's Horizon 2020 Research and Innovation Programme, Call H2020-SFS-23-2016, grant agreement no. 727315 (http://www.medaid-h2020.eu/).

## ACKNOWLEDGMENTS

The authors would like to thank Gillian Forlivesi Heywood for English language editing and Antonina De Marco for assistance in fish maintenance during her master thesis degree accomplishment.

## SUPPLEMENTARY MATERIAL

The Supplementary Material for this article can be found online at: https://www.frontiersin.org/articles/10.3389/fmars.2021.779053/full#supplementary-material

## REFERENCES

AOAC (2010). *Officials Methods of Analysis*, 17th Edn. Washington, DC: Association of Official Analytical Chemists.

Bagni, M., Civitareale, C., Priori, A., and Ballerini, A. (2007). Pre-slaughter crowding stress and killing procedures affecting quality and welfare in sea bass (*Dicentrarchus labrax*) and sea bream (*Sparus aurata*). *Aquaculture* 263, 52–60. doi: 10.1016/j.aquaculture.2006.07.049

Balasch, J. C., and Tort, L. (2019). Netting the stress responses in fish. *Front. Endocrinol.* 10:62. doi: 10.3389/fendo.2019.00062

Barton, B. A. (2002). Stress in fishes: a diversity of responses with particular reference to changes in circulating corticosteroids. *Integr. Compar. Biol.* 42, 517–525. doi: 10.1093/icb/42.3.517

Barton, B. A., Ribas, L., Acerete, L., and Tort, L. (2005). Effects of chronic confinement on physiological responses of juvenile gilthead sea bream, *Sparus aurata L* ., to acute handling. *Aquac. Res.* 36, 172–179. doi: 10.1111/j.1365-2109.2004.01202.x

Bligh, E. G., and Dyer, W. J. (1959). A rapid method of total lipid extraction and purification. *Can. J. Biochem. Physiol.* 37, 911–917. doi: 10.1139/o59-099

Bonvini, E., Parma, L., Badiani, A., Fontanillas, R., Gatta, P. P., Sirri, F., et al. (2018c). Integrated study on production performance and quality traits of European sea bass (*Dicentrarchus labrax*) fed high plant protein diets. *Aquaculture* 484, 126–132. doi: 10.1016/J.aquaculture.2017.10.041

Bonvini, E., Bonaldo, A., Mandrioli, L., Sirri, R., Dondi, F., Bianco, C., et al. (2018a). Effects of feeding low fishmeal diets with increasing soybean meal levels on growth, gut histology and plasma biochemistry of sea bass. *Animal* 12, 923–930. doi: 10.1017/S1751731117002683

Bonvini, E., Bonaldo, A., Parma, L., Mandrioli, L., Sirri, R., Grandi, M., et al. (2018b). Feeding European sea bass with increasing dietary fibre levels: Impact on growth, blood biochemistry, gut histology, gut evacuation. *Aquaculture* 494, 1–9. doi: 10.1016/j.aquaculture.2018.05.017

Bonvini, E., Parma, L., Mandrioli, L., Sirri, R., Brachelente, C., Mongile, F., et al. (2015). Feeding common sole (*Solea solea*) juveniles with increasing dietary lipid levels affects growth, feed utilization and gut health. *Aquaculture* 449, 87–93. doi: 10.1016/j.aquaculture.2015.01.013

Boyd, C. E., D'Abramo, L. R., Glencross, B. D., Huyben, D. C., Juarez, L. M., Lockwood, G. S., et al. (2020). Achieving sustainable aquaculture: historical and current perspectives and future needs and challenges. *J. World Aquac. Soc.* 51, 578–633. doi: 10.1111/jwas.12714

Bradford, M. M. (1976). A rapid and sensitive method for the quantitation of microgram quantities of protein utilizing the principle of protein-dye binding. *Anal. Biochem.* 72, 248–254.

Busti, S., Bonaldo, A., Dondi, F., Cavallini, D., Yúfera, M., Gilannejad, N., et al. (2020). Effects of different feeding frequencies on growth, feed utilisation, digestive enzyme activities and plasma biochemistry of gilthead sea bream (*Sparus aurata*). *Aquaculture* 529, 735616. doi: 10.1016/j.aquaculture.2020.735616

Castillo, J., Teles, M., Mackenzie, S., and Tort, L. (2009). Stress-related hormones modulate cytokine expression in the head kidney of gilthead seabream (*Sparus aurata*). *Fish Shellf. Immunol.* 27, 493–499. doi: 10.1016/j.fsi.2009.06.021

Castro, C., Peréz-jiménez, A., Coutinho, F., and Corraze, G. (2018). Nutritional history does not modulate hepatic oxidative status of European sea bass (*Dicentrarchus labrax*) submitted to handling stress. *Fish Physiol. Biochem.* 44, 911–918. doi: 10.1007/s10695-018-0480-6

Coeurdacier, J. L., Dutto, G., Gasset, E., and Blancheton, J. P. (2011). Is total serum protein a good indicator for welfare in reared sea bass (*Dicentrarchus labrax*)? *Aquat. Liv. Resourc.* 24, 121–127. doi: 10.1051/alr/2011130

Cordero, H., Morcillo, P., Cuesta, A., Brinchmann, M. F., and Esteban, M. A. (2016). Differential proteome profile of skin mucus of gilthead seabream (*Sparus aurata*) after probiotic intake and/or overcrowding stress. *J. Proteomics* 132, 41–50. doi: 10.1016/j.jprot.2015.11.017

Coutinho, F., Simões, R., Oliva-Teles, A., Oliva-Teles, A., Peres, H., Monge-Ortiz, R., et al. (2017). Effects of dietary methionine and taurine supplementation to low-fish meal diets on growth performance and oxidative status of European sea bass (*Dicentrarchus labrax*) juveniles. *Aquaculture* 479, 447–454. doi: 10.1016/J.aquaculture.2017.06.017

De Kloet, E. R., Joëls, M., and Holsboer, F. (2005). Stress and the brain: from adaptation to disease. *Nat. Rev. Neurosci.* 6, 463–475. doi: 10.1038/nrn1683

De Kloet, E. R., Karst, H., and Joëls, M. (2008). Corticosteroid hormones in the central stress response: quick-and-slow. *Front. Neuroendocrinol.* 29:268–272. doi: 10.1016/j.yfrne.2007.10.002

Di Marco, P., Priori, A., Finoia, M. G., Massari, A., Mandich, A., and Marino, G. (2008). Physiological responses of European sea bass *Dicentrarchus labrax* to different stocking densities and acute stress challenge. *Aquaculture* 275, 319–328. doi: 10.1016/j.aquaculture.2007.12.012

Djordjevic, B., Morales-Lange, B., Press, C. M., Olson, J., Lagos, L., Mercado, L., et al. (2021). Comparison of circulating markers and mucosal immune parameters from skin and distal intestine of Atlantic salmon in two models of acute stress. *Int. J. Mol. Sci.* 22, 1–13. doi: 10.3390/ijms22031028

d'Orbcastel, E. R., Lemarié, G., Breuil, G., Petochi, T., Marino, G., Triplet, G., et al. (2010). Effects of rearing density on sea bass (*Dicentrarchus labrax*) biological performance, blood parameters and disease resistance in a flow through system. *Aquat. Liv. Resourc.* 23, 109–117. doi: 10.1051/alr/2009056

Eissa, N., and Wang, H.-P. (2016). Transcriptional stress responses to environmental and husbandry stressors in aquaculture species. *Rev. Aquac.* 8, 61–88. doi: 10.1111/raq.12081

El Aamri, F., Real, F., Acosta, F., Bravo, J., Román, L., Déniz, S., et al. (2015). Differential innate immune response of European seabass (*Dicentrarchus labrax*) against *Streptococcus iniae*. *Fish Shellf. Immunol.* 46, 436–441. doi: 10.1016/j.fsi.2015.05.054

Ellis, T., Yildiz, H. Y., López-Olmeda, J., Spedicato, M. T., Tort, L., Øverli, Ø, et al. (2012). Cortisol and finfish welfare. *Fish Physiol. Biochem.* 38, 163–188. doi: 10.1007/s10695-011-9568-y

Fanouraki, E., Divanach, P., and Pavlidis, M. (2007). Baseline values for acute and chronic stress indicators in sexually immature red porgy (*Pagrus pagrus*). *Aquaculture* 265, 294–304. doi: 10.1016/j.aquaculture.2007.01.006

Fanouraki, E., Mylonas, C. C., Papandroulakis, N., and Pavlidis, M. (2011). Species specificity in the magnitude and duration of the acute stress response in Mediterranean marine fish in culture. *Gen. Compar. Endocrinol.* 173, 313–322. doi: 10.1016/j.ygcen.2011.06.004

Geay, F., Ferraresso, S., Zambonino-Infante, J. L., Bargelloni, L., Quentel, C., Vandeputte, M., et al. (2011). Effects of the total replacement of fish-based diet with plant-based diet on the hepatic transcriptome of two European sea bass (*Dicentrarchus labrax*) half-sibfamilies showing different growth rates with the plant-based diet. *BMC Genomics* 12:522. doi: 10.1186/1471-2164-12-522

Gisbert, E., Fournier, V., Solovyev, M., Skalli, A., and Andree, K. B. (2018). Diets containing shrimp protein hydrolysates provided protection to European sea bass (*Dicentrarchus labrax*) affected by a Vibrio pelagius natural infection outbreak. *Aquaculture* 495, 136–143. doi: 10.1016/j.aquaculture.2018.04.051

Gornati, R., Papis, E., Rimoldi, S., Terova, G., Saroglia, M., and Bernardini, G. (2004). Rearing density influences the expression of stress-related genes in sea bass (*Dicentrarchus labrax*, L.). *Gene* 341, 111–118. doi: 10.1016/j.gene.2004.06.020

Guardiola, F. A., Cuesta, A., Abellán, E., Meseguer, J., and Esteban, M. A. (2014a). Comparative analysis of the humoral immunity of skin mucus from several marine teleost fish. *Fish Shellf. Immunol.* 40, 24–31. doi: 10.1016/j.fsi.2014.06.018

Guardiola, F. A., Cuesta, A., and Esteban, M. A. (2016). Using skin mucus to evaluate stress in gilthead seabream (*Sparus aurata* L.). *Fish Shellf. Immunol.* 59, 323–330. doi: 10.1016/j.fsi.2016.11.005

Guardiola, F. A., Cuesta, A., Arizcun, M., Meseguer, J., and Esteban, M. A. (2014b). Comparative skin mucus and serum humoral defence mechanisms in the teleost gilthead seabream (*Sparus aurata*). *Fish Shellf. Immunol.* 36, 545–551. doi: 10.1016/j.fsi.2014.01.001

Guardiola, F. A., Saraiva-Fraga, M., Cuesta, A., and Esteban, M. A. (2018). Changes in natural haemolytic complement activity induced by stress in gilthead seabream (*Sparus aurata L.*). *Fish Shellf. Immunol.* 78, 317–321. doi: 10.1016/j.fsi.2018.04.056

Guo, H., and Dixon, B. (2021). Understanding acute stress-mediated immunity in teleost fish. *Fish Shellf. Immunol. Rep.* 2:100010. doi: 10.1016/j.fsirep.2021.100010

Hall, T. (1999). BioEdit: a user-friendly biological sequence alignment editor and analysis program for Windows 95/98/NT. *Nucleic Acids Symp. Ser.* 41, 95–98.

Hanif, A., Bakopoulos, V., and Dimitriadis, G. J. (2004). Maternal transfer of humoral specific and non-specific immune parameters to sea bream (*Sparus aurata*) larvae. *Fish Shellf. Immunol.* 17, 411–435. doi: 10.1016/j.fsi.2004.04.013

Hardy, R. W. (2010). Utilization of plant proteins in fish diets: effects of global demand and supplies of fishmeal. *Aquac. Res.* 41, 770–776. doi: 10.1111/j.1365-2109.2009.02349.x

Henry, M. A., Fountoulaki, E., Vasilaki, A., Rigos, G., Kokou, F., and Karalazos, V. (2020). Dietary micronutrient supplementation in low fishmeal based diets for optimum growth and immune status of European sea bass (*Dicentrarchus labrax*) juveniles. *Aquaculture* 528:735479. doi: 10.1016/j.aquaculture.2020.735479

Hoseinifar, S. H., Sharifian, M., Vesaghi, M. J., Khalili, M., and Esteban, M. A. (2014). The effects of dietary xylooligosaccharide on mucosal parameters, intestinal microbiota and morphology and growth performance of Caspian white fish (*Rutilus frisii kutum*) fry. *Fish Shellf. Immunol.* 39, 231–236. doi: 10.1016/j.fsi.2014.05.009

Hrubec, T. C., and Smith, S. S. (2010). "Hematology of fishes," in *Schalm's Veterinary Hematology*, 6th Edn, eds D. Weiss, K. Wardrop, and O. Schalm (Hoboken, NJ: Wiley-Blackwell), 994–1003.

Islam, M. J., Kunzmann, A., and Slater, M. J. (2021). Extreme winter cold-induced osmoregulatory, metabolic, and physiological responses in European seabass (*Dicentrarchus labrax*) acclimatized at different salinities. *Sci. Total Environ.* 771:145202. doi: 10.1016/j.scitotenv.2021.145202

Jia, R., Liu, B.-L., Han, C., Huang, B., and Lei, J.-L. (2016). Influence of stocking density on growth performance, antioxidant status, and physiological response of juvenile turbot, *Scophthalmus maximus*, reared in land-based recirculating aquaculture system. *J. World Aquac. Soc.* 47, 587–599. doi: 10.1111/jwas.12295

Jung, T. S., Del Castillo, C. S., Javaregowda, P. K., Dalvi, R. S., Nho, S. W., Park, S. B., et al. (2012). Seasonal variation and comparative analysis of non-specific humoral immune substances in the skin mucus of olive flounder (*Paralichthys olivaceus*). *Dev. Compar. Immunol.* 38, 295–301. doi: 10.1016/j.dci.2012.06.005

Kaushik, S. J., Covès, D., Dutto, G., and Blanc, D. (2004). Almost total replacement of fish meal by plant protein sources in the diet of a marine teleost, the European seabass, *Dicentrarchus labrax*. *Aquaculture* 230, 391–404. doi: 10.1016/S0044-8486(03)00422-8

Kwasek, K., Thorne-Lyman, A. L., and Phillips, M. (2020). Can human nutrition be improved through better fish feeding practices? A review paper. *Crit. Rev. Food Sci. Nutr.* 60, 3822–3835. doi: 10.1080/10408398.2019.1708698

Lall, S. P. (2002). "The minerals," in *Fish Nutrition*, 3rd Edn, eds J. E. Halver and R. W. Hardy (Cambridge, MA: Academic Press), 824.

Machado, M., Castro, C., Oliva-Teles, A., and Costas, B. (2019). Interactive effects of dietary vegetable oil and carbohydrate incorporation on the innate immune response of European seabass (*Dicentrarchus labrax*) juveniles subjected to acute stress. *Aquaculture* 498, 171–180. doi: 10.1016/j.aquaculture.2018.08.050

Maricchiolo, G., Mirto, S., Caruso, G., Caruso, T., Bonaventura, R., Celi, M., et al. (2011). Welfare status of cage farmed European sea bass (*Dicentrarchus labrax*): a comparison between submerged and surface cages. *Aquaculture* 314, 173–181. doi: 10.1016/j.aquaculture.2011.02.001

Masek, T., Vopalensky, V., Suchomelova, P., and Pospisek, M. (2005). Denaturing RNA electrophoresis in TAE agarose gels. *Anal. Biochem.* 336, 46–50. doi: 10.1016/j.ab.2004.09.010

Médale, F., and Kaushik, S. (2009). Les sources protéiques dans les aliments pour les poissons d'élevage. *Cah. Agric.* 18, 103–111. doi: 10.1684/agr.2009.0279

Meloni, M., Candusso, S., Galeotti, M., and Volpatti, D. (2015). Preliminary study on expression of antimicrobial peptides in European sea bass (*Dicentrarchus labrax*) following in vivo infection with *Vibrio anguillarum*. A time course experiment. *Fish Shellf. Immunol.* 43, 82–90. doi: 10.1016/j.fsi.2014.12.016

Mommsen, T. P., Vijayan, M. M., and Moon, T. W. (1999). Cortisol in teleosts: dynamics, mechanisms of action, and metabolic regulation. *Rev. Fish Biol. Fish.* 9, 211–268. doi: 10.1023/a:1008924418720

Montero, D., and Izquierdo, M. (2010). "Welfare and health of fish fed vegetable oils as alternative lipid sources to fish oil," in *Fish Oil Replacement and Alternative Lipid Sources in Aquaculture Feeds*, eds G. M. Turchini, W.-K. Ng, and D. R. Tocher (Boca Raton, FL: CRC Press), 439–485.

Montero, D., Izquierdo, M. S., Tort, L., Robaina, L., and Vergara, J. M. (1999). High stocking density produces crowding stress altering some physiological and biochemical parameters in gilthead seabream, *Sparus aurata*, juveniles. *Fish Physiol. Biochem.* 20, 53–60. doi: 10.1023/a:1007719928905

Montero, D., Kalinowski, T., Obach, A., Robaina, L., Tort, L., Caballero, M. J., et al. (2003). Vegetable lipid sources for gilthead seabream (*Sparus aurata*): effects on fish health. *Aquaculture* 225, 353–370. doi: 10.1016/S0044-8486(03)00301-6

Mosca, F., Ciulli, S., Volpatti, D., Romano, N., Volpe, E., Bulfon, C., et al. (2014). Defensive response of European sea bass (*Dicentrarchus labrax*) against *Listonella anguillarum* or Photobacterium damselae subsp. piscicida experimental infection. *Vet. Immunol. Immunopathol.* 162, 83–95. doi: 10.1016/j.vetimm.2014.10.002

Nasopoulou, C., and Zabetakis, I. (2012). Benefits of fish oil replacement by plant originated oils in compounded fish feeds. A review. *LWT* 47, 217–224. doi: 10.1016/j.lwt.2012.01.018

Parma, L., Pelusio, N. F., Gisbert, E., Esteban, M. A., D'Amico, F., Soverini, M., et al. (2020). Effects of rearing density on growth, digestive conditions, welfare indicators and gut bacterial community of gilthead sea bream (*Sparus aurata, L.* 1758) fed different fishmeal and fish oil dietary levels. *Aquaculture* 518:734854. doi: 10.1016/j.aquaculture.2019.734854

Parma, L., Yúfera, M., Navarro-Guillén, C., Moyano, F. J., Soverini, M., D'Amico, F., et al. (2019). Effects of calcium carbonate inclusion in low fishmeal diets on growth, gastrointestinal pH, digestive enzyme activity and gut

bacterial community of European sea bass (*Dicentrarchus labrax* L.) juveniles. *Aquaculture* 510, 283–292. doi: 10.1016/j.aquaculture.2019.05.064

Parry, R. M., Chandan, R. C., and Shahani, K. M. (1965). A Rapid and sensitive assay of muramidase. *Exp. Biol. Med.* 119, 384–386. doi: 10.3181/00379727-119-30188

Pavlidis, M., Karantzali, E., Fanouraki, E., Barsakis, C., Kollias, S., and Papandroulakis, N. (2011). Onset of the primary stress in European sea bass *Dicentrarhus labrax*, as indicated by whole body cortisol in relation to glucocorticoid receptor during early development. *Aquaculture* 315, 125–130. doi: 10.1016/j.aquaculture.2010.09.013

Pelusio, N. F., Scicchitano, D., Parma, L., Dondi, F., Brini, E., D'Amico, F., et al. (2021). Interaction between dietary lipid level and seasonal temperature changes in gilthead sea bream *Sparus aurata*: effects on growth, fat deposition, plasma biochemistry, digestive enzyme activity, and gut bacterial community. *Front. Mar. Sci.* 8:664701. doi: 10.3389/fmars.2021.664701

Peres, H., Santos, S., and Oliva-Teles, A. (2013). Selected plasma biochemistry parameters in gilthead seabream (*Sparus aurata*) juveniles. *J. Appl. Ichthyol.* 29, 630–636. doi: 10.1111/j.1439-0426.2012.02049.x

Peres, H., Santos, S., and Oliva-Teles, A. (2014). Blood chemistry profile as indicator of nutritional status in European seabass (*Dicentrarchus labrax*). *Fish Physiol. Biochem.* 40, 1339–1347. doi: 10.1007/s10695-014-9928-5

Pérez-Jiménez, A., Guedes, M. J., Morales, A. E., and Oliva-Teles, A. (2007). Metabolic responses to short starvation and refeeding in *Dicentrarchus labrax*. Effect of dietary composition. *Aquaculture* 265, 325–335. doi: 10.1016/j.aquaculture.2007.01.021

Pfaffl, M. W. (2004). "Quantification strategies in real-time PCR," in *AZ of Quantitative PCR*, ed. S. A. Bustin (La Jolla, CA: International University Line), 89–113.

Poltronieri, C., Maccatrozzo, L., Simontacchi, C., Bertotto, D., Funkenstein, B., Patruno, M., et al. (2007). Quantitative RT-PCR analysis and immunohistochemical localization of HSP70 in sea bass *Dicentrarchus labrax* exposed to transport stress. *Eur. J. Histochem.* 51, 125–136. doi: 10.4081/1134

Quade, M. J., and Roth, J. A. (1997). A rapid, direct assay to measure degranulation of bovine neutrophil primary granules. *Vet. Immunol. Immunopathol.* 58, 239–248. doi: 10.1016/s0165-2427(97)00048-2

Reverter, M., Tapissier-Bontemps, N., Sarter, S., Sasal, P., and Caruso, D. (2021). Moving towards more sustainable aquaculture practices: a meta-analysis on the potential of plant-enriched diets to improve fish growth, immunity and disease resistance. *Rev. Aquac.e* 13, 537–555. doi: 10.1111/raq.12485

Reyes-López, F. E., Aerts, J., Vallejos-Vidal, E., Ampe, B., Dierckens, K., Tort, L., et al. (2018). Modulation of innate immune-related genes and glucocorticoid synthesis in gnotobiotic full-sibling European sea bass (*Dicentrarchus labrax*) larvae challenged with *Vibrio anguillarum*. *Front. Immunol.* 9:914. doi: 10.3389/fimmu.2018.00914

Roosta, Z., and Hoseinifar, S. H. (2016). The effects of crowding stress on some epidermal mucus immune parameters, growth performance and survival rate of tiger barb (*Pentius tetrazona*). *Aquac. Res.* 47, 1682–1686. doi: 10.1111/are.12616

Roque, A., Yildiz, H. Y., Carazo, I., and Duncan, N. (2010). Physiological stress responses of sea bass (*Dicentrarchus labrax*) to hydrogen peroxide (H2O2) exposure. *Aquaculture* 304, 104–107. doi: 10.1016/j.aquaculture.2010.03.024

Ross, N. W., Firth, K. J., Wang, A., Burka, J. F., and Johnson, S. C. (2000). Changes in hydrolytic enzyme activities of naïve Atlantic salmon Salmo salar skin mucus due to infection with the salmon louse *Lepeophtheirus salmonis* and cortisol implantation. *Dis. Aquat. Org.* 41, 43–51. doi: 10.3354/dao041043

Ruane, N. M., Huisman, E. A., and Komen, J. (2002). The influence of feeding history on the acute stress response of common carp (*Cyprinus carpio*). *Aquaculture* 210, 245–257. doi: 10.1016/S0044-8486(01)00819-5

Saccol, E. M. H., Parrado-Sanabria, Y. A., Gagliardi, L., Jerez-Cepa, I., Mourão, R. H. V., Heinzmann, B. M., et al. (2018). Myrcia sylvatica essential oil in the diet of gilthead sea bream (*Sparus aurata L.*) attenuates the stress response induced by high stocking density. *Aquac. Nutr.* 24, 1381–1392. doi: 10.1111/anu.12675

Sales, J., and Glencross, B. (2011). A meta-analysis of the effects of dietary marine oil replacement with vegetable oils on growth, feed conversion and muscle fatty acid composition of fish species. *Aquac. Nutr.* 17, e271–e287. doi: 10.1111/j.1365-2095.2010.00761.x

Samaras, A., Pavlidis, M., Lika, K., Theodoridi, A., and Papandroulakis, N. (2017). Scale matters: performance of European sea bass, *Dicentrarchus labrax*, L. (1758), reared in cages of different volumes. *Aquac. Res.* 48, 990–1005. doi: 10.1111/are.12942

Samaras, A., Santo, C. E., Papandroulakis, N., Mitrizakis, N., Pavlidis, M., Höglund, E., et al. (2018). Allostatic load and stress physiology in European seabass (*Dicentrarchus labrax* L .) and gilthead seabream (*Sparus aurata* L .). *Front. Endocrinol.* 9:451. doi: 10.3389/fendo.2018.00451

Sanahuja, I., Fernández-Alacid, L., Ordóñez-Grande, B., Sánchez-Nuño, S., Ramos, A., Araujo, R. M., et al. (2019). Comparison of several non-specific skin mucus immune defences in three piscine species of aquaculture interest. *Fish Shellf. Immunol.* 89, 428–436. doi: 10.1016/j.fsi.2019.04.008

Serradell, A., Torrecillas, S., Makol, A., Valdenegro, V., Fernández-Montero, A., Acosta, F., et al. (2020). Prebiotics and phytogenics functional additives in low fish meal and fish oil based diets for European sea bass (*Dicentrarchus labrax*): effects on stress and immune responses. *Fish Shellf. Immunol.* 100, 219–229. doi: 10.1016/j.fsi.2020.03.016

Sheikhzadeh, N., Heidarieh, M., Karimi Pashaki, A., Nofouzi, K., Ahrab Farshbafi, M., and Akbari, M. (2012a). Hilyses®, fermented *Saccharomyces cerevisiae*, enhances the growth performance and skin non-specific immune parameters in rainbow trout (*Oncorhynchus mykiss*). *Fish Shellf. Immunol.* 32, 1083–1087. doi: 10.1016/j.fsi.2012.03.003

Sheikhzadeh, N., Karimi Pashaki, A., Nofouzi, K., Heidarieh, M., and Tayefi-Nasrabadi, H. (2012b). Effects of dietary Ergosan on cutaneous mucosal immune response in rainbow trout (*Oncorhynchus mykiss*). *Fish Shellf. Immunol.* 32, 407–410. doi: 10.1016/j.fsi.2011.11.028

Sinuani, I., Beberashvili, I., Averbukh, Z., and Sandbank, J. (2013). Role of IL-10 in the progression of kidney disease. *World J. Transplant.* 3, 91–98. doi: 10.5500/wjt.v3.i4.91

Sitjà-Bobadilla, A., Peña-Llopis, S., Gómez-Requeni, P., Médale, F., Kaushik, S., and Pérez-Sánchez, J. (2005). Effect of fish meal replacement by plant protein sources on non-specific defence mechanisms and oxidative stress in gilthead sea bream (*Sparus aurata*). *Aquaculture* 249, 387–400. doi: 10.1016/j.aquaculture.2005.03.031

Stevens, M. G., Kehrli, M. E., and Canning, P. C. (1991). A colorimetric assay for quantitating bovine neutrophil bactericidal activity. *Vet. Immunol. Immunopathol.* 28, 45–56. doi: 10.1016/0165-2427(91)90042-b

Sutili, F. J., Gatlin, D. M., Heinzmann, B. M., and Baldisserotto, B. (2018). Plant essential oils as fish diet additives: benefits on fish health and stability in feed. *Rev. Aquac.* 10, 716–726. doi: 10.1111/raq.12197

Torrecillas, S., Betancor, M. B., Caballero, M. J., Rivero, F., Robaina, L., Izquierdo, M., et al. (2018). Supplementation of arachidonic acid rich oil in European sea bass juveniles (Dicentrarchus labrax) diets: effects on growth performance, tissue fatty acid profile and lipid metabolism. *Fish Physiol. Biochem.* 44, 283–300. doi: 10.1007/s10695-017-0433-5

Torrecillas, S., Mompel, D., Caballero, M. J., Montero, D., Merrifield, D., Rodiles, A., et al. (2017a). Effect of fishmeal and fish oil replacement by vegetable meals and oils on gut health of European sea bass (*Dicentrarchus labrax*). *Aquaculture* 468, 386–398. doi: 10.1016/j.aquaculture.2016.11.005

Torrecillas, S., Montero, D., Domínguez, D., Robaina, L., and Izquierdo, M. (2019). Skin mucus fatty acid composition of gilthead sea bream (*Sparus aurata*): a descriptive study in fish fed low and high fish meal diets. *Fishes* 4:15. doi: 10.3390/fishes4010015

Torrecillas, S., Robaina, L., Caballero, M. J., Montero, D., Calandra, G., Mompel, D., et al. (2017b). Combined replacement of fishmeal and fish oil in European sea bass (*Dicentrarchus labrax*): production performance, tissue composition and liver morphology. *Aquaculture* 474, 101–112. doi: 10.1016/j.aquaculture.2017.03.031

Tort, L., and Teles, M. (2012). Genomic responses to stress challenges in fish. *Funct. Genom. Aquac.* 7, 147–168. doi: 10.1002/9781118350041.ch7

Tsalafouta, A., Papandroulakis, N., and Pavlidis, M. (2015). Early life stress and effects at subsequent stages of development in European sea bass (*D. labrax*). *Aquaculture* 436, 27–33. doi: 10.1016/j.aquaculture.2014.10.042

Valero, Y., Arizcun, M., Cortés, J., Ramírez-Cepeda, F., Guzmán, F., Mercado, L., et al. (2020). NK-lysin, dicentracin and hepcidin antimicrobial peptides in European sea bass. Ontogenetic development and modulation in juveniles by nodavirus. *Dev. Compar. Immunol.* 103:103516. doi: 10.1016/j.dci.2019.103516

Valero, Y., García-Alcázar, A., Esteban, M. A., Cuesta, A., and Chaves-Pozo, E. (2015). Antimicrobial response is increased in the testis of European sea bass,

but not in gilthead seabream, upon nodavirus infection. *Fish Shellf. Immunol.* 44, 203–213. doi: 10.1016/j.fsi.2015.02.015

Van Anholt, R. D., Spanings, F. A. T., Koven, W. M., Nixon, O., and Wendelaar Bonga, S. E. (2004). Arachidonic acid reduces the stress response of gilthead seabream *Sparus aurata L. J. Exp. Biol.* 207, 3419–3430. doi: 10.1242/jeb.01166

Volpatti, D., Bulfon, C., Tulli, F., and Galeotti, M. (2013). Growth parameters, innate immune response and resistance to *Listonella* (Vibrio) anguillarum of *Dicentrarchus labrax* fed carvacrol supplemented diets. *Aquac. Res.* 45, 31–44. doi: 10.1111/j.1365-2109.2012.03202.x

**Conflict of Interest:** The authors declare that the research was conducted in the absence of any commercial or financial relationships that could be construed as a potential conflict of interest.

**Publisher's Note:** All claims expressed in this article are solely those of the authors and do not necessarily represent those of their affiliated organizations, or those of the publisher, the editors and the reviewers. Any product that may be evaluated in this article, or claim that may be made by its manufacturer, is not guaranteed or endorsed by the publisher.

frontiers in Physiology

ORIGINAL RESEARCH
published: 27 January 2022
doi: 10.3389/fphys.2021.771951

# Assessing Stress Resilience After Smolt Transportation by Waterborne Cortisol and Feeding Behavior in a Commercial Atlantic Salmon (*Salmo salar*) Grow-Out Recirculating Aquaculture System

*Erik Höglund[1,2]*, Paulo Fernandes[1], Paula Rojas-Tirado[1], Jan Thomas Rundberget[1] and Ole-Kristian Hess-Erga[1]*

*[1] Norwegian Institute for Water Research (NIVA), Oslo, Norway, [2] Center of Coastal Research, University of Agder, Kristiansand, Norway*

OPEN ACCESS

**Edited by:**
*Marce Herrera,*
*IFAPA Centro Agua del Pino, Spain*

**Reviewed by:**
*Sunil Kadri,*
*Universidad Austral de Chile, Chile*
*Patrick Prunet,*
*Institut National de Recherche pour l'Agriculture, l'Alimentation et l'Environnement (INRAE), France*

***Correspondence:**
*Erik Höglund*
*Erik.hoglund@niva.no*

**Specialty section:**
*This article was submitted to Aquatic Physiology, a section of the journal Frontiers in Physiology*

**Received:** *07 September 2021*
**Accepted:** *09 December 2021*
**Published:** *27 January 2022*

**Citation:**
*Höglund E, Fernandes P, Rojas-Tirado P, Rundberget JT and Hess-Erga O-K (2022) Assessing Stress Resilience After Smolt Transportation by Waterborne Cortisol and Feeding Behavior in a Commercial Atlantic Salmon (Salmo salar) Grow-Out Recirculating Aquaculture System. Front. Physiol. 12:771951. doi: 10.3389/fphys.2021.771951*

Sampling protocols and water quality sensors have been developed to assess fish health and welfare in recirculating aquaculture systems (RASs). Still, the use of fish-based non-invasive welfare indicators, reflecting the physiological state of the fish, is limited in this type of system. Cortisol, the major stress-coping hormone in fish, diffuses through the gills. Consequently, waterborne cortisol is a potential fish-based non-invasive welfare indicator in RAS. However, its use in commercial rearing systems is sparse. In this study, we evaluated water cortisol levels and feeding behavior as welfare indicators of newly inserted smolt in a commercial RAS for harvest size Atlantic salmon. The RAS consisted of two parallel fish rearing raceways, raceways 1 and 2, sharing the same water treatment with common outlets and inlets. The smolts were inserted in raceway 1 while salmon that have been in the system for 6 months or more were kept in raceway 2. The smolt insertion period was 3 days. Samples for water cortisol levels were withdrawn the day before, 1 and 3 days after the smolt insertion period. Smolt insertion resulted in elevated water cortisol concentrations in the entire system, with the highest values in raceway 1, one day after smolt insertion. Estimated cortisol production in newly inserted smolt decreased over time, was similar to what has been reported in salmon adapting to experimental tanks. Feeding behavior indicated that the appetite was not fully resumed in the newly inserted smolts, while the appetite of fish in raceway 2 was unaffected by smolt insertion. These results, obtained in a highly intensive commercial RAS, suggest that waterborne cortisol together with feeding behavior can be used as indicators for adaptive processes associated with stress resilience in farmed fish. Thus, they are promising non-invasive indicators for assessing the impact of potential stressors on fish welfare in this type of rearing system.

**Keywords: waterborne cortisol, fish welfare, behavior, close containment rearing, welfare indicators**

## INTRODUCTION

Generally, recirculating aquaculture systems (RASs) minimize the environmental impact and provide a venue to balance aquaculture growth and environmental/ethical considerations (Martins et al., 2010). However, fish health and welfare issues related to water quality and rearing densities in this type of rearing system have been raised (van de Vis et al., 2020). Accordingly, water quality sampling protocols and sensor technologies have been developed to ensure cost-effective production (Su et al., 2020), supported by maintaining good rearing conditions in terms of water quality and fish health and welfare. In addition to water quality-based health and welfare indicators, techniques for monitoring the physiological state of the fish provide important information needed to safeguard the health and welfare of farmed fish (Baretto et al., 2022). Currently, fish-based non-invasive welfare indicators are often based on behavioral and respiratory changes, and the use of other measures is limited (Baretto et al., 2022).

There are several studies showing that hormone levels in the water reflect the physiological status of fish (Ellis et al., 2004; Scott and Ellis, 2007). Since steroids are quite stable in water and play a central role in stress coping and health of fish, many of the studies on water-borne hormones focus on these types of hormones or their metabolites in the rearing water (reviewed by Scott and Ellis, 2007). Generally, waterborne steroids and their metabolites are directly related to steroid clearance in fish, which in-turn depend on steroid lipophilicity; free steroids (lipid-soluble) diffuse into the water across the gills whereas sulfate and glucuronide steroids (lipid-insoluble steroids) are excreted more slowly through the kidneys (Vermeirssen and Scott, 1996; Ellis et al., 2005). Accordingly, several studies show a strong relationship between blood plasma levels of cortisol, the main stress-coping hormone in fish, and the release of free cortisol to the rearing water [for references see review by Scott and Ellis (2007)]. Following this, waterborne cortisol has been used as a noninvasive indicator of stress in laboratory studies (Scott and Ellis, 2007; Félix et al., 2013) and experimental aquaculture facilities (Mota et al., 2017a,b). Still, its use as a non-invasive fish-based welfare indicator in commercial RAS is limited.

In addition to reflecting the physiological status of the fish, steroids, and their metabolites can induce behavioral and physiological changes in fish by acting as pheromones. Indeed, water-borne steroids and their metabolites are detected with great sensitivity and specificity by the olfactory organs of fish and exert important effects on behavior and physiology in major taxa, such as carps (goldfish), catfishes, salmon, and gobies (Chung-Davidson et al., 2010; Good and Davidson, 2016). Considering that cortisol and other steroids have been shown to accumulate in RAS, concerns about the impact of these water-borne hormones on farmed fish have been raised (Mota et al., 2014, 2017b; Good and Davidson, 2016).

In RAS production of slaughter size salmon, smolts are transferred from an external or internal smolt production site. Such transfer/transport consists of several traumatic perturbations, including capture, loading, transport, unloading, and re-stocking. Thus, transfer/transport can initiate a severe stress response in farmed fish (Barton and Iwama, 1991), including release of the stress hormone cortisol (Iversen et al., 1998, 2005). Generally, this hormone redistributes energy from maintenance functions, including growth and immune reactions, towards processes needed for coping with perturbations (Sapolsky et al., 2000). In accordance with this, mortality during the sea phase of the Atlantic salmon production cycle have been associated with transportation stress during the smolt stage (Iversen et al., 2005). However, information on the impact of smolt transport on stress coping and resilience in the sea phase of the production cycle is sparse. However, information on the impact of smolt transport on stress coping and resilience in the sea phase of the rearing cycle is sparse.

In RAS, the dynamics of waterborne cortisol offers a potential indicator of how smolt transportation affects stress resilience in the seawater phase of salmon rearing. Thus, in this study, we evaluated if water-borne cortisol could be used as an indicator for stress resilience in newly inserted smolt in commercial RAS. In addition, potential physiological, and behavioral effects of being exposed to water from newly inserted smolt were investigated. This was done by measuring water cortisol concentrations before and after smolt insertion at a commercial grow-out salmon RAS. In this system, smolts were inserted in one of the two circular parallel raceways with shared water treatment. Cortisol production rate before and after smolt insertion in the two raceways was estimated. In addition, the potential effects of smolt insertion on feeding behavior were quantified.

## MATERIALS AND METHODS

### Study Site

The study was performed in one of the two separate RAS modules at Fredrikstad Seafoods (Nordic Aquafarms, Fredriksstad, Norway). The total annual production capacity of these two modules was 1,500 metric tons of 3.5–6 kg Atlantic salmon. Each RAS module has a total water volume of 7,300 $m^3$ each, with two circular raceways (1 and 2) for holding fish, **Figure 1**. Raceway 1 was 4.5 m x 4.7 m x 75 m (width x depth x length) with a total volume of 1,700 $m^3$ and a fish production volume of 1,400 $m^3$. Raceway 2 was 6.5 m x 4.7 m x 115 m (width x depth x length) with a total water volume of 3,300 $m^3$ and a fish production volume of 3,200 $m^3$. The two raceways shared the same water treatment with common water in- and out-lets. There was no other mixing of water between the raceways. In addition to the raceways, each RAS module consisted of 6 drum filters of different mesh sizes (ranging from 20 to 50 μm), a moving bed biofilter reactor with 5 chambers, and a degassing unit (**Figure 1**). The water entered raceways 1 and 2 (point 11, **Figure 1**) from the water treatment, where it was circulated at speed of 2 and 4 $ms^{-1}$, respectively. The hydraulic retention time (HRT) was 40 min in each raceway. From the outlet of raceways 1 and 2, the water entered the water treatment by flowing into the drum filters (point 13, **Figure 1**). Thereafter the permeate water was split and flowed either directly into the biofilters (90% of flow) or the biofilter *via* a UV contact

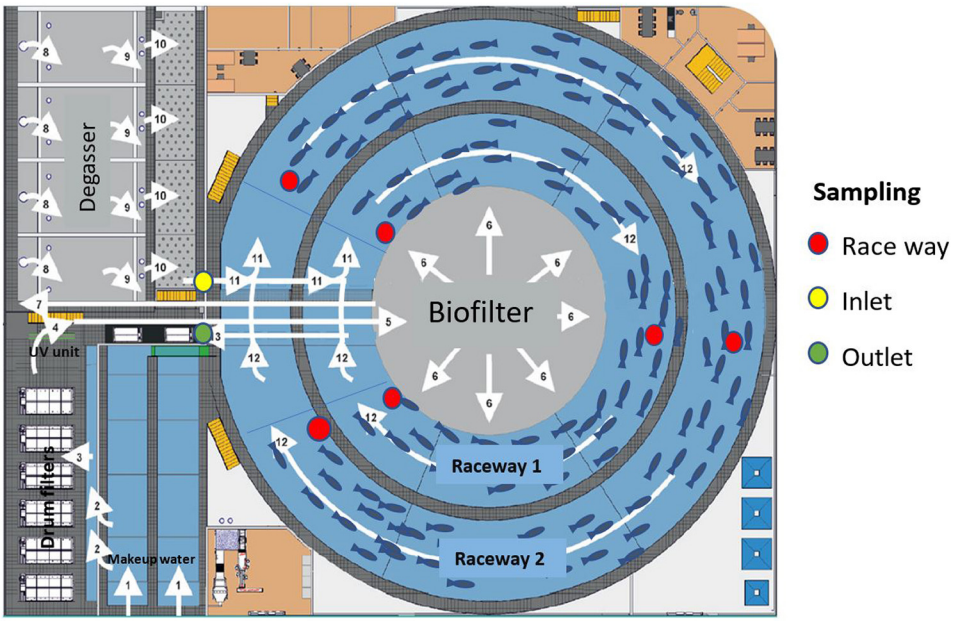


**FIGURE 1 |** Illustration of a RAS module at Fredrikstad Seafood – water flow through the water treatment loop (white arrows show the direction of flow). The system is comprised of circular raceways for holding fish with a volume of 7,300 $m^3$, six drum filters of different mesh sizes (ranging from 20 to 50 μm), a biofilter with five chambers, and a degassing unit. New water (1–2) enters the systems and goes (3) through six drum filters of different mesh sizes (20–50 μm). The permeate from the drum filters is split (10%) into a UV contact chamber (4) and (90%) in a 5-chamber biofilter (5–6). The water is re-mixed (7) at the entrance to a degassing unit (8–10). After the degasser, the water then enters a 7,300 $m^3$ fish tank (11) and is split between an inner and outer raceway ring. The water exits in the fish tanks (12) and re-enters the water treatment loop *via* the drum filters (13). RAS, recirculating aquaculture systems.

chamber (10% of flow). After the biofilter, the water entered the degasser, and then it was pumped back into the raceways. The HRT in the water treatment loop was 22 min. The inflow of new water in the system (make-up water) was 30 $m^3\ h^{-1}$. Fish were kept in continuous artificial light and continuously fed with Bio Mar orbit X feed. The feeding ratio was 0.5% biomass $day^{-1}$ in raceway 1 with newly inserted smolt. Raceway 2 was divided into two compartments up and down streams each other. Fish were fed 1% biomass $day^{-1}$ in one of the compartments. In the other compartment, fish were starved due to slaughter pretreatment. Moreover, in raceway 2, the average weight and number of fish in the compartment containing fed fish that were fed was 4.3 kg and 30,300 fish. The average weight and number of fish in the compartment where fish were pretreated for slaughter were 6.3 kg and 9,500–8,200 fish. The estimated rearing density was about 65 kg $m^{-3}$ in both of these compartments.

## Smolt Insertion and Water Sampling

Smolt insertion was done in raceway 1 during the period of 27–29 of April. Before smolt insertion, the smolts were transported on a truck for approximately 3.5 h. Ten truckloads were inserted over 3 days between 10:00 and 22:00 each day. The smolts had an average weight of 180 g at arrival and were inserted in 850 $m^3$ compartment of raceway 1, resulting in a rearing density of 33 kg $m^{-3}$ at the end of the smolt insertion. The reminding of this raceway was kept empty during the period of the study.

Triplicate 0.5 L water grab samples were withdrawn at the inlet and outlet of the raceways. In addition, grab samples collected in the water were sampled in the start, middle, and end sections of the raceways (**Figure 1**). Water was sampled between 07:00 and 07:30 at depth of 2 m, before the daily husbandry routines started, the day before (April 26), the day after (April 30), and 3 days after (May 2) smolt insertion. The water samples were frozen and kept at $-20^oC$ before being analyzed.

## Water Cortisol Analysis

Analysis of cortisol followed a method described by McWhinney et al. (2010) with some modifications. Water samples were spiked with 10 ng internal standard (cortisol d4) to correct for matrix effects and for losses in sample extraction, concentration, and analysis. Samples were loaded onto activated Oasis HLB 6 cc (200 mg) solid-phase extraction cartridges (Waters, Milford, MA, United States). After loading 200–300 mL of the samples, the columns were washed with 3 ml milliQ water followed by 3 ml of 20% methanol. Samples were eluted with 5 ml 100% ethyl acetate, dried at 50°C, and reconstituted in 200 μL of 40% methanol with 5 mmol/L ammonium formate and 0.1% formic acid. Separation was achieved on a BEH C8 column (Waters, Milford, MA, United States) using a solvent gradient consisting of 5 mmol/L ammonium formate and 0.1% formic acid in water and methanol. Cortisol content was analyzed with a tandem mass spectrometer (Waters TQ-S, Milford, MA, United States) operated in negative electron spray ionization mode with the following MRM acquisition parameters (precursor

and product ions); 407.1 > 331.05, 407.1 > 331.1 for cortisol and 411.1 > 335.05, 411.1 > 335.1 for cortisol d4 (IS).

Quantification was done using response factors (Cortisol/Cis) calculated by a 6-point calibration curve from 0.05 to 10 ng/ml. Samples were analyzed in groups with at least one standard addition sample and a blank seawater control. Recovery of spiked cortisol was typically 95–105%. The limit of detection (LOD) of 0.1 ng/L cortisol was estimated as three times the signal to noise (S/N) using spiked control samples.

## Cortisol Production Rate, Clearance Rate, Release Rate, and Clearance Efficacy

For estimation of cortisol clearance rate (CCR; mg cortisol $h^{-1}$) and cortisol release rate (CRR; ng cortisol g fish $biomass^{-1}$ $h^{-1}$), a quasi-steady-state in cortisol was assumed (Good et al., 2014).

Cortisol clearance rate was estimated by multiplying the difference between mean cortisol concentration at the inlet to water treatment [$\bar{x}$ ($cortisol_{water\ treatment}$); green in **Figure 1**] and the cortisol concentration in the three samples withdrawn at the inlet to the raceway [(cortisol $_{inlet}$); yellow in **Figure 1**] with the total volume of the water in the water treatment ($V_{treatment}$; total volume-production volume). This was then divided by the HRT of the water treatment.

$$CCR = \frac{\left(\left[\bar{x}\,\mathrm{Cortisol}_{\mathrm{water\ treatment}}\right] - \left[\mathrm{Cotisol}_{\mathrm{inlet}}\right]\right) \times V_{\mathrm{water\ treatment}}}{\mathrm{HRT}_{\mathrm{water\ treatment}}}$$

Cortisol release rate in each raceway ($CRR_{raceway}$) was estimated by multiplying the difference between the mean inlet concentration [$\bar{x}$ $_{(cortisol\ inlet)}$; yellow in **Figure 1**] and concentration of the three samples withdrawn in the production volume of the raceway [(cortisol start), (cortisol mid), and (cortisol end); red in **Figure 1**] with the volume of the raceway ($V_{raceway}$). This was then divided by the biomass in the raceway ($W_{raceway}$, **Table 1**) and the hydraulic retention time ($HRT_{raceway}$) of the raceway.

$$CRR_{raceway} = \frac{\left(\bar{x}\left[Cortisol_{inlet}\right] - \left[Cortisol_{raceway}\right]\right) \times V_{raceway}}{W_{raceway} \times HRT_{raceway}}$$

Moreover, cortisol clearance efficiencies were calculated based on the differences between the mean total cortisol production (sum of cortisol production in raceways 1 and 2; mg $h^{-1}$) and mean CCR. Efficiencies were expressed as a percent.

**TABLE 1 |** Biomass present in the commercial RAS 1 day before, the day after, and 3 days after smolt insertion.

| | Biomass (tons) | |
|---|---|---|
| | Raceway 1 | Raceway 2 |
| Day before smolt insertion | 0 | 191 |
| Day after smolt insertion | 28 | 214 |
| Three days after smolt insertion | 28 | 231 |

## Feeding Behavior

A husbandry practice response to feeding was routinely quantified by hand-feeding 3–9 times a day. All personal scoring behaviors were trained to rank behavior by the following scale:

1. Non to low locomotor activity when feeding and non to a few fish responds to feeding.
2. Fish responded with a low locomotor activity to hand-feeding and most of the fish do not eat.
3. Fish responded with a medium locomotor activity to hand-feeding and most of the observed fish eats.
4. Fish responded with a high locomotor activity to hand-feeding: all observed fish eats.
5. Fish responded with an even higher locomotor activity to hand-feeding and all observed fish eats.
6. Fish responded with high intensity to hand-feeding, aggression, and all fish eats.

In this feeding score system, feeding score 4 was considered normal feeding behavior.

Because fish were starved before harvested in one of the two rearing compartments in raceway 2, feeding behavior was quantified in the rearing compartment where fish were fed.

## Statistical Analyses

Data from one of the two RAS modules are illustrated in **Figure 1**. To include individual variances between samples withdrawn in the start, middle, and end sections of the raceways in the analysis, effects of smolt insertion on water cortisol concentrations and CRR in raceways 1 and 2 were analyzed with repeated measure ANOVAs with sampling date as independent variables and sampling place in the raceway as dependent variables.

Effects of smolt insertion on water cortisol concentrations at the inlet to the fish keeping raceways, the inlet to the water treatment, and cortisol removal, were analyzed by ANOVA with sampling date as independent variables. The ANOVA was followed by a Tukey-HSD *post-hoc* test when required. Feeding behavior was analyzed using Kruskal-Wallis tests with sampling dates as an independent variable, followed by Mann-Whitney U tests for testing differences between dates. The values of $p$ from the Mann-Whitney U test were corrected for multiple comparisons by Bonferroni correction (α/n), resulting in corrected values of $p$ for significant differences ($p < 0.05$) in the inner raceway $p < 0.01$ and the outer raceway $p < 0.008$.

# RESULTS

## Water Cortisol

The cortisol concentrations were changed significantly over time in raceway 1 [ANOVA: $F_{(2,6)} = 165$, $p < 0.001$] and increased significantly compared to values before smolt insertion ($p < 0.001$). Moreover, this increase was highest the day after smolt insertion, showing significantly higher values compared to water sampled 3 d after smolt insertion ($p < 0.05$), **Table 2**. In addition, cortisol concentrations changed significantly over time in raceway 2, the inlet of fish keeping raceways and the

**TABLE 2 |** Concentrations of cortisol in the rearing water in a commercial RAS for slaughter size salmon the day before, the day after, and 3 days after a smolt insertion period of 3 days.

| | Water cortisol (ng $l^{-1}$) | | |
|---|---|---|---|
| | **Day before smolt insertion (26 April)** | **Day after smolt insertion (30 April)** | **Three days after smolt insertion (2 May)** |
| In to raceways | $0.37 \pm 0.01^{a}$ | $0.87 \pm 0.03^{b}$ | $0.81 \pm 0.06^{b}$ |
| Raceway 1 | $0.37 \pm 0.03^{a}$ | $1.6 \pm 0.1^{b}$ | $1.3 \pm 0.08^{c}$ |
| Raceway 2 | $0.44 \pm 0.03^{a}$ | $0.98 \pm 0.02^{b}$ | $1.1 \pm 0.06^{b}$ |
| To water treatment | $0.45 \pm 0.01^{a}$ | $1.1 \pm 0.08^{b}$ | $1.1 \pm 0.06^{b}$ |

*Smolts were inserted in raceway 1. This raceway was empty before smolt insertion. Values are averages of three samples ± SEM. Different letters indicate significant differences ($p < 0.05$) between sampling occasions at each sampling point.*

inlet to water treatment [ANOVAs: $F_{(2,4)} = 290$, $p < 0.001$; $F_{(2,6)} = 118$, $p < 0.001$; $F_{(2,6)} = 50$, $p < 0.001$; respectively]. At all these sampling locations, cortisol values were significantly higher after 1 day and 3 days of smolt insertion, compared to the start ($p < 0.001$). However, there were no significant differences in water cortisol concentrations between samples taken after 1 day and 3 days of smolt insertion at raceway 2 ($p < 0.15$), the inlet to the fish keeping raceways ($p < 0.29$), and the inlet to the water treatment ($p < 0.94$).

## Cortisol Release Rate

Cortisol release rate from fish in raceway 1 decreased significantly between the day after and after 3 days of smolt insertion [ANOVA: $F_{(43)}$, $p < 0.05$; **Figure 2A**]. Also in raceway 2, the CRR changed over time [ANOVA: $F_{(2,4)} = 8.4$, $p < 0.01$], leading to significantly higher values after 3 days of smolt insertion compared to values before $p < 0.05$) and after ($p < 0.05$) smolt insertion. However, CRR 1 day after smolt insertion did not differ significantly from values before smolt insertion ($p < 0.63$) in this raceway (**Figure 2B**).

## Cortisol Clearance Rate and Clearance Efficacy

Cortisol clearance rates were $0.6 \pm 0.1$ the day before, $2.0 \pm 0.2$ the day after, and $2.2 \pm 0.24$ (mg $h^{-1}$) 3 days after smolt insertion (values are mean ± SE).

Cortisol clearance efficacies were 99.8% the day before smolt insertion, 39.1% the day after smolt insertion, and 43% 3 days after smolt insertion.

## Feeding Behavior

In raceway 1, the feeding score changed over time [Kruskal-Wallis test; H (4) = 16, $p < 0.003$]. This was reflected in significant differences in lower values ($p < 0.01$) scored during smolt insertion (April 28–29) compared to values scored in the two last days following smolt insertion (April 30–May 2; **Figure 3**). The feeding score also differed significantly between days in raceway 2 [Kruskal-Wallis test; H (5) = 15, $p < 0.01$]. Moreover, in this raceway, the feeding score was significantly higher ($p < 0.008$) on the third day of smolt insertion (April 29) when compared to feeding behavior scored on the first day of smolt insertion (April 27).

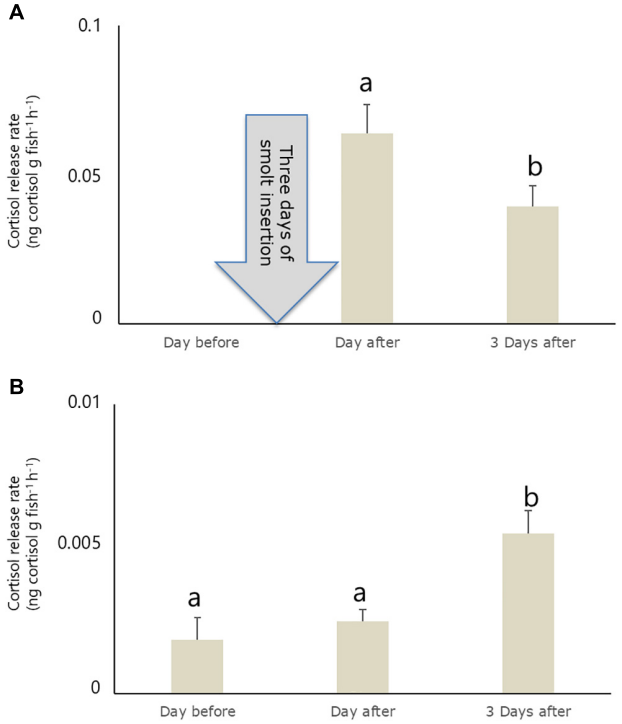


**FIGURE 2 |** Cortisol release rate in raceway 1 **(A)** and raceway 2 **(B)** before and after a 4 days smolt insertion period in raceway 1. Raceway 1 was emptied before smolt insertion. Different lowercase letters indicate a significant difference ($p < 0.05$) between sampling occasions within a raceway. Values are averages of three samples ± SEM.

# DISCUSSION

In the present study, the water cortisol stayed high for 3 days after smolt insertion in a commercial grow-out RAS for salmon. Moreover, the estimated CRR was approximately ten times higher in newly inserted smolts compared to already stocked fish. Interestingly, salmon acclimatizing to experimental tanks show a similar CRR, ranging from 0.03 to 0.2 ng $g^{-1}$ $h^{-1}$ 1–7 d after being inserted in the tanks, as in the current study (Ellis et al., 2007). Underlaying factors for such relative slow adaption have been associated to reduced space, unfamiliar physical environment, and changed social environment (Pottinger and Pickering, 1992). Generally, the transfer to seawater in commercial production consists of several potential stressors, such as capture, loading, transport, unloading, adaption to seawater, new environment, and social structures. In addition, generally, an elevation of plasma cortisol is associated with the process of smoltification (McCormick et al., 2000; Ebbesson et al., 2008). Thus, this suggests that the smoltification process contributed to the increased level of waterborne cortisol in the current study. Still, decreased CRR after smolt insertion

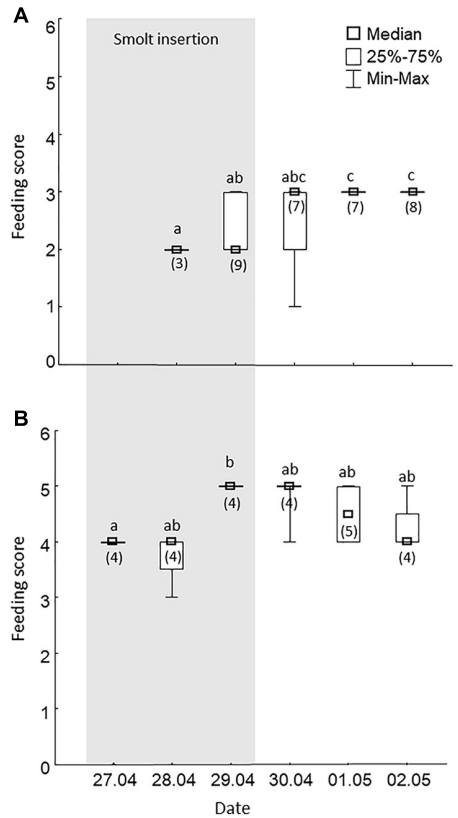


**FIGURE 3 |** Behavioral response to feeding in Atlantic salmon reared in two raceways in a commercial RAS for slaughter size salmon during a 3-days smolt insertion period (April 27–29) and the three following days (30 April–2 May). Smolts were inserted in raceway 1 **(A)**. This raceway was empty before smolt insertion. Salmon that were established in the system were kept in raceway 2 **(B)**. A feed score of four corresponds to all pellets eaten without observations of aggressive behavior. The feeding score under four score corresponds to that not all pellets are eaten, and the feeding score above four corresponds to that all pellets are eaten and aggressive behavior is observed. More details about the feeding score are shown in section "Materials and Methods." Numbers within parenthesis denotes the number of daily observations. Different lowercase letters indicate significant differences ($p = 0.05$) between daily feeding scores within a raceway. RAS, recirculating aquaculture systems.

in raceway 1 indicates ongoing adaptive processes in the newly inserted smolts.

Mota et al. (2014) estimated cortisol clearance efficacy to be <99% in commercial RAS during baseline conditions. Still, studies comparing steroid concentrations in the make-up water (new water into the system) with concentrations in the rearing water have shown that waterborne cortisol and other steroids accumulate in the rearing water of commercial and experimental RAS (Mota et al., 2014; Good et al., 2017). In the present study, cortisol clearance efficacy was 99.8% 1 day before smolt insertion. However, clearance efficacy decreased to approximately 40% the day after and 3 days after smolt insertion, when cortisol release was increased in the raceways. This demonstrates that the increased water cortisol levels exceeded the cortisol clearance capacity of the system, and contributed to the water cortisol concentrations stayed high after smolt insertion.

A characteristic behavioral response to stress in all vertebrates appears to be a reduction in food intake (Carr, 2002). This is reflected in laboratory studies showing that salmon can respond with a stress-induced anorexia to a new environment (Vaz-Serrano et al., 2011) and resume normal feeding behavior within a week. In accordance with this, the feeding motivation score in the current study raised from score 2 to 3 indicated that the smolts were in the process of adapting to the rearing environment 3 days after being inserted in the raceway. This, together with a reduced water cortisol concentration and release rate 3 days after smolt insertion in raceway 1, suggests that smolts are in the process of adapting to highly intensive seawater rearing in a commercial RAS facility. "However, it is important to note that both feeding score and CRR suggest that fish was not fully adapted during the timespan of the study. Thus, further studies are needed to investigate the time smolt need to fully adapt in a highly intensive RAS."

Since steroids induce behavioral and physiological changes in fish by acting as pheromones, concerns regarding the behavioral and physiological effects of waterborne steroids in RAS have been raised (Mota et al., 2014; Good and Davidson, 2016; Good et al., 2017). However, these effects seems mainly to be induced by the sex steroids, and whether waterborne cortisol affects fish, has been questioned (Mota et al., 2017b). Interestingly, there was a small increase in cortisol release on day three in raceway 2, containing fish established in the system. However, the current experimental setup did not allow the investigations of whether, and to what extent, this rise in cortisol release was induced by water-borne cortisol. Furthermore, the fish in one of the compartments in raceway 2 were pre-treated for slaughter, such as starvation and handling, and the increased cortisol release may be related to this treatment.

In conclusion, the current results, obtained in a highly intensive commercial RAS, indicate that water cortisol concentrations and CRR are sensitive to system perturbations. Moreover, together with behavioral responses to feed, water cortisol measurements are promising non-invasive indicators of adaptive processes associated with stress resilience in this type of rearing system. As such, they can be used for evaluating the impact of potential stressors, such as compromised water quality, crowding and handling, on fish welfare. However, it is important to keep in mind that cortisol release and clearance rate were estimated assuming a quasi-steady state of hormone release during a smolt insertion event, while the results show a highly dynamic response to this perturbation. Other factors, which can contribute to the dynamics of waterborne cortisol in RAS, include changes in clearance capacity of water treatment processes, amount of new water into the system, and hormone concentrations in this make-up water (Good et al., 2017). Altogether, this accentuates the need for further studies on the underlying mechanisms of the dynamics of water cortisol concentrations, to refine waterborne cortisol as a non-invasive fish-based welfare indicator in commercial RAS.

## DATA AVAILABILITY STATEMENT

The original contributions presented in the study are included in the article/**Supplementary Material**, further inquiries can be directed to the corresponding author.

## ETHICS STATEMENT

We used non-invasive welfare indicators (waterborne cortisol and feeding behavior) to study the impact of smolt insertion in a commercial RAS. All fish treatments in the study are parts of the commercial rearing practice.

## AUTHOR CONTRIBUTIONS

EH contributed to plan the experiment, draft the manuscript, and data analyses. PF contributed to draft the manuscript and data analyses. PR-T and O-KH-E drafted the manuscript. JR contributed to plan the experiment and data analyses. All authors contributed to the article and approved the submitted version.

## FUNDING

This study was funded by the Norwegian Research Council, project number; 160016/F4.

## ACKNOWLEDGMENTS

We thank the personal at Fredrikstad Seafoods for access to their RAS facility, data on feeding behavior, and excellent help with water sampling.

## SUPPLEMENTARY MATERIAL

The Supplementary Material for this article can be found online at: https://www.frontiersin.org/articles/10.3389/fphys.2021.771951/full#supplementary-material

## REFERENCES

Baretto, M. O., Rey Planellas, S., Yang, Y., Phillips, C., and Descovich, K. (2022). Emerging indicators of fish welfare in aquaculture. *Rev. Aquac.* 14, 343–361. doi: 10.1111/raq.12601

Barton, B. A., and Iwama, G. K. (1991). Physiological changes in fish from stress in aquaculture with emphasis on the response and effects of corticosteroids. *Annu. Rev. Fish. Dis.* 1, 3–26.

Carr, J. A. (2002). Stress, neuropeptides, and feeding behavior: a comparative perspective. *Integr. Comp. Biol.* 42, 582–590. doi: 10.1093/icb/42.3.582

Chung-Davidson, Y. W., Huertas, M., and Li, W. (2010). "A review of research in fish pheromones," in *Chemical Communication in Crustaceans*, eds T. Breithaupt and M. Thiel (New York Dordrecht Heidelberg London: Springer), 467–482. doi: 10.1007/978-0-387-77101-4

Ebbesson, L. O., Björnsson, B. T., Ekström, P., and Stefansson, S. O. (2008). Daily endocrine profiles in parr and smolt Atlantic salmon. *Comp. Biochem. Physiol. A. Mol. Integr. Physiol.* 151, 698–704. doi: 10.1016/j.cbpa.2008.08.017

Ellis, T., James, J. D., and Scott, A. P. (2005). Branchial release of free cortisol and melatonin by rainbow trout. *J. Fish Biol.* 67, 535–540. doi: 10.1111/j.0022-1112.2005.00740.x

Ellis, T., James, J. D., Stewart, C., and Scott, A. P. (2004). A non-invasive stress assay based upon measurement of free cortisol released into the water by rainbow trout. *J. Fish Biol.* 65, 1233–1252. doi: 10.1111/j.0022-1112.2004.00499.x

Ellis, T., James, J. D., Sundh, H., Fridell, F., Sundell, K., and Scott, A. P. (2007). Non-invasive measurement of cortisol and melatonin in tanks stocked with seawater Atlantic salmon. *Aquaculture* 272, 698–706. doi: 10.1016/j.aquaculture.2007.07.219

Félix, A. S., Faustino, A. I., Cabral, E. M., and Oliveira, R. F. (2013). Noninvasive measurement of steroid hormones in zebrafish holding-water. *Zebrafish* 10, 110–115. doi: 10.1089/zeb.2012.0792

Good, C., and Davidson, J. (2016). A review of factors influencing maturation of Atlantic salmon, Salmo salar, with focus on water recirculation aquaculture system environments. *J. World. Aquac. Soc.* 47, 605–632. doi: 10.1111/jwas.12342

Good, C., Davidson, J., Earley, R. L., Lee, E., and Summerfelt, S. (2014). The impact of water exchange rate and treatment processes on water-borne hormones in recirculation aquaculture systems containing sexually maturing Atlantic salmon Salmo salar. *J. Aquac. Res. Dev.* 5:1. doi: 10.4172/2155-9546.1000260

Good, C., Davidson, J., Earley, R. L., Styga, J., and Summerfelt, S. (2017). The effects of ozonation on select waterborne steroid hormones in recirculation aquaculture systems containing sexually mature Atlantic salmon *Salmo salar*. *Aquac. Eng.* 79, 9–16. doi: 10.1016/j.aquaeng.2017.08.004

Iversen, M., Finstad, B., and Nilssen, K. J. (1998). Recovery from loading and transport stress in Atlantic salmon (*Salmo salar* L.) smolts. *Aquaculture* 168, 387–394. doi: 10.1016/s0044-8486(98)00364-0

Iversen, M., Finstad, B., McKinley, R. S., Eliassen, R. A., Carlsen, K. T., and Evjen, T. (2005). Stress responses in Atlantic salmon (*Salmo salar* L.) smolts during commercial well boat transports, and effects on survival after transfer to sea. *Aquaculture* 243, 373–382. doi: 10.1016/j.aquaculture.2004.10.019

Martins, C. I. M., Eding, E. H., Verdegem, M. C., Heinsbroek, L. T., Schneider, O., Blancheton, J. P., et al. (2010). New developments in recirculating aquaculture systems in Europe: a perspective on environmental sustainability. *Aquacl. Eng.* 43, 83–93.

McCormick, S. D., Moriyama, S., and Bjornsson, B. T. (2000). Low temperature limits photoperiod control of smolting in Atlantic salmon through endocrine mechanisms. *Am. J. Physiol. Regul. Integr. Comp. Physiol.* 278, R1352–R1361. doi: 10.1152/ajpregu.2000.278.5.R1352

McWhinney, B. C., Briscoe, S. E., Ungerer, J. P., and Pretorius, C. J. (2010). Measurement of cortisol, cortisone, prednisolone, dexamethasone and 11-deoxycortisol with ultra high performance liquid chromatography–tandem mass spectrometry: application for plasma, plasma ultrafiltrate, urine and saliva in a routine laboratory. *J. Chromatogr.* 878, 2863–2869. doi: 10.1016/j.jchromb.2010.08.044

Mota, V. C., Martins, C. I., Eding, E. H., Canário, A. V., and Verreth, J. A. (2014). Steroids accumulate in the rearing water of commercial recirculating aquaculture systems. *Aquac. Eng.* 62, 9–16. doi: 10.1016/j.aquaeng.2014.07.0040144-8609

Mota, V. C., Martins, C. I., Eding, E. H., Canário, A. V., and Verreth, J. A. (2017a). Cortisol and testosterone accumulation in a low pH recirculating aquaculture system for rainbow trout (*Oncorhynchus mykiss*). *Aquac. Res.* 48, 3579–3588. doi: 10.1111/are.13184

Mota, V. C., Martins, C. I., Eding, E. H., Canário, A. V., and Verreth, J. A. (2017b). Water cortisol and testosterone in Nile tilapia (*Oreochromis niloticus*) recirculating aquaculture systems. *Aquaculture* 468, 255–261. doi: 10.1016/j.aquaculture.2016.10.023

Pottinger, T. G., and Pickering, A. D. (1992). The influence of social interaction on the acclimation of rainbow trout, *Oncorhynchus mykiss* (Walbaum) to chronic stress. *J. Fish Biol.* 41, 435–447. doi: 10.1111/j.1095-8649.1992.tb02672.x

Sapolsky, R. M., Romero, L. M., and Munck, A. U. (2000). How do glucocorticoids influence stress responses? Integrating permissive, suppressive, stimulatory, and preparative actions. *Endocr. Rev.* 21, 55–89. doi: 10.1210/edrv.21.1.0389

Scott, A. P., and Ellis, T. (2007). Measurement of fish steroids in water—a review. *Gen. Comp. Endocrinol.* 153, 392–400. doi: 10.1016/j.ygcen.2006.11.006

Su, X., Sutarlie, L., and Loh, X. J. (2020). Sensors, biosensors, and analytical technologies for aquaculture water quality. *Research* 2020:8272705. doi: 10.34133/2020/8272705

van de Vis, H., Kolarevic, J., Stien, L. H., Kristiansen, T. S., Gerritzen, M., Van De Braak, K., et al. (2020). "Welfare of farmed fish in different production systems and operations," in *The Welfare of Fish*, eds T. S. Kristiansen, A. Fernö, M. A. Pavlidis, and H. van de Vis (Switzerland AG: Springer Nature), 323–361. doi: 10.1007/978-3-030-41675-1

Vaz-Serrano, J., Ruiz-Gomez, M. D. L., Gjøen, H., Skov, P. V., Huntingford, F., Øverli, Ø, et al. (2011). Consistent boldness behaviour in early emerging fry of domesticated Atlantic salmon (*Salmo salar*): decoupling of behavioural and physiological traits of the proactive stress coping style. *Physiol. Behav.* 103, 359–364. doi: 10.1016/j.physbeh.2011.02.025

Vermeirssen, E. L., and Scott, A. P. (1996). Excretion of free and conjugated steroids in rainbow trout (*Oncorhynchus mykiss*): evidence for branchial excretion of the maturation-inducing steroid, 17, 20β-dihydroxy-4-pregnen-3-one. *Gen. Comp. Endocrin.* 101, 180–194. doi: 10.1006/gcen.1996.0020

**Conflict of Interest:** The authors declare that the research was conducted in the absence of any commercial or financial relationships that could be construed as a potential conflict of interest.

**Publisher's Note:** All claims expressed in this article are solely those of the authors and do not necessarily represent those of their affiliated organizations, or those of the publisher, the editors and the reviewers. Any product that may be evaluated in this article, or claim that may be made by its manufacturer, is not guaranteed or endorsed by the publisher.

frontiers in Physiology

ORIGINAL RESEARCH
published: 09 February 2022
doi: 10.3389/fphys.2021.775771

# Effects of Dietary Phenylalanine and Tyrosine Supplements on the Chronic Stress Response in the Seabream (*Sparus aurata*)

*Natalia Salamanca[1]*, Oscar Moreno[1], Inmaculada Giráldez[2], Emilio Morales[2], Ignacio de la Rosa[3] and Marcelino Herrera[1,3]*

[1] IFAPA Centro Agua del Pino, Cartaya, Spain, [2] Faculty of Experimental Sciences, University of Huelva, Huelva, Spain, [3] Escuela Superior de Ingeniería, University of Huelva, Huelva, Spain

The increase of aquaculture production is associated with a growing interest in improving physiological status and welfare in fish. For this reason, the search for strategies for mitigating stress has been intensified, with one of these strategies being food supplementation with different amino acids (AA). The objective of this study was to evaluate the effects of dietary phenylalanine (Phe) and tyrosine (Tyr) supplements on the endocrine and physiological state of seabreams (*Sparus aurata*) subjected to chronic stress. The fish were stocked at 30 fish/tank in a recirculation aquatic system, fed one control diet and two diets supplemented with 5% Phe or Tyr for 90 days. Blood was drawn from 10 fish per tank every 30 days, and the weight and length were measured every 15 days. At the end of the experiment, length/weight of the fish were measured, and they were sacrificed for the extraction of blood, head kidney, liver, and brain. Classic plasma stress markers (glucose, lactate, proteins, and cortisol), as well as hormones derived from Phe and Tyr (adrenaline, norepinephrine, and dopamine) and the accumulation of AA were analyzed. Fish fed with diets supplemented with Phe or Tyr showed a reduction in various stress markers and physiological parameters. In addition, the stress condition favored a mobilization of AA toward the tissues, especially in supplemented diets, so this excess of AA could be used as an energy substrate to cope with stress.

**Keywords: *Sparus aurata*, stress, welfare, phenylalanine, tyrosine, feed supplement**

OPEN ACCESS

***Edited by:***
*Luciana Mandrioli, University of Bologna, Italy*

***Reviewed by:***
*Albamaria Parmeggiani, University of Bologna, Italy*
*Nicholas Romano, University of Arkansas at Pine Bluff, United States*

****Correspondence:***
*Natalia Salamanca*
*natalia.salamanca@juntadeandalucia.es*

***Specialty section:***
*This article was submitted to Aquatic Physiology, a section of the journal Frontiers in Physiology*

***Received:*** *14 September 2021*
***Accepted:*** *25 October 2021*
***Published:*** *09 February 2022*

***Citation:***
*Salamanca N, Moreno O, Giráldez I, Morales E, de la Rosa I and Herrera M (2022) Effects of Dietary Phenylalanine and Tyrosine Supplements on the Chronic Stress Response in the Seabream (Sparus aurata). Front. Physiol. 12:775771. doi: 10.3389/fphys.2021.775771*

## INTRODUCTION

In recent years, aquaculture studies have focused on finding new strategies for minimizing stress and increasing animal welfare in the main species of interest, such as the gilthead seabream (*Sparus aurata*), whose culture is carried out in different marine farms along the Mediterranean and South-Atlantic areas, both onshore and offshore (AGAPA, 2019). In 2020, the production of seabream in the world experienced a decrease of 1.3% compared to 2020, reaching 249,200 tons, according to statistics from APROMAR (2020) (Spanish Association of Aquaculturists). Seabream farms exist in 18 countries, the top producers being Turkey (33.7% of total production), Greece (25.9% of total production), and Spain (9.3% of total production). Despite the position occupied by the Spanish

production of seabream, it dropped off 9.4% in 2019, which represented an important decrease after the slight rebound occurred in 2017. The main Spanish region in seabream production is Valencia, which produces 49% of the total. Andalusia ranks third with a production of 1,606 tons in 2019. Besides important growth and reproductive indexes, this species' success relies on its high domestication level (Teletchea, 2015).

Stress is a factor that may determine the success of fish culture. The primary physiological response to stress involves rises in plasma catecholamines and cortisol (Barton, 2002). Following, these hormones induce secondary responses, which are detected by the reduction in hepatic reserves (mainly glycogen) and increased plasma glucose levels, mobilizing glucose (and other energy substrates) to tissues for recovering homeostasis (Barton et al., 2002). If stress condition continues, the tertiary response can appear, being related to failures at organism level (reproduction, growth, survival, etc.) (Iwama et al., 2006).

Changes in salinity and environmental temperature, transport, and culture stocking density are some of the factors that can cause stress situations in marine farms, the most common being transport stress (acute stress) and culture stocking density (chronic stress) (Arends et al., 1999; Montero et al., 1999; Feidantsis et al., 2009; Martos-Sitcha et al., 2014; Jerez-Cepa et al., 2019). For this reason, stress reduction in fish has been widely studied using anesthetics, essential oils, or food additives (Ross and Ross, 2008; Zahl et al., 2012; Vanderzwalmen et al., 2018; Hoseini et al., 2019; Herrera et al., 2020; Salamanca et al., 2020, 2021).

Proteins constitute the essential part of the diet since they provide the amino acids (AA) necessary for the sustenance of the body. The AA which are a part of the cellular processes are called functional AA. A deficit of these AA can affect the body's metabolism and homeostasis. In this sense, it has been shown that AA improve resistance to disease, reproduction, or behavior (Li et al., 2009; Wu, 2009). With the aim of optimizing the performance of aquaculture facilities and the quality of the final product, there has been an increase in the study of fish functional foods based on AA during the last years (Herrera et al., 2012, 2019; Andersen et al., 2016; Salamanca et al., 2020, 2021). In this sense, according to various authors, some amino acid dietary supplements could attenuate the stress response in different fish species and enhance the immune response (Herrera et al., 2016; Gonzalez-Silvera et al., 2018; Fernández-Alacid et al., 2019; Salamanca et al., 2020).

The effects of phenylalanine (Phe) and tyrosine (Tyr) have hardly been studied in fish (Herrera et al., 2016; Salamanca et al., 2021). Phe is an essential amino acid that is metabolized through two metabolic pathways, namely oxidation to Tyr and transamination to phenylpyruvate (Shafik et al., 2014). Tyr is a precursor of the catecholamine (adrenaline, noradrenaline, and dopamine) and thyroid (triiodothyronine and thyroxine) hormones, which are involved in the stress response (Reid et al., 1998). In this sense, it has been described that thermal stress rises the circulating levels of catecholamines in the rainbow trout (*Oncorhynchus mykiss*) (LeBlanc et al., 2011, 2012), and the concentration of plasma thyroid hormones could be a stress indicator (Hoseini et al., 2014). As stress is an energy-demanding process, Tyr also could be catabolized to hydroxyphenyl pyruvate and becomes a part of the energy metabolism.

It has been reported that Phe- and Tyr-enriched diets can mitigate the effects of acute stress in mammals (Brady et al., 1980; Lehnert et al., 1984; Banderet and Lieberman, 1989). In fact, Cotoia et al. (2014) have shown that hydroxyphenyl pyruvate improves cell survival under stress conditions in rats. In fish, both AA decrease the cases of bone deformity in *Diplodus sargus* larvae (Saavedra et al., 2010). Only Salamanca et al. (2021) have described the stress-attenuating effects of Phe and Tyr in meagre (*Argyrosomus regius*) and seabream (*S. aurata*) after submitting to acute stress. However, there are no studies on how Phe or Tyr supplements influence physiological responses to chronic stress. Therefore, the objective of this study is to analyze the effects of diets supplemented with Phe and Tyr on stress markers in situations of chronic stress in gilthead seabream (*S. aurata*).

# MATERIALS AND METHODS

## Experimental Culture and Sampling

Gilthead seabreams *S. aurata* ($n$ = 180), with a body weight of 33.93 ± 0.93 g and a total length of 12.87 ± 0.16 cm (mean ± standard error, SE), came from CULMASUR (Isla Cristina, Spain). The fish batch was divided into 30 fish/tank in six 500-L flat bottom circular tanks at a stocking density of 2 kg $m^{-3}$. The culture water was recirculated, the flow rate, mean temperature, salinity, and dissolved oxygen levels were 300 L $h^{-1}$, 21.47 ± 1°C, 37 ± 1 g $L^{-1}$, and above 5 ppm, respectively. Water quality was checked weekly through Spectroquant kits (MERCK, Darmstadt, Germany), maintaining the following values (mg $L^{-1}$) in each experimental tank: total ammonia <0.04; total nitrite <0.02; and total nitrate <0.03.

Before the experiment began, the fish were fed commercial feed (L2 Alterna® Skretting, Burgos, Spain) with daily rations of 2% of biomass for 2 weeks. The experimental treatment consisted of two physiological statuses (basal and stress) fed with three types of feeding (control, food enriched with 5% Phe, and food enriched with 5% Tyr) for 90 days. The stressed groups were submitted to confinement and netting/chasing stress. This procedure consisted of fish that were randomly net-chased and netted (with no exposure to air) daily for 5 min three times a day (adapted from Gonzalez-Silvera et al., 2018 and Herrera et al., 2020). Those tanks had a water column of 20 cm, and thus an initial stocking density of 4 Kg $m^{-3}$. The basal group tanks had a water volume of 500 L (40 cm water height, 2 kg $m^{-3}$) and were not disturbed along the experiment. All tanks were supervised daily for cleaning (light siphoning). Fifteen fish from each tank were individually ink-tagged according to Rodiles et al. (2015) so the experimental unit was every individual fish (15 replicates) and tank replicates were not necessary.

Fish feed was provided through automatic feeders and the ration was adjusted to 2% of the tank biomass daily; the feeders supplied food 24 h a day. The rations were adjusted after each biometric sampling. The tanks were cleaned and checked daily for possible dead fish. Biometric samplings were carried out every 15 days and blood (0.1 mL) was drawn every

30 days, previously anesthetizing marked fish ($n$ = 10) in a 2-phenoxyethanol bath (200 μL $L^{-1}$). At the end of the 90-day trial, fish were sacrificed with 2-phenoxyethanol overdose (1 mL $L^{-1}$) for blood and tissue extraction (10 fish per treatment). Prior to each sampling, the fish were fasted for 24 h and without manipulation that caused stress effects. Blood was collected from the caudal vein with 1 mL heparinized syringes (25,000 units of ammonium heparin/3 mL of 0.6% NaCl saline, Sigma H6279, Saint Louis, MO, United States). Plasma was separated from cells by whole blood centrifugation with an Eppendorf 5415R centrifuge (Hamburg, Germany) (3 min; 10,000 × $g$; 4°C) and stored at −80°C until analyzes were performed. The next biometric parameters were calculated: specific growth rate (% $day^{-1}$), SGR = 100·(ln Wf − ln Wi)/t; conversion factor, CF = FS/(Wf − Wi); condition factor, $K$ = 100·BW/TL3; and hepatosomatic index, HSI = 100·(Lw/BW); where Wf, Wi are individual final and initial weight (g); Lw is individual liver weight (g); BW and TL, individual body weight (g) and total length (cm); t, time (days); and FS is individual mean supplied food (g). No fish mortality was detected during the experiment.

The IFAPA facilities are certified and have the necessary authorization for the breeding and husbandry of animals for scientific purposes (REGA Code ES210210000303). All procedures involving the handling and treatment of the fish were approved as far as the care and use of experimental animals are concerned (authorization code 11/05/2021/073), by the European Union (2010/63/EU) and the Spanish Government (Real Decreto 53/2013, de 1 de febrero, por el que se establecen las normas básicas aplicables para la protección de los animales utilizados en experimentación y otros fines científicos, incluyendo la docencia).

## Experimental Food Making

Commercial fish feed (L2 Alterna® Skretting, Burgos, Spain), with a size of 2.2 mm, was used as the control diet. L-phenylalanine and L-tyrosine (dry powder) were purchased from ThermoFisher (Kandel, Germany). The commercial control diet was finely ground and mixed with AA and later water (300 mL $Kg^{-1}$ dry feed). The amount of phenylalanine and tyrosine in each experimental diet was 5% (on dry feed) except for the control diet which did not have any amino acid. The mixture was thread pelleted into 2 mm diameter and 20–25 cm length strips. These were cut to get 2–3 mm size pellets. Finally, these food strips were dried at 30°C for 48 h and stored at 4°C.

Analysis of AA was performed as reported previously (Herrera et al., 2020; Salamanca et al., 2020). According to the above method, the final amino acid concentrations in the experimental diets are shown in **Table 1**.

**TABLE 1 |** Amino acid composition (g amino acid/Kg wet food) for every experimental fish feed.

| Amino acid | Control | 5% Phe | 5% Tyr |
|---|---|---|---|
| Alanine | 0.52 | 0.76 | 0.76 |
| Glycine | 0.98 | 1.30 | 1.10 |
| Valine | 0.53 | 0.71 | 0.72 |
| Leucine | 0.63 | 0.90 | 0.87 |
| Isoleukin | 0.99 | 1.23 | 1.21 |
| Proline | 2.39 | 3.46 | 3.33 |
| Threonine | 0.01 | 0.01 | 0.01 |
| Aspartic acid | 1.14 | 1.58 | 1.50 |
| Methionine | 0.09 | 0.12 | 0.11 |
| Glutamic acid | 4.91 | 6.69 | 6.37 |
| Phenylalanine | 1.05 | 3.74 | 1.41 |
| Lysine | 0.84 | 1.24 | 1.09 |
| Tyrosine | 0.89 | 1.37 | 5.21 |

## Plasma Analysis

Plasma glucose, proteins, lactate, and catecholamines (adrenaline, noradrenaline, and dopamine) levels were measured using commercial kits from Química Analitica Aplicada S.A. (QCA Glucose Liquid Ref. 998,225, QCA Total Proteins Ref. 997,180, Tarragona, Spain), Spinreact (Lactate Ref. 1,001,330, Barcelona, Spain), and 2-CAT (A-N) Research ELISA (Ref. BA E-5400, Nordhorn, Germany) adapted to 96-well microplates (Herrera et al., 2012). All assays were performed with a Varioskan Lux reader, using Skantt software for microplate readers v.6.0 (Thermo Fisher Scientific, MA, United States). Plasma cortisol levels were quantified by an ELISA kit (EA65, Oxford Biomedical Research, MI, United States) modified and adapted to fish. Cortisol was extracted from 20 μL plasma in 200 μL diethyl ether. The lower limit of detection (88.2% of binding) was 0.005 ng $mL^{-1}$ plasma. The interassay coefficient of variation was 9.8%, while the mean intraassay coefficient of variation was 4.6%. The mean percentage of recovery was 90%. The main cross reactivities (>5%; given by the supplier) were detected with prednisolone (66.9%), 11-deoxycortisol (58.1%), cortisone (15.9%), prednisone (13.7%), and 17-hydroxyprogesterone (5.4%).

## Tissue Analysis

For brain catecholamines, 20–50 mg of brain tissue was homogenized by ultrasonic disruption with 150 μL of perchloric acid (PCA), and then mixed with 150 μL of potassium dichromate 0.15 M. Following this, the mixture was centrifuged (1200 $g$; 4°C; 10 min) and the supernatant removed. The precipitate was air-dried for 2 h at 25°C. Finally, 250 μL of distilled water was added to the tube and the solution used for ELISA kit determination according to the above section "Plasma Analysis."

For analyzing Phe and Tyr concentrations, tissue samples (20–50 mg) were dissolved in an acid hydrolysis and basic hydrolysis. The solution was diluted to 1:20 to avoid high concentration. Derivatization procedure was based on the method described by Zhao et al. (2017) with some modifications. An aliquot (100 μL) of working standard solution or sample extract was placed in a 2-mL vial, and 400 μL of a NaOH (3%):ethanol:pyridine (60:32:8) mixture and 40 μL of ethyl chloroformate were added. It was capped and vigorously shaken with a vortex mixer for 60 s at room temperature. Gas evolution (carbon dioxide) usually occurs. Then, 200 μL of chloroform (containing 1% ethyl chloroformate, ECF) and 200 μL 50 mM sodium bicarbonate solution were added. The derivatives were extracted into the

organic phase by striking the tube against a pad for about 30 s. The organic phase was dried with anhydrous sodium sulfate. Another 200 μL of chloroform (containing 1% ECF) were added and shaken for 30 s. The organic phase was dried with anhydrous sodium sulfate, and transferred to a new gas chromatography (GC) vial.

Aliquots (1 μL) of the derivative extracts were injected into a Shimadzu GCMS-TQ8030 equipped with an Agilent HP-5MS fused silica capillary column (60 m × 0.25 mm i.d., 0.25 mm film thickness). The gas chromatograph system was equipped with a split/splitless injection port operating in Splitless mode. The column was kept at 120°C for 1 min, ramped at 15°C $min^{-1}$ to 285°C and held for 3 min, then the temperature was increased at 15°C $min^{-1}$ to 300°C and held for 2 min. The carrier gas was helium with a constant flow of 1.2 mL $min^{-1}$. The temperature of the injector, transfer line, and ion source was maintained at 250, 290, and 230°C, respectively, and a solvent delay of 10 min was selected. The mass spectrophotometry (MS) was tuned to *m/z* 69, 219, and 502 for EI corresponding to perfluorotributylamine (PFTBA). Each compound was identified

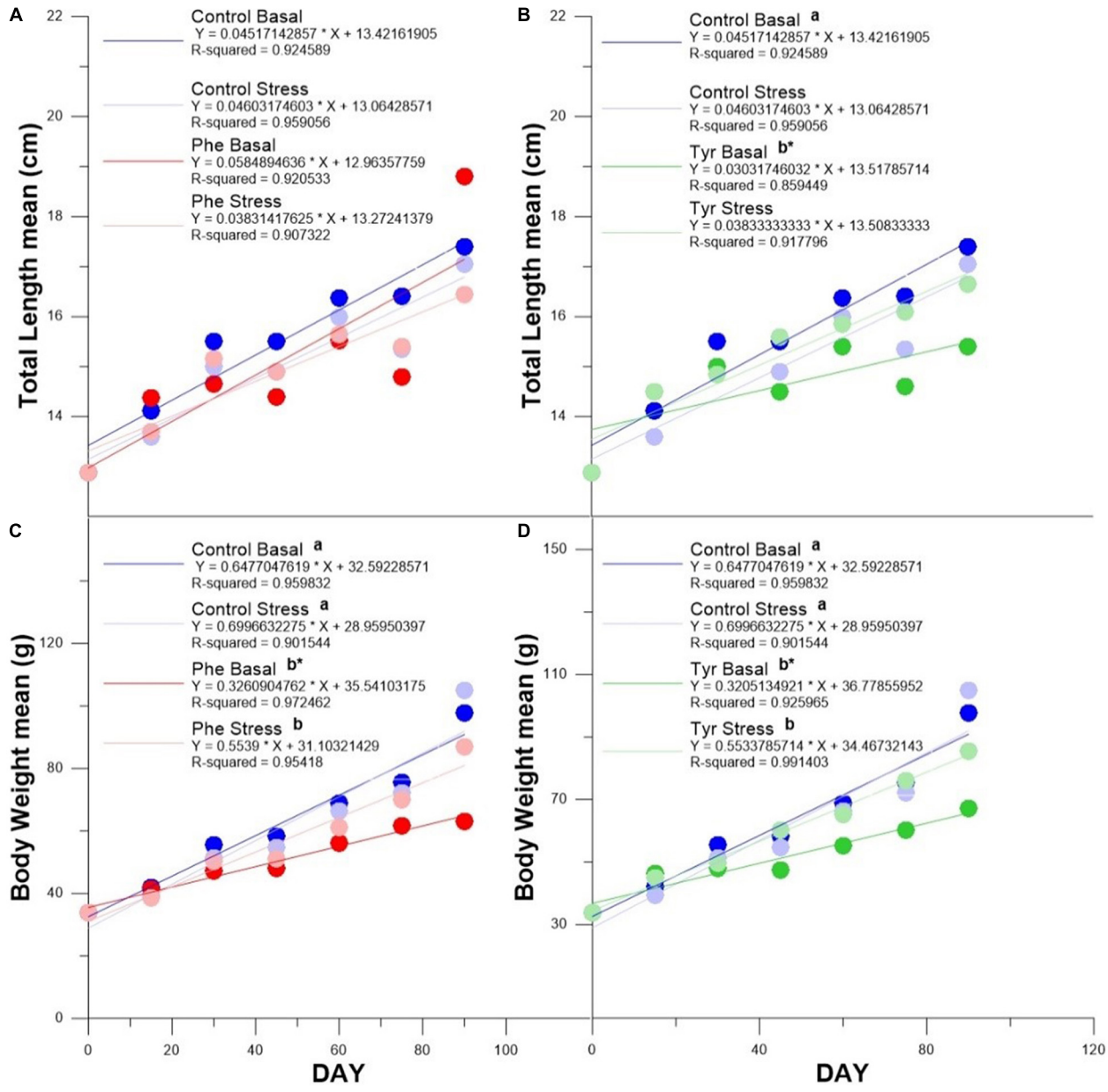


**FIGURE 1 |** Total length curve for Phe enriched **(A)** and Tyr enriched **(B)** diets. Body weight curve for Phe enriched **(C)** and Tyr enriched **(D)** diets. Asterisks indicate significant differences in curve slope between basal and stress for the same feed, and different letters indicate differences in curve slope between control and phenylalanine or tyrosine within every state (stress or basal).

**TABLE 2 |** Biometric parameters for the experiment (mean ± SE).

| | SGR (% day$^{-1}$) | CF | *K* | HSI |
|---|---|---|---|---|
| Ctrl basal | 0.89 ± 0.47 | 2.32 ± 2.12 | 1.89 ± 0.09$^{a*}$ | 0.94 ± 0.18$^{a}$ |
| Ctrl stress | 1.06 ± 0.41 | 1.15 ± 0.63 | 2.10 ± 0.02$^{a}$ | 1.21 ± 0.54 |
| Phe basal | 0.55 ± 0.19 | 1.89 ± 0.40$^{*}$ | 1.58 ± 0.17$^{b}$ | 1.24 ± 0.29$^{b}$ |
| Phe stress | 0.73 ± 0.38 | 1.21 ± 0.53 | 1.94 ± 0.09$^{b}$ | 1.18 ± 0.51 |
| Tyr basal | 0.63 ± 0.20 | 1.68 ± 0.39 | 1.85 ± 0.14$^{a}$ | 1.15 ± 0.33$^{ab}$ |
| Tyr stress | 0.82 ± 0.21 | 1.67 ± 0.55 | 1.86 ± 0.01$^{b}$ | 1.10 ± 0.29 |

*SGR, specific growth rate; CF, conversion factor; K, condition factor; HSI, hepatosomatic index. Different letters indicate significant differences between the different diets. Asterisks indicate significant differences between stress and basal within every diet.*

using three characteristic ions, a quantifier, two qualifier ions, and the relative intensity of qualifier to quantifier ion (±20%). For phenylalanine *m/z* 176 (quantifier), *m/z* 102, *m/z* 91, and tyrosine *m/z* 107 (quantifier), *m/z* 192, *m/z* 264 were used. Quantification was conducted by the standard external calibration method following the same procedure for all samples. The detection limits of phenylalanine and tyrosine were 0.35 and 0.05 ng mL$^{-1}$, respectively (Huang et al., 1993; Qiu et al., 2007; Zhao et al., 2017).

## Statistical Analysis

Normality and homoscedasticity of all data sets were checked through the Kolmogorov–Smirnov and Levene tests, respectively (SPSS v.21.0, IBM, Armonk, NY, United States). Body weight and total length values over time were adjusted to a linear equation (best curve fit) by curve estimation regression models (SPSS v.21.0, IBM, Armonk, NY, United States). Differences among curve slopes from weight and length were detected through an ANOVA analysis using treatment (control or supplemented feed) as factor and time as covariate. Differences among treatments (marked fish) were detected through paired-samples T or measures repeated ANOVA tests. Data are expressed as mean ± SEM. The significance level was 0.05.

# RESULTS

## Biometric Parameters

There were no differences in the slope of the length curve in the specimens fed with Phe compared to the control (**Figure 1A**). The slope of the length curve in fish fed tyrosine at basal (Tyr basal) was significantly less than that of fish fed a control diet. Furthermore, the slope of the length curve was less than that of the fish subjected to stress and fed the same amino acid (**Figure 1B**). With respect to weight, the slope of the curve of the specimens fed AA was significantly lower than those fed the control diet both in stress and basal state. Samples fed with AA and subjected to stress showed a significantly greater weight curve than those fed with the same amino acid within the basal state (**Figures 1C,D**).

The fish fed control diet and in the basal state presented higher condition factor than those fed amino acid-enriched diets (**Table 2**). Moreover, fish fed control diet and subjected to stress presented a higher condition factor than those fed amino acid-enriched diets. In the basal state, the specimens fed a diet supplemented with phenylalanine showed a higher hepatosomatic index than those fed control diet. The specific

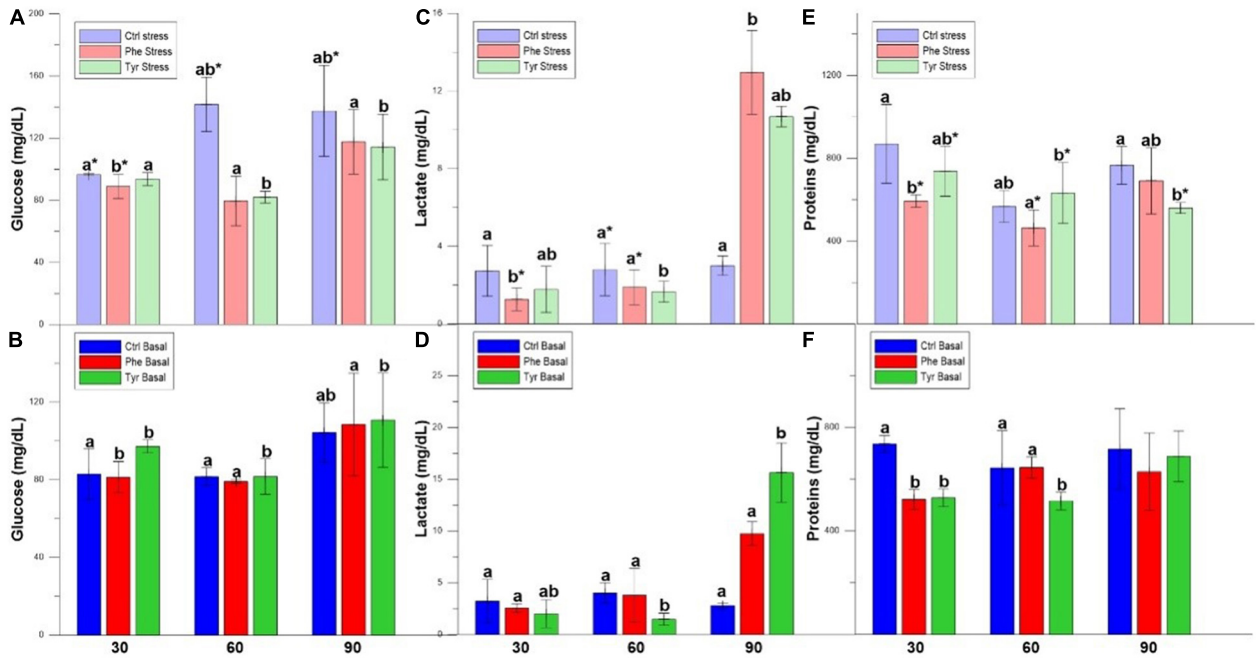


**FIGURE 2 |** Glucose **(A,B)**, lactate **(C,D)**, and proteins **(E,F)** values (mean ± SEM) for the experimental cultures. Different letters indicate significant differences between the different diets. Asterisks indicate significant differences for the same diet between stress and basal.

growth rate did not present any significant difference between any of the experimental group.

## Classical Stress Markers Over Time

After 30 days of feeding, the plasma glucose values were higher in the specimens subjected to stress except for those fed with a diet supplemented with Tyr (**Figure 2A**). Furthermore, the control was significantly different from those fed the amino-acid-supplemented diet (**Figures 2A,B**). In the fish subjected to stress and fed the diet enriched with phenylalanine, lactate was significantly lower compared to the rest of the specimens in the basal state (**Figures 2C,D**). The proteins were significantly higher in the specimens subjected to stress with respect to the basal one, and also in the specimens fed with the control diet with respect to those fed with a diet enriched with AA (**Figures 2E,F**). After 60 days of feeding, the plasma glucose in the fish fed the diet supplemented with tyrosine was significantly different with respect to the other treatments (**Figure 2A**). For lactate and protein, the values for those fed phenylalanine and subjected to stress were different from those fed the same diet at basal. After 90 days, the plasma metabolites of the tyrosine-fed samples were significantly different from the other treatments, except for proteins at basal, where there was no difference.

The plasma cortisol of those specimens subjected to stress did not show significant differences between the control and those fed the diet supplemented with AA at all sampling points. During days 30 and 90, the cortisol values for stressed fish were significantly different when compared with the basal treatment ones for the control diet. In basal state, plasma cortisol in specimens fed the control diet was higher than those fed with AA on day 30. During day 90, this hormone in specimens fed the diet supplemented with phenylalanine were significantly higher than the other treatments (**Figure 3**).

## End-Point Hormone Concentrations

The plasma adrenaline values after 90 days were significantly lower in the specimens fed the diet supplemented with tyrosine for both states (stress and basal). At the end of the experiment, the plasma noradrenaline values in the specimens fed phenylalanine diet, in both states, were significantly different than the other treatments (**Figure 4**).

**Figure 5** shows the catecholamine hormone values in the brain. The adrenaline (**Figure 5A**) and noradrenaline (**Figure 5C**)

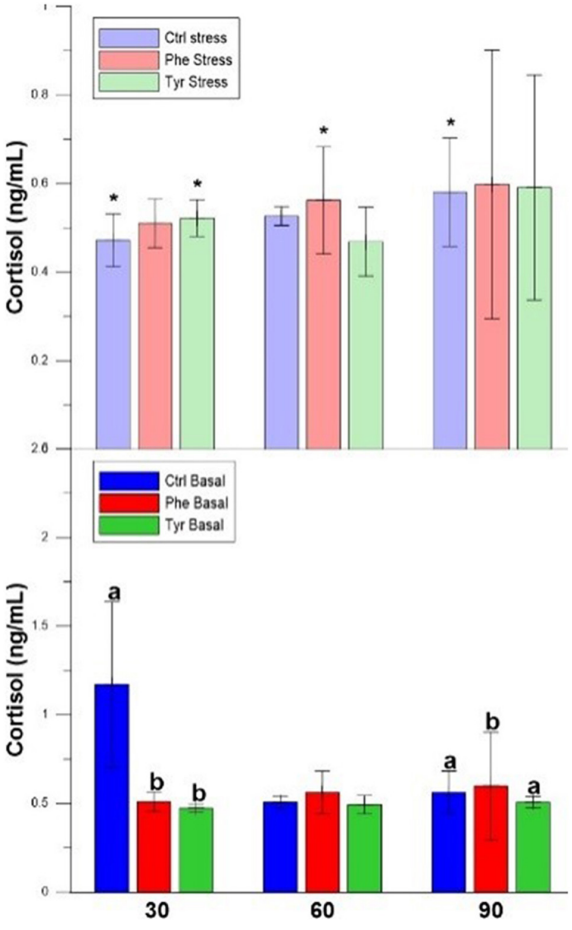


**FIGURE 3 |** Cortisol values for the experimental cultures (mean ± SEM). Different letters indicate significant differences between the different diets. The asterisks indicate significant differences for the same diet between stress and basal.

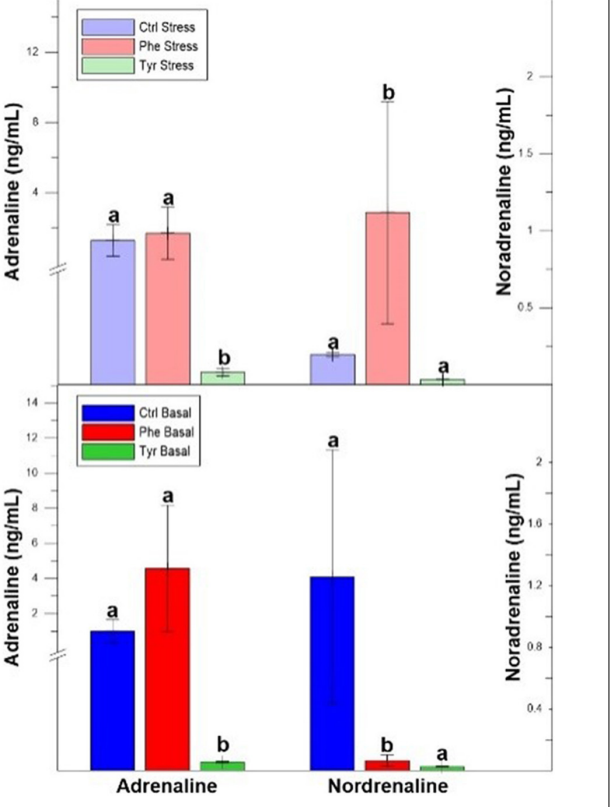


**FIGURE 4 |** Plasma adrenaline and noradrenaline after 90 days values (mean ± SEM). Different letters indicate significant differences between the different diets.

values of the specimens subjected to stress and fed the diet supplemented with tyrosine were significantly higher than those fed the control diets or supplemented with phenylalanine. For noradrenaline (**Figures 5C,D**) and dopamine (**Figures 5E,F**), the specimens fed the diet supplemented with phenylalanine showed significant differences between the stress and basal state. In the basal state, the specimens fed the control diet presented dopamine levels that were higher than the other treatments (**Figure 5F**).

There were significant differences in adrenaline for the head kidney both in stress and basal state, with the concentration of this hormone being higher in those fed Tyr (**Figures 6A,B**). The concentration of noradrenaline in those subjected to stress was higher in those fed with the diet supplemented with Phe

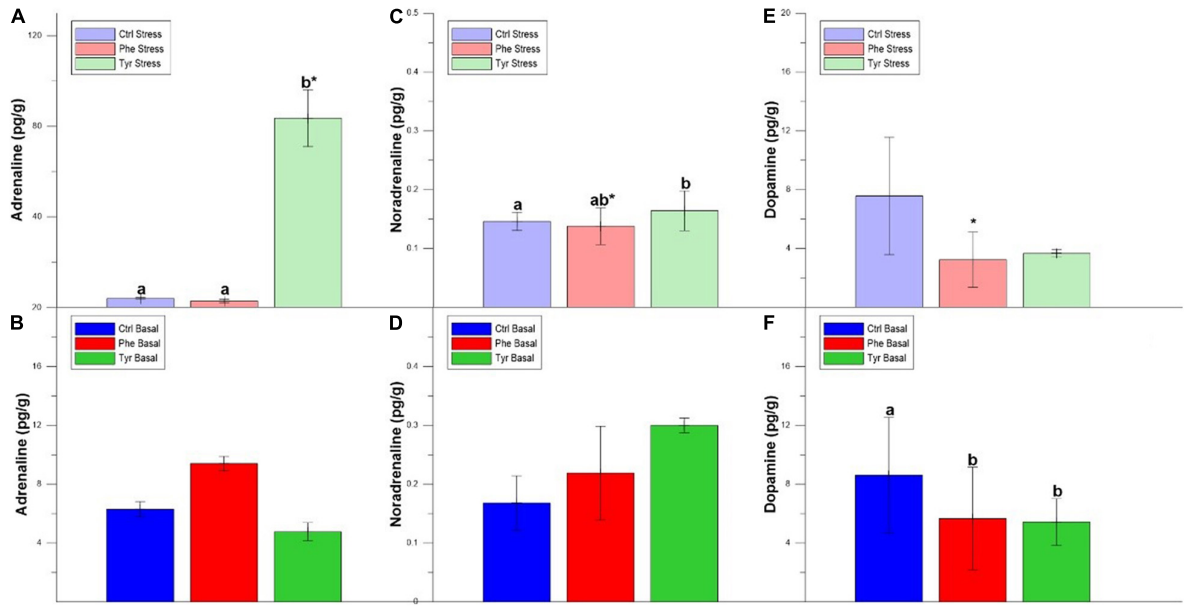


**FIGURE 5 |** Brain adrenaline **(A,B)**, noradrenaline **(C,D)**, and dopamine **(E,F)** values after 90 days (mean ± SEM), per grams of tissue. Different letters indicate significant differences between the different diets. Asterisks indicate significant differences for the same diet between stress and basal.

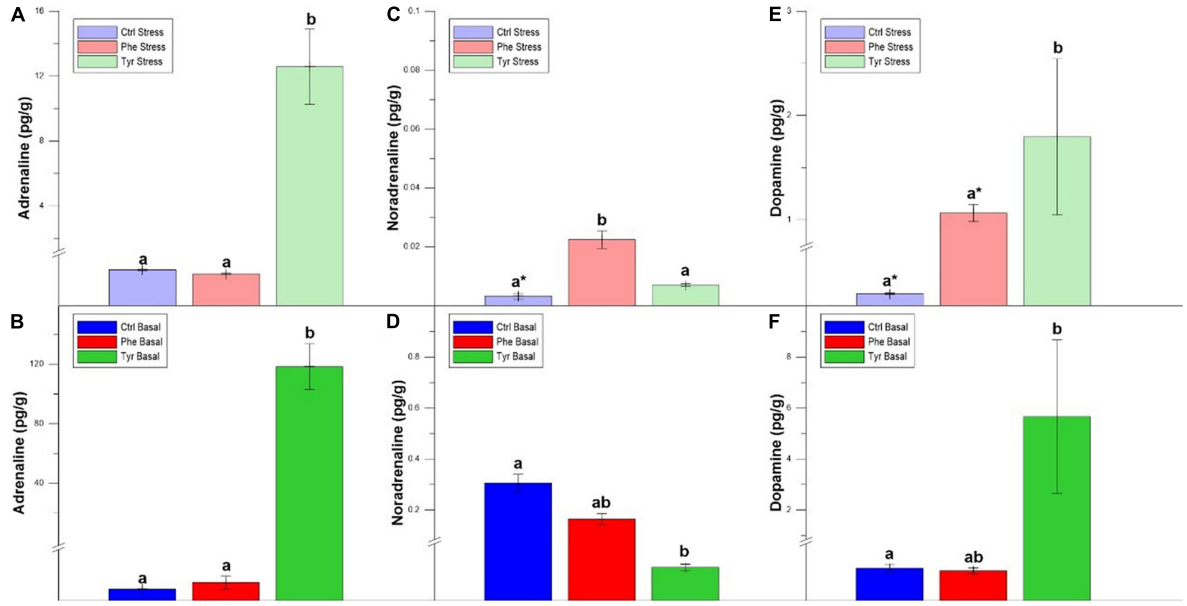


**FIGURE 6 |** Head kidney adrenaline **(A,B)**, noradrenaline **(C,D)**, and dopamine **(E,F)** values after 90 days (mean ± SEM). Different letters indicate significant differences between the different diets. The asterisks indicate significant differences for the same diet between stress and basal.

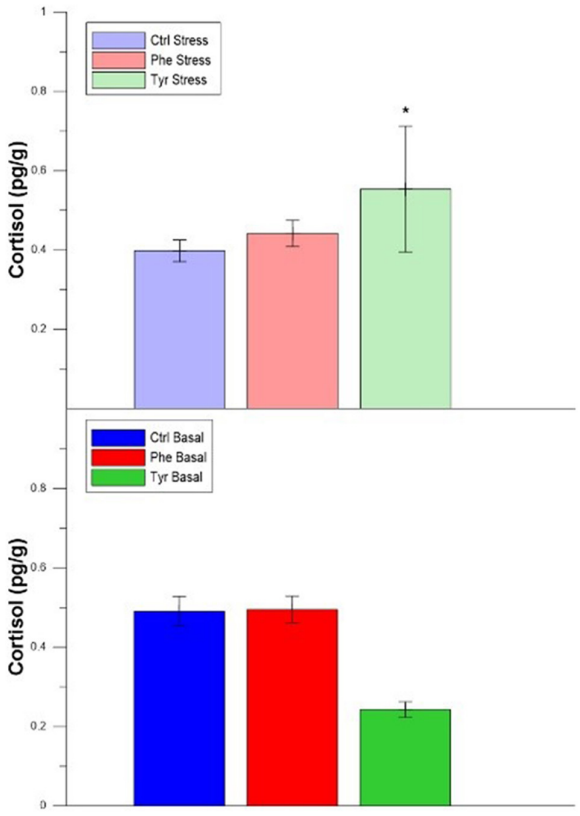


**FIGURE 7 |** Head kidney cortisol after 90 days (mean ± SEM). The asterisks indicate significant differences for the same diet between stress and basal.

compared to the other treatments (**Figure 6C**). However, in those specimens that were not subjected to stress and fed with Tyr, the concentration of this hormone was inferior to the other treatments (**Figure 6D**). The dopamine values in the samples fed with tyrosine were significantly higher than in the rest of the diets for both stress and basal states (**Figures 6E,F**). Furthermore, there were significant differences between stress and basal treatments for fish fed the control diet or the phenylalanine-supplemented diet.

Regarding the cortisol concentration in the head kidney, differences were only detected between stress and basal treatments for fish fed the diet supplemented with tyrosine (**Figure 7**).

## Phenylalanine and Tyrosine Concentration in Tissues

The concentration of Phe in the liver was higher in fish fed the control diet compared to those fed the diet enriched with Phe. In addition, there was a decrease in the liver Phe concentration of the fish subjected to stress compared to the basal within the Phe-supplemented diet (**Figures 8A,B**). The same happened for the liver Tyr concentration in specimens fed the diet enriched with Phe (**Figures 9A,B**). **Figures 8C,D** show the Phe concentration in the muscle, where there was no difference except for fish fed the control diet and where the specimens subjected to stress had a higher Phe concentration. There was no difference in muscle Tyr concentration within any treatment (**Figures 9C,D**). There was no difference in the brain Phe concentration (**Figures 8E,F**). However, there were differences in the brain Tyr concentration for the stressed fish fed the control or Phe-enriched diets compared to those fed the Tyr diet (**Figures 9E,F**).

# DISCUSSION

In our study, Phe and Tyr supplementation in the diet reduced fish growth and biometric parameters, in addition to modulated classical stress markers. It also produced an accumulation of both AA in liver, brain, and muscle that could be limiting to activate some metabolic pathways, since it has been shown that an increase in dietary Tyr decreases the body's Phe requirements (Li et al., 2009).

The effects of dietary supplementation with Tyr and its metabolic products on the stress system and growth has been studied by various authors (Garg, 2007; Herrera et al., 2017; Salamanca et al., 2021). Phe supplementation in the diet has been studied in a few fish species (*Catla catla, Megalobrama ambycephala*, and *Gadus morhua*) (Zehra and Khan, 2014; Ren et al., 2015; Herrera et al., 2016).

According to Garg (2007), an increase in T4 (thyroxine), a product of Tyr metabolism, causes a decrease in body growth parameters. Similarly, Saavedra et al. (2010) showed that an increase in Phe and Tyr supplementation in the diet of white seabream (*D. sargus*) larvae reduced the growth rate. Something similar happened in our study since the specimens fed the Tyr diet showed a decrease in specific growth rate and growth curve slope. The SGR presented a decreasing tendency in non-stressed fish in the Phe-enriched treatment, which may be due to the Tyr formation pathway that was stimulated from Phe (Li et al., 2009). This is supported by other results (see below) since the accumulation of Tyr in the liver in those specimens was higher than the specimens subjected to stress. Moreover, the continuous feeding through an unbalanced diet (amino acid excess) could result in malnutrition and, hence, poor growth (Wu, 2009).

According to Herrera et al. (2016), the concentration of plasma stress markers (glucose, lactate, and proteins) in Atlantic cod (*G. morhua*) fed diets supplemented with Phe high levels presented a significant drop. Our results showed similar patterns since there was a decrease in glucose, lactate, and proteins with respect to the control at all sampling points. Nevertheless, this did not occur in lactate values after 90 days when there was a significant increase in those specimens fed the diet enriched with AA. According to Li et al. (2009), an increase in the amount of Tyr supplied in the body produces a decrease in the Phe requirement, which causes its accumulation. Consequently, our fish could have an excess of Phe that caused the lactate rise, as stated by Schuck et al. (2015) in humans and mice having phenylketonuria (an increased Phe concentration).

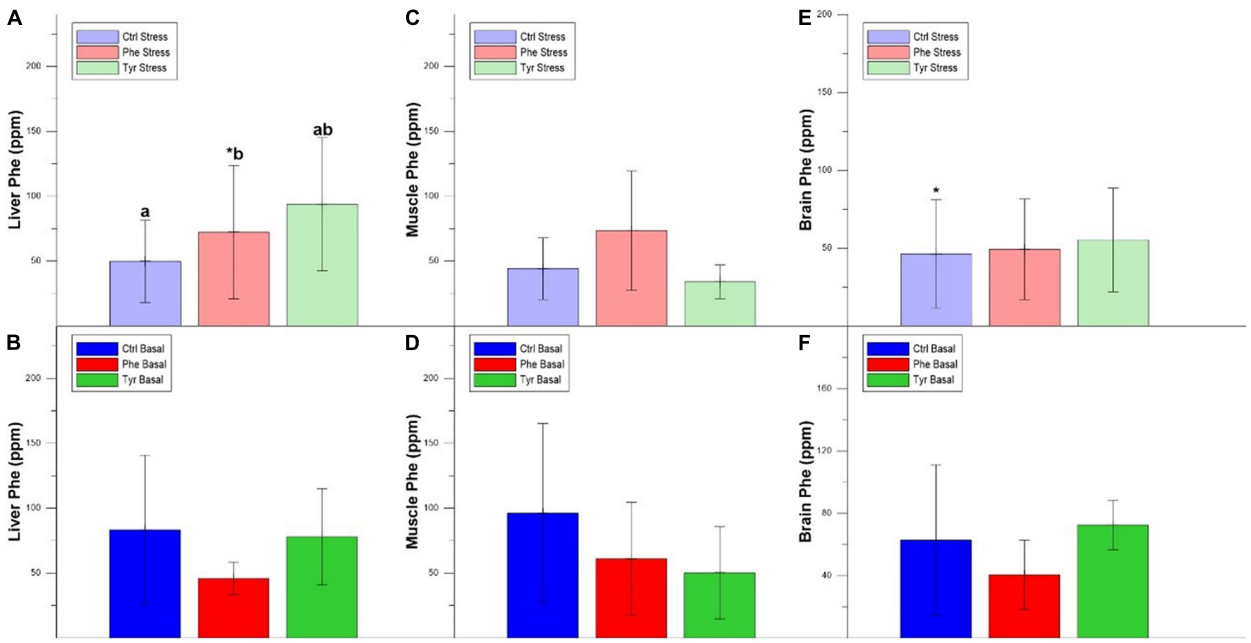


**FIGURE 8 |** Liver Phe stress **(A)**, liver Phe basal **(B)**, muscle Phe stress **(C)**, and muscle Phe basal **(D)**, brain Phe stress **(E)**, and brain Phe basal **(F)** values after 90 days (mean ± SEM). Different letters indicate significant differences between the different diets. The asterisks indicate significant differences for the same diet between stress and basal.

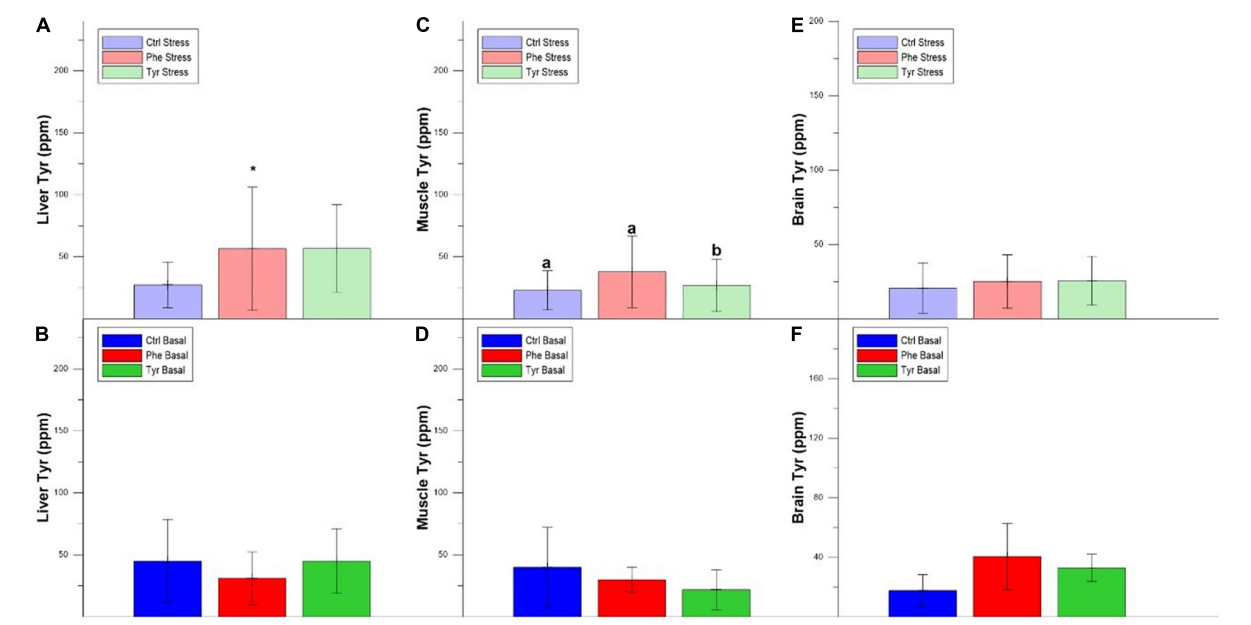


**FIGURE 9 |** Liver Tyr stress **(A)**, liver Tyr basal **(B)**, muscle Tyr stress **(C)** and muscle Tyr basal **(D)**, brain Tyr stress **(E)**, and brain Tyr basal **(F)** values after 90 days (mean ± SEM). Different letters indicate significant differences between the different diets. The asterisk indicates significant differences for the same diet between stress and basal.

Plasma cortisol only showed differences in non-stressed specimens at 30 and 90 days between the control and the specimens fed amino acid diets and between the specimens fed with Phe and with other treatments, respectively. It is probable that enriched foods could attenuate the cortisol increase related to the stress response since it only varied significantly between basal and stress states in the Phe treatment; in this sense, previous studies have demonstrated that the cortisol levels did not show differences in seabreams (*S. aurata*) which were fed with Phe and Tyr supplemented diets (Salamanca et al., 2021). As the

present experiment was based on chronic stress, the absence of cortisol changes after 3 months could have been expectable due to the acclimation of the hypothalamic–pituitary–interrenal (HPI) axis (Montero et al., 1999; Procarione et al., 1999; Haukenes and Barton, 2004; Barton et al., 2005). However, the differences between stressed and non-stressed control fish were evident at the end of the experimental culture, as well as the attenuating effects of the enriched diets.

It has been shown that the supplementation of AA in the diet attenuates stress in *A. regius* and *M. ambycephala* (Ren et al., 2015; Fernández-Alacid et al., 2019). In the present work, this effect produced by Phe and Tyr may be because both the AA are precursors of hormones involved in stress processes, such as adrenaline, noradrenaline, and dopamine (Zehra and Khan, 2014). However, Salamanca et al. (2021) did not detect significant differences in plasma adrenaline and noradrenaline in seabreams fed amino acid supplements. These differences may be because the fish were fed for a short period of time (7 days) in that work, as opposed to the 90 days of feeding in our experiment.

The stress response involves the recognition of a threat by the central nervous system, with a rapid increase in plasma catecholamines (Reid et al., 1998; Gallo and Civinini, 2003). In turn, the activation of these endocrine pathways is derived from changes in the plasma and tissue metabolites to cope with the energy imposed by the stressor. In teleost fish, the activity of the HPI axis, involved in the stress response, is stimulated by noradrenaline (Höglund et al., 2000; Li et al., 2009).

In our stress condition, plasma adrenaline and noradrenaline values were higher in those specimens fed the Phe-supplemented diet. It has been reported that there is an inverse relationship between Phe concentration and norepinephrine and dopamine values (Güttler and Lou, 1986). In fact, the increase of Phe concentration in the diet decreased the concentration of catecholamine hormones in plasma, since increasing the concentration of this amino acid in the blood favors its passage through the blood–brain barrier compared to other AA, including tyrosine, hence, the synthesis of catecholamines is not stimulated (Salamanca et al., 2021). However, this did not occur in the present study. This may be due to the fact that, when feeding for a long period with Phe-enriched diets, this amino acid is catabolized to Tyr, which causes the catecholamine hormone formation pathway to be stimulated. Furthermore, in our work, this favored the accumulation of Tyr in the different tissues. The brain adrenaline and noradrenaline concentrations were slightly higher in those specimens fed Tyr-enriched diets. In this sense, the accumulation of Tyr in brain could have enhanced the catecholamine formation (Damasceno-Oliveira et al., 2007).

An increase in adrenaline and dopamine concentrations occurred in the head kidney, which also could be due to the increase in the concentration of Tyr in this tissue (Damasceno-Oliveira et al., 2007). The level of dopamine present in the head kidney of seabream was higher in the diet supplemented with Tyr; hence this amino acid enhanced this hormonal response, since Tyr seems to be limiting for the production of the catecholamine hormones (Cotoia et al., 2014). According to Øverli et al. (1999) and Höglund et al. (2001), an increase in L-Dopa (precursor of dopamine) enhanced the plasma cortisol in Arctic char (*Salvelinus alpinus*). In this sense, in our study there was a cortisol increase in the head kidney of fish fed the diet supplemented with Tyr and subjected to stress, coinciding with a dopamine raise in this tissue.

## CONCLUSION

In conclusion, to our knowledge, this is the first work on the effects of the Phe- or Tyr-enriched diets on the response to chronic stress in fish. Both the AA altered the stress response and the zootechnical parameters in the seabream (*S. aurata*). The hormonal stress markers were significantly attenuated in different tissues. Nevertheless, the experimental diets could decrease the growth parameters due to the unbalanced formulation (amino acid excess) and the long feeding time. Therefore, it is highly probable that this type of feed supplements should be applied in short-time basis, just before a stressing condition, as previously assayed in previous works. Future research should be focused on finding a balanced diet, including nutritional supplements for long-term feeding which does not affect growth and, in addition, improve the chronic stress response. In addition, this research line could study the inclusion of both AA for detecting synergistic or antagonistic effect.

## DATA AVAILABILITY STATEMENT

The original contributions presented in the study are included in the article/supplementary material, further inquiries can be directed to the corresponding author.

## ETHICS STATEMENT

The animal study was reviewed and approved by REGA Code ES210210000303.

## AUTHOR CONTRIBUTIONS

NS and MH: methodology. IG and EM: software and formal analysis. IR: resources. NS: writing – original draft preparation. NS, OM, IG, EM, IR, and MH: writing – review and editing. MH: supervision and project administration. MH and OM: funding acquisition. All authors have read and agreed to the published version of the manuscript.

## FUNDING

This research was funded by the projects INIA RTA2015-00025-C03-01 and 0750_AQUA_AMBI_2_5_P (INTERREG VA). MH and NS belong to the Fish Welfare and Stress Network (AGL2016-81808-REDT), supported by the Agencia Estatal de Investigación (AEI, MICINN, Spanish Government). NS's predoc contract is confinanced by the European Social Fund (FSE) through the call "Ayudas para contratos predoctorales para la formación de doctores 2017" from the AEI.

## REFERENCES


AGAPA (2019). *La Acuicultura Marina en Andalucía 2018; Agencia de Gestión Agraria y Pesquera de Andalucía; Consejería de Agricultura, Ganadería, Pesca y Desarrollo Sostenible*. Sevilla: España.

Andersen, S. M., Waagbø, R., and Espe, M. (2016). Functional amino acids in fish health and welfare. *Front. Bio.* 8:143–169.doi: 10.2741/757

APROMAR (2020). *La acuicultura en España 2020*. Spain: Asociación de empresas de acuicultura.

Arends, R. J., Mancera, J. M., Munoz, J. L., Bonga, S. W., and Flik, G. (1999). The stress response of the gilthead sea bream (*Sparus aurata L.*) to air exposure and confinement. *J. Endocrinol.* 163, 149. doi: 10.1677/joe.0.1630149

Banderet, L. E., and Lieberman, H. R. (1989). Treatment with tyrosine, a neurotransmitter precursor, reduces environmental stress in humans. *Brain Res. Bull.* 22, 759–762. doi: 10.1016/0361-9230(89)90096-8

Barton, B. A. (2002). Stress in fishes: a diversity of responses with particular reference to changes in circulating corticosteroids. *Integ. Com. Bio.* 42, 517–525. doi: 10.1093/icb/42.3.517

Barton, B. A., Morgan, J. D., and Vijayan, M. M. (2002). *Physiological and condition-related indicators of environmental stress in fish. Biological indicators of aquatic ecosystem stress*. Bethesda: American Fisheries Society, 111–148.

Barton, B. A., Ribas, L., Acerete, L., and Tort, L. (2005). Effects of chronic confinement on physiological responses of juvenile gilthead sea bream, Sparus aurata L., to acute handling. *Aquac. Res.* 36, 172–179.

Brady, K., Brown, J. W., and Thurmond, J. B. (1980). Behavioral and neurochemical effects of dietary tyrosine in young and aged mice following cold-swim stress. *Pharmacol. Biochem. Behav.* 12, 667–674. doi: 10.1016/0091-3057(80)90146-x

Cotoia, A., Scrima, R., Gefter, J. V., Piccoli, C., Cinnella, G., Dambrosio, M., et al. (2014). p-Hydroxyphenylpyruvate, an intermediate of the Phe/Tyr catabolism, improves mitochondrial oxidative metabolism under stressing conditions and prolongs survival in rats subjected to profound hemorrhagic shock. *PLoS One* 9:e90917. doi: 10.1371/journal.pone.0090917.

Damasceno-Oliveira, A., Fernández-Durán, B., Gonçalves, J., Serrão, P., Soares-da-Silva, P., Reis-Henriques, M. A., et al. (2007). Effects of cyclic hydrostatic pressure on the brain biogenic amines concentrations in the flounder, Platichthys flesus. *Gen. Comp. Endocrinol.* 153, 385–389. doi: 10.1016/j.ygcen.2007.05.017

Feidantsis, K., Pörtner, H. O., Lazou, A., Kostoglou, B., and Michaelidis, B. (2009). Metabolic and molecular stress responses of the gilthead seabream Sparus aurata during long-term exposure to increasing temperatures. *Mar. Biol.* 156, 797–809. doi: 10.1186/1471-2164-15-765

Fernández-Alacid, L., Sanahuja, I., Ordóñez-Grande, B., Sánchez-Nuño, S., Herrera, M., and Ibarz, A. (2019). Skin mucus metabolites and cortisol in meagre fed acute stress-attenuating diets: correlations between plasma and mucus. *Aquaculture* 499, 185–194. doi: 10.1016/j.aquaculture.2018.09.039

Gallo, V. P., and Civinini, A. (2003). Survey of the adrenal homolog in teleosts. *Int. Rev. Cytol.* 230, 89–187. doi: 10.1016/s0074-7696(03)30003-8

Garg, S. K. (2007). Effect of oral administration of l-thyroxine (T 4) on growth performance, digestibility, and nutrient retention in Channa punctatus (Bloch) and *Heteropneustes fossilis* (Bloch). *Fish Physiol. Biochem.* 33, 347–358. doi: 10.1007/s10695-007-9166-1

Gonzalez-Silvera, D., Herrera, M., Giráldez, I., and Esteban, Á (2018). Effects of the dietary tryptophan and aspartate on the immune response of meagre (*Argyrosomus regius*) after stress. *Fishes* 3, 6.

Güttler, F., and Lou, H. (1986). Dietary problems of phenylketonuria: effect on CNS transmitters and their possible role in behaviour and neuropsychological function. *J. Inherit. Metab. Dis.* 9, 169–177. doi: 10.1007/BF01799701

Haukenes, A. H., and Barton, B. A. (2004). Characterization of the cortisol response following an acute challenge with lipopolysaccharide in yellow perch and the influence of rearing density. *J. Fish Biol.* 64, 851–862. doi: 10.1111/j.1095-8649.2004.00354.x

Herrera, M., Aragão, C., Hachero, I., Ruiz-Jarabo, I., Vargas-Chacoff, L., Mancera, J. M., et al. (2012). Physiological short-term response to sudden salinity change in the Senegalese sole (*Solea senegalensis*). *Fish Physiol. Biochem.* 38, 1741–1751. doi: 10.1007/s10695-012-9671-8

Herrera, M., Fernández-Alacid, L., Sanahuja, I., Ibarz, A., Salamanca, N., Morales, E., et al. (2020). Physiological and metabolic effects of a tryptophan-enriched diet to face up chronic stress in meagre (*Argyrosomus regius*). *Aquaculture* 522, 735102. doi: 10.1016/j.aquaculture.2020.735102

Herrera, M., Herves, M. A., Giráldez, I., Skar, K., Mogren, H., Mortensen, A., et al. (2017). Effects of amino acid supplementations on metabolic and physiological parameters in Atlantic cod (*Gadus morhua*) under stress. *Fish Physiol. Biochem.* 43, 591–602. doi: 10.1007/s10695-016-0314-3

Herrera, M., Miró, J. M., Giráldez, I., Salamanca, N., Martos-Sitcha, J. A., Mancera, J. M., et al. (2019). Metabolic and stress responses in Senegalese soles (*Solea senegalensis Kaup*) fed tryptophan supplements: effects of concentration and feeding period. *Animals* 9, 320. doi: 10.3390/ani9060320

Herrera, M., Rodiles, A., Sánchez, B., López, J. M., and de La Roca, E. (2016). Physiological stress responses to captivity in early developmental stages of the wedge sole Dicologoglossa cuneata (*Moreau*). *Aquac. Res.* 47, 732–740.

Höglund, E., Balm, P. H., and Winberg, S. (2000). Skin darkening, a potential social signal in subordinate arctic charr (*Salvelinus alpinus*): the regulatory role of brain monoamines and pro-opiomelanocortin-derived peptides. *J. Exp. Biol.* 203, 1711–1721. doi: 10.1242/jeb.203.11.1711

Höglund, E., Kolm, N., and Winberg, S. (2001). Stress-induced changes in brain serotonergic activity, plasma cortisol and aggressive behavior in Arctic charr (*Salvelinus alpinus*) is counteracted by L-DOPA. *Physiol. Behave.* 74, 381–389. doi: 10.1016/s0031-9384(01)00571-6

Hoseini, S. M., Hedayati, A., and Ghelichpour, M. (2014). Plasma metabolites, ions and thyroid hormones levels, and hepatic enzymes× activity in Caspian roach (*Rutilus rutilus caspicus*) exposed to waterborne manganese. *Ecotoxicol. Environ. Saf.* 107, 84–89. doi: 10.1016/j.ecoenv.2014.05.002

Hoseini, S. M., Taheri Mirghaed, A., and Yousefi, M. (2019). Application of herbal anaesthetics in aquaculture. *Rev. Aquac.* 11, 550–564. doi: 10.1080/15548627.2020.1797280

Huang, Z. H., Wang, J., Gage, D. A., Watson, J. T., Sweeley, C. C., and HuSek, P. (1993). Characterization of N-ethoxycarbonyl ethyl esters of amino acids by mass spectrometry. *J. Chromatogr.* 635, 271–281. doi: 10.1016/0021-9673(93)80370-n

Iwama, G. K., Afonso, L. O. B., and Vijayan, M. M. (2006). "Stress in fish," in *Physiology of fishes*, eds D. H. Evans, and J. B. Claiborne, (Boca Raton: CRC press), 320–342.

Jerez-Cepa, I., Fernández-Castro, M., Del Santo, O., Neill, T. J., Martos-Sitcha, J. A., Martínez-Rodríguez, G., et al. (2019). Transport and recovery of gilthead seabream (*Sparus aurata* L.) sedated with clove oil and MS-222: effects on stress axis regulation and intermediary metabolism. *Front. Physiol.* 10:612.doi: 10.3389/fphys.2019.00612

LeBlanc, S., Höglund, E., Gilmour, K. M., and Currie, S. (2012). Hormonal modulation of the heat shock response: insights from fish with divergent cortisol stress responses. *Am. J. Physiol.* 302, R184–R192. doi: 10.1152/ajpregu.00196.2011

LeBlanc, S., Middleton, S., Gilmour, K. M., and Currie, S. (2011). Chronic social stress impairs thermal tolerance in the rainbow trout (*Oncorhynchus mykiss*). *J. Exp. Biol.* 214, 1721–1731. doi: 10.1242/jeb.056135

Lehnert, H., Reinstein, D. K., Strowbridge, B. W., and Wurtman, R. J. (1984). Neurochemical and behavioral consequences of acute, uncontrollable stress: effects of dietary tyrosine. *Brain Res.* 303, 215–223. doi: 10.1016/0006-8993(84)91207-1

Li, P., Mai, K., Trushenski, J., and Wu, G. (2009). New developments in fish amino acid nutrition: towards functional and environmentally oriented aquafeeds. *Amino Acids* 37, 43–53. doi: 10.1007/s00726-008-0171-1

Martos-Sitcha, J. A., Wunderink, Y. S., Straatjes, J., Skrzynska, A. K., Mancera, J. M., and Martínez-Rodríguez, G. (2014). Different stressors induce differential responses of the CRH-stress system in the gilthead sea bream (*Sparus aurata*). *Com. Biochem. Phys. A* 177, 49–61. doi: 10.1016/j.cbpa.2014.07.021

Montero, D., Izquierdo, M. S., Tort, L., Robaina, L., and Vergara, J. M. (1999). High stocking density produces crowding stress altering some physiological and biochemical parameters in gilthead seabream, *Sparus aurata*, juveniles. *Fish Physiol. Biochem.* 20, 53–60.

Øverli, Ø, Harris, C. A., and Winberg, S. (1999). Short-term effects of fights for social dominance and the establishment of dominant-subordinate relationships on brain monoamines and cortisol in rainbow trout. *Brain Behav. Evol.* 54, 263–275. doi: 10.1159/000006627

Procarione, L. S., Barry, T. P., and Malison, J. A. (1999). Effects of high rearing densities and loading rates on the growth and stress responses of juvenile

rainbow trout. *N. Am. J. Aquacult.* 61, 91–96. doi: 10.1577/1548-8454(1999)061<0091:eohrda>2.0.co;2

Qiu, Y., Su, M., Liu, Y., Chen, M., Gu, J., Zhang, J., et al. (2007). Application of ethyl chloroformate derivatization for gas chromatography–mass spectrometry based metabonomic profiling. *Anal. Chimic. Acta* 583, 277–283. doi: 10.1016/j.aca.2006.10.025

Reid, S. G., Bernier, N. J., and Perry, S. F. (1998). The adrenergic stress response in fish: control of catecholamine storage and release. *Com. Biochem. Physiol. C* 120, 1–27. doi: 10.1016/s0742-8413(98)00037-1

Ren, M., Liu, B., Habte-Tsion, H. M., Ge, X., Xie, J., Zhou, Q., et al. (2015). Dietary phenylalanine requirement and tyrosine replacement value for phenylalanine of juvenile blunt snout bream, *Megalobrama amblycephala*. *Aquaculture* 442, 51–57.

Rodiles, A., Herrera, M., Hachero-Cruzado, I., Ruiz-Jarabo, I., Mancera, J. M., Cordero, M. L., et al. (2015). Tissue composition, blood biochemistry and histology of digestive organs in Senegalese sole (*Solea senegalensis*) juveniles fed diets containing different plant protein ingredients. *Aqua. Nutr.* 21, 767–779.

Ross, L. G., and Ross, B. (2008). *Anaesthetic and Sedative Techniques for Aquatic Animals*. Hoboken, NJ: John Wiley & Sons.

Saavedra, M., Conceição, L. E., Barr, Y., Helland, S., Pousão-Ferreira, P., Yúfera, M., et al. (2010). Tyrosine and phenylalanine supplementation on *Diplodus sargus* larvae: effect on growth and quality. *Aquac. Res.* 41, 1523–1532.

Salamanca, N., Giráldez, I., Morales, E., de La Rosa, I., and Herrera, M. (2021). Phenylalanine and Tyrosine as Feed Additives for Reducing Stress and Enhancing Welfare in Gilthead Seabream and Meagre. *Animals* 11:45. doi: 10.3390/ani11010045

Salamanca, N., Morales, E., Ruiz-Azcona, P., and Herrera, M. (2020). Endocrine and metabolic effects of Trp-enriched diets for attenuation of chronic stress in the Senegal soles (*Solea senegalensis*). *Aquaculture* 523:735173. doi: 10.1016/j.aquaculture.2020.735173

Schuck, P. F., Malgarin, F., Cararo, J. H., Cardoso, F., Streck, E. L., and Ferreira, G. C. (2015). Phenylketonuria pathophysiology: on the role of metabolic alterations. *Aging Disease* 6:390. doi: 10.14336/AD.2015.0827

Shafik, M., Ibrahime, H., Elyazeid, I. A., Abass, O., and Saad, H. M. (2014). The stress of phenylalanine on rats to study the phenylketonuria at biochemical and molecular level. *J. Appl. Pharm. Sci.* 4, 24–29.

Teletchea, F. (2015). Domestication of marine fish species: update and perspectives. *J. Mar. Sci. Eng.* 3, 1227–1243. doi: 10.3390/jmse3041227

Vanderzwalmen, M., Eaton, L., Mullen, C., Henriquez, F., Carey, P., Snellgrove, D., et al. (2018). The use of feed and water additives for live fish transport. *Rev. Aquac.* 11, 263–278. doi: 10.1038/s41598-019-39316-w

Wu, G. (2009). Amino acids: metabolism, functions, and nutrition. *Amino Acids* 37, 1–17. doi: 10.1007/s00726-009-0269-0

Zahl, I. H., Samuelsen, O., and Kiessling, A. (2012). Anaesthesia of farmed fish: implications for welfare. *Fish Physiol. Biochem.* 38, 201–218. doi: 10.1007/s10695-011-9565-1

Zehra, S., and Khan, M. A. (2014). Dietary phenylalanine requirement and tyrosine replacement value for phenylalanine for fingerling *Catla catla* (Hamilton). *Aquaculture* 433, 256–265. doi: 10.1016/j.aquaculture.2014.06.023

Zhao, L., Ni, Y., Su, M., Li, H., Dong, F., Chen, W., et al. (2017). High throughput and quantitative measurement of microbial metabolome by gas chromatography/mass spectrometry using automated alkyl chloroformate derivatization. *Anal. Chem.* 89, 5565–5577. doi: 10.1021/acs.analchem.7b00660

**Conflict of Interest:** The authors declare that the research was conducted in the absence of any commercial or financial relationships that could be construed as a potential conflict of interest.

**Publisher's Note:** All claims expressed in this article are solely those of the authors and do not necessarily represent those of their affiliated organizations, or those of the publisher, the editors and the reviewers. Any product that may be evaluated in this article, or claim that may be made by its manufacturer, is not guaranteed or endorsed by the publisher.

frontiers in Physiology

ORIGINAL RESEARCH
published: 02 March 2022
doi: 10.3389/fphys.2022.781519

# Cohabitation With Atlantic Salmon (*Salmo salar*) Affects Brain Neuromodulators But Not Welfare Indicators in Lumpfish (*Cyclopterus lumpus*)

*Fredrik R. Staven[1,2]*, Manuel Gesto[3], Martin H. Iversen[1], Per Andersen[2], Deepti M. Patel[1], Jarle T. Nordeide[1] and Torstein Kristensen[1]*

*[1] Faculty of Biosciences and Aquaculture, Nord University, Bodø, Norway, [2] Department of Research and Development, Aqua Kompetanse AS, Flatanger, Norway, [3] Section for Aquaculture, Technical University of Denmark, Hirtshals, Denmark*

Lumpfish are utilized to combat ectoparasitic epidemics in salmon farming. Research gaps on both cleaning behavior and client preferences in a natural environment, emphasizes the need to investigate the physiological impacts on lumpfish during cohabitation with piscivorous Atlantic salmon. Lumpfish (39.9 g, S.D ± 8.98) were arranged in duplicate tanks (*n* = 40 per treatment) and exposed to Live Atlantic salmon (245.7 g, S.D ± 25.05), salmon Olfaction or lifelike salmon Models for 6 weeks. Growth and health scores were measured every second week. In addition, the final sampling included measurements of neuromodulators, body color, and plasma cortisol. A stimulation and suppression test of the hypothalamic-pituitary-interrenal (HPI) axis was used for chronic stress assessment. Results showed that growth, health scores, and body color remained unaffected by treatments. Significant reductions in levels of brain dopamine and norepinephrine were observed in Live compared to Control. Plasma cortisol was low in all treatments, while the stimulation and suppression test of the HPI axis revealed no indications of chronic stress. This study presents novel findings on the impact on neuromodulators from Atlantic salmon interaction in the lumpfish brain. We argue that the downregulation of dopamine and norepinephrine indicate plastic adjustments to cohabitation with no negative effect on the species. This is in accordance with no observed deviations in welfare measurements, including growth, health scores, body color, and stress. We conclude that exposure to salmon or salmon cues did not impact the welfare of the species in our laboratory setup, and that neuromodulators are affected by heterospecific interaction.

**Keywords: lumpfish, Atlantic salmon, cleaner fish, aquaculture, welfare, neuromodulators, habituation**



***Edited by:***
*Marce Herrera,*
*IFAPA Centro Agua del Pino, Spain*

***Reviewed by:***
*William G. Willmore,*
*Carleton University, Canada*
*Natalia Salamanca,*
*IFAPA Centro Agua del Pino, Spain*

****Correspondence:***
*Fredrik R. Staven*
*fredrik@aqua-kompetanse.no*

***Specialty section:***
*This article was submitted to Aquatic Physiology, a section of the journal Frontiers in Physiology*

***Received:*** *22 September 2021*
***Accepted:*** *27 January 2022*
***Published:*** *02 March 2022*

***Citation:***
*Staven FR, Gesto M, Iversen MH, Andersen P, Patel DM, Nordeide JT and Kristensen T (2022) Cohabitation With Atlantic Salmon (Salmo salar) Affects Brain Neuromodulators But Not Welfare Indicators in Lumpfish (Cyclopterus lumpus). Front. Physiol. 13:781519. doi: 10.3389/fphys.2022.781519*

## INTRODUCTION

The presence of predators induces multiple behavioral and physiological responses in prey animals. Among teleost fish, such responses involve freezing, fight, or flight; each strategy or a mix of strategies aimed at enhancing the likelihood for survival (Eaton et al., 1977; Clinchy et al., 2013; Rupia et al., 2016). Recognition of potential predators can be inherited and entails adapted systems

for both sensory detection and defensive responses to external threats (Brown and Godin, 1999; Berejikian et al., 2003; Brown, 2003). Both olfaction and vision are essential sensory detection systems in aquatic prey fish, due to variable turbidity and light conditions in the environment (Chivers and Smith, 1998; Ferrari et al., 2010). For a prey fish, the time spent on high alert is time lost on fitness-related activities such as foraging and reproduction (Schreck, 2010). As a counter mechanism, habituation and threat-sensitive predator avoidance occur through plastic cognitive development when physiological and behavioral mechanisms are altered to no longer respond to a repeated non-specific risk (Brown et al., 2006; Rankin et al., 2009). A textbook example of adaptive plasticity to predators is observed among cleaner fish. Cleaner fish are specialized in the removal of ectoparasites from other fish, here called clients. Natural selection on habituation to client interactions have earned cleaner fish unique access to both parasite food items and nipping of nutrient rich skin mucus, delicately balancing mutualism over parasitism (Grutter, 1999; Bshary, 2001; Gingins et al., 2017). The behavioral approach sometimes involves cleaner fish signaling to the client fish, who respond with a non-aggressive behavior before parasites are removed (Grutter, 2004). In a cleaner fish–client fish interaction, the importance of habituation might thus seem apparent. To access ectoparasites, cleaners can approach much larger predator clients and perform behaviors most perilous, such as entering the clients mouth cavity in search of food items (Brown and Godin, 1999; Bshary and Würth, 2001).

In Atlantic salmon (*Salmo salar*) aquaculture, certain wrasse species (Labridae) and lumpfish (*Cyclopterus lumpus*) are utilized as cleaner fish to combat ectoparasites (Bjordal, 1990; Imsland et al., 2014a; Blanco Gonzalez and de Boer, 2017). Failing to control epidemics of the sea lice copepod *Lepheophteirus salmonis* have both economic and environmental consequences (Costello, 2009; Torrissen et al., 2013; Øverli et al., 2014). Today, one of the most common species of cleaner fish used in Atlantic salmon farming is lumpfish (Powell et al., 2017). Studies in commercial large-scale sea cages with Atlantic salmon, revealed significant reductions in sea lice numbers when juvenile lumpfish were added, where 13–36% of the lumpfish stock had sea lice in their stomach (Eliasen et al., 2018; Imsland et al., 2018a). Why sea lice grazing on Atlantic salmon is not homogeneous among all lumpfish individuals is uncertain, but variation between family strains have been observed (Imsland et al., 2016a). Ontogeny is also relevant for sea lice consumption, where small individuals (20–50 g) have been observed with a higher total count of sea lice in their stomach (Imsland et al., 2016b; Eliasen et al., 2018). With individual variation in behavior, it is thus relevant to assess physiological mechanisms involved in social situations.

The main challenges of using lumpfish in aquaculture are high mortality rates and the maintenance of good welfare during the commercial sea phase together with Atlantic salmon. It is necessary to investigate each part of the puzzle related to increased mortality in the myriad of stressors capable of impeding the resting state of lumpfish. One such stressor is social interaction with Atlantic salmon and the ability to habituate to the presence of a larger, potentially predatory, species. Whether lumpfish has been documented to be predated upon by Atlantic salmon in a commercial fish farm is uncertain. Nonetheless, Imsland et al. (2014b) observed no antagonistic behavior during cohabitation with the two species. While cleaner-client behavioral interactions have been documented for decades in aquaculture (Bjordal, 1990), including almost 10 years of research on lumpfish (Imsland et al., 2014a), knowledge gaps still exist on the underlying mechanisms that regulate sea lice grazing. Recently, the neurobiological, and neuro-molecular mechanisms involved in interspecific interaction have been investigated in other cleaner fish species (Soares, 2017; Ramírez-Calero et al., 2021). These novel approaches have accentuated the role of neuromodulators in social contexts (Soares et al., 2012, 2017; Paula et al., 2015; de Abreu et al., 2018, 2020). Neurotransmitters of relevance are dopamine, which influence Bluestreak wrasse (*Labroides dimidiatus*) learning capacity in cooperative investment, and time spent in physical contact with clients (Messias et al., 2016a, b; Soares et al., 2017). Serotonin has multiple roles including regulation of hypothalamic-pituitary-interrenal (HPI) activity in teleost fish, cleaner fish social stress, cooperation, and learning (Winberg et al., 1997; Paula et al., 2015; Soares et al., 2016; Winberg and Thörnqvist, 2016; Backström and Winberg, 2017). A third neurotransmitter, associated with acute stress in multiple species of fish, as reviewed by Gamperl et al. (1994) is norepinephrine. The role of norepinephrine in association with cleaner fish behavior and physiological change to client interaction is nonetheless undetermined.

Individual variation in wild parental brood fish during rearing, and a breeding program in early development, both emphasize the importance of investigating lumpfish responses to Atlantic salmon. While acute responses in lumpfish exposed to Atlantic salmon or salmon sensory cues have been investigated to evaluate behavioral and physiological plasticity (Staven et al., 2019, 2021), the following study aimed to investigate how lumpfish responded to the presence of Atlantic salmon or salmon sensory cues over a period of 6 weeks. We measured physiological parameters relevant to stress and habituation including (1) growth, (2) health score assessment, (3) body color, (4) neurotransmitters, and (5) HPI axis responses.

# MATERIALS AND METHODS

## Ethics Statement

Use of research animals was accepted for experimental purposes by the Norwegian Food Safety Authority (FDU #17231). Animals were carefully handled based on the Norwegian law on Regulation of Animal Experimentation (FOR-1996-01-15-23). Personnel involved were certified with FELASA-C, developed by the Federation of European Laboratory Animal Science Association. The experiment was conducted based on the three R's and the ARRIVE guidelines (Kilkenny et al., 2010).

## Research Animals and Tagging

### Lumpfish

Lumpfish used in the study originated from wild mature lumpfish captured in Troms and Finnmark county, Norway. Milt and roe

were collected, fertilized, hatched, and reared from February 2018 at Mørkvedbukta AS. Lumpfish were fed with pellets based on standard recommendations given by a commercial feed producer (Skretting, Stavanger, Norway). All lumpfish were vaccinated with AMarine micro 4-2® (Pharmaq, Overhalla, Norway) and given 300 day-degrees immunization before they were transferred to the Mørkvedbukta research station. Lumpfish used were juvenile individuals with low gonadal development, indicating no maturation. Lumpfish were tagged 1 week prior to experiment start with Floy tag t-bars (Floy Tag and Mfg Inc., Seattle, WA, United States). Tags were attached in the dorsal crest using a t-bar pistol after fish had been anesthetized with 100 mg $l^{-1}$ benzocaine (ACD Pharmaceuticals, Leknes, Norway) based on recommendations in Skår et al. (2017).

### Atlantic Salmon

Atlantic salmon used in the study were produced from an 11th generation Aquagen strain, hatched at Sundsfjord Smolt AS in Nordland, Norway. Smolts were transported to Mørkvedbukta research station in Bodø during the spring of 2017. At the station, feeding was conducted in same manners as later during the experiment. This included the use of automatic feeders (Arvo-Tec Oy, Huutokoski, Finland) containing Gemma diamond 150 (Skretting, Stavanger, Norway) split across three dosages adding up to a daily amount of 2% biomass. A total of eight Atlantic salmon (246.7 g, S.D ± 25.50) were used in the experiment and had no previous experience with lumpfish.

## Experimental Preparation

On the first day of the experiment (October 30, 2018), 160 lumpfish (39.7 g, S.D ± 8.99) were morphologically measured (see section "Growth"), photographed (see section "Skin Coloration"), and health assessed (see section "Health Assessment"). Next, lumpfish were randomly distributed in eight gray tank units (1 × 1 × 1 m, 480 L) with lids to avoid visual disturbance. With three different treatments in addition to a control group, the distribution of lumpfish were 20 individuals per tank with two tanks per treatment ($n$ = 40). During the 6-week experimental period, the water flow in each tank was 500 L $h^{-1}$ while mean ± SD oxygen saturation and water temperature from all eight tanks was 91.6 ± 1.84% and 7.5 ± 0.07°C, respectively. The photoperiod during the experiment was 24:0. Fish were fed 2% of their biomass separated into three meals served 08:00, 11:00, and 14:00 with 30 doses of pellets for each meal (Arvo-Tec Oy, Finland). Spilled feed and feces were removed once a week, but not within 4 days prior to sampling dates to avoid disturbance. Every second week, each individual lumpfish was morphologically measured and assessed for health scores. To avoid stress during handling, fish were quickly hand netted from the experimental tank to a 30 L tank with 5 mg $L^{-1}$ of cortisol blocking metomidate (Aquacalm™, Western Chemical Inc, Ferndale, United States). This concentration causes rapid anesthesia and stops further increase of plasma cortisol (Iversen et al., 2003; Iversen and Eliassen, 2014). Fish were moved back to their respective tanks after the measurements were done.

## Treatments

The different treatments in the duplicate tanks were named "Live," "Model," and "Olfaction." The duration of the treatments was 6 weeks. Two remaining tanks ("Control") contained lumpfish exposed to no specific treatment. The Live treatment included cohabitation with two Atlantic salmon per tank. Model treatments involved two silicone salmonid models (*3D Line Thru 15 cm,* Savage Gear™, United States). Models were the same size as the initial size of Atlantic salmon used in the Live treatment. Each salmon model was attached to a nylon string and a swivel above the tank, which caused the models to move with the water current in the surface center area of the tank during the entire experiment. In the Olfaction treatment, the water input was connected to an adjacent tank containing four Atlantic salmon. Without disturbing flow or environmental parameters, the duplicate tanks were provided with a stable influx of water representing the presence of Atlantic salmon without any visual cues.

## Data Analysis

### Growth

Weight ($W$) was measured with 0.1 g accuracy, while length ($L$) was measured to the nearest 0.1 cm, one fish at the time. Specific growth rates (SGR % $day^{-1}$) were calculated using the formulae developed by Houde and Schekter (1981):

$$SGR = \left(e^{g} - 1\right) * 100$$

where $g = [\ln(W_2) - \ln(W_1)/(t_2 - t_1)]$. $W_2$ refers to weight on the last day of measurement for the respective period, while $W1$ refers to weight on the first day. $t_2$ and $t_1$ refer to the time period described as number of days.

Formula for condition factor ($K$) was:

$$K = 100 * W/L^3$$

It was decided to use SGR and K-factor in the present study to compare findings with previous studies on lumpfish involving growth (Nytrø et al., 2014; Jørgensen et al., 2017; Imsland et al., 2018b, 2019).

### Skin Coloration

Skin color analysis of lumpfish epidermal skin was assessed using methods described in Staven et al. (2021). Each lumpfish was photographed, and later analyzed for pixel counts within a defined area of the lateral side of the fish. Mean values of each of the three primary colors red (R), green (G), and blue (B) were measured using the histogram function in ImageJ, version 1.53e (NIH, Bethesda, MD, available at https://imagej.nih.gov/ij/). Eventually, the mean value for each of the three colors were added together, referred to as mean R + G + B.

### Health Assessment

External health was scored based on health assessment criteria specifically developed for lumpfish (Imsland et al., 2020). This involved scoring (from 0 to 4) body conditions, tail fins, other fins, deformities, cataract, eye ulceration and the condition factor

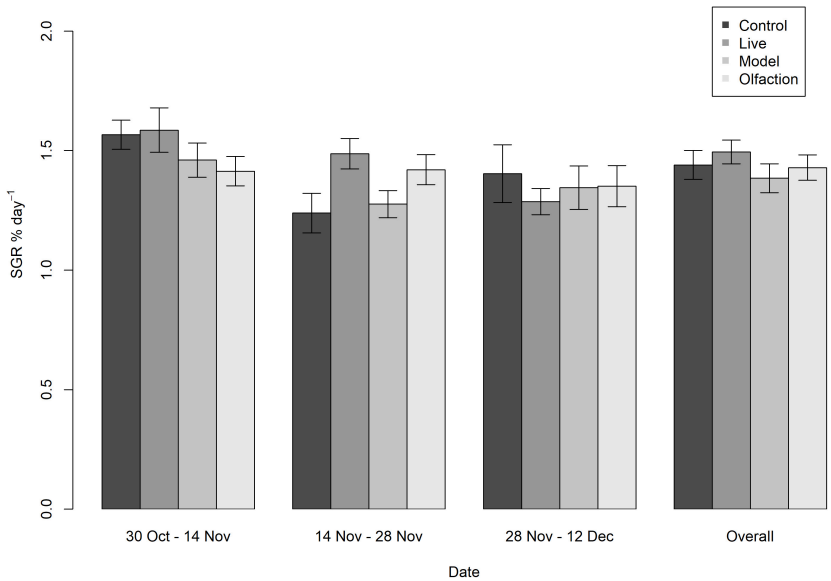


**FIGURE 1 |** Specific growth rate (SGR % day$^{-1}$) in lumpfish ($n$ = 40 per treatment) during 6 weeks of interaction with Live, Model or Olfaction treatments or Control. Mean measurements with 95% confidence interval error bars revealed no difference between treatments measured every second week, including an overall measurement comparing initial weight with endpoint weight.

($K$). For each parameter, a lower score indicated less deviations from normal health conditions. Individual scores were summated and the mean score per treatment calculated. Mean welfare score from 0 to 11 suggested "no to minimal deterioration," while mean welfare score from 11 to 16 suggested "higher incidence of compromised health." A score above 16 indicated "evidence of further extensive health deterioration." For a detailed scoring description, see Imsland et al. (2020).

### Blood and Brain Sampling for Plasma Cortisol and Neurotransmitters

Blood and brains were sampled after 6 weeks of experiment. To avoid activation of the HPI-axis during the final handling, water supply was stopped and 5 mg L$^{-1}$ metomidate (Aquacalm$^{TM}$, Western Chemical Inc., Canada) quickly added to one tank at the time. Amnesia (hypnosis) occurred within 2 min in lumpfish. Next, fish were removed from the tank with a hand net before blood was sampled from the caudal vessel using 0.33 × 12.7 mm syringes (BD Micro-fine®). Anticoagulating heparin (Leo Pharma, Malmø, Sweden) was added to the syringes by pulling the plunger out and back again into its initial position, thus leaving a small amount of heparin in the dead space of the syringe (approximately 0.08 mL). Samples were centrifuged at 5000 RPM (2000 × $g$) for 10 min in a Mini Star centrifuge (VWR$^{TM}$, United Kingdom). After centrifugation, the plasma was separated with a pipette, transferred to a 1.8 mL Nunc Cryo Tube® and stored at −40°C. Plasma cortisol levels were later analyzed using radioimmunoassay, based on methods described in Iversen et al. (1998). Next, fish were euthanized by spinal transection and gills were cut. Left hemisphere brains were removed, separated along the sagittal plane, and stored on dry ice, while right hemisphere brains were designated for other experiments and not included in the study. Concentrations of norepinephrine (NE), dopamine (DA), 3,4-dihydroxyphenylacetic acid (DOPAC), serotonin (5-hydroxytryptamine, 5-HT), and 5-hydroxyindoleacetic acid (5-HIAA) in left hemisphere brain tissue were later quantified by means of high performance liquid chromatography (HPLC) with electrochemical detection as previously described (Alfonso et al., 2019).

### Stimulation and Suppression Test of Hypothalamic-Pituitary-Interrenal Axis

To investigate treatment impact on the HPI-axis feedback system, a stimulation and suppression test using adrenocorticotropic hormone (ACTH) and dexamethasone (DEX), respectively, was conducted in accordance with the previous study by Pottinger and Carrick (2001), with some minor modifications as described in Iversen and Eliassen (2014).

## STATISTICS

All statistical tests were performed using the R software$^{TM}$ R.3.2.2 (R Development Core Team, 2013) at a 95% level of significance. Data were tested for normality using the Shapiro–Wilk test (Shapiro and Wilk, 1965) while variance was tested using Levene's $F$-test (Gastwirth et al., 2009). Treatments and control were analyzed with a one-way ANOVA test. When assumptions of normality or homoscedasticity were not met, a non-parametric Kruskal–Wallis test were used instead. If significant differences occurred, a *post hoc* test was used to compare treatments and control with one another. A Tukey test was used after one-way ANOVA, while a Dunn test was used after a Kruskal–Wallis test. Results were presented using mean values ± standard

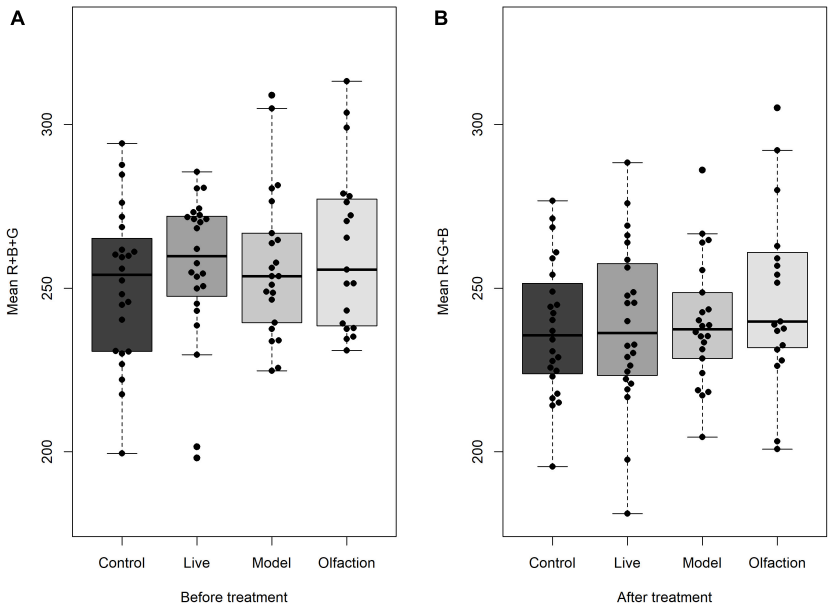


**FIGURE 2 |** Lumpfish skin color ($n$ = 24) measured as mean Red + Green + Blue pixels **(A)** before and **(B)** after treatment exposure. Mean R + G + B did not deviate between treatments before or between treatments after the experiment. Lumpfish were reared in experimental tanks with Live Atlantic salmon or different salmon sensory cues (Olfaction and Model). Boxplots describe median values with quantiles and outliers.

deviation (mean ± S.D). Figures were graphically depicted as bar graphs with means and 95% confidence intervals, or as boxplots with a median central line and whiskers covering 95% of values, while separate dots indicated outliers. Letters were used to illustrate significant differences from *post hoc* tests, while no letters indicated no significant difference from the ANOVA or Kruskal–Wallis tests. From 20 lumpfish in each experimental tank, 12 were used for real time measurements of plasma cortisol, including six lumpfish also used for measurements of brain neurotransmitters. The remaining eight in each tank were used for stimulation and suppression test of HPI axis.

# RESULTS

## Morphometric Parameters

### Growth and Condition of Lumpfish

Initial measurements of mean weight did not differ between treatments and control [$F(3,157) = 0.950$, $p = 0.44$]. During the experiment, specific growth rates did not differ between treatments after 2 weeks [$K(158) = 159$, $p = 0.467$], 4 weeks [$K(158) = 159$, $p = 0.485$], 6 weeks [$K(158) = 159$, $p = 0.485$], or overall [$K(160) = 160$, $p = 0.485$; **Figure 1**]. Also, the condition factors ($K$) measured after experimental termination in Control (3.93 ± 0.44), Live (3.93 ± 0.34), Models (4.01 ± 0.44), and Olfaction (3.91 ± 0.48) did not significantly differ [$F(3,157) = 0.388$, $p = 0.76$].

### Mortality and Health Score Assessments

No mortality was observed during the experiment. Health score assessments done after the experiment was terminated, revealed no visible damage (score = 0) for mouth, skin, gills, fins, or eyes in all fish, with exception of a single fish in the Live treatment, that had a skin score of 1. Skin penetration in the dorsal crest from Floy tag t-bars did not cause wounds. Mean condition factor ($K$) for each treatment, including Control, were within the score range of 3.5–4.5, which was defined as in "moderate condition," giving a health score of "1."

### Skin Coloration

Skin coloration measured on the first day of experiment did not differ when comparing mean R + G + B in treatments and control [$F(3,85) = 1.35$, $p = 0.261$; **Figure 2A**]. Similarly, the 6 weeks of cohabitation did not induce any change in mean R + G + B measurements between treatments and control [$F(3,85) = 0.727$, $p = 0.539$; **Figure 2B**].

## Neurotransmitters

### Dopamine

The levels of dopamine (DA) in treatments and control were significantly different [$F(3,44) = 3.\ 97$, $p = 0.013$] and a *post hoc* comparison revealed significantly lower concentrations ($p = 0.010$) in Live (92.7 ± 42.60 ng/g) compared to Control (140.2 ± 27.26 ng/g). The dopaminergic activity index (the DOPAC:DA ratio) was significantly different between treatments and control [$H(3) = 9.67$, $p = 0.021$], and a *post hoc* comparison revealed significant increase ($p = 0.002$) of the DOPAC:DA ratio in the Live treatment (DOPAC:DA = 13.0% ± 7.58) compared to the Control (DOPAC:DA = 7.0% ± 2.70). Levels of the metabolite 3,4-dihydroxyphenylacetid acid (DOPAC) did not differ between treatments and control [$F(3,44) = 0.21$, $p = 0.889$; **Figures 3A–C**].

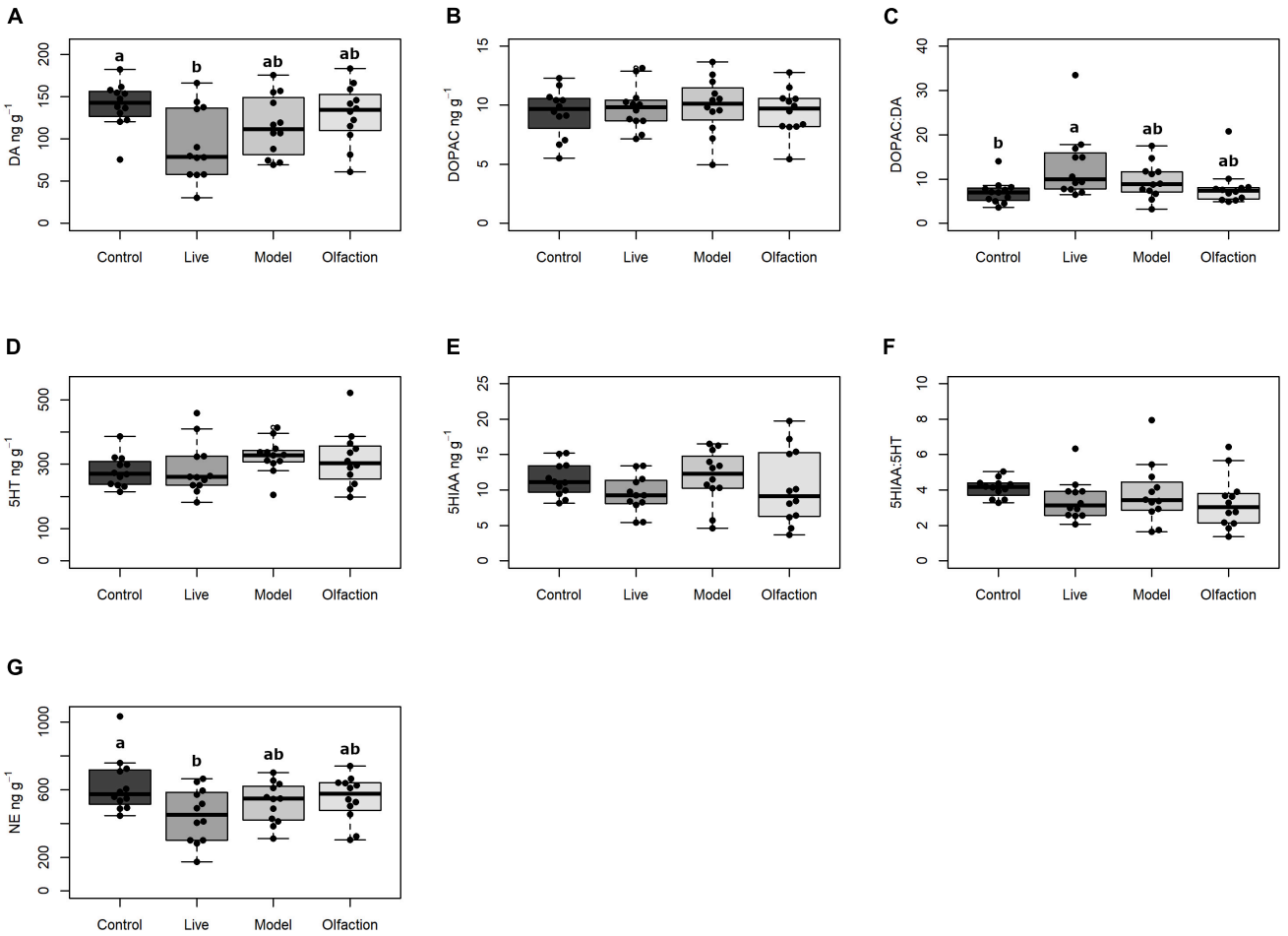


**FIGURE 3 |** The levels of neurotransmitters (ng $g^{-1}$) in ft hemisphere of brains from lumpfish ($n$ = 12) exposed to Live, Model, or Olfaction treatments in addition to a Control. Neurotransmitters include **(A)** DA (dopamine), **(B)** DOPAC (3,4-dihydroxyphenylacetic acid), **(C)** the DOPAC:DA turnover ratio, **(D)** 5HT (serotonin), **(E)** 5HIAA (5-hydroxyindoleacetic acid), **(F)** the 5HIAA:5HT turnover ratio, and **(G)** NE (Norepinephrine). Treatments that share a letter were not significantly different ($p < 0.05$).

### Serotonin

No difference between treatments and control were observed for serotonin (5-HT) [$F(3,44) = 1.26$, $p = 0.3$], the serotonin metabolite (5HIAA) [$F(3,44) = 1.03$, $p = 0.387$] or the serotonergic activity index (5HIAA:5-HT) [$F(3,44) = 0.94$, $p = 0.425$] (**Figures 3D–F**).

### Norepinephrine

A significant difference in levels of norepinephrine (NA) was observed between treatments and control [$F(3,44) = 3.08$, $p = 0.036$; **Figure 3G**], and a *post hoc* test showed that the difference ($p = 0.021$) occurred between Live (455.8 ± 159.49) and Control (624.4 ± 170.64).

## Hypothalamic-Pituitary-Interrenal Axis Responses

### Basal Levels

Basal levels of plasma cortisol concentrations were similar between lumpfish ($n = 24$) in treatments and control [$H(3) = 6.23$, $p = 0.1$]. Mean ± SD plasma cortisol for the treatments were lowest in Live (3.0 ± 3.92 nmol $L^{-1}$) and highest in Control (26.6 ± 48.11 nmol $L^{-1}$), while Model and Olfaction were 11.7 ± 49.24 nmol $L^{-1}$ and 12.1 ± 35.15 nmol $L^{-1}$, respectively (**Figure 4**).

### Stimulation and Suppression Test of Hypothalamic-Pituitary-Interrenal Axis

The remaining lumpfish ($n$ = 16) per treatment that were used to evaluate the stimulation and suppression of the HPA axis showed no significant difference in plasma cortisol levels after phosphate-saline injection (PBS) [$H(3) = 7.11$, $p = 0.07$], while injection with adrenocorticotrophic hormone (ACTH) revealed different responses between treatments and control [$H(3) = 11.51$, $p = 0.009$; **Figure 5**]. A *post hoc* test found significant differences between Model (76.7 ± 118.40 nmol $L^{-1}$) and Live (14.7 ± 18.60 nmol $L^{-1}$) ($p = 0.006$), Model and Olfaction (8.0 ± 6.43 nmol $L^{-1}$) ($p = 0.001$), and Olfaction and Control (30.6 ± 26.73 nmol $L^{-1}$) ($p = 0.017$).

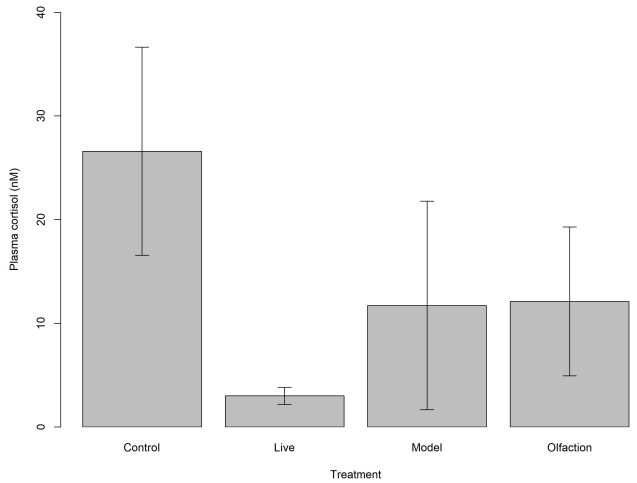


**FIGURE 4 |** Mean basal plasma cortisol (nM) levels with 95% confidence intervals in lumpfish ($n$ = 24) after 6 weeks of treatment exposure. Treatments involved interaction with two Atlantic salmon (Live), two salmon models (Model) or salmon smell from a tank containing four Atlantic salmon (Olfaction).

## DISCUSSION

The study evaluated physiological effects in lumpfish exposed to Atlantic salmon or to different salmon sensory cues over a duration of 6 weeks. Live, Model, and Olfaction treatments induced no change in growth, body coloration, health assessments, or basal levels of plasma cortisol. Brain analysis revealed significant changes in concentrations of neurotransmitters observed in lumpfish cohabiting with Live Atlantic salmon. Both dopamine and norepinephrine concentrations were significantly lower in the Live treatment compared to Control. The stimulation and suppression test of the HPI axis found oversensitivity from the ACTH injection in one lumpfish from the Model treatment, while the Live and Olfaction treatments did not show any indications of oversensitivity. The present findings coincide with previously observed physiological acute impacts on lumpfish exposed to the same, or similar treatment protocols, and adds novel perspectives on how the species coexist over longer time periods without impeding the resting state or the welfare of the species (Staven et al., 2019, 2021). Below, we elaborate each specific investigated parameter.

### Growth

In aquaculture, specific growth rate (SGR) and the condition factor ($K$) can be used as indicators on the wellbeing of farmed fish (North et al., 2006; Calabrese et al., 2017). Deviations from a normal resting state can alter the metabolic scope and energy expenditure in fish due to the relocation of energy surpluses (e.g., gluconeogenic effect of corticosteroids) (Barton and Iwama, 1991). In lumpfish, SGR has been previously studied in relationship with temperature and fish size (Nytrø et al., 2014), families (Imsland et al., 2021), diet types (Imsland et al., 2019), water exchange, and oxygen saturation (Jørgensen et al., 2017). In the present study we investigated if predator cues could impact lumpfish to an extent where growth was affected. After 6 weeks of interaction, lumpfish showed no change in SGR or condition factors ($K$) from salmon sensory cues or

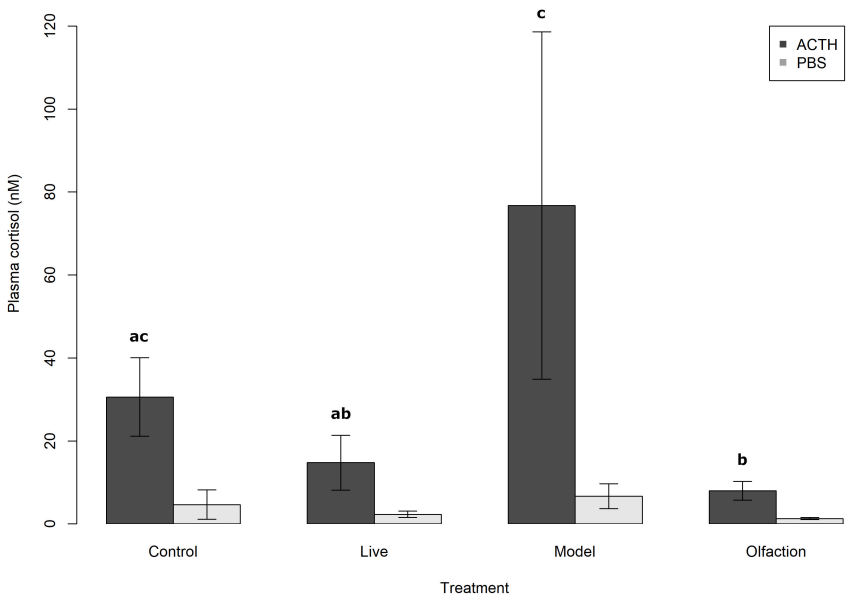


**FIGURE 5 |** Mean plasma cortisol (nM) levels with 95% confidence intervals in lumpfish ($n$ = 16) 2 h post-intraperitoneal injection with either 0.5 mL $kg^{-1}$ phosphate-buffered saline (PBS) or 45 $\mu g$ $mL^{-1}$ adrenocorticotropic hormone (ACTH). 24 h prior to sampling, lumpfish were injected with 1 mg $kg^{-1}$ dexamethasone in ethanol: PBS; 1:3; 1 $\mu g$ $L^{-1}$ (DEX) and relocated to dark tanks with the same environmental conditions as during the experiment. Treatments involved interaction with Live Atlantic salmon, salmon Models or salmon smell from a tank containing four Atlantic salmon. Treatments that share a letter were not significantly different ($p < 0.05$).

cohabitation with Atlantic salmon in comparison with the Control. In other prey fish, or fish relatively small, the presence of predatory cues caused reduced growth performance (Strand et al., 2007; Sunardi et al., 2007) or impairments on the capacity of prey fish to obtain and preserve energy resources (Lima and Dill, 1990). When lumpfish are utilized in aquaculture, the transition from rearing conditions with conspecifics only to interaction with large Atlantic salmon induces elevated levels of plasma cortisol, increased swimming activity, and avoidance behavior (Staven et al., 2019). A follow up study revealed that swimming activity rapidly increased upon exposure to salmon cues before dropping again within the first hour of interaction (Staven et al., 2021). In accordance with both Staven et al. (2019) and Staven et al. (2021), salmon cues can initiate moderate acute stress responses, while these responses diminished during a prolonged interaction and did not affect growth. Overall SGR in treatments were approximately 0.6 points lower in comparison with Nytrø et al. (2014). Both studies had similar light regimes, temperatures, and oxygen saturations, yet Nytrø et al. (2014) conducted an optimal feeding trial with more lumpfish per tank and lower initial individual variation in weight. This shows that SGR is a relatively stable measurement of expected growth in a tank experiment and thus a good welfare indicator based on the given environment. The overall importance of our findings on SGR and condition factor was the limited effect from Atlantic salmon or salmon cues alone.

## Skin Coloration

Lumpfish express variation in skin coloration both early in ontogeny and after maturation (Davenport and Thorsteinsson, 1989; Davenport and Bradshaw, 1995). While skin coloration and pigmentation have previously been observed to alter based on background color and hue (Davenport and Bradshaw, 1995), acute changes within an hour of interaction were previously detected in both parameters when juvenile lumpfish were exposed to Atlantic salmon olfaction (Staven et al., 2021). In the current study, lumpfish color (measured as mean R + G + B) did not differ between any of the three treatments compared to Control. Acute stress has been associated with mediation and aggregation of melanosomes inside melanophore cells in fish, regulating both color and darkening (Fujii, 2000; Aspengren et al., 2003; Nilsson Sköld et al., 2013). Given that mechanisms of color change require energy, the physiological process of habituation to salmon cues would cause an overall reduction in unnecessary energy expenditure in lumpfish. Overall, the long-term interaction with salmon cues revealed a novel understanding of skin coloration change from social interaction and suggests that lumpfish induce little visual alterations when the resting state is not disrupted, while acute stress responses can increase both darkening and the vividness of the skin (Staven et al., 2021).

## Health Assessment and Mortality

Health scores were assessed before, during, and after the experiment based on methods described in Imsland et al. (2020). The experiment did not cause any deterioration in health score from interaction with the different salmon cues in comparison to the health scores observed in Control. This is the first experiment to measure the effect on health for lumpfish in interaction with Atlantic salmon or exposure to salmon sensory cues in a confined tank experiment. Previous studies on health scores in lumpfish were conducted in commercial scale sea pens together with Atlantic salmon and were not designed to measure solely the effect from salmon interaction or salmon cues (Imsland et al., 2020; Gutierrez Rabadan et al., 2021). In general, the little negative impacts on health scores were in accordance with the physiological measurements. With no clinical or physiological indications of negative impacts from treatments, zero mortalities in lumpfish were as expected.

## Neurotransmitters

Monoaminergic neuromodulators have important roles in the regulation of different physiological and behavioral processes, both in vertebrates and invertebrates. This includes learning and memory, wakefulness and arousal, stress responses, social interactions, and aggression, among others (Swallow et al., 2016; Ranjbar-Slamloo and Fazlali, 2020). Recent studies have shown that brain monoamines might be important in regulating interspecific patterns of behavior such as those between cleaner fish and their clients (Soares, 2017; de Abreu et al., 2018). In our study, the 6-week cohabitation with Live salmon induced a decrease in the levels of catecholamines, dopamine, and norepinephrine in the brain of the lumpfish. Both compounds share a biosynthetic route from the amino acid tyrosine and seem to functionally overlap to a certain extent in vertebrates (Ranjbar-Slamloo and Fazlali, 2020). The dopaminergic system in fish is known to be involved in processes such as locomotor activity, learning, motivation, reward, reproduction, stress, and social behavior including aggression, dominance, and interspecific interactions, as observed between cleaner and client fish (Summers and Winberg, 2006; Gesto et al., 2013; Soares, 2017; Ganesh, 2021). Among those functions, both stress-related factors and the social interaction with the introduced salmon might have been involved in the observed changes in the lumpfish brain. Furthermore, based on the results of this and a previous study (Staven et al., 2021), the social factor was likely the most important. Social factors were considered the most relevant because stress related alterations in the brain monoaminergic systems are usually more prominent in the serotonergic than in the dopaminergic system, both in situations of acute and prolonged stress (Øverli et al., 2001; Gesto et al., 2013; Conde-Sieira et al., 2018; López-Patiño et al., 2021), and no alterations were found in the serotonergic system in this study. Furthermore, our previous study (Staven et al., 2021) showed that both Live and Olfaction treatment were equally able to acutely modify the swimming activity of the lumpfish (in a kind of "startling" response), while only the Live treatment significantly affected the lumpfish brain in the current study. Even if the observed brain alterations could be the result of social factors related to the presence of salmon, the precise physiological significance of the reduced levels of

both dopamine and norepinephrine in the lumpfish exposed to live salmon are difficult to interpret. Reduced levels of the parent catecholamines could be the result of a reduced synthesis rate, a sustained higher release and subsequent oxidation, or both. In the Live group, despite the reduction in dopamine, the DOPAC levels remained unaltered, thus resulting in a higher DOPAC/DA turnover ratio. The higher turnover ratio suggests that DAergic neurons had a higher firing rate in the Live group. Acute changes in the dopamine system have been observed before in specific brain areas upon acute exposure to stress or social interaction (Gesto et al., 2013; Teles et al., 2013; de Abreu et al., 2018). However, the comparison of the current data with those studies is complex since we did not perform a brain region-specific analysis. Furthermore, prolonged exposure to the same events might result in different alterations, since the brain will have time to finely modulate the release of neurotransmitters to adjust to the new situation by using different feedback mechanisms (Best et al., 2009, 2010). In addition, prolonged exposure periods would include potential effects of other brain processes related to memory, learning, and motivation/reward mechanisms to adjust fish behavior to the new situation. In this regard, it can be even questioned whether the turnover ratios (metabolite/amine) are still good estimators of neuron firing rates, since other factors could be having a relevant effect on the levels of the metabolite; for example, alterations in the monoamine oxidase activity cannot be ruled out (Higuchi et al., 2017, 2019). Interestingly, a long-term increase in overall brain catecholaminergic activity was observed in gilthead seabream after early life exposure to stress for 2 weeks (Vindas et al., 2018). In that study, however, the DAergic ratio was increased in the brain because of increased levels of the metabolite DOPAC, and not because of a decrease in dopamine amounts, so the mechanism behind the alterations is likely different. Together with the lack of differences in terms of growth performance and health scores, brain data suggest that lumpfish were able to cope with the treatments, and only the Live group required some adjustment in the brain pathways involved in behavioral regulation. The fact that dopamine adjustments were observed only in Live and not in the Model or Olfaction treatments, demonstrate that single cues were not having a relevant effect on the lumpfish brain in the long term, also supporting the view that dopamine alterations were likely the result of interspecific social contact.

## Effects on the Hypothalamic-Pituitary-Interrenal Axis

In mammals, several changes in the HPI-axis have been documented during a chronic stress state. This includes weight loss, proliferation of the corticotrope cells in the anterior pituitary, inhibition of ACTH synthesis by cortisol, reduction of the feedback effect of glucocorticoid receptor agonists on ACTH release, increase of the size of the adrenal glands and of the response of the adrenals to ACTH (Mormède et al., 2007). This resetting of the HPI axis at a new level of activity (set points), that Selye (1975) described as the stage of resistance, is also known as allostasis (McEwen, 1998; McEwen and Wingfield, 2003; Goymann and Wingfield, 2004; Wingfield, 2005). Different approaches can be used to detect these changes as described above, including stimulation tests (activating corticotropic releasing hormone, vasopressin, ACTH, and insulin-induced hypoglycemia) that measure the relative sensitivity of the pituitary and the interrenal cells, and the use of an inhibition test utilizing DEX to demonstrate the reduced efficiency of the negative feedback by corticosteroids (Mormède et al., 2007). In this experiment, the treatment exposure induced variations in mean concentrations of plasma cortisol after administration of a weight-adjusted dose of ACTH. At first observation, lumpfish exposed to Models revealed oversensitivity to administration of a weight-adjusted dose of ACTH compared to the other treatments. Data unveiled a single outlier (strong stress response of 366.85 nM), which increased mean plasma cortisol level of the Model treatment from 18.34 to 32.86 nM. While removal of the outlier would have impacted the statistical outcome, resulting in no significant difference between Model, Olfaction and Live treatments, individual variation in stress responses in fish should be accounted for. This is due to the reality of different behavioral strategies observed between individuals within the same species referred to as bold or shy, proactive, or reactive, or as differences in personalities (Schjolden and Winberg, 2007; Toms et al., 2010; Yuan et al., 2018). In lumpfish, differences in personality have recently been observed when individuals were exposed to novel objects and later introduced to Atlantic salmon (Whittaker et al., 2021). Variation in stress responses in lumpfish during novel heterospecific interactions could be associated with why only certain lumpfish graze sea lice when deployed in net pens with Atlantic salmon, especially in the context of neurotransmitters associated with cooperative establishment and social behavior. Overall, few studies on ACTH sensitivity have been done on fish. However, Pottinger and Carrick (2001) showed that two strains of rainbow trout selected for high (HR) and low (LR) responsiveness to a standard crowding test had different responsiveness to a weight-adjusted dose of ACTH. The LR strain had significant lower production of plasma cortisol compared to the HR strain. In domesticated mammals, an injection of ACTH has shown an increased cortisol response in animals reared in poor conditions or subjected to repeated stressors. Similarly, Iversen and Eliassen (2014) showed that salmon that were stressed daily over a 4-week period became oversensitive to ACTH, regardless of whether the fish were vaccinated before or after applied stressor. One can only speculate how the Model treatment triggered the HPI axis in a single individual. However, the models used were novel, and the introduction of novel objects is a common method used to distinguish different individual responses in fish (Castanheira et al., 2013; White et al., 2013; Whittaker et al., 2021). Exposure to Models were not enough to elicit at full blown allostasis type 2 response, referred to as chronical stress, recognized by an oversensitive ACTH axis linked with non-functioning negative feedback (DEX) as described by Iversen and Eliassen (2014). Plasma cortisol measured in lumpfish sampled from the experimental tanks after 6 weeks of treatment exposure revealed

no significant difference between the different treatments and the control. Still, a tendency of reduced plasma cortisol levels in the Live treatment was observed, similar what was seen as reduced concentrations of norepinephrine and dopamine after coexisting with Atlantic salmon. The combination of the stimulation and suppression test together with overall low basal levels of plasma cortisol suggested that treatments and interaction with Atlantic salmon induced a plastic change in lumpfish where the threshold of activation of the HPI-axis was downregulated.

## CONCLUSION

We investigated how lumpfish responded to the presence of carnivorous Atlantic salmon or salmon sensory cues through analysis of multiple physiological parameters relevant to welfare, social interaction, and stress during a 6-week tank experiment. Results showed that growth, health scores, and skin coloration remained unaltered. The stimulation and suppression test of HPI-axis and the overall low plasma cortisol levels suggested no indication of allostasis type 2 chronic stress or acute stress, respectively. Interaction with live salmon induced alterations in the brain of the lumpfish, which revealed reduced levels of brain catecholamines, namely norepinephrine and dopamine. The cause and function of these alterations are not completely understood but could be part of a necessary process to adjust lumpfish behavior to cohabiting with free-roaming salmon. Lumpfish behavior was not assessed during the experiment, and a future focus on potential relationships between altered neurotransmission and behavioral adjustment would be necessary to test if that was the case. The novel findings on the plastic change in neuromodulators could be utilized in future work identifying targets for breeding selection, considering the importance of their role in social interaction in other species of cleaner fish. Overall, this study showed that lumpfish were not negatively impacted by cohabitation or exposure to salmon cues, which suggested that welfare disruption in commercial production is probably related to a combination of Atlantic salmon exposure with other stressors.

## DATA AVAILABILITY STATEMENT

The raw data supporting the conclusions of this article will be made available by the authors, without undue reservation.

## ETHICS STATEMENT

The animal study was reviewed and approved by Norwegian Food Safety Authority (FDU#17231).

## AUTHOR CONTRIBUTIONS

FS, TK, and JN contributed to the design of the study. FS conducted the study with help from DP and PA and made the first manuscript draft. MG and MI were in charge of brain analysis and cortisol measurements, and wrote sections of the manuscript. All authors contributed to manuscript revision, read, and approved the submitted version.

## FUNDING

Financial support was given by the Research Council of Norway/Norges Forskningsråd with grant number ES610697, as part of the main authors industrial Ph.D. programme.

## ACKNOWLEDGMENTS

We would like to thank the staff at Mørkvedbukta research station in Bodø, the CycLus R&D team and colleagues in Aqua Kompetanse AS.

## REFERENCES

Alfonso, S., Sadoul, B., Gesto, M., Joassard, L., Chatain, B., Geffroy, B., et al. (2019). Coping styles in European sea bass: the link between boldness, stress response and neurogenesis. *Physiol. Behav.* 207, 76–85. doi: 10.1016/j.physbeh.2019.04.020

Aspengren, S., Sköld, H. N., Quiroga, G., Mårtensson, L., and Wallin, M. (2003). Noradrenaline- and melatonin-mediated regulation of pigment aggregation in fish melanophores. *Pigm. Cell Res.* 16, 59–64. doi: 10.1034/j.1600-0749.2003.00003.x

Backström, T., and Winberg, S. (2017). Serotonin coordinates responses to social stress - what we can learn from fish. *Front. Neurosci.* 11:595. doi: 10.3389/fnins.2017.00595

Barton, B. A., and Iwama, G. K. (1991). Physiological changes in fish from stress in aquaculture with emphasis on the response and effects of corticosteroids. *Annu. Rev. Fish Dis.* 1, 3–26. doi: 10.1016/0959-8030(91)90019-G

Berejikian, B. A., Tezak, E. P., and LaRae, A. L. (2003). Innate and enhanced predator recognition in hatchery-reared chinook salmon. *Environ. Biol. Fishes.* 67, 241–251. doi: 10.1023/A:1025887015436

Best, J., Nijhout, H. F., and Reed, M. (2010). Serotonin synthesis, release and reuptake in terminals: a mathematical model. *Theor. Biol. Med. Model.* 7:34. doi: 10.1186/1742-4682-7-34

Best, J. A., Nijhout, H. F., and Reed, M. C. (2009). Homeostatic mechanisms in dopamine synthesis and release: a mathematical model. *Theor. Biol. Med. Model.* 6:21. doi: 10.1186/1742-4682-6-21

Bjordal, Å (1990). Sea lice infestation on farmed salmon: possible use of cleaner-fish as an alternative method for de-lousing. *Can. Tech. Rep. Fish. Aquat. Sci.* 1761, 85–89.

Blanco Gonzalez, E., and de Boer, F. (2017). The development of the norwegian wrasse fishery and the use of wrasses as cleaner fish in the salmon aquaculture industry. *Fish. Sci.* 83, 661–670. doi: 10.1007/s12562-017-1110-4

Brown, G. E. (2003). Learning about danger: chemical alarm cues and local risk assessment in prey fishes. *Fish Fish.* 4, 227–234. doi: 10.1046/j.1467-2979.2003.00132.x

Brown, G. E., and Godin, J. G. J. (1999). Who dares, learns: chemical inspection behaviour and acquired predator recognition in a characin fish. *Anim. Behav.* 57, 475–481. doi: 10.1006/anbe.1998.1017

Brown, G. E., Rive, A. C., Ferrari, M. C. O., and Chivers, D. P. (2006). The dynamic nature of antipredator behavior: prey fish integrate threat-sensitive antipredator

responses within background levels of predation risk. *Behav. Ecol. Sociobiol.* 61, 9–16. doi: 10.1007/s00265-006-0232-y

Bshary, R. (2001). "The cleaner fish market," in *Economics in Nature*, eds R. Noë, J. A. R. Van Hooff, and P. Hammerstein (Cambridge: University Press), 146–172. doi: 10.1086/707519

Bshary, R., and Würth, M. (2001). Cleaner fish (*Labroides dimidiatus*) manipulate client reef fish by providing tactile stimulation. *Proc. R. Soc. Lond.* 268, 1495–1501. doi: 10.1098/rspb.2001.1495

Calabrese, S., Nilsen, T. O., Kolarevic, J., Ebbesson, L. O. E., Pedrosa, C., Fivelstad, S., et al. (2017). Stocking density limits for post-smolt Atlantic salmon (*Salmo salar* L.) with emphasis on production performance and welfare. *Aquaculture* 468, 363–370. doi: 10.1016/j.aquaculture.2016.10.041

Castanheira, M. F., Herrera, M., Costas, B., Conceição, L. E. C., and Martins, C. I. M. (2013). Can we predict personality in fish? Searching for consistency over time and across contexts. *PLoS One* 8:e62037. doi: 10.1371/journal.pone.0062037

Chivers, D. P., and Smith, R. J. F. (1998). Chemical alarm signalling in aquatic predator-prey systems: a review and prospectus. *Écoscience* 5, 338–352. doi: 10.1080/11956860.1998.11682471

Clinchy, M., Sheriff, M. J., and Zanette, L. Y. (2013). Predator-induced stress and the ecology of fear. *Funct. Ecol.* 27, 56–65. doi: 10.1111/1365-2435.12007

Conde-Sieira, M., Valente, L. M. P., Hernández-Pérez, J., Soengas, J. L., Míguez, J. M., and Gesto, M. (2018). Short-term exposure to repeated chasing stress does not induce habituation in *Senegalese sole*, *Solea senegalensis*. *Aquaculture* 487, 32–40. doi: 10.1016/j.aquaculture.2018.01.003

Costello, M. J. (2009). The global economic cost of sea lice to the salmonid farming industry. *J. Fish. Dis.* 32, 115–118. doi: 10.1111/j.1365-2761.2008.01011.x

Davenport, J., and Bradshaw, C. (1995). Observations on skin colour changes in juvenile lumpsuckers. *J. Fish. Biol.* 47, 143–154. doi: 10.1111/j.1095-8649.1995.tb01880.x

Davenport, J., and Thorsteinsson, V. (1989). Observations on the colours of lumpsuckers, *Cyclopterus lumpus* L. *J. Fish. Biol.* 35, 829–838. doi: 10.1111/j.1095-8649.1989.tb03034.x

de Abreu, M. S., Maximino, C., Cardoso, S. C., Marques, C. I., Pimentel, A. F. N., Mece, E., et al. (2020). Dopamine and serotonin mediate the impact of stress on cleaner fish cooperative behavior. *Horm. Behav.* 125:104813. doi: 10.1016/j.yhbeh.2020.104813

de Abreu, M. S., Messias, J. P. M., Thörnqvist, P.-O., Winberg, S., and Soares, M. C. (2018). The variable monoaminergic outcomes of cleaner fish brains when facing different social and mutualistic contexts. *PeerJ* 6:e4830. doi: 10.7717/peerj.4830

Eaton, R. C., Bombardieri, R. A., and Meyer, D. L. (1977). The mauthner-initiated startle response in teleost fish. *J. Exp. Biol.* 66, 65–81. doi: 10.1242/jeb.66.1.65

Eliasen, K., Danielsen, E., Johannesen, Á, Joensen, L. L., and Patursson, E. J. (2018). The cleaning efficacy of lumpfish (*Cyclopterus lumpus* L.) in *Faroese salmon* (*Salmo salar* L.) farming pens in relation to lumpfish size and seasonality. *Aquaculture* 488, 61–65. doi: 10.1016/j.aquaculture.2018.01.026

Ferrari, M. C., Wisenden, B. D. W., and Chivers, D. P. C. (2010). Chemical ecology of predator - prey interactions in aquatic ecosystems: a review and prospectus. *Can. J. Zool.* 88, 698–724. doi: 10.1139/z10-029

Fujii, R. (2000). The regulation of motile activity in fish chromatophores. *Pigment Cell Res.* 13, 300–319. doi: 10.1034/j.1600-0749.2000.130502.x

Gamperl, A. K., Vijayan, M. M., and Boutilier, R. G. (1994). Experimental control of stress hormone levels in fishes: techniques and applications. *Rev. Fish Biol. Fisher.* 4, 215–255. doi: 10.1007/BF00044129

Ganesh, C. B. (2021). The stress – reproductive axis in fish: the involvement of functional neuroanatomical systems in the brain. *J. Chem. Neuroanat.* 112:101904. doi: 10.1016/j.jchemneu.2020.101904

Gastwirth, J. L., Gel, Y. R., and Miao, W. (2009). The impact of Levene's test of equality of variances on statistiacal theory and practice. *Stat. Sci.* 24, 343–360. doi: 10.1214/09-STS301

Gesto, M., López-Patiño, M. A., Hernández, J., Soengas, J. L., and Míguez, J. M. (2013). The response of brain serotonergic and dopaminergic systems to an acute stressor in rainbow trout: a time course study. *J. Exp. Biol.* 216, 4435–4442. doi: 10.1242/jeb.091751

Gingins, S., Roche, D. G., and Bshary, R. (2017). Mutualistic cleaner fish maintains high escape performance despite privileged relationship with predators. *Proc. R. Soc. B.* 284:2469. doi: 10.1098/rspb.2016.2469

Goymann, W., and Wingfield, J. C. (2004). Allostatic load, social status and stress hormones: the costs of social status matter. *Anim. Behav.* 67, 591–602. doi: 10.1016/j.anbehav.2003.08.007

Grutter, A. S. (1999). Cleaner fish really do clean. *Nature* 398, 672–673. doi: 10.1038/19443

Grutter, A. S. (2004). Cleaner fish use tactile dancing behavior as a preconflict management strategy. *Curr. Biol.* 14, 1080–1083. doi: 10.1016/j.cub.2004.05.048

Gutierrez Rabadan, C., Spreadbury, C., Consuegra, S., and Garcia de Leaniz, C. (2021). Development, validation and testing of an operational welfare score index for farmed lumpfish *Cyclopterus lumpus* L. *Aquaculture* 531:735777. doi: 10.1016/j.aquaculture.2020.735777

Higuchi, Y., Soga, T., and Parhar, I. S. (2017). Regulatory pathways of monoamine oxidase a during social stress. *Front. Neurosci.* 11:604. doi: 10.3389/fnins.2017.00604

Higuchi, Y., Soga, T., and Parhar, I. S. (2019). Social defeat stress decreases mRNA for monoamine oxidase A and increases 5-HT turnover in the brain of male Nile tilapia (*Oreochromis niloticus*). *Front. Pharmacol.* 9:1549. doi: 10.3389/fphar.2018.01549

Houde, E. D., and Schekter, R. D. (1981). Growth rates, rations and cohort consumption of marine fish larvae in relation to prey concentrations. rapp. P.-v. *Reun. Cons. Int. Explor. Mer* 178, 441–453.

Imsland, A. K., Reynolds, P., Eliassen, G., Hangstad, T. A., Foss, A., Vikingstad, E., et al. (2014a). The use of lumpfish (*Cyclopterus lumpus* L) to control sea lice (*Lepeophtheirus salmonis* Kroyer) infestations in intensively farmed Atlantic salmon (*Salmo salar* L). *Aquaculture* 424, 18–23. doi: 10.1016/j.aquaculture.2013.12.033

Imsland, A. K., Reynolds, P., Eliassen, G., Hangstad, T. A., Nytro, A. V., Foss, A., et al. (2014b). Notes on the behaviour of lumpfish in sea pens with and without Atlantic salmon present. *J. Ethol.* 32, 117–122. doi: 10.1007/s10164-014-0397-1

Imsland, A. K., Reynolds, P., Eliassen, G., Mortensen, A., Hansen, ØJ., Puvanendran, V., et al. (2016a). Is cleaning behaviour in lumpfish (*Cyclopterus lumpus*) parentally controlled? *Aquaculture* 459, 156–165. doi: 10.1016/j.aquaculture.2016.03.047

Imsland, A. K., Reynolds, P., Nytrø, A. V., Eliassen, G., Hangstad, T. A., Jónsdóttir, Ó. D. B., et al. (2016b). Effects of lumpfish size on foraging behaviour and co-existence with sea lice infected Atlantic salmon in sea cages. *Aquaculture* 465, 19–27. doi: 10.1016/j.aquaculture.2016.08.015

Imsland, A. K., Hanssen, A., Nytrø, A. V., Reynolds, P., Jonassen, T. M., Hangstad, T. A., et al. (2018a). It works! lumpfish can significantly lower sea lice infestation in large-scale salmon farming. *Biol. Open* 7:bio036301. doi: 10.1242/bio.036301

Imsland, A. K., Reynolds, P., Hangstad, T. A., Jónsdóttir, ÓD. B., Noble, T., Wilson, M., et al. (2018b). Feeding behaviour and growth of lumpfish (*Cyclopterus lumpus* L.) fed with feed blocks. *Aquac. Res.* 49, 2006–2012. doi: 10.1111/are.13657

Imsland, A. K. D., Reynolds, P., Hangstad, T. A., Kapari, L., Maduna, S. N., Hagen, S. B., et al. (2021). Quantification of grazing efficacy, growth and health score of different lumpfish (*Cyclopterus lumpus* L.) families: possible size and gender effects. *Aquaculture* 530:735925. doi: 10.1016/j.aquaculture.2020.735925

Imsland, A. K. D., Reynolds, P., Jonassen, T. M., Hangstad, T. A., Adron, J., Elvegård, T. A., et al. (2019). Comparison of diet composition, feeding, growth and health of lumpfish (*Cyclopterus lumpus* L.) fed either feed blocks or pelleted commercial feed. *Aquac. Res.* 50, 1952–1963. doi: 10.1111/are.14083

Imsland, A. K. D., Reynolds, P., Lorentzen, M., Eilertsen, R. A., Micallef, G., and Tvenning, R. (2020). Improving survival and health of lumpfish (*Cyclopterus lumpus* L.) by the use of feed blocks and operational welfare indicators (OWIs) in commercial Atlantic salmon cages. *Aquaculture* 527:735476. doi: 10.1016/j.aquaculture.2020.735476

Iversen, M., Finstad, B., McKinley, R. S., and Eliassen, R. A. (2003). The efficacy of metomidate, clove oil, Aqui-S ™ and Benzoak ® as anaesthetics in Atlantic salmon (*Salmo salar* L.) smolts, and their potential stress-reducing capacity. *Aquaculture* 221, 549–566. doi: 10.1016/s0044-8486(3)00111-x

Iversen, M., Finstad, B., and Nilssen, K. J. (1998). Recovery from loading and transport stress in Atlantic salmon (*Salmo salar* L.) smolts. *Aquaculture* 168, 387–394. doi: 10.1016/s0044-8486(98)00364-0

Iversen, M. H., and Eliassen, R. A. (2014). The effect of allostatic load on hypothalamic–pituitary–interrenal (HPI) axis before and after secondary vaccination in Atlantic salmon postsmolts (*Salmo salar* L.). *Fish Physiol. Biochem.* 40, 527–538. doi: 10.1007/s10695-013-9863-x

Jørgensen, E. H., Haatuft, A., Puvanendran, V., and Mortensen, A. (2017). Effects of reduced water exchange rate and oxygen saturation on growth and stress indicators of juvenile lumpfish (*Cyclopterus lumpus* L.) in aquaculture. *Aquaculture* 474, 26–33. doi: 10.1016/j.aquaculture.2017.03.019

Kilkenny, C., Browne, W., Cuthill, I. C., Emerson, M., and Altman, D. G. (2010). Animal research: reporting *in vivo* experiments: the ARRIVE guidelines. *Br. J. Pharmacol.* 160, 1577–1579. doi: 10.1111/j.1476-5381.2010.00872.x

Lima, S. L., and Dill, L. M. (1990). Behavioral decisions made under the risk of predation: a review and prospectus. *Can. J. Zool.* 68, 619–640. doi: 10.1139/z90-092

López-Patiño, M. A., Skrzynska, A. K., Naderi, F., Mancera, J. M., Míguez, J. M., and Martos-Sitcha, J. A. (2021). High stocking density and food deprivation increase brain monoaminergic activity in gilthead sea bream (*Sparus aurata*). *Animals* 11:1503. doi: 10.3390/ani11061503

McEwen, B. S. (1998). Stress, adaptation, and disease. allostasis and allostatic load. *Ann. N.Y. Acad. Sci.* 840, 33–44. doi: 10.1111/j.1749-6632.1998.tb09546.x

McEwen, B. S., and Wingfield, J. C. (2003). The concept of allostasis in biology and biomedicine. *Horm. Behav.* 43, 2–15. doi: 10.1016/s0018-506x(02)00024-7

Messias, J. P. M., Paula, J. R., Grutter, A. S., Bshary, R., and Soares, M. C. (2016a). Dopamine disruption increases negotiation for cooperative interactions in a fish. *Sci. Rep*. 6:20817. doi: 10.1038/srep20817

Messias, J. P. M., Santos, T. P., Pinto, M., and Soares, M. C. (2016b). Stimulation of dopamine D1 receptor improves learning capacity in cooperating cleaner fish. *Proc. R. Soc. B.* 283:20152272. doi: 10.1098/rspb.2015.2272

Mormède, P., Andanson, S., Aupérin, B., Beerda, B., Guémené, D., Malmkvist, J., et al. (2007). Exploration of the hypothalamic-pituitary-adrenal function as a tool to evaluate animal welfare. *Physiol. Behav.* 92, 317–339. doi: 10.1016/j.physbeh.2006.12.003

Nilsson Sköld, H., Aspengren, S., and Wallin, M. (2013). Rapid color change in fish and amphibians - function, regulation, and emerging applications. *Pigment Cell Melanoma Res.* 26, 29–38. doi: 10.1111/pcmr.12040

North, B. P., Turnbull, J. F., Ellis, T., Porter, M. J., Migaud, H., Bron, J., et al. (2006). The impact of stocking density on the welfare of rainbow trout (*Oncorhynchus mykiss*). *Aquaculture* 255, 466–479. doi: 10.1016/j.aquaculture.2006.01.004

Nytrø, A. V., Vikingstad, E., Foss, A., Hangstad, T. A., Reynolds, P., Eliassen, G., et al. (2014). The effect of temperature and fish size on growth of juvenile lumpfish (*Cyclopterus lumpus* L.). *Aquaculture* 434, 296–302. doi: 10.1016/j.aquaculture.2014.07.028

Øverli, Ø, Nordgreen, J., Mejdell, C. M., Janczak, A. M., Kittilsen, S., Johansen, I. B., et al. (2014). Ectoparasitic sea lice (*Lepeophtheirus salmonis*) affect behavior and brain serotonergic activity in Atlantic salmon (*Salmo salar* L.): perspectives on animal welfare. *Physiol. Behav.* 132, 44–50. doi: 10.1016/j.physbeh.2014.04.031

Øverli, Ø, Pottinger, T. G., Carrick, T. R., Øverli, E., and Winberg, S. (2001). Brain monoaminergic activity in rainbow trout selected for high and low stress responsiveness. *Brain Behav. Evol.* 57, 214–224. doi: 10.1159/000047238

Paula, J. R., Messias, J. P., Grutter, A. S., Bshary, R., and Soares, M. C. (2015). The role of serotonin in the modulation of cooperative behavior. *Behav. Ecol.* 26, 1005–1012. doi: 10.1093/beheco/arv039

Pottinger, T. G., and Carrick, T. R. (2001). Stress responsiveness affects dominant-subordinate relationships in rainbow trout. *Horm. Behav.* 40, 419–427. doi: 10.1006/hbeh.2001.1707

Powell, A., Treasurer, J. W., Pooley, C. L., Keay, A. J., Lloyd, R., Imsland, A. K., et al. (2017). Use of lumpfish for sea-lice control in salmon farming: challenges and opportunities. *Rev. Aquac.* 10:12194. doi: 10.1111/raq.12194

R Development Core Team (2013). *R: A Language and Environment for Statistical Computing*. Available online at: https://www.r-project.org (accessed February 15, 2021)

Ramírez-Calero, S., Paula, J. R., Otjacques, E., Rosa, R., Ravasi, T., and Schunter, C. (2021). *Neuro-Molecular Characterization of Fish Cleaning Interactions*. Available online at: https://www.biorxiv.org/content/10.1101/2021.06.22.449532v1 (accessed August 13, 2021)

Ranjbar-Slamloo, Y., and Fazlali, Z. (2020). Dopamine and noradrenaline in the brain; overlapping or dissociate functions? *Front. Mol. Neurosci.* 12:334. doi: 10.3389/fnmol.2019.00334

Rankin, C. H., Abrams, T., Barry, R. J., Bhatnagar, S., Clayton, D. F., Colombo, J., et al. (2009). Habituation revisited: an updated and revised description of the behavioral characteristics of habituation. *Neurobiol. Learn. Mem.* 92, 135–138. doi: 10.1016/j.nlm.2008.09.012

Rupia, E. J., Binning, S. A., Roche, D. G., and Lu, W. (2016). Fight-flight or freeze-hide? Personality and metabolic phenotype mediate physiological defence responses in flatfish. *J. Anim. Ecol.* 85, 927–937. doi: 10.1111/1365-2656.12524

Schjolden, J., and Winberg, S. (2007). Genetically determined variation in stress responsiveness in rainbow trout: behavior and neurobiology. *Brain Behav. Evol.* 70, 227–238. doi: 10.1159/000105486

Schreck, C. B. (2010). Stress and fish reproduction: the roles of allostasis and hormesis. *Gen. Comp. Endocrinol.* 165, 549–556. doi: 10.1016/j.ygcen.2009.07.004

Selye, H. (1975). "«Homeostasis and heterostasis»," in *Trauma: Clinical and Biological Aspects*, ed. S. B. Day (Boston, MA: Springer), 25–29. doi: 10.1007/978-1-4684-2145-3_2

Shapiro, S. S., and Wilk, M. B. (1965). An analysis of variance test for normality (complete samples). *Biometrika* 52, 591–611. doi: 10.2307/2333709

Skår, M. W., Haugland, G. T., Powell, M. D., Wergeland, H. I., and Samuelsen, O. B. (2017). Development of anaesthetic protocols for lumpfish (*Cyclopterus lumpus* L.): effect of anaesthetic concentrations, sea water temperature and body weight. *PLoS One* 12:e0179344. doi: 10.1371/journal.pone.0179344

Soares, M. C. (2017). The neurobiology of mutualistic behavior: the cleanerfish swims into the spotlight. *Front. Behav. Neurosci.* 11:191. doi: 10.3389/fnbeh.2017.00191

Soares, M. C., Bshary, R., Mendonça, R., Grutter, A. S., and Oliveira, R. F. (2012). Arginine vasotocin regulation of interspecific cooperative behaviour in a cleaner fish. *PLoS One* 7:e39583. doi: 10.1371/journal.pone.0039583

Soares, M. C., Paula, J. R., and Bshary, R. (2016). Serotonin blockade delays learning performance in a cooperative fish. *Anim. Cogn.* 19, 1027–1030. doi: 10.1007/s10071-016-0988-z

Soares, M. C., Santos, T. P., and Messias, J. P. M. (2017). Dopamine disruption increases cleanerfish cooperative investment in novel client partners. *R. Soc. Open Sci.* 4:160609. doi: 10.1098/rsos.160609

Staven, F. R., Nordeide, J. T., Gesto, M., Andersen, P., Patel, D. M., and Kristensen, T. (2021). Behavioural and physiological responses of lumpfish (*Cyclopterus lumpus*) exposed to Atlantic salmon (*Salmo salar*) sensory cues. *Aquaculture* 544:737066. doi: 10.1016/j.aquaculture.2021.737066

Staven, F. R., Nordeide, J. T., Imsland, A. K., Andersen, P., Iversen, N. S., and Kristensen, T. (2019). Is habituation measurable in lumpfish *Cyclopterus lumpus* when used as cleaner fish in Atlantic salmon *Salmo salar* aquaculture? *Front. Vet. Sci.* 6:227. doi: 10.3389/fvets.2019.00227

Strand, Å, Alanärä, A., Staffan, F., and Magnhagen, C. (2007). Effects of tank colour and light intensity on feed intake, growth rate and energy expenditure of juvenile Eurasian perch, Perca fluviatilis L. *Aquaculture* 272, 312–318. doi: 10.1016/j.aquaculture.2007.08.052

Summers, C. H., and Winberg, S. (2006). Interactions between the neural regulation of stress and aggression. *J. Exp. Biol.* 209, 4581–4589. doi: 10.1242/jeb.02565

Sunardi, A. T., Manatunge, J., and Fujino, T. (2007). The effects of predation risk and current velocity stress on growth, condition and swimming energetics of Japanese minnow (*Pseudorasbora parva*). *Ecol. Res.* 22, 32–40. doi: 10.1007/s11284-006-0186-6

Swallow, J. G., Bubak, A. N., Grace, J. L., and Editors, G. (2016). The role of monoamines in modulating behavior. *Cur. Zool.* 62, 253–255. doi: 10.1093/cz/zow046

Teles, M. C., Dahlbom, S. J., Winberg, S., and Oliveira, R. F. (2013). Social modulation of brain monoamine levels in zebrafish. *Behav. Brain Res.* 253, 17–24. doi: 10.1016/j.bbr.2013.07.012

Toms, C. N., Echevarria, D. J., and Jouandot, D. J. (2010). A methodological review of personality-related studies in fish: focus on the shy-bold axis of behavior. *Int. J. Comput. Psychol.* 23, 1–25.

Torrissen, O., Jones, S., Asche, F., Guttormsen, A., Skilbrei, O. T., Nilsen, F., et al. (2013). Salmon lice - impact on wild salmonids and salmon aquaculture. *J. Fish Dis.* 36, 171–194. doi: 10.1111/jfd.12061

Vindas, M. A., Fokos, S., Pavlidis, M., Höglund, E., Dionysopoulou, S., Ebbesson, L. O. E., et al. (2018). Early life stress induces long-term changes in limbic areas of a teleost fish: the role of catecholamine systems in stress coping. *Sci. Rep.* 8:5638. doi: 10.1038/s41598-018-23950-x

White, J. R., Meekan, M. G., McCormick, M. I., and Ferrari, M. C. O. (2013). A comparison of measures of boldness and their relationships to survival in young fish. *PLoS One* 8:e68900. doi: 10.1371/journal.pone.0068900

Whittaker, B. A., Consuegra, S., and de Leaniz, C. G. (2021). *Personality Profiling May Help Select Better Cleaner Fish for Sea-Lice Control In Salmon Farming*. Available online at: https://www.biorxiv.org/content/10.1101/2021.05.21.444956v1 (accessed August 15, 2021)

Winberg, S., Nilsson, A., Hylland, P., Söderstöm, V., and Nilsson, G. E. (1997). Serotonin as a regulator of hypothalamic-pituitary-interrenal activity in teleost fish. *Neurosci. Lett.* 230, 113–116. doi: 10.1016/S0304-3940(97)00488-6

Winberg, S., and Thörnqvist, P.-O. (2016). Role of brain serotonin in modulating fish behavior. *Cur Zool.* 62, 317–323. doi: 10.1093/cz/zow037

Wingfield, J. C. (2005). The concept of allostasis: coping with a capricious environment. *J. Mammal.* 86, 248–254. doi: 10.1644/bhe-004.1

Yuan, M., Chen, Y., Huang, Y., and Lu, W. (2018). Behavioral and metabolic phenotype indicate personality in zebrafish (Danio rerio). *Front. Physiol.* 9:653. doi: 10.3389/fphys.2018.00653

**Conflict of Interest:** FS and PA were employed by Aqua Kompetanse AS.

The remaining authors declare that the research was conducted in the absence of any commercial or financial relationships that could be construed as a potential conflict of interest.

frontiers in Marine Science

REVIEW
published: 07 March 2022
doi: 10.3389/fmars.2022.854888

# Revising the Impact and Prospects of Activity and Ventilation Rate Bio-Loggers for Tracking Welfare and Fish-Environment Interactions in Salmonids and Mediterranean Farmed Fish

OPEN ACCESS

**Edited by:**
*Enric Gisbert, Institute of Agrifood Research and Technology (IRTA), Spain*

**Reviewed by:**
*Lluis Tort, Universitat Autònoma de Barcelona, Spain*
*Marce Herrera, IFAPA Centro Agua del Pino, Spain*

***Correspondence:**
*Jaume Pérez-Sánchez*
*jaime.perez.sanchez@csic.es*

**Specialty section:**
*This article was submitted to Aquatic Physiology, a section of the journal Frontiers in Marine Science*

**Received:** *14 January 2022*
**Accepted:** *09 February 2022*
**Published:** *07 March 2022*

**Citation:**
*Calduch-Giner J, Holhorea PG, Ferrer MÁ, Naya-Català F, Rosell-Moll E, Vega García C, Prunet P, Espmark ÅM, Leguen I, Kolarevic J, Vega A, Kerneis T, Goardon L, Afonso JM and Pérez-Sánchez J (2022) Revising the Impact and Prospects of Activity and Ventilation Rate Bio-Loggers for Tracking Welfare and Fish-Environment Interactions in Salmonids and Mediterranean Farmed Fish. Front. Mar. Sci. 9:854888. doi: 10.3389/fmars.2022.854888*

***Josep Calduch-Giner[1], Paul George Holhorea[1], Miguel Ángel Ferrer[2], Fernando Naya-Català[1], Enrique Rosell-Moll[1], Carlos Vega García[3], Patrick Prunet[4], Åsa M. Espmark[5], Isabelle Leguen[6], Jelena Kolarevic[7], Aurelio Vega[3], Thierry Kerneis[8], Lionel Goardon[8], Juan Manuel Afonso[9] and Jaume Pérez-Sánchez[1]****

*[1] Nutrigenomics and Fish Growth Endocrinology Group, Institute of Aquaculture Torre de la Sal (IATS-CSIC), Castellón, Spain, [2] Technological Centre for Innovation in Communications (iDeTIC), University of Las Palmas de Gran Canaria (ULPGC), Las Palmas, Spain, [3] Institute for Applied Microelectronics (IUMA), University of Las Palmas de Gran Canaria, Las Palmas, Spain, [4] INRAE, Laboratoire de Physiologie et de Génomique des Poissons (LPGP), Rennes, France, [5] Nofima AS, Tromsø, Norway, [6] MARBEC, Univ. Montpellier, CNRS, Ifremer, IRD, Palavas-les-Flots, France, [7] Faculty of Biosciences, Fisheries and Economics, The Norwegian College of Fishery Science, UiT The Arctic University of Norway, Tromsø, Norway, [8] INRAE, PEIMA, Sizun, France, [9] Aquaculture Research Group, Institute of Sustainable Aquaculture and Marine Ecosystems (IU-ECOAQUA), University of Las Palmas de Gran Canaria, Las Palmas, Spain*

Behavioral parameters are reliable and useful operational welfare indicators that yield information on fish health and welfare status in aquaculture. However, aquatic environment is still constraining for some solutions based on underwater cameras or echo sounder transmitters. Thus, the use of bio-loggers internally or externally attached to sentinel fish emerges as a solution for fish welfare monitoring in tanks- and sea cages-rearing systems. This review is focused on the recently developed AEFishBIT, a small and light data storage tag designed to be externally attached to fish operculum for individual and simultaneous monitoring of swimming activity and ventilation rates under steady and unsteady swimming conditions for short-term periods. AEFishBIT is a tri-axial accelerometer with a frequency sampling of 50–100 Hz that is able to provide proxy measurements of physical and metabolic activities validated by video recording, exercise tests in swim tunnel respirometers, and differential operculum and body tail movements across fish species with differences in swimming capabilities. Tagging procedures based on tag piercing and surgery procedures are adapted to species anatomical head and operculum features, which allowed trained operators to quickly complete the tagging procedure with a fast post-tagging recovery of just 2.5–7 h in both salmonid (rainbow trout, Atlantic salmon) and non-salmonid (gilthead sea bream, European sea bass) farmed fish. Dual recorded data are processed by on-board algorithms, providing valuable information on adaptive behavior through

the productive cycle with the changing environment and genetics. Such biosensing approach also provides valuable information on social behavior in terms of adaptive capacities or changes in daily or seasonal activity, linking respiratory rates with changes in metabolic rates and energy partitioning between growth and physical activity. At short-term, upcoming improvements in device design and accompanying software are envisaged, including energy-harvesting techniques aimed to prolong the battery life and the addition of a gyroscope for the estimation of the spatial distribution of fish movements. Altogether, the measured features of AEFishBIT will assist researchers, fish farmers and breeders to establish stricter welfare criteria, suitable feeding strategies, and to produce more robust and efficient fish in a changing environment, helping to improve fish management and aquaculture profitability.

**Keywords: bio-loggers, welfare indicator, activity patterns, ventilation rate, fish behavior, fish robustness**

## INTRODUCTION

To meet the increasing global demand of fish protein, aquaculture production is becoming more intensified, which requires the selection of non-aggressive individuals that perform well at high densities (Huntingford, 2004; Huntingford et al., 2006). The potential benefits are obvious because fish with high stress resilience are less susceptible to diseases, show better growth performance, and provide a better-quality product (Ashley, 2007). However, animal health and welfare issues are of increasing public concern, and livestock industries and aquaculture in particular require to project a welfare-friendly image of their products (Hemsworth and Coleman, 2011; Toni et al., 2019; Barreto et al., 2021). The challenge is that fish aquaculture involves a huge number of species and the understanding of their welfare biology is limited, which explains why relatively few operational welfare indicators (OWI) are used to assess welfare status on commercial aquaculture facilities (Segner et al., 2019). Major advances on the establishment of OWIs have been achieved in Atlantic salmon (Noble et al., 2018; Rey et al., 2019), trout (Noble et al., 2020), and tilapia (Pedrazzani et al., 2020). Less standardized are the welfare assessment protocols in other farmed fish, such as gilthead sea bream and European sea bass (Papaharisis et al., 2019; Sadoul et al., 2021), though specific key performance indicator-based benchmarking systems have been recently validated within the framework of MedAID[1] and PerformFISH[2] H2020 EU projects. All this will contribute to ensure that fish welfare is properly assessed in different aquaculture production systems to warrant that currently cultured fish strains are not far from their optimum welfare (Saraiva et al., 2018; Saraiva and Arechavala-Lopez, 2019). It is thereby important to encompass the development of aquaculture with novel and stricter criteria of welfare for the simultaneous improvement of the productivity and the welfare of group-housed animals. This includes the use of both animal-based indicators (something you monitor from the fish) and indirect resource-based indicators (measurements of rearing environment), but further research is needed for a full and rapid transition from highly informative laboratory-based welfare indicators (LABWI) to OWI (Noble et al., 2018). A good example of a fast transition is the portable MinION nanopore sequencer, which allows fish farmers and researchers to obtain rapid microbial profiles and RNA viruses diagnoses of reared fish (Gallagher et al., 2018; Gonçalves et al., 2020). Hence, with the advent of new technologies it will be relatively easy to integrate insights from the environment, microbial loads, and fish behavior and appearance, which can be then scored according to the suggested welfare status from 0 (worst) to 1 (best) (Noble et al., 2018, 2019).

Behavioral indicators are becoming especially useful for alerting farmers that something is potentially wrong and warrants further investigation before significant welfare issues and mortality occur (Martins et al., 2012; Sharma, 2019). Thus, exploratory behavior or feed anticipatory activities are considered indicators of good welfare. By contrast, abnormal swimming and poor response to feed or novel objects are indicators of disease and stressful conditions, depending on how a particular animal perceives handling and restraint on the previous experiences and inherited traits. Thus, selective breeding of more social animals resulted in the improved behavior of the offspring (de Goede et al., 2013; Balasch and Tort, 2019). The challenge is that very often behavioral indicators are difficult to quantify in the aquatic environment (absolute changes in swimming speed, aggression levels, and gill beat frequency) and proper assessment of fish welfare often requires additional physiological measurements (Sadoul et al., 2021). Moreover, these analysis becomes tedious and laborious, though underwater cameras and echo sounder technology are relatively inexpensive and provide the opportunity for real time observation of fish behavior and intelligent feeding (Hung et al., 2016; Li et al., 2020; An et al., 2021; Georgopoulou et al., 2021). Therefore, to turn quantitative behavioral analysis into practical OWI, technological advances on machine vision, biotelemetry and miniaturized bio-loggers need to be applied and adapted to the demand of fish welfare monitoring. Thus, as reviewed by Macaulay et al. (2021), electronic transmitter tags

[1] www.medaid.eu

[2] www.performfish.eu

(e.g., acoustic accelerometers) were first developed for studying wild fish behavior, but they are now rapidly transitioned into the world of farmed fish for an individual-based behavioral assessment, acting tagged individuals as "sentinel fish" to provide useful welfare-related information for monitoring and managing feeding, growth and disease outbreaks (Kolarevic et al., 2016; Føre et al., 2017, 2018; Warren-Myers et al., 2021). In any case, the proposed monitoring solutions should be different depending on the asked question, the species biology, and the culture system (tank-based systems, ponds, lagoons, sea cages, etc.).

A primary assumption of "smart farming" is that the behavior of tagged individuals is representative of that of untagged individuals, but tagging can be a stressful experience causing altered behavior and increased mortality (Jepsen et al., 2015; Newton et al., 2016; Vollset et al., 2020; Macaulay et al., 2021. Such negative effects should be mitigated as transmitter tags evolve and become more miniaturized. Meanwhile, the smaller size of Data Storage Tags (DST) (working in standalone mode) makes it easier to monitor small fish, while minimizing the negative impact of tagging protocols for a reliable underscore of welfare in fish exposed to different aquaculture stressors (Rosell-Moll et al., 2021). However, the retrieval of DST devices for data download remains a major constraint (especially in the case of sea-cage aquaculture). Besides, tagging procedures should be refined and improved using species-specific approaches for minimizing not only animal discomfort and data skew, but also the success of tag recovery for the download of recorded and/or pre-processed data by on-board algorithms. Otherwise, energy harvesting, energy storage, micro-power management of DST tags and their system integration need to be addressed in depth to define the best trade-off between battery power life and the accuracy of data recording, processing and transmitting. Each sensing system has thereby different advantages and disadvantages, and the aim of this review is to revisit the use of DST devices as an alternative and some times more accurate solution for progressing toward the use of IoT in aquaculture by both academic and industry researchers. Attention was focused on accelerometer technology with special emphasis on the DST prototype (AEFishBIT), designed and validated within the framework of AQUAEXCEL$^{2020}$ H2020 EU project for the individual and simultaneous monitoring of physical activity and gill ventilation rates (two in one). AEFishBIT battery is rechargeable and it can be re-used several times with reprogrammable data sampling schedules. This device has been tested in European sea bass and more extensively in gilthead sea bream under a wide range of experimental conditions (Martos-Sitcha et al., 2019b; Ferrer et al., 2020; Rosell-Moll et al., 2021). It has thereby a Technology Readiness Level (TLR) higher than 7, and current studies in rainbow trout and Atlantic salmon have proven its potential in other farmed fish using species-specific procedures for the device operculum tagging (see below). We discuss here how further research and technological improvements in fish sensing can contribute to associate different activity and behavior patterns with better performance or differences in stress and disease resilience, emphasizing the importance of the better understanding of the species and genotype-by-environment interactions for the improvement of fish health and welfare in the framework of AQUAEXCEL3.0 EU project.

## DATA RECORDING AND ON-BOARD ALGORITHM DATA PROCESSING

The assessment of fish welfare through behavior and movement analyses requires a precise and accurate representation of movements. This is initiated by neuronal electrical impulses, causing muscle contractions that produce a mechanical impulse or jerk. In this way, the wave-like swimming activity is an overlap of jerks caused by the repetitive electrical stimulation of the muscles by the neurons. This sequence of jerks causes a bell-shaped speed representation with a period similar to the period of the electrical stimulation. A proper sampling frequency of these bell-shaped changes in speed is essential for an accurate description of fish movements. Most devices in the market rely on a low sampling frequency and average the accelerometer data over a sampling window of usually 20–40 s. This average corresponds to a low pass filtering of the absolute acceleration values, and they are adequate to represent changes in the tendency of swimming speed, as variation from steady to unsteady swimming will result in differences in the averaged data. Low sampling frequencies are also convenient for a real-time transmission of the averaged accelerations. Thus, the use of low frequency sampling devices is adequate for a continuous fish monitoring in sea cages of unsteady movements and to transmit low bit rate data in real time *via* acoustic communication channels, though they are less informative about other subtler events that can be of importance for the assessment of the overall welfare status (Murchie et al., 2011; Wilson et al., 2013; Arechavala-Lopez et al., 2021). Indeed, the capture of sustained movement with an accelerometer requires not only an adequate tag implantation location (Alfonso et al., 2021), but also high sampling rates that have been usually established to be higher than 30 Hz (Broell et al., 2013). Higher sampling frequencies are free of any aliasing distortion (Chen and Bassett, 2005) and allow to work out the fish velocity by integration of the acceleration and the real distance covered by the fish by integration of the velocity. Similarly, the time derivation of the acceleration will be the jerk and the jerk derivation the snap of the fish. These principles were taken into account for the design and use of the low power AEFishBIT device, a tri-axial accelerometer intended to be attached to the operculum of small fish for data recording at a sampling frequency of 100 and 50 Hz (Martos-Sitcha et al., 2019b; Ferrer et al., 2020) for raw data and on-board data processing, respectively.

Briefly, the recorded z-axis acceleration from AEFishBIT device generates positive and negative signals, related to the operculum opening and closing that serves as a direct measure of respiratory frequency. This signal was band pass filtered between 0.5 and 8 Hz to reduce the noise, to attenuate the influence of other movements and to highlight the periodic properties

of the signal. Afterward, the number of crosses through zero was divided by two to obtain the signal period, which was then averaged over several frames for 2 min to reduce the bias and estimate respiratory frequency. Similarly, description of physical activity was based on the simple optimization principle that human and livestock try to perform maximally smooth movements by minimizing the first temporal derivative of acceleration, while constraining all higher derivatives to zero (Flash and Hogan, 1985; Hamäläinen et al., 2011). Thus, *x*- and *y*-axis accelerations were derived to obtain the jerk, being considered their averaged energy over 2 min a representative indicator of physical activity. Software development also offers the possibility to process the recorded data by on-board algorithms (no memory consuming process), increasing the autonomy of the system up to 6 h of continuous data recording with different short-time programmable schedules, routinely reduced to 2–4 days with 2 min measures each 15–30 min windows. This dual recording system (activity and gill breathing) has been validated in a swim tunnel respirometer, which yielded strong correlations of AEFishBIT outputs with data of forced swimming speed and $O_2$ consumption in juveniles of European sea bass and gilthead sea bream (Martos-Sitcha et al., 2019b). As part of the validation procedure, fish species differences (gilthead sea bream vs. European sea bass) in the amplitude and frequency of operculum and body tail movements were also evidenced using recorded raw data from exercised fish, which highlighted the anatomical and metabolic adaptive features of European sea bass as a fast swimming predator (Ferrer et al., 2020). Additionally, in Atlantic salmon, good correlations between AEFishBIT and video recording data have been provided by Kolarevic et al. (2021), providing additional evidence for a reliable use of AEFishBIT as a smart tool for sensing farmed fish of high economic value for aquaculture. The tracking of these validation/calibration procedures is summarized in **Figure 1**. Of note, the device is not initially intended for extended recording periods, though future improvements in AEFishBIT miniaturization, energy harvest and battery auto-recharge will result in a smaller and lighter device that will facilitate fish sensing from earlier life stages and extended periods of time.

## TAGGING METHODS: HOW AND WHERE

As pointed out in previous reviews (Lucas and Baras, 2000; Cooke et al., 2013; Jepsen et al., 2015), there are three main methods for attaching electronic tags to fish: surgical implantation into the body cavity, external attachment, and gastric insertion *via* the mouth. Each method offers different advantages and disadvantages that need to be considered in each particular case. Surgical implantation of the tag does not attract predators and it is ideal for long-term studies, but it requires longer recovery times and generally more practice and skills than other tagging methods. Alternatively, gastric insertion can be a less invasive and quick tagging method, though it is mainly suitable at life stages with growth and feed cessation, and thereby of limited interest in fish farming where a continuous feeding at different rates mostly occurs through all the productive cycle. Conversely, the most commonly reported problems with external tags are tissue damage, tag loss and decreased swimming capacity, but external tagging has the advantage to be used rapidly after tagging or in fish with a body shape not suitable for surgical implantation due to gonadal development or lateral or dorso-ventral compression (flat fish). Otherwise, external tagging is especially useful if sensors are used to record not only external variables (i.e., $O_2$, temperature, light intensity), but also some physiological features such as gill breathing. In particular, the dual recording of AEFishBIT (physical activity and respiratory frequency) requires it to be externally attached to fish operculum, minimizing as much as possible tissue damage, and physiological and behavioral disturbances to ensure that tagged animals are representative of the untagged population in challenging farming conditions and that the tagging procedure does not impact the

| Species | Method | Outcome | References |
|---|---|---|---|
| Gilthead sea bream, European sea bass  | Exercise test in swim tunnel respirometer | Correlation between oxygen consumption and AEFishBIT measurements with increased water flow | Martos-Sitcha et al (2019a) |
| Gilthead sea bream  | Functional tests | Effects of genetics, developmental stage, disease progressin and space and oxygen availability on behaviour and swimming | Rosell-Moll et al. (2021), Perera et al. (2021a) |
| Gilthead sea bream, European sea bass  | Species comparison in swimming capabilities | Differences in amplitude and frequency of operculum and body tail movements highlight the anatomical and metabolic features of sea bass as a fast swimming predator | Ferrer et al. (2020) |
| Atlantic salmon  | Validation of behaviour data by video recording | Activity changes in response to change in light intensity regime agree with video recording results | Kolarevic et al. (2021) |

**FIGURE 1 |** AEFishBIT validation procedures summary.

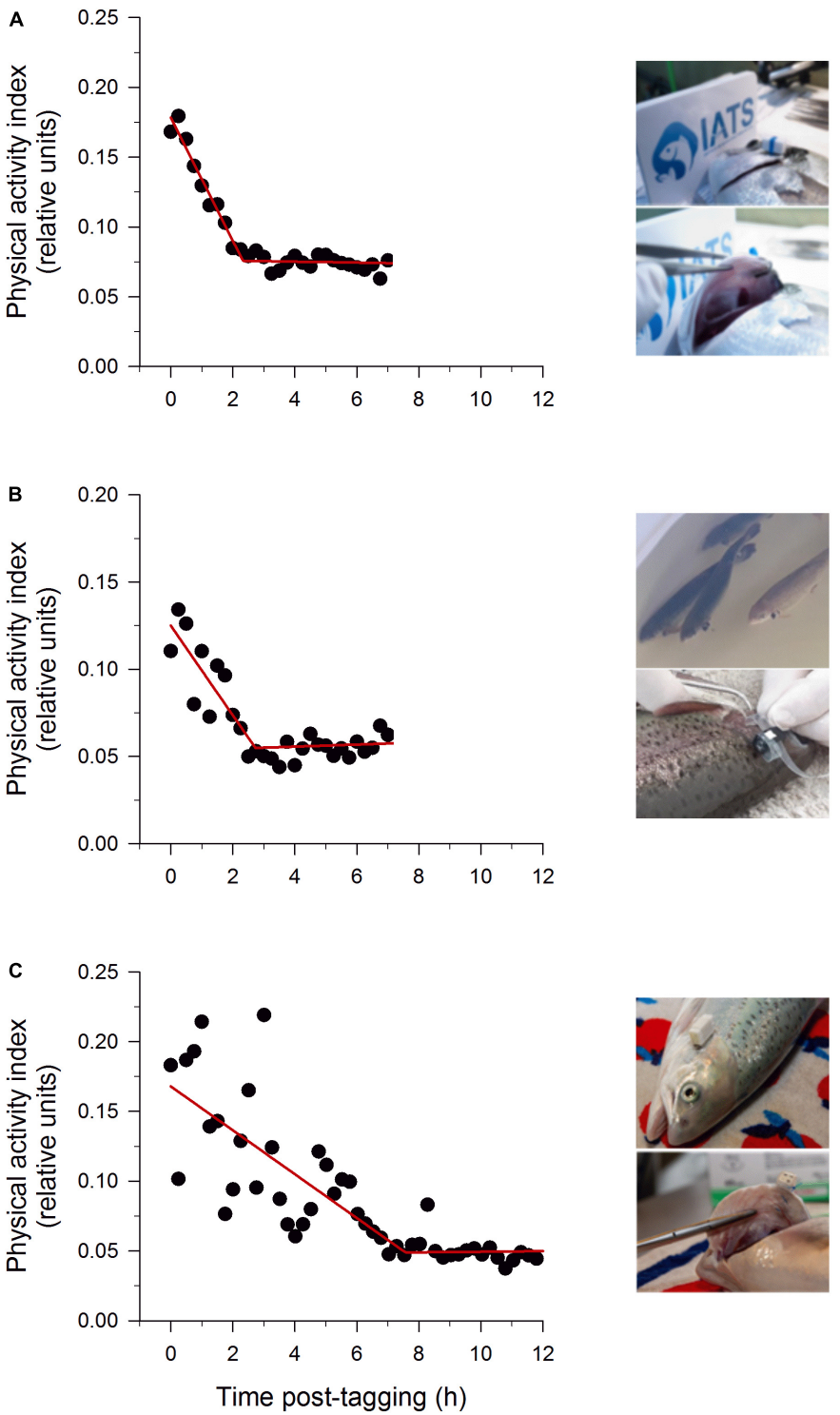


**FIGURE 2 |** AEFishBIT records of physical activity of a representative individual, **(A)** gilthead sea bream; **(B)** rainbow trout; **(C)** Atlantic salmon) after tagging and return to the tank. Measures (black circles) were taken every 15 min. Lines represent piecewise linear fit of data with one break point. Inserts show the operculum attachment in 200–300 g gilthead sea bream (monel tags with a flexible heat shrink polyethylene tube), 550–650 rainbow trout (heat shrink polyethylene tube ring 2 weeks after suture) and 700–800 g Atlantic salmon (suture and heat shrink polyethylene tube ring in a single step). Partially adapted from data of Kolarevic et al. (2021) and Rosell-Moll et al. (2021).

reliability of the recorded data (Macaulay et al., 2021). In that sense, the AEFishBIT device benefits of a small size and weight (15 × 6 × 6 mm, 1.1 g in air), though the tagging method needs to be adapted to each species to make it a reliable tool for smart sensing farmed fish.

In gilthead sea bream and European sea bass, the AEFishBIT attachment was initially attained using laboratory tags for identification of experimentation animals (RapID tags), which were rapidly pierced to operculum and on which a polyamide pocket was fixed in juvenile fish of 50–100 g onward (Martos-Sitcha et al., 2019b). This attachment procedure did not alter significantly plasma levels of cortisol, glucose and lactate after 1 week of tagging. However, after 10 days, the appearance of macroscopic indications of damage and necrosis at the piercing location were evident in a high percentage of individuals reared in a tank-based system. This undesirable effect was solved by using corrosion-resistant self-piercing fish tags with a flexible heat shrink polyethylene tube to fit the device, which avoided growth impairment or pathological signs of hemorrhage or tissue damage after 1–3 weeks of tagging (Rosell-Moll et al., 2021). Such approach also works well in flat fish (turbot, sole), but it is not feasible in rainbow trout or Atlantic salmon, probably due to differences in head shape and operculum ossification (Huby and Parmentier, 2019). Indeed, following this tagging protocol, significant tissue damage and necrosis were observed few days post-tagging in both trout and salmon at the level of the piercing location and also on the gill tissue located below. Thus, alternative surgery approaches were developed for trout and salmon (400–500 g onward), using a flexible heat shrink polyethylene tube ring sutured on the operculum and with AEFishBIT held in this ring. This tagging method led to 100% retention rate (7 days post-tagging) with no significant tissue

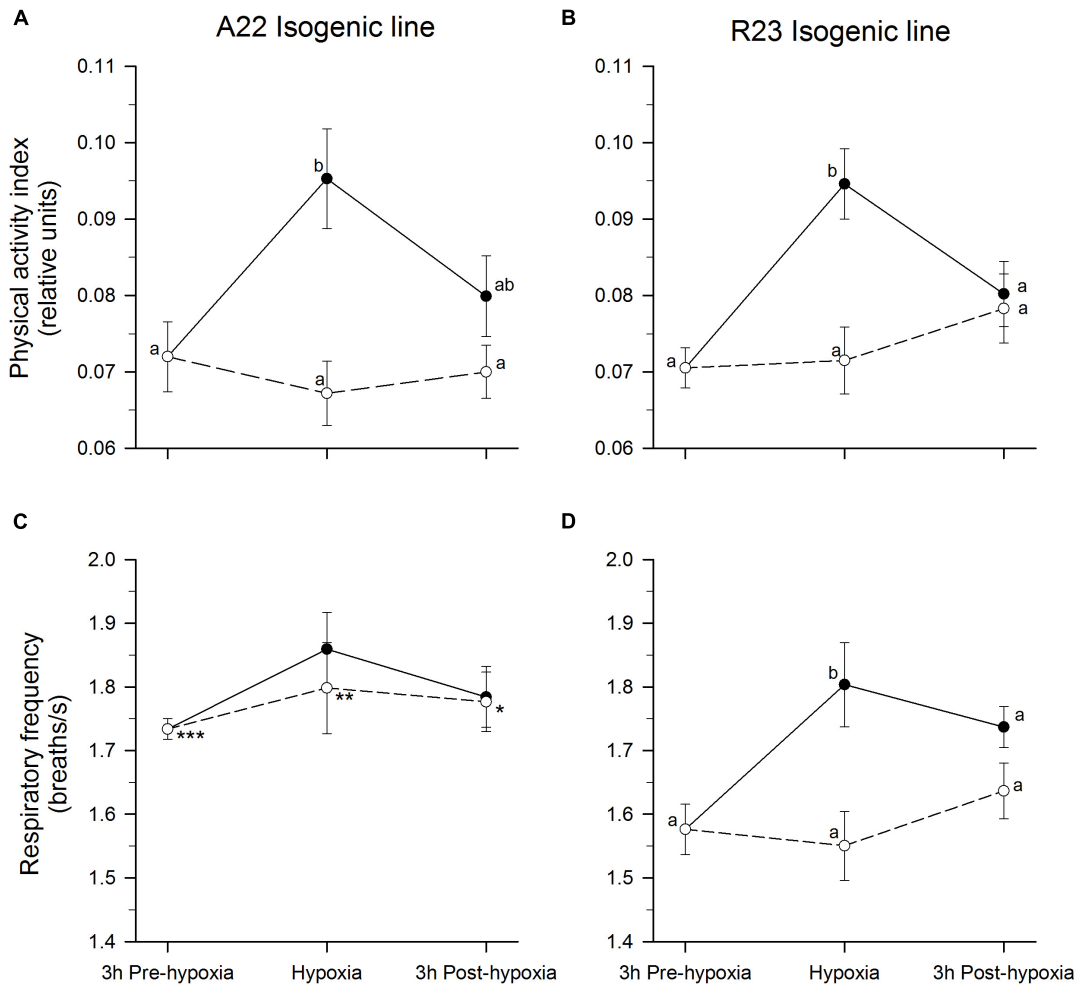


**FIGURE 3 |** AEFishBIT records of physical activity **(A,B)** and respiratory frequency **(C,D)** of rainbow trout isogenic lines A22 **(A,C)** and R23 **(B,D)** exposed to a 3 h hypoxia (from 8.0–9.0 ppm to 2.8–3.0 $O_2$ ppm) challenge. For each individual (598 ± 10 g body weight), measures taken every 15 min are averaged at each time point (3 h pre-challenge, 3 h hypoxia, 3 h post-challenge). Black circles are the values of hypoxia-challenged fish, whereas white circles are those of unchallenged fish. Values are expressed as mean ± SEM ($n$ = 10 for hypoxia and post-challenge groups, $n$ = 20 for pre-challenge fish). Different letters represent significant ($P < 0.05$, ANOVA, SNK test) differences among challenge time points. Asterisks represent significant (*$P < 0.05$; **$P < 0.01$; ***$P < 0.001$, $t$-test) between trout lines at the same time point and challenge.

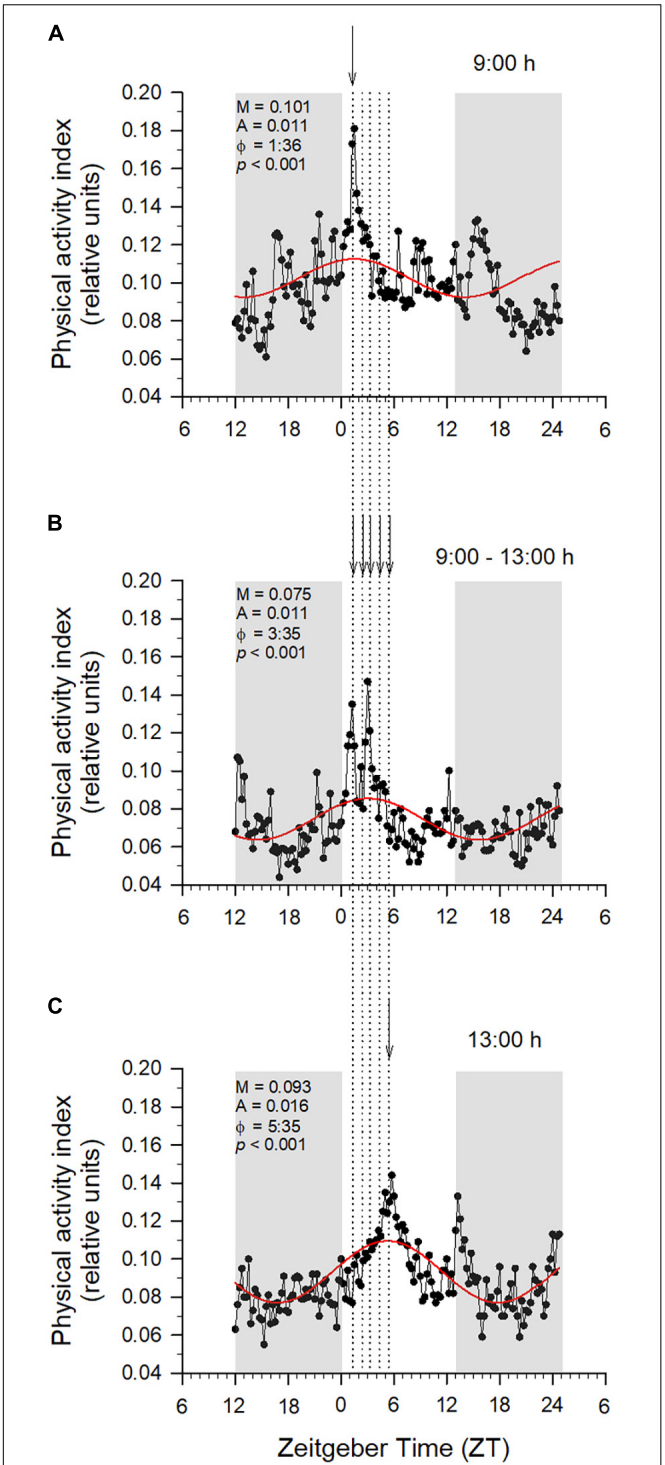


**FIGURE 4 |** Gilthead sea bream (mean body weight 305 g) activity synchronization by feeding with different schedules: 9:00 h **(A)**, once per hour between 9:00 and 13:00 h **(B)**, and at 13:00 h **(C)**. In each panel, the best-fit curve derived from cosinor analysis of physical activity AEFishBIT data (measures taken every 15 min along 2 days) of representative individuals is shown as a continuous solid line. Values of mesor (M), amplitude (A), acrophase (ϕ), and *p*-value (P) of best-fit curves are shown. Gray shaded areas represent dark phases. Arrows in vertical dotted lines indicates the mealtimes.

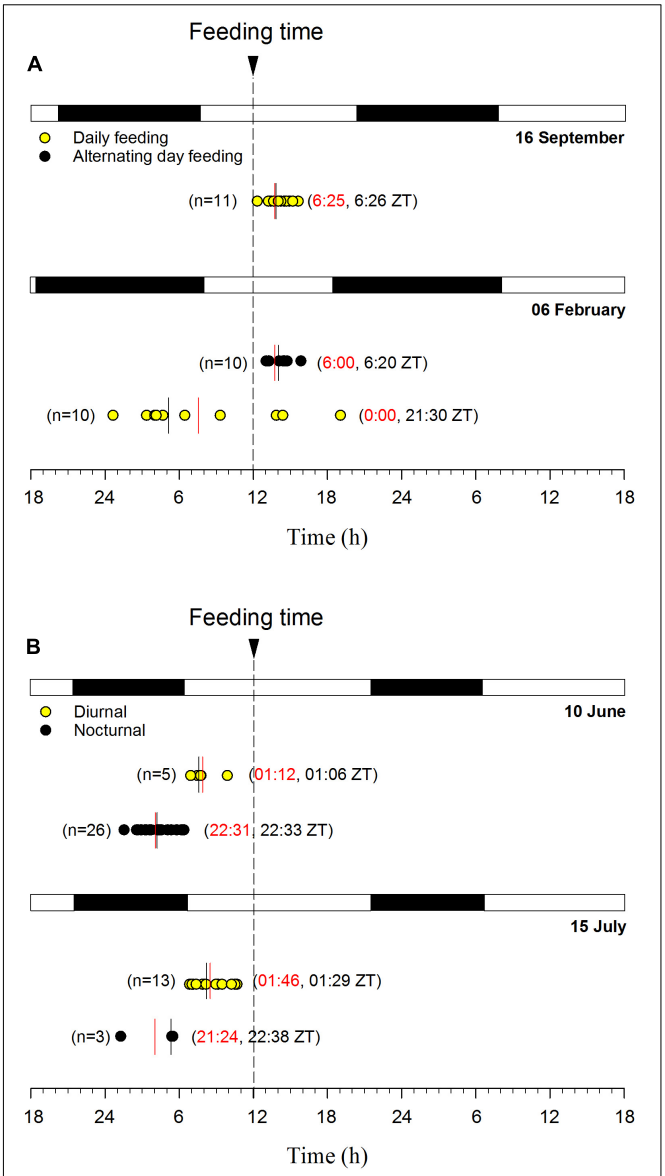


**FIGURE 5 |** Seasonal activity synchronization by feeding in gilthead sea bream **(A)** and European sea bass **(B)**. Circles represent the activity acrophase of the best-fit curve derived from cosinor analysis of physical activity AEFishBIT data (measures taken every 15 min along 2 days) of each individual. At each month, light and dark phases (natural photoperiod) are represented, as well as the feeding time. For gilthead sea bream, fish fed daily (mean body weight 225 g in September, 390 g in February) are represented by red circles, and fish fed during alternate days (mean body weight 385 g) are represented by black circles. For European sea bass fed daily, individuals with diurnal (yellow circles, mean body weight 295 g in June and 345 g in July) and nocturnal (black circles, mean body weight 250 g in June and 255 g in July) behavior are represented. For each group, green bar marks the mean acrophase, and black bar the median. The number of individuals is stated for each group.

lesions or gill lamellae necrosis in salmon of 400–600 g body weight (Kolarevic et al., 2021). This procedure still provoked some tissue damages in trout, though it can be prevented by means of a suture step at operculum 2 weeks before the

implantation of the heat shrink polyethylene ring with the AEFishBIT device. The success of the different tagging protocols was evidenced by a fast achievement of a steady state for the AEFishBIT measurements of physical activity, which was found within 2.5–3 h post-tagging in gilthead sea bream and trout, whereas 7 h were required for salmon with a lasting surgery tagging procedure in a single step (**Figure 2**). In any case, the tagging recovery after AEFishBIT implantation was fast in all species, which makes feasible to start data recording few hours after the completion of tagging procedure.

# EVALUATING HOW IS FISH SENSING AND RESPONDING

## Problems and Pitfalls in Spatial Cognition and Physical Swimming Activity

Natural stressors tend to be brief and/or avoidable, while stressors in captivity are often prolonged or repetitive, activating in a repeated manner physiological stress responses detrimental to the animal (Fraser and Duncan, 1998; Veissier and Boissy, 2007). This becomes especially evident in the case of random aquaculture stressors (Bermejo-Nogales et al., 2014), showing transcriptomic meta-analysis that mitochondria are among the first responders to environmental and nutritional stress stimuli in fish (Calduch-Giner et al., 2014; Healy et al., 2017; Sokolova, 2018). Particularly in gilthead sea bream, several mitochondrial markers with a role in oxidative phosphorylation, antioxidant defense and respiration uncoupling have been used as reference values of well-being to monitor and mitigate the negative impacts of captive rearing (Pérez-Sánchez et al., 2011; Bermejo-Nogales et al., 2015; Magnoni et al., 2017; Martos-Sitcha et al., 2017, 2019a). However, this interest has now expanded into recognizing the importance of positive effects of environmental enrichment (EE) as a promising tool to guarantee or improve the welfare of laboratory and farmed fish (Brydges and Braithwaite, 2009; Evans et al., 2015; Stevens et al., 2021). Such approach provides the opportunity to experience new situations typical of the species in the wild, and it is generally accepted that well-designed EE (e.g., stones, roots, logs, plants, algae, sand, sessile animals, ice, artificial objects, etc.) improves behavioral flexibility and cognitive ability of fish by changes in physical activity. Indeed, modifications in swimming behavior reflect how a fish is sensing and responding to its environment, which is reflected by changes in spatial distribution and ventilation activity to ensure the supply of $O_2$ at the exact rate required by the organism (Martins et al., 2012; Zupa et al., 2015; Arechavala-Lopez et al., 2021). Thus, video recording analysis highlighted that physical EE promoted the increase of antioxidant enzyme activity, exploratory behavior and learning abilities of gilthead sea bream juveniles reared in tank-based systems (Arechavala-Lopez et al., 2020). Likewise, the provision of EE in sea cages promoted the overall improvement of gilthead sea bream welfare, reducing aggressiveness and interactions with the net, which might serve to reduce the incidence of fish escapes (Arechavala-Lopez et al., 2019; Muñoz et al., 2020). However, data records from independent studies are often poorly consistent and it remains difficult to establish a general pattern of space occupancy and physical swimming activity as valuable insights in the behavior, but also in the physiological well-being and resilience of farmed fish around the world and Mediterranean fish in particular.

The above findings reinforce the need of further research addressing the type of body movements that are recorded from the externally or internally implanted fish sensors. Certainly, Palstra et al. (2021) pointed out that gilthead sea bream accelerations from acoustic transmitter tags (ventrally implanted) are a good proxy of unsteady swimming activity (e.g., escape reactions and aggressive or foraging behavior) in experimental sea cages, but not of sustained swimming exercise. This assumption is based on the correlations between accelerations and the weight of heart and mesenteric fat weight, which were the opposite to that found and expected in exercised training fish (Blasco et al., 2015; Rodnick and Planas, 2016; Palstra et al., 2020). Indeed, most commercially available acoustic accelerometers work at low data recording frequency, and they mainly record deviations from sustained activity in swim-tunnel exercised fish at different flow speeds (Arechavala-Lopez et al., 2021). In contrast, as indicated before, the inferred physical activity from on-board AEFishBIT outputs in exercised juveniles of gilthead sea bream and European sea bass is able to characterize the whole jerk produced by the muscular twitching that impulse the fish and reconstruct the bell-shaped acceleration of the muscular jerk. High sampling frequency also allows detecting consistent differences in sustained swimming at various speeds (1–6 body length/s) (Martos-Sitcha et al., 2019b). Moreover, in depth analysis of raw data from exercised fish highlighted that the large amplitude of operculum aperture and body tail movements of European sea bass is part of the adaptive features of this fish species as a fast swimming predator (Ferrer et al., 2020), linked to the natural evolution and behavioral ecology in a predator-prey system (Berger, 2010; de Matos Dias et al., 2018). Besides, selection for growth within the PROGENSA® gilthead sea bream breeding program modified behavioral and physical activity traits, priming growth in genetically fast-growing fish and swimming performance in genetically slow-growing fish (Perera et al., 2021a). This was supported by the improved resistance to fatigue in swim tunnels, but also by the more active swimming behavior of free-swimming fish assessed by AEFishBIT measurements of grouped-housed fish in rearing tanks. Likewise, AEFishBIT outputs revealed a more continuous physical swimming activity of younger fish when comparisons were made between gilthead sea bream individuals of class of age + 1 and class of age + 3 (Rosell-Moll et al., 2021). Older fish also showed a significant reduction of operculum beats, supporting a reduction of metabolic rates with the age-mediated decrease in growth rates. Also in this study, jerk accelerations of fish allocated in 90 L, 500 L and 3,000 L tanks increased with the decrease of available space as a result of erratic and chaotic trajectories, which again indicates that AEFishBIT outputs of swimming activity are a good proxy for both unsteady and

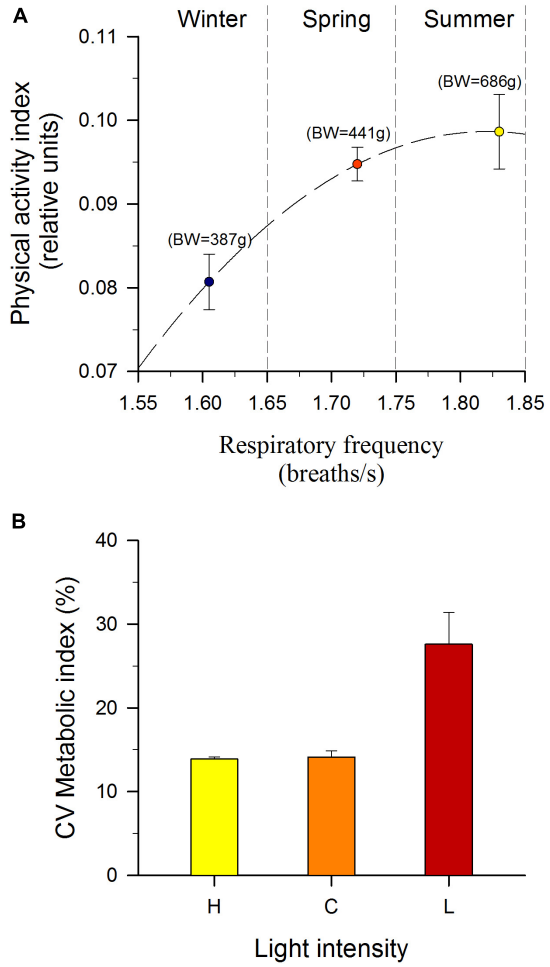


**FIGURE 6 | (A)** Seasonal correlation plot between physical activity index and respiratory frequency in cultured gilthead sea bream (measures taken every 15 min along 2 days). Each value represents the mean mesor of 10–12 individuals **(B)** Coefficient of variation (CV) of the metabolic index (respiratory frequency/physical activity) of Atlantic salmon exposed to different light intensities: H (High, yellow bar, 18.90 $\mu mol.m^{-2}.s^{-1}$), C (Control, orange bar, 6.83 $\mu mol.m^{-2}.s^{-1}$) and L (Low, red bar, 0.28 $\mu mol.m^{-2}.s^{-1}$). Each value is the mean ± SEM of the daily coefficient of variation of 6–7 individuals for 3 days. Different letters indicate significant differences ($P < 0.01$, ANOVA). Partially adapted from data of Kolarevic et al. (2021).

sustained swimming activity. Indeed, monitoring of physical activity is becoming a useful tool for meeting the behavioral needs (e.g., optimal space availability regardless of density), or time of adaptation of farmed fish for reducing stress, aggressiveness and anxiety after stressful aquaculture operations (Stevens et al., 2021).

## Adaptive Capacities and Robustness

In a time of rapid environmental changes, with increases in ocean temperatures and in the frequency and severity of hypoxic events, serious concerns are arising about the profitability of some aquaculture production systems (Brander, 2007; Gamperl et al., 2020; Burke et al., 2021). Therefore, the better understanding of the mechanisms operating in fish to mitigate heat stress in combination with mild hypoxia is becoming a challenge. Recently, important advances have been made in this field, and a number of genes have been identified in Atlantic salmon as molecular biomarkers for the quantification of hypoxia, but also for the detection of epigenetic markers that can predict thermotolerance (Beemelmanns et al., 2021). There is also now evidence in zebrafish that paternal hypoxia exposure primes offspring for increased hypoxia resistance (Ragsdale et al., 2020). As a general pattern, these hypoxic adaptive features involve the induction of hypo-metabolic states, the increased $O_2$-mitochondria affinity, and the aerobic/anaerobic switches in substrate preference as metabolic fuels according to the metabolic capabilities of each tissue (Hoppeler and Vogt, 2001; Murray, 2009; Gamboa and Andrade, 2012; Martos-Sitcha et al., 2017, 2019a). However, in gilthead sea bream juveniles, this process is more complex than initially envisaged. Thus, the resetting of the skeletal muscle transcriptome by mild hypoxia condition first primed an increased contribution of lipid metabolism to the whole energy supply to preserve the aerobic energy production, and thereafter (with the restoration of normoxia) a reduced protein turnover and improved anaerobic fitness (Naya-Català et al., 2021b). How fish physiologists, farmers and breeders can fully exploit this metabolic plasticity remains open, though it becomes clear that it can serve to preserve an efficient nutrient utilization but also the swimming performance under predictable hypoxic stress episodes.

It is also known that the different growing within gilthead sea bream families from the PROGENSA® breeding program are associated with differences in resistance to fatigue and probably with different aerobic/anaerobic fitness to cope with a low $O_2$ availability (Perera et al., 2021b). These traits are co-selected with a growth pattern that promoted growth spurts in summer rather than a more continuous growth across season (Perera et al., 2019). However, the genetic variability of current farmed gilthead sea bream populations remains high enough and individual tracking of physical activity patterns with AEFishBIT served to differentiate active and inactive behaviors after exposure to acute hypoxia (Rosell-Moll et al., 2021). Active individuals typically show dynamic avoidance in response to challenges and are more aggressive and socially dominant. On the contrary, inactive (or passive) individuals generally respond to challenges with caution and immobility, being socially subordinate, and generally more flexible in their behavioral responses to environmental change (Koolhaas et al., 1999; Korte et al., 2005; Huntingford et al., 2010). AEFishBIT determined that all hypoxic fish increased their ventilation rates almost equally in our challenge, but jerk accelerations highlighted the enhanced physical activity of a subset of fish that will support their escape reactions (active fish) during hypoxia episodes.

Robustness, defined as the ability to combine high production potential with resilience to stressors, becomes a key trait for selection in aquaculture (Knap, 2005). Physiological and behavioral resistance and resilience to environmental challenges are thereby considered a robustness feature. Robustness typology has been studied in two divergent isogenic lines of trout,

namely A22 and R23, with a different ability to cope with plant-based diets (Geurden et al., 2013). These fish are also a good model for studying differences in hypothalamus-pituitary-interrenal (HPI) reactivity, as an alternative to the previously studied high and low cortisol responsive fish strains of trout (Pottinger and Carrick, 1999; Øverli et al., 2005). Indeed, animals of line R23 were described as less aggressive and more robust fish showing a low cortisol response to crowding stress in comparison to reactive individuals (line A22) that showed a strong corticosteroid response (Sadoul et al., 2015). Nevertheless, comparisons between different environmental stressors pointed out that animals can modulate their responses depending on the type of stressor. Thus, line R23 showed a higher sensitivity than A22 to an acute $CO_2$ (hypercapnia) challenge (Sadoul et al., 2017). These divergences in adaptive capabilities are further corroborated by AEFishBIT measurements in hypoxic exposed fish. In fact, the two trout isogenic lines highlighted an increased physical activity during hypoxia, and this response was more persistent in reactive A22 fish (**Figures 3A,B**). Regarding respiratory frequency, it was noticeable that R23 fish displayed a lower basal activity than A22, and this feature could facilitate an enhanced respiration responsiveness in fish facing a hypoxic challenge, whereas respiratory frequency of challenged A22 fish remained closer to normoxia values prior the challenge (**Figures 3C,D**). These data illustrate the different behavioral and physiological strategies developed by the two isogenic trout lines when exposed to acute hypoxia stress and confirm the notion that differences in basal behavior determined with AEFishBIT help to establish different fish adaptive capabilities. Indeed, comparison of fish species differences in hypoxia tolerance and responsiveness highlighted that, contrarily to gilthead sea bream, the primary response to hypoxia in trout is the increase of locomotor activity rather than ventilation rates. This would reflect the prioritization of the escape reactions in a fish species with a well-known limited tolerance to a hypoxic environment (Dunn and Hochachka, 1986; Hou et al., 2020). Altogether, AEFishBIT can serve to determine differences in basal behavior and how robust are the current domesticated/selected farmed fish when they are facing perturbations associated to common culture practice.

## Daily Patterns of Diurnal/Nocturnal Behavior

Feeding in wild life takes place periodically during a certain temporal niche (e.g., day-time or night-time), depending on whether the species is diurnal or nocturnal. This timing system is comprised of a network of endogenous circadian clocks that generate, *via* their local or distributed outputs, an internal rhythmicity close to 24 h (Challet, 2013). Hence, when food access is limited to a few hours every day at the same time (temporal restricted feeding), most organisms display a food-anticipatory activity, accompanied of food-appetitive behaviors and hormonal responses prior to the expected food presentation (Bloch et al., 2013; Skvortsova et al., 2021). Moreover, disruption of the circadian cycle is strongly associated with metabolic imbalances in rodent models of circadian arrhythmia (Eckel-Mahan and Sassone-Corsi, 2013). Indeed, the pervasiveness of circadian rhythms in life suggests that circadian clocks are adaptive in nature, functioning as a timing reference that allow organisms to anticipate the diel fluctuations in their environments, being also the basis for the transduction of seasonality from the changing photoperiod (Van der Zee et al., 2008). Certainly, it is becoming apparent from metabolites to transcription factors that circadian clock interacts with metabolism in numerous ways that are essential in a multitude of processes related to cellular metabolism, stress, and senescence (Tevy et al., 2013; Majeed et al., 2020), which can operate in the absence of the transcriptional/translational circadian clockwork as reported for instance for ubiquitous antioxidant enzymes (e.g., peroxiredoxins) and $NAD^+$-dependent histone deacetylases (sirtuins). Overall, it opens discussions about the etiological mechanisms regulating food anticipatory responses and metabolic disorders arising from the loss of circadian rhythms. In this regard, early studies in Atlantic salmon highlighted that acute stress can be measured in terms of changes to feeding motivation, becoming this criterion a more sensitive indicator of stress than measurements of changes in cortisol excretion (Folkedal et al., 2012). Certainly, locomotor and feeding rhythms are of endogenous origin, as they can persist under constant conditions without external time cues (Madrid et al., 2001; Sánchez-Vázquez and Madrid, 2001). However, it is also known that vertebrate animals in polar regions show highly diverse activity patterns ranging from entrained circadian rhythms to arrhythmicity patterns (Cockrem, 1990; Ashley et al., 2012), as reported for AEFishBIT measurements of locomotor activity and respiratory rates in Atlantic salmon under continuous light regimes and hourly access to food excess (Kolarevic et al., 2021).

The above findings contrast with the observations made in most other fish studies, showing daily rhythms in locomotor and feeding behavior that can be diurnal or nocturnal depending of the species biology (Madrid et al., 2001; Reebs, 2002). In addition, some fish display a clear seasonal change of diurnal/nocturnal behavior, having European sea bass a nocturnal feeding behavior in winter that is changing to be diurnal in summer and autumn (Azzaydi et al., 2007). Otherwise, using self-feeding system specially designed for small fish, del Pozo et al. (2011) pointed out an independent phasing between locomotor and feeding activities in zebrafish, which were mostly nocturnal or diurnal, respectively. This dualism has also been reported in gilthead sea bream, where the scheduled-feeding drove the self-feeding pattern (López-Olmeda et al., 2009), as it became diurnal or nocturnal under day- or night-feeding, respectively. In contrast, in the same study, the locomotor activity (measured by means of infrared photocells) was little affected by feeding time, and remained mostly diurnal with a photoperiod set at 12 h light: 12 h dark. However, AEFishBIT outputs evidenced the high ability of gilthead sea bream to concentrate self-feeding activity around the programmed meals in fish taught to different temporal restricted feeding schedules (one single meal at 9 or 12 h; hourly feeding times from 9 to 12 h) (**Figure 4**). In addition, feeding would serve to synchronize the phase of locomotor and metabolic rhythms (respiratory rates), which are not necessarily in the same phase in adults of European sea bass feeding at

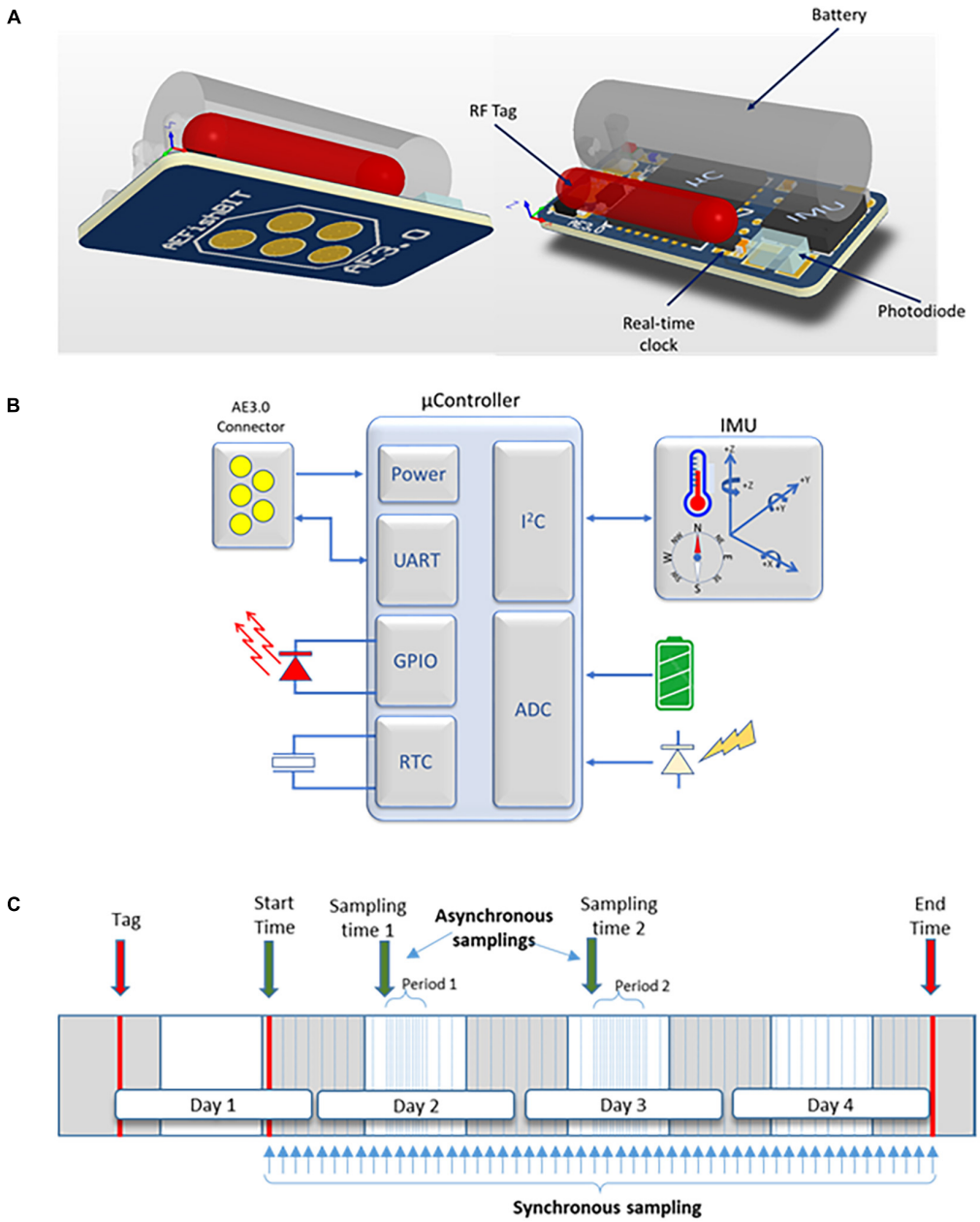


**FIGURE 7 | (A)** 3D view of unencapsulated AEFishBIT prototype. Connection pins are shown in the left image. Prototype includes a real-time clock and a photodiode to ensure device functioning under insulation conditions in aquatic environment. IMU: inertial measurement unit (accelerometer, gyroscope, magnetometer, thermometer). μC: microcontroller. **(B)** Blocks diagram of AEFishBIT functioning. UART: universal asynchronous receiver-transmitter. GPIO: general purpose input/output. RTC: real-time clock. $I^2C$: inter-integrated circuit. ADC: analog to digital converter for battery monitoring. **(C)** Diagram representation of AEFishBIT synchronous and asynchronous schedules.

midday (Ferrer et al., 2020). How the synchronization of feeding, locomotor and metabolic rhythms can contribute to improve aquaculture profit is under debate, but the methodological advances in fish monitoring in a tank-based system can also be extrapolated to the field. For instance, gilthead sea bream in winter becomes mostly arrhythmic with feeding schedules and physiological rhythms of physical activity and respiratory rates out of phase. However, current studies highlight that the use of feeding schedules with alternating days (maintaining constant the total food intake, but with an increased feed supply the feeding day), served to restore the typical feeding behavior of summer with an enhanced activity around the feeding time (**Figure 5A**). By contrast, this daily synchronization is more difficult in European sea bass than in gilthead sea bream, as feeding level by itself does not act as a main synchronizer in actively feeding fish. Indeed, 2-year old European sea bass, taught

to feed at a fixed time at 12:00 h under natural photoperiod and temperature conditions displayed (84% of population) a nocturnal behavior with a peak of activity at 5:01 h (22:31 ZT) during late spring, but only 19% of population remained nocturnal at midsummer with feeding levels of the same order of magnitude (1.0–1.1% body weight) (**Figure 5B**). It is likely that the predator nature of this species drives it to shift its activity behavior according to the longer phase (nocturnal/diurnal) of photoperiod. In any case, how these behavioral features can be used as a suitable indicator of fish welfare and/or domestication success of farmed fish under intensive aquaculture production requires further research.

## Energy Partitioning for Growth and Locomotor Activity

How genetics and environment affect individual size variation and growth compensatory processes in fish with different heritable growth also evolves as a valuable criterion to evaluate and improve growth, production and welfare under intensive fish farming. Certainly, gilthead sea bream families characterized as fast, intermediate and slow growing within the PROGENSA® breeding program had differences in growth trajectories, size heterogeneity, swimming capabilities and gut microbiota composition across the production cycle (Perera et al., 2019, 2021a,b; Piazzon et al., 2020). This is also susceptible of an effective environmental programing that can produce different growth and survival phenotypes depending for instance on the time window of hypoxia episodes. Hence, early mild hypoxia exposure (60–81 dph, 3.6–3.8 ppm) did not compromise growth compensation processes driving a reduced size heterogeneity during early life juvenile stages (Perera et al., 2021b). However, growth compensation becomes constrained with recurrent or late hypoxia episodes in life, which impaired the capacity to reduce size variation during the dominant phase of muscle growth hyperplasia. Such considerations are especially relevant to discriminate the main source of variation in growth rates along time or between different fish families, helping to avoid the use of confounding criteria for improving fish management and aquaculture profitability (Power et al., 2011). Indeed, selective breeding would lead the selection of animals that are not necessarily the fastest growers, but that have a positive effect on the group as a whole (Devlin et al., 2004; de Goede et al., 2013). In this regard, it must be noted that measures of critical swimming speed (defined as the speed that can theoretically be maintained without exhaustion) in swim tunnel tests negatively correlated with growth in gilthead sea bream (Perera et al., 2021a). Likewise, AEFishBIT outputs of group-housed fish highlighted changes in swimming behavior, priming fast growth rather than swimming performance, as reported for highly domesticated strains of salmon and trout that becomes athletically less robust than wild fish (Anttila and Mänttäri, 2009; Bellinger et al., 2014; Zhang et al., 2016). This reveals a complex trade-off that would prime growth in genetically fast-growing fish, or swimming performance (and maybe escape reactions) in genetically slow-growing fish, resulting in a lower capacity of larger fish to cope with the increased water temperature and reduced $O_2$ availability around the entire world due to global warming. How current farmed fish have evolved for adapting to global climate change is thereby a key issue, and welfare indicators informing, directly or indirectly, of this phenotypic plasticity are of high applicability in aquaculture for fish farmers and breeders.

The general thinking is that there is a positive relationship between metabolism and food availability (Reid et al., 2011). However, this relationship can also vary among studies and species (Auer et al., 2015; Liu and Fu, 2017), showing different types of rearrangements between growth and metabolism. For instance, in a common garden system with all fish under identical environmental conditions in the same experimental tank, respiratory rates are negatively or positively correlated with body mass in gilthead sea bream juveniles having slow- and fast-growing phenotypes, respectively (Perera et al., 2021a). This feature highlighted a higher contribution of energy to growth in fast growing fish, which was also evidenced when AEFishBIT comparisons were made between salmon and gilthead sea bream (Kolarevic et al., 2021). Likewise, measurements of respiratory rates in gilthead sea bream varied with growth changes across season and development, while changes in locomotor activity appeared less variable (**Figure 6A**), a feature that reinforces the concept of AEFishBIT respiratory frequency as an indirect measure of basal metabolism and hence growth potentiality among fish species and studies. In other words, the ratio between respiratory frequency and physical activity values can be considered as a metabolic index whose variations can be indicative of differences in the energy partitioning. Indeed, the variations of this metabolic index have been proven useful to assess the adaptation of salmon to different light regimes (**Figure 6B**; Kolarevic et al., 2021). How this knowledge can be used to define new algorithms based on the combination of physical activity and respiratory frequency as integrative welfare indicators is underway to better dissociate the growth changes related to development, natural environmental cues, and aquaculture stressors, with an impact among other factors on the optimization of water quality and available space for the interaction of individuals with the environment and their congeners.

# CONCLUDING REMARKS AND FUTURE PROSPECTS

AEFishBIT provides reproducible and accurate measurements of behavior and welfare status of farmed fish in tank-based systems. This is different of what we expect of electronic transmitter tags that are especially suitable for the real-time monitoring of unsteady swimming activity, associated for instance to feeding behavior or escape reactions in sea cages. Otherwise, the use of DST allows monitoring of small fish, which is of special relevance for farmed species with a harvest body weight of 500–800 g. This is the reason why the miniaturized AEFishBIT device was initially tested and validated on Mediterranean farmed fish rather than in salmonids with a harvest weight at commercialization too much higher than gilthead sea bream or European sea bass.

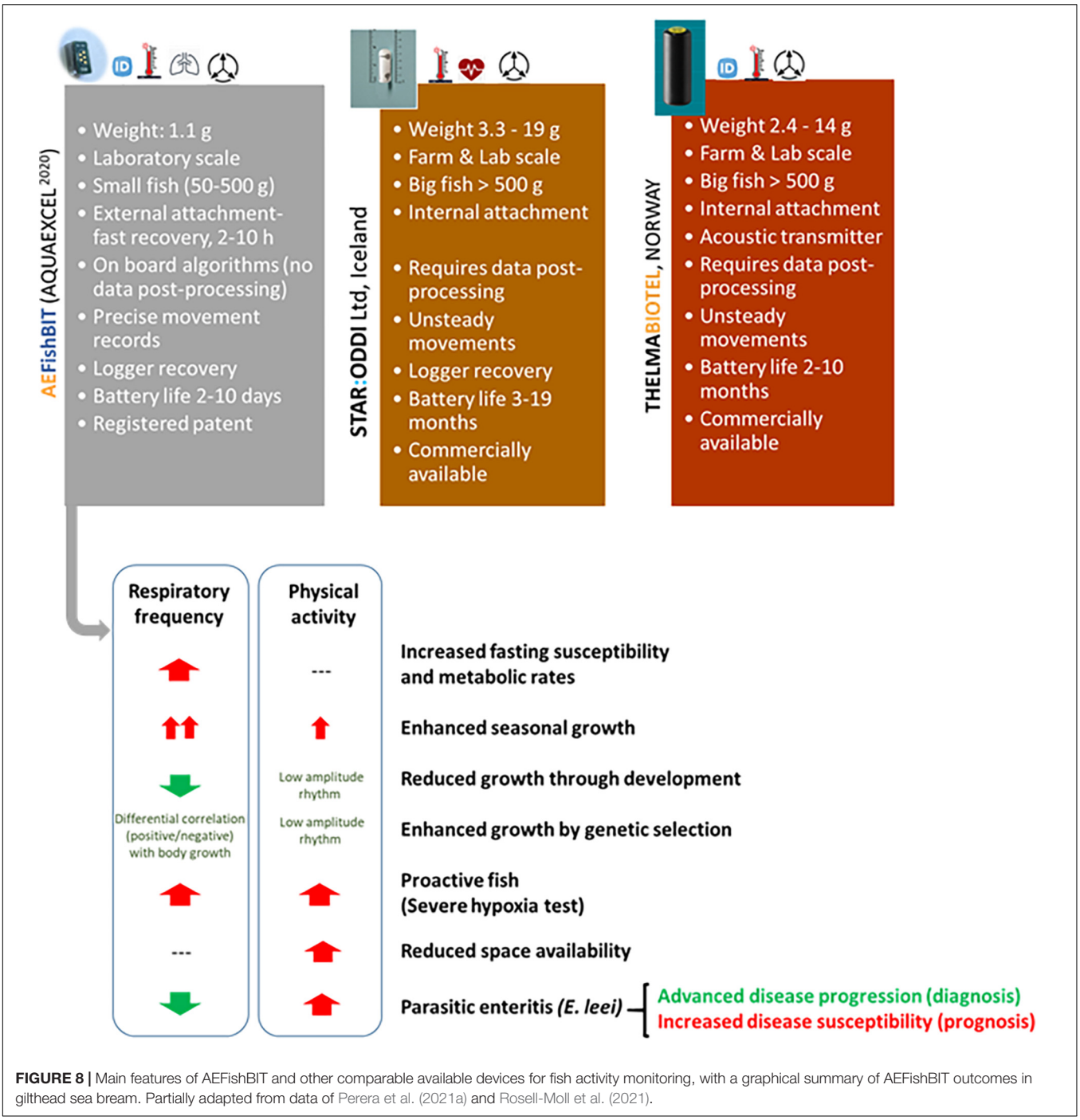


**FIGURE 8 |** Main features of AEFishBIT and other comparable available devices for fish activity monitoring, with a graphical summary of AEFishBIT outcomes in gilthead sea bream. Partially adapted from data of Perera et al. (2021a) and Rosell-Moll et al. (2021).

In any case, a critical step in fish biosensing is the tagging procedure, being the adopted solution dependent on anatomical features, developmental stage, rearing system, duration of study, and more importantly on the research question. Altogether, these factors limit the current threshold size for fish AEFishBIT monitoring, which is ranging between 50 and 100 g in gilthead sea bream and European sea bass, and 400–500 g for salmonids. Future improvements in device design and miniaturization are envisaged at short-term to expand species and recording period through the production cycle. A major constraint factor for this achievement is the size and weight of the battery, whose life could be extended using different energy harvesting approaches that are under evaluation within the EnABLES H2020 EU project. The ultimate goal is to take advantage of fish movement to adopt self-powered technologies that would remove the large battery in the device design. This zero power approach would further minimize the impact of device attachment and allow monitoring of smaller fish. Additionally, it is planned to include a gyroscope,

so the inertial unit (gyroscope and accelerometer) would be able to provide a "three-in-one": physical activity, respiratory frequency and angular acceleration (and hence fish trajectory). Moreover, the information drawn from the gyroscope could be of utility to refine the currently used on-board algorithms for the calculus of respiratory frequency and physical activity. Additionally, the current user-friendly accompanying software for device programming and data recovery will be updated to include these new features, improving the programmed schedule features for a more dynamic fish monitoring with different sleep and recordings periods, synchronous and asynchronous, by means of a real-time clock (**Figure 7**).

As sum up in **Figure 8**, the main features of the current AEFishBIT device are different of those of other small gadgets available in the market, serving for different but also complementary purposes. Indeed, routine remote monitoring in large cage systems is mostly useful for real-time detection of unsteady fish reactions in response to predictable or unpredictable events, whereas AEFishBIT recording would assist farmers, breeders and physiologists for accurate phenotyping of behavior and whole metabolic traits under highly controlled conditions. Thus, this system is able to give useful information about how a fish is sensing and responding to changes in age, genetics and environment as a good proxy of both unsteady and sustained states of swimming and metabolic rates in a context of climate change, with cultured fish exposed to high temperatures and limited oxygen availability. The challenge is how this information at laboratory scale can be extrapolated and used to the field level for the improvement of aquaculture sustainability and profitability. In that sense, behavior changes related to the acceptance of new feed formulations and changing environmental conditions can be mimicked and tested at laboratory scale for merging genetics, nutrition, health and environmental science into a single transdisciplinary and fundamental knowledge system, supporting the future and viable growth of aquaculture. All this will serve to ensure the use of behavior monitoring as a reliable and routine approach to evaluate new fish feed formulations, largely based on sustainability and circular economy principles (Aragão et al., 2020; Naya-Català et al., 2021a).

Future prospects on behavior and emotional indicators can also serve to measure and interpret the positive reactions of fish to the environmental enrichment. Otherwise, regarding disease outcomes, it is of particular interest that the reduction of respiratory frequency was a consistent marker of the progression of parasitic enteritis in gilthead sea bream experimentally infected with the myxozoan parasite *Enteromyxum leei* (Rosell-Moll et al., 2021). This intestinal parasite is responsible of severe epizooties and production losses in Mediterranean fish farms (Sitjà-Bobadilla and Palenzuela, 2012), and there is now experimental evidence showing that differences in the basal behavior and physical activity are indicative of their predisposition to infection (unpublished results). This feature would add a predictive value to AEFishBIT records, which becomes especially interesting for driving selective breeding toward tailored productive traits. Finally, major efforts for the integration of complex data informing of the host response to nutritional inputs and genetics and microbiota interactions have been accomplished recently in farmed fish and gilthead sea bream in particular (Piazzon et al., 2017, 2019, 2020; Naya-Català et al., 2021a; Solé-Jiménez et al., 2021), but how this also affects to behavioral traits remains mostly unknown. Altogether, this opens new research opportunities for incorporating measurements of organism behavior as a routine procedure of academia researchers as well as fish farmers, and fish feed producers and breeders.

## AUTHOR CONTRIBUTIONS

JP-S: conceptualization. JC-G, MÁF, PP, and JP-S: writing-original manuscript. All authors writing-review and editing, read and approved the final manuscript.

## FUNDING

This work was supported by the EU H2020 Research Innovation Program under grant agreement no. 871108 (AQUAEXCEL3.0). This output reflects only the author's view and the European Union cannot be held responsible for any use that may be made of the information contained therein. Additional funding was obtained by the Spanish MCIN project Bream-AquaINTECH (RTI2018–094128-B-I00, AEI/FEDER, UE) to JP-S and JC-G. This study forms part of the ThinkInAzul programme and was supported by MCIN with funding from European Union NextGenerationEU (PRTR-C17.I1) and by Generalitat Valenciana (THINKINAZUL/2021/024) to JP-S.

## REFERENCES

Alfonso, S., Zupa, W., Spedicato, M. T., Lembo, G., and Carbonara, P. l (2021). Mapping the energetic costs of free-swimming gilthead sea bream (*Sparus aurata*), a key species in European marine aquaculture. *Biology* 10:1357. doi: 10.3390/biology10121357

An, D., Huang, J., and Wei, Y. (2021). A survey of fish behaviour quantification indexes and methods in aquaculture. *Rev. Aquacult.* 13, 2169–2189. doi: 10.1111/raq.12564

Anttila, K., and Mänttäri, S. (2009). Ultrastructural differences and histochemical characteristics in swimming muscles between wild and reared Atlantic salmon. *Acta Physiol.* 196, 249–257. doi: 10.1111/j.1748-1716.2008.01911.x

Aragão, C., Cabano, M., Colen, R., Fuentes, J., and Dias, J. (2020). Alternative formulations for gilthead seabream diets: towards a more sustainable production. *Aquac. Nutr.* 26, 444–455. doi: 10.1111/anu.13007

Arechavala-Lopez, P., Caballero-Froilán, J. C., Jiménez-García, M., Capó, X., Tejada, S., Saraiva, J. L., et al. (2020). Enriched environments enhance cognition, exploratory behaviour and brain physiological functions of *Sparus aurata*. *Sci. Rep.* 10:11252. doi: 10.1038/s41598-020-68306-6

Arechavala-Lopez, P., Diaz-Gil, C., Saraiva, J. L., Moranta, D., Castanheira, M. F., Nuñez-Velázquez, S., et al. (2019). Effects of structural environmental enrichment on welfare of juvenile seabream (*Sparus aurata*). *Aquac. Rep.* 15:100224. doi: 10.1016/j.aqrep.2019.100224

Arechavala-Lopez, P., Lankheet, M. J., Díaz-Gil, C., Abbink, W., and Palstra, A. P. (2021). Swimming activity of gilthead seabream (*Sparus aurata*) in swim-tunnels: acoustic accelerometry, oxygen consumption and body motion. *Front. Anim. Sci.* 2:25. doi: 10.3389/fanim.2021.679848

Ashley, N. T., Schwabl, I., Goymann, W., and Buck, C. L. (2012). Keeping time under the midnight sun: behavioral and plasma melatonin profiles of free-living lapland longspurs (*Calcarius lapponicus*) during the Arctic Summer. *J. Exp. Zool. A Ecol. Genet. Physiol.* 319, 10–22. doi: 10.1002/jez.1768

Ashley, P. J. (2007). Fish welfare: current issues in aquaculture. *Appl. Anim. Behav. Sci.* 104, 199–235. doi: 10.1016/j.applanim.2006.09.001

Auer, S. K., Salin, K., Rudolf, A. M., Anderson, G. J., and Metcalfe, N. B. (2015). The optimal combination of standard metabolic rate and aerobic scope for somatic growth depends on food availability. *Funct. Ecol.* 29, 479–486. doi: 10.1111/1365-2435.12396

Azzaydi, M., Rubio, V. C., Martínez López, F. J., Sánchez-Vázquez, F. J., Zamora, S., and Madrid, J. A. (2007). Effect of restricted feeding schedule on seasonal shifting of daily demand-feeding pattern and food anticipatory activity in European sea bass (*Dicentrarchus labrax* L.). *Chronobiol. Int.* 24, 859–874. doi: 10.1080/07420520701658399

Balasch, J. C., and Tort, L. (2019). Netting the stress responses in fish. *Front. Endocrinol.* 10:62. doi: 10.3389/fendo.2019.00062

Barreto, M. O., Rey Planellas, S., Yang, Y., Phillips, C., and Descovich, K. (2021). Emerging indicators of fish welfare in aquaculture. *Rev. Aquac.* 107, 2411–2502. doi: 10.1111/raq.12601

Beemelmanns, A., Zanuzzo, F. S., Xue, X., Sandrelli, R. M., Rise, M. L., and Gamperl, A. K. (2021). The transcriptomic responses of Atlantic salmon (*Salmo salar*) to high temperature stress alone, and in combination with moderate hypoxia. *BMC Genomics* 22:261. doi: 10.1186/s12864-021-07464-x

Bellinger, K. L., Thorgaard, G. H., and Carter, P. A. (2014). Domestication is associated with reduced burst swimming performance and increased body size in clonal rainbow trout lines. *Aquaculture* 420, 154–159. doi: 10.1016/j.aquaculture.2013.10.028

Berger, J. (2010). "Fear-mediated food webs," in *Trophic Cascades: Predators, Prey and the Changing Dynamics of Nature*, eds J. Terborgh and J. A. Estes (Washington, DC: Island Press), 241–254.

Bermejo-Nogales, A., Calduch-Giner, J. A., and Pérez-Sánchez, J. (2015). Unraveling the molecular signatures of oxidative phosphorylation to cope with the nutritionally changing metabolic capabilities of liver and muscle tissues in farmed fish. *PLoS One* 10:e0122889. doi: 10.1371/journal.pone.0122889

Bermejo-Nogales, A., Nederlof, M., Benedito-Palos, L., Ballester-Lozano, G. F., Folkedal, O., Olsen, R. E., et al. (2014). Metabolic and transcriptional responses of gilthead sea bream (*Sparus aurata* L.) to environmental stress: new insights in fish mitochondrial phenotyping. *Gen. Comp. Endocrinol.* 205, 305–315. doi: 10.1016/j.ygcen.2014.04.016

Blasco, J., Moya, A., Millán-Cubillo, A., Vélez, E. J., Capilla, E., Pérez-Sánchez, J., et al. (2015). Growth-promoting effects of sustained swimming in fingerlings of gilthead sea bream (*Sparus aurata* L.). *J. Comp. Physiol. B* 185, 859–868. doi: 10.1007/s00360-015-0933-5

Bloch, G., Barnes, B. M., Gerkema, M. P., and Helm, B. (2013). Animal activity around the clock with no overt circadian rhythms: patterns, mechanisms and adaptive value. *Proc. R. Soc. B* 280:20130019. doi: 10.1098/rspb.2013.0019

Brander, K. M. (2007). Global fish production and climate change. *Proc. Natl. Acad. Sci.* 104, 19709–19714. doi: 10.1073/pnas.0702059104

Broell, F., Noda, T., Wright, S., Domenici, P., Steffensen, J. F., Auclair, J.-P., et al. (2013). Accelerometer tags: detecting and identifying activities in fish and the effect of sampling frequency. *J. Exp. Biol.* 216, 1255–1264. doi: 10.1242/jeb.077396

Brydges, N. M., and Braithwaite, V. A. (2009). Does environmental enrichment affect the behaviour of fish commonly used in laboratory work? *Appl. Anim. Behav. Sci.* 118, 137–143. doi: 10.1016/j.applanim.2009.02.017

Burke, M., Grant, J., Filgueira, R., and Stone, T. (2021). Oceanographic processes control dissolved oxygen variability at a commercial Atlantic salmon farm: application of a real-time sensor network. *Aquaculture* 533:736143. doi: 10.1016/j.aquaculture.2020.736143

Calduch-Giner, J. A., Echasseriau, Y., Crespo, D., Baron, D., Planas, J. V., Prunet, P., et al. (2014). Transcriptional assessment by microarray analysis and large-scale meta-analysis of the metabolic capacity of cardiac and skeletal muscle tissues to cope with reduced nutrient availability in gilthead sea bream (*Sparus aurata* L.). *Mar. Biotechnol.* 16, 423–435. doi: 10.1007/s10126-014-9562-3

Challet, E. (2013). Circadian clocks, food intake, and metabolism. *Prog. Mol. Biol. Transl. Sci.* 119, 105–135. doi: 10.1016/B978-0-12-396971-2.00005-1

Chen, K. Y., and Bassett, D. R. Jr. (2005). The technology of accelerometry-based activity monitors: current and future. *Med. Sci. Sports Exerc.* 37, S490–S500. doi: 10.1249/01.mss.0000185571.49104.82

Cockrem, J. F. (1990). "Circadian rhythms," in *Antarctic Penguins. Penguin biology*, eds L. S. Davis and J. T. Darby (San Diego, CA: Academic Press), 319–344.

Cooke, S. J., Nguyen, V. M., Murchie, K. J., Thiem, J. D., Donaldson, M. R., Hinch, S. G., et al. (2013). To tag or not to tag: animal welfare, conservation, and stakeholder considerations in fish tracking studies that use electronic tags. *J. Int. Wildlife Law Policy* 16, 352–374. doi: 10.1080/13880292.2013.805075

de Goede, D., Gremmen, B., Rodenburg, T. B., Bolhuis, J. E., Bijma, P., Scholten, M., et al. (2013). Reducing damaging behaviour in robust livestock farming. *NJAS Wagen. J. Life. Sci.* 66, 49–53. doi: 10.1016/j.njas.2013.05.006

de Matos Dias, D., de Campos, C. B., and Rodrigues, F. H. G. (2018). Behavioural ecology in a predator-prey system. *Mamm. Biol.* 92, 30–36. doi: 10.1016/j.mambio.2018.04.005

del Pozo, A., Sánchez-Férez, J. A., and Sánchez-Vázquez, F. J. (2011). Circadian rhythms of self-feeding and locomotor activity in zebrafish (*Danio rerio*). *Chronobiol. Int.* 28, 39–47. doi: 10.3109/07420528.2010.530728

Devlin, R. H., D'Andrade, M., Uh, M., and Biagi, C. A. (2004). Population effects of growth hormone transgenic coho salmon depend on food availability and genotype by environment interactions. *Proc. Natl. Acad. Sci. U. S. A.* 101, 9303–9308. doi: 10.1073/pnas.0400023101

Dunn, J. F., and Hochachka, P. W. (1986). Metabolic responses of trout (*Salmo gairdneri*) to acute environmental hypoxia. *J. Exp. Biol.* 123, 229–242.

Eckel-Mahan, K., and Sassone-Corsi, P. (2013). Metabolism and the circadian clock converge. *Physiol. Rev.* 93, 107–135. doi: 10.1152/physrev.00016.2012

Evans, M. L., Hori, T. S., Rise, M. L., and Fleming, I. A. (2015). Transcriptomic responses of Atlantic Salmon (*Salmo salar*) to environmental enrichment during juvenile rearing. *PLoS One* 10:e0118378. doi: 10.1371/journal.pone.0118378

Ferrer, M. A., Calduch-Giner, J. A., Díaz, M., Sosa, J., Rosell-Moll, E., Santana Abril, J., et al. (2020). From operculum and body tail movements to different coupling of physical activity and respiratory frequency in farmed gilthead sea bream and European sea bass. Insights on aquaculture biosensing. *Comput. Electron. Agric.* 175:105531. doi: 10.1016/j.compag.2020.105531

Flash, T., and Hogan, N. (1985). The coordination of arm movements: an experimentally confirmed mathematical model. *J. Neurosci.* 5, 1688–1703. doi: 10.1523/JNEUROSCI.05-07-01688.1985

Folkedal, O., Stien, L. H., Torgersen, T., Oppedal, F., Olsen, R. E., Fosseidengen, J. E., et al. (2012). Food anticipatory behaviour as an indicator of stress response and recovery in Atlantic salmon post-smolt after exposure to acute temperature fluctuation. *Physiol. Behav.* 105, 350–356. doi: 10.1016/j.physbeh.2011.08.008

Føre, M., Frank, K., Dempster, T., Alfredsen, J. A., and Høy, E. (2017). Biomonitoring using tagged sentinel fish and acoustic telemetry in commercial salmon aquaculture: a feasibility study. *Aquac. Eng.* 78, 163–172. doi: 10.1016/j.aquaeng.2017.07.004

Føre, M., Frank, K., Norton, T., Svendsen, E., Alfredsen, J. A., Dempster, T., et al. (2018). Precision fish farming: a new framework to improve production in aquaculture. *Biosyst. Eng.* 173, 176–193. doi: 10.1016/j.biosystemseng.2017.10.014

Fraser, D., and Duncan, I. J. (1998). 'Pleasures','pains' and animal welfare: toward a natural history of affect. *Anim. Welf.* 1998, 383–396.

Gallagher, M. D., Matejusova, I., Nguyen, L., Ruane, N. M., Falk, K., and Macqueen, D. J. (2018). Nanopore sequencing for rapid diagnostics of salmonid RNA viruses. *Sci. Rep.* 8:16307. doi: 10.1038/s41598-018-34464-x

Gamboa, J. L., and Andrade, F. H. (2012). Muscle endurance and mitochondrial function after chronic normobaric hypoxia: contrast of respiratory and limb muscles. *Pflügers Arch. Eur. J. Physiol.* 463, 327–338. doi: 10.1007/s00424-011-1057-8

Gamperl, A. K., Ajiboye, O. O., Zanuzzo, F. S., Sandrelli, R. M., Ellen de Fátima, C. P., and Beemelmanns, A. (2020). The impacts of increasing temperature

and moderate hypoxia on the production characteristics, cardiac morphology and haematology of Atlantic Salmon (*Salmo salar*). *Aquaculture* 519, 1–14. doi: 10.1016/j.aquaculture.2019.734874

Georgopoulou, D. G., Stavrakidis-Zachou, O., Mitrizakis, N., and Papandroulakis, N. (2021). Tracking and analysis of the movement behavior of European seabass (*Dicentrarchus labrax*) in aquaculture systems. *Front. Anim. Sci.* 2:754520. doi: 10.3389/fanim.2021.754520

Geurden, I., Borchert, P., Balasubramanian, M. N., Schrama, J. W., Dupont-Nivet, M., Quillet, E., et al. (2013). The positive impact of the early-feeding of a plant-based diet on its future acceptance and utilisation in rainbow trout. *PLoS One* 8:e83162. doi: 10.1371/journal.pone.0083162

Gonçalves, A. T., Collipal-Matamal, R., Valenzuela-Muñoz, V., Nuñez-Acuña, G., Valenzuela-Miranda, D., and Gallardo-Escárate, C. (2020). Nanopore sequencing of microbial communities reveals the potential role of sea lice as a reservoir for fish pathogens. *Sci. Rep.* 10:2895. doi: 10.1038/s41598-020-59747-0

Hamäläinen, W., Järvinen, M., Martiskainen, P., and Mononen, J. (2011). "Jerk-based feature extraction for robust activity recognition from acceleration data," in *Proeedings of the 2011 11th International Conference on Intelligent Systems Design and Applications* (Cordoba: IEEE), 831–836. doi: 10.1109/ISDA.2011.6121760

Healy, T. M., Chung, D. J., Crowther, K. G., and Schulte, P. M. (2017). Metabolic and regulatory responses involved in cold acclimation in Atlantic killifish, *Fundulus heteroclitus*. *J. Comp. Physiol. B.* 187, 463–475. doi: 10.1007/s00360-016-1042-9

Hemsworth, P. H., and Coleman, G. J. (2011). "Human-animal interactions and animal productivity and welfare," in *Human-livestock interactions. The Stockperson and the Productivity of Intensively Farmed Animals*, eds P. H. Hemsworth and G. J. Coleman (Oxford: CAB International), 47–83. doi: 10.1079/9781845936730.0047

Hoppeler, H., and Vogt, M. (2001). Muscle tissue adaptations to hypoxia. *J. Exp. Biol.* 204, 3133–3139. doi: 10.1242/jeb.204.18.3133

Hou, Z. S., Wen, H. S., Li, J. F., He, F., Li, Y., and Qi, X. (2020). Environmental hypoxia causes growth retardation, osteoclast differentiation and calcium dyshomeostasis in juvenile rainbow trout (*Oncorhynchus mykiss*). *Sci. Total Environ.* 705:135272. doi: 10.1016/j.scitotenv.2019.135272

Huby, A., and Parmentier, E. (2019). "Actinopterygians: head, jaws and muscles," in *Heads, Jaws, and Muscles. Fascinating Life Sciences*, eds J. Ziermann, R. Jr. Diaz, and R. Diogo (Cham: Springer), doi: 10.1007/978-3-319-93560-7_5C

Hung, C. C., Tsao, S. C., Huang, K. H., Jang, J. P., Chang, H. K., and Dobbs, F. C. (2016). A highly sensitive underwater video system for use in turbid aquaculture ponds. *Sci. Rep.* 6:31810. doi: 10.1038/srep31810

Huntingford, F. A. (2004). Implications of domestication and rearing conditions for the behaviour of cultivated fishes. *J. Fish Biol.* 65, 122–142. doi: 10.1111/j.0022-1112.2004.00562.x

Huntingford, F. A., Adams, C., Braithwaite, V. A., Kadri, S., Pottinger, T. G., Sandøe, P., et al. (2006). Current issues in fish welfare. *J. Fish Biol.* 68, 332–372. doi: 10.1111/j.0022-1112.2006.001046.x

Huntingford, F. A., Andrew, G., Mackenzie, S., Morera, D., Coyle, S. M., Pilarczyk, M., et al. (2010). Coping strategies in a strongly schooling fish, the common carp *Cyprinus carpio*. *J. Fish Biol.* 76, 1576–1591. doi: 10.1111/j.1095-8649.2010.02582.x

Jepsen, N., Thorstad, E. B., Havn, T., and Lucas, M. C. (2015). The use of external electronic tags on fish: an evaluation of tag retention and tagging effects. *Anim. Biotelem.* 3:49. doi: 10.1186/s40317-015-0086-z

Knap, P. W. (2005). Breeding robust pigs. *Aust. J. Exp. Agric.* 45, 763–773. doi: 10.1071/EA05041

Kolarevic, J., Aas-Hansen, Ø, Espmark, Å, Baeverfjord, G., Terjesen, B. F., and Damsgård, B. (2016). The use of acoustic acceleration transmitter tags for monitoring of Atlantic salmon swimming activity in recirculating aquaculture systems (RAS). *Aquat. Eng.* 72, 30–39. doi: 10.1016/j.aquaeng.2016.03.002

Kolarevic, J., Calduch-Giner, J., Espmark, ÅM., Evensen, T., Sosa, J., and Pérez-Sánchez, J. (2021). A novel miniaturized biosensor for monitoring Atlantic salmon swimming activity and respiratory frequency. *Animals* 11:2403. doi: 10.3390/ani11082403

Koolhaas, J. M., Korte, S. M., De Boer, S. F., Van Der Vegt, B. J., Van Reenen, C. G., Hopster, H., et al. (1999). Coping styles in animals: current status in behavior and stress-physiology. *Neurosci. Biobehav. Rev.* 23, 925–935. doi: 10.1016/S0149-7634(99)00026-3

Korte, S. M., Koolhaas, J. M., Wingfield, J. C., and McEwen, B. S. (2005). The Darwinian concept of stress: benefits of allostasis and costs of allostatic load and the trade-offs in health and disease. *Neurosci. Biobehav. Rev.* 29, 3–38. doi: 10.1016/j.neubiorev.2004.08.009

Li, D. L., Wang, Z. H., Wu, S. Y., Miao, Z., Du, L., and Duan, Y. Q. (2020). Automatic recognition methods of fish feeding behavior in aquaculture: a review. *Aquaculture* 528:735508. doi: 10.1016/j.aquaculture.2020.735508

Liu, S., and Fu, S. J. (2017). Effects of food availability on metabolism, behaviour, growth and their relationships in a triploid carp. *J. Exp. Biol.* 220, 4711–4719. doi: 10.1242/jeb.167783

López-Olmeda, J. F., Montoya, A., Oliveira, C., and Sánchez-Vázquez, F. J. (2009). Synchronization to light and restricted-feeding schedules of behavioral and humoral daily rhythms in gilthead sea bream (*Sparus aurata*). *Chronobiol. Int.* 26, 1389–1408. doi: 10.3109/07420520903421922

Lucas, M. C., and Baras, E. (2000). Methods for studying spatial behaviour of freshwater fishes in the natural environment. *Fish Fish.* 1, 283–316. doi: 10.1046/j.1467-2979.2000.00028.x

Macaulay, G., Warren-Myers, F., Barrett, L. T., Oppedal, F., Føre, M., and Dempster, T. (2021). Tag use to monitor fish behaviour in aquaculture: a review of benefits, problems and solutions. *Rev. Aquac.* 13, 1565–1582. doi: 10.1111/raq.12534

Madrid, J. A., Boujard, T., and Sánchez-Vázquez, F. J. (2001). "Feeding rhythms," in *Food intake in fish*, eds D. Houlihan, T. Boujard, and M. Jobling (Oxford: Blackwell Science Ltd), 189–215. doi: 10.1002/9780470999516.ch8

Magnoni, L. J., Martos-Sitcha, J. A., Queiroz, A., Calduch-Giner, J. A., Magalhàes Gonçalves, J. F., Rocha, C. M. R., et al. (2017). Dietary supplementation of heat-treated *Gracillaria* and *Ulva* seaweeds enhanced acute hypoxia tolerance in gilthead seabream (*Sparus aurata*). *Biol. Open* 6, 897–908. doi: 10.1242/bio.024299

Majeed, N., Panigrahi, K. C., Sukla, L. B., John, R., and Panigrahy, M. (2020). Regulatory mechanisms across networks of the circadian clock and senescence pathways. *J. Plant Biochem. Biotechnol.* 29, 665–674. doi: 10.1007/s13562-020-00612-6

Martins, C. I. M., Galhardo, L., Noble, C., Damsgård, B., Spedicato, M. T., Zupa, W., et al. (2012). Behavioural indicators of welfare in farmed fish. *Fish Physiol. Biochem.* 38, 17–41. doi: 10.1007/s10695-011-9518-8

Martos-Sitcha, J. A., Bermejo-Nogales, A., Calduch-Giner, J. A., and Pérez-Sánchez, J. (2017). Gene expression profiling of whole blood cells supports a more efficient mitochondrial respiration in hypoxia-challenged gilthead sea bream (*Sparus aurata*). *Front. Zool.* 14:34. doi: 10.1186/s12983-017-0220-2

Martos-Sitcha, J. A., Simó-Mirabet, P., de las Heras, V., Calduch-Giner, J. A., and Pérez-Sánchez, J. (2019a). Tissue-specific orchestration of gilthead sea bream resilience to hypoxia and high stocking density. *Front. Physiol.* 10:840. doi: 10.3389/fphys.2019.00840

Martos-Sitcha, J. A., Sosa, J., Ramos-Valido, D., Bravo, F. J., Carmona-Duarte, C., Gomes, H. L., et al. (2019b). Ultra-low power sensor devices for monitoring physical activity and respiratory frequency in farmed fish. *Front. Physiol.* 10:667. doi: 10.3389/fphys.2019.00667

Muñoz, L., Aspillaga, E., Palmer, M., Saraiva, J. L., and Arechavala-Lopez, P. (2020). Acoustic telemetry: a tool to monitor fish swimming behavior in sea-cage aquaculture. *Front. Mar. Sci.* 7:645. doi: 10.3389/fmars.2020.00645

Murchie, K. J., Cooke, S. J., Danylchuk, A. J., and Suski, C. D. (2011). Estimates of field activity and metabolic rates of bonefish (*Albula vulpes*) in coastal marine habitats using acoustic tri-axial accelerometer transmitters and intermittent-flow respirometry. *J. Exp. Mar. Biol. Ecol.* 396, 147–155. doi: 10.1016/j.jembe.2010.10.019

Murray, A. J. (2009). Metabolic adaptation of skeletal muscle to high altitude hypoxia: how new technologies could resolve the controversies. *Genome Med.* 1:117. doi: 10.1186/gm117

Naya-Català, F., do Vale Pereira, G., Piazzon, M. C., Fernandes, A. M., Calduch-Giner, J. A., Sitjà-Bobadilla, A., et al. (2021a). Cross-talk between intestinal microbiota and host gene expression in gilthead sea bream (*Sparus aurata*)

Juveniles: insights in fish feeds for increased circularity and resource utilization. *Front. Physiol.* 12:748265. doi: 10.3389/fphys.2021.748265

Naya-Català, F., Simó-Mirabet, P., Calduch-Giner, J., and Pérez-Sánchez, J. (2021b). Transcriptomic profiling of Gh/Igf system reveals a prompted tissue-specifc diferentiation and novel hypoxia responsive genes in gilthead sea bream. *Sci. Rep.* 11:16466. doi: 10.1038/s41598-021-95408-6

Newton, M., Barry, J., Dodd, J. A., Lucas, M. C., Boylan, P., and Adams, C. E. (2016). Does size matter? A test of size-specific mortality in Atlantic salmon *Salmo salar* smolts tagged with acoustic transmitters. *J. Fish Biol.* 89, 1641–1650. doi: 10.1111/jfb.13066

Noble, E. C., Gismervik, K., Iversen, M. H., Kolarevic, J., Nilsson, J., Stien, L. H., et al. (2018). *Welfare Indicators for Farmed Atlantic Salmon—Tools for Assessing Fish Welfare*. Tromso: Nofima, 351.

Noble, E. C., Gismervik, K., Iversen, M. H., Kolarevic, J., Nilsson, J., Stien, L. H., et al. (2020). *Welfare Indicators for Farmed Rainbow Trout: Tools for Assessing Fish Welfare*. Tromso: Nofima, 310.

Noble, E. C., Iversen, M. H., Lein, I., Kolarevic, J., Johansen, L. H., Burgerhout, E., et al. (2019). *Rensevel OWI Fact Sheet Series: an Introduction to Operational and Laboratory based Welfare Indicators for Ballan wrasse (Labrus bergylta)*. Tromso: Nofima.

Øverli, Ø, Winberg, S., and Pottinger, T. G. (2005). Behavioral and neuroendocrine correlates of selection for stress responsiveness in rainbow trout—a review. *Integr. Comp. Biol.* 45, 463–474. doi: 10.1093/icb/45.3.463

Palstra, A. P., Arechavala-Lopez, P., Xue, Y., and Roque, A. (2021). Accelerometry of seabream in a sea-cage: Is acceleration a good proxy for activity? *Front. Mar. Sci.* 8:144. doi: 10.3389/fmars.2021.639608

Palstra, A. P., Roque, A., Kruijt, L., Jéhannet, P., Pérez-Sánchez, J., and Dirks, R. P. (2020). Physiological effects of water flow induced swimming exercise in seabream *Sparus aurata*. *Front. Physiol.* 11:610049. doi: 10.3389/fphys.2020.610049

Papaharisis, L., Tsironi, T., Dimitroglou, A., Taoukis, P., and Pavlidis, M. (2019). Stress assessment, quality indicators and shelf life of three aquaculture important marine fish, in relation to harvest practices, water temperature and slaughter method. *Aquac. Res.* 50, 2608–2620. doi: 10.1111/are.14217

Pedrazzani, A. S., Quintiliano, M. H., Bolfe, F., Sans, E. C. D. O., and Molento, C. F. M. (2020). Tilapia on-farm welfare assessment protocol for semi-intensive production systems. *Front. Vet. Sci.* 7:991. doi: 10.3389/fvets.2020.606388

Perera, E., Rosell-Moll, E., Martos-Sitcha, J. A., Naya-Català, F., Simó-Mirabet, P., Calduch-Giner, J. A., et al. (2021a). Physiological trade-offs associated with fasting weight loss, resistance to exercise and behavioral traits in farmed gilthead sea bream (*Sparus aurata*) selected by growth. *Aquac. Rep.* 20:100645. doi: 10.1016/j.aqrep.2021.100645

Perera, E., Rosell-Moll, E., Naya-Català, F., Simó-Mirabet, P., Calduch-Giner, J., and Pérez-Sánchez, J. (2021b). Effects of genetics and early-life mild hypoxia on size variation in farmed gilthead sea bream (*Sparus aurata*). *Fish Physiol. Biochem.* 47, 121–133. doi: 10.1007/s10695-020-00899-1

Perera, E., Simó-Mirabet, P., SukShin, H., Rosell-Moll, E., Naya-Català, F., De las Heras, V., et al. (2019). Selection for growth is associated in gilthead sea bream (*Sparus aurata*) with diet flexibility, changes in growth patterns and higher intestine plasticity. *Aquaculture* 507, 349–360. doi: 10.1016/j.aquaculture.2019.04.052

Pérez-Sánchez, J., Bermejo-Nogales, A., Calduch-Giner, J. A., Kaushik, S., and Sitjà-Bobadilla, A. (2011). Molecular characterization and expression analysis of six peroxiredoxin paralogous genes in gilthead sea bream (*Sparus aurata*): insights from fish exposed to dietary, pathogen and confinement stressors. *Fish Shellfish Immunol.* 31, 294–302. doi: 10.1016/j.fsi.2011.05.015

Piazzon, M. C., Calduch-Giner, J. A., Fouz, B., Estensoro, I., Simó-Mirabet, P., Puyalto, M., et al. (2017). Under control: how a dietary additive can restore the gut microbiome and proteomic profile, and improve disease resilience in a marine teleostean fish fed vegetable diets. *Microbiome* 5:164. doi: 10.1186/s40168-017-0390-3

Piazzon, M. C., Naya-Català, F., Perera, E., Palenzuela, O., Sitjà-Bobadilla, A., and Pérez-Sànchez, J. (2020). Genetic selection for growth drives differences in intestinal microbiota composition and parasite disease resistance in gilthead sea bream. *Microbiome* 8:168. doi: 10.1186/s40168-020-00922-w

Piazzon, M. C., Naya-Català, F., Simó-Mirabet, P., Picard-Sánchez, A., Roig, F. J., Calduch-Giner, J. A., et al. (2019). Sex, age, and bacteria: how the intestinal microbiota is modulated in a protandrous hermaphrodite fish. *Front. Microbiol.* 10:2512. doi: 10.3389/fmicb.2019.02512

Pottinger, T. G., and Carrick, T. R. (1999). Modification of the plasma cortisol response to stress in rainbow trout by selective breeding. *Gen. Comp. Endocrinol.* 116, 122–132. doi: 10.1006/gcen.1999.7355

Power, D. M., Louro, B., Houston, R., Anjos, L., and Cardoso, J. C. R. (2011). "Genomic-proteomic research in Sparidae and its application to genetic improvement," in *Sparidae: Biology and Aquaculture of Gilthead Sea Bream and other Species*, 1st Edn, eds M. A. Pavlidis and C. C. Mylonas (Oxford: Wiley-Blackwell), 359–381.

Ragsdale, A., Ortega-Recalde, O., Dutoit, L., Besson, A. A., Chia, J. H., King, T., et al. (2020). Paternal hypoxia exposure primes offspring for increased hypoxia resistance. *bioRxiv* [Preprint]. doi: 10.1101/2020.12.09.416727

Reebs, S. G. (2002). Plasticity of diel and circadian activity rhythms in fishes. *Rev. Fish Biol. Fish.* 12, 349–371. doi: 10.1023/A:1025371804611

Reid, D., Armstrong, J. D., and Metcalfe, N. B. (2011). Estimated standard metabolic rate interacts with territory quality and density to determine the growth rates of juvenile Atlantic salmon. *Funct. Ecol.* 25, 1360–1367. doi: 10.1111/j.1365-2435.2011.01894.x

Rey, S., Little, D. C., and Ellis, M. A. (2019). *Farmed Fish Welfare Practices: Salmon Farming as a Case Study. GAA publications*. Available online at: https://www.aquaculturealliance.org/wp-content/uploads/2020/05/FarmedFishWelfarePractices_26_May_2020.pdf [accessed on May 26, 2020]

Rodnick, K. J., and Planas, J. V. (2016). The stress and stress mitigation effects of exercise: cardiovascular, metabolic, and skeletal muscle adjustments. *Fish Physiol.* 35, 251–294.

Rosell-Moll, E., Piazzon, M. C., Sosa, J., Ferrer, M. A., Cabruja, E., Vega, A., et al. (2021). Use of accelerometer technology for individual tracking of activity patterns, metabolic rates and welfare in farmed gilthead sea bream (*Sparus aurata*) facing a wide range of stressors. *Aquaculture* 539:736609. doi: 10.1016/j.aquaculture.2021.736609

Sadoul, B., Alfonso, S., Cousin, X., Prunet, P., Bégout, M. L., and Leguen, I. (2021). Global assessment of the response to chronic stress in European sea bass. *Aquaculture* 544:737072. doi: 10.1016/j.aquaculture.2021.737072

Sadoul, B., Friggens, N. C., Valotaire, C., Labbé, L., Colson, V., Prunet, P., et al. (2017). Physiological and behavioral flexibility to an acute $CO_2$ challenge, within and between genotypes in rainbow trout. *Comp. Biochem. Physiol. Part A* 209, 25–33. doi: 10.1016/j.cbpa.2017.04.002

Sadoul, B., Leguen, I., Colson, V., Friggens, N. C., and Prunet, P. (2015). A multivariate analysis using physiology and behavior to characterize robustness in two isogenic lines of rainbow trout exposed to a confinement stress. *Physiol. Behav.* 140, 139–147. doi: 10.1016/j.physbeh.2014.12.006

Sánchez-Vázquez, F. J., and Madrid, J. A. (2001). "Feeding anticipatory activity," in *Food Intake in Fish*, eds D. Houlihan, T. Boujard, and M. Jobling (Oxford: Blackwell Science), 216–232.

Saraiva, J. L., and Arechavala-Lopez, P. (2019). Welfare of fish-no longer the elephant in the room. *Fishes* 4, 39. doi: 10.3390/fishes4030039

Saraiva, J. L., Castanheira, M. F., Arechavala-Lopez, P., Volstorf, J., and Studer, B. H. (2018). "Domestication and Welfare in Farmed Fish," in *Animal Domestication*, ed. F. Teletchea (London: IntechOpen).

Segner, H., Reiser, S., Ruane, N., Rösch, R., Steinhagen, D., and Vehanen, T. (2019). *Welfare of Fishes in Aquaculture. FAO Fisheries and Aquaculture Circular No. C1189*. Budapest: FAO.

Sharma, M. (2019). Behavioural responses in effect to chemical stress in fish: a review. *Int. J. Fish. Aquat. Stud.* 7, 1–5.

Sitjà-Bobadilla, A., and Palenzuela, O. (2012). "Enteromyxum species," in *Fish Parasites: Pathology and Protection*, eds P. T. K. Woo and K. Buchmann (Oxfordshire: CAB International), 163–176. doi: 10.1079/9781845938062.0163

Skvortsova, A., Veldhuijzen, D. S., Kloosterman, I. E., Pacheco-López, G., and Evers, A. W. (2021). Food anticipatory hormonal responses: a systematic review of animal and human studies. *Neurosci. Biobehav. Rev.* 126, 447–464. doi: 10.1016/j.neubiorev.2021.03.030

Sokolova, I. (2018). Mitochondrial adaptations to variable environments and their role in animals' stress tolerance. *Integr. Comp. Biol.* 58, 519–531. doi: 10.1093/icb/icy017

Solé-Jiménez, P., Naya-Català, F., Piazzon, M. C., Estensoro, I., Calduch-Giner, J. À, Sitjà-Bobadilla, A., et al. (2021). Reshaping of gut microbiota in gilthead sea bream fed microbial and processed animal proteins as the main dietary protein source. *Front. Mar. Sci.* 8:842. doi: 10.3389/fmars.2021.705041

Stevens, A., Doneley, R., Cogny, A., and Phillips, C. J. (2021). The effects of environmental enrichment on the behaviour of cockatiels (*Nymphicus hollandicus*) in aviaries. *Appl. Anim. Behav. Sci.* 235:105154. doi: 10.1016/j.applanim.2020.105154

Tevy, M. F., Giebultowicz, J., Pincus, Z., Mazzoccoli, G., and Vinciguerra, M. (2013). Aging signaling pathways and circadian clock-dependent metabolic derangements. *Trends Endocrinol. Metab.* 24, 229–237. doi: 10.1016/j.tem.2012.12.002

Toni, M., Manciocco, A., Angiulli, E., Alleva, E., Cioni, C., and Malavasi, S. (2019). Review: assessing fish welfare in research and aquaculture, with a focus on European directives. *Animal* 13, 161–170. doi: 10.1017/S1751731118000940

Van der Zee, E. A., Havekes, R., Barf, R. P., Hut, R. A., Nijholt, I. M., Jacobs, E. H., et al. (2008). Circadian time-place learning in mice depends on Cry genes. *Curr. Biol.* 18, 844–848. doi: 10.1016/j.cub.2008.04.077

Veissier, I., and Boissy, A. (2007). Stress and welfare: two complementary concepts that are intrinsically related to the animal's point of view. *Physiol. Behav.* 92, 429–433. doi: 10.1016/j.physbeh.2006.11.008

Vollset, K. W., Lennox, R. J., Thorstad, E. B., Auer, S., Bär, K., Larsen, M. H., et al. (2020). Systematic review and meta-analysis of PIT tagging effects on mortality and growth of juvenile salmonids. *Rev. Fish Biol. Fish.* 30, 553–568. doi: 10.1007/s11160-020-09611-1

Warren-Myers, F., Hvas, M., Vågseth, T., Dempster, T., and Oppedal, F. (2021). Sentinels in salmon aquaculture: heart rates across seasons and during crowding events. *Front. Physiol.* 12:755659. doi: 10.3389/fphys.2021.755659

Wilson, S. M., Hinch, S. G., Eliason, E. J., Farrell, A. P., and Cooke, S. J. (2013). Calibrating acoustic acceleration transmitters for estimating energy use by wild adult Pacific salmon. *Comp. Biochem. Physiol. Part A Mol. Integr. Physiol.* 164, 491–498. doi: 10.1016/j.cbpa.2012.12.002

Zhang, Y., Timmerhaus, G., Anttila, K., Mauduit, F., Jørgensen, S. M., Kristensen, T., et al. (2016). eDomestication compromises athleticism and respiratory plasticity in response to aerobic exercise training in Atlantic salmon (*Salmo salar*). *Aquaculture* 463, 79–88. doi: 10.1016/j.aquaculture.2016.05.015

Zupa, W., Carbonara, P., Spedicato, M. T., and Lembo, G. (2015). Modelling swimming activities and energetic costs in European sea bass (*Dicentrarchus labrax* L., 1758) during critical swimming tests. *Mar. Freshw. Behav. Physiol.* 48, 341–357. doi: 10.1080/10236244.2015.1073456

**Author Disclaimer:** This output reflects only the authors' view and the European Union cannot be held responsible for any use that may be made of the information contained therein.

**Conflict of Interest:** The authors declare that the research was conducted in the absence of any commercial or financial relationships that could be construed as a potential conflict of interest.

**Publisher's Note:** All claims expressed in this article are solely those of the authors and do not necessarily represent those of their affiliated organizations, or those of the publisher, the editors and the reviewers. Any product that may be evaluated in this article, or claim that may be made by its manufacturer, is not guaranteed or endorsed by the publisher.

frontiers in Marine Science

BRIEF RESEARCH REPORT
published: 08 March 2022
doi: 10.3389/fmars.2022.828050

# The Direct Exposure of Cortisol Does Not Modulate the Expression of Immune-Related Genes on Tissue Explants of Mucosal Surfaces in Rainbow Trout (*Oncorhynchus mykiss*) Nor in Gilthead Sea Bream (*Sparus aurata*)

*Eva Vallejos-Vidal[1,2,3†], Ali Reza Khansari[1†], Lluc Soliva-Dueso[1], Joan Carles Balasch[1], Lluis Tort[1] and Felipe E. Reyes-López[1,2*]*

[1] Department of Cell Biology, Physiology, and Immunology, Faculty of Biosciences, Universitat Autonoma de Barcelona, Barcelona, Spain, [2] Centro de Biotecnología Acuícola, Facultad de Química y Biología, Universidad de Santiago de Chile, Santiago, Chile, [3] Facultad de Medicina Veterinaria y Agronomía, Universidad de Las Américas, Santiago, Chile

The stress response in fish is characterized by the activation of the HPI axis resulting in the release of cortisol. Previous studies in rainbow trout (*Oncorhynchus mykiss*) and gilthead sea bream (*Sparus aurata*) have shown that an acute stressor modulates the expression of immune- and stress-related genes in mucosal-associated lymphoid tissues (MALTs), particularly in the skin (SALT), gills (GIALT), and gut (GALT). However, there are no antecedents on whether the modulation on the mucosal transcriptomic profile is coordinated through the local presence of cortisol in the mucosal tissue surface. Thus, the aim of this study was to evaluate the effect of cortisol upon the modulation of a set of immune- (*il-1β, il-6, tnf-α*, and *cox-2*) and stress-related (*hsp70, gr1*) genes. For this purpose, tissue explants cultures were incubated with cortisol (100 ng/100 mg tissue) for 2-, 4-, and 24 h and the gene expression profile was evaluated at each time-point by real-time PCR. No differences were found in the gene expression between cortisol-incubated tissue explants and mock-incubated tissues in any of the time-points tested for both species. These results suggest that the quick modulation of the gene expression during the first 24 h after the exposure to stressor challenge reported in previous studies, is probably coordinated and mediated through a systemic-dependent mechanism but not through a peripheral/local response on mucosal tissue surfaces.

**Keywords: glucocorticoids, fish stress, immune response, gene expression, mucosal tissues, fish physiology, teleosts**

OPEN ACCESS

***Edited by:***
*Benjamin Costas, University of Porto, Portugal*

***Reviewed by:***
*Mahmoud A. O. Dawood, Kafrelsheikh University, Egypt*
*Luis Vargas-Chacoff, Austral University of Chile, Chile*

***Correspondence:**
*Felipe E. Reyes-López*
*Felipe.Reyes@uab.cat;*
*felipe.reyes.l@usach.cl*

*† These authors have contributed equally to this work and share first authorship*

***Specialty section:***
*This article was submitted to Aquatic Physiology, a section of the journal Frontiers in Marine Science*

***Received:*** *02 December 2021*
***Accepted:*** *31 January 2022*
***Published:*** *08 March 2022*

***Citation:***
*Vallejos-Vidal E, Khansari AR, Soliva-Dueso L, Balasch JC, Tort L and Reyes-López FE (2022) The Direct Exposure of Cortisol Does Not Modulate the Expression of Immune-Related Genes on Tissue Explants of Mucosal Surfaces in Rainbow Trout (Oncorhynchus mykiss) Nor in Gilthead Sea Bream (Sparus aurata). Front. Mar. Sci. 9:828050. doi: 10.3389/fmars.2022.828050*

## INTRODUCTION

The stress response is a physiological complex mechanism activated by a stimulus that is perceived by the organism as a potential threat (Tort, 2011). It involves a sum of sequential and coordinated activation mechanisms at different functional levels including molecular processes with direct repercussions on gene expression and protein synthesis that, at the end, will activate the responses from cellular to systemic and performance levels (Parra et al., 2015).

Once an external (i.e., fluctuation on water parameters, contaminants, xenobiotics, endocrine disruptors, crowding, and predator attack) or internal stimuli (i.e., homeostasis imbalance, an opportunistic pathogen, increases on the virus/bacterial load) is perceived as a stressor, this information is immediately transmitted to the central nervous system (CNS) for its processing. In case the stimulus is greater than the minimum threshold required, the activation of the Hypothalamus-Pituitary-Interrenal (HPI) and Sympathetic Adreno-Medullar (SAM) axes occurs. The SAM axis is characterized by the neuronal signaling to secrete catecholamines (adrenaline and noradrenaline) by chromaffin cells. This response is also known as the fight-or-flight reaction and it takes place in a matter of seconds to a few minutes (Schreck and Tort, 2016). On the other hand, the HPI axis activation is responsible for the synthesis of hypothalamic corticotrophin-releasing hormone (CRH) from the hypothalamic paraventricular nucleus (PVN), which in turn promotes the secretion of adrenocorticotropic hormone (ACTH) by the pituitary gland (Khansari et al., 2017a). The ACTH is then recognized by the melanocortin receptor 2 (MC2R) of the interrenal cells, thus activating the steroidogenic signaling pathway responsible for cortisol synthesis.

The fate of these two main stress hormones is diametrically different in terms of average lifetime in response to a stressor challenge. While catecholamines are rapidly cleared from circulation, cortisol level remains elevated within minutes to hours in the bloodstream (Vijayan et al., 2010), thus allowing interaction with cortisol receptors in most tissues and also an easier analytical assessment. For this reason, cortisol has been used as the most common physiological indicator of stress in fish (Schreck and Tort, 2016; Reyes-López et al., 2018). The main functions of cortisol include energy homeostasis, osmotic balance maintenance, and metabolic reorganization. In this way, cortisol modulates the normal function of other biological processes including the host defense through a delay or reduction of the immune response (Tort, 2011). There is a generalized consensus that immune suppressive mechanisms in response to stressors in teleost species is more typical of a chronic than an acute stress response (Sunyer and Tort, 1995; Vazzana et al., 2002; Verburg-van Kemenade et al., 2009; Tort, 2011; Schreck and Tort, 2016). This pattern of response is associated to continuous and long-time energy and biological requirements to cope with the stressor challenge (Tort, 2011). By contrast, when fish face up an acute short-term stressor it may happen that the pattern of response is preferentially stimulatory, activating particularly the innate humoral immunity (Sunyer and Tort, 1995; Demers and Bayne, 1997). However, other immune-related processes may not be significantly affected (Tort, 2011). Despite these antecedents, less consensus exists in regard to the effects of the acute stress response in fish. In fact, it has been shown that the magnitude and dynamics of cortisol secretion and the modulation of immune- and stress-related genes against the same stressor are different between different teleost species (Khansari et al., 2019).

In the last years, special attention has focused on the mucosal-associated lymphoid tissues (MALTs) because: (a) their role as a physical barrier in intimate contact with the aquatic environment (Parra et al., 2015); (b) their wide range of biological functions including immune response (Bakke et al., 2010; Nelson and Dehn, 2010; Zhang et al., 2011; Xu et al., 2013; Salinas, 2015); (c) their potential utilization as target tissues for the development of new vaccine administration strategies (Salinas et al., 2015); and (d) their use as an interesting alternative for the less-invasive sampling collection for the evaluation of fish health indicators (Rajan et al., 2013; Cordero et al., 2015; Sanahuja and Ibarz, 2015). In teleost species, four MALTs have been described: nose-associated lymphoid tissue (NALT), skin-associated lymphoid tissue (SALT), gill-associated lymphoid tissue (GIALT), and gut-associated lymphoid tissue (GALT) (Parra et al., 2015). These tissues have attracted increasing interest for the evaluation of different stress indicators, including cortisol, particularly skin mucus (Guardiola et al., 2016; Fernández-Alacid et al., 2018). Previous studies in rainbow trout (*Oncorhynchus mykiss*) and gilthead sea bream (*Sparus aurata*) have shown that an acute stressor is able to increase the cortisol in skin mucus (Khansari et al., 2018). Moreover, there is a correlation between plasmatic and skin mucus cortisol levels in the first 24 h after an intense activation of the HPI axis (Carbajal et al., 2019). Importantly, this acute response modulates the expression of MALT immune- and stress-related genes in time-, and species-specific manner (Khansari et al., 2018). Several studies have reported the local effect of cortisol on the modulation of immune- and stress-related genes in the head kidney because of its neuroendocrine function, as an effector organ in the HPI axis activation cascade, as well as for its role as lymphohematopoietic tissue (Castillo et al., 2009; Khansari et al., 2017b,c). Nonetheless, there is no antecedents on whether the modulation of the mucosal transcriptomic profile is coordinated through the local presence of cortisol on the mucosal tissue surface. Thus, the aim of this study was to evaluate the effect of cortisol upon the modulation of a set of immune- and stress-related genes in MALT, including skin (SALT), gills (GIALT), and gut (GALT). For this purpose, tissue explants cultures were incubated with cortisol for 2-, 4-, and 24 h and the gene expression profile was evaluated at each time-point. For this purpose, the study included two commercially relevant species that inhabit two distinct milieus: rainbow trout (a freshwater teleost) and gilthead sea bream (marine teleost), and that have been model species for the study of stress (chronic and acute) and the immune response (Tort, 2011; Balasch and Tort, 2019).

# MATERIALS AND METHODS

## Fish

Juvenile rainbow trout (*Oncorhynchus mykiss*) (130 ± 10 g; $n_{total}$ = 36) and gilthead sea bream (*Sparus aurata*) (65 ± 5.0 g; $n_{total}$ = 36) were purchased from commercial hatcheries (TROUTFACTORY, Lleida, Spain; Aquicultura els ALFACS, S.L., Tarragona, Spain) and maintained at the AQUAB-Fish facility (Universitat Autónoma de Barcelona, Cerdanyola del Vallès, Spain). Fish were acclimatized to laboratory conditions for 21 days before the start of the experiment in conic tanks (2.0 $m^3$ total volume capacity) with water pump, recirculating chiller cooling system, sand filter, and biofilter. Fish were maintained at a photoperiod of 12L:12D and at their respective environmental temperature (15°C for trout; 20°C for sea bream). Fish were fed a commercial pellet (Skretting) at 1.5% of total body weight/day. Water quality indicators (dissolved oxygen, ammonia, nitrite, and pH for both species; salinity in the case of sea bream) were analyzed and controlled periodically.

## Ethics Statement

The experiment complied with the Guiding Principles for Biomedical Research Involving Animals (EU2010/63), the guidelines of the Spanish laws (law 32/2007 and RD 53/2013) and authorized by the Ethical Committee of the UAB CEEAH (Spain) for the use of laboratory animals (Ref. OH4218_4219).

## Tissue Sampling

Rainbow trout ($n$ = 6) and gilthead sea bream ($n$ = 6) were euthanized by MS-222 (Sigma) overdose (200 mg/l). Before tissue sampling collection, blood was harvested in order to avoid the systemic influence of cortisol on mucosal tissues. After blood sampling, the same piece of skin, gills, and gut were taken from each fish according to Khansari et al. (2018) with minor modifications. Skin tissue samples were taken from the upper lateral line area behind the dorsal fin, left side, and roughly the same size. The skin samples were carefully taken to avoid muscle contamination. Thereafter, the body cavity was opened laterally and the gills were perfused with 1X Phosphate-buffered saline (PBS) (Sigma) according to Xu et al. (2016) in order to avoid blood contamination, thus discarding any systemic response influence on data. Then, gills (first lamella from the left side) were also sampled. For gut analysis, the body cavity was opened laterally, and the midgut and hindgut were sampled using a sterile scalpel and forceps. These harvested gut sections were open longitudinally and feces and mucus were carefully removed with forceps. Then, all the tissue sections were immediately transferred to 50-ml tubes and maintained with 20 ml DMEM – high glucose (Sigma; product num. 08168), and kept on ice.

## Tissue Explants Culture and Incubation With Cortisol

The mucosal tissues (gills, skin, and gut) from each fish were divided into six sections of 100 mg each [one sample per experimental group (negative control and cortisol-incubated) and time-point evaluated (2-, 4-, and 24 h of incubation); $n_{total}$ = 6 fish for each fish species)]. Each piece of tissue was disposed individually in 24-well culture plate (Jet Biofil). All the samples were submerged in 70% ethanol for 20 sec to eliminate any potential bacteria present on the tissue surface, according to Xu et al. (2016). Then, the tissue was rinsed twice in 1X PBS for 2 min, and immediately placed in a new 24-well culture plate (Jet Biofil) and kept on ice with 1 ml DMEM - high glucose supplemented with 10% heat inactivated fetal bovine serum (Gibco) and penicillin (100 IU/l) per well until the beginning of the incubation with cortisol.

Cortisol (Hydrocortisone; Sigma cat #H2882-1G) was dissolved in appropriate solvent (absolute ethanol; Sigma-Aldrich cat #E7023) according to manufacturer's instructions. Each mucosal tissue sample (gills, skin, and gut) was incubated with cortisol (100 ng/100 mg tissue/1 ml DMEM – high glucose supplemented) and incubated for 2-, 4-, and 24 h under optimal temperature culture conditions (16°C for rainbow trout; 18°C for sea bream; 5% $CO_2$), according to Khansari et al., 2017b,c). The concentration of cortisol used in this current study was chosen because it corresponds to the plasma concentration level of acute stress-subjected fish (for rainbow trout and sea bream) (Castillo et al., 2008; Khansari et al., 2019). This concentration of cortisol has been previously used and its effect has been evaluated in similar approaches (Castillo et al., 2009; Kelly and Chasiotis, 2011; Khansari et al., 2017b,c). The time-points analyzed in this current study were chosen based on the highest cortisol effect on *in vitro* cell cultures (2 h post-incubation) (Castillo et al., 2009), the recovery limit time period for exogenously elevated cortisol levels (4 h post-incubation) (Algera et al., 2017), and the time established as accepted limit for the recovery of a situation of acute stress of high intensity and short duration (Khansari et al., 2018, 2019; Carbajal et al., 2019). As negative control, the mucosal tissue was mock-incubated under the same conditions. After treatment, the whole tissue was immediately frozen to −80°C until the RNA extraction.

## Total RNA Extraction and Complementary DNA Synthesis

Total RNA extraction was carried out from the whole frozen MALT using 1 ml of TriReagent (Sigma, cat#T9424) following manufacturer's instructions. Total RNA concentration was determined by NanoDrop-1000 spectrophotometer (Thermo Scientific, Waltham, MA, United States) and the integrity was measured by Agilent 2100 Bioanalyzer (Agilent Technologies, Santa Clara, CA, United states). Only those samples with RIN values > 7.5 were chosen for gene expression analysis. One μg of total RNA from all samples were used to synthesize cDNA with High-Capacity cDNA Reverse Transcription Kit (Applied Biosystems) according to the manufacturer's instructions. The cDNA was used as template for absolute quantification by real-time PCR (qRT-PCR) expression analysis.

## Gene Expression Analysis

Real-time PCR (qRT-PCR) was carried out in rainbow trout and sea bream MALTs to analyze the expression pattern of genes associated to pro- (*il-1β, il-6, tnf-α, cox-2*) and anti-inflammatory

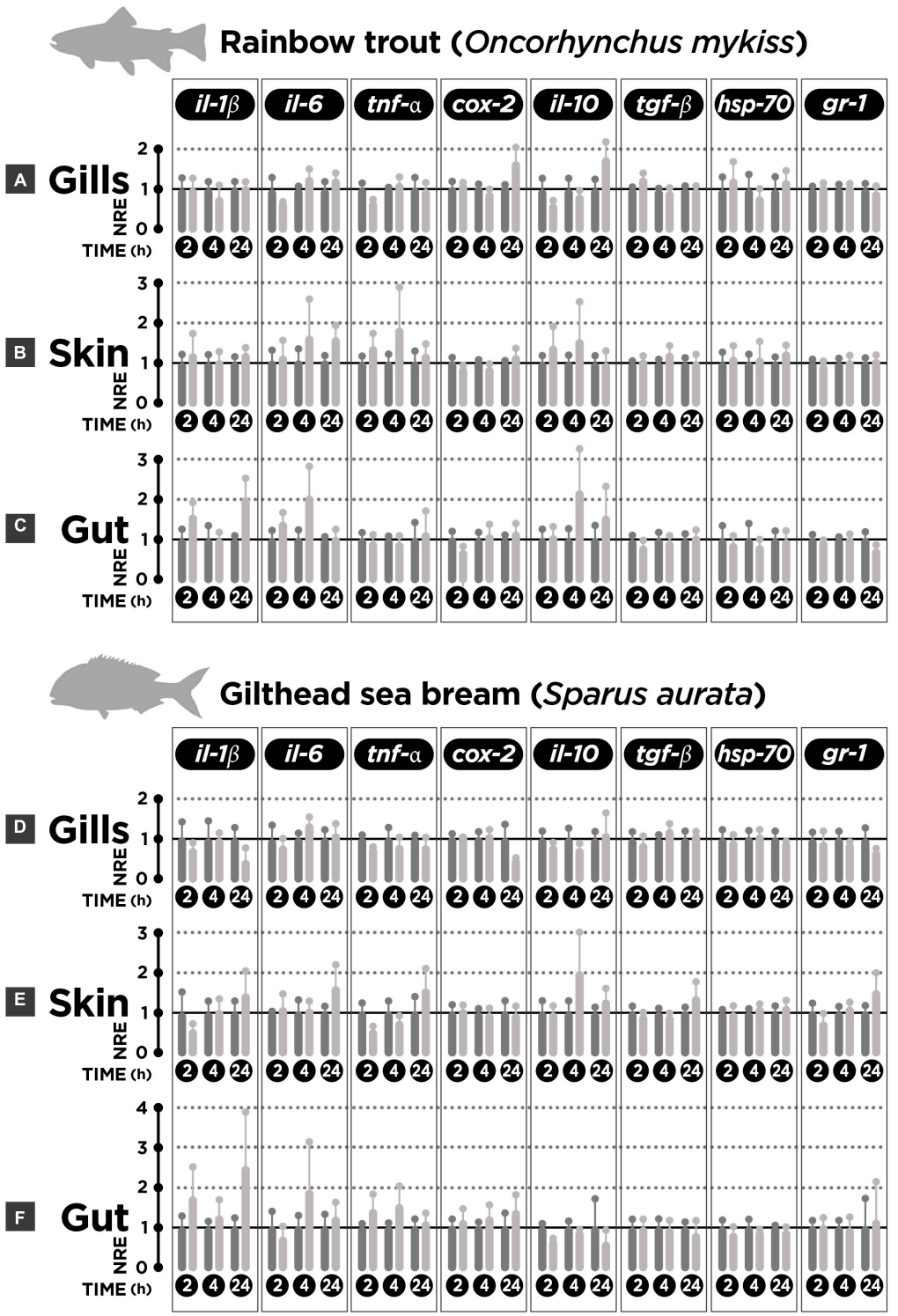


**FIGURE 1 |** Normalized relative expression (NRE) in rainbow trout ($n$ = 6) and gilthead sea bream ($n$ = 6) skin-(SALT), gills-(GIALT), and gut-associated lymphoid tissue (GALT) explants incubated with cortisol. **(A)** Rainbow trout gills. **(B)** Rainbow trout skin. **(C)** Rainbow trout gut. **(D)** Sea bream gills. **(E)** Sea bream skin. **(F)** Sea bream gut. The gene expression pattern for pro- (*il-1β, il-6, tnf-α*, and *cox-2*) and anti-inflammatory cytokines (*il-10, tgf-β*), and stress-related genes (*hsp70*, *gr1*) after 2, 4, and 24 h of incubation with cortisol. Bars represent mean ± SEM ($n$ = 6 fish per condition and time-point assessed). For each time-point, the left bars represents the mock-incubated tissue explant (control); the right bar represents the tissue explant incubated with cortisol. Two-way ANOVA and Sidak's post-test was used to explore differences ($p$-value $< 0.05$) in each time-point between mock-incubated (control) and cortisol treatment groups for each MALT tissue assessed. No significant differences were obtained ($p$-value $> 0.05$).

response (*il-10, tgf*-β), and stress response [*gr isoform 1 (gr1), hsp-70*]. The details about specific primers used for all genes tested including thermal conditions and reagent concentrations, are indicated in Khansari et al. (2017b, 2018). Real-time PCR was carried out using 1:20 as optimum cDNA dilution for each tissue based on the set of serial dilutions contained in the primer efficiency curve. All reactions were performed using Bio-Rad CFX384 Real-Time PCR Detection System (Bio-Rad Laboratories, Hercules, CA, United States) and data output was obtained from Bio-Rad CFX Manager software (version 3.1). We tested several candidates for reference genes in rainbow trout (*ef1*α and β-*actin*) and sea bream (*18s*, *ef1*α, and *rpl27*) to elucidate which one had less variation. β-Actin (for rainbow trout) and 18s (for sea bream) was included on gene expression analysis. Quantification was done according to Pfaffl (2001) corrected by each primer efficiency using a specific reference gene for each species (β-actin for rainbow trout; 18S for sea bream) and normalized to the control group.

## Statistical Analysis

Assumptions were tested for normality (D'Agostino-Pearson normality test), and homogeneity of variance (Spearman test for homoscedasticity). Two-way ANOVA and Sidak's post-test were used to explore differences in each time-point between the control group and cortisol treatment for each MALT tissue assessed. GraphPad software v6.0 was used to calculate the mean and standard error (SEM), and to perform statistical tests. In the analyses, a $p$-value $< 0.05$ was considered statistically significant.

# RESULTS

In order to evaluate the cortisol local effect on gills-, skin-, and gut-associated lymphoid tissues, the tissue explants were incubated with the hormone. No differences were found between cortisol-incubated explants and mock-incubated tissues for the expression of genes associated to immune (pro- [*il-1*β*, il-6, tnf*-α*, cox-2*] and anti-inflammatory cytokines [*il-10, tgf*-β]) or stress response [*gr isoform 1 (gr1), hsp-70*] for any of the time-points tested (2-, 4-, 24 h of incubation with cortisol) in rainbow trout gills (**Figure 1A**), skin (**Figure 1B**), nor gut (**Figure 1C**). No differences were either registered for gilthead sea bream gills (**Figure 1D**), skin (**Figure 1E**), nor gut (**Figure 1F**). The $p$-values obtained from *post-hoc* Sidak's test for comparison of NRE values between control and cortisol treatment is listed in **Supplementary Table 1**. These results suggest that exogenous cortisol has no local effect upon the modulation of the genes tested in gills, skin, nor gut mucosal tissues.

# DISCUSSION

In this study, the local effect of cortisol upon the modulation of immune- and stress-related genes in gills (GIALT), skin (SALT), and gut (GALT) was evaluated. Our results clearly show that cortisol by itself does not significantly modulate the expression of the genes evaluated in mucosal surfaces of either rainbow trout and gilthead sea bream at any of the time-points tested (2-, 4-, and 24 h post-incubation) compared to the mock-incubated group. These results suggest that the individual, isolated, and local action of cortisol on MALTs is not sufficient to promote the modulation of the genes tested in this study, and therefore that the relevant physiological modulation would be probably performed through the HPI systemic axis.

It has been well documented that in most fishes, a plasmatic concentration of 100 ng/ml of cortisol is associated with an acute stress response event (Castillo et al., 2008; Khansari et al., 2018, 2019). This concentration is currently measured in the first hour after subjecting rainbow trout to stressors of different nature, or a few hours post-stress (6 h in the case of sea bream) (Khansari et al., 2018, 2019). For this reason, it is not surprising that in several studies the concentration of 100 ng/ml of cortisol was used to evaluate local effects on the modulation of genes associated with immune and stress response (Castillo et al., 2009; Khansari et al., 2017b,c). The local effect of cortisol has been evaluated in the head kidney because (1) its endocrine function associated to the secretion of cortisol and catecholamines; (2) its role in immunity as lymphopoietic tissue; and (3) its role in preserving the physiological and energetic status due to its responsibility as hematopoietic tissue. Previous work showed that the incubation of sea bream head kidney primary cell culture (HKPCC) with 100 ng/ml cortisol induced a down-regulatory effect on the expression of pro- (*il-1*β, *il-6*, *tnf*α) and anti-inflammatory cytokines (*il-10*, *tgf*β) after 2 h (Castillo et al., 2009; Khansari et al., 2017b). These antecedents indicate a high influence of cortisol on the expression of pro- and anti-inflammatory cytokines. However, no regulatory effects upon the expression of those genes were observed in rainbow trout HKPCC incubated with cortisol (100 ng/ml) (Khansari et al., 2017b), suggesting differential sensitivity to cortisol at local level between rainbow trout and sea bream.

It is widely accepted that the perception of a stressor is a centralized mechanism that generates a coordinated response. The stimulus is perceived by sensory elements of the CNS that, once processed and depending on its magnitude and intensity, may conduct to the activation of the HPI axis and the subsequent release of corticosteroids to the bloodstream. These stress hormones, in turn, will be responsible for the effector response at the periphery. At the systemic level, the increase of plasma cortisol has been associated to the *in vivo* modulation of some genes involved in stress and immunity. In comparative analyses between rainbow trout and sea bream subjected to acute stressors, a differential expression pattern was observed both in magnitude and also response kinetics in the liver and spleen (Khansari et al., 2019). These antecedents suggest that the differential stress reactions among fishes may depend not only on the stressor intensity but on the environmental factors (i.e., salinity and thermopreferendum) and species specificities. In addition, sensitivity to stressors may also depend on the individual response or coping strategy, i. e., a proactive versus reactive response (Vargas et al., 2018). This suggests that more comparative approaches are necessary among teleost species in order to assess the short-term responsiveness to stressors and

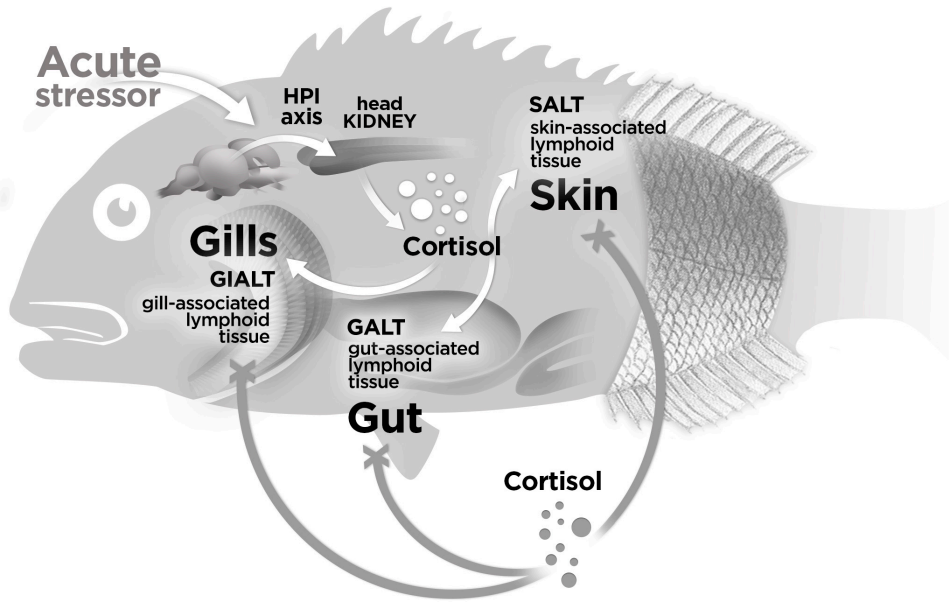


**FIGURE 2 |** Model of response for the modulation of genes in MALT in response to cortisol. In our study, no effect was registered on gills-(GIALT), skin-(SALT), and gut-associated lymphoid tissue (GALT) explants incubated with exogenous cortisol (represented with gray spheres) upon the modulation of a set of immune- and stress-related genes (represented with a "X" instead an arrow head). In a previous study (23) has been reported that the endogenous cortisol released (represented with white spheres) at the first 24 h in response to a stressor challenge modulates the expression of genes associated to immune and stress response in the same MALTs evaluated in this current study. These antecedents suggest that the modulation of genes on mucosal surfaces associated to a stress response is mainly influenced by the sum of systemic mechanisms activated in response to a stressor challenge but not by the direct exposure of the exogenous cortisol. The fish representation (gilthead sea bream) is merely explicative and also applicable for rainbow trout.

their eventual common characteristics associated to the acute stress response.

Because of the potential stressor effect of blood sampling, the interest in applying less-invasive sampling techniques associated to welfare issues, and the specific time presence (minutes to hours) of cortisol in the bloodstream (Vijayan et al., 2010), new strategies have been explored to identify cortisol in other biological matrices than in plasma. In this way, cortisol has been measured in the skin mucus of trout and sea bream (Guardiola et al., 2016; Fernández-Alacid et al., 2018; Khansari et al., 2018; Carbajal et al., 2019). Along with the cortisol increased levels both in plasma and skin mucus after acute stress, differences between rainbow trout and sea bream were observed on the expression pattern of genes associated to immune and stress response in gills (*il-6*, *il-10*, *tgf*-β, *hsp70*), skin (*il-6*, *tnf*-α, *il-10*, *tgf*-β, *hsp70*), and gut mucosal tissues (*il-6*, *il-10*, *hsp70*). By contrast, only the upregulation of *il-1*β and *cox-2* showed the same expression pattern in all these mucosal surfaces (Khansari et al., 2018). In gills the upregulation of *tnf*-α was also registered, while in the gut the upregulation of *il-1*β, *cox-2,* and *tnf*-α was accompanied with the upregulation of *tgf*-β (Khansari et al., 2018). This differential modulation of genes in mucosal tissues could be directly associated with the systemic (bloodstream) cortisol increase and, in consequence, with the concomitant modulation of the physiological response on the whole organism to recover homeostasis. On the other hand, the presence of cortisol in the mucus matrix could influence the subsequent immediate modulation of the transcriptional machinery. However, in our study, no modulatory local effect of cortisol was observed on a set of immune (*il-1*β, *il-6*, *tnf*-α, *cox-2*, *il-10*, *tgf*-β) nor stress genes (*hsp70*, *gr-1*) after incubating mucosal tissue explants with cortisol (100 ng). The absence of the direct effect of cortisol on the transcriptomic tissue explant profile suggests that cortisol is not able to carry out a relevant direct and local influence on mucosal tissues. This antecedent, together with the previous report (Khansari et al., 2018) indicating a modulatory gene expression effect after acute stress in rainbow trout and gilthead sea bream mucosal tissues, suggest that the expression profile associated to stress response in mucosal surfaces would be more influenced by the sum of systemic mechanisms activated in response to a stressor challenge rather than the direct exposure to the exogenous cortisol (**Figure 2**).

In summary, our results suggest that the quick modulation of the gene expression in the first 24 h after the exposure to stressor challenge reported in previous studies (Khansari et al., 2018) is probably coordinated and mediated through a systemic dependent mechanism but not so through a peripheral local response on mucosal tissues surfaces.

## DATA AVAILABILITY STATEMENT

The original contributions presented in the study are included in the article/**Supplementary Material**, further inquiries can be directed to the corresponding author.

## ETHICS STATEMENT

The animal study was reviewed and approved by the UAB CEEAH (Spain) for the use of laboratory animals (Reference number OH4218_4219).

## AUTHOR CONTRIBUTIONS

EV-V, AK, LT, and FER-L performed the conceptualization of the experiment. EV-V, AK, LS-D, and LT carried out the experiments. EV-V and FER-L performed the data analysis. EV-V, JCB, LT, and FER-L conceptualized the figures. EV-V, LT, and FER-L wrote the original draft. All authors participated in the interpretation of the results and corrected, read, and approved the final manuscript.

## FUNDING

This study was funded by the AGL2016-76069-C2-2-R and PID2020-117557RB-C21, AEI-MINECO (Spain) grants. EV-V thanks the support of Fondecyt iniciación grant (project number 11221308; Agencia Nacional de Investigación y Desarrollo de Chile, Government of Chile). AK was recipient of a Ministry of Science, Research, and Technology (Iran) fellowship. FER-L thanks the support of Fondecyt regular grant (project number: 1211841; Agencia Nacional de Investigación y Desarrollo de Chile, Government of Chile).

## ACKNOWLEDGMENTS

We thank Joan Baró (Trout Factory) for the trout supply.

## SUPPLEMENTARY MATERIAL

The Supplementary Material for this article can be found online at: https://www.frontiersin.org/articles/10.3389/fmars.2022.828050/full#supplementary-material

## REFERENCES

Algera, D. A., Brownscombe, J. W., Gilmour, K. M., Lawrence, M. J., Zolderdo, A. J., and Cooke, S. J. (2017). Cortisol treatment affects locomotor activity and swimming behaviour of male smallmouth bass engaged in paternal care: a field study using acceleration biologgers. *Physiol. Behav.* 181, 59–68. doi: 10.1016/j.physbeh.2017.08.026

Bakke, A. M., Glover, C., and Krogdahl, Å (2010). Feeding, digestion and absorption of nutrients. *Fish Physiol.* 30, 57–110. doi: 10.1016/S1546-5098(10)03002-5

Balasch, J. C., and Tort, L. (2019). Netting the Stress Responses in Fish. *Front. Endocrinol.* 10:62. doi: 10.3389/fendo.2019.00062

Carbajal, A., Reyes-López, F. E., Tallo-Parra, O., Lopez-Bejar, M., and Tort, L. (2019). Comparative assessment of cortisol in plasma, skin mucus and scales as a measure of the hypothalamic-pituitary-interrenal axis activity in fish. *Aquaculture* 506, 410–416. doi: 10.1016/j.aquaculture.2019.04.005

Castillo, J., Castellana, B., Acerete, L., Planas, J. V., Goetz, F. W., Mackenzie, S., et al. (2008). Stress-induced regulation of steroidogenic acute regulatory protein expression in head kidney of Gilthead seabream (Sparus aurata). *J. Endocrinol.* 196, 313–322. doi: 10.1677/JOE-07-0440

Castillo, J., Teles, M., Mackenzie, S., and Tort, L. (2009). Stress-related hormones modulate cytokine expression in the head kidney of gilthead seabream (Sparus aurata). *Fish Shellfish Immunol.* 27, 493–499. doi: 10.1016/j.fsi.2009.06.021

Cordero, H., Brinchmann, M. F., Cuesta, A., Meseguer, J., and Esteban, M. A. (2015). Skin mucus proteome map of European sea bass (Dicentrarchus labrax). *Proteomics* 15, 4007–4020. doi: 10.1002/pmic.201500120

Demers, N. E., and Bayne, C. J. (1997). The immediate effects of stress on hormones and plasma lysozyme in rainbow trout. *Dev. Comp. Immunol.* 21, 363–373. [pii], doi: 10.1016/s0145-305x(97)00009-8

Fernández-Alacid, L., Sanahuja, I., Ordóñez-Grande, B., Sánchez-Nuño, S., Viscor, G., Gisbert, E., et al. (2018). Skin mucus metabolites in response to physiological challenges: a valuable non-invasive method to study teleost marine species. *Sci. Total Environ.* 644, 1323–1335. doi: 10.1016/j.scitotenv.2018.07.083

Guardiola, F. A., Cuesta, A., and Esteban, M. Á (2016). Using skin mucus to evaluate stress in gilthead seabream (Sparus aurata L.). *Fish Shellfish Immunol.* 59, 323–330. doi: 10.1016/j.fsi.2016.11.005

Kelly, S. P., and Chasiotis, H. (2011). Glucocorticoid and mineralocorticoid receptors regulate paracellular permeability in a primary cultured gill epithelium. *J. Exp. Biol.* 214, 2308–2318. doi: 10.1242/jeb.055962

Khansari, A. R., Balasch, J. C., Reyes-lópez, F. E., and Tort, L. (2017a). Stressing the Inflammatory Network?: immuno-endocrine Responses to Allostatic Load in Fish. *J. Mar. Sci. Res. Technol.* 1:2.

Khansari, A. R., Parra, D., Reyes-López, F. E., and Tort, L. (2017b). Cytokine modulation by stress hormones and antagonist specific hormonal inhibition in rainbow trout (Oncorhynchus mykiss) and gilthead sea bream (Sparus aurata) head kidney primary cell culture. *Gen. Comp. Endocrinol.* 250, 122–135. doi: 10.1016/j.ygcen.2017.06.005

Khansari, A. R., Parra, D., Reyes-López, F. E., and Tort, L. (2017c). Modulatory in vitro effect of stress hormones on the cytokine response of rainbow trout and gilthead sea bream head kidney stimulated with Vibrio anguillarum bacterin. *Fish Shellfish Immunol.* 70, 736–749. doi: 10.1016/j.fsi.2017.09.009

Khansari, A. R., Balasch, J. C., Vallejos-Vidal, E., Parra, D., Reyes-López, F. E., and Tort, L. (2018). Comparative Immune- and Stress-Related Transcript Response Induced by Air Exposure and Vibrio anguillarum Bacterin in Rainbow Trout (Oncorhynchus mykiss) and Gilthead Seabream (Sparus aurata) Mucosal Surfaces. *Front. Immunol.* 9:856. doi: 10.3389/fimmu.2018.00856

Khansari, A. R., Balasch, J. C., Vallejos-Vidal, E., Teles, M., Fierro-Castro, C., Tort, L., et al. (2019). Comparative study of stress and immune-related transcript outcomes triggered by Vibrio anguillarum bacterin and air exposure stress in liver and spleen of gilthead seabream (Sparus aurata), zebrafish (Danio rerio) and rainbow trout (Oncorhynchus mykiss). *Fish Shellfish Immunol.* 86, 436–448. doi: 10.1016/j.fsi.2018.11.063

Nelson, J. A., and Dehn, A. M. (2010). The GI tract in air breathing. *First Edit. Elsevier Inc.* 30, 395–433. doi: 10.1088/0031-8949/2005/T121/007

Parra, D., Reyes-Lopez, F. E., and Tort, L. (2015). Mucosal Immunity and B Cells in Teleosts: effect of Vaccination and Stress. *Front. Immunol.* 6:354. doi: 10.3389/fimmu.2015.00354

Pfaffl, M. W. (2001). A new mathematical model for relative quantification in real-time RT-PCR. *Nucleic Acids Res.* 29:e45. doi: 10.1093/nar/29.9.e45

Rajan, B., Lokesh, J., Kiron, V., and Brinchmann, M. F. (2013). Differentially expressed proteins in the skin mucus of Atlantic cod (Gadus morhua) upon natural infection with Vibrio anguillarum. *BMC Vet. Res.* 9:103. doi: 10.1186/1746-6148-9-103

Reyes-López, F. E., Aerts, J., Vallejos-Vidal, E., Ampe, B., Dierckens, K., Tort, L., et al. (2018). Modulation of Innate Immune- Related Genes and Glucocorticoid Synthesis in Gnotobiotic Full-Sibling European Sea Bass (Dicentrarchus labrax) Larvae Challenged With Vibrio anguillarum. *Front. Immunol.* 9:914. doi: 10.3389/fimmu.2018.00914

Salinas, I. (2015). The Mucosal Immune System of Teleost Fish. *Biology* 4, 525–539. doi: 10.3390/biology4030525

Salinas, I., LaPatra, S. E., and Erhardt, E. B. (2015). Nasal vaccination of young rainbow trout (Oncorhynchus mykiss) against infectious hematopoietic

necrosis and enteric red mouth disease. *Dev. Comp. Immunol.* 53, 105–111. doi: 10.1016/j.dci.2015.05.015

Sanahuja, I., and Ibarz, A. (2015). Skin mucus proteome of gilthead sea bream: a non-invasive method to screen for welfare indicators. *Fish Shellfish Immunol.* 46, 426–435. doi: 10.1016/j.fsi.2015.05.056

Schreck, C. B., and Tort, L. (2016). "The concept of stress in fish", in *Biology of Stress in* Fish. First edit, eds A. P. Farrell and C. J. Brauner (London: Academic Press).

Sunyer, J. O., and Tort, L. (1995). Natural hemolytic and bactericidal activities of sea bream Sparus aurata serum are effected by the alternative complement pathway. *Vet. Immunol. Immunopathol.* 45, 333–345.

Tort, L. (2011). Stress and immune modulation in fish. *Dev. Comp. Immunol.* 35, 1366–1375. doi: 10.1016/j.dci.2011.07.002

Vargas, R., Balasch, J. C., Brandts, I., Reyes-López, F., Tort, L., and Teles, M. (2018). Variations in the immune and metabolic response of proactive and reactive Sparus aurata under stimulation with Vibrio anguillarum vaccine. *Sci. Rep.* 8:17352. doi: 10.1038/s41598-018-35863-w

Vazzana, M., Cammarata, M., Cooper, E. L., and Parrinello, N. (2002). Confinement stress in sea bass (Dicentrarchus labrax) depresses peritoneal leukocyte cytotoxicity. *Aquaculture* 210, 231–243. doi: 10.1016/S0044-8486(01)00818-3

Verburg-van Kemenade, B. M. L., Stolte, H. H., Metz, J. R., and Chadzinska, M. K. (2009). "Neuroendocrine-immune interactions in teleost fish," in *Fish Neuroendocrinology Fish Physiology?: 28*, eds N. J. Bernier, G. Van der Kraak, A. P. Farrell, and C. J. Brauner (London: Academic Press), 313–364. doi: 10.1016/s1546-5098(09)28007-1

Vijayan, M. M., Aluru, N., and Leatherland, J. F. (2010). "Stress response and the role of cortisol. Vol 2: non-Infectious Disorders," in *Fish Diseases and Disorders*, eds J. F. Leatherland and P. Woo (Oxfordshire: CAB), 182–201. doi: 10.1079/9781845935535.0182

Xu, Z., Parra, D., Gómez, D., Salinas, I., Zhang, Y.-A., Jørgensen, L. V. G., et al. (2013). Teleost skin, an ancient mucosal surface that elicits gut-like immune responses. *Proc. Natl. Acad. Sci. U.S.A.* 110, 13097–13102. doi: 10.1073/pnas.1304319110

Xu, Z., Takizawa, F., Parra, D., Gómez, D., Jørgensen, L. V. G., LaPatra, S. E., et al. (2016). Mucosal immunoglobulins at respiratory surfaces mark an ancient association that predates the emergence of tetrapods. *Nat. Commun.* 7:10728. doi: 10.1038/ncomms10728

Zhang, Y.-A., Salinas, I., and Oriol Sunyer, J. (2011). Recent findings on the structure and function of teleost IgT. *Fish Shellfish Immunol.* 31, 627–634. doi: 10.1016/j.fsi.2011.03.021

**Conflict of Interest:** The authors declare that the research was conducted in the absence of any commercial or financial relationships that could be construed as a potential conflict of interest.

**Publisher's Note:** All claims expressed in this article are solely those of the authors and do not necessarily represent those of their affiliated organizations, or those of the publisher, the editors and the reviewers. Any product that may be evaluated in this article, or claim that may be made by its manufacturer, is not guaranteed or endorsed by the publisher.

frontiers in Marine Science

ORIGINAL RESEARCH
published: 18 March 2022
doi: 10.3389/fmars.2022.797507

# From Embryo to Adult Life: Differential Expression of Visual Opsins in the Flatfish *Solea senegalensis* Under Different Light Spectra and Photoperiods

*Sara Frau[1†], José A. Paullada-Salmerón[1,2,3†], Isabella Paradiso[1], Mairi E. Cowan[1,4], Águeda J. Martín-Robles[2,3,5*] and José A. Muñoz-Cueto[1,2,3*]*

[1] Department of Biology, Faculty of Marine and Environmental Sciences, University of Cádiz, Puerto Real, Spain, [2] INMAR Research Institute, Marine Campus of International Excellence (CEIMAR), Agrifood Campus of International Excellence (ceiA3), Puerto Real, Spain, [3] European University of the Seas SEA-EU, Cádiz, Spain, [4] Scottish Association for Marine Science, Oban, United Kingdom, [5] Biochemistry and Molecular Biology Area, Department of Biomedicine, Biotechnology and Public Health, Faculty of Sciences, University of Cádiz, Puerto Real, Spain

OPEN ACCESS

**Edited by:**
Enric Gisbert,
Institute of Agrifood Research and Technology (IRTA), Spain

**Reviewed by:**
Ignacio Fernández,
Instituto Tecnológico Agrario de Castilla y León, Spain
F. Javier Sanchez Vazquez,
University of Murcia, Spain

***Correspondence:**
Águeda J. Martín-Robles
agueda.jimena@uca.es
José A. Muñoz-Cueto
munoz.cueto@uca.es

[†] These authors have contributed equally to this work and share first authorship

**Specialty section:**
This article was submitted to Aquatic Physiology, a section of the journal Frontiers in Marine Science

**Received:** 18 October 2021
**Accepted:** 17 January 2022
**Published:** 18 March 2022

**Citation:**
Frau S, Paullada-Salmerón JA, Paradiso I, Cowan ME, Martín-Robles ÁJ and Muñoz-Cueto JA (2022) From Embryo to Adult Life: Differential Expression of Visual Opsins in the Flatfish Solea senegalensis Under Different Light Spectra and Photoperiods. Front. Mar. Sci. 9:797507. doi: 10.3389/fmars.2022.797507

Visual photoreceptors in fish are usually adjusted to the light environment to ensure the highest efficiency and best adaptation. In the Senegalese sole, metamorphosis determines migration from pelagic to benthic habitats, with marked differences in both light intensity and spectrum. Here, we analysed the ontogeny of six visual photopigments, namely, rod opsin (*rh1*), short wavelength-sensitive (*sws1* and *sws2*), medium wavelength-sensitive (*rh2.3* and *rh2.4*), and long wavelength-sensitive (*lws*) cone opsins, in sole specimens maintained in light-dark cycles of white (LDW), blue (LDB), red (LDR), and continuous white (LL) lights by using RT-qPCR and *in situ* hybridisation. Most of the opsins displayed a similar developmental expression pattern under all tested conditions. However, lower transcripts were detected under LDR and LL compared to LDW and LDB. A significant increase in gene expression was detected before and after metamorphosis, reaching minimum transcript levels at hatching and during metamorphosis. Interestingly, green opsins (*rh2.3* and *rh2.4*) displayed a significant increase only before metamorphosis, with their expression remaining low during and after metamorphosis. The rod opsin and short-, medium-, and long-wavelength sensitive cone opsins were detected in retinal photoreceptors of the sole from pre-metamorphic to adult stages by *in situ* hybridisation. In adults, the short-wavelength cone opsins (*sws1* and *sws2*) were found in single cones, whereas the medium- (*rh2.4*) and long-wavelength (*lws*) cone opsins were present in double cones. The results obtained by *in situ* hybridisation in the retina of developing sole, in terms of number of positive cells and/or intensity of labelling, were consistent with the ontogenetic transcript patterns found by RT-qPCR, suggesting that most of the visual opsin expressions detected in the whole specimens could correspond to retinal expression. Taken together, our results pointed out that the ontogeny of the Senegalese sole is accompanied by remodelling in opsin gene expression, with the green-cone

opsins being the most abundant photopigments in pre-metamorphosis and rod opsin the dominant visual photopigment from the completion of metamorphosis onwards. These results enlarge our knowledge of flatfish metamorphosis and ecology and provide useful information to develop light protocols adapted to different ontogenetic stages that could improve welfare and production in sole aquaculture.

**Keywords: ontogeny, photoreception, flatfish metamorphosis, retina, cones, rods (retina), sole (*Solea senegalensis*)**

## INTRODUCTION

Particularly diverse light environments are present in aquatic marine habitats. When sunlight hits the ocean, some photons are reflected off the surface back into the atmosphere, but water absorbs most of them. In a very shallow layer, longer wavelengths are absorbed more quickly than shorter wavelengths (Jerlov, 1968). Light with short and medium wavelengths, such as blue and green lights, can penetrate more deeply. At 40 m, ocean water has absorbed nearly all the red and orange visible lights. However, blue and green lights are still able to penetrate beyond these depths (up to 200 m) in open ocean waters. Factors such as suspended sediments and dissolved organic matters can alter the quality of underwater light and consequently modify the absorption of different spectra (Jerlov, 1968). These changes in the physical environment require an organism to adapt to new abiotic conditions and modify its physiology and behaviour to survive.

Many fish species present variations in retinal sensitivity during development in response to altered or changing light conditions in the early stages compared to adult life (Evans and Fernald, 1990). These differences in light intensity and spectrum affect the wavelength absorption of photoreceptor cells, resulting in altered retinal mosaics and changes in the number of different photoreceptor cells and the expression of opsins in the retina. Five visual opsin subfamilies have been reported in vertebrates, including medium wavelength-sensitive rhodopsin (RH1) expressed in rods, UV-sensitive or very-short-wavelength-sensitive 1 (SWS1), blue-sensitive or short-wavelength-sensitive 2 (SWS2), medium wavelength-sensitive rhodopsin-like 2 (RH2), and long wavelength-sensitive (LWS) opsins expressed in cones (Carleton et al., 2020; Musilova et al., 2021). In teleost fish, gene duplication events result in multiple copies of opsin genes compared to other vertebrates. Thus, up to two *sws1*, three *sws2*, eight *rh2*, five *lws,* and two *rh1* opsin genes have been described in teleosts, although some deep-sea fish exhibit a much higher number of *rh1* gene copies (up to 38) as an adaptation to the dim light of mesopelagic habitats (Carleton et al., 2020; Musilova et al., 2021). Fish such as the eel (*Anguilla anguilla*), salmon (*Oncorhynchus gorbuscha*), and rainbow trout (*Oncorhynchus mykiss*) that undergo important life cycle transformations (i.e., metamorphosis, smoltification) were also reported to exhibit opsin plasticity associated with these changes. This could occur in a number of different ways like shifts in chromophore or absorbance spectrum, and loss, substitution, or addition of other types of opsins during these processes, coinciding with drastic changes in the environment (Cheng and Novales Flamarique, 2004; Veldhoen et al., 2006; Bowmaker et al., 2008; Temple et al., 2008).

Similarly, flatfish species are widely affected by physical and environmental changes (Evans and Fernald, 1990; Dufour et al., 2012; Iwanicki et al., 2017). The Senegalese sole, *Solea senegalensis*, is exposed to different environmental light depending on the ontogenetic phase. Larvae live on the surface of the seawater column exposed to a vast range of visible light spectra, while juveniles and adults live in the bottom, mainly in coastal areas of up to 100 m depth dominated by blue and green lights (Muñoz-Cueto et al., 2019). A number of studies have focused on the plasticity of opsins in pre-metamorphic and post-metamorphic flatfish species (Evans et al., 1993; Helvik et al., 2001a,b; Mader and Cameron, 2004; Hoke et al., 2006; Ferraresso et al., 2013; Chen et al., 2014; Savelli et al., 2018; Wang et al., 2021), even though it is still not clear whether these changes are driven by genetic forces or by environmental factors.

In a recent study, we characterised the mosaic, the type, and the distribution of the cones in the retina of two *Solea* spp. including *Solea senegalensis*, evidencing a loss of regular cone mosaic patterning compared to other fishes adapted to different light environments and habitats (Frau et al., 2020a). In a second study, we demonstrated that light regimes clearly affected phases, amplitudes, and/or significance of opsin daily rhythms in the Senegalese sole. We revealed that the alternation in light-dark (LD) cycles of appropriate wavelengths are very important for the optimal development of opsin repertoire in the sole, with blue light representing the most adequate for early establishment of robust visual opsin daily rhythms (Frau et al., 2020b). In this study, we continued to collect information on the topic by investigating ontogenetic patterns of expression of visual opsins and their retinal localisation in this metamorphic flatfish species, the Senegalese sole, and how they are affected when exposed to different light conditions during development, by using real-time qPCR and *in situ* hybridisation. Considering the importance that both photoperiod and light spectrum play in the early stages of the sole (Blanco-Vives et al., 2010, 2011, Martín-Robles et al., 2012), as well as the high commercial value and wide consumption of this species (Howell and Dinis, 2019), the information obtained in this study could be relevant for deciphering whether opsin usage is driven by environmental factors or genetically preprogrammed (or both), for improving the welfare of animals and proper development and breeding of the Senegalese sole in the aquaculture industry.

# MATERIALS AND METHODS

## Animals and Rearing System

Senegalese sole fertilised eggs were provided by the Spanish Institute of Oceanography (Santander, Cantabria, Spain) in the spring reproductive season and brought to the University of Cadiz under dark conditions. They arrived at our facilities 1 day before hatching, and they were distributed into eight 15-L cylindroconical tanks. Water temperature was maintained under a natural thermocycle of 21 ± 0.5°C during the day and 18 ± 0.5°C during the night and continuously recorded with an underwater sensor and a data logger (HOBO Pendant; Onset Computer Corporation, Bourne, MA, United States) placed in each tank. All the tanks were sustained under continuous water and oxygen renovation, 35 ppt of salinity, and pH 7.5–8.2.

Food protocol administration to the larvae was conducted according to Frau et al. (2020b). To feed the larvae, rotifers were cultured and enriched with green algae at a proportion of 300 cells/ml/day of *Nannochloropsis gaditana* and 50 cells/ml/day of *Isochrysis galbana*. Enriched rotifers were added to the tanks as live food at a density of 10 individuals/ml/day from 3 to 6 days post-hatching (dph) and at a density of 15 individuals/ml/day from dph 7 to 9. *Artemia* nauplii were added to the tanks at a density of 1 to 5 nauplii/ml/day and were provided from 7 to 31 dph. For the whole experiment, the alive food was provided to the larvae four times a day to ensure their constant circulation. Rotifers, algae, and *Artemia* were provided by the fish facility of the "Servicio Central de Investigación en Cultivos Marinos" (REGA ESII0280003I2, University of Cádiz).

## Experimental Setup and Sampling

Upon acclimation to our facilities, fertilised eggs were exposed to different light wavelengths and photoperiod conditions: LD cycles of blue light (LDB, λ peak = 463 nm, half-peak bandwidth 435–500 nm), red light (LDR, λ peak = 665 nm half-peak, bandwidth 628–692 nm), white light (LDW, ∼ 100 lx), and constant white light (LL). The white light possessed a broad spectrum of 95% irradiance within the range of 367 to 757 nm. A photoperiod of 14 h of light and 10 h of darkness was set in the LDW, LDB, and LDR tanks, while the LL group was kept with continuous (24 h) white light. LDW represented the control group mimicking the current fish hatchery protocol. Two biological replicates (tanks) were analysed for each light condition. All the tanks were covered with a thick black screen to avoid the effects of any background light on the experiments. Details regarding the light setup of the experiments are indicated in the Materials and methods section of Frau et al. (2020b).

For the qPCR experiment, pools of larvae were sampled in different developmental stages: days post hatching (dph) –1 (before hatching), dph 0 (hatching), dph 4, dph 7, dph 9, dph 17, dph 21, and dph 32. Twenty specimens/sample were collected for dph –1, 0, 4, and 7; ten specimens/sample for dph 9 and 17; and five specimens/sample for dph 21 and 32 ($n$ = 3–5 per stage, obtained from both tanks of each light condition). In each stage, sampling was performed at zeitgeber/circadian time (ZT/CT) 4 (12:00 h local time) for specimens maintained under LD cycles and constant conditions, respectively. ZT0 corresponds to lights on and ZT14 to lights off. All the samples were immediately frozen in liquid nitrogen and stored at –80°C until they were used.

*In situ* hybridisation (ISH) analysis was performed in sole specimens at dph 7 (pre-metamorphosis), dph 13 (metamorphosis), dph 32 (post-metamorphosis), and 2-year-old (adult) stages, which were maintained under LDW condition and sampled at ZT4 (12:00 h local time).

All animals were manipulated following the guidelines of the Animal Experimentation and Ethics Committee of the University of Cádiz (Spain) and the Directorate General for Agricultural and Livestock Production of the Regional Government of Andalusia (approval number 15/12/2020/142) and in accordance with international ethical standards and the European Union regulation (EC Directive 86/609/EEC).

## RNA Extraction and cDNA Synthesis

Total RNA from sole larvae was extracted using TRIsure Reagent®(Bioline, London, United Kingdom), as described in Frau et al. (2020b). Briefly, the samples were resuspended and homogenised, and the RNA was precipitated, isolated, cleaned and stored at –80°C until it was used. Total RNA yield and quality were determined by the 260/280-nm absorbance ratio with a NanoDrop 2000 Spectrophotometer (Thermo Fisher Scientific, Wilmington, DE, United States). For cDNA synthesis, aliquots of 1 μg of total RNA were treated with DNase-I to remove genomic DNA and reverse transcribed using a QuantiTect Reverse transcription kit (Qiagen, Hilden, Germany) following manufacturer instructions.

## Gene Expression Analysis

Real-time quantitative PCR (RT-qPCR) was performed to analyse the relative mRNA expression of visual opsins. RT-qPCR reactions were performed in a Bio-Rad CFX96 Touch detection system (Bio-Rad, Richmond, CA, United States) using SYBRPremix Ex TaqII (TliRnaseH Plus; TAKARA BIO INC., Otsu, Japan). Specific forward and reverse primers were used and amplification conditions were described in Frau et al. (2020b) as follows: 1 min at 95°C (initial denaturation) and 40 cycles of 15 s at 95°C (denaturation), 15 s at annealing temperature (58.8°C for *sws2*; 60°C for *sws1*, *rh2.3*, *lws,* and *housekeeping genes*; 62.5°C for *rh1* and *rh2.4*), and 10 s at 65°C (extension). Non-template control and non-retro-transcribed total RNA samples were used as negative controls. Duplicates of each sample were analysed in the same assay, and melting curves were determined for each sample to confirm that a single product was amplified. The ΔΔCt method was used to determine relative mRNA opsin expression (Livak and Schmittgen, 2001). Data obtained were normalised to the dph –1 group. Senegalese sole *elongation factor 1 alpha* (*eef1a1*) and *ubiquitin* (*ubq*) (gene bank accession numbers AB326302.1 and AB291588.1, respectively) were used as housekeeping genes for normalisation (Infante et al., 2008).

## Riboprobe Synthesis

Messenger RNAs used for the synthesis of specific riboprobes corresponded to the ORF-coding region of *Solea senegalensis*

visual opsins. The probes consisted of 486 nt for the rod opsin (*rh1*), 680 nt for the ultraviolet (UV) cone opsin (*sws1*), 485 nt for the blue cone opsin (*sws2*), 432 nt for the green cone opsin (*rh2.4*), and 624 nt for the red cone opsin (*lws*). Specific riboprobes were synthesised using a pSpark II vector (Canvax Biotech, Córdoba, Spain) containing DNA sequences of sole opsins synthesised by Bio Basic Inc. (Markham, Canada). Antisense and sense single-stranded mRNA probes were obtained with DIG RNA labelling MIX (Sigma Aldrich, Madrid, Spain) by transcription with T7 and SP6 RNA polymerases (Promega Biotech Ibérica S.L., Alcobendas, Spain) on plasmids linearised with *Sac*I and *Sac*II restriction enzymes. The size of the DIG-labeled riboprobes was checked by 1% agarose gel electrophoresis under denaturing conditions, and their concentration was evaluated by spectrophotometric analysis.

## *In situ* Hybridisation

The precise localisation of visual opsin expression (*rh1*, *sws1*, sws2, *rh2.4,* and *lws*) was analysed by *in situ* hybridisation (ISH) in the retina of the sole in 4 different developmental stages: pre-metamorphosis, metamorphosis, post-metamorphosis, and adult. Whole larva (pre-metamorphosis, metamorphosis), juvenile (post-metamorphosis), and adult retinas were fixed by immersion in 4% paraformaldehyde in PBS (pH 7.4). After cryoprotection overnight in a 15% sucrose solution in PBS, whole specimens and retinas were embedded in Tissue-Tek and quickly frozen in cold isopentane, and transverse 7-μm-thick serial sections were obtained with a cryostat.

The protocol for ISH was as described in Servili et al. (2012), but was slightly modified. Before hybridisation, cryostat sections were washed in 1 × PBS (pH 7.4) two times and postfixed for 20 min in 4% paraformaldehyde (PAF) diluted in PBS. After postfixation, the sections were washed in PBS and incubated with proteinase K for 5 min at 37°C in PBS, rinsed, and postfixed again in 4% PAF. Afterward, the sections were rinsed two times in 2 × SSC at room temperature for 10 min. The DIG-labeled probes were preheated at 75°C for 5 min before the hybridisation procedure. Hybridisation was carried out at 60–65°C in a humidified chamber using 60 μl of a hybridisation buffer (2 × SSC; 2.5% dextran sulfate; 50% deionised formamide; 5 × Denhardt's solution; 50 μg/ml of yeast tRNA, pH 8; 4 mM EDTA) containing the DIG-labeled riboprobes (500 ng–1 μg/ml). Subsequently, the slides were rinsed in 2 × SSC at 60–65°C, followed by two rinses at 60–65°C for 30 min in 2 × SSC/50% deionised formamide. The sections were rinsed in 0.2 and 0.1 × SSC at room temperature and then blocked for 1 h in a solution of 100mM Tris-HCl buffer, 150 mM NaCl (pH 7.5) with 0.5% BSA, and 0.2% Triton X-100. The slides were incubated overnight at room temperature with an alkaline phosphatase-conjugated anti-DIG antibody (1:500; Sigma Aldrich, Madrid, Spain). On the next day, the sections were incubated for 40 min in NBT/BCIP (stock solution; Sigma Aldrich, Madrid, Spain). Same riboprobe concentration, and same conditions and incubation/developing times for each opsin were systematically used in our ISH study in all the stages analyzed, permitting us to obtain some comparative information on the amount of transcript levels present in tissue sections. The specificity of the hybridisation signal was systematically checked by hybridising parallel sections with corresponding sense probes. *In situ* hybridisation slides were analysed on an Axio Imager (Zeiss, Oberkochen, Germany) microscope, and pictures were processed with the Zen software (Zeiss, Oberkochen, Germany) and Adobe Photoshop (Adobe Systems, San Jose, CA, United States) without any modification except for light or contrast adjustments.

## Statistical Analyses

Statistical differences in the expression of the visual opsin genes between samples of the two tanks from the same condition and stage were analysed by Student's *t*-test. Statistical differences in developmental expression of visual opsin genes under each particular light photoperiod and spectrum condition were analysed by one-way ANOVA and represented in **Figures 1**, **3**, **5**, **7**, **8**, **10**. A comparison of visual opsin expression among different light conditions in a given developmental stage was also performed by one-way ANOVA and represented in **Supplementary Tables 1–6**. Significant ANOVAs were followed by Tukey's *post hoc* comparison test to determine differences among means, with $p < 0.05$ as statistically significant threshold. When needed, values were transformed to match the normal distribution and homogeneity of variances. When data did not accomplish the ANOVA conditions, the non-parametric Kruskal-Wallis test was applied, followed by multiple contrasts of range test (Bonferroni). All the statistical analyses were performed using the Statgraphics Plus 5.1 software (Statpoint Technologies, Warrenton, VA, United States). The data were presented as the mean ± SEM. All the graphics were created by Prism version 6.00 for Mac (GraphPad Software, La Jolla, CA, United States).

# RESULTS

Visual monitoring of eye migration, position in the water column (pelagic vs. benthic), locomotor activity (diurnal vs. nocturnal), and total length of the specimens were registered in different light regimes to follow the progression of metamorphosis, using LDW as a control condition (**Table 1**). A delay in development was observed under the LDR regime, with the animals exhibiting shorter length and retardation in the course of metamorphosis, particularly on dph 21 (S2, middle metamorphosis under LDR vs. S3, late metamorphosis/S4, early post-metamorphosis under LDW, LDB, and LL; **Table 1**). High mortality was also observed in larvae reared under LDR conditions; as a result, this condition was not possible to be analysed in the last post-metamorphic stage (dph 32). Visual opsin expression during Senegalese sole development and effects of photoperiod and light spectrum were analysed by RT-qPCR (**Figures 1**, **3**, **5**, **7**, **8**, **10**). No statistical differences were found in opsin expression among the samples of different tanks from the same condition and stage (Student's *t*-test, $p > 0.05$). In turn, the localisation of visual opsin-expressing cells was revealed by *in situ* hybridisations in the retina of the sole in the pre-metamorphic, metamorphic, post-metamorphic, and adult stages (**Figures 2**, **4**, **6**, **9**, **11**, **12**). The

**TABLE 1 |** Total length (TL) and main developmental stages of Senegalese sole under the different light regimes tested.

| | | LDW | LDB | LDR | LL |
|---|---|---|---|---|---|
| dph 6 | TL (mm) | 3.11 ± 0.15 | 3.23 ± 0.17 | 2.94 ± 0.12 | 3.15 ± 0.18 |
| | Developmental stage | Pre-metamorphosis (S0) | Pre-metamorphosis (S0) | Pre-metamorphosis (S0) | Pre-metamorphosis (S0) |
| dph 9 | TL (mm) | 4.13 ± 0.18 | 4.15 ± 0.13 | 4.01 ± 0.12 | 4.10 ± 0.20 |
| | Developmental stage | Early metamorphosis (S1) | Early metamorphosis (S1) | Pre-metamorphosis/Early metamorphosis (S0/S1) | Early metamorphosis (S1) |
| dph 21 | TL (mm) | 7.13 ± 0.21 | 7.29 ± 0.23 | 5.98 ± 0.21 | 7.23 ± 0.20 |
| | Developmental stage | Late metamorphosis/Early post-metamorphosis (S3/S4) | Late metamorphosis/Early post-metamorphosis (S3/S4) | Middle metamorphosis (S2) | Late metamorphosis/Early post-metamorphosis (S3/S4) |

*The classification into different larval developmental phases and metamorphic stages in Solea senegalensis was determined by visual monitoring of eye migration, position in the water column (pelagic vs. benthic) and locomotor activity (diurnal vs. nocturnal) according to Blanco-Vives et al. (2010; 2011; 2012), Sarasquete et al. (2019) dph, days post-hatching; TL, total length.*

results obtained by ISH in the retina of the developing sole, in terms of the number of positive cells and/or intensity of the labelling, were highly consistent with those found by RT-qPCR. There were no marked differences in labelling between the right and left retinas in any of the developmental stages analysed (**Figures 2A,C**, **6A,C**, **11D,F**). No labelling was observed in sections incubated with sense riboprobes (**Figures 2G,H**, **4G,H**, **6G,H**, **9C,D**, **11B,C**), confirming the specificity of the staining evidenced in antisense sections.

## Rod Opsin

Rod opsin (*rh1*) transcript levels exhibited a comparable temporal expression pattern in all the groups analysed but had slight differences (**Figures 1A–D** and **Supplementary Table 1**). The lowest transcript levels were found in embryos (dph –1) and at hatching (dph 0). A significant increase in expression was evident in the pre-metamorphic stage, in particular on dph 7 (except under LDW conditions), followed by a significant decrease during metamorphosis (dph 9 and/or 17), which was not evident either under LDW conditions, and further increase in later stages under all conditions (dph 21 and/or 32, **Figures 1A–D**). However, *rh1* expression levels were markedly affected by light conditions, with differences particularly evident on dph 21 and 32 (**Figure 1** and **Supplementary Table 1**). In these stages, the highest *rh1* expression was reached under LDW conditions, followed by LDB, LL, and LDR. In LDW, the expression was between three (dph 32) and ten (dph 21) times higher than the expression in LDB, around three times higher compared to that in LDR (dph 21), and seven times higher in relation to LL conditions (dph 32). In contrast, during hatching (dph 0), pre-metamorphosis (dph 7), and metamorphosis (dph 17), transcript levels were quite similar among the different light conditions (**Supplementary Table 1**).

*In situ* hybridisation permitted us to identify a conspicuous rod opsin expression in the cell bodies and inner segments of photoreceptors present in the outer nuclear layer of the retina in the four ontogenetic stages analysed (**Figure 2**). The number of rod opsin-expressing cells and intensity of the labelling was lower in pre-metamorphic (**Figures 2A,B**) and metamorphic (**Figures 2C,D**) specimens compared to post-metamorphic (**Figures 2E,F**) and adult animals, in which *rh1* represented the most expressed photopigment in densely packed cell bodies of the outer nuclear layer (**Figures 2I,J**).

## Short-Wavelength Opsins: Ultraviolet and Blue Opsins

Ultraviolet (*sws1*) and blue (*sws2*) cone opsin transcripts were also detected in Senegalese sole embryos, larvae, and juveniles in all the stages analysed and under all light spectra and photoperiod regimes (**Figures 3–6**).

The temporal expression pattern of *sws1* resembles that found for *rh1* and is quite similar in most tested conditions but relative expression levels are much lower and ontogenetic variations are less pronounced. In LDW, LDB, and LL, *sws1* expression exhibited its lowest levels in embryos (dph –1) and hatched larvae (dph 0) (**Figures 3A,B,D**). A significant increment in mRNA levels was observed during pre-metamorphosis (dph 4 and/or 7). During metamorphosis (dph 9 and 17), *sws1* expression levels remained constant (**Figures 3A,B,D**), with further elevation after completion of the metamorphic process (dph 21 and/or 32) (**Figures 3A,B,D**). Under LDR conditions, *sws1* transcript levels did not present any differences from embryos to early metamorphosis, but the expression increased significantly on dph 21 (**Figure 3C**). The light spectra and photoperiod also affected the expression levels of *sws1*. The highest expression of this opsin was detected under LDB conditions in most of the developmental stages, followed by LL/LDW conditions, being particularly low in LDR (**Figures 3A–D** and **Supplementary Table 2**).

Almost no UV opsin labelling was detected by *in situ* hybridisation in the retina of pre-metamorphic (**Figure 4A**) and metamorphic soles (**Figure 4B**, white arrowheads) using *sws1* antisense riboprobes. As observed for *rh1*, the number of positive cells and intensity of the labelling increased in post-metamorphic specimens (**Figures 4C,D**). In adults, a moderate *sws1* expression appeared restricted to the base of the inner segments of single cone photoreceptors (**Figures 4E,F**, white arrowheads), which occupied an intermediate position between larger double cones devoid of labelling (**Figure 4F**, black arrowheads) and cell bodies of rods present in the outer nuclear layer.

Regarding *sws2*, the temporal pattern of expression resembles that of *rh1* rather than that of *sws1*, with a significant increase during pre-metamorphosis (dph 4 and/or dph 7), a decrease during metamorphosis (dph 9 and 17), and a subsequent rise

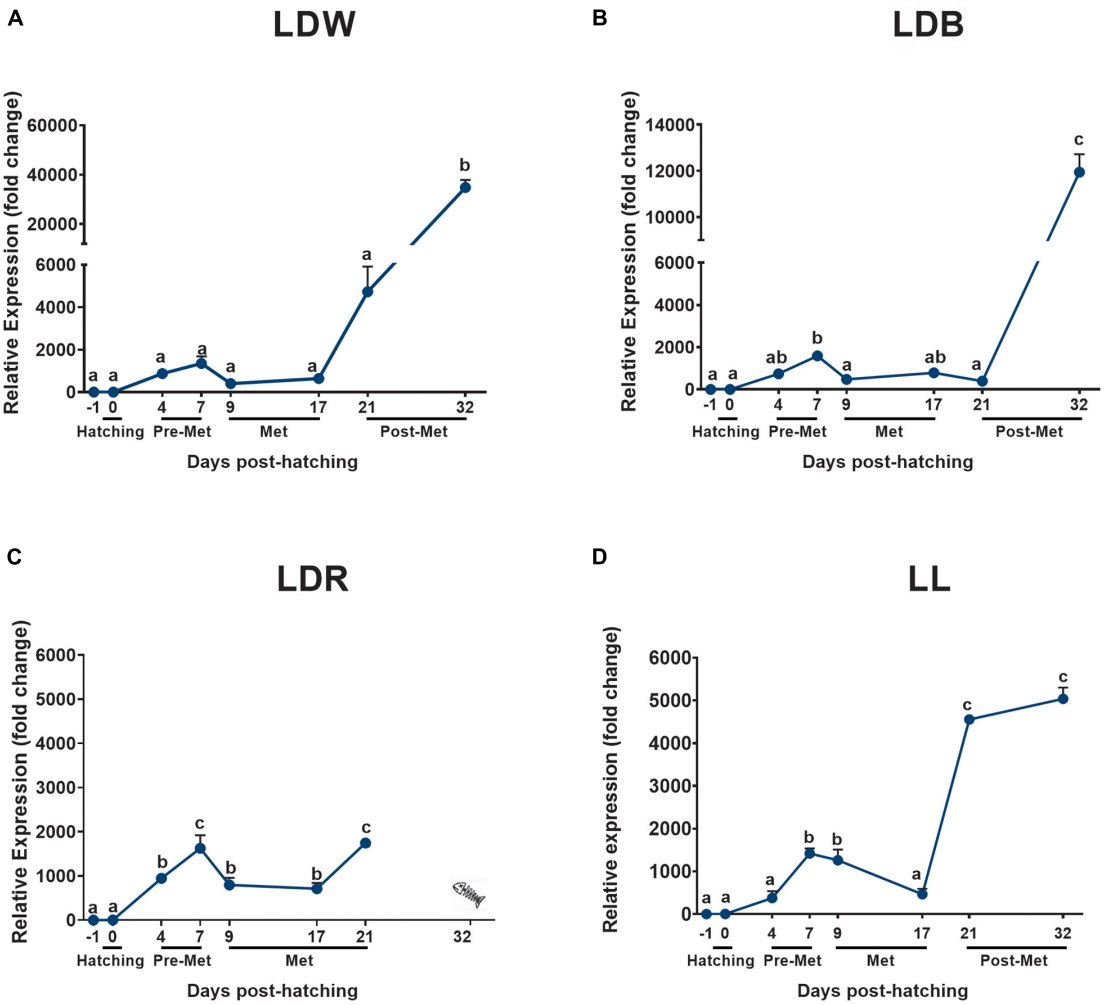


**FIGURE 1 |** Expression of rod opsin (*rh1*) in embryos, larvae, and juveniles of the Senegalese sole –1 day post-hatching (dph) or dph –1 (embryos), dph 0 (hatching), dph 4–7 (pre-metamorphosis, Pre-Met), dph 9–17 (metamorphosis, Met), and dph 21–32 (post-metamorphosis, Post-Met) analysed by real-time quantitative polymerase chain reaction (RT-qPCR). It should be noted that the animals under LDR conditions showed delayed development, remaining in the metamorphic phase (S2-middle metamorphosis) on dph 21. Therefore, the bar indicating the metamorphic stage has been extended to dph 21 in panel **(C)**. Each value represents the mean ± SEM ($n$ = 3–5). Relative expression was normalised to the dph –1 group, and using *ef1a1* and *ubq* as housekeeping genes. Senegalese sole specimens were maintained under different photoperiods and light spectra: light/dark (LD) cycles of white (LDW; **A**), blue (LDB; **B**), and red (LDR; **C**) lights, or under constant light conditions (LL; **D**). Different letters indicate statistically significant differences between mean values ($p < 0.05$). The Fishbone symbol in the LDR condition indicated that larvae died before the completion of metamorphosis.

in transcript levels in late post-metamorphosis (dph 32), which was evident under all light conditions except for LDR specimens that did not reach this stage (**Figures 5A–D**). This pattern of expression was influenced by the light spectrum and photoperiod. Thus, in LDW, the rise in *sws2* expression was advanced in pre-metamorphosis to dph 4, and the peak of expression found in the post-metamorphic stage (dph 32) reached higher levels (**Figure 5A** and **Supplementary Table 3**) in relation to LDB (**Figure 5B** and **Supplementary Table 3**) and, in particular, compared to constant light conditions in which these values were significantly lower than those attained in pre-metamorphosis (**Figure 5D** and **Supplementary Table 3**).

Blue opsin expression in the retina of the sole was higher than that of UV opsins in all developmental stages analysed, as revealed by *in situ* hybridisation (**Figure 6**). In the early stages (pre-metamorphosis and metamorphosis), positive *sws2* cells were more abundant in the ventral and medial surfaces of the retina (**Figures 6A–D**, white arrowheads), which were also evident in the dorsal retina of post-metamorphic animals (**Figures 6E,F**). In adults, the *sws2* visual pigment was also

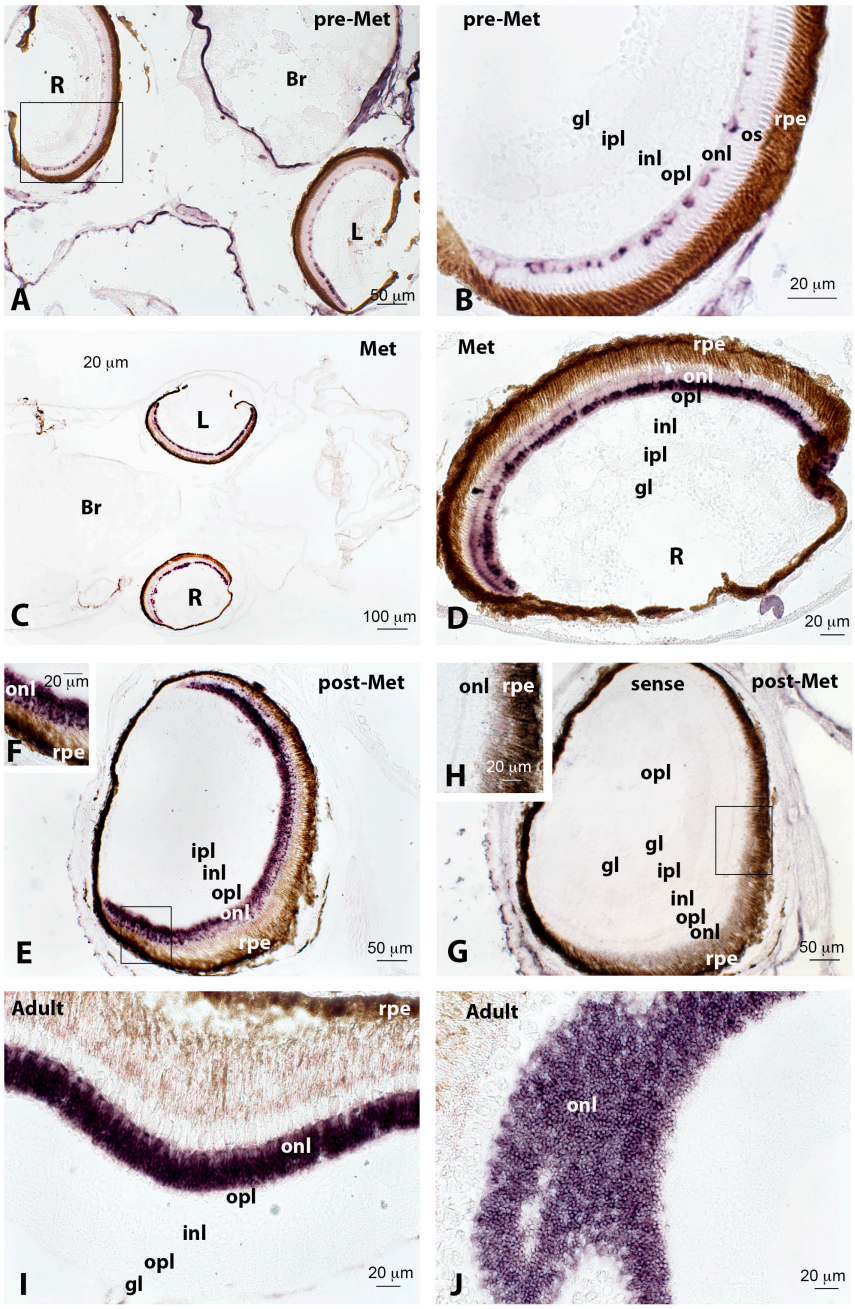


**FIGURE 2 |** Localisation of rod opsin (*rh1*) expression in the retina of pre-metamorphic (pre-Met; **A,B**), metamorphic (Met; **C,D**), post-metamorphic (post-Met; **E–H**), and adult **(I,J)** Senegalese sole specimens revealed by *in situ* hybridisation. All the photomicrographs represent antisense sections, with the exception of panels **(G,H)**, which show sense control sections. The photomicrograph represented in panel **(J)** shows a tangential section through the outer nuclear layer (onl), exhibiting abundant positive *rh1*-expressing cells. Squares in panels **(A,E,G)** mark the areas magnified in photomicrographs **(B,F,H)**, respectively. Note how the expression of *rh1* in rods of onl increases markedly in the post-metamorphic and adult retina compared to the previous stages. Other abbreviations: Br, brain; gl, glomerular layer; inl, internal nuclear layer; ipl, internal plexiform layer; L, left retina; opl, outer plexiform layer; os, outer segment of photoreceptors; R, right retina; rpe, retinal pigment epithelium. Scale bars represent 20 µm in panels **(B,D,F,H,I,J)**; 50 µm in panels **(A,E,G)**; and 100 µm in panel **(C)**.

confined to the single cones (**Figures 6I–M**, white arrowheads), with labelling being evident at the base of the inner segments of photoreceptors (myoid region), which have a pear-like appearance in radial sections (**Figures 6J,K**) and a rounded aspect in oblique (**Figure 6L**) and tangential (**Figure 6M**) sections. These *sws2*-positive single cones appeared surrounded by larger and unlabelled double (**Figures 6K–M**, black arrowheads and asterisks) and triple (**Figure 6M**, black arrow) cones, probably

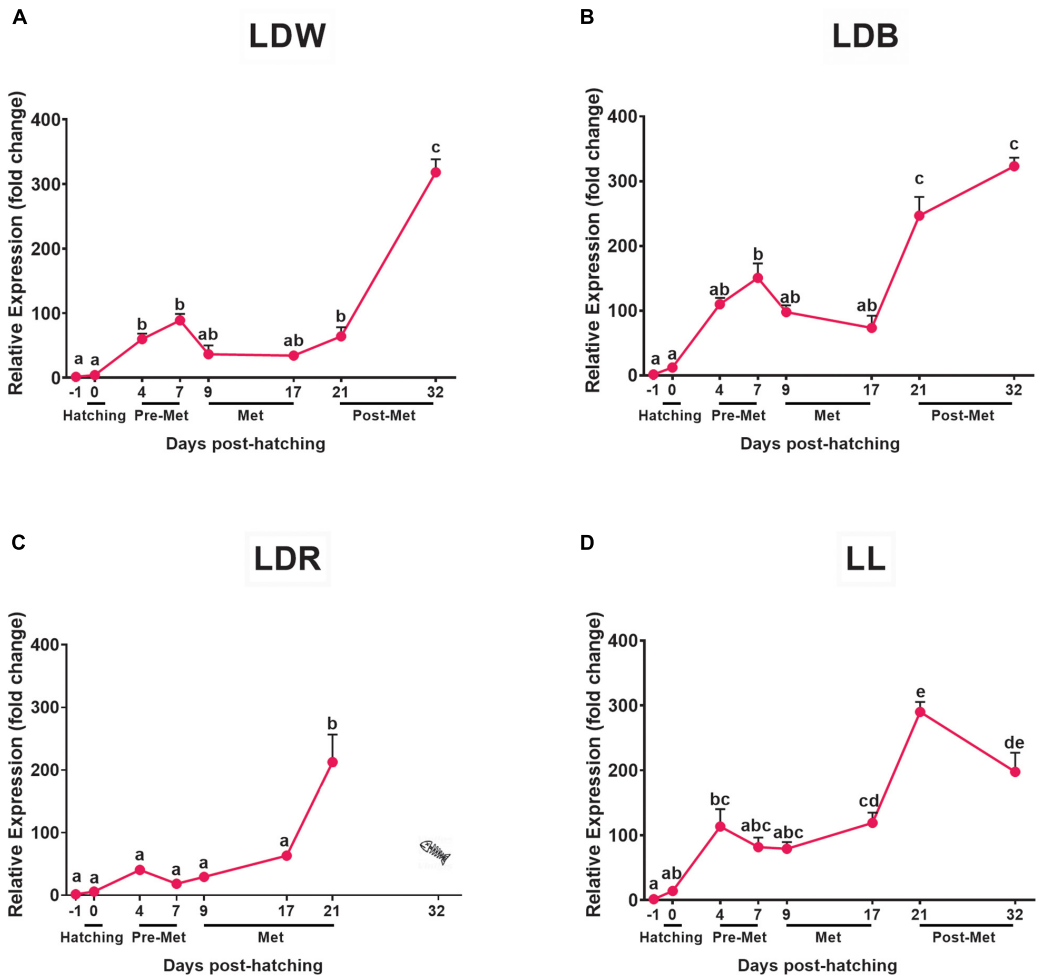


**FIGURE 3 |** Expression of ultraviolet cone opsin (*sws1*) in embryos, larvae, and juveniles of the Senegalese sole on dph –1 (embryos), dph 0 (hatching), dph 4–7 (pre-metamorphosis, Pre-Met), dph 9–17 (metamorphosis, Met), and dph 21–32 (post-metamorphosis, Post-Met) analysed by RT-qPCR. For further information, see the legend in **Figure 1**.

expressing medium wavelength- (*rh2.3* and/or *rh2.4*) and long wavelength- (*lws*) sensitive opsins.

## Medium-Wavelength Opsins: Green Opsins

The developmental expression pattern of both green opsins (*rh2.3* and *rh2.4*) was similar but exhibited important differences in transcript levels between them (much higher expression for *rh2.4*), and when compared with the other opsins analysed, because their expression did not increase in the post-metamorphic stage like the other opsins (**Figures 7**, **8**). In this way, the highest expression values for both *rh2.3* and *rh2.4* were observed in pre-metamorphosis (dph 4 or dph 7, **Figures 7**, **8** and **Supplementary Tables 4**, **5**), when the green opsins represented the most abundant photopigments. Light spectrum affected differentially the expression of both green opsins, with blue lights (LDB) determining an increase of around 10 times in mRNA peak levels of *rh2.3*, but not of *rh2.4* (**Figures 7B**, **8B** and **Supplementary Tables 4**, **5**) when compared to the other light regimes (**Figures 7A,C,D**, **8A,C,D** and **Supplementary Tables 4**, **5**). Concerning *rh2.4*, LDW was the light regime more efficient in increasing its transcript levels in both pre-metamorphosis (dph 4) and post-metamorphosis (dph 21 and 32) (**Figure 8** and **Supplementary Table 5**). Photoperiod also influenced the expression of the green opsins, with lower peak levels of both *rh2.3* and *rh2.4* in pre-metamorphosis under constant light conditions (LL, **Figures 7D**, **8D** and **Supplementary Tables 4**, **5**) in relation to the light-dark conditions tested (**Figures 7A–C**, **8A–C** and **Supplementary Tables 4**, **5**).

The presence of green opsins in retinal cells of the sole was identified by *in situ* hybridisation only for *rh2.4* because *rh2.3*

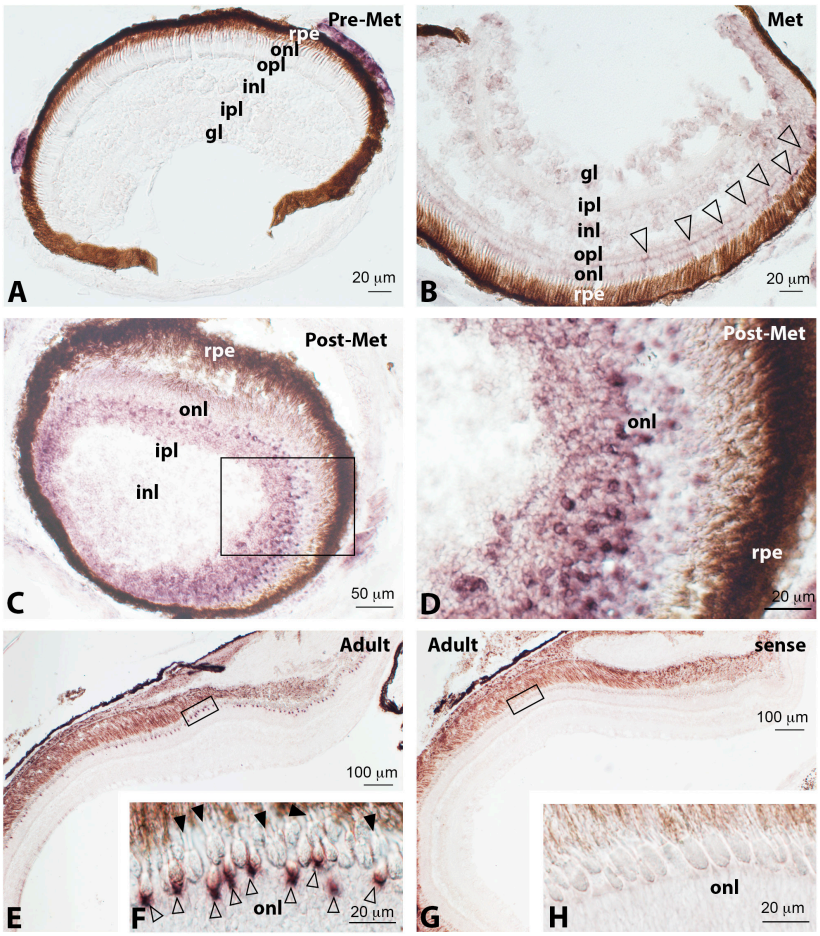


**FIGURE 4 |** Localisation of ultraviolet cone opsin (*sws1*) expression in the retina of pre-metamorphic (Pre-Met; **A**), metamorphic (Met; **B**), post-metamorphic (Post-Met; **C,D**), and adult **(E–H)** Senegalese sole specimens revealed by *in situ* hybridisation. All the photomicrographs represent antisense sections, with the exception of panels **(G)** and **(H)**, which show sense control sections. Squares in panels **(C,E,G)** mark the areas magnified in photomicrographs **(D,F,H)**, respectively. Note the absence of positive cells in pre-metamorphic specimens **(A)**, faint labelling of photoreceptors in metamorphic animals (white arrowheads in panel **B**), and how the number of labelled photoreceptors and intensity of this labelling increase in post-metamorphic **(C,D)**, and adult **(E,F)** retina. In the adult retina, *sws1* expression appears evident at the base of inner segments of single cones (white arrowheads in panel **F**). In contrast, double cones were devoid of labelling (**F**, black arrowheads). For abbreviations, see the legend in **Figure 2**. Scale bars represent 20 μm in panels **(A,B,D,F,H)**; 50 μm in panel **(C)**; and 100 μm in panels **(E,G)**.

transcript levels were much lower in most of the developmental stages analysed, as revealed by Cts in the qPCR study. In contrast to that observed by qPCR, no marked differences in the expression of *rh2.4* were observed among the retinas of pre-metamorphic (**Figures 9A,B**) and metamorphic animals (**Figures 9E,F**) by *in situ* hybridisation. Abundant positive green opsin-expressing cells were evident in the outer nuclear layer of the retina in both stages, with more intense labelling in the external half of the outer nuclear layer, closer to the retinal pigment epithelium (**Figures 9B,F**). However, in agreement with the qPCR results, a marked reduction in *rh2.4* expression was observed in post-metamorphic specimens (**Figures 9G,H**). In adults, intense *rh2.4* labelling was present at the base of the inner segments of double cones (**Figures 9I,J**, black arrowheads), at the level of the external limiting membrane, whereas single cones appeared unlabelled (**Figures 9I,J**, white arrowheads). The presence of double cones with inner segments devoid of green opsin labelling was also evident in the retina of the adult sole (**Figure 9K**, black arrows).

## Long-Wavelength Opsins: Red Opsin

Finally, the expression of the red opsin (*lws*) followed a similar developmental trend than that reported for most of the opsins studied, i.e., the lowest levels in the embryo (dph –1) and hatching (dph 0) stages, a significant increase during pre-metamorphosis (dph 4 and/or dph 7), drop in transcript levels during metamorphosis (non-significant under LDW conditions), and a further increase in later stages (dph 21 and/or dph 32) (**Figures 10A–D**). The light regime also influenced *lws* expression. In this case, light-dark cycles of white lights (LDW) were the most efficient in increasing *lws* transcript levels in the pre-metamorphic stage (dph 4), with two to five times higher expression than the remaining light conditions (**Figures 10A–D** and **Supplementary Table 6**). In the later stages, the peak

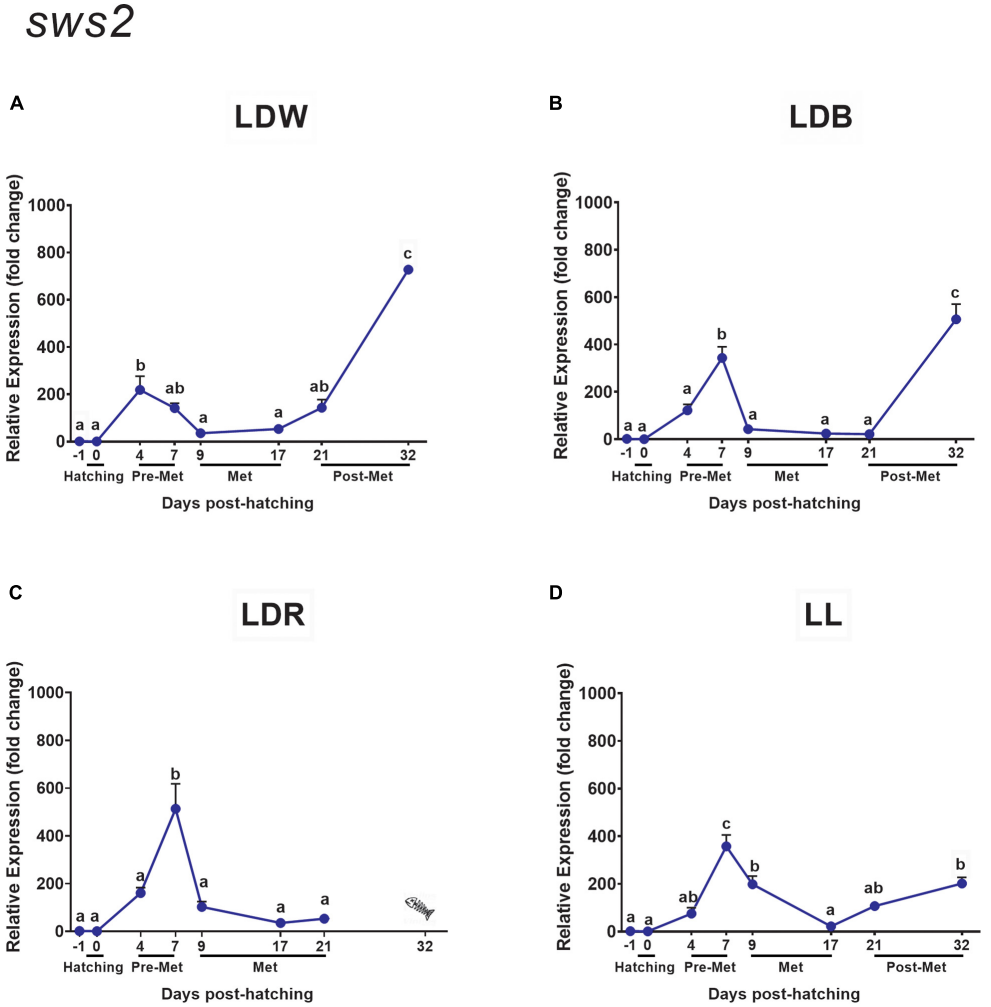


**FIGURE 5 |** Expression of blue cone opsin (*sws2*) in embryos, larvae, and juveniles of the Senegalese sole on dph –1 (embryos), dph 0 (hatching), dph 4–7 (pre-metamorphosis, Pre-Met), dph 9–17 (metamorphosis, Met), and dph 21–32 (post-metamorphosis, Post-Met) analysed by RT-qPCR. For further information, see the legend in **Figure 1**.

of *lws* expression was also higher under the LDW regime (dph 32), followed by LDB (dph 32), LL (dph 32), and LDR (dph 21) (**Figures 10A–D** and **Supplementary Table 6**). It should be noted that the latter increase was already evident in LDW, LDR, and LL on dph 21 (**Figures 10A,C,D** and **Supplementary Table 6**) but was not significant under LDB conditions until 32 dph (**Figure 10B** and **Supplementary Table 6**).

The red opsin was detected by *in situ* hybridisation in the retina of the sole in all the developmental stages analysed (**Figure 11**). However, in pre-metamorphosis (**Figure 11A**) and metamorphosis (**Figures 11D–G**), labelling was much more evident in the ventromedial part of the retina, being the dorsal area almost devoid of positive cells, whereas in post-metamorphic (**Figures 11H,I**) and adult (**Figures 11J–L**) animals, the dorsal retina also exhibited conspicuous labelling. The expression of *lws* was detected in double cones showing intense labelling in both double cone pairs (**Figures 11K,L**), although some of them were labelled only in one of the double cone members (**Figure 11L**, black arrows). These positive cells appear intermingled with unlabelled single cones (**Figures 11K,L**, white arrowheads) and unlabelled double cones (**Figure 11L**, asterisks), probably containing short-wavelength opsins and medium-wavelength opsins, respectively.

**Figure 12** illustrates the comparative distribution of cells expressing the five visual opsins analysed by *in situ* hybridisation in haematoxylin-eosin stained sections of the retina of the adult sole. The number of rod opsin (*rh1*)-expressing cells and intensity of the labelling were markedly higher than those observed in serial sections of the retina processed with riboprobes against the other visual pigments (**Figures 12A,B**). Medium-wavelength sensitive opsin-expressing cells (green opsin *rh2.4*, **Figures 12G,H**) were also abundant in cones of the outer nuclear layer of the retina, where a moderate number of intensely stained long wavelength-sensitive opsin-expressing cones (red opsin *lws*, **Figures 12I,J**) were also found. In contrast, short-wavelength sensitive opsin-expressing cells containing the blue

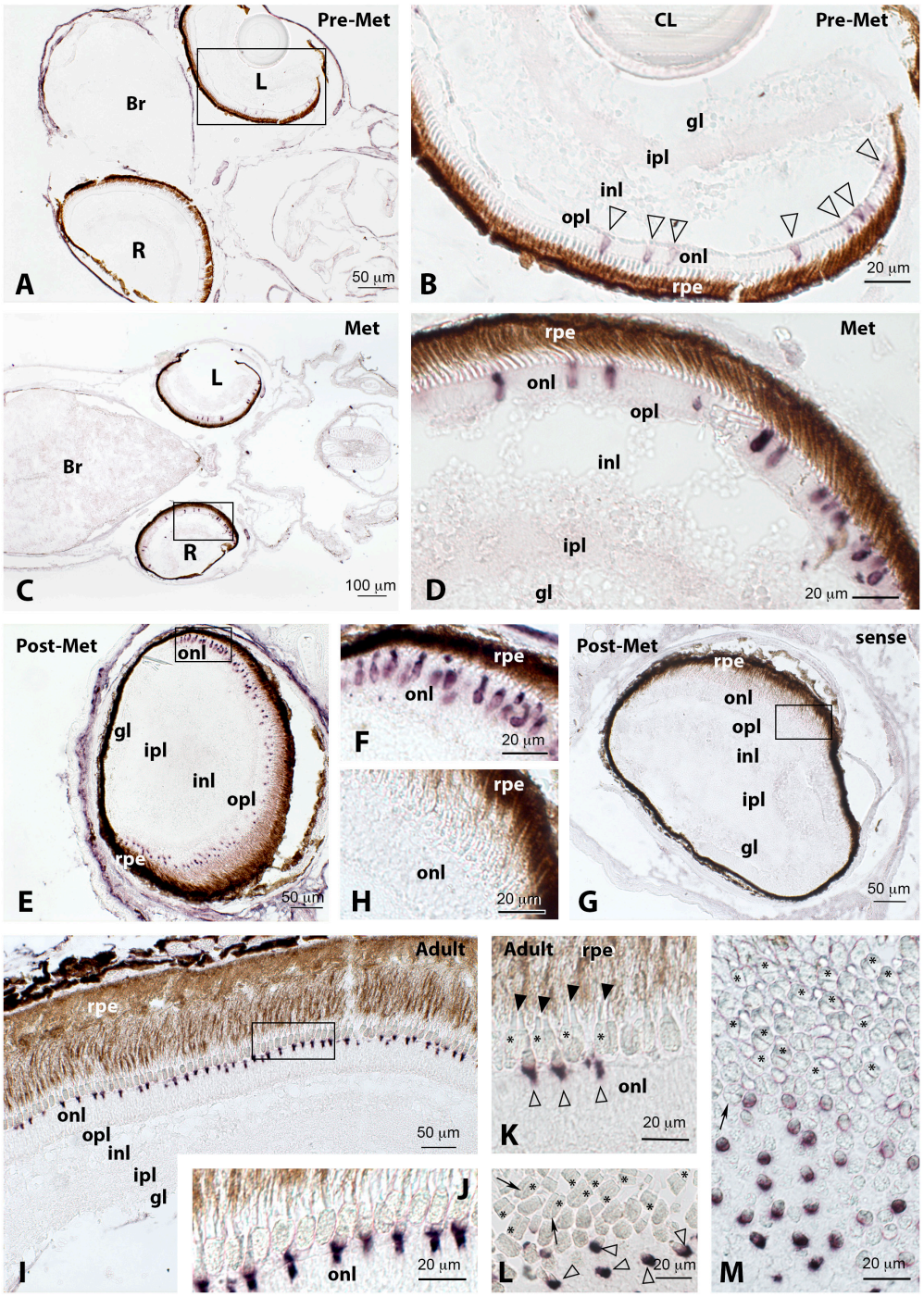


**FIGURE 6 |** Localisation of blue cone opsin (*sws2*) expression in the retina of pre-metamorphic (Pre-Met; **A,B**), metamorphic (Met; **C,D**), post-metamorphic (Post-Met; **E–H**), and adult **(I–M)** Senegalese sole specimens revealed by *in situ* hybridisation. All the photomicrographs represent antisense sections, with the exception of panels **(G)** and **(H)**, which show sense control sections. Squares in panels **(A,C,E,G,I)** mark the areas magnified in photomicrographs **(B,D,F,H,J)**, respectively. Note the low number of positive cells and faint labelling of cones in pre-metamorphic specimens (**B**, white arrowheads), how the intensity of this labelling increases in metamorphic animals **(C,D)**, and subsequent increase in the number of labelled cones in post-metamorphic **(E,F)** and adult **(I,J)** retinas. In the adult retina, *sws2* expression appears evident at the base of inner segments of single cones (white arrowheads in panels **K,L**). In contrast, double cones (asterisks in panels **K–M**), which exhibit their characteristic double outer segments (black arrowheads in panel **K**), were devoid of labelling. Most of the unlabelled double cones exhibited straight partitions **(L,M)**, although a few of them showed a bent partition (black arrows in panel **L**). Black arrow in panel **(M)** marks an unlabelled triple cone revealed in a radial section. **(L,M)** photomicrographs represent oblique and tangential sections, respectively, whereas the remaining pictures corresponded to radial sections. CL, crystalline lens. For other abbreviations, see the legend in **Figure 2**. Scale bars represent 20 μm in panels **(B,D,F,H,J–M)**; 50 μm in panels **(A,E,G,I)**; and 100 μm in panel **(C)**.

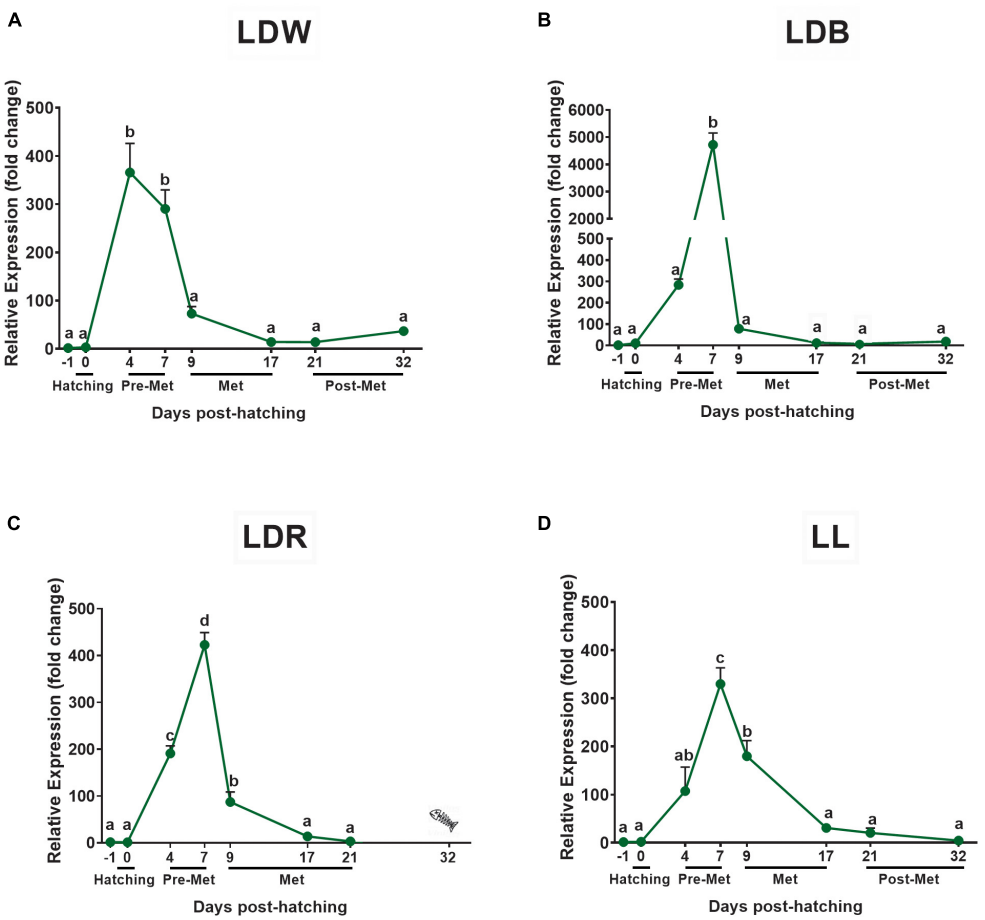


**FIGURE 7 |** Expression of green cone opsin (*rh2.3*) in embryos, larvae, and juveniles of the Senegalese sole on dph –1 (embryos), dph 0 (hatching), dph 4–7 (pre-metamorphosis, Pre-Met), dph 9–17 (metamorphosis, Met), and dph 21–32 (post-metamorphosis, Post-Met) analysed by RT-qPCR. For further information, see the legend in **Figure 1**.

cone opsin (*sws2*, **Figures 12E,F**) and the UV cone opsin (*sws1*, **Figures 12C,D**) were less represented in the retina of the adult sole.

## DISCUSSION

In the Senegalese sole, as in other flatfish species, metamorphosis causes morphological, cellular, molecular, physiological, and behavioural changes (e.g., migration of left eye to the right side, skin stratification, remodelling of axial muscle, mouth, head, and forebrain, gas-exchange efficiency, gastrointestinal tract compartmentalization, the shift from diurnal to nocturnal locomotor activity, and feeding), which accompany its vertical migration from the surface of the water column to the bedside and determine a switch from planktonic to benthonic habits (Rodríguez-Gómez et al., 2000; Fernández-Díaz et al., 2001; Blanco-Vives et al., 2012; Campinho, 2019). In this study, our main goal was to understand if these morphological, behavioural, and ecological changes match physiological and adaptive changes in visual opsin expression and the number of visual opsin-expressing cells from the embryo to the juvenile/adult stages of the Senegalese sole. As summarised in **Figure 13**, visual opsin expression was significantly upregulated in pre-metamorphosis (dph 4–7) just after the functional differentiation of the retina (Bejarano-Escobar et al., 2010), and in post-metamorphosis (dph 21–32), when the shift from pelagic to benthic habitats and from diurnal to nocturnal behaviour is already accomplished (Blanco-Vives et al., 2012). In between, a generalised decline in visual opsin expression was detected, coinciding with the metamorphic process (dph 9–17). The overall patterns of expression of the six opsins analysed follow a similar developmental trend regardless of the light regime, suggesting that opsin usage could be genetically preprogrammed during sole development, as has been previously proposed in other fish species such as the cod, *Gadus morhua* (Valen et al., 2014, 2018). However, photoperiod and

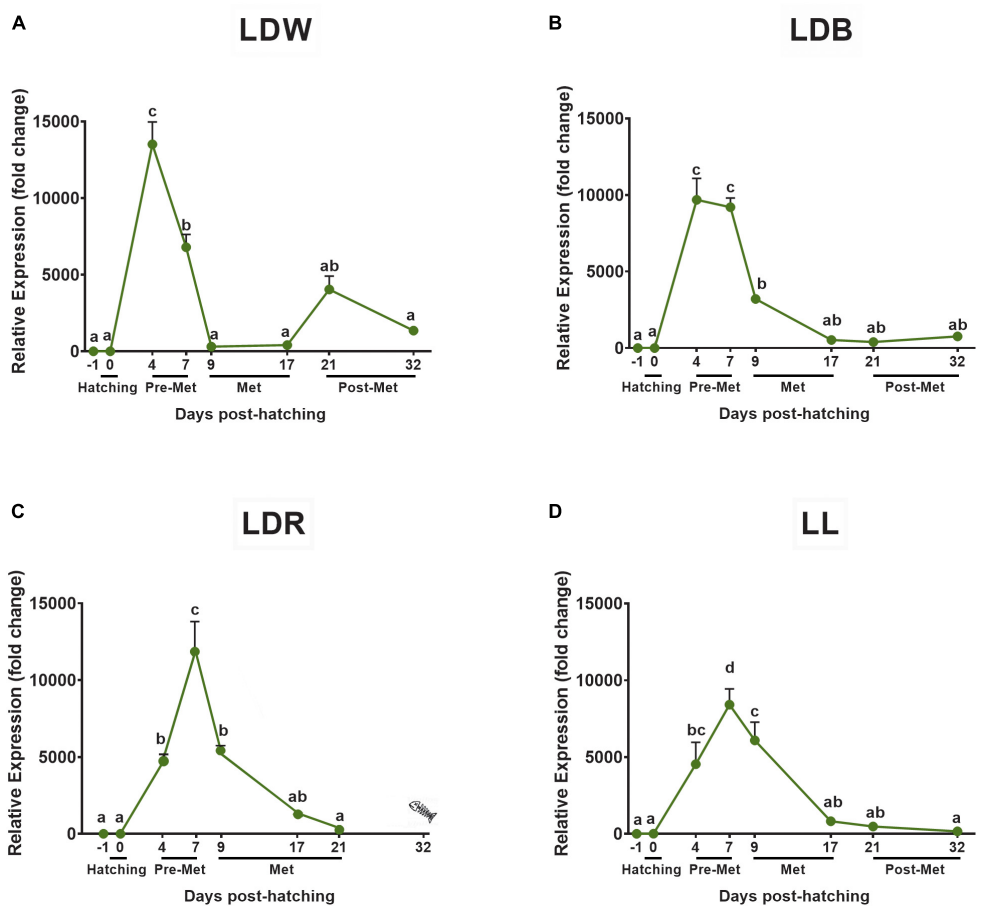


**FIGURE 8 |** Expression of green cone opsin (*rh2.4*) in embryos, larvae, and juveniles of the Senegalese sole on dph –1 (embryos), dph 0 (hatching), dph 4–7 (pre-metamorphosis, Pre-Met), dph 9–17 (metamorphosis, Met), and dph 21–32 (post-metamorphosis, Post-Met) analysed by RT-qPCR. For further information, see the legend in **Figure 1**.

light spectrum affected the peak in transcript levels of most of the visual opsins analysed. Overall, the ontogeny of visual opsin-expressing cells and intensity of the labelling present in the retina of the sole, as revealed by *in situ* hybridisation, provided very consistent results compared to the developmental pattern observed in the whole body by RT-qPCR, which suggests that retinal transcripts account for most visual opsin expressions in this species. These anatomical results also fit well with our previous study, showing that the Senegalese sole did not exhibit the characteristic highly ordered, lattice-like mosaics of other flatfish species (see **Figure 11L**), and confirming that the short-wavelength sensitive opsins (*sws1* and *sws2*) were expressed in single cones, whereas the middle wavelength (*rh2.4*)- and long wavelength (*lws*)-sensitive photopigments were present in double cones (Frau et al., 2020a). From a practical point of view, an important conclusion could be drawn, i.e., both the pre-metamorphosis (dph 4–7) and post-metamorphosis (dph 21–32) stages appear to represent two developmental windows with increased light sensitivity in the sole, as the number of transcript levels of molecules detecting photic stimuli is significantly higher. Therefore, extra care should be taken with the light protocols used when handling larvae and juveniles in these stages in aquaculture practise.

In this study, the expression of all the visual opsins analysed was detected already in sole embryos and larvae one day before hatching (dph –1) and at hatching (dph 0). Several studies have shown that many fish species present advanced eye development already at hatching (Evans and Browman, 2004). However, according to Bejarano-Escobar et al. (2010), new-born Senegalese sole larvae still have unpigmented and rudimentary eyes, consisting of just a neuroepithelial optic cup, similar to other flatfish species such as the turbot, *Psetta maxima,* and halibut, *Hippoglossus hippoglossus* (Kvenseth et al., 1996; De Miguel Villegas et al., 1997). On dph 3, the sole larval retina is not yet fully differentiated, although it might be able to sustain a limited visual function, being completely functional on dph

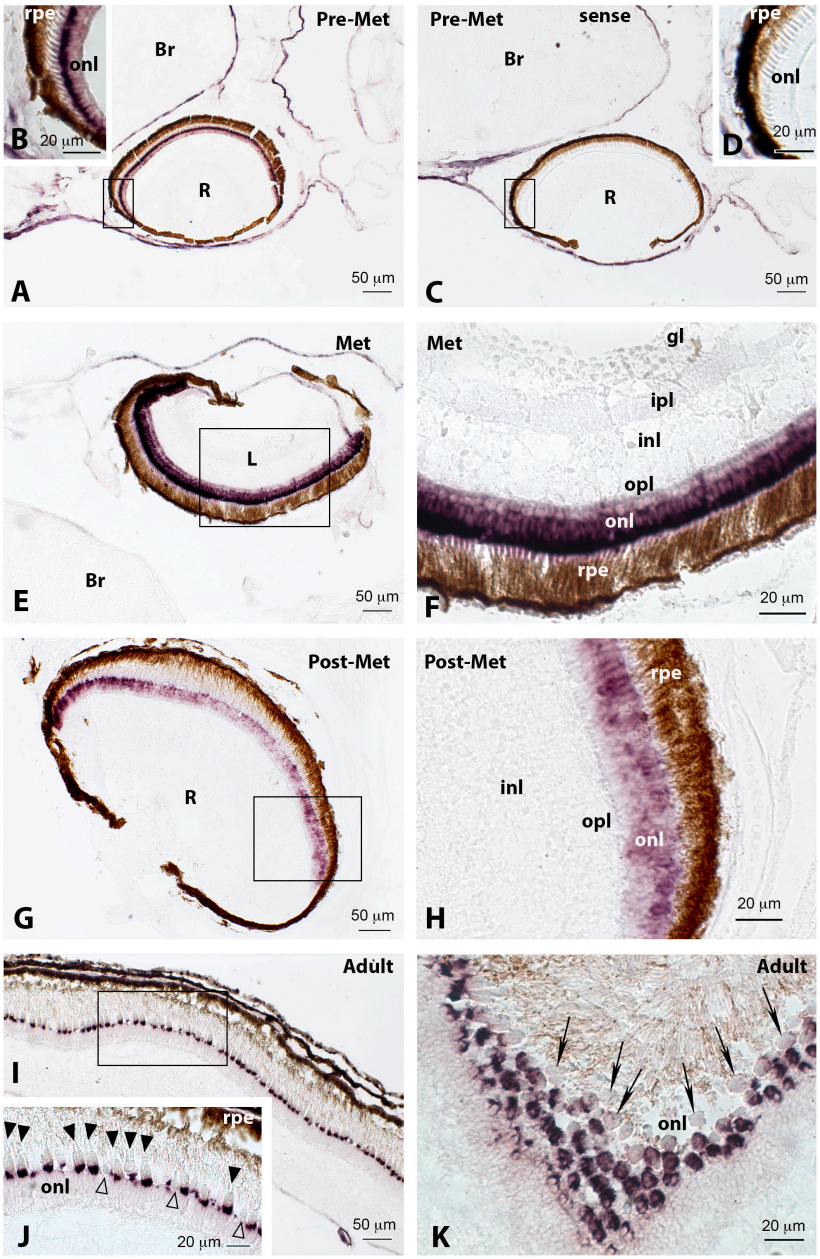


**FIGURE 9 |** Localisation of green cone opsin (*rh2.4*) expression in the retina of pre-metamorphic (Pre-Met; **A–D**), metamorphic (Met; **E,F**), post-metamorphic (Post-Met; **G,H**), and adult **(I–K)** Senegalese sole specimens revealed by *in situ* hybridisation. All the photomicrographs represent antisense sections, with the exception of panels **(C,D)**, which show sense control sections. Squares in panels **(A,C,E,G,I)** mark the areas magnified in photomicrographs **(B,D,F,H,J)**, respectively. Note the intense labelling in the retina of pre-metamorphic **(A)** and metamorphic **(E,F)** animals, compared to post-metamorphic **(G,H)** and adult **(I–K)** specimens. In the adult retina, *rh2.4* expression appears evident in the basal region of the inner segments of double cones (**J**, black arrowheads), with the single cones being devoid of labelling (**J**, white arrowheads). Some double cones appear unlabelled, as seen in photomicrograph **(K)** (black arrows). For abbreviations, see the legend in **Figure 2**. Scale bars represent 20 µm in panels **(B,D,F,H,J,K)**; and 50 µm in panels **(A,C,E,G,I)**.

4 (Bejarano-Escobar et al., 2010; Padrós et al., 2011; Sarasquete et al., 2019). Moreover, the pineal organ of the Senegalese sole, the other well-known photoreceptive structure, becomes differentiated 2 days post-fertilisation (corresponding to dph 1) (El M'Rabet et al., 2008; Isorna et al., 2009). Our results suggest that sole embryos and early-staged larvae could activate the molecular machinery to perceive lights of different wavelengths even before the complete differentiation and functionality of light-sensitive structures, and as soon as one day before hatching (dph –1). This is consistent with our previous study, where the expression of visual opsins was also detected very early during development on dph 0 (hatching) (Frau et al., 2020b). The early

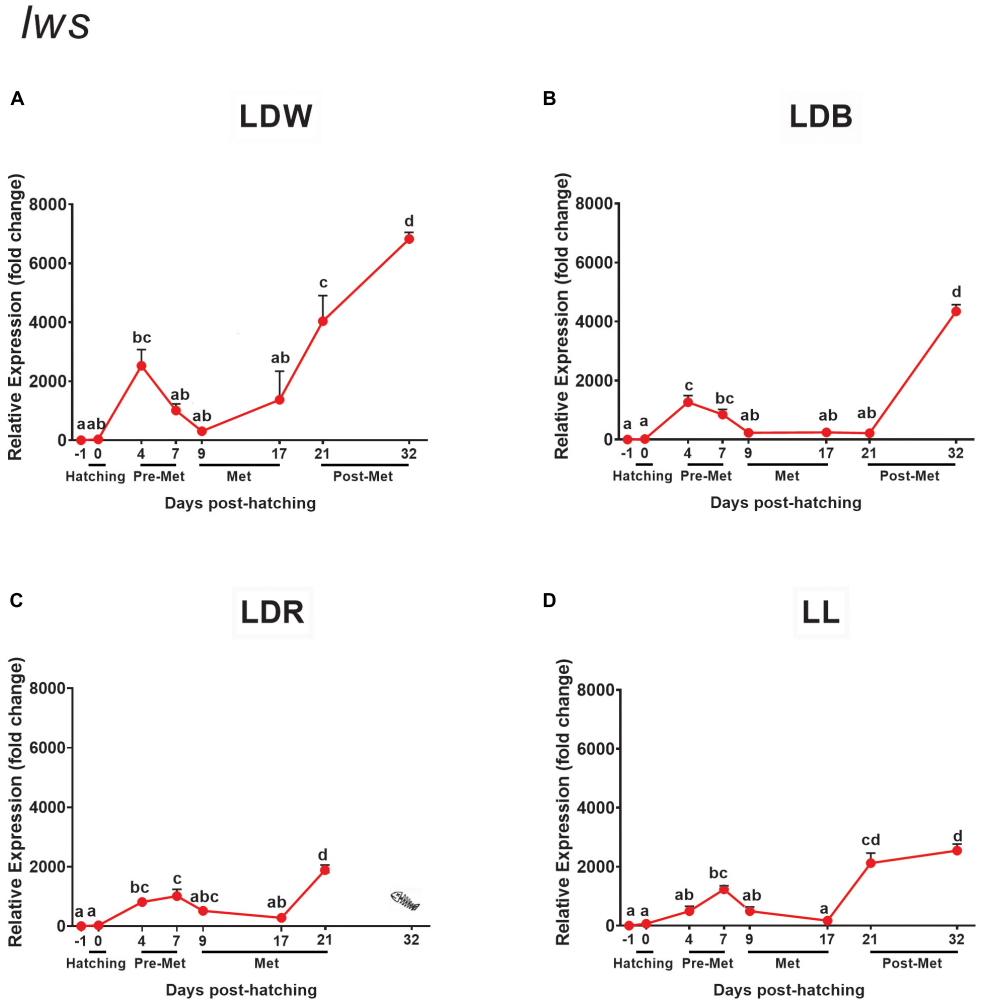


**FIGURE 10 |** Expression of red cone opsin (*lws*) in embryos, larvae, and juveniles of the Senegalese sole on dph –1 (embryos), dph 0 (hatching), dph 4–7 (pre-metamorphosis, Pre-Met), dph 9–17 (metamorphosis, Met), and dph 21–32 (post-metamorphosis, Post-Met) analysed by RT-qPCR. For further information, see the legend in **Figure 1**.

expression of visual opsins in sole embryos could also be related to direct light sensitivity at the cellular level. It is known that fish organs and fish-derived embryonic cell lines are sensitive to light (Whitmore et al., 2000; Tamai et al., 2005; Vergès-Castillo et al., 2021), and it has been recently shown that they express a wide number of opsin photopigments, which may support their ability to respond directly to photic stimuli (Davies et al., 2015; Steindal and Whitmore, 2020).

The increment in all visual opsin mRNA levels prior to metamorphosis (dph 4–7), when pelagic larvae are swimming in the upper part of the water column exposed to all wavelengths of incident light (**Figure 13**), coincides with the complete development of the retina, mouth opening, and onset of exogenous feeding in the sole (Bejarano-Escobar et al., 2010; Blanco-Vives et al., 2011; Padrós et al., 2011). This opsin expression could be mediating the light synchronisation of diverse rhythms (e.g., rhythms in the molecular clock, embryonic development, hatching, locomotor, and feeding activities) that appear very early during development in this and other fish species (Blanco-Vives et al., 2010, 2011, 2012; Martín-Robles et al., 2012; Villamizar et al., 2013; Rosa et al., 2015; Frau et al., 2020b). In fact, this increase in visual opsin transcript levels is concurrent with the complete organisation of molecular clock loops in sole larvae and climax of the expression of melatonin-synthesising enzymes *aanat1a* and *aanat2* at early ontogeny, thus contributing to the functionality and entraining of the sole circadian system in early stages (Isorna et al., 2009, 2011; Martín-Robles et al., 2012). The early expression of rod opsin (*rh1*) detected in the sole by both RT-qPCR and *in situ* hybridisation is in agreement with that described by Bejarano-Escobar et al. (2010) by immunohistochemistry using an antiserum against bovine rod opsin. However, it is in contrast with previous results reported on flatfish species and most teleosts, in which cones generally anticipate the formation of rods, and rod opsin expression is not detected in the retina in the pre-metamorphic stage, being evident only in the juvenile

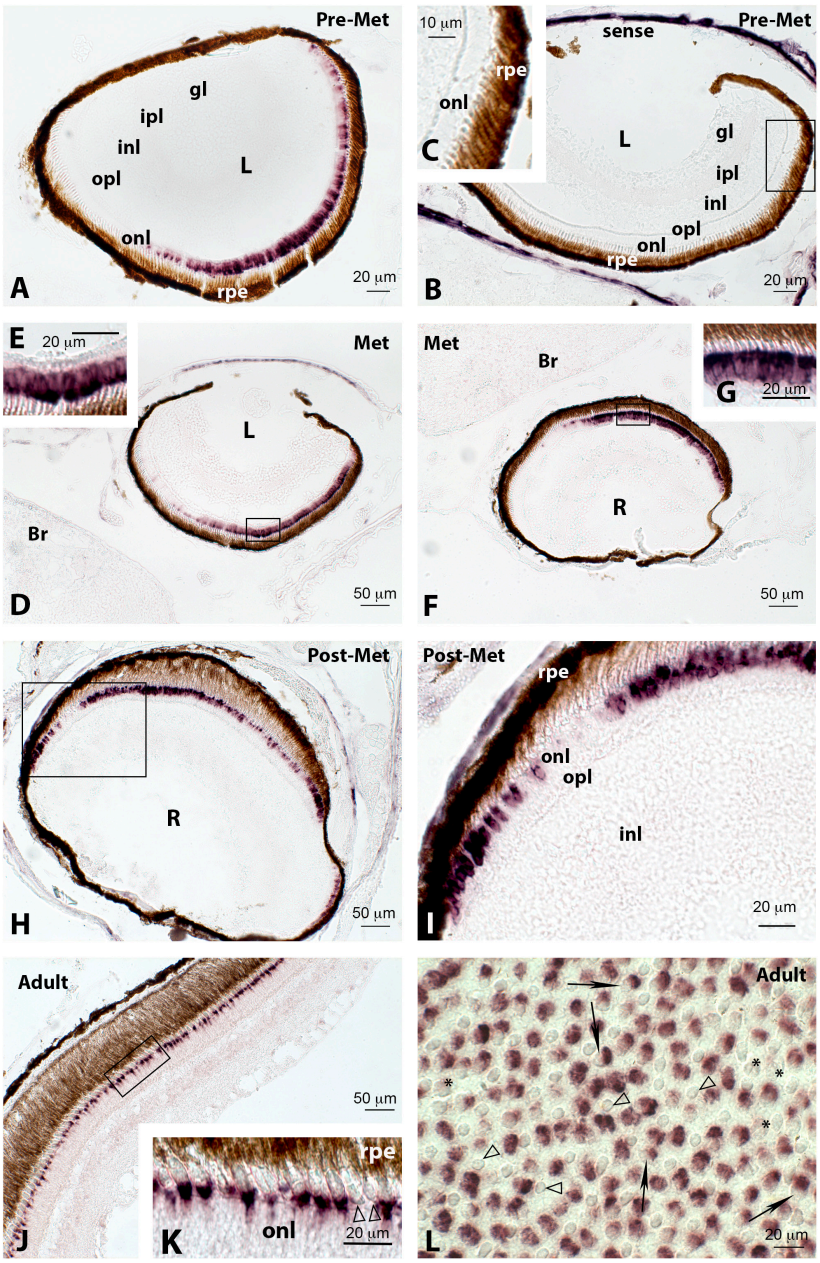


**FIGURE 11 |** Localisation of red cone opsin (*lws*) expression in the retina of pre-metamorphic (Pre-Met; **A–C**), metamorphic (Met; **D–G**), post-metamorphic (Post-Met; **H,I**), and adult **(J–L)** Senegalese sole specimens revealed by *in situ* hybridisation. All the photomicrographs represent antisense sections, with the exception of panels **(B,C)**, which show sense control sections. Squares in panels **(B,D,F,H,J)** mark the areas magnified in photomicrographs **(C,E,G,I,K)**, respectively. Note that some parts of the retina (dorsal margin) appear devoid of labelling in pre-metamorphic **(A)** and metamorphic **(D,F)** specimens, both in the left and right retinas. Positive red opsin-expressing cells become evident in the dorsal retina of post-metamorphic animals **(H,I)**. In the adult retina, this expression is evident in double cones, with smaller single cones being devoid of labelling (**K,L**, white arrowheads). Some double cones appear unlabelled (**L**, asterisks) while others only exhibit one of the pairs labelled (**L**, black arrows). All pictures corresponded to radial sections, with the exception of **(L)** that represents a tangential section. For abbreviations, see the legend in **Figure 2**. Scale bars represent 10 μm in panel **(C)**; 20 μm in panels **(A,B,E,G,I,K,L)**; and 50 μm in panels **(D,F,H,J)**.

phase (Evans et al., 1993; Helvik et al., 2001a,b; Mader and Cameron, 2004). Strong overexpression of the rod opsin (7-fold increase) was also identified in common sole (*Solea solea* L.) larvae from hatching to dph 4 in a transcriptomic study (Ferraresso et al., 2013). During this period, flatfish larvae actively feed, and the developmental process is at its highest rate, with maximum growth rates (Ribeiro et al., 1999; Fernández-Díaz et al., 2001). As vision plays an important role in prey detection and feeding in fish larvae (Blaxter, 1969; Govoni et al., 1986; Falk-Petersen, 2005), increased levels of visual opsin transcripts could

contribute to enhancing light sensitivity for foraging behaviour and active feeding and contribute to predator avoidance during this critical period.

On the contrary, flatfish metamorphosis, a highly energy-demanding process, is characterised by a significant decrease in growth, energy content, and feeding rates. Metamorphic specimens have to rely on stored reserves, reducing their growth performance (Yúfera et al., 1999; Fernández-Díaz et al., 2001; Cañavate et al., 2006; Geffen et al., 2007). In addition, sole metamorphosis is associated with shift in swimming duration, prey attack rate, and capture success rate from diurnal to nocturnal (Blanco-Vives et al., 2012), which could be associated with the remodelling in photoreceptors and changes in visual acuity and sensitivity to adapt to new lighting environment. Consistent with these facts, we have observed a significant downregulation of all the visual opsins analysed during this period. Decreasing expression levels of clock genes, melatonin-synthesising enzymes (*aanat1* and *aanat2*), and melatonin receptors (*mt1* and *mt2*) have also been described during metamorphosis (Isorna et al., 2009, 2011; Martín-Robles et al., 2013; Lan-Chow-Wing et al., 2014), as well as a transient lost in clock genes and visual opsin rhythms (Martín-Robles et al., 2012; Frau et al., 2020b). Therefore, the input, clock, and output elements of the circadian systems appear to work at a lower rate and reorganise during metamorphosis.

As mentioned above, visual opsins significantly rose again in post-metamorphic specimens, excluding the green opsins *rh2.3* and *rh2.4* that remain at low levels at these ages. In this stage, eye migration and metamorphosis are completed, and asymmetrical juveniles have already started their benthic life (Fernández-Díaz et al., 2001; Blanco-Vives et al., 2012). Active feeding restarts again in sole juveniles, and a complete repertoire of visual opsins would be beneficial to detect prey. In fish, it has been demonstrated that the UV cone opsin (*sws1*) enhanced foraging performance (Novales Flamarique, 2013). The Senegalese sole feed mostly on small, bottom-dwelling invertebrates, and the increase in *sws1* expression could help to improve the catching and intake rates of prey as an adaptation to the new environment.

Although we found a conspicuous *rh1* expression in the Senegalese sole at pre-metamorphosis, a significant increase was evident in all the experimental groups after metamorphosis. In this sense, a proliferation of rods in fish has been shown as essential for the capacity to see under dim light (Evans and Browman, 2004; Musilova et al., 2019). Matsuda et al. (2008) made a comparison among three flatfish species of different ecotypes, and they found that a nocturnal fish, the pointhead flounder (*Hippoglossoides pinetorum*), has higher rod density in the outer nuclear layer than either slime flounder (*Microstomus achne*) or red halibut (*Hippoglossoides dubius*), which are both diurnal fishes. A correlation between a high proportion of rods and reduced light environment conditions was also reported in eels. Epipelagic freshwater eel possesses *rh2* and *sws2* cones; however, when it goes through metamorphosis and becomes deep-sea eel, the vision becomes rod-based in the new scotopic environment, and cones are almost lost (Bowmaker et al., 2008). In the half-smooth tongue sole, *Cynoglossus semilaevis*, transcript levels of rod pigment (*rh1*) were also significantly higher in benthic stages when compared to pelagic specimens (Chen et al., 2014). Accordingly, our *in situ* hybridisation study showed a progressive increase in the number of *rh1*-labelled cells and in the intensity of labelling in the outer nuclear layer of the retina from pelagic pre-metamorphic larvae to benthic post-metamorphic juveniles, with rods being the most abundant photoreceptors in the retina of the adult sole (see **Figure 12**).

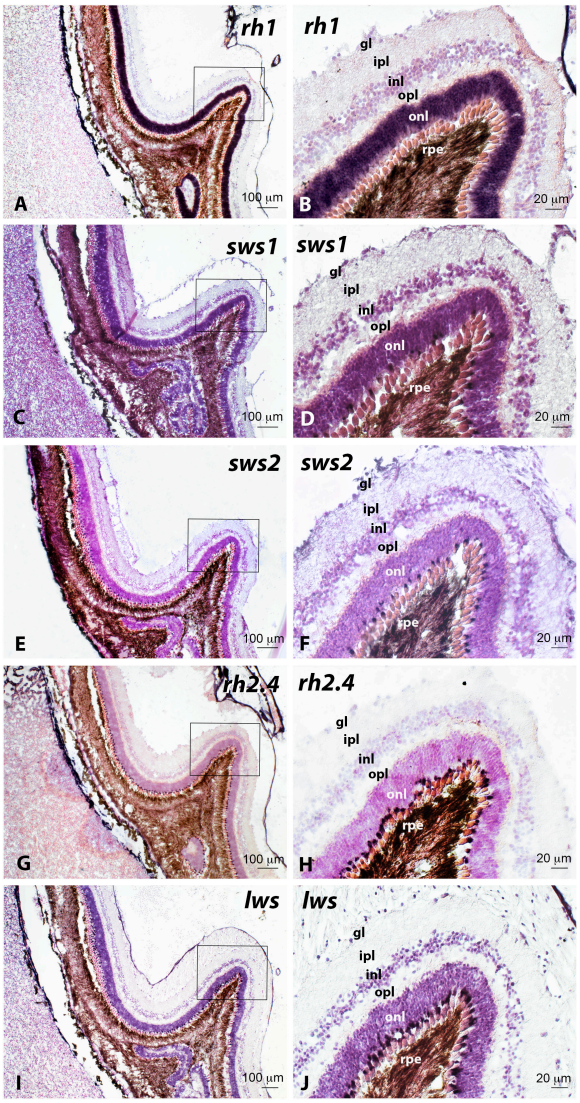


**FIGURE 12 |** Localisation of rod (*rh1*; **A,B**), ultraviolet cone (*sws1*; **C,D**), blue cone (*sws2*; **E,F**), green cone (*rh2.4*; **G,H**) and red cone (*lws*; **I,J**) opsin-expressing cells in serial haematoxylin-eosin stained sections of the retina of adult Senegalese sole specimens revealed by *in situ* hybridisation. All the photomicrographs represent antisense sections. Squares in panels **(A,C,E,G,I)** mark the areas magnified in photomicrographs **(B,D,F,H,J)**, respectively. Note the presence of abundant *rh1*-positive cells in the outer nuclear layer (onl, **A,B**), important amount of *rh2.4*- **(G,H)**, and *lws*- **(I,J)** expressing cells and lower number of *sws1*- **(C,D)** and *sws2*- **(E,F)** expressing cells in the retina of adult specimens. For other abbreviations, see the legend in **Figure 2**. Scale bars represent 20 µm in panels **(B,D,F,H,J)**; and 100 µm in panels **(A,C,E,G,I)**.

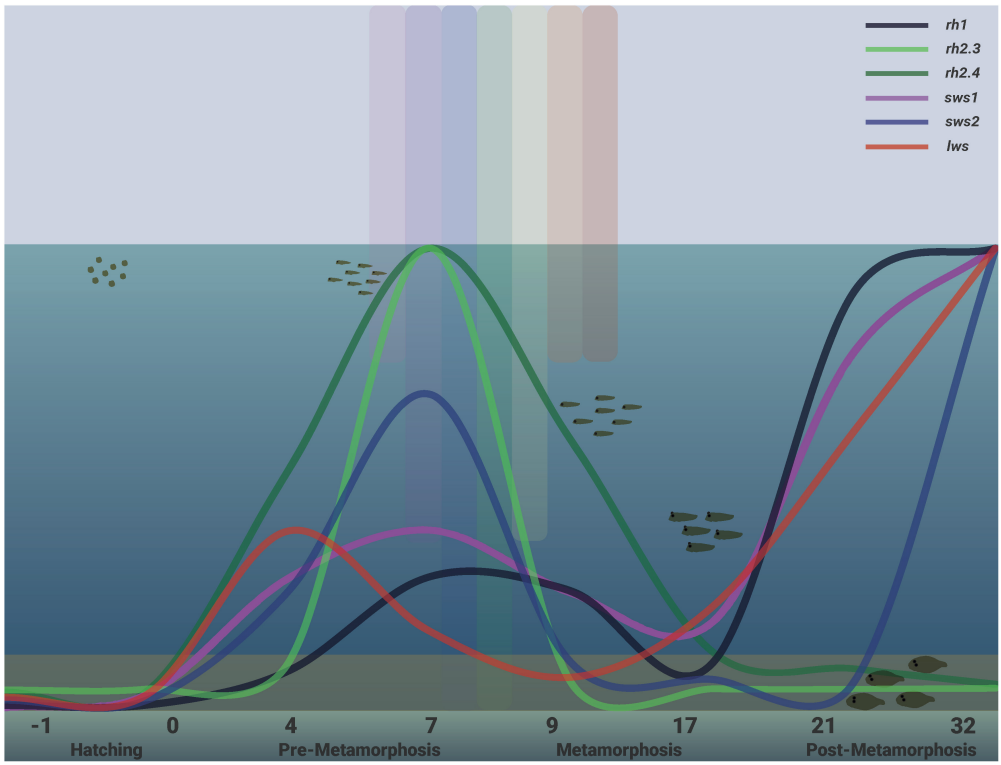


**FIGURE 13 |** Summary of the profile of visual opsins for *rh1, sws1, sws2, rh2.3, rh2.4, and lws* transcript levels obtained in this study in developing sole. This figure does not intend to compare expression levels among different opsins but the ontogenetic expression pattern for each visual photopigment. All the visual opsins exhibited early increase in expression during pre-metamorphosis and subsequent decrease in transcript levels during metamorphosis. Note how *rh2.3* and *rh2.4* green opsin expressions remain at low levels in post-metamorphic juvenile specimens. On the contrary, at this moment, all the other opsin transcript levels increase considerably. The different stages of Senegalese sole development analysed in this study by RT-qPCR are shown in this Figure (hatching, pre-metamorphosis, metamorphosis, and post-metamorphosis), indicating the position that specimens occupy in the water column in each stage. The differential penetration of lights of the visible spectrum into the ocean water column is also represented. Longer wavelengths, such as red light, are the first to be completely absorbed while shorter and medium wavelengths, such as blue and green lights, penetrate deeper. Eggs, embryos, and early larvae of the Senegalese sole live in the upper part of the water column, thus receiving irradiation that contains all wavelengths present in sun light. During metamorphosis, they start to migrate vertically to the bottom, receiving fewer wavelengths; finally, after the completion of the metamorphic process, they live in the seabed in an environment dominated by green and blue lights.

Together with blue light, green wavelengths penetrate deeply into the water column. Fish species tend to possess visual pigments that are related to the most abundant wavelengths (Douglas et al., 2003). In this sense, the significant increase in *sws2* observed in the post-metamorphic sole could contribute to perceiving blue lights reaching these benthic habitats. However, for the same reason, the sole was expected to have high levels of green sensitive opsins after metamorphosis. Surprisingly, whereas all other opsins increased their expression after completion of the metamorphic process, the downregulation of green opsins detected during metamorphosis was maintained in early post-metamorphic juveniles for *rh2.4*, and especially for *rh2.3*, which was barely detected in this stage. It is interesting to note that the expression of the middle-wavelength sensitive pigment gene (*rh2*) in the half-smooth tongue sole was also significantly higher in pelagic larvae compared to benthic juveniles (Chen et al., 2014). Whether another type of middle-wavelength-sensitive opsin could be activated in the sole after this drop in *rh2.3* and *rh2.4* expression remains to be elucidated, because up to eight rhodopsin-like 2 (*rh2*) genes have been described in teleosts (Carleton et al., 2020; Musilova et al., 2021). Ontogenetic chromophore switches have been reported previously in the literature. Thus, Cheng et al. (2009) described widely the shift that occurs in salmons from *sws1* to *sws2a* when they change from larvae to juvenile life stages. Further investigation performing HPLC analysis on different opsins before and after metamorphosis, and even during older juvenile and adult stages, is needed to test this hypothesis on the Senegalese sole. Nevertheless, a conspicuous expression of *rh2.3* and *rh2.4* was evident in the retina of older juvenile Senegalese sole specimens (180–250 days old; i.e., over 5 months after metamorphosis), and two middle-wavelength-sensitive visual pigments (λmax 523 and 536 nm, respectively) were found by microspectrophotometry in the juvenile retina of a closely related species living in the same habitats, the common sole *Solea solea* (Frau et al., 2020a). Therefore, the downregulation of green opsins observed during metamorphosis and in early post-metamorphic juveniles could represent a transient event in Senegalese sole life cycle. In fact, *in situ* hybridisation analysis performed on the retina of the 2-year-old adult sole (present

study) revealed the presence of an important number of intensely labelled *rh2.4*-expressing cells (see **Figure 12** for comparison with other opsins). The high proportion of M-type cones present in the retina of the juvenile and adult soles is consistent with the fact that middle- rather than short-wavelengths are preferentially transmitted in turbid coastal waters (Jerlov, 1968), where the sole inhabits in these older stages. The cone mosaic without a lattice-like structure found in the sole, with packing significantly greater than that found in other flatfish species (Frau et al., 2020a), appears suitable for life in these low-light environments. In any case, metamorphosis in the Senegalese sole is also associated with a shift from cone opsin- to rod opsin-dominated vision, which is characterised by higher sensitivity but lower spatial and temporal resolutions (Ebrey and Koutalos, 2001). Thus, as revealed in our laboratory, rod opsin transcript levels were high in the retina of the juvenile sole (present study, Frau et al., 2020a), and rod opsin-expressing cells were the most abundant photoreceptors in the retina of post-metamorphic and adult animals (present study). Interestingly, in a previous microspectrophotometry analysis (Frau et al., 2020a), we identified the presence of a rod visual photopigment in the retina of a juvenile common sole with λmax of 511 nm, which is close to the wavelengths of maximum absorbance of the two visual pigments measured in the outer segment of green cone opsin photoreceptors (λmax nm and 536 nm). Therefore, rod opsin photopigments could be sensing green wavelengths reaching the seabed until green cone opsins are up-regulated again.

In turn, we could expect a severe downregulation of red-sensitive opsins after metamorphosis, as the red colour absorbance at the bottom of the seabed appears to be negligible (**Figure 13**). However, we detected an up-regulation of *lws* transcript levels in the post-metamorphic sole, in particular, under LDW and LDB regimes. This result was confirmed anatomically in the retina of the sole by our *in situ* hybridisation study, in which we detected an important number of red opsin-expressing cells in double cones of the post-metamorphic and adult sole. Furthermore, microspectrophotometry absorbance measurements from individual photoreceptors of the juvenile common sole revealed the existence of a long-wavelength-sensitive visual pigment with λ peak of 559 nm and bandwidth from 490 to 640 nm (Frau et al., 2020a). According to our results, the expression of long-wavelength-sensitive opsin *lws1* in tongue sole was higher in the benthic animals than in the pelagic specimens (Chen et al., 2014). In a recent study by Chang and Yan (2019), the red shiner (*Cyprinella lutrensis*) was exposed to four water turbidity treatments. Turbid waters often create red light-abundant surroundings (Doxaran et al., 2002) and, accordingly, an elevated proportional expression of *lws* in the cone was observed, indicating that the visual spectrum of the red shiner displays a redshift in response to increased turbidity (Chang and Yan, 2019). The guppy (*Poecilia reticulata*) also has higher proportional and relative *lws* opsin expression when it is reared in turbid waters (Ehlman et al., 2015). All these considerations are particularly important considering that post-metamorphic *Solea senegalensis* lives in a low-light environment strongly influenced by turbidity, which could support the increased expression of red-sensitive opsins to adapt to the new environment. Alternatively, these red-sensitive opsins could play a role in perceiving long wavelengths when sole specimens experience vertical migrations in the water column at dawn and dusk, and/or perceiving nocturnal moonlight, aspects that will require further investigation in the future. In any case, stimulation of these red-sensitive opsins alone does not seem to be sufficient to guarantee the optimal development of the sole, because, as shown in this and previous studies (Blanco-Vives et al., 2011, 2012; Frau et al., 2020b), animals reared under LDR conditions exhibited impaired hatching, feeding performance and foraging behaviour, delayed development and lower growth, and less robust visual opsin rhythms, dying before the completion of metamorphosis.

Interestingly, the expression pattern of most of the visual opsins during sole ontogeny exhibited an inverse correlation with developmental levels of thyroid hormones (THs), which sharply increase at the beginning of metamorphosis and reach maximum at the metamorphic climax, and decrease progressively until post-metamorphosis (Klaren et al., 2008; Isorna et al., 2009). THs and their receptors are widely described in the literature to be responsible for changes at all levels of metamorphic animals. They also regulate cell migration, neuronal differentiation, and alter profoundly the visual system, and are crucial for optimal maturation of the retina (Mader and Cameron, 2006; Galay-Burgos et al., 2008; Cheng et al., 2009). Cheng et al. (2009) investigated the role of THs in triggering opsin remodelling and demonstrated that THs are responsible for the depopulation of UV cones by inducing a UV-to-blue opsin switch in the retina of juvenile salmonid fishes, as occurs during natural development. Taken together, these results suggest that THs could be modulating the repertoire of visual opsins and their plastic changes in the sole during development. Further studies on *Solea senegalensis* larvae treated with THs and/or THs antagonists during metamorphosis could give us valuable information to understand this possible correlation.

In this study, we also found significant effects of the light spectrum and photoperiod on modulating the ontogenetic expression of visual opsins, with blue (for *sws1* and *rh2.3*) and white (for *rh1*, *sws2*, *rh2.4,* and *lws*) light-dark cycles producing the highest peaks in their transcript levels. In previous studies, we showed that LD cycles of blue and white lights represented optimal photic conditions for the proper development of biological functions and behaviour of sole larvae (Blanco-Vives et al., 2011, 2012). In agreement with these results, LD cycles of blue and white lights also constituted the best light regimes for visual opsin development. The improved performance in these light regimes harmonises well with the natural adaptation of sole larvae and juveniles to blue-green dominated light environments in their natural ecosystem. A study by Sierra-Flores et al. (2016) on cod and turbot larvae also showed improved growth and survival under blue/green light compared to red light. This aspect is also highlighted in a review by Villamizar et al. (2011) describing how European sea bass, *Dicentrarchus labrax,* and sole larvae achieved the best performance and showed the fastest development and lowest degree of deformity using blue light/dark cycles. Our present and previous results, evidencing that the early development of Senegalese sole embryos and larvae is strongly affected by

light characteristics, reinforce the assumption that both light photoperiod and spectrum should be taken into account in sole rearing for the proper development of the visual opsin system.

## CONCLUSION

In conclusion, this study provides novel results showing how visual opsin transcript levels change during Senegalese sole ontogeny depending on developmental stages and light regimes. These changes appear to be modulated by environmental, hormonal, and genetic factors. We found common trends in the expression patterns of most of the opsins analysed, with significant increases during pre-metamorphosis and after metamorphosis. Although the visual system remains functional, downregulation of all the opsins was detected during the metamorphic process. The results obtained reveal that green-cone opsins represent the most abundant photopigments in the pre-metamorphic stage, declining thereafter, with rod opsin (sensitive to light in the blue-green spectrum) being the dominant visual photopigment from the completion of metamorphosis onwards. Together with previous results, the data obtained in this study could be of basic interest for better knowledge of the metamorphic process and development of the visual system of *Solea senegalensis* and could also contribute to more efficient rearing of embryos, larvae, and juveniles of this species in the aquaculture industry. The present results reinforce those obtained in previous studies showing the benefits of using blue/green lights as an alternative to white lights in sole rearing protocols in the early stages. At present, LED technologies permit to adapt the lighting protocols in fish aquaculture to those encountered by the animals in the natural environment in different stages of development, which could contribute to the adequate development of their visual opsins repertoire and improve considerably animal welfare and production.

## DATA AVAILABILITY STATEMENT

The original contributions presented in the study are included in the article/**Supplementary Material**. Further inquiries can be directed to the corresponding author/s.

## ETHICS STATEMENT

The animal study was reviewed and approved by the Ethics Committee of the University of Cádiz and the General Directorate for Agricultural and Livestock Production of the Regional Government of Andalusia, Spain (Approval Number 15/12/2020/142).

## AUTHOR CONTRIBUTIONS

JAM-C and ÁJM-R contributed to the conception of the study. SF and JAP-S performed the experiments and data analysis with the help of IP and MEC. SF, JAP-S, ÁJM-R, and JAM-C wrote the manuscript. All authors contributed to the article and approved the submitted version.

## FUNDING

This work was funded by a grant from the Spanish Ministry of Science, Innovation and Universities (AGL2017-82582-C3-1-R) to JAM-C. SF was a FPI fellow funded by the CEIMAR at UCA. MEC was a recipient of a Marie Curie contract from the UE (FP7/2007-2013, Grant No. 331964).

## ACKNOWLEDGMENTS

We would like to thank the staff from the "Planta de Cultivos Marinos" (University of Cádiz) for their help in the husbandry of the experimental animals in this developmental study. We also thank M. Manchado for the helpful assistance with sole opsin sequences.

## SUPPLEMENTARY MATERIAL

The Supplementary Material for this article can be found online at: https://www.frontiersin.org/articles/10.3389/fmars.2022.797507/full#supplementary-material

## REFERENCES

Bejarano-Escobar, R., Blasco, M., DeGrip, W. J., Oyola-Velasco, J. A., Martín-Partido, G., and Francisco-Morcillo, J. (2010). Eye development and retinal differentiation in an altricial fish species, the Senegalese sole (*Solea senegalensis*, Kaup 1858). *J. Exp. Zool. B, Mol. Dev. Evol.* 314, 580–605. doi: 10.1002/jez.b.21363

Blanco-Vives, B., Aliaga-Guerrero, M., Cañavate, J. P., García-Mateos, G., Martín-Robles, A. J., Herrera-Pérez, P., et al. (2012). Metamorphosis induces a light-dependent switch in Senegalese sole (*Solea senegalensis*) from diurnal to nocturnal behavior. *J. Biol. Rhythms.* 27, 135–144. doi: 10.1177/0748730411435303

Blanco-Vives, B., Aliaga-Guerrero, M., Cañavate, J. P., Muñoz-Cueto, J. A., and Sánchez-Vázquez, F. J. (2011). Does lighting manipulation during incubation affect hatching rhythms and early development of sole? *Chronobiol. Int.* 28, 300–306. doi: 10.3109/07420528.2011.560316

Blanco-Vives, B., Villamizar, N., Ramos, J., Bayarri, M. J., Chereguini, O., and Sánchez-Vázquez, F. J. (2010). Effect of daily thermo- and photo-cycles of different light spectrum on the development of Senegal sole (*Solea senegalensis*) larvae. *Aquaculture* 306, 137–145.

Blaxter, J. H. S. (1969). Visual thresholds and spectral sensitivity of flatfish larvae. *J. Exp. Biol.* 51, 221–230. doi: 10.1242/jeb.51.1.221

Bowmaker, J. K., Semo, M., Hunt, D. M., and Jeffery, G. (2008). Eel visual pigments revisited: the fate of retinal cones during metamorphosis. *Vis. Neurosci.* 25, 249–255. doi: 10.1017/S0952523808080152

Campinho, M. A. (2019). Teleost metamorphosis: the role of thyroid hormone. *Front. Endocrinol.* 10:383. doi: 10.3389/fendo.2019.00383

Cañavate, J. P., Zerolo, R., and Fernández-Díaz, C. (2006). Feeding and development of Senegal sole (*Solea senegalensis*) larvae reared in different photoperiods. *Aquaculture* 258, 368–377.

Carleton, K. L., Escobar-Camacho, D., Stieb, S. M., Cortesi, F., and Marshall, N. J. (2020). Seeing the rainbow: mechanisms underlying spectral sensitivity

in teleost fishes. *J. Exp. Biol.* 223(Pt 8):jeb193334. doi: 10.1242/jeb.193334

Chang, C.-H., and Yan, H. Y. (2019). Plasticity of opsin gene expression in the adult red shiner (Cyprinellalutrensis) in response to turbid habitats. *PLoS One* 14:e0215376. doi: 10.1371/journal.pone.0215376

Chen, S., Zhang, G., Shao, C., Huang, Q., Liu, G., Zhang, P., et al. (2014). Whole-genome sequence of a flatfish provides insights into ZW sex chromosome evolution and adaptation to a benthic lifestyle. *Nat. Genet.* 46, 253–260. doi: 10.1038/ng.2890

Cheng, C. L., and Novales Flamarique, I. (2004). Opsin expression: new mechanism for modulating colour vision. *Nature* 428:279. doi: 10.1038/428279a

Cheng, C. L., Gan, K. J., and Flamarique, I. N. (2009). Thyroid hormone induces a time-dependent opsin switch in the retina of salmonid fishes. *Invest. Ophthalmol. Vis. Sci.* 50, 3024–3032. doi: 10.1167/iovs.08-2713

Davies, W. I. L., Tamai, T. K., Zheng, L., Fu, J. K., Rihel, J., Foster, R. G., et al. (2015). An extended family of novel vertebrate photopigments is widely expressed and displays a diversity of function. *Genome Res.* 25, 1666–1679. doi: 10.1101/gr.189886.115

De Miguel Villegas, E., Dans, M. J. D., Paz-Andrade Castillo, C., and Alvarez, R. A. (1997). Development of the eye in the turbot Psetta maxima (Teleosti) from hatching through metamorphosis. *J. Morphol.* 233, 31–42. doi: 10.1002/(SICI)1097-4687(199707)233:1<31::AID-JMOR3>3.0.CO;2-R

Douglas, R. H., Hunt, D. M., and Bowmaker, J. K. (2003). "Spectral sensitivity tuning in the deep-sea," in *Sensory Processing in Aquatic Environments*, eds S. P. Collin and N. J. Marshall (New York, NY: Springer), 323–342.

Doxaran, D., Froidefond, J.-M., and Castaing, P. (2002). A reflectance band ratio used to estimate suspended matter concentrations in sediment-dominated coastal waters. *Int. J. Remote Sensing* 23, 5079–5085.

Dufour, S., Rousseau, K., and Kapoor, B. G. (2012). *Metamorphosis in Fish*. Boca Raton, FL: CRC Press.

Ebrey, T., and Koutalos, Y. (2001). Vertebrate photoreceptors. *Prog. Retin. Eye Res.* 20, 49–91.

Ehlman, S. M., Sandkam, B. A., Breden, F., and Sih, A. (2015). Developmental plasticity in vision and behavior may help guppies overcome increased turbidity. *J. Comp. Physiol. A Neuroethol. Sens. Neural. Behav. Physiol.* 201, 1125–1135. doi: 10.1007/s00359-015-1041-4

El M'Rabet, A., Confente, F., Ouarour, A., and Muñoz-Cueto, J. A. (2008). "Ontogenia del órgano pineal del lenguado, Solea senegalensis", in *Avances en Endocrinología Comparada*, eds J.A. Muñoz-Cueto, J.M. Mancera, G. Martínez. (Cádiz: Servicio de Publicaciones de la Universidad de Cádiz), 4, 179–181.

Evans, B. I., and Fernald, R. D. (1990). Metamorphosis and fish vision. *J. Neurobiol.* 21, 1037–1052. doi: 10.1002/neu.480210709

Evans, B. I., Hárosi, F. I., and Fernald, R. D. (1993). Photoreceptor spectral absorbance in larval and adult winter flounder (*Pseudopleuronectes americanus*). *Vis. Neurosci.* 10, 1065–1071. doi: 10.1017/s0952523800010178

Evans, B., and Browman, H. (2004). Variation in the development of the fish retina. *Am. Fish. Soc. Symp.* 40, 145–166.

Falk-Petersen, I. B. (2005). Comparative organ differentiation during early life stages of marine fish. *Fish Shellfish Immunol.* 19, 397–412. doi: 10.1016/j.fsi.2005.03.006

Fernández-Díaz, C., Yúfera, M., Cañavate, J. P., Moyano, F. J., Alarcón, F. J., and Díaz, M. (2001). Growth and physiological changes during metamorphosis of Senegal sole reared in the laboratory. *J. Fish Biol.* 58, 1086–1097. doi: 10.1111/j.1095-8649.2001.tb00557.x

Ferraresso, S., Bonaldo, A., Parma, L., Cinotti, S., Massi, P., Bargelloni, L., et al. (2013). Exploring the larval transcriptome of the common sole (*Solea solea* L.). *BMC Genomics* 14:315. doi: 10.1186/1471-2164-14-315

Frau, S., Flamarique, I. N., Keeley, P. W., Reese, B. E., and Muñoz-Cueto, J. A. (2020a). Straying from the flatfish retinal plan: cone photoreceptor patterning in the common sole (*Solea solea*) and the Senegalese sole (*Solea senegalensis*). *J. Comp. Neurol.* 528, 2283–2307. doi: 10.1002/cne.24893

Frau, S., Loentgen, G., Martín-Robles, ÁJ., and Muñoz-Cueto, J. A. (2020b). Ontogenetic expression rhythms of visual opsins in Senegalese sole are modulated by photoperiod and light spectrum. *J. Comp. Physiol. B.* 190, 185–204. doi: 10.1007/s00360-020-01264-7

Galay-Burgos, M., Power, D. M., Llewellyn, L., and Sweeney, G. E. (2008). Thyroid hormone receptor expression during metamorphosis of Atlantic halibut (*Hippoglossushippoglossus*). *Mol. Cell. Endocrinol.* 281, 56–63.

Geffen, A. J., van der Veer, H. W., and Nash, R. D. M. (2007). The cost of metamorphosis in flatfishes. *J. Sea Res.* 58, 35–45. doi: 10.1016/j.seares.2007.02.004

Govoni, J. J., Boehlert, G. W., and Watanabe, Y. (1986). The physiology of digestion in fish larvae. *Environ. Biol. Fish.* 16, 59–77. doi: 10.1007/bf00005160

Helvik, J. V., Drivenes, Ø, Harboe, T., and Seo, H.-C. (2001a). Topography of different photoreceptor cell types in the larval retina of Atlantic halibut (*Hippoglossus hippoglossus*). *J. Exp. Biol.* 204, 2553–2559.

Helvik, J. V., Drivenes, Ø, Næss, T. H., Fjose, A., and Seo, H.-C. (2001b). Molecular cloning and characterization of five opsin genes from the marine flatfish Atlantic halibut (*Hippoglossus hippoglossus*). *Vis. Neurosci.* 18, 767–780. doi: 10.1017/s095252380118510x

Hoke, K. L., Evans, B. I., and Fernald, R. D. (2006). Remodeling of the cone photoreceptor mosaic during metamorphosis of flounder (*Pseudopleuronectes americanus*). *Brain Behav. Evol.* 68, 241–254. doi: 10.1159/000094705

Howell, B. R., and Dinis, M. T. (2019). "An overview of soleid (*Pleuronectiformes*) fisheries and aquaculture," in *The Biology of Sole*, eds J. A. Muñoz-Cueto, E. L. Mañanos-Sánchez, and F. J. Sánchez-Vázquez (Boca Raton, FL: CRC Press, Taylor & Francis Group), 3–22.

Infante, C., Matsuoka, M. P., Asensio, E., Cañavate, J. P., Reith, M., and Manchado, M. (2008). Selection of housekeeping genes for gene expression studies in larvae from flatfish using real-time PCR. *BMC Mol. Biol.* 9:28. doi: 10.1186/1471-2199-9-28

Isorna, E., Aliaga-Guerrero, M., M'Rabet, A. E., Servili, A., Falcón, J., and Muñoz-Cueto, J. A. (2011). Identification of two arylalkylamine N-acetyltranferase 1 genes with different developmental expression profiles in the flatfish Solea senegalensis. *J. Pineal Res.* 51, 434–444. doi: 10.1111/j.1600-079X.2011.00907.x

Isorna, E., M'Rabet, A. E., Confente, F., Falcón, J., and Muñoz-Cueto, J. A. (2009). Cloning and expression of arylalkylamine N-acetyltranferase-2 during early development and metamorphosis in the sole Solea senegalensis. *Gen. Comp. Endocrinol.* 161, 97–102. doi: 10.1016/j.ygcen.2008.10.007

Iwanicki, T. W., Flamarique, I. N., Ausiü, J., Morris, E., and Taylor, J. S. (2017). Fine-tuning light sensitivity in the starry flounder (*Platichthys stellatus*) retina: regional variation in photoreceptor cell morphology and opsin gene expression. *J. Comp. Neurol.* 525, 2328–2342. doi: 10.1002/cne.24205

Jerlov, N. G. (1968). *Optical Oceanography*. Amsterdam: Elsevier.

Klaren, P. H. M., Wunderink, Y. S., Yúfera, M., Mancera, J. M., and Flik, G. (2008). The thyroid gland and thyroid hormones in Senegalese sole (*Solea senegalensis*) during early development and metamorphosis. *Gen. Comp. Endocrinol.* 155, 686–694. doi: 10.1016/j.ygcen.2007.09.014

Kvenseth, A. M., Pittman, K., and Helvik, J. V. (1996). Eye development in Atlantic halibut (*Hippoglossus hippoglossus*): differentiation and development of the retina from early yolk sac stages through metamorphosis. *Can. J. Fish. Aquat. Sci.* 53, 2524–2532. doi: 10.1139/f96-205

Lan-Chow-Wing, O., Confente, F., Herrera-Pérez, P., Isorna, E., Chereguini, O., Rendón, M. C., et al. (2014). Distinct expression profiles of three melatonin receptors during early development and metamorphosis in the flatfish *Solea senegalensis*. *Int. J. Mol. Sci.* 15, 20789–20799. doi: 10.3390/ijms151120789

Livak, K. J., and Schmittgen, T. D. (2001). Analysis of relative gene expression data using real-time quantitative PCR and the 2(-Delta Delta C(T)) Method. *Methods* 25, 402–408. doi: 10.1006/meth.2001.1262

Mader, M. M., and Cameron, D. A. (2004). Photoreceptor differentiation during retinal development, growth, and regeneration in a metamorphic vertebrate. *J. Neurosci.* 24, 11463–11472. doi: 10.1523/JNEUROSCI.3343-04.2004

Mader, M. M., and Cameron, D. A. (2006). Effects of induced systemic hypothyroidism upon the retina: regulation of thyroid hormone receptor alpha and photoreceptor production. *Mol. Vis.* 12, 915–930.

Martín-Robles, ÁJ., Aliaga-Guerrero, M., Whitmore, D., Pendón, C., and Muñoz-Cueto, J. A. (2012). The circadian clock machinery during early development of Senegalese sole (*Solea senegalensis*): effects of constant light and dark conditions. *Chronobiol. Int.* 29, 1195–1205. doi: 10.3109/07420528.2012.719963

Martín-Robles, ÁJ., Whitmore, D., Pendón, C., and Muñoz-Cueto, J. A. (2013). Differential effects of transient constant light-dark conditions on daily rhythms of Period and Clock transcripts during *Senegalese sole* metamorphosis. *Chronobiol. Int.* 30, 699–710. doi: 10.3109/07420528.2013.782313

Matsuda, K., Torisawa, S., Hiraishi, T., and Yamamoto, K. (2008). Comparison of visual acuity and visual axis of three flatfish species with different ecotypes. *Fish. Sci.* 74, 562–572. doi: 10.1111/j.1444-2906.2008.01559.x

Muñoz-Cueto, J. A., Mañanos-Sánchez, E. L., and Sánchez-Vázquez, F. J. (2019). *The Biology of Sole*. Boca Raton: CRC Press, Taylor & Francis Group.

Musilova, Z., Cortesi, F., Matschiner, M., Davies, W. I. L., Patel, J. S., Stieb, S. M., et al. (2019). Vision using multiple distinct rod opsins in deep-sea fishes. *Science* 364, 588–592. doi: 10.1126/science.aav4632

Musilova, Z., Salzburger, W., and Cortesi, F. (2021). The visual opsin gene repertoires of teleost fishes: evolution, ecology, and function. *Annu. Rev. Cell. Dev. Biol.* 37, 441–468. doi: 10.1146/annurev-cellbio-120219-024915

Novales Flamarique, I. (2013). Opsin switch reveals function of the ultraviolet cone in fish foraging. *Proc. Royal Soc. B: Biol. Sci.* 280:20122490. doi: 10.1098/rspb.2012.2490

Padrós, F., Villalta, M., Gisbert, E., and Estévez, A. (2011). Morphological and histological study of larval development of the Senegal sole *Solea senegalensis*: an integrative study. *J. Fish Biol.* 79, 3–32. doi: 10.1111/j.1095-8649.2011.02942.x

Ribeiro, L., Zambonino-Infante, J. L., Cahu, C., and Dinis, M. T. (1999). Development of digestive enzymes in larvae of Solea senegalensis, Kaup 1858. *Aquaculture* 179, 465–473. doi: 10.1016/j.cbpb.2014.11.011

Rodríguez-Gómez, F. J., Sarasquete, C., and Muñoz-Cueto, J. A. (2000). A morphological study of the brain of *Solea senegalensis*. I. the telencephalon. *Histol. Histopathol.* 15, 355–364. doi: 10.14670/HH-15.355

Rosa, V. D., Frigato, E., López-Olmeda, J. F., Sánchez-Vázquez, F. J., and Bertolucci, C. (2015). The light wavelength affects the ontogeny of clock gene expression and activity rhythms in zebrafish larvae. *PLoS One* 10:e0132235. doi: 10.1371/journal.pone.0132235

Sarasquete, C., Gisbert, E., and Ortiz-Delgado, J. B. (2019). "Embryonic and larval ontogeny of the Senegalese sole, Solea senegalensis: normal patterns and pathological alterations," in *The Biology of Sole*, eds J. A. Muñoz-Cueto, E. L. Mañanos-Sánchez, and F. J. Sánchez-Vázquez (Boca Raton, FL: CRC Press, Taylor & Francis Group), 216–252. doi: 10.1201/9781315120393-11

Savelli, I., Novales Flamarique, I., Iwanicki, T., and Taylor, J. S. (2018). Parallel opsin switches in multiple cone types of the starry flounder retina: tuning visual pigment composition for a demersal life style. *Sci. Rep.* 8:4763. doi: 10.1038/s41598-018-23008-y

Servili, A., Herrera-Pérez, P., Kah, O., and Muñoz-Cueto, J. A. (2012). The retina is a target for GnRH-3 system in the European sea bass, *Dicentrarchus labrax*. *Gen. Comp. Endocrinol.* 175, 398–406. doi: 10.1016/j.ygcen.2011.11.007

Sierra-Flores, R., Davie, A., Grant, B., Carboni, S., Atack, T., and Migaud, H. (2016). Effects of light spectrum and tank background colour on Atlantic cod (*Gadus morhua*) and turbot (*Scophthalmus maximus*) larvae performance. *Aquaculture* 450, 6–13. doi: 10.1016/j.aquaculture.2015.06.041

Steindal, I. A. F., and Whitmore, D. (2020). Zebrafish circadian clock entrainment and the importance of broad spectral light sensitivity. *Front. Physiol.* 11:1002. doi: 10.3389/fphys.2020.01002

Tamai, T. K., Carr, A. J., and Whitmore, D. (2005). Zebrafish circadian clocks: cells that see light. *Biochem. Soc. Trans.* 33, 962–966. doi: 10.1042/BST20050962

Temple, S. E., Veldhoen, K. M., Phelan, J. T., Veldhoen, N. J., and Hawryshyn, C. W. (2008). Ontogenetic changes in photoreceptor opsin gene expression in coho salmon (*Oncorhynchus kisutch*. Walbaum). *J. Exp. Biol.* 211, 3879–3888. doi: 10.1242/jeb.020289

Valen, R., Edvardsen, R. B., Søviknes, A. M., Drivenes, Ø, and Helvik, J. V. (2014). Molecular evidence that only two opsin subfamilies, the blue light- (SWS2) and green light-sensitive (RH2), drive color vision in Atlantic cod (*Gadus morhua*). *PLoS One* 9:e115436. doi: 10.1371/journal.pone.0115436

Valen, R., Karlsen, R., and Helvik, J. V. (2018). Environmental, population and life-stage plasticity in the visual system of Atlantic cod. *J. Exp. Biol.* 221(Pt1):jeb165191. doi: 10.1242/jeb.165191

Veldhoen, K., Allison, W. T., Veldhoen, N., Anholt, B. R., Helbing, C. C., and Hawryshyn, C. W. (2006). Spatio-temporal characterization of retinal opsin gene expression during thyroid hormone-induced and natural development of rainbow trout. *Vis. Neurosci.* 23, 169–179. doi: 10.1017/S0952523806232139

Vergès-Castillo, A., González-Vargas, I. A., Muñoz-Cueto, J. A., Martín-Robles, ÁJ., and Pendón, C. (2021). Establishment and characterisation of single cell-derived embryonic stem cell lines from the gilthead seabream, *Sparus aurata*. *Comp. Biochem. Physiol. B, Biochem. Mol. Biol.* 256:110626. doi: 10.1016/j.cbpb.2021.110626

Villamizar, N., Blanco-Vives, B., Migaud, H., Davie, A., Carboni, S., and Sánchez-Vázquez, F. J. (2011). Effects of light during early larval development of some aquaculturedteleosts: a review. *Aquaculture* 315, 86–94.

Villamizar, N., Blanco-Vives, B., Oliveira, C., Dinis, M. T., Rosa, V. D., Negrini, P., et al. (2013). Circadian rhythms of embryonic development and hatching in fish: a comparative study of zebrafish (diurnal), Senegalese sole (nocturnal), and Somalian cavefish (blind). *Chronobiol. Int.* 30, 889–900. doi: 10.3109/07420528.2013.784772

Wang, Y., Zhou, L., Wu, L., Song, C., Ma, X., Xu, S., et al. (2021). Evolutionary ecology of the visual opsin gene sequence and its expression in turbot (*Scophthalmus maximus*). *BMC Ecol. Evol.* 21:114. doi: 10.1186/s12862-021-01837-1832

Whitmore, D., Foulkes, N. S., and Sassone-Corsi, P. (2000). Light acts directly on organs and cells in culture to set the vertebrate circadian clock. *Nature* 404, 87–91. doi: 10.1038/35003589

Yúfera, M., Pascual, E., and Fernández-Dıìaz, C. (1999). A highly efficient microencapsulated food for rearing early larvae of marine fish. *Aquaculture* 177, 249–256.

**Conflict of Interest:** The authors declare that the research was conducted in the absence of any commercial or financial relationships that could be construed as a potential conflict of interest.

**Publisher's Note:** All claims expressed in this article are solely those of the authors and do not necessarily represent those of their affiliated organizations, or those of the publisher, the editors and the reviewers. Any product that may be evaluated in this article, or claim that may be made by its manufacturer, is not guaranteed or endorsed by the publisher.

frontiers | Frontiers in Marine Science

ORIGINAL RESEARCH
published: 20 April 2022
doi: 10.3389/fmars.2022.861691

# Alternative Splicing of the Lobster (*Homarus americanus*) Crustacean Hyperglycemic Hormone A and B Genes Produce 2 Protein Variants Involved in Vitellogenin Inhibition

*Cheng Gui Wang*[1,2], *Wei Wang*[1], *Li Li Shi*[1], *Yu Chun Shen*[2*] and *Siuming F. Chan*[1*]

[1] Laboratory of Shrimp Genetic Breeding, College of Fisheries, Guangdong Ocean University, Zhanjiang, China,
[2] Key Laboratory of Marine Ecology and Aquaculture Environment of Zhanjiang, College of Fisheries, Guangdong Ocean University, Zhanjiang, China

OPEN ACCESS

**Edited by:**
Benjamin Costas,
University of Porto, Portugal

**Reviewed by:**
Piero Giulio Giulianini,
University of Trieste, Italy
Ting Chen,
Chinese Academy of Sciences, China

***Correspondence:**
Yu Chun Shen
shenyuchun@163.com
Siuming F. Chan
siuming573@sina.com

**Specialty section:**
This article was submitted to Aquatic Physiology, a section of the journal Frontiers in Marine Science

**Received:** 25 January 2022
**Accepted:** 11 March 2022
**Published:** 20 April 2022

**Citation:**
Wang CG, Wang W, Shi LL, Shen YC and Chan SF (2022) Alternative Splicing of the Lobster (Homarus americanus) Crustacean Hyperglycemic Hormone A and B Genes Produce 2 Protein Variants Involved in Vitellogenin Inhibition. Front. Mar. Sci. 9:861691. doi: 10.3389/fmars.2022.861691

Current BLASTP search analysis results suggested that the lobster (*Homarus americanus*) *HaCHH-A* and *HaCHH-B* may be derived from two different four-exon genes. Repeated tissue expression studies have revealed much different expression patterns of these two genes from those reported in the past. With RT-PCR, rapid amplification of complementary DNA (cDNA) ends (RACE), and genomic DNA cloning, we confirmed that the *HaCHH-A* and *HaCHH-B* transcripts were derived from two different four-exon CHH genes. By an alternative splicing mechanism, each gene can produce different but larger transcript variants (i.e., *sHaCHH-A* and *sHaCHH-B*) mainly in different non-eyestalk tissues of the females. The larger and unspliced transcripts can be detected in the hepatopancreas, gill, heart, nerve cord, brain, ovary, and thoracic ganglion of the reproductive females. The expression patterns of *sHaCHH-A* and *sHaCHH-B* in other non-eyestalk tissues suggest that these transcripts have a wide spectrum of expressions during the female reproductive cycle. An *in vitro* organ explant culture system was developed to investigate the reproductive function of these cDNAs. The results showed that the recombinant proteins for *sHaCHH-A* and *sHaCHH-B* inhibited the gene expression of vitellogenin, whereas the double-stranded RNA (dsRNA) for *sHaCHH-A* and *sHaCHH-B* stimulated the expression of the vitellogenin gene *in vitro*. The results of the study may provide insights for the development of techniques to induce gonad development without using eyestalk ablation operation. This is the first in-depth report of the characterization of two four-exon CHH genes in a crustacean.

**Keywords: shrimp, eyestalk, crustacean hyperglycemic hormone, alternative splicing, vitellogenin**

## HIGHLIGHTS

1. Multiple *CHH-A* and *CHH-B* genes exist in the lobster *Homarus americanus*, and these genes consist of four exons and are interrupted by three introns.

2. The previously reported lobster *CHH-A* and *CHH-B* cDNAs were derived from alternative splicing of the third intron, and the newly identified *sCHH-A* and *sCHH-B* transcripts were products of four-exon transcripts that exist mainly in non-eyestalk neuronal tissues.

3. The expression patterns of the newly reported *sHaCHH-A* and *sHaCHH-B* suggested that they may have a reproductive stage-related function in the biannual reproductive cycle of females.

4. Recombinant proteins for *sHaCHH-A* and *sHaCHH-B* inhibited the expression of vitellogenin, and gene knockdown of *sHaCHH-A* and/or *sHaCHH-B* caused a significant increase in the gene expression of vitellogenin in the hepatopancreas and ovary.

## INTRODUCTION

Reproduction is an important physiological process and requires a large amount of energy in crustaceans. Crustacean reproduction is tightly regulated by the interactions of hormones (i.e., peptides, neuropeptides, juvenoids, and steroids) (Fingerman, 1987; Huberman, 2000; Diwan, 2005). The neuropeptides most popularly studied in crustacean endocrine research are the crustacean hyperglycemic hormone (CHH), molt-inhibiting hormone (MIH), and gonad-inhibiting hormone (GIH). Together, these hormones belong to a large group of neuropeptides of the CHH/MIH/GIH family (Keller, 1992). These hormones are synthesized in the X-organ sinus gland complex located in the optical ganglia of the eyestalk. The eyestalk sinus gland is a neurohemal organ consisting of clustered axon endings of the neurosecretory cell somata (Chan et al., 2003; Chung et al, 2020; Keller, 1992; Montagné et al., 2008; Tensen et al., 1991; Webster et al., 2012). Many studies have shown that the removal of eyestalks could induce gonad maturation in decapods (Panouse, 1943; Primavera, 1978; Okumura uand Aida, 2001; Uawisetwathana, et al., 2011; Magaña-Gallegos et al., 2021). Removal of the eyestalk could remove the source of GIH and result in rapid ovary development. However, the use of this technique has raised serious animal welfare concerns in recent years. In lobster (*Homarus americanus*), two highly similar HaCHH isoforms (i.e., *HaCHH-A* and *HaCHH-B*) have been characterized (Tensen et al., 1991; De Kleijn et al., 1994; De Kleijn and Van Herp, 1995; Chang et al., 1999). They are known to play a role in the reproduction of the female lobster. The *HaCHH-A* and *HaCHH-B* isoforms share a high overall amino acid sequence identity and differ only by eight amino acid residues for the deduced pro-hormone. Despite the high sequence homology, each CHH has been reported to regulate reproduction during the biannual reproductive cycle of adult females (De Kleijin et al., 1995). Many CHH family neuropeptides from other crustacean species were discovered in the eyestalk from 1990 to 2000; subsequent studies indicated that the transcripts of these neuropeptides can be found in other non-eyestalk neuronal tissues (Chan et al., 2003; Diwan, 2005; Huberman, 2000; Keller, 1992; Spanings-Pierrot et al., 2000; Webster et al., 2012; Loredo-Ranjel et al., 2017) and even in many non-neuronal tissues (Chen et al., 2004; Shi et al., 2018). Although the discovery of the two lobster CHH isoforms has been reported for 25 years, little information has been acquired since their first discovery. At the time when the complementary DNAs (cDNAs) of *HaCHH-A* and *HaCHH-B* were cloned, only a few CHH family neuropeptide sequences have been reported in the GenBank. With the exponential increase in the total number of CHH family neuropeptides reported in recent years, it is important to obtain additional specific information on the gonad maturation of the lobster.

In recent years, China has imported large quantities of *H. americanus* as high-priced seafood from the US and Canada. Because of the increased need for this species as food, growing interest to develop a large-scale commercial complete aquaculture of *H. americanus* in China has arisen. One major constraint for the successful aquaculture of this species is the lack of information on the endocrine control of reproduction. Knowledge on its reproduction, larval rearing, and broodstock management is inadequate. For this reason, investigations into the involvement of CHHs in the reproductive cycle of the female lobster are urgently needed. In this study, we further characterized *HaCHH-A* and *HaCHH-B* from the study of gene structure and expression. We report new findings for two additional CHH-related peptides and confirm that they are derived from two different four-exon *CHH* genes that also gave rise to the originally discovered *HaCHH-A* and *HaCHH-B* cDNAs. We also demonstrate the potential functions of *sHaCHHs* during the reproductive cycle of the female lobster.

## MATERIALS AND METHODS

### Animals

Female lobsters (average carapace length = 70 ± 3 cm, weight = 500 ± 50 g) were purchased from the local seafood market. These animals were imported from the US or Canada to China. They were brought back to the Marine Research Station of the Guangdong Ocean University, Zhanjiang, China. The lobsters were acclimatized (>1 week) in 1-mt circular fiberglass tanks equipped with running seawater (salinity = 32 ± 5‰), temperature of 20 ± 3°C, and an aeration system under conditions of natural photoperiod. They were fed twice daily with commercial pellet diets and fresh oysters. The molt stages of the lobsters were determined by setogenesis specifically for lobster (Helluy and Beltz, 1991). Except for the tissue extraction studies, females were used in all cloning and expression experiments. Before dissection, the lobsters were anesthetized in ice for 30 min. All experiments were conducted

in compliance with the guidelines of the Animal Care and Use Committee of Guangdong Ocean University.

## Cloning of *HaCHH-A* and *HaCHH-B* Genes

To avoid cloning of multiple highly homologous CHH isoforms and highly polymorphic gene transcripts from different individuals, genomic DNA from a single animal was used as the template. For genomic DNA extraction, tissues from the hepatopancreas (Hp) or testis were dissected from the animal and extracted in an extraction buffer. Purified high-quality genomic DNA was used as the template for PCR. Gene-specific primers were designed to specifically amplify either the *HaCHH-A* or the *HaCHH-B* gene, and these primers were located in the exon of the published CHH gene from other decapods (**Table 1**).

## Cloning of the *sHaCHH-A* and *sHaCHH-B* cDNA

Total RNA was extracted from various tissues using TransZol Up Plus RNA spin column-based kit (TransGen, Beijing, China). The RNA concentration was determined using a NanoDrop spectrophotometer, and 1 μg of total RNA was reverse transcribed using the SMART RACE cDNA Amplification Kit (TaKaRa, Shiga, Japan). PCR amplification of RACE (rapid amplification of cDNA ends) products was performed using a 5′- and 3′-RACE Kit (TaKaRa, Shiga, Japan). The forward primers CHH-F1A: 5′-CGTCATGTTCGCCTGC AGAACTCTG-3′ and CHH-F1B: TCATGATGGCCTGCAGAGCGCTGT and the common reverse primer CHH-RP: 5′-TTACTTG CCGACCATCTGGACG-3′ were used. The internal primers used to generate *HaCHH-A* and *HaCHH-B* isoform-specific RT-PCR products were as follows: full-length *HaCHH-A* and *HaCHH-B* were generated using the forward primer 5′-CCCATTTGCAAAGCGATGAGTTCG-3′ and the reverse primer 5′-TGTGCCAA ATGGCTCACAGAA-3′; the amplified fragment was cloned into the pMD19 TA cloning vector (Sangon Biotech, Shanghai, China). All the clones were confirmed by nucleotide sequencing analyses.

To determine the messenger RNA (mRNA) expression profiles of *sHaCHH-A* and *sHaCHH-B* in the biannual ovarian development cycle, females at different reproductive stages were sacrificed for total RNA extraction. The reproductive stages of these animals were determined based on the coloration of the ovary and the Gonadosomatic Index (GSI) as previously reported (Tiu et al., 2009).

The amino acid sequences of the positive clones were analyzed using ORF Finder (NCBI; http://www.ncbi.nlm.nih.gov/projects/gorf/orfig.cgi). Sequence identities were verified using BLAST (http://blast.ncbi.nlm.nih.gov/Blast.cgi). Multiple sequence alignment was performed using the amino acid sequence, and the online Multiple Sequence Alignment software ClustalW (genome.jp) was employed for the various CHH sequences chosen to represent the major subgroups of the type I CHH genes, using only the most highly conserved orthologous amino acids within the CHH/MIH/GIH from representative decapods. The amino acid sequences used in our phylogenetic analysis are listed in **Supplemental Data File 1**. The amino acid sequences of *HaCHH-A* and *HaCHH-B* were compared to those of other decapods to confirm the identification of each family member.

## Real-Time Quantitative PCR

The transcript levels of *HaCHH-A*, *sHaCHH-A*, *HaCHH-B*, and *sHaCHH-B* were determined by both semi-quantitative PCR and real-time quantitative PCR (RT-qPCR). For the semi-quantitative PCR, each PCR was carried out in a final volume of 10 μl containing 5 μl of 2× PCR Master Mix (ABI, Richmond Hill, Canada), 0.3 μl of forward and reverse primers, 2.4 μl of nuclease-free water, and 2 μl of cDNA template. For the internal control, we

**TABLE 1** | Primer sequences used in the RT-PCR, RACE, gDNA PCR ad RNAi for the lobster CHH.

| Name | Sequence | Description:genomic/RTPCR/RNAi |
|---|---|---|
| HaCHH-F4 | TCAGGTGTTCGACCAGGCGTGT | Common primer for geomic,RT-PCR |
| HaCHHRP | TTACTTGCCGACCATCTGGACG | |
| HaCHH-F1A | CGTCATGTTCGCCTGCAGAACTCTG | Specific primer for HaCHH-A |
| HaCHH-F1B: | TCATGATGGCCTGCAGAGCGCTGT | Specific primer for HaCHH-A |
| HaCHH-R2: | GTTGTAACAGTCCTCACACACACGG | Common primer for geomic,RT-PCR |
| T7HaCHHAex3F: | TAATACGACTCACTATAGGGAAACCTTTCGTCGCCACCACCTG | dsRNA |
| T7HaCHHAex3R: | TAATACGACTCACTATAGGGTGATCATATCCCTGATCTCGAGGT | |
| T7HaCHHBex3F: | TAATACGACTCACTATAGGGAAACCTTTCATCGTCACCACCTG | dsRNA |
| T7HaCHHBex3R: | TAATACGACTCACTATAGGGTTGATCATATCCCTGAACTCAAGGA | |
| sHaCHH-A_F: | CTCGTCCAATTCGCCGTCGT | qT-PCR |
| sHaCHH-A_R: | TCCTTCCTCCTCACCAACCACTTAAAGT | |
| HaCHH-A_F: | CTCGTCCAATTCGCCGTCGT | qT-PCR |
| HaCHH-A_R: | CGAGACATTGACGGAACACCCAATTAC | |
| sHaCHH-B_F: | CTCGTCCAATTCGCCGTCGT | qT-PCR |
| sHaCHH-B_R: | CATCACACACCTCGGGAATGTGT | |
| HaCHH-B_F | CTCGTCCAATTCGCCGTCGT | qT-PCR |
| HaCHH-B_R: | CGTTGGAGACGTACTCGTCGAT | |
| HaEF1aF | AATACCGCGGCCCTTTAGTTTG | qT-PCR |
| HaEF1aR: | TTGGTGTGGGTTAAGGAACTCG | |
| Ha1VgF: | AGACGGACGTGGTAGGGAAGTG | qT-PCR |
| Ha1VgR: | CAGACTACCTTGAGGGATGGCAG | |

have used the elongation factor 1 (*EF1α*) and the β-actin gene of the lobster. The PCR conditions were as follows: 94°C for 5 min, 34 cycles at 94°C for 30 s, 60°C for 30 s, 72°C for 1 min, and 72°C for 3 min. For RT-qPCR, the CFX96 Real Time System (Bio-Rad, Hercules, CA, USA) and qPCR Master Mix (TaKaRa) were used. Total RNA was extracted from the different tissues of mature lobsters. Total RNA from each tissue (1 μg) was treated with gDNA Eraser at 37°C for 15 min to avoid contamination with genomic DNA. Total RNAs were used for cDNA synthesis using the PrimeScript RT reagent kit with gDNA Eraser (TaKaRa). The cDNAs from females with vitellogenic oocytes were used for tissue distribution. The relative mRNA abundance of each gene was calculated using the $\Delta\Delta^{Ct}$ method, then normalized to that of the *Ef1α* and β-actin for each sample. Measurements of the expression levels were performed in triplicate or duplicate.

## *sHaCHH-A* and *sHaCHH-B* Functional Study by *In vitro* Bioassay

Recombinant protein and RNAi technologies were used to study the function of *sHaCHH-A* and *sHaCHH-B* in lobster gonad vitellogenesis. For the detailed protocol of recombinant protein production, see Liang et al. (2019). Briefly, the restriction enzyme site sequence-linked primers for *sHaCHH-A* (expHaCHH-AF: GGATCCCGGTCTGTAGAAGGAGCATC; expHaCHH-AR: GAGCTCCTACCCCTTGATCATATCC) and *sHaCHH-B* (*sHaCHH-B*; rHaCHH-B: GGATCCCGGTCAGTAGAAGG AGCGGATATGATCAAGGGGTAGGAGCTC) (**Table 1**) were used to amplify the mature peptide of *sHaCHH-A* or *HaCHH-B*. The cDNA template was derived from the cDNA clones from the above cDNA cloning procedure. The PCR-amplified cDNA fragments were digested with the same enzyme and ligated to the pET32A vector plasmid digested previously with the same restriction enzymes (*Bam*HI and *Sac*I). After bacterial transformation, positive clones were screened by PCR using the T7 promoter and T-terminator primers. The positive clones were verified by PCR with a gene-specific primer for either the *HaCHH-A* or *HaCHH-B* gene and DNA sequence determination. The recombinant proteins were produced using *Escherichia coli* DE21 strain and subsequently purified. The purified and re-natured recombinant proteins for *sHaCHH-A* and *sHaCHH-B* were used for *in vitro* bioassay to study their potential functions.

RNA interference approaches were used to knock down the functions of *sHaCHH-A* or *sHaCHH-B*. For double-stranded RNA (dsRNA) synthesis, primers amplifying exon 3 of *sHaCHH-A* and *sHaCHH-B* were designed (**Table 1**). The templates were the cDNAs for *sHaCHH-A* and *sHaCHH-B* from the cDNA cloning described above. DsRNAs were synthesized using the T7 RNA Transcription Kit (Vazyme, Nanjing, China). For control, the dsRNA for the tiger frog virus ATPase gene was used (Tiu et al., 2008). The dsRNA template for each gene was amplified (PCR amplification procedure: 95°C for 5 min, followed by 30 cycles of 95°C for 30 s, 57°C for 30 s, and 72°C for 30 s, then 72°C for 10 min) with the above primers and purified using the FastPure Gel DNA Extraction Mini Kit (Vazyme). After detection of the concentrations of the DNA templates (NanoDrop 2000; Thermo Fisher Scientific, Inc., Waltham, MA, USA), dsRNA was produced with DNA templates using the T7 RNA Transcription Kit (Vazyme). The final dsRNA was diluted to an appropriate concentration (1 μg/μl) with phosphate-buffered saline (PBS). *In vitro* RNA interference experiments ($n = 8$) were then performed.

The lobsters were dissected and the ovary developmental stage was determined. Individuals with ovary at the early (yellow) and middle (light green) stages were dissected for the Hp and ovary (i.e., 50–80 $mm^3$). The tissues were first rinsed with ice-cold PBS and then placed into the wells of a sterile culture plate containing 1.5 ml nutrient medium (M199; Sigma, St. Louis, MO, USA). Individual wells were treated with either the tested recombinant proteins, dsRNAs, or the control (Tiu et al., 2008). The culture plate was then shaken on the platform of an orbital shaker at 24–26°C for 3 h. At the end of the culture period, the tissues were extracted for total RNA and for cDNA synthesis. The expression of the lobster vitellogenin gene was monitored by RT-PCR, as previously described. The *HaVg1* primers were derived from the lobster vitellogenin cDNA (GenBank no. EF422415.1).

# RESULTS

## Characterization of *sHaCHH-A* and *sHaCHH-B*

Current GenBank BLASTP sequence homology search results for *HaCHH-A* (GenBank no. P19806.3) and *HaCHH-B* (GenBank no. 2105187B) indicated that they are most similar to the prepro-CHH isoform A of the lobster *Nephrops norvegicus* (GenBank no. AAQ22391.1) and the CHH isoform B (GenBank no. AAQ22392.1). Compared to the crayfish, *HaCHH-A* and *HaCHH-B* are most similar to the CHH of *Procambarus clarkii* (GenBank no. Q25683.3). Compared to the CHH of shrimps, *HaCHH-A* and *HaCHH-B* are most similar to the CHH-like of *Litopenaeus vannamei* (GenBank no. AAN86055.1) and *Penaeus monodon* (GenBank no. XP037787977), sharing 68%–69% sequence identity in the mature peptide region. Moreover, the *HaCHH-A* and *Ha-CHH-B* sequences are more similar to the CHH of the freshwater shrimp *Macrobrachium rosenbergii* (GenBank no. AAF29534.1). Compared to the crab CHH, the lobster sequences shared the highest sequence identity with the CmCHH (GenBank no. P14944) of *Carcinus maenas*. Further analysis of these decapod CHH sequences revealed that they were derived from four-exon genes. Alternative splicing of the pre-mRNA for these CHHs gave rise to the transcripts being analyzed. Therefore, the results suggested that the lobster *HaCHH-A* and *HaCHH-B* may also be derived from different four-exon genes. Unlike a previous report (DeKleijn et al., 1995), the current RT-PCR results showed that two transcripts can be detected in the eyestalk cDNA (**Figure 1A**). The small cDNA fragment was about 150 bp, and a larger and more abundant DNA fragment of 310 bp was also amplified. Similar results were observed for the *HaCHH-B* gene when primers *HaCHH1b* and

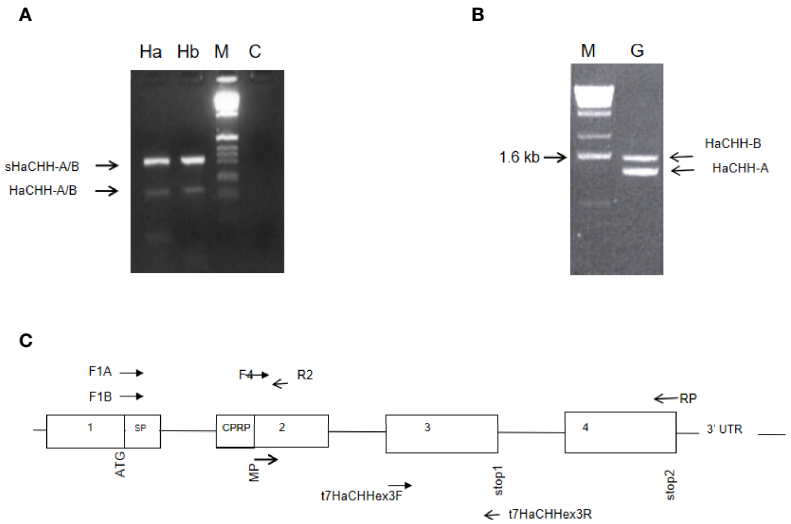


**FIGURE 1** | **(A)** Identification of transcript variants for the *HaCHH-A* and *HaCHH-B* genes. Gene-specific forward primers for *HaCHH-A* (*F1A*) and *HaCHH-B* (*F1B*) were paired with common reverse primer (*R2*) in the RT-PCR amplification of cDNA from eyestalk (*Es*). Two major fragments were amplified by each pair of primers. The larger fragment (*upper arrow*) is the *sHaCHH-A* or the *sHaCHH-B* transcript variant; the smaller band (*lower arrow*) is for transcripts *HaCHH-A* and *HaCHH-B*. **(B)** Gene from eyestalk cDNA of female lobster. *Lane Ha*: PCR results using primer pair F1A and RP; *lane Hb*: results for primer F1B/RP; *M*: DNA size marker; and *C*: negative, no template control. **(B)** Genomic PCR detection of multiple *HaCHH-A* and *HaCHH-B* genes. The primer pair F4/RP (**Figure 2** and **Table 1**) was used and two distinctive DNA fragments (i.e., 1.4 and 1.6 kb) were amplified. **(C)** Schematic diagram showing the locations of the primers and the proposed gene structure of the HaCHH genes used in this study.

*HaCHH-RP* were used in PCR (**Figure 1A**). These two DNA fragments were subcloned into pMD19 in *E. coli* for DNA sequencing. The results revealed that the smaller cDNAs carried coding sequences for the matured peptide of the previously reported *HaCHH-A* (GenBank no. P198063) and *HaCHH-B* (GenBank no. 2105187B). The 5′ end of the larger cDNA carried a coding sequence identical to the corresponding *HaCHH-A* or *HaCHH-B*, but the 3′ end carried a peptide sequence different from the original *HaCHH-A* and *HaCHH-B* cDNA (see below).

## *HaCHH-A* and *HaCHH-B* Gene Organization

To study the *HaCHH-A* and *CHH-B* genes, PCR amplification of genomic DNA was performed with the DNA templates and cDNAs from a single individual (**Figures 1B, C** and **Table 1**). Two major DNA bands with sizes of 1,600 and 1,450 bp were amplified. Because the intensity of the smaller band in the agarose gel was stronger, more copy numbers for the smaller genomic DNA were expected. Sequence determination of the bands revealed that each DNA fragment carries the coding and non-coding sequences for the *HaCHH-A* (1.4 kb) or the HaCHH-B (1.6 kb) gene (**Figures 1B, C**). These fragments carry coding sequences for partial exon 2, exon 3, and exon 4 and the interrupting non-coding introns 2 and 3. We employed genomic PCR to attempt to recover the partial exon 1 coding sequence and non-coding intron 1 of both genes, without success. As a comparative study of these CHH genes, genomic information of the four-exon CHH genes from other decapods was collected (**Figure 2**). Except for the complete CHH gene structure of *L. vannamei* (from the *L. vannamei* genome project), the other CHH gene structures were incomplete. Most of these genes lacked information on the first intron. In the *L. vannamei* CHH gene, intron 1 consisted of several highly repeated microsatellite sequences [i.e., (AT)*n*, (CT)*n*, and (GT)*n*] along the span of a 3.34 intronic region (*L. vannamei* genomic database, GenBank no. LOC113815764).

The RT-PCR and 5′ and 3′RACE cloning approaches were used to clone the large and small fragments, as described above. The four cDNA sequences were cloned and the sequences determined. The amino acid sequences of two smaller cDNAs were identical to the previously reported *HaCHH-A* and *HaCHH-B*. The two larger cDNAs (i.e., *sHaCHH-A* and *sHaCHH-B*) represented the newly discovered transcript variants (**Figure 3**). As expected, *HaCHH-A* and *sHaCHH-A* shared identical amino acids in the N-terminal end, but major amino acid sequence variations occurred in the C-terminal end. Similar results were found for *HaCHH-B* and *sHaCHH-B*. For the multiple alignment and phylogenetic study, other CHH subtype I sequences and MIH/GIH subtype II group neuropeptides were included in the ClustalW analysis together with the four HaCHH variants. Within the same color block, a much higher degree of sequence identity was observed in the signal mature peptide region (**Figure 4**). For the mature peptide, the degree of homology was much higher in the coding sequence of exon 2 and was much lower in the C-terminal end of the protein encoded by exon 3. The amino acid similarity at the N-terminal end of the mature peptide for *HaCHH-A* and *HaCHH-B* was much higher, i.e., >97% amino acid identity, but the homology decreased to only 63.5% at the C-terminal end.

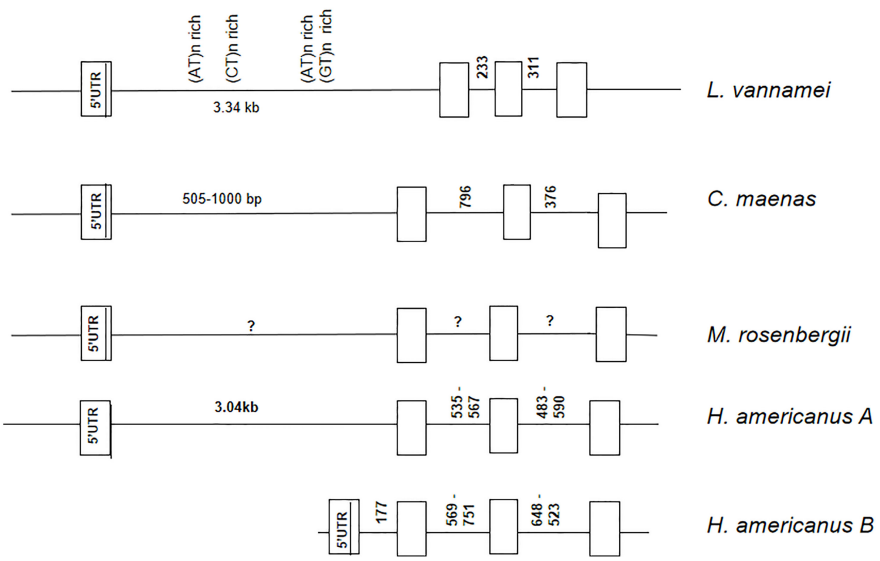


**FIGURE 2** | Comparison of the four-exon CHH genes from the lobster *Homarus americanus*, crab *Carcinus maenas*, and shrimp *Litopenaeus vannamei* and *Macrobrachium rosenbergii*. Exons are indicated by the *open boxes* and introns are indicated by the *horizontal line* in between the exons. The first exon consists of the 5′-ÚTR and the ATG start codon. Unknown intron sizes are indicated by an a *question mark*. Highly repetitive sequence (satellite DNA) clusters were identified in the promoter region of *L. vannamei* CHH-like gene.

Despite the similar molecular characteristics of these CHHs, the p*I* values (ExPASy Compute p*I*/$M_w$ tool) of these isoforms were quite different. For example, the estimated p*I* value of *sHaCHH-A* (i.e., p*I* = 5.27) was the smallest compared to those of the rest.

The phylogenetic tree results revealed that the crustacean CHH can be divided into three different subgroups: CHH group, CHH-like group, and CHH-L/S group. The CHH group is the three-exon CHH gene consisting of the typical signal peptide–

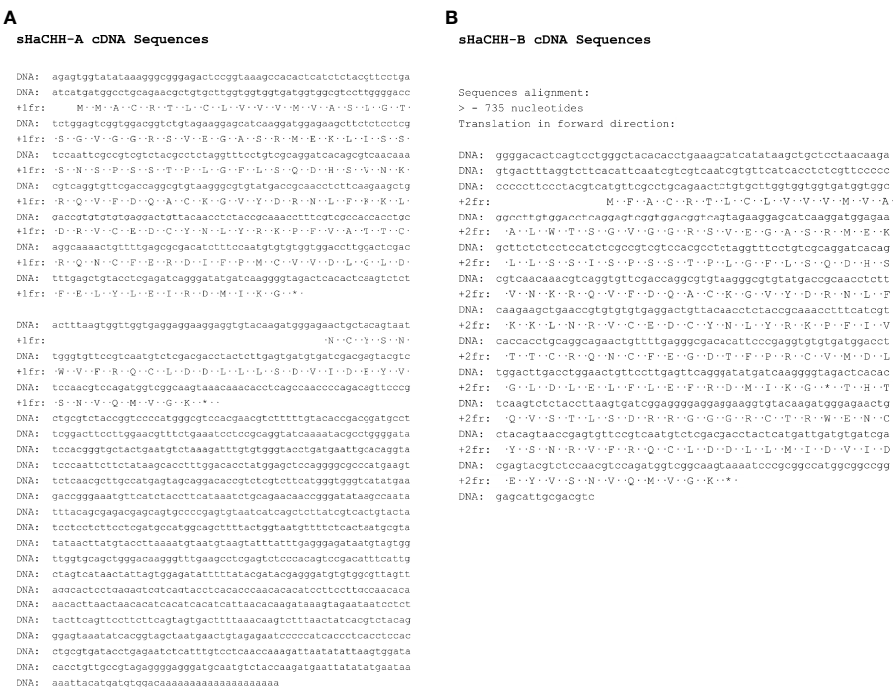


**FIGURE 3** | Nucleotide and deduced amino acid sequences of the computed cDNA for *sHaCHH-A* **(A)** and *sHaCHH-B* **(B)**. A one-letter amino acid code was used to indicate the amino acid residues.

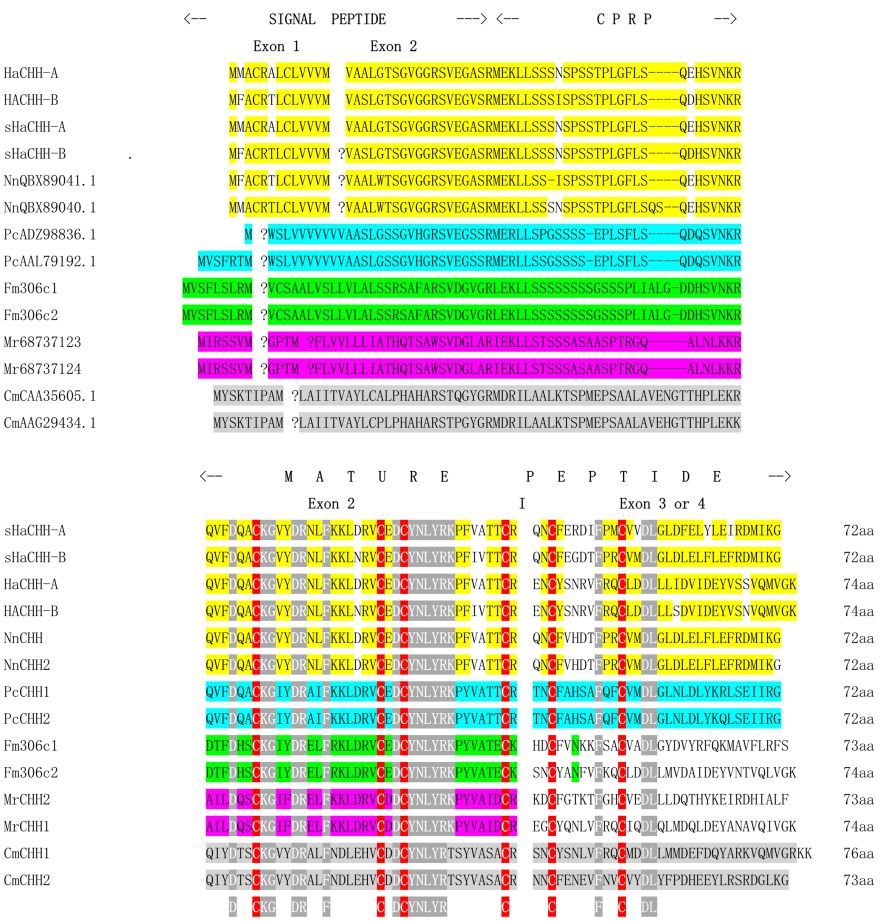


**FIGURE 4** | Alignment of the lobster four-exon CHH genes with that of other decapods, including lobster (*yellow*: *HaCHH-A* and *HaCHH-B*; *NnCHH-1* and *NnCHH-2*), crab (*gray*: *CmCHH-1* and *CmCHH2*), shrimp (*green*: *Fm306-c1* and *Fm306-c2*) (Shi et al., 2018), freshwater shrimp (*pink*: *MrCHH1* and *MrCHH2*), and crayfish (*blue*: *PcCHH1*, *PcCHH2*). The *same block color* indicates the same groups of decapods. Signal peptides and mature peptides are indicated. Gaps are introduced in the boundary of the exons in lobster, shrimp, and crab CHH-like genes. A *question mark* is inserted in the locations of potential intron insertion sites in the CHH-like genes from other decapods. In addition to the conserved cysteine residues (*highlighted in red*), several conserved amino acids (*highlighted in gray*) may be important for motif structure formation of the peptide.

CPRP–mature peptide structure. The CHH-Like group is the more recently discovered CHHs having the signal peptide–mature peptide structure. The CHH-L/S group comprise the four-exon CHH genes that produce alternative transcripts, as described in this study. The lobster *sHaCHH-A* and *sHaCHH-B* were closely related to the crayfish CHH, followed by those of the shrimp and crab (**Figure 5**). As a reference, the MIH/GIH subtype evolved from a common ancestor, giving rise to the three-exon CHH and the four-exon CHH-L/S. It was observed that the four-exon CHH-L/S gene cluster represented a small number relative to the CHH group since only a few (i.e., LvCHH2 and MeCHH-B) of the CHH type were selected for phylogenetic tree construction (**Figure 5**).

## Expression of Lobster *sHaCHH-A* and *sHaCHH-B* Transcripts

Both semi-quantitative RT-PCR and RT-qPCR were used to study the expression of the HaCHH gene. For semi-quantitative PCR, multiple DNA fragments were amplified by F1A/R4 and F1B/R4 primers from different tissues. The smaller transcripts (i.e., 158 bp) represent the originally reported *HaCHH-A* or *HaCHH-B* cDNA, and they can be detected in the eyestalks of non-reproductive females. No specific pattern of these short transcripts was observed during the different stages of the reproductive cycle. The larger transcripts (i.e., 317 bp, which produced *sHaCHH-A* and *sHaCHH-B*) can be detected mainly in the Hp and thoracic ganglion. However, DNA fragments of different sizes were also amplified (i.e., especially in the thoracic ganglion) (**Figure 6A**). Further study by qPCR was performed using females in the early reproductive stages. The results confirmed that *HaCHH-A* and *HaCHH-B* were mainly expressed in the eyestalk. Also, *sHaCHH-A* and *sHaCHH-B* transcripts were detected in the non-eyestalk neuronal and in non-neuronal tissues, including the Hp, ovary, brain, and thoracic ganglion. However, the transcripts were not detected in the Hp (**Figure 6B**). The 158- and 317-bp PCR products were also subcloned and DNA sequencing was

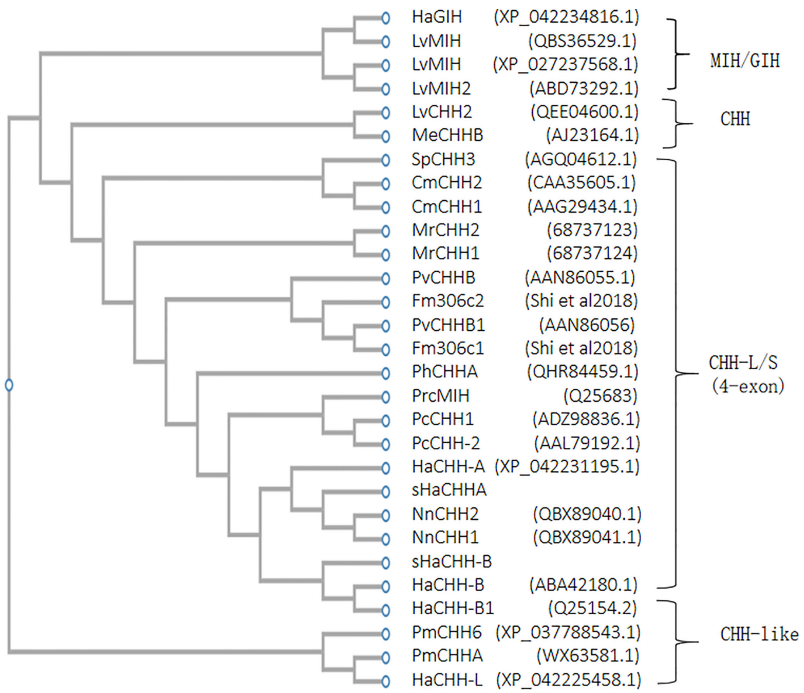


**FIGURE 5** | Phylogenetic tree analysis of lobster *HaCHH-A* and *HaCHH-B* cDNA within the major subfamilies of decapod CHH/MIH/GIH. The sequences included the lobster (*Homarus americanus*, *Ha*) PhCHH-A (QHR84459.1), HaCHH-L (XP_042225458.1), HaGIH (XP_042234816.1), HaCHH-A (XP_042231195.1), sHaCHH-A, NnCHH2 (QBX89040.1), NnCHH1 (QBX89041.1), sHaCHH-B, (ABA42180.1), and HaCHH-B1 (Q25154.2); crab (*Carcinus maenas*, *Cm*) CmCHH2 (CAA35605.1), CmCHH1 (AAG29434.1), and SpCHH3 (AGQ04612.1); shrimp (*Litopenaeus vannamei*, *Lv*) LvMIH (QBS36529.1), LvMIH (XP_027237568.1), LvMIH2 (ABD73292.1), LvCHH2 (QEE04600.1), PvCHHB (AAN86055.1), Fm306c2 (Shi et al., 2018), PvCHHB1 (AAN86056), Fm306c1 (Shi et al., 2018), PmCHH6 (XP_037788543.1) PmCHHA (WX63581.1), and MeCHHB (AJ23164.1); freshwater shrimp (*Macrobrachium rosenbergii*, *Mr*) MrCHH2 (68737123) and MrCHH1(68737124); and crayfish (*Procambarus clarkii*, *Prc*) PrcMIH (Q25683), PcCHH1 (ADZ98836.1), and PcCHH-2 (AAL79192.1). GenBank accession numbers are shown in *parentheses*.

performed, which confirmed that they were specific for the *HaCHH-A* and *HaCHH-B* and the *sHaCHH-A* and *sHaCHH-B* isoform sequences, respectively. Nucleotide sequence analysis of 12 clones generated from the PCR products revealed five *HaCHH-A* and two *sHaCHH-A* clones and two *HaCHH-B* and one *sHaCHH-B* clone, confirming that the large sized clones were from the *sHaCHH-A* and/or *sHaCHH-B* and the small sized clones were from the *HaCHH-A* and/or *HaCHH-B*.

Because previous tissue expression results suggested that neuronal tissues express relatively large amounts of *sHaCHH-A* and *sHaCHH-B*, we studied their expressions at different gonad maturation stages of the female lobster. The RT-PCR results indicated that they are the predominant transcripts during the different stages of maturation (i.e., stages I to IV). Although both *sHaCHH-A* and *sHaCHH-B* were expressed, the transcript level for *sHaCHH-B* was much lower than that of the original *HaCHH-A* and *HaCHH-B* transcripts. In contrast, the other non-eyestalk neuronal tissues (i.e., brain, thoracic ganglion, and nerve cord) expressed mainly the larger transcripts consisting of exons 1–4 (**Figure 7A**). In the thoracic ganglion and the nerve cord, the expression level of *sHaCHH-A* was consistently low. The expression level of *HaCHH-B* appeared higher during the early and active stages of vitellogenesis (**Figure 7B**). However, no specific expression pattern for *sHaCHH-A*/*sHaCHH-B* was recognized in the neuronal tissues. In summary, the expression study indicated that *sHaCHH-A* and *sHaCHH-B* are both expressed in non-eyestalk neuronal tissues, including the brain, thoracic ganglion, and ventral nerve cord. The expressions of *sHaCHH-A* and *sHaCHH-B* in other non-neuronal tissues, such as the Hp and ovary, during ovarian maturation suggested that these proteins are important in ovary maturation. Moreover, the expressions of these genes are stage-specific as lower transcript levels were detected during the immature stage, but much higher levels of expression in lobster undergo reproduction.

## Functional Study of *sHaCHH-A* and *sHaCHH-B* by *In Vitro* Tissue Culture of the Hepatopancreas and Ovary Fragments

Purified recombinant protein and dsRNA were added to the nutrient medium in the tissue explant bioassay experiments (**Figure 8**). In stage I Hp, recombinant *sHaCHH-A* (i.e., 2 μg) caused a decrease in the transcript level of *HaVg1*. Despite the lower expression of *HaVg1* in the ovary compared to that in the hepatopacreas, an increase in the concentration of rsHaCHH-A caused a decrease in the expression of *HaVg1* in a dose-dependent manner ($p < 0.05$). In stage I Hp and ovary, the dsRNAs for *sHaCHH-A* caused a significant increase in the expression of *HaVg1* ($p < 0.05$) (**Figure 9A**). In stage III Hp,

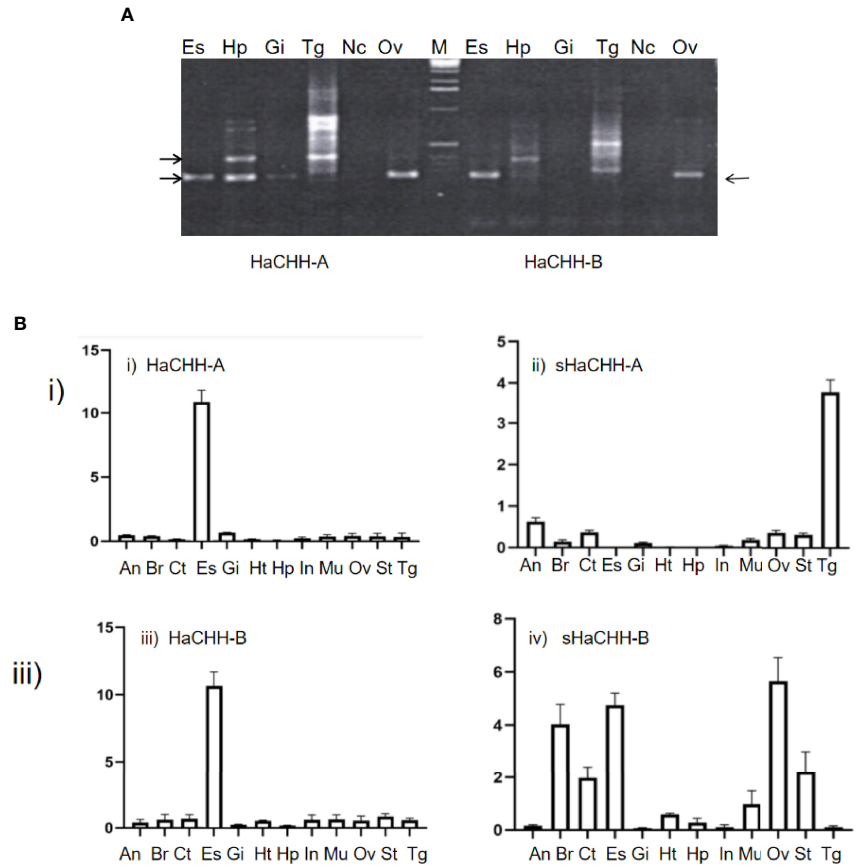


**FIGURE 6** | **(A)** RT-PCR expression study of the *HaCHH-A*, *sHaCHH-A*, *HaCHH-B*, and *sHaCHH-B* genes in different tissues of the lobster female. The primers F1A and RP were used to amplify *HaCHH-A* and *sHaCHH-A*, while primers F1B and RP were used to detect the transcripts of *HaCHH-B* and *sHaCHH-B* in the different tissues [eyestalk (*Es*), hepatopancreas (*Hp*), gill, (*Gi*), thoracic ganglion (*Tg*), nerve cord (*Nc*), and ovary (*Ov*)] of lobster during the early reproductive stage (stage I). **(A)** Representative agarose gels showing the detection of *HaCHH-A*. *HaCHH-B*, *sHaCHH-A*, and *sHaCHH-B*. The larger (317 bp) fragment is the *sHaCHH-A* or *sHaCHH-B* and the smaller (158 bp) fragment is the amplified partial *HaCHH-A* and *HaCHH-B* cDNA. **(B)** qPCR expression study of the i) *HaCHH-A*, ii) *sHaCHH-A*, iii) *HaCHH-B*, and iv) *sHaCHH-B* genes in different tissues of the female lobster. Primers HaCHH-AF/HaCHH-AR and sHaCHHAF/sHaCHHAR were used to amplify *HaCHH-A* and *sHaCHH-A*. Primers HaCHHAF/HaCHHAR and sHaCHH-BF/sHaCHH-BR were used to detect the transcripts of *HaCHH-B* and *sHaCHH-B* in the different tissues [abdominal nerve (*An*), brain (*Br*), cuticle (*Ct*), eyestalk (*Es*), hepatopancreas (*Hp*), heart (*Ht*), gill (*Gi*), intestine (*In*), muscle (*Mu*), stomach (*St*), thoracic ganglion (*Tg*), nerve cord (*Nc*), and ovary (*Ov*)] of lobster during the middle stage of reproduction (II).

rsHaCHH-A caused a decrease of *HaVg1* in a dose-dependent manner ($p < 0.05$). However, the expression level of *HaVg1* in the ovary was not affected. When dssHaCHH-A was added to the medium, the expression levels of *HaVg1* in the Hp and ovary increased (**Figure 9B**).

When the recombinant protein for *sHaCHH-B* was added to the medium, a decrease in the level of *HaVg1* was observed in the Hp and ovary from stages I and III (**Figures 9C, D**). When the dsRNAs for *sHaCHH-B* were added, the expression levels of *HaVg1* also increased in the Hp and ovary fragments. It appears that the level of stimulation was much higher for the dssHaCHH-B-treated Hp. In summary, the results indicated that the recombinant proteins of *sHaCHH-A* and *sHaCHH-B* inhibited the expression of *HaVg1*, but gene knockdown of *sHaCHH-A* and *sHaCHH-B* stimulated the expression of *HaVg1* in the Hp and ovary fragments (**Figure 9**).

# DISCUSSION

## Transcript Variants of CHH in Lobsters and Other Decapods

Major advancement occurred in crustacean endocrinology in the recent application of the next-generation sequencing technique in transcriptome and genome studies. As a result, the number of CHH family genes identified in the same species and the total number of CHH in crustaceans have greatly increased (Havird and Santos, 2016; Chang and Lai, 2018; Oliphant et al., 2018; Hyde et al., 2020; Mykles and Chang, 2020). Therefore, many new CHH sequences have been reported in recent years. However, most CHH sequencing projects mainly focused on economically important species. Therefore, the number of CHH family members identified in lobster is fewer than that of the shrimps and other decapods (Hyde et al., 2020). Based on

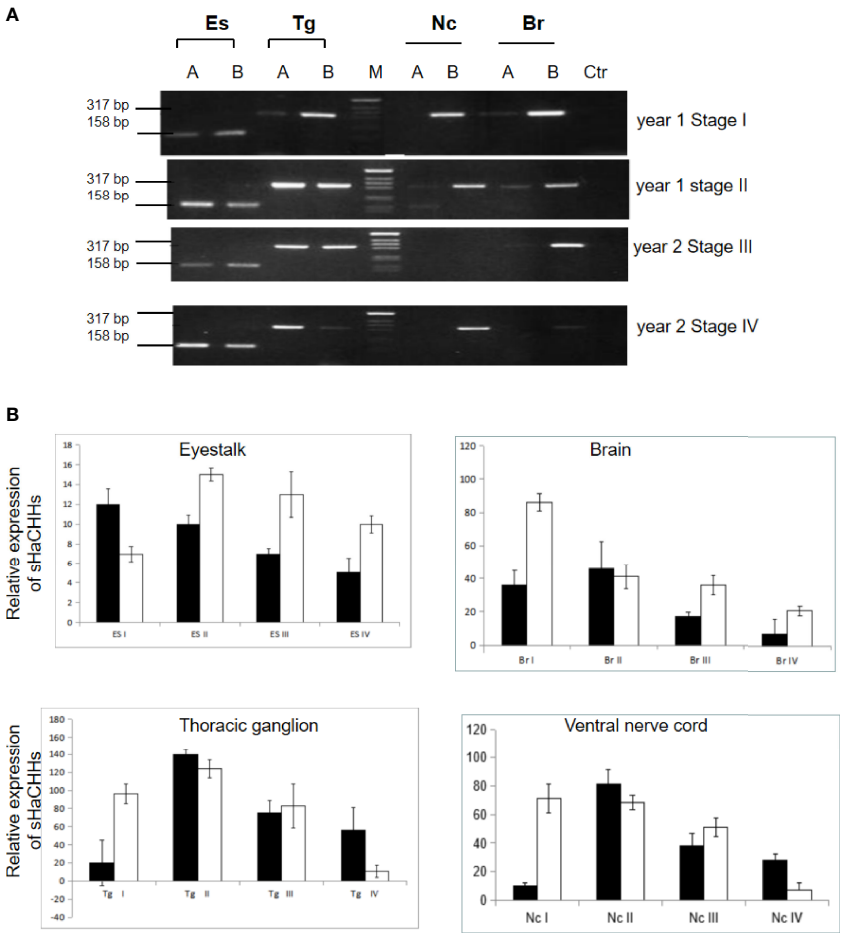


**FIGURE 7** | Expression study of sHaCHH-A and sHaCHH-B by Semi-quantitative **(A)** and **(B)** qPCR. **(A)** Agarose gel analysis of the PCR products and detection of the sHaCHH-A, HaCHH-A sHaCHH-B, HaCHH-B. The lanes A used primers for HaCHH-A gene and lane B used primers for HaCHH-B forcDNA from eyestalk (Es), thoracic ganglion (Tg), ventral nerve cord (Nc) and brain (Br).

genomic and transcriptomic sequence data from *L. vannamei* and *P. monodon*, it is evident that the CHH family consists of multiple gene members. In *L. vannamei*, it is estimated that at least >65 CHH family genes are present in the genome (Zhang et al., 2019). However only a small portion of the CHH genes had the four-exon gene organization. Therefore, the four-exon CHH genes from the decapods shown in the phylogenetic tree in **Figure 4** represent a very small portion of the same species within the same gene family. Although the number of CHH genes reported in lobster was fewer, it is unlikely that *H. americanus* consists of only two highly homologous four-exon CHH genes. From the recent lobster genome project (Polinski et al., 2021), we only identified <5 CHH-related genes. Moreover, no positive sequence was returned when we used several lobster genes (from our lobster transcriptome project) as the query sequence to the BLAST search against the lobster genome. Therefore, additional lobster CHH-like sequences may exist, but were missed in the lobster genome project. Despite the ambiguity, the lobster genome should consist of fewer number of CHH/MIH/GIH genes compared to the shrimps. From the expression and multiple alignment results (**Figure 5**), some generalizations can be proposed. The non-eyestalk expressed transcript is usually the larger CHH variant derived from the four-exon transcript. In addition, due to the broad distribution of the transcripts in the non-eyestalk and non-neuronal tissues, it is suggested that they may have a broad spectrum of functions.

Structurally, the *sHaCHH-A* and *sHaCHH-B* identified in this study had the major features of the CHH neuropeptide, and they shared identical lengths with the mature peptides and are conserved in other lobsters. In the lobster *N. norvegicus*, despite two *NnCHH* being cloned, the two cDNAs shared >98% amino acid identity in the mature peptide region; a second CHH that shares similar exon 3 has not been reported. In *L. vannamei* (GenBank no. AAK69346.1) and *P. monodon* (GenBank no. XP_037787978) CHH-like, they also consisted of identical amino acid residues in the mature peptide region. All the short/smaller CHH-like variants were derived from longer transcripts consisting of exons 1–4. For example, in *Fenneropenaeus merguiensis*, the gill form CHH-like was derived from a longer transcript (i.e., exons 1–4) and the larger

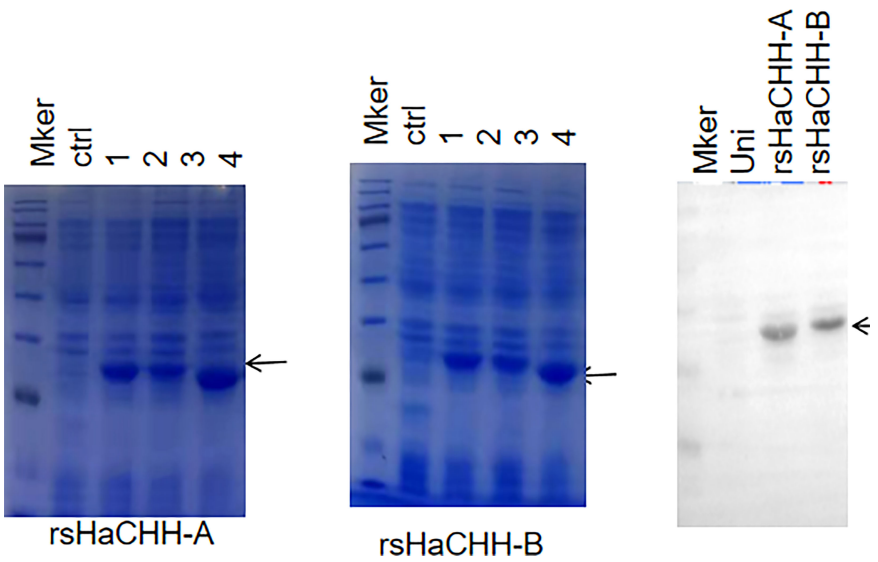


**FIGURE 8** | SDS-PAGE (12.5%) analysis of the prokaryotic (*Escherichia coli*) expression of the recombinant proteins rsHaCHH-A (*left*) and rsHaCHH-B (*middle*) after induction by IPTG. *Ctrl*: uninduced (*uni*); *lanes 1–4*: induced and sampled at 2, 4, 6, and 8 h, respectively. Western blot detection of the poly-His-tagged recombinant proteins sHaCHH-A and sHaCHH-B (*arrow*). *Right*: The antibody used is the anti-polyhistidine peroxidase conjugate antibody (Sangon Biotech, Shanghai, China).

CHH-like was derived from a smaller transcript consisting of exons 1, 2, and 4 (Shi et al., 2018). The mature peptides of *sHaCHH-A* and *sHaCHH-B*, and *sNnCHH-A* and *sNnCHH-B* consisted of 73 and 74 amino acid sequences, respectively (Mettulio et al., 2004). The phylogenetic tree also revealed that the four-exon *CHH-L/S* gene (**Figure 5**) may be derived from the common ancestor gene that gave rise to the more abundant three-exon CHH genes (i.e., *LvCHH2*; GenBank no. QEE046000.1) and the *MIH/GIH* subtype. In the lobster *H. americanus*, a three-exon *HaCHH* gene was identified from the recent genome sequencing project (GenBank no. XP_042225458.1) and can be grouped into the CHH-like class, as indicated in **Figure 5**.

## Four-Exon CHH Gene in Decapod Crustaceans

Although the four-exon CHH family genes have been reported in several decapods, but only the complete gene structure of *L. vannamei* is known. For the other decapods—the crab, freshwater shrimp, and crayfish—only the partial gene structure was revealed, and sequence information for the first intron was missing. We speculated that the gene organizations of these four-exon CHHs among decapods are highly similar. The sequence for the first intron of the CHH gene in *L. vannamei* was obtained from a genome sequencing project. The first intron of the CHH gene is 4.65 kb, and within this region, several highly repetitive simple sequence repeats (SSRs) exist. This highly repetitive sequence would affect the PCR reaction and, therefore, cause failure in genomic PCR (GenBank no. LOC113815764). Therefore, it is likely that the first exon of these decapod CHH genes is also made up of a large intron 1 and may consist of highly repetitive SSRs within the intron that hinder/disrupt the PCR amplification.

## CHH Sequence Comparison

In terms of the evolutionary relationship of the CHH family genes, it was speculated that their original prototype consisted of three exons and two introns. The evolution of the CHH family genes began from gene duplication and mutation (Chan et al., 2003; Montagné et al., 2008; Chung et al., 2010; Chen et al., 2020). Alignment of the four-exon CHH neuropeptide genes revealed both similarities and differences among decapods. The lobster *HaCHH-A* and *HaCHH-B* shared >95%–100% amino acid identity with the lobster CHHs. The similarity was much higher (i.e., 99% amino acid identity) in the mature peptide region. In the Norway lobster *Nephrops norvegius*, two CHHs were cloned (i.e., GenBank nos. AY285782 and AY285783), which differed only in the signal peptide region, but the mature peptide showed 100% sequence identity (Mettulio et al., 2004). *HaCHH-A* and *HaCHH-B* shared only 77%–78% amino acid identity with the crayfish *P. clarkii* CHH-like (78.1%; GenBank no. Q25683) and *Astacus leptodactyl* (i.e., 77.3%; GenBank no. AAX09331). In earlier studies, the CHH family neuropeptides were reported to be expressed only in the eyestalks. Increasing evidence from recent expression studies has confirmed the expression of CHH family members in other non-eyestalk neuronal and non-neuronal tissues. So far, *H. americanus* is the only decapod consisting of two 4-exon CHH family genes, and these two genes could produce four different transcripts.

The original *HaCHH-A* and *HaCHH-B* transcripts are abundant in the eyestalk; therefore, RT-PCR cannot amplify

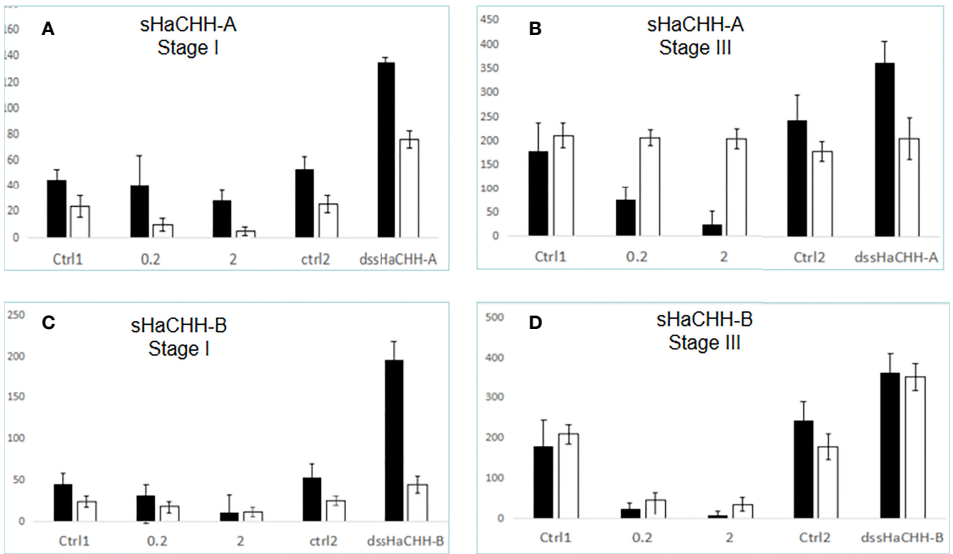


**FIGURE 9** | Effect of recombinant proteinand dsRNA for sHaCHH **(A, B)** and sHaCHH-B **(C, D)** on HaVg1 gene expression. The *Y*-axis shows the relative expression level of the *HaVg1* gene in the hepatopancreas (*black bar*) and ovary (*open white bar*). Triplicate tests (*N* = 4 samples) were performed for each animal. The lobsters used were in the early stage of vitellogenesis (stage I) and middle–late stage (stage III) of the gonad maturation cycle. Tissue fragments were placed inside the well containing 1.5 ml of the nutrient medium M199 with either the control recombinant protein (0, 0.2, or 2.0 μg/PBS) and ctrl2 dsTFV, 2 μg dssHaCHH-A, or dssHaCHH-B. After incubating for 3 h, the hepatopancreas and ovary fragments were analyzed for the expression of *HaVg1*. The vitellogenin gene-specific primer was derived from the *HaVg1* cDNA, as reported earlier (Tiu et al., 2008). Data are the mean ± SE.

the larger transcripts in the eyestalk. In early studies, polyclonal antibodies for *HaCHH-A* and *HaCHH-B* were produced to determine the titer of CHH during the reproductive cycle of females. For example, in *N. norvegicus*, CHH antibodies have been generated to localize the neuropeptide by immunocytochemistry (Giulianini et al., 2002). Other antibodies for CHH were produced, and ELISA was performed to measure the concentration of CHH-A in the hemolymph (Chang et al., 1998; Chang et al., 1999). The cross-reactivity of the polyclonal antibody to *sHaCHH-A* and *sHaCHH-B* has not been evaluated. Therefore, it is necessary to reexamine the protein level of CHH during the reproductive cycle using more specific antisera against specific isoforms. The role of *sHaCHH-A* and *sHaCHH-B* in other neuronal tissues, i.e., brain, thoracic ganglion, and ventral nerve cord, has not been examined. In short, more specific antibody is needed to determine the protein expression patterns of sHaCHH during the lobster reproductive cycle.

The two CHH genes reported in this study can produce a total of four different transcripts (i.e., *HaCHH-A*, *sHaCHH-A*, *HaCHH-B*, and *sHaCHH-B*). However, the expressions of these transcript variants appeared to be tightly regulated as they may exist in a specific temporal and spatial manner. One of the major controversies in the study of *HaCHH-A* expression and protein level was the lack of correlation in both the mRNA and peptide levels in the hemolymph during the pre-vitellogenic stage (de Kleijn et al., 1998). For *HaCHH-B*, the total mRNA and hemolymph CHH peptide levels increased in the mature stage, and there were no differences in peptide storage that may suggest that synthesis is not related to storage (de Kleijn et al., 1998). The interpretation was hampered by the lack of information for these transcripts' variants. The expression study was focused only on the mRNA in the eyestalk, and the antibody used to detect *HaCHH-A* and *HaCHH-B* may not be able to differentiate *sHaCHH-A* and/or *sHaCHH-B*. Therefore, a more systematic approach for the study of the titer and expression patterns must be reinvestigated to fully elucidate the roles of these hormones in lobster reproduction control.

Alternative splicing is a method used to create more proteins from the same gene (Baralle and Giudice, 2017; Gallego-Paez et al., 2017; Modrek and Lee, 2002). It is an essential mechanism increasing the complexity of gene expression, and it plays an important role in cellular differentiation and organism development. There are several reports for the alternative splicing of the CHH gene in crustaceans (Dircksen et al., 2003; Chen et al., 2004; Jeon et al., 2012; Shi et al., 2018; Sun et al., 2019). In the Morotoge shrimp *Pandalopsis japonica*, an eyestalk form and a pericardial organ isoform were identified. Although the reproductive function of the CHH variant was not studied, eyestalk ablation would reduce the expression of *Pj-CHH1ES* in the brain and *Pj-CHH1*PO and *Pj-CHH2* in the thoracic ganglion (Jeon et al., 2012). The *Mar-CHH* gene of *M. rosenbergii* also consists of four exons. The eyestalk transcript (*chh*) contains exons I, II, and IV, whereas the *CHH-l* transcript in the heart, gills, antennal glands, and thoracic ganglion contains all four exons. Similarly, the *sHaCHH-A* and *sHaCHH-B* transcripts are mainly expressed in non-eyestalk tissues. The production of alternatively spliced variants from a single gene, therefore, would increase the number of proteins in a cell and increase the overall proteome content within the cell. Additionally, these

spliced variants may be produced at different stages of the life cycle (Wang et al., 2015). The differential stage-specific expression of the transcripts in lobster might contribute to its regulation during the reproductive cycle in the biannual reproductive pattern of *H. americanus*. Despite that a similar 3D structure was predicted between HaCHH-A *vs*. *HaCHH-B* and *sHaCHH-A vs*. *sHaCHH-B*, the p*I* values (i.e., hydrophobicity) of the corresponding proteins were quite different. The differences in the hydrophobicity may have allowed different isoforms to work optimally in different pH conditions of the Hp and ovary. Therefore, we hypothesized that, with a lower p*I* value (i.e., 5.27), *sHaCHH-A* may work optimally under a more acidic condition in the Hp, which has a lower pH for the function of the acidic digestive enzyme.

A major challenge in the research on the CHH/MIH/GIH family is the lack of functional studies for most of the members. Therefore, the bioassay/functional confirmation of most CHHs was not performed. The use of recombinant protein and RNAi technique to study the function of the CHH family genes has been reported for the MIH-like in the sand shrimp and the MIH-like in the banana shrimp *F. merguiensis* type II neuropeptide (Gu et al., 2000; Tiu et al., 2008; Liang et al., 2019). Opposing results of the dsRNAs and recombinant proteins were demonstrated in the sand shrimp and in the lobster in this study. Since there are multiple numbers of genes in the CHH/MIH/GIH family, the antagonistic results from the recombinant proteins and dsRNAs may provide a tool to investigate the role of this neuropeptide superfamily.

## CONCLUSION

The present study has confirmed that the previously reported *HaCHH-A* and *HaCHH-B* cDNAs were derived from alternative splicing of two 4-exon CHH genes. The retention of intron 3 and exon 4 produced the transcript variants *sHaCHH-A* and *sHACHH-B*, as reported in this study. Results of the functional study indicated that *sHaCHH-A* and *sHaCHH-B* can regulate the gene expression of vitellogenin. The findings in this study have provided new information on the gene structure organization, precise expression patterns for the transcript variants, and the vitellogenin-inhibiting function of *sHaCHH-A* and *sHaCHH-B*. The results of this report have also provided a basis for reassessing the expression patterns and hemolymph titers of these transcripts during the reproductive cycle of the female lobster.

## DATA AVAILABILITY STATEMENT

The raw data supporting the conclusions of this article will be made available by the authors, without undue reservation.

## AUTHOR CONTRIBUTIONS

SC: conceptualization, writing—original draft preparation, project administration, and funding acquisition. SC, CGW, and YS: methodology. CGW: software and resources. WW: validation. YS and WW: formal analysis. WG and SC: writing—review and editing. LLS: visualization. YS and SC: supervision. All authors contributed to the article and approved the submitted version.

## FUNDING

This study was funded in part by the National Natural Science Foundation of China (#31572606) and Zhanjiang City Fund.

## REFERENCES

Baralle, F. E., and Giudice, J. (2017). Alternative Splicing as a Regulator of Development and Tissue Identity. *Nat. Rev. Mol. Cell Biol.* 18, 437–451. doi: 10.1038/nrm

Chang, E. S., Chang, S. A., Beltz, B. S., and Kravitz, E. A. (1999). Crustacean Hyperglycemic Hormone in the Lobster Nervous System: Localization and Release From Cells in the Subesophageal Ganglion and Thoracic Second Roots. *J. Comp. Neurol.* 414, 50–56. doi: 10.1002/(SICI)1096-9861(19991108)414:1<50::AID-CNE4>3.0.CO;2-Q

Chang, E. S., Keller, R., and Chang, S. A. (1998). Quantification of Crustacean Hyperglycemic Hormone by ELISA in Hemolymph of the Lobster, *Homarus Americanu*s, Following Various Stresses. *Gen. Comp. Endocrinol.* 111, 359–366. doi: 10.1006/gcen.1998.7120

Chang, W. H., and Lai, A. G. (2018). Comparative Genomic Analysis of Crustacean Hyperglycemic Hormone (CHH) Neuropeptide Genes Across Diverse Crustacean Species. *F1000Res* 7, 100. doi: 10.12688/f1000research.13732.1

Chan, S. M., Gu, P. L., and Chu, K. H. (2003). Crustacean Neuropeptide Genes of the CHH/MIH/GIH Family: Implications From Molecular Studies. *Gen. Comp. Endocrinol.* 134, 214–219. doi: 10.1016/S0016-6480(03)00263-6

Chen, S. H., Lin, C. Y., and Kuo, C. M. (2004). Cloning of Two Crustacean Hyperglycemic Hormone Isoforms in Freshwater Giant Prawn (*Macrobrachium Rosenbergii*): Evidence of Alternative Splicing. *Mar Biotechnol. (NY)* 6, 83–94. doi: 10.1007/s10126-003-0014-8

Chen, H. Y., Toullec, J. Y., and Lee, C. Y. (2020). The Crustacean Hyperglycemic Hormone Superfamily: Progress Made in the Past Decade. *Front. Endocrinol. (Lausanne)* 11. doi: 10.3389/fendo.2020.578958

Chung, J. S., Christie, A., and Flynn, E. (2020). Molecular Cloning of Crustacean Hyperglycemic Hormone (CHH) Family Members (CHH, Molt-Inhibiting Hormone and Mandibular Organ-Inhibiting Hormone) and Their Expression Levels in the Jonah Crab. *Cancer Borealis Gen. Comp. Endocrinol.* 1 (295), 113522. doi: 10.1016/j.ygcen.2020.113522

Chung, J. S., Zmora, N., Katayama, H., and Tsutsui, N. (2010). Review. Crustacean Hyperglycemic Hormone (CHH) Neuropeptides Family: Functions, Titer, and Binding to Target Tissues. *Gen. Comp. Endocrinol.* 166, 447–454. doi: 10.1016/j.ygcen.2009.12.011

De Kleijn, D. P., De Leeuw, E. P., Van den Berg, M. C., Martens, G. J., and Van Herp, F. (1995). Cloning and Expression of Two mRNAs Encoding Structurally Different Crustacean Hyperglycemic Hormone Precursors in the Lobster. *Homarus Americanus Biochim. Biophys. Acta* 1260, 62–66.

de Kleijn, D. P., Janssen, K. P., Waddy, S. L., Hegeman, R., Lai, W. Y., Martens, G. J., and Van Herp, F. (1998). Expression of the Crustacean Hyperglycaemic Hormones and the Gonad-Inhibiting Hormone During the Reproductive Cycle of the Female American Lobster Homarus Americanus. *J. Endocrinol.* 156 (2), 291–298. doi: 10.1677/joe.0.1560291

De Kleijn, D. P., Janssen, K. P., Martens, G. J., and Van Herp, F. (1994). Cloning and Expression of Two Crustacean Hyperglycemic-Hormone mRNAs in the Eyestalk of the Crayfish. *Orconectes Limosus Eur. J. Biochem.* 224, 623–629. doi: 10.1111/j.1432-1033.1994.00623.x

De Kleijn, D. P., and Van Herp, F. (1995). Molecular Biology of Neurohormone Precursors in the Eyestalk of. *Crustacea. Comp. Biochem. Physiol. B. Biochem. Mol. Biol.* 112, 573–579. doi: 10.1016/0305-0491(95)00126-3

Dircksen, H., Böcking, D., Heyn, U., Mandel, C., Chung, J. S, Baggerman, G., et al. (2003). Crustacean Hyperglycaemic Hormone (CHH)-Like Peptides and CHH-Precursor-Related Peptides From Pericardial Organ Neurosecretory Cells in the Shore Crab, Carcinus Maenas, are Putatively Spliced and Modified Products of Multiple Genes. *Biochem. J.* 356, 159–170. doi: 10.1042/bj3560159

Diwan, A. D. (2005). Current Progress in Shrimp Endocrinology. *Indian J. Exp. Biol.* 43, 209–223.

Fingerman, M. (1987). The Endocrine Mechanisms of Crustaceans. *J. Crustacean Biol.* 7, 1–24. doi: 10.2307/1548622

Gallego-Paez, L. M., Bordone, M. C., Leote, A. C., Saraiva-Agostinho, N., Ascensão-Ferreira, M., and Barbosa-Morais, N. L. (2017). Alternative Splicing: The Pledge, the Turn, and the Prestige: The Key Role of Alternative Splicing in Human Biological Systems. *Hum. Genet.* 136, 1015–1042. doi: 10.1007/s00439-017-1790-y

Giulianini, P. G., Pandolfelli, N., Lorenzon, S., Ferrero, E. A., and Edomi, P. (2002). An Antibody to Recombinant Crustacean Hyperglycaemic Hormone of *Nephrops Norvegicus* Cross-Reacts With Neuroendocrine Organs of Several Taxa of Malacostracan Crustacea. *Cell Tissue Res.* 307, 243–254. doi: 10.1007/s00441-001-0484-9

Gu, P. L., Yu, K. L., and Chan, S. M. (2000). Molecular Characterization of an Additional Shrimp Hyperglycemic Hormone: cDNA Cloning, Gene Organization, Expression and Biological Assay of Recombinant Proteins. *FEBS Lett.* 472, 122–128. doi: 10.1016/S0014-5793(00)01420-4

Havird, J. C., and Santos, S. R. (2016). Here We Are, But Where Do We Go? A Systematic Review of Crustacean Transcriptomic Studies From 2014-2015. *Integr. Comp. Biol.* 56 (6), 1055–1066. doi: 10.1093/icb/icw061

Helluy, S. M., and Beltz, B. S. (1991). Embryonic Development of the American Lobster (*Homarus Americanus*): Quantitative Staging and Characterization of an Embryonic Molt Cycle. *Biol. Bull.* 180, 355–371. doi: 10.2307/1542337

Huberman, A. (2000). Shrimp Endocrinology: A Review. *Aquaculture* 191, 191–208. doi: 10.1016/S0044-8486(00)00428-2

Hyde, C. J., Fitzgibbon, Q. P., Elizur, A., Smith, G. G., and Ventura, T. (2020). CrustyBase: An Interactive Online Database for Crustacean Transcriptomes. *BMC Genomics* 21, 637. doi: 10.1186/s12864-020-07063-2

Jayasankar, V., Tomy, S., and Wilder, M. N. (2020). Insights on Molecular Mechanisms of Ovarian Development in Decapod Crustacea: Focus on Vitellogenesis-Stimulating Factors and Pathways. *Front. Endocrinol. (Lausanne)* 11. doi: 10.3389/fendo.2020.577925

Jeon, J.-M., Kim, B.-K., Lee, J. H., Kim, H. K., Kang, C.-K., Mykles, D. L., et al. (2012). Two Type I Crustacean Hyperglycemic Hormone (CHH) Genes in Morotoge Shrimp (*Pandalopsis Japonica*): Cloning and Expression of Eyestalk and Pericardial Organ Isoforms Produced by Alternative Splicing and a Novel Type I CHH With Predicted Structure Shared With Type II CHH Peptides Comp. *Biochem. Physiol. B Biochem. Mol. Biol.* 162 (4), 88–99. doi: 10.1016/j.cbpb.2012.04.003

Keller, R. (1992). Crustacean Neuropeptides: Structures, Functions and Comparative Aspects. *Experientia* 48, 439–448. doi: 10.1007/BF01928162

Liang, H. F., Liu, Y., Zhou, T. T., Li, ,. X. Y., Li, B., Chan, S.F, et al. (2019). Molecular Characterization, RNA Interference and Recombinant Protein Approach to Study the Function of the Putative Molt Inhibiting Hormone (FmMIH1) Gene From the Shrimp *Fenneropenaeus Merguiensis*. *Peptides* 122, 1–12. doi: 10.1016/j.peptides.2017.10.017

Loredo-Ranjel, R., Fanjul-Moles, M. L., and Escamilla-Chimal, E. G. (2017). Crustacean Hyperglycemic Hormone Is Synthesized in the Eyestalk and Brain of the Crayfish *Procambarus Clarkii*. *PloS One* 12 (4), e0175046. doi: 10.1371/journal.pone.0175046

Magaña-Gallegos, E., Arévalo, M., Cuzon, G., and Gaxiola, G. (2021). Effects of Using the Biofloc System and Eyestalk Ablation on Reproductive Performance and Egg Quality of *Litopenaeus Vannamei* (Boon) (Decapoda: Dendrobranchiata: Penaeidae). *Anim. Reprod. Sci.* 228, 106749. doi: 10.1016/j.anireprosci.2021.106749

Mettulio, R., Edomi, P., Ferrero, E. A., Lorenzon, S., and Giulianini, P. G. (2004). The Crustacean Hyperglycemic Hormone Precursors a and B of the Norway Lobster Differ in the Preprohormone But Not in the Mature Peptide. *Peptides* 25, 1899–1907. doi: 10.1016/j.peptides.2004.06.013

Modrek, B., and Lee, C. (2002). A Genomic View of Alternative Splicing. *Nat. Genet.* 30, 13–19. doi: 10.1038/ng0102-13

Montagné, N., Soyez, D., Céline, D., Jean-Yves, G., and Toullec, O. (2008). New Insights Into Evolution of Crustacean Hyperglycaemic Hormone in Decapods–First Characterization in Anomura. *FEBS J.* 275, 1039–1052. doi: 10.1111/j.1742-4658.2007.06245.x

Mykles, D. L., and Chang, E. S. (2020). Hormonal Control of the Crustacean Molting Gland: Insights From Transcriptomics and Proteomics. *Gen. Comp. Endocrinol.* 294, 113493. doi: 10.1016/j.ygcen.2020.113493

Okumura,,. T., and Aida, K. (2001). Effects of Bilateral Eyestalk Ablation on Molting and Ovarian Development in the Giant Freshwater Prawn. *Macrobrachium Rosenbergii Fish Sci.* 67, 1125–1135. doi: 10.1046/j.1444-2906.2001.00370.x

Oliphant, A., Alexander, J. L., Swain, M. T., Webster, S. G., and Wilcockson, D. C. (2018). Transcriptomic Analysis of Crustacean Neuropeptide Signaling During the Moult Cycle in the Green Shore Crab, *Carcinus Maenas*. *BMC Genomics* 19, 711–720. doi: 10.1186/s12864-018-5057-3

Panouse, J. B. (1943). Influence De L'ablation Du Pédoncle Oculaire Sur La Croissance De L'ovaire Chez La Crevette *Leander Serratus*. *Comptes Rendus l'Académie Des. Sci.* 217, 553–555.

Polinski, J. M., Zimin, A. V., Clark, K. F., Kohn, A. B., Sadowski, N., and Timp, W. (2021). The American Lobster Genome Reveals Insights on Longevity, Neural, and Immune Adaptations. *Sci. Adv.* 7 (26). doi: 10.1126/sciadv.abe8290.

Primavera, J. H. (1978). Induced Maturation and Spawning in Five-Month-Old *Penaeus Monodon* Fabricius by Eyestalk Ablation. *Aquacult* 13, 355–359. doi: 10.1016/0044-8486(78)90184-9

Reddy, P. R., and Kishori, B. (2017). Mini Review. Crustacean Endocrinology: Intriguing Towards Quality Protein Production. *J. Endocrinol. Thyroid Res.* 1 (2), 555556. doi: 10.19080/JETR.2017.01.555556

Shi, L., Li, B., Zhou, T. T., Wang, W., and Chan, S. F. (2018). Functional and Evolutionary Implications From the Molecular Characterization of Five Spermatophore CHH/MIH/GIH Genes in the Shrimp. *Fenneropenaeus Merguiensis PloS One* 19, 13(3):e0193375. doi: 10.1371/journal.pone.0193375

Sun, D., Lv, J., Gao, B., Liu, P., and Li, J. (2019). Crustacean Hyperglycemic Hormone of *Portunus Trituberculatus*: Evidence of Alternative Splicing and Potential Roles in Osmoregulation. *Cell Stress Chaperones* 24, 517–525. doi: 10.1007/s12192-019-00980-6

Tensen, C. P., Verhoeven, A. H., Gaus, G., Janssen, K. P., Keller, R., and Van Herp, F. (1991). Isolation and Amino Acid Sequence of Crustacean Hyperglycemic Hormone Precursor-Related Peptides. *Peptides* 12, 673–681. doi: 10.1016/0196-9781(91)90119-A

Tiu, S. H. K., and Chan, S.-M. (2007). The Use of Recombinant Protein and RNA Interference Approaches to Study the Reproductive Functions of a Gonad-Stimulating Hormone From the Shrimp *Metapenaeus Ensis*. *FEBS J.* 274, 4385–4395. doi: 10.1111/j.1742-4658.2007.05968.x

Tiu, S. H., Hui, H. L., Tsukimura, B., Tobe, S. S., He, J. G., and Chan, S. M. (2009). Cloning and Expression Study of the Lobster (*Homarus Americanus*) Vitellogenin: Conservation in Gene Structure Among Decapods. *Gen. Comp. Endocrinol.* 160, 36–46. doi: 10.1016/j.ygcen.2008.10.014

Uawisetwathana, U., Leelatanawit, R., Klanchui, A., Prommoon, J., Klinbunga, S., and Karoonuthaisiri, N. (2011). Insights Into Eyestalk Ablation Mechanism to Induce Ovarian Maturation in the Black Tiger Shrimp. *PloS One* 6, e24427. doi: 10.1371/journal.pone.0024427

Wang, Y., Liu, J., Huang, B. O., Xu, Y. M., Li, J., Huang, L. F., et al. (2015). Mechanism of Alternative Splicing and its Regulation. *Biomed. Rep.* 3, 152–158. doi: 10.3892/br.2014.407

Webster, S. G. (2001). Crustacean Hyperglycaemic Hormone (CHH)-Like Peptides and CHH-Precursor-Related Peptides From Pericardial Organ Neurosecretory Cells in the Shore Crab, Carcinus Maenas, are Putatively Spliced and Modified Products of Multiple Genes. *Biochem. J.* 356, 159–170. doi: 10.1042/bj3560159

Webster, S. G., Keller, R., and Dircksen, H. (2012). The CHH-Superfamily of Multifunctional Peptide Hormones Controlling Crustacean Metabolism, Osmoregulation, Moulting, and Reproduction. *Gen. Comp. Endocrinol.* 175, 217–233. doi: 10.1016/j.ygcen.2011.11.035

Zhang, X., Yuan, J., Sun, Y., Li, S., Gao, Y., Yu, Y., et al. (2019). Penaeid Shrimp Genome Provides Insights Into Benthic Adaptation and Frequent Molting. *Nat. Commun.* 10, 356. doi: 10.1038/s41467-018-08197-4

**Conflict of Interest:** The authors declare that the research was conducted in the absence of any commercial or financial relationships that could be construed as a potential conflict of interest.

**Publisher's Note:** All claims expressed in this article are solely those of the authors and do not necessarily represent those of their affiliated organizations, or those of the publisher, the editors and the reviewers. Any product that may be evaluated in this article, or claim that may be made by its manufacturer, is not guaranteed or endorsed by the publisher.

frontiers | Frontiers in Physiology

ORIGINAL RESEARCH
published: 28 April 2022
doi: 10.3389/fphys.2022.883621

# Low Omega-3 Levels in the Diet Disturbs Intestinal Barrier and Transporting Functions of Atlantic Salmon Freshwater and Seawater Smolts

*Kristina Sundell*[1], *Gerd Marit Berge*[2], *Bente Ruyter*[2,3] *and Henrik Sundh*[1]*

[1]Swedish Mariculture Research Center, Department of Biological and Environmental Sciences, University of Gothenburg, Gothenburg, Sweden, [2]Norwegian Institute of Food, Fisheries and Aquaculture Research (Nofima), Nofima, Sjølsengen, Sunndalsøra, Norway, [3]Nofima, Ås, Norway

Due to a limited access to marine raw materials from capture fisheries, Atlantic salmon feeds are currently based on mainly plant ingredients (75%) while only 25% come from traditional marine ingredients including marine fish meal and fish oil. Thus, current feeds contain less of the essential omega-3 fatty acids. The aim of the study was to assess the impact of different omega-3 levels in fish feed on intestinal barrier and transporting functions of Atlantic salmon freshwater and seawater smolts. Atlantic salmon were fed three levels of omega-3 (2, 1 and 0.5%) and fish performance was followed through smoltification and the subsequent seawater acclimation. Intestinal barrier and transporting functions were assessed using Ussing chamber methodology and combined with transcript analysis of tight junction related proteins and ion transporters. A linear decrease in growth was observed with decreasing omega-3 levels. Low (0.5%) inclusion of omega-3 impaired the barrier function of the proximal intestine compared to 2% inclusion. Further, low levels of omega-3 decrease the transepithelial electrical potential across the epithelium indicating disturbed ion transport. It can be concluded that low dietary levels of omega-3 impair somatic growth and intestinal function of Atlantic salmon.

**Keywords: omega-3, Atlantic salmon, intestinal transport, intestinal barrier function, tight junctions**

OPEN ACCESS

***Edited by:***
*Marce Herrera,*
*IFAPA Centro Agua del Pino, Spain*

***Reviewed by:***
*Yang Jin,*
*Norwegian University of Life Sciences, Norway*
*Anne Marie Bakke,*
*Waltham Petcare Science Institute, United Kingdom*

***Correspondence:**
*Henrik Sundh*
*henrik.sundh@bioenv.gu.se*

***Specialty section:***
*This article was submitted to Aquatic Physiology, a section of the journal Frontiers in Physiology*

***Received:*** *25 February 2022*
***Accepted:*** *08 April 2022*
***Published:*** *28 April 2022*

***Citation:***
*Sundell K, Berge GM, Ruyter B and Sundh H (2022) Low Omega-3 Levels in the Diet Disturbs Intestinal Barrier and Transporting Functions of Atlantic Salmon Freshwater and Seawater Smolts. Front. Physiol. 13:883621. doi: 10.3389/fphys.2022.883621*

## INTRODUCTION

The long chain omega-3 fatty acids EPA (20:5 n-3; eicosapentaenoic acid) and DHA (22:6 n-3; docosahexaenoic acid) are essential for the health and normal development of Atlantic salmon (Ruyter et al., 2000a, 2000b; Bou et al., 2017a, 2017b). These fatty acids play a key role in maintenance of proper structure and function of the cell membranes, being parts of the amphipathic lipids constituting the membranes and precursors for signaling molecules like eicosanoids and resolvins as well as regulators of the transcription of genes involved in lipid metabolism (Miyazaki and Ntambi, 2008; Smith and Murphy, 2015). Fish oil and fish meal have traditionally been the main sources of EPA and DHA for the Atlantic salmon (*Salmo salar* L.) aquaculture industry (Ytrestøyl et al., 2015; Aas et al., 2019). Due to a limited access to marine raw materials as well as ethical considerations regarding capture fisheries and the utilization of human food grade fish for fish feed production,

salmon feed have developed to substitute marine ingredients with plant-based alternatives and currently most salmon feeds contain ca. 25% marine ingredients and 75% plant ingredients (Aas et al., 2019).

The intestine is a multifunctional organ, where the intestinal epithelium absorbs ions, fluid and nutrients in a controlled manner while efficiently restricts harmful agents in the intestinal lumen to reach the circulatory system (Veillette et al., 1993, 1995; Sundell et al., 2003; Tipsmark et al., 2010a, 2010b; Sundell and Rønnestad, 2011; Sundell and Sundh, 2012; Sundh et al., 2014; Sundh and Sundell, 2015). The Atlantic salmon intestine thus act as a selective primary barrier towards the environment. The intrinsic intestinal barrier consists of the epithelial cells (enterocytes), connected at the apical side through intercellular protein complexes collectively known as the tight junction (TJ). The TJ consists of a range of different integral membrane proteins (e.g. occludin and claudins) and associated cytoplasmic proteins such as ZO-1 (Günzel and Fromm, 2012). TJs provide two types of barrier functions, 1) a fence, that sustain epithelial polarity by restricting lateral diffusion of membrane proteins from the apical to the basolateral membrane and vice versa and 2) a gate, that maintain a high selectivity for passive transfer of substances (diffusion) through the paracellular pathway (Günzel and Fromm, 2012). The gate function is mainly determined by the type of claudin isoforms present in the TJ (Anderson and Van Itallie, 2009; Günzel and Yu, 2013). In fish, 63 claudin isoforms have been described in 16 different species (Kolosov et al., 2013). Recent findings suggest that at least 26 claudin isoforms are expressed in tissues of the Atlantic salmon (Tipsmark et al., 2008), where claudin-15, and 25b are suggested to be specific for the intestine (Tipsmark et al., 2010a).

Intestinal barrier and transporting functions are essential for fish health and welfare (Segner et al., 2012; Sundh and Sundell, 2015). Impaired intestinal barrier function, *i.e.* a leaky gut, is correlated to intestinal inflammation and a disturbed intestinal immune barrier of Atlantic salmon (Knudsen et al., 2008; Sundh et al., 2010, 2019; Niklasson et al., 2011) and may result in decreased disease resistance (Sundh et al., 2009). In this perspective, the composition of the feed is essential for the intestinal health as the intestine is the first organ to be exposed to the digested feed. A suboptimal feed with poor nutritional value or which contain anti nutrient factors impairs the intestinal barrier function (Knudsen et al., 2008; Vidakovic et al., 2015; Estensoro et al., 2016).

To ensure a healthy salmon, there has been an increasing focus on studying the effects of the current development of commercial salmon feed with lower and lower levels of EPA and DHA. In trout deprived of essential fatty acids, reduced apical uptake of $Na^+$ (Nonnotte et al., 1987) and modulated osmoregulatory ability after transfer to seawater have been reported (Finstad and Thomassen, 1991). Further, a lack of essential fatty acids is reported to reduce growth and increase lipid accumulation in the intestine (Olsen et al., 1999, 2003; Bou et al., 2017a) as well as reduce the stress coping ability of salmonids (Bou et al., 2017b; Løvmo et al., 2021). Low dietary levels of EPA and DHA also lead to reduced levels of EPA and DHA in the enterocyte plasma membrane phospholipids (PLs), whereas the pro-inflammatory n-6 fatty acids levels increase (Bou et al., 2017a; 2017b). In gilthead seabream, intestinal barrier functions are negatively affected by low levels of omega-3 in feed (Estensoro et al., 2016). If and how the intestinal health of the Atlantic salmon is affected by low levels of EPA and DHA in the feed is currently unknown.

The aim of the present study was to assess the impact of different omega-3 levels in fish feed on general fish health and welfare and intestinal barrier and transporting functions of Atlantic salmon fresh- and seawater smolts. Fish growth and mortality as well as plasma ion levels are well known indicators for fish health and welfare and osmoregulatory capacity (Noble et al., 2018). Further, as the intestine is the first organ to potentially be affected by the fatty acid composition of the feed, the fatty acid composition of the phospholipids (PLs) in intestinal tissue was determined. Intestinal barrier and transporting functions were assessed using the Ussing-chamber methodology. Finally, the expression of key TJ proteins was determined using qPCR.

# MATERIALS AND METHODS

## Experimental Fish and Rearing Conditions

Atlantic salmon parr with an average weight of 60 g, originating from the SalmoBreed strain, were used for the trial. At the beginning of the trial, 120 fish were stocked in each of nine experimental units, 500 L cylindrical fiberglass tanks supplied with recirculating freshwater at 12.4 (std 0.6)°C. The fish were initially held at short day-length (12 h light:12 h dark) for 6 weeks, followed by another 4 weeks with 24 h light to induce smoltification. When fish were ready for transfer to seawater (salinity 32–33 ppt and temperature 13.0 (std.1.0)°C), all fish groups were moved to nine larger, 3,2 $m^3$ tanks for the seawater period of the trial. The entire feeding trial was done in the Nofima Centre for Recirculation in Aquaculture (NCRA) in Sunndalsøra, Norway, using recirculated water. The RAS systems are described in detail by (Terjesen et al., 2013). The experiment was terminated 96 days after seawater transfer. The experiment was performed in compliance with the Norwegian national regulation for use of experimental animals (NARA, FOR-2015-06-18-761) and the National Guidelines for Animal Care and Welfare published by the Norwegian Ministry of Education and Research and approved by Norwegian Food Safety Authority (FOTS); approval nr. 11666.

## Experimental Diets and Feeding

Three experimental diets with different levels of the omega-3 fatty acids EPA and DHA were produced at Nofimas Feed Technology Center in Bergen, Norway. Composition of the diets is presented in **Table 1**, and fatty acid profiles in **Table 2**.

Each of the test diets were fed to triplicate groups of fish, through both periods of the experiment. Feeding was planned according to estimated growth rate, but adjusted according to observed appetite. The fish were fed approximately 15–20% in

**TABLE 1 |** Composition of experimental diets.

| | 2% EPA + DHA | 1% EPA + DHA | 0.5% EPA + DHA |
|---|---|---|---|
| g 100 $g^{-1}$ | | | |
| Fish meal[a] | 16.00 | 16.00 | 16.00 |
| Wheat[b] | 7.10 | 7.10 | 7.10 |
| Wheat gluten[c] | 14.40 | 14.40 | 14.40 |
| Soy protein concentrate[d] | 19.00 | 19.00 | 19.00 |
| Corn gluten[e] | 10.00 | 10.00 | 10.00 |
| Horse beans[f] | 4.00 | 4.00 | 4.00 |
| Oil mix[g] | 20.40 | 20.40 | 20.40 |
| Soy lecithin[h] | 1.00 | 1.00 | 1.00 |
| Vitamin mix[i] | 2.00 | 2.00 | 2.00 |
| Mono sodium phosphate[j] | 2.50 | 2.50 | 2.50 |
| Carophyll pink. 10% Ax[k] | 0.05 | 0.05 | 0.05 |
| Yttrium oxide[l] | 0.01 | 0.01 | 0.01 |
| L-lysine[m] | 1.40 | 1.40 | 1.40 |
| Mineral mix without zink[n] | 0.555 | 0.555 | 0.555 |
| Zink[o] | 0.087 | 0.087 | 0.087 |
| Threonine[p] | 0.20 | 0.20 | 0.20 |
| Betafine[q] | 0.50 | 0.50 | 0.50 |
| DL-methionine[r] | 0.80 | 0.80 | 0.80 |
| Chemical content, g 100 $g^{-1}$ | | | |
| Dry matter | 94.4 | 94.3 | 94.0 |
| Total lipid | 26.7 | 26.8 | 26.8 |
| Crude protein | 45.5 | 45.3 | 45.1 |
| Ash | 6.9 | 6.9 | 6.9 |
| Energy, MJ $kg^{-1}$ | 23.0 | 23.0 | 23.0 |

[a]*Fish meal—LT, Fishmeal, Vedde, Norge.*
[b]*Wheat, Møllerens, Norge.*
[c]*Wheat gluten—Vital wheat gluten, Tereos Syral, Belgium.*
[d]*SPC – Soy protein concentrate, Agrokorn, Denmark.*
[e]*Corn gluten—Corn gluten meal, Agrokorn, Denmark.*
[f]*Horse beans, Socomac Rouen, France.*
[g]*Rapeseed oil, Emmelev, Denmark, and Fish oil, Pelagia, Norway.*
[h]*Soy lecithin—Denothin 62, Denofa, Norway.*
[i]*Vitamin-mix—Vilomix, Norway.*
[j]*MSP – Vilomix, Norway.*
[k]*Carophyll pink, 10% Ax—DSM, France.*
[l]*Yttrium oxide—VWR, Norway.*
[m]*L-lysine—Vilomix, Norway.*
[n]*Mineralmix uten Zn—Vilomix, Norway.*
[o]*Organic Zn—Alltech, Norway.*
[p]*Threonine—Vilomix, Norway.*
[q]*Betafine—Vilomix, Norway.*
[r]*DL-methionine—Vilomix, Norway.*

excess to secure *ad libitum* conditions. Fish were weighed at start, at transfer to seawater, and at termination of the seawater feeding period. Specific growth rate (SGR) was calculated according to the following formula:

SGR, % pr day = $(\ln W_2 - \ln W_1)\ (t)^{-1} * 100$; where $W_1$ and $W_2$ are average body weight (g) at start and end of the trial, and t is the number of days in the trial. Mortality was registered daily in each tank, dead fish were removed and individually weighed. Total accumulated mortality was calculated in % of initial number of fish.

## Sampling

Fish were randomly and gently netted and instantly euthanized by an overdose of MS-222. Samples were taken for analysis of plasma ions, fatty acid composition of phospholipids, intestinal gene expression and Ussing chamber analysis of intestinal functions, as described below.

## Plasma Ions

Whole blood was sampled from the caudal vessels using Vacuette® heparinized vacuum tubes (Greiner Bio-One, Kremsmuster, Austria) from five fish in each tank in freshwater 2–4 days before seawater transfer and at 5 and 68 days after transfer to seawater. The blood was centrifuged at 3500 g for 10 min, plasma separated and stored at −80°C until further analyses. Photometric analyses of $Na^+$, $Cl^-$ and $K^+$ were done by Nofima, Sunndalsøra (Pentra C400 HORIBA; HORIBA medical, Montpellier, France).

## Fatty Acid Composition of Phospholipids

Samples of proximal intestines (the region from just after the pyloric caeca to the thicker distal intestine with complex circular folds) for lipid analyses were collected from five fish per tank, after 5 and 68 days in seawater. A pooled sample of five fish per tank was homogenized making in total three pooled samples per dietary

**TABLE 2 |** Fatty acid content in experimental diets, g * 100 $g^{-1}$.

| | 2% EPA + DHA | 1% EPA + DHA | 0.5% EPA + DHA |
|---|---|---|---|
| C 14:0 | 0.66 | 0.30 | 0.14 |
| C 16:0 | 1.81 | 1.48 | 1.35 |
| C 18:0 | 0.31 | 0.34 | 0.36 |
| C 20:0 | 0.06 | 0.08 | 0.09 |
| C 22:0 | 0,04 | 0,05 | 0,05 |
| C 24:0 | 0.03 | 0.02 | 0.02 |
| Sum SFA[a] | 2.96 | 2.32 | 2.04 |
| C 16:1 n-7 | 0.50 | 0.26 | 0.14 |
| C 18:1 n-9 | 4.95 | 7.40 | 8.54 |
| C 18:1 n-7 | 0.41 | 0.51 | 0.54 |
| C 20:1 n-9 | 1.18 | 0.66 | 0.40 |
| C 22:1 n-7 | 0.06 | 0.03 | 0.01 |
| C 22:1 n-11 | 1.59 | 0.73 | 0.30 |
| C 24:1 n-9 | 0.00 | 0.02 | 0.02 |
| Sum MUFA[b] | 8.82 | 9.67 | 9.99 |
| C 18:2 n-6 | 2.71 | 3.65 | 4.23 |
| C 18:3 n-3 | 0.85 | 1.24 | 1.40 |
| C 20:4 n-3 | 0.08 | 0.04 | 0.02 |
| C 20:2 n-6 | 0.02 | 0.02 | 0.02 |
| C 20:4 n-6 | 0.03 | 0.02 | 0.01 |
| C 20:5 n-3 | 0.90 | 0.48 | 0.26 |
| C 22:5 n-3 | 0.09 | 0.06 | 0.04 |
| C 22:6 n-3 | 0.86 | 0.45 | 0.24 |
| Sum PUFA[c] | 5.57 | 5.96 | 6.24 |
| Sum EPA + DHA | 1.76 | 0.92 | 0.50 |
| Sum n-3 | 2.79 | 2.26 | 1.97 |
| Sum n-6 | 2.77 | 3.69 | 4.26 |
| n6/n3 ratio | 0.99 | 1.63 | 2.16 |

[a]*Sum SFA includes C15:0, C17:0.*
[b]*Sum MUFA includes C14:1n-5, C16:1n-9, C16:1n-5, C17:1n-7, C20:1n-11.*
[c]*Sum PUFA includes C16:3n-4.*

group ($n = 3$). Total lipids were extracted by the Folch method (Folch et al., 1957). The chloroform phase with the total lipid fraction was used to analyse the phospholipids (PLs). The chloroform was evaporated under nitrogen gas and then the total lipid fraction was re-dissolved in hexane. PLs were thereafter separated from non-polar lipids using thin layer chromatography with petroleum ether: diethyl ether: acetic acid (113:20:2, by vol.) as mobile phase. The PL fraction was visualised by spraying the TLC plates with 0.2% (w/v) 2′,7′-dichlorofluorescein in methanol, and by comparing the retention factor (Rf) with known standards under UV light. The PL fraction was thereafter scraped off and used for analysis of fatty acid composition. Briefly, the extract was dried under nitrogen gas and methyl esters of fatty acids were made with 2′,2′-methoxypropane, methanolic HCl and benzene by following the method of Mason and Waller (Mason and Waller, 1964). The fatty acid methyl esters were separated in a gas chromatograph (Hewlett Packard 6,890) equipped with a split injector by using an SGE BPX70 capillary column (length, 60 m; internal diameter, 0.25 mm; and film thickness, 0.25 μm; SGE Analytical Science), flame ionisation detector and HP Chem Station software. The carrier gas was helium, and the temperature of injector and detector was 280°C. The oven temperature was increased from 50 to 180°C at the rate of 10°C/min, and then increased to 240°C at a rate of 0.7°C/min. Standards were used to identify individual fatty acid methyl esters. The relative amount of each fatty acid was expressed as a percentage of the total amount of fatty acids in the analysed sample, and the absolute amount of fatty acids per g of tissue was calculated using the fatty acid 23:0 methyl ester as the internal standard.

## Intestinal Function

Assessment of intestinal function using the Ussing chamber technique were performed on four fish from each tank ($n = 12$) at peak smolt in freshwater, 2–4 days before transfer to seawater, and 94–96 days in seawater. The body cavity was opened laterally and the intestine, from just posterior to the last pyloric caeca to the rectum was carefully removed. The intestine was separated into a proximal region with simple folds only and a distal part with simple and complex folds, and placed in an ice-cold salmon Ringer solution (140 mM NaCl, 2.5 mM KCl, 15 mM $NaHCO_3$, 1.5 mM $CaCl_2$, 1 mM $KH_2PO_4$, 0.8 mM $MgSO_4$, 5 mM HEPES, 10 mM D-glucose, 0.5 mM L-lysine and 20 mM L-glutamine (pH 7.8) for freshwater smolts, and 150 mM NaCl, 2.5 mM KCl, 2.5 mM $CaCl_2$, 1.0 mM $MgCl_2$, 7.0 mM $NaHCO_3$, 0.7 mM $NaH_2PO_4$, 5 mM HEPES, 10 mM D-glucose, 0.5 mM L-methionine and 20 mM L-glutamine (pH 7.8) for the smolts in seawater aerated with 99.7% air and 0.3% $CO_2$.

The intestinal segments were mounted into modified Ussing chambers, filled with the appropriate salmon Ringer solution and the temperature was kept at the acclimation temperature of the fish by a cooling mantle. Mixing and oxygenation was maintained by a gas lift, driven by a gas mixture of 99.7% air and 0.3% $CO_2$. The exposed tissue surface area was 0.75 $cm^2$ and the half-chamber volume 4 ml. After mounting, the intestinal segments were allowed 60 min of recovery for stabilisation of the electrical parameters. To assess the paracellular permeability of the intestinal segments the transepithelial electrical resistance (TER) as well as the apparent permeability ($P_{app}$) of the hydrophilic marker molecule $^{14}$C-mannitol were monitored using an Ussing chamber system as previously described (Sundell and Sundh, 2012). Together with TER, continuous monitoring of the transepithelial electrical resistance (TEP; mV) and short-circuit current (SCC; μA/$cm^2$) was used as monitoring of preparation viability and indicators of net ion distribution and net ion flow respectively. After the 60 min acclimation period the experiment was started by renewing the Ringer solution on the serosal side, and replacing the Ringer solution on the mucosal side with Ringer containing 40 kBq $ml^{-1}$ of the hydrophilic marker molecule $^{14}$C-mannitol (0.1 mCi $ml^{-1}$ and 55.5 mCi $mmol^{-1}$; PerkinElmer, Boston, MA, United States). For the freshwater smolts also 0.14 MBq $mol^{-1}$ of $^{3}$H-L-lysine in presence of 0.5 mM unlabelled L-lysine was added to the freshwater Ringer. L-lysine could not be used in seawater acclimated fish due to supply issues. The fish sampled in seawater had the same activity as well as unlabelled amino acid concentrations added to the seawater Ringer, but using L-methionine instead. A 100 μL sub-sample was taken from the mucosal half chamber at t = 0 and from the serosal Ringer at time points 0, 20, 25 30, 60, 80, 85 and 90 min. The serosal samples were replaced with equal volume of fresh Ringer solution to maintain same hydrostatic pressure across the intestinal tissue. Radioactivity was assessed in a liquid scintillation counter (Wallac 1409, Turku, Finland) after adding 5 ml Ultima Gold™ (PerkinElmer, Boston,United States). Apparent permeability coefficient for mannitol ($P_{app;}$ cm/s) was calculated using **Eq. 1**

$$Papp = dQ/dT \times 1/ACo \quad (1)$$

where d$Q$/d$T$ is the appearance rate of the molecule in the serosal compartment of the Ussing chamber, A is the area ($cm^2$) of intestinal surface exposed in the chamber and $C_o$ is the initial concentration (mol $ml^{-1}$) on the mucosal side. Amino acid transport was calculated using **Eq. 2**

$$(dQ/dT)/A \quad (2)$$

where d$Q$/d$T$ is the appearance rate of the nutrient in the serosal compartment of the Ussing chamber (mol/min) and A is the area ($cm^2$) of intestinal surface exposed. The electrical parameters TER, TEP and SCC are reported as mean value of the last five measurements between 130–150 min.

## qPCR

From fish sampled for Ussing chamber analysis, a small ring of proximal and distal intestine respectively (FW: $n = 6$; SW: $n = 12$) were cut open, cleaned from feces and the mucosa was scraped off using objective glass (100–200 mg) and placed into tubes that contained 1 ml of RNAlater® (Sigma-Aldrich Co.), which was stored at −80°C after 24 h in +4°C. Upon mRNA extraction, mucosa samples were separated from RNAlater® and lysed in 600 µL RLT Plus buffer with 5 mm steel beads using a TissueLyser II homo-geniser (Qiagen NV, Hilden, Germany) for two cycles of 3 min at 25 rotations $sec^{-1}$. Samples were centrifuged for 3 min at 17,000 g and supernatant was pipetted into spin columns for mRNA extraction using RNeasy© Plus Mini kits (Qiagen NV), according to the manufacture's manual. RNAse-free water was used to elute the mRNA and quantity was determined by Nanodrop (Thermo Fisher Scientific Inc.). RNA quality was assessed on random subsamples using a 2,100 Bioanalyzer system (Agilent Technologies). Samples were diluted twice to obtain 1,000 ng of mRNA. The cDNA was synthesized by reverse transcriptase using iScript™ Synthesis kits (Bio-Rad Laboratories Inc., Copenhagen, Denmark) with random primers in 20 µL reactions in one cycle of 5 min at 25°C, 30 s at 42°C and 5 min at 85°C in a thermocycler (Bio-Rad Lab Inc.). The primers sequences used for *claudin-15* and *-25b* was previously published by (Tipsmark et al., 2010a), *tricellulin* and *occludin* in (Tipsmark and Madsen, 2012) and *nka α1c* by (Nilsen et al., 2007). Primers were verified using NCBIs Primer-BLAST tool (https://www.ncbi.nlm.nih.gov/tools/primer-blast) and obtained from Eurofins MWG operon (Ebersberg, Germany). Efficiencies of each primer pair were confirmed to be between 90 and 105% using a dilution series of 2–50 ng cDNA pooled from six random samples. For each sample, duplicate 10 µL reactions of 10 ng cDNA, 0.5 µM of each primer pair (0.3 µM for β-actin) and SYBRGreen Supermix (Bio-Rad Lab Inc.) were pipetted into a reaction plate. Plates were analysed for 40 cycles with initial denaturation at 95°C for 3 min, followed by 40 cycles of 95°C for 10 s and 57–61°C for 30 s using a CFX Connect Real-time PCR Detection System (Bio-Rad Lab Inc.). The reference gene, ribosomal protein L 23 (*rpl23*), was used (Stefansson et al., 2012) and did not differ between freshwater or seawater acclimated fish [threshold cycle (CT) value 20.2 ± 0.18 and 20.2 ± 0.14 respectively (mean ± SEM)] in this study. The ratio of relative expression between the target and reference gene was calculated based on the CT: relative ex-pression = 2-[C (target)−CTT (reference)] using the 2−ΔC T′ method (Livak and Schmittgen, 2001).

**TABLE 3 |** Plasma ion levels (mM) of Atlantic salmon fed different levels of omega-3, in freshwater smolts 2–4 days before seawater transfer, 5 and 68 days after transfer of fish to seawater.

| | 2% EPA + DHA | 1% EPA + DHA | 0.5% EPA + DHA | *p*-value |
|---|---|---|---|---|
| Freshwater smolt | | | | |
| $Cl^-$ | 101.8 ± 1.7 | 101.3 ± 1.6 | 105.3 ± 1.6 | 0.15 |
| $Na^+$ | 157.7 ± 0.7 | 158.0 ± 0.7 | 159.4 ± 1.6 | 0.38 |
| $K^+$ | 3.8 ± 0.2 | 3.1 ± 0.3 | 3.9 ± 0.5 | 0.06 |
| 5 days in seawater | | | | |
| $Cl^-$ | 137.9 ± 0.8 | 139.4 ± 0.8 | 138.7 ± 0.6 | 0.81 |
| $Na^+$ | 157.8 ± 0.6 | 157.9 ± 0.4 | 157.9 ± 0.7 | 0.99 |
| $K^+$ | 3.3 ± 0.2 | 3.1 ± 0.1 | 3.2 ± 0.4 | 0.95 |
| 68 days in seawater | | | | |
| $Cl^-$ | 131.4 ± 0.6 | 134.3 ± 1.0 | 131.7 ± 0.5 | 0.12 |
| $Na^+$ | 161.0 ± 0.8 | 161.4 ± 0.8 | 160.4 ± 0.6 | 0.79 |
| $K^+$ | 1.5 ± 0.1 | 1.6 ± 0.2 | 1.5 ± 0.2 | 0.91 |

## Statistical Analyses

Data on specific growth rate were first analysed by a One-way ANOVA, to assess the effect of diet. Secondly, a linear regression model was applied, using level of EPA + DHA in the diet as the independent variable. Individual data on plasma ion levels were analysed by a mixed model with diet as fixed effect and tank as random effect (GLM procedure in SAS 9.4 Software, SAS Institute Inc., Cary, NC, United States). The levels of fatty acids in intestinal phospholipids were analysed by a One-way ANOVA. Electrical parameters and mannitol data from the Ussing chamber analyses and transcript levels were analyzed using a 2-way ANOVA including omega-3 levels and salinity as fixed factors and analysing possible interactions between factors. Significant main effects were analysed using Tukey´s multiple comparisons test and significant interactions using Sidak´s multiple comparisons test. Amino acid transport was analysed in freshwater and seawater separately using 2-way ANOVA with intestinal region and omega-3 levels as fixed factors. A non-parametric frequency analysis was performed on the distribution of serosa positive/negative TEP (Chi-square test for trends). Normality and homoscedasticity were analysed using Shapiro-Wilk test and Spearmans´s test respectively. Data not fulfilling the assumptions for statistical analyses were log-transformed. All analyses were performed using GraphPad Prism version 8.0.2 for Windows, GraphPad Software, San Diego, California United States, www.graphpad.com. Significant effects were considered at $p < 0.05$.

# RESULTS

## Growth, Mortality and Plasma Ions

The mortality during the entire experiment was 2.9%, and there were no differences between dietary treatments. The statistical analyses by One-way ANOVA did not reveal any significant differences in specific growth rate (SGR) between the three dietary groups ($p = 0.13$). However, the linear regression analysis revealed that there was a significant ($p = 0.03$) linear

**TABLE 4 |** Fatty acid (FA) composition (% of total) in the phospholipid (PL) fraction of Atlantic salmon proximal intestine first sampling (5 days after transfer to seawater).

| | FA in Proximal intestine | | | Aanova | Regression omega-3 in feed | |
|---|---|---|---|---|---|---|
| | 2% EPA + DHA | 1% EPA + DHA | 0.5% EPA + DHA | *p*-value | *p*-value | R-square |
| ∑ SFA | 30.2 ± 0.34 | 30.2 ± 0.37 | 29.3 ± 0.46 | 0.24 | 0.23 | 0.19 |
| 18:1 n-9 | 11.5 ± 0.24$^{b}$ | 13.7 ± 0.22$^{a}$ | 14.6 ± 0.67$^{a}$ | 0.006 | 0.0008 | 0.82 |
| ∑ MUFA | 19.4 ± 0.36 | 20.3 ± 0.21 | 21.2 ± 1.05 | 0.23 | 0.08 | 0.37 |
| 18:2 n-6 | 4.0 ± 0.20 | 4.3 ± 0.36 | 4.4 ± 0.34 | 0.66 | 0.35 | 0.12 |
| 20:4 n-6 | 2.7 ± 0.02$^{c}$ | 3.4 ± 0.07$^{b}$ | 4.5 ± 0.05$^{a}$ | <0.0001 | <0.0001 | 0.90 |
| 20:5 n-3 | 4.4 ± 0.17$^{a}$ | 3.6 ± 0.05$^{b}$ | 3.6 ± 0.15$^{b}$ | 0.006 | 0.003 | 0.75 |
| 22:6 n-3 | 32.5 ± 0.38 | 31.5 ± 0.36 | 29.7 ± 1.30 | 0.12 | 0.05 | 0.45 |
| ∑ PUFA | 51.7 ± 0.23 | 51.9 ± 0.22 | 52.7 ± 0.63 | 0.27 | 0.17 | 0.25 |
| ∑ EPA DHA | 37.0 ± 0.44$^{a}$ | 35.1 ± 0.32$^{ab}$ | 33.3 ± 1.15$^{b}$ | 0.04 | 0.008 | 0.66 |
| n6/n3 | 0.2 ± 0.01$^{b}$ | 0.2 ± 0.01$^{ab}$ | 0.3 ± 0.02$^{a}$ | 0.01 | 0.003 | 0.73 |

*Data are shown as mean values using tank as a statistical unit (n = 3, being each sample represented by a pool of five fish) with their standard errors. Different superscript letters indicate statistically significant differences with one-way anova (p < 0.05). The table also shows the p-value and R-square for the regression analyses of increasing omega-3 fatty acids in feed.*

**TABLE 5 |** Fatty acid (FA) composition (% of total) in phospholipid (PL) fraction of Atlantic salmon proximal intestine second sampling (68 days after transfer to seawater.

| | FA in Proximal intestine | | | Anova | Regression omega-3 in feed | |
|---|---|---|---|---|---|---|
| | 2% EPA + DHA | 1% EPA + DHA | 0.5% EPA + DHA | *p*-value | *p*-value | R-square |
| ∑ SFA | 28.5 ± 0.61 | 28.6 ± 1.78 | 26.4 ± 0.86 | 0.42 | 0.32 | 0.14 |
| 18:1 n-9 | 13.5 ± 0.17$^{c}$ | 17.3 ± 0.38$^{b}$ | 18.8 ± 0.40$^{a}$ | <0.0001 | <0.0001 | 0.95 |
| ∑ MUFA | 18.6 ± 0.40$^{b}$ | 21.8 ± 0.39$^{a}$ | 23.2 ± 0.57$^{a}$ | 0.001 | 0.0001 | 0.90 |
| 18:2 n-6 | 6.8 ± 0.16$^{b}$ | 8.9 ± 0.43$^{a}$ | 9.8 ± 0.16$^{a}$ | 0.0007 | <0.0001 | 0.91 |
| 20:4 n-6 | 1.7 ± 0.38 | 2.6 ± 0.50 | 3.2 ± 0.22 | 0.08 | 0.02 | 0.57 |
| 20:5 n-3 | 9.0 ± 0.82$^{a}$ | 6.0 ± 0.34$^{b}$ | 5.4 ± 0.15$^{b}$ | 0.005 | 0.01 | 0.80 |
| 22:6 n-3 | 23.8 ± 0.26$^{a}$ | 18.5 ± 1.57$^{b}$ | 18.2 ± 1.04$^{b}$ | 0.02 | 0.006 | 0.68 |
| ∑ PUFA | 48.1 ± 0.13 | 45.4 ± 2.38 | 47.3 ± 1.78 | 0.54 | 0.60 | 0.04 |
| ∑ EPA DHA | 32.9 ± 0.89$^{a}$ | 24.5 ± 1.83$^{b}$ | 23.5 ± 1.19$^{b}$ | 0.005 | 0.002 | 0.78 |
| n6/n3 | 0.3 ± 0.02$^{b}$ | 0.5 ± 0.03$^{a}$ | 0.6 ± 0.02$^{a}$ | 0.0002 | <0.0001 | 0.92 |

*Data are shown as mean values using tank as a statistical unit (n = 3, being each sample represented by a pool of five fish) with their standard errors. Different superscript letters indicate statistically significant differences with one-way anova (p < 0.05). The table also shows the p-value and R-square for the regression analyses of increasing omega-3 fatty acids in feed.*

increase in SGR in relation to increased dietary content of EPA and DHA. SGR increased from 1.08 in the lowest (0.5%) to 1.11 in the intermediate (1%) and further to 1.19 in the high (2%) omega-3 diet. Levels of plasma ions did not show any dietary effects either in freshwater or the two samplings in seawater (**Table 3**).

## Fatty Acids in Intestinal Phospholipids

In samples collected 5 days after transfer to seawater, there were no change in the relative distribution between total saturated (SAT), monounsaturated (MUFA) and polyunsaturated (PUFA) fatty acids between the dietary groups (**Table 4**). However, the levels of EPA and 18:1n-9 (oleic acid; OA) in percentage of total fatty acids was higher and the level of 20:4n-6 (arachidonic acid; ARA) was lower, in fish from the high omega-3 diet group as compared to the two other dietary groups. At the end of the trial (**Table 5**), there were still no change in the relative distribution of total SAT between the dietary groups. But also at this time point the relative levels of EPA and DHA increased and the relative levels of the fatty acids 18:1n-9, 18:2n-6 (alpha-linolenic acid; ALA) and ARA as well as the n-6/n-3 ratio decreased, with increasing dietary levels of EPA and DHA (regression analyses).

## Intestinal Barrier Function

A functional intestinal barrier is essential for fish health and welfare (Sundh and Sundell, 2015). Intestinal barrier function towards ions and small water-soluble substances were assessed as transepithelial electrical resistance (TER; $\Omega^{*}cm^{2}$) and the apparent permeability coefficient ($P_{app}$; cm/s) for $^{14}$C-mannitol, respectively. Main effects were observed for TER in the proximal intestine (**Figure 1A**) for diet ($p < 0.05$) and salinity ($p < 0.001$) while no interaction was observed. Tukeys' multiple comparisons test revealed significantly lower TER in the 0.5% group compared to 2% group ($p < 0.01$), while the 1% omega-3 was similar to the other diets groups ($p = 0.1022$). In the distal intestine (**Figure 1B**), no effects were observed regarding diet ($p = 0.908$) whereas the TER was significantly increased by salinity ($p < 0.001$) in all dietary groups as there were no interactions ($p = 0.539$). The diffusion rate of $^{14}$C-mannitol ($P_{app}$) in the proximal intestine (**Figure 1C**), was not affected by omega-3 levels, but was significantly reduced after seawater acclimation ($p < 0.001$). In the distal intestine (**Figure 1D**), a significant interaction between diet and salinity was observed ($p < 0.05$) and the following post-hoc test showed that the $P_{app}$ in the 1% omega-3 were lower compared to 2% omega-3. In

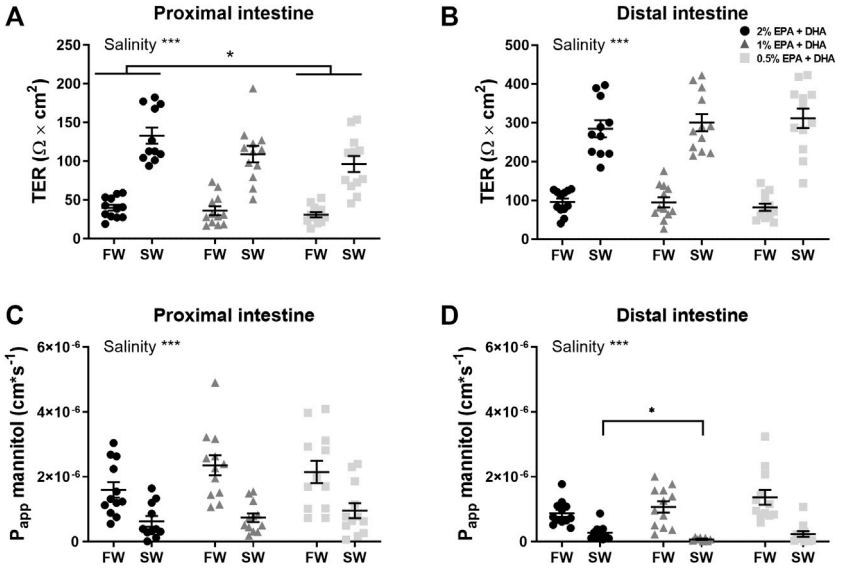


**FIGURE 1 |** Barrier function assessed as transepithelial electrical resistance (TER; **(A,B)** and apparent permeability coefficient ($P_{app}$) for $^{14}$C-mannitol **(C,D)** in proximal and distal intestine of freshwater (FW) smolts and seawater (SW) acclimated Atlantic salmon fed different levels of omega-3. Statistics: 2-way ANOVA where main effects were compared with Tukey´s multiple comparisons test. Significant effects from the post-hoc test are reported as $^{*}p < 0.05$ and $^{***}p < 0.001$. Data are presented as individual values with the horizontal line representing the mean and the vertical lines SEM.

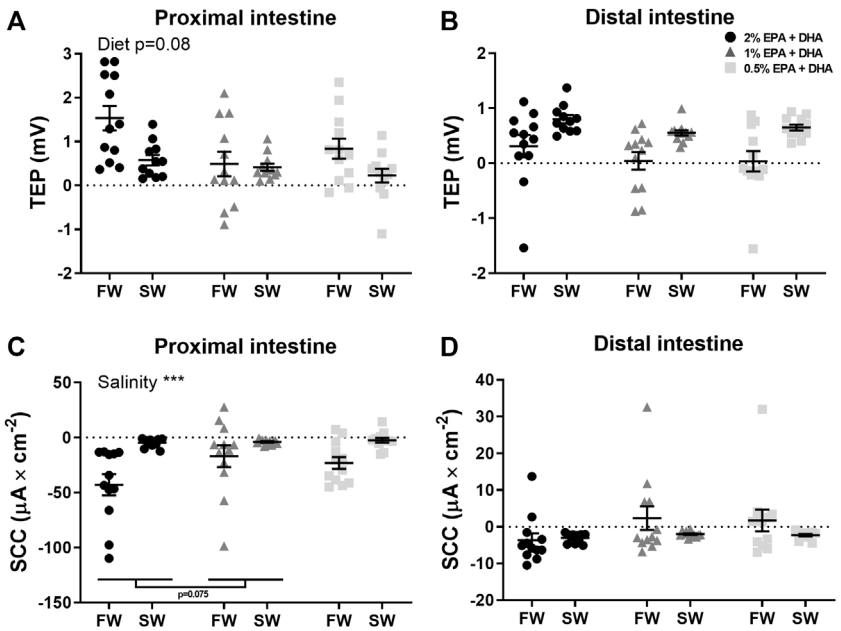


**FIGURE 2 |** Active intestinal ion transport assessed as transepithelial potential difference (TEP; **(A,B)** and short-circuit current (SCC; **(C,D)** in freshwater (FW) smolts and seawater (SW) acclimated Atlantic salmon fed different levels of omega-3. Statistics: 2-way ANOVA where main effects were compared with Tukey´s multiple comparisons test. Significant effects from the post-hoc test are reported as $^{*}p < 0.05$ and $^{***}p < 0.001$. Data are presented as individual values with the horizontal line representing the mean and the vertical lines SEM.

**TABLE 6 |** Number of intestines displaying serosa positive TEP values in Atlantic salmon freshwater smolts and seawater post-smolts.

| | Proximal intestine | | | Chi-square | Distal intestine | | | Chi-square |
|---|---|---|---|---|---|---|---|---|
| | 2% EPA + DHA | 1% EPA + DHA | 0.5% EPA + DHA | | 2% EPA + DHA | 1% EPA + DHA | 0.5% EPA + DHA | |
| Freshwater | 12 of 12 | 9 of 12 | 10 of 12 | 0.24 | 10 of 12 | 8 of 12 | 5 of 12 | 0.03 |
| Seawater | 12 of 12 | 12 of 12 | 9 of 12 | 0.03 | 12 of 12 | 12 of 12 | 12 of 12 | 1 |

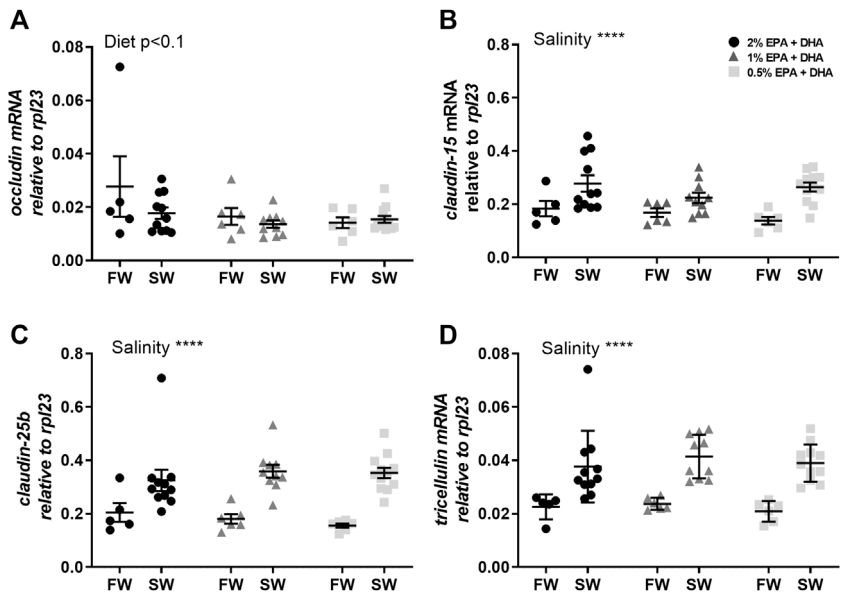


**FIGURE 3 |** Transcript levels of **(A)** *occludin*, **(B)** *claudin-15*, **(C)** *claudin-25b* and **(D)** *tricellulin* in the proximal intestine of freshwater (FW) smolts and seawater (SW) acclimated Atlantic salmon fed different levels of omega-3. Statistics: two-way ANOVA. Significant effects are reported as *$p < 0.05$ and ***$p < 0.001$. Data are presented as individual values with the horizontal line representing the mean and the vertical lines SEM.

addition, similarly as for the proximal intestine, the $P_{app}$ in the distal region was significantly lower after seawater acclimation ($p < 0.001$).

## Intestinal Transport

In the proximal intestine (**Figure 2A**), overall effects on TEP were observed for salinity ($p < 0.001$) while the effect of diet was not significant ($p = 0.08$). In the distal intestine (**Figure 2B**), the TEP was in general more serosa-positive in seawater compared to in freshwater. Further, a marked diet effect could be observed in the net-ion distribution across both intestinal regions, as decreased omega-3 levels reduced the occurrence of serosa-positive TEP's in the distal intestine of freshwater fish and in the proximal intestine of seawater fish ($p < 0.05$; chi-square, **Table 6**). In neither the proximal (**Figure 2C**) nor the distal intestine (**Figure 2D**), any statistical differences were found in response to diets regarding SCC. Salinity significantly increased (less negative) SCC in the proximal intestine ($p < 0.001$), while no effects of salinity were observed in the distal intestine. Amino acid transport was assessed as an indicator for possible effects on active nutrient transport. In freshwater, the L-lysine transport was not affected by diet but was significantly higher in the proximal compared to the distal region (0.4 ± 0.02 nmol*min$^{-1}$*cm$^{-2}$ and 0.1 ± 0.005 nmol*min$^{-1}$*cm$^{-2}$ respectively; $p < 0.001$). Similarly, L-methionine transport in seawater was not affected by diet but was significantly higher in the proximal compared to the distal region (0.5 ± 0.07 nmol*min$^{-1}$*cm$^{-2}$ and 0.09 ± 0.009 nmol*min$^{-1}$*cm$^{-2}$ respectively; $p < 0.001$).

## qPCR

In the proximal intestine, *occludin* transcript levels were not statistically affected by diet ($p < 0.1$) or salinity (**Figure 3A**). The other tight junction proteins, *claudin-15* (**Figure 3B**), *claudin-25b* (**Figure 3C**) and *tricellulin* (**Figure 3D**), were significantly upregulated after in seawater compared to freshwater smolts ($p < 0.001$). In the distal intestine, the expression of *occludin* was significantly upregulated by salinity in the 1 and 0.5% omega-3 groups, but not in the 2% omega-3 group (**Figure 4A**). The *claudin-25b* (**Figure 4C**) and *tricellulin* (**Figure 4D**) were significantly upregulated in seawater compared to freshwater smolts ($p < 0.001$). No effects were observed for *claudin-15* (**Figure 4B**).

The $Na^+/K^+$-ATPase (NKA) is the main driver of active ion, fluid and nutrient transport in the intestinal epithelium. The *nka*

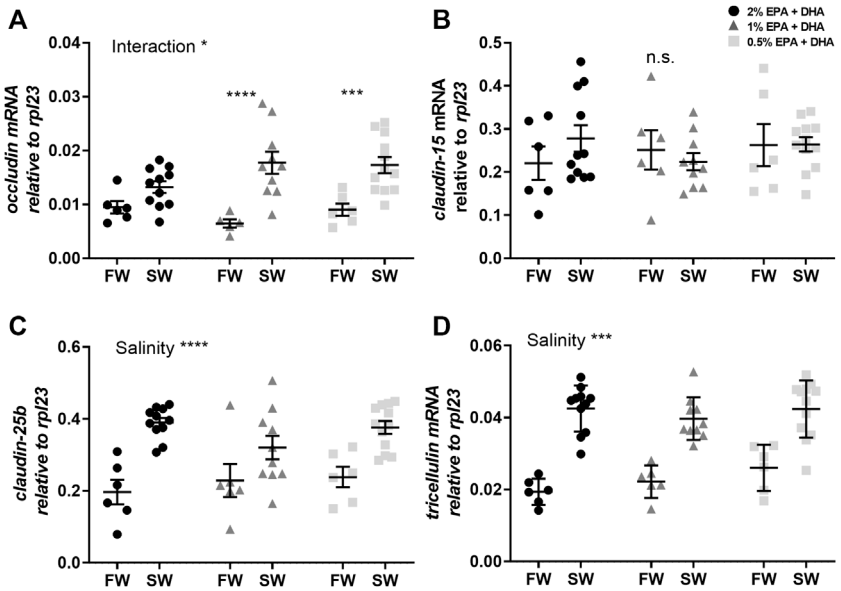


**FIGURE 4 |** Transcript levels of **(A)** *occludin*, **(B)** *claudin-15*, **(C)** *claudin-25b* and **(D)** *tricellulin* in the distal intestine of freshwater (FW) smolts and seawater (SW) acclimated Atlantic salmon smolts fed different levels of omega-3. Statistics: two-way ANOVA where significant interaction was analysed using Sidak's multiple comparisons test. Significant effects are reported as $^{*}p < 0.05$ and $^{***}p < 0.001$. Data are presented as individual values with the horizontal line representing the mean and the vertical lines SEM.

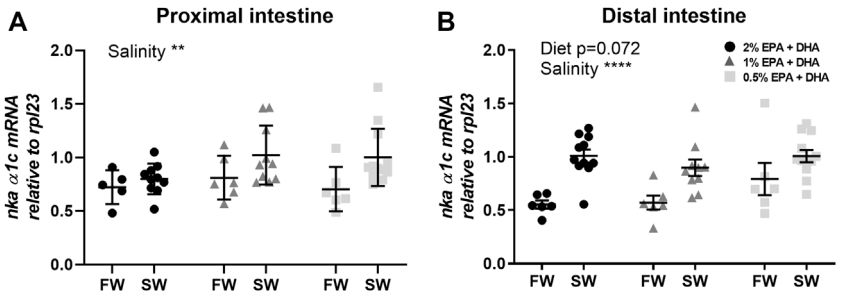


**FIGURE 5 |** Transcript levels of $Na^{+}/K^{+}$-ATPase (*nka*) isoform *α1c* in the proximal **(A)** and distal **(B)** intestine of freshwater (FW) smolts and seawater (SW) acclimated Atlantic salmon fed different levels of omega-3. Statistics: 2-way ANOVA where main effects were compared with Tukey's multiple comparisons test. Significant effects from the post-hoc test are reported as $^{*}p < 0.05$ and $^{***}p < 0.001$. Data are presented as individual values with the horizontal line representing the mean and the vertical lines SEM.

*α1c* transcript levels were upregulated after seawater acclimation in both proximal (**Figure 5A**) and distal intestine ($p < 0.01$; **Figure 5B**) while no significant diet effects were observed.

## DISCUSSION

Total SGR in the current study was well in line with previously published studies on Atlantic salmon (Føre et al., 2016), and increasing dietary level of EPA and DHA from 0.5% up to 2% did cause a linear increase in SGR. Earlier studies have shown differing results regarding the effect of omega-3 fatty acids on growth rate dependent on environment and size of the fish (Ruyter et al., 2000a; Rosenlund et al., 2016; Bou et al., 2017a, 2017b). Ion levels were in the normal range of Atlantic salmon smolts in freshwater and both shortly (5 days) after transfer to seawater and at termination of the feeding trial. Thus, low omega-3 levels do not seem to lead to any sever osmoregulatory problems. However, decreased growth rate with decreasing omega-3 levels indicate that the physiology of the fish was affected, and may be a result of an increased allostatic load on the fish.

The significant increase in TER of both intestinal regions after seawater acclimation is in line with previous observations of salmonids acclimated to seawater (Sundell et al., 2003; Sundell and Sundh, 2012). The reduction in TER in both freshwater and

seawater smolts in the low omega-3 diet group, on the other hand, clearly indicate that the intestinal barrier is impaired. The role of the observed marked increase in TER after seawater acclimation is not fully characterized but has been hypothesized to have a role in the intestine when the intestinal fluid uptake increases in seawater (Sundell and Sundh, 2012). According to this hypothesis, a high osmotic coupling compartment must be created in the lateral intercellular space (LIS) to attract fluid from the lumen across the intestinal epithelium to the blood side (Grosell, 2010; Sundell and Sundh, 2012; Whittamore, 2012). The high osmolality is mainly created by laterally located NKAs resulting in high $Na^+$ levels in the LIS. The increased TER in SW aids in maintaining the high intercellular osmolality. The decrease in TER, as seen in the 0.5% omega group, most likely reflects an increased $Na^+$ permeability across the TJ. A consequence therefore of the impaired barrier towards ions in the low dietary levels of EPA and DHA may be impaired intestinal fluid uptake.

The proximal region of the intestine, together with the pyloric caeca, is the most important regions for nutrient uptake while both proximal and distal intestinal regions are important for fluid uptake. The TEP in the current study were in general serosa positive, which is in agreement with previous studies on freshwater and seawater acclimated Atlantic salmon (Sundh et al., 2010). The seawater acclimated Atlantic salmon, on the other hand, often deviates from most stenohaline seawater teleosts, normally showing a serosa negative TEP. This discrepancy in TEP between different seawater living teleosts is most probably the result of differing ion selectivity's of the TJs. Leaky epithelia, like in the fish proximal intestine, is in general more permeable to $Na^+$ than to $Cl^-$ which allows some of the $Na^+$ transported by the NKA to the LIS to leak back to the intestinal lumen (Field et al., 1978; Loretz, 1995). This gives rise to a less positive (or negative) TEP depending on the balance between electroneutral (eg. NKCC2/NCC) and electrogenic transport (eg. $Na^+$-driven nutrient uptake) across the epithelium (Jiang et al., 1998; Usami et al., 2001, 2003). Thus, the decrease in TEP seen in the proximal intestine with decreasing omega-3 levels further supports an increased $Na^+$-permeability across the TJ as a result of low dietary EPA and DHA levels. A decrease in TEP caused by intestinal barrier impairment will in many instances be compensated for by an increased activity of the lateral NKAs in order to try to maintain an optimal osmolality in the LIS. However, no support could be found in the current study for such a compensation in increased active transport, neither as an increase SCC nor any effect mRNA levels of NKA1c.

Different fatty acids have direct impact on the function of the tight junction complexes and thus intestinal barrier function (Jiang et al., 1998; Usami et al., 2001, 2003). In the current study, increased levels of OA (oleic acid) and linoleic acid (LA) may provide a plausible explanation for the intestinal barrier impairment seen with this diet, as these FAs all have been connected to barrier dysfunction in mammalian model systems. Mammalian *in vitro* models have investigated the impact of specific FA on intestinal barrier function. LA, γ-linoleic acid (GLA) and ALA, but not OA, resulted in decreased TER, *i.e.* impaired barrier function of Caco-2 cells (Usami et al., 2001, 2003). In a vascular endothelial cell line, LA and OA decreased TER while ARA and ALA had no effect (Jiang et al., 1998). In contrast, GLA, dihomo- γ-linoleic acid (DGLA), and ARA, increased TER, *i.e.* strengthened the barrier, in the T84 human intestinal cell line whereas LA, ALA and DGLA had no effect (Willemsen et al., 2008). The results from these mammalian model systems and the present study suggest that different FA exert different effects in different types of cells. Also, the marine, long omega-3 FAs, EPA and DHA, were suggested to induce barrier dysfunction in Caco-2 cells (Usami et al., 2001, 2003). However, these negative effects maybe the result of lipid peroxidation as DHA supplemented with antioxidants mitigated the dysfunction (Roig-Pérez et al., 2004). In agreement, both DHA and EPA tightens the epithelium when human intestinal epithelial cells (T84) were supplemented with vitamin D and E (Willemsen et al., 2008). These data highlight that both the type and the quality of the fatty acids are crucial for maintaining the beneficial effects of PUFAs on intestinal barrier functions. Taking these previous observations in mammalian tissues and cell-lines into account suggest that the observed impairment of the intestinal barrier function in the current study may be due to the decreased relative levels of EPA and DHA in combination with increased relative levels of OA, ALA and ARA, with decreasing dietary levels of EPA and DHA in the feed.

Increased intestinal permeability is directly linked to intestinal inflammation in fish (Knudsen et al., 2008; Sundh et al., 2009, 2010, 2019; Niklasson et al., 2011; Venkatakrishnan et al., 2019) as in mammals, where impaired intestinal barrier function is one of several risk factors behind chronic intestinal inflammatory diseases (Michielan and D'Incà, 2015). Different fatty acids may also have indirect impact on the function of the tight junction complexes and thus intestinal barrier function through generation of secondary active compounds (Huang et al., 2020). The link between barrier dysfunction and relative level of different FAs such as ARA, is suggested to be through their effect on the inflammatory state. ARA is used as a substrate by cyclooxygenase (COX), lipoxygenase (LOX) and cytochrome P450 enzymes and converted into eicosanoids (Ricciotti and Fitzgerald, 2011). Increased levels of ARA in the cell membranes result in increased production of eicosanoid family molecules that can mediate pro-inflammatory processes, resulting in increased inflammation, a state that can be connected to intestinal barrier dysfunction in mammals including humans (Ricciotti and Fitzgerald, 2011; Huang et al., 2020). In the current study, ARA doubled in the intestinal FAs in the low compared to high omega-3 levels. This suggests that the reduced intestinal barrier function seen in the Atlantic salmon, at least in part, is a result of an increase in the pro-inflammatory FA, ARA. Yet another support for the correlation between long chain omega-3 FA and reduced inflammation in mammals is that increased levels of DHA and EPA decreases ARA in mammals (Calder, 2017). This may reduce a pro-inflammatory reaction through decreased production of potent eicosanoids, and possibly also through reduced production of pro-inflammatory cytokines, also known to induce intestinal barrier dysfunction (Calder, 2017). Further studies are however needed to elucidate if the observed intestinal barrier dysfunction of Atlantic salmon fed low, 0.5%, omega-3 levels also is mediated by increased pro-inflammatory reactions as a result of increased eicosanoid production from ARA.

The molecular mechanism behind epithelial permeability and selectivity across the intestine is determined by the main intercellular

tight junction proteins, claudin, occludin and tricellulin (Chasiotis et al., 2012; Sundell and Sundh, 2012; Kolosov et al., 2013; Sundh and Sundell, 2015). Thus, another possible explanation for the barrier effects of dietary omega-3 levels is through changed expression of specific tight junction proteins. Mammalian claudins are broadly divided into barrier- or pore-forming isoforms, where the specific character is attributed to their effect on specific anions or cations (Krug et al., 2014; Krug, 2017; Rosenthal et al., 2017). To date, there are very few functional studies regarding the selectivity and permeability characteristics of fish claudins in general and none regarding Atlantic salmon intestinal claudins. However, Tipsmark et al. (2010a) suggested that claudin-25b is a barrier forming isoform and claudin-15 a pore forming isoform in the Atlantic salmon intestine. These suggestions are based on a sequence analysis comparing the Atlantic salmon claudins to mammalian and zebrafish claudins, which both were verified to be ion selective. Based on this assumption, the increased TER in both intestinal regions after seawater transfer may be due to an up-regulation of a barrier-forming claudin, which is also supported by the drastic up-regulation of claudin-25b in seawater. On the other hand, claudin-15, a suggested pore-forming isoform, also increased in response to the seawater acclimation in the proximal intestine concomitant with increased TER, which makes this assumption elusive. In addition, no dietary effects were observed in the expression of tight junction proteins, therefore the claudin-25b or claudin-15 differential expression patterns cannot explain the impaired barrier function seen in response to low EPA and DHA levels in the feed.

Occludin and tricellulin are both important tight junction proteins contributing to the barrier against uncharged macromolecules and mediating an increase of the TER (Krug, 2017). This is supported by studies using the mammalian MDCK cell-line where overexpression of occludin resulted in increased TER and thus a tighter epithelium (McCarthy et al., 1996). The tendency towards decreased expression of occludin in the proximal intestine with low omega-3 levels, may suggest that occludin is involved in the barrier formation towards ions in this intestinal region. Interestingly, in the distal intestine of the Atlantic salmon there was an upregulation of the occludin expression in the lower, 1 and 0.5%, omega-3 groups concomitant with a lack of dietary effects on barrier function in this region of the seawater acclimated fish. This may suggest that the distal intestine is able to compensate for a reduction in TER caused by low the omega-3 levels through up-regulation of occludin.

In conclusion, this study shows that low levels of omega-3 in the diet impairs the intestinal functions and reduce Atlantic salmon health and welfare. The low inclusion level do not affect osmoregulation assessed as plasma ion levels, but it reduce growth and changes the FA composition of the proximal intestine. Low omega-3 dietary levels further results in decreased omega-3 content of the intestinal epithelial membranes as well as in impaired intestinal barrier function and decreased TEP in the proximal intestine. The potentially pro-inflammatory FA, ARA, on the other hand, increased with decreasing omega-3 dietary levels. Transfer of Atlantic salmon from freshwater to seawater in general increased the transcript levels of tight junction proteins concomitant with increased barrier function, assessed as TER.

## DATA AVAILABILITY STATEMENT

The original contributions presented in the study are included in the article/Supplementary Materials, further inquiries can be directed to the corresponding author.

## ETHICS STATEMENT

The animal study was reviewed and approved by the experiment was terminated 96 days after seawater transfer. The experiment was performed in compliance with the Norwegian national regulation for use of experimental animals (NARA, FOR-2015-06-18-761) and the National Guidelines for Animal Care and Welfare published by the Norwegian Ministry of Education and Research and approved by Norwegian Food Safety Authority (FOTS); approval nr. 11666.

## AUTHOR CONTRIBUTIONS

Conceptualization, GB and BR; methodology, KS, GB, BR, and HS, validation, KS, GB, BR, and HS; formal analysis, KS, GB, BR, and HS investigation, KS, GB, BR, and HS; resources, KS, GB, BR, and HS; data curation, GB, BR, and HS; writing—original draft preparation, KS and HS; writing—review and editing, KS, GB, BR, and HS; visualization, GB, BR, and HS; project administration, GB; funding acquisition, GB and BR; All authors have read and agreed to the published version of the manuscript.

## FUNDING

This research was funded by Norwegian Seafood Research Fund (FHF), grant number 901265.

## ACKNOWLEDGMENTS

We would like to thank Linda Hasselberg-Frank for technical help during the qPCR measurements and the technical staff at NOFIMA.

## REFERENCES

Aas, T. S., Ytrestøyl, T., and Åsgård, T. (2019). Utilization of Feed Resources in the Production of Atlantic salmon (*Salmo salar*) in Norway: An Update for 2016. *Aquaculture Rep.* doi:10.1016/j.aqrep.2019.100216

Anderson, J. M., and Van Itallie, C. M. (2009). Physiology and Function of the Tight junction. *Cold Spring Harbor Perspect. Biol.* 1, a002584. doi:10.1101/cshperspect.a002584

Bou, M., Berge, G. M., Baeverfjord, G., Sigholt, T., Østbye, T.-K., Romarheim, O. H., et al. (2017a). Requirements Ofn-3 Very Long-Chain PUFA in Atlantic salmon (Salmo salarL): Effects of Different Dietary Levels of EPA and DHA on

Fish Performance and Tissue Composition and Integrity. *Br. J. Nutr.* 117, 30–47. doi:10.1017/S0007114516004396

Bou, M., Berge, G. M., Baeverfjord, G., Sigholt, T., Østbye, T.-K., and Ruyter, B. (2017b). Low Levels of Very-Long-Chain N-3 PUFA in Atlantic salmon (*Salmo salar*) Diet Reduce Fish Robustness under Challenging Conditions in Sea Cages. *J. Nutr. Sci.* 6. doi:10.1017/jns.2017.28

Calder, P. C. (2017). Omega-3 Fatty Acids and Inflammatory Processes: From Molecules to Man. *Biochem. Soc. Trans.* 45, 1105–1115. doi:10.1042/BST20160474

Chasiotis, H., Kolosov, D., Bui, P., and Kelly, S. P. (2012). Tight Junctions, Tight junction Proteins and Paracellular Permeability across the Gill Epithelium of Fishes: A Review. *Respir. Physiol. Neurobiol.* 184, 269–281. doi:10.1016/j.resp.2012.05.020

Estensoro, I., Ballester-Lozano, G., Benedito-Palos, L., Grammes, F., Martos-Sitcha, J. A., Mydland, L.-T., et al. (2016). Dietary Butyrate Helps to Restore the Intestinal Status of a marine Teleost (*Sparus Aurata*) Fed Extreme Diets Low in Fish Meal and Fish Oil. *PLoS ONE* 11, e0166564–21. doi:10.1371/journal.pone.0166564

Field, M., Karnaky, K. J., Jr., Smith, P. L., Bolton, J. E., and Kinter, W. B. (1978). Ion Transport across the Isolated Intestinal Mucosa of the winter Flounder,*Pseudopleuronectes americanus*. *J. Membrain Biol.* 41, 265–293. doi:10.1007/bf01870433

Finstad, B., and Thomassen, M. S. (1991). Does Dietary Lipid Composition Affect the Osmoregulatory Ability of Rainbow trout (*Oncorhynchus mykiss*) at High and Low Temperatures? *Comp. Biochem. Physiol. A: Physiol.* 99, 463–471. doi:10.1016/0300-9629(91)90034-A

Folch, J., Lees, M., and Stanley, G. H. S. (1957). A Simple Method for the Isolation and Purification of Total Lipides from Animal Tissues. *J. Biol. Chem.* 226, 497–509. doi:10.1016/s0021-9258(18)64849-5

Føre, M., Alver, M., Alfredsen, J. A., Marafioti, G., Senneset, G., Birkevold, J., et al. (2016). Modelling Growth Performance and Feeding Behaviour of Atlantic salmon (*Salmo salar* L.) in Commercial-Size Aquaculture Net Pens: Model Details and Validation through Full-Scale Experiments. *Aquaculture* 464, 268–278. doi:10.1016/j.aquaculture.2016.06.045

Grosell, M. (2010). "The Role of the Gastrointestinal Tract in Salt and Water Balance," in *Fish Physiology*. Editors M. Grosell, A. P. Farrell, and J. B. Colin (Academic Press), 135–164. doi:10.1016/s1546-5098(10)03004-9

Günzel, D., and Fromm, M. (2012). Claudins and Other Tight junction Proteins. *Compr. Physiol.* 2, 1819–1852. doi:10.1002/cphy.c110045

Günzel, D., and Yu, A. S. L. (2013). Claudins and the Modulation of Tight junction Permeability. *Physiol. Rev.* 93, 525–569. doi:10.1152/physrev.00019.2012

Huang, N., Wang, M., Peng, J., and Wei, H. (2020). Role of Arachidonic Acid-Derived Eicosanoids in Intestinal Innate Immunity. *Crit. Rev. Food Sci. Nutr.* 61, 2399–2410. doi:10.1080/10408398.2020.1777932

Jiang, W. G., Bryce, R. P., Horrobin, D. F., and Mansel, R. E. (1998). Regulation of Tight junction Permeability and Occludin Expression by Polyunsaturated Fatty Acids. *Biochem. Biophysical Res. Commun.* 244, 414–420. doi:10.1006/bbrc.1998.8288

Knudsen, D., Jutfelt, F., Sundh, H., Sundell, K., Koppe, W., and Frøkiær, H. (2008). Dietary Soya Saponins Increase Gut Permeability and Play a Key Role in the Onset of Soyabean-Induced Enteritis in Atlantic salmon (*Salmo salar* L.). *Br. J. Nutr.* 100, 120–129. doi:10.1017/S0007114507886338

Kolosov, D., Bui, P., Chasiotis, H., and Kelly, S. P. (2013). Claudins in Teleost Fishes. *Tissue Barriers* 1, e25391. doi:10.4161/tisb.25391

Krug, S. M. (2017). Contribution of the Tricellular Tight junction to Paracellular Permeability in Leaky and Tight Epithelia. *Ann. N.Y. Acad. Sci.* 1397, 219–230. doi:10.1111/nyas.13379

Krug, S. M., Schulzke, J. D., and Fromm, M. (2014). Tight junction, Selective Permeability, and Related Diseases. *Semin. Cel Developmental Biol.* 36, 166–176. doi:10.1016/j.semcdb.2014.09.002

Livak, K. J., and Schmittgen, T. D. (2001). Analysis of Relative Gene Expression Data Using Real-Time Quantitative PCR and the 2−ΔΔCT Method. *Methods* 25, 402–408. doi:10.1006/meth.2001.1262

Loretz, C. A. (1995). "2 Electrophysiology of Ion Transport in Teleost Intestinal Cells," in *Cellular and Molecuar Approaches to Fish Ionic Regulation*. Editors M. W. Chris, and J. S. Trevor (Academic Press), 25–56. doi:10.1016/s1546-5098(08)60241-1

Løvmo, S. D., Whatmore, P., Sundh, H., Sigholt, T., Madaro, A., Bardal, T., et al. (2021). Effects of Atlantic salmon (*Salmo salar*) Fed Low- and High HUFA Diets on Growth and Midgut Intestinal Health. *Aquaculture* 539, 736653. doi:10.1016/j.aquaculture.2021.736653

Mason, M. E., and Waller, G. R. (1964). Dimethoxypropane Induced Transesterification of Fats and Oils in Preparation of Methyl Esters for Gas Chromatographic Analysis. *Anal. Chem.* 36, 583–586. doi:10.1021/ac60209a008

McCarthy, K. M., Skare, I. B., Stankewich, M. C., Furuse, M., Tsukita, S., Rogers, R. A., et al. (1996). Occludin Is a Functional Component of the Tight junction. *J. Cel Sci* 109, 2287–2298. doi:10.1242/jcs.109.9.2287

Michielan, A., and D'Incà, R. (20152015). Intestinal Permeability in Inflammatory Bowel Disease: Pathogenesis, Clinical Evaluation, and Therapy of Leaky Gut. *Mediators Inflamm.* 2015, 1–10. doi:10.1155/2015/628157

Miyazaki, M., and Ntambi, J. M. (2008). Fatty Acid Desaturation and Chain Elongation in Mammals. *Biochem. Lipids Lipoproteins Membranes*, 191–211. doi:10.1016/b978-044453219-0.50009-x

Niklasson, L., Sundh, H., Fridell, F., Taranger, G. L., and Sundell, K. (2011). Disturbance of the Intestinal Mucosal Immune System of Farmed Atlantic salmon (*Salmo salar*), in Response to Long-Term Hypoxic Conditions. *Fish Shellfish Immunol.* 31, 1072–1080. doi:10.1016/j.fsi.2011.09.011

Nilsen, T. O., Ebbesson, L. O. E., Madsen, S. S., McCormick, S. D., Andersson, E., Björrnsson, B. T., et al. (2007). Differential Expression of Gill Na+,K+-ATPaseα- and β-subunits, Na+,K+,2Cl-cotransporter and CFTR Anion Channel in Juvenile Anadromous and Landlocked Atlantic salmon *Salmo salar*. *J. Exp. Biol.* 210, 2885–2896. doi:10.1242/jeb.002873

Noble, C., Gismervik, K., Iversen, M. H., Kolarevic, J., Nilsson, J., Stien, L. H., et al. (2018). *Welfare Indicators for Farmed Atlantic salmon: Tools for Assessing Fish Welfare*. 978-82-8296-556-9.

Nonnotte, G., Aubree-Pelletier, A., and Colin, D. A. (1987). Na+ Transport in Perfused Intestine and in Isolated Enterocytes of Freshwater trout Deprived of Essential Fatty Acid. *Comp. Biochem. Physiol. Part A: Physiol.* 88, 431–436. doi:10.1016/0300-9629(87)90058-2

Olsen, R. E., Myklebust, R., Kaino, T., and Ringø, E. (1999). Lipid Digestibility and Ultrastructural Changes in the Enterocytes of Arctic Char (*Salvelinus alpinus* L.) Fed Linseed Oil and Soybean Lecithin. *Fish Physiol. Biochem.* 21, 35–44. doi:10.1023/a:1007726615889

Olsen, R. E., Tore Dragnes, B., Myklebust, R., and Ringø, E. (2003). Effect of Soybean Oil and Soybean Lecithin on Intestinal Lipid Composition and Lipid Droplet Accumulation of Rainbow trout, *Oncorhynchus mykiss* Walbaum. *Fish Physiol. Biochem.* 29, 181–192. doi:10.1023/B:FISH.0000045708.67760.43

Ricciotti, E., and FitzGerald, G. A. (2011). Prostaglandins and Inflammation. *Atvb* 31, 986–1000. doi:10.1161/ATVBAHA.110.207449.Prostaglandins

Roig-Pérez, S., Guardiola, F., Moretó, M., and Ferrer, R. (2004). Lipid Peroxidation Induced by DHA Enrichment Modifies Paracellular Permeability in Caco-2 Cells. *J. Lipid Res.* 45, 1418–1428. doi:10.1194/jlr.M300513-JLR200

Rosenlund, G., Torstensen, B. E., Stubhaug, I., Usman, N., and Sissener, N. H. (2016). Atlantic salmon Require Long-Chain N-3 Fatty Acids for Optimal Growth throughout the Seawater Period. *J. Nutr. Sci.* 5, 1–13. doi:10.1017/jns.2016.10

Rosenthal, R., Günzel, D., Theune, D., Czichos, C., Schulzke, J.-D., and Fromm, M. (2017). Water Channels and Barriers Formed by Claudins. *Ann. N.Y. Acad. Sci.* 1397, 100–109. doi:10.1111/nyas.13383

Ruyter, B., RØsjØ, C., Einen, O., and Thomassen, M. S. (2000a). Essential Fatty Acids in Atlantic salmon: Effects of Increasing Dietary Doses of N-6 and N-3 Fatty Acids on Growth, Survival and Fatty Acid Composition of Liver, Blood and Carcass. *Aquaculture Nutr.* 6, 119–127. doi:10.1046/j.1365-2095.2000.00137.x

Ruyter, B., RØsjØ, C., Einen, O., and Thomassen, M. S. (2000b). Essential Fatty Acids in Atlantic salmon: Time Course of Changes in Fatty Acid Composition of Liver, Blood and Carcass Induced by a Diet Deficient in N-3 and N-6 Fatty Acids. *Aquaculture Nutr.* 6, 109–117. doi:10.1046/j.1365-2095.2000.00136.x

Segner, H., Sundh, H., Buchmann, K., Douxfils, J., Sundell, K. S., Mathieu, C., et al. (2012). Health of Farmed Fish: Its Relation to Fish Welfare and its Utility as Welfare Indicator. *Fish. Physiol. Biochem.* 38, 85–105. doi:10.1007/s10695-011-9517-9

Smith, W. L., and Murphy, R. C. (2015). The Eicosanoids: Cyclooxygenase, Lipoxygenase and Epoxygenase Pathways. *Sixth Edit. Elsevier* 2016, 259–296. doi:10.1016/B978-0-444-63438-2.00009-2

Stefansson, S. O., Haugland, M., Björnsson, B. T., McCormick, S. D., Holm, M., Ebbesson, L. O. E., et al. (2012). Growth, Osmoregulation and Endocrine Changes in Wild Atlantic salmon Smolts and post-smolts during marine Migration. *Aquaculture* 362-363, 127–136. doi:10.1016/j.aquaculture.2011.07.002

Sundell, K., Jutfelt, F., Ágústsson, T., Olsen, R.-E., Sandblom, E., Hansen, T., et al. (2003). Intestinal Transport Mechanisms and Plasma Cortisol Levels during normal and Out-Of-Season Parr-Smolt Transformation of Atlantic salmon, *Salmo salar*. *Aquaculture* 222, 265–285. doi:10.1016/S0044-8486(03)00127-3

Sundell, K. S., and Rønnestad, I. (2011). "INTEGRATED FUNCTION and CONTROL of the GUT | Intestinal Absorption," in *Encyclopedia of Fish Physiology*. *In-Chief*: *Anthony*. Editor P. F. Editor (San Diego: Academic Press), 1311–1321. doi:10.1016/b978-0-12-374553-8.00072-1

Sundell, K. S., and Sundh, H. (2012). Intestinal Fluid Absorption in Anadromous Salmonids: Importance of Tight Junctions and Aquaporins. *Front. Physio.* 3, 388. doi:10.3389/fphys.2012.00388

Sundh, H., Finne-fridell, F., Ellis, T., Taranger, G. L., Niklasson, L., Pettersen, E. F., et al. (2019). Reduced Water Quality Associated with Higher Stocking Density Disturbs the Intestinal Barrier Functions of Atlantic salmon (*Salmo salar* L.). *Aquaculture* 512, 734356. doi:10.1016/j.aquaculture.2019.734356

Sundh, H., Kvamme, B., Fridell, F., Olsen, R., Ellis, T., Taranger, G., et al. (2010). Intestinal Barrier Function of Atlantic salmon (*Salmo salar* L.) post Smolts Is Reduced by Common Sea Cage Environments and Suggested as a Possible Physiological Welfare Indicator. *BMC Physiol.* 10, 22. doi:10.1186/1472-6793-10-22

Sundh, H., Nilsen, T. O., Lindström, J., Hasselberg-Frank, L., Stefansson, S. O., McCormick, S. D., et al. (2014). Development of Intestinal Ion-Transporting Mechanisms during Smoltification and Seawater Acclimation in Atlantic salmon *Salmo salar*. *J. Fish. Biol.* 85, 1227–1252. doi:10.1111/jfb.12531

Sundh, H., Olsen, R.-E., Fridell, F., Gadan, K., Evensen, Ø., Glette, J., et al. (2009). The Effect of Hyperoxygenation and Reduced Flow in Fresh Water and Subsequent Infectious Pancreatic Necrosis Virus challenge in Sea Water, on the Intestinal Barrier Integrity in Atlantic salmon,Salmo salarL. *J. Fish. Dis.* 32, 687–698. doi:10.1111/j.1365-2761.2009.01047.x

Sundh, H., and Sundell, K. S. (2015). "Environmental Impacts on Fish Mucosa," in *Mucosal Health in Aquaculture*. Editor E. Peatman (Elsevier), 171–197. doi:10.1016/B978-0-12-417186-2.00007-8

Terjesen, B. F., Summerfelt, S. T., Nerland, S., Ulgenes, Y., Fjæra, S. O., Megård Reiten, B. K., et al. (2013). Design, Dimensioning, and Performance of a Research Facility for Studies on the Requirements of Fish in RAS Environments. *Aquacultural Eng.* 54, 49–63. doi:10.1016/j.aquaeng.2012.11.002

Tipsmark, C. K., Kiilerich, P., Nilsen, T. O., Ebbesson, L. O. E., Stefansson, S. O., and Madsen, S. S. (2008). Branchial Expression Patterns of Claudin Isoforms in Atlantic salmon during Seawater Acclimation and Smoltification. *Am. J. Physiology-Regulatory, Integr. Comp. Physiol.* 294, R1563–R1574. doi:10.1152/ajpregu.00915.2007

Tipsmark, C. K., and Madsen, S. S. (2012). Tricellulin, Occludin and Claudin-3 Expression in salmon Intestine and Kidney during Salinity Adaptation. *Comp. Biochem. Physiol. A: Mol. Integr. Physiol.* 162, 378–385. doi:10.1016/j.cbpa.2012.04.020

Tipsmark, C. K., Sørensen, K. J., Hulgard, K., and Madsen, S. S. (2010a). Claudin-15 and -25b Expression in the Intestinal Tract of Atlantic salmon in Response to Seawater Acclimation, Smoltification and Hormone Treatment. *Comp. Biochem. Physiol. Part A: Mol. Integr. Physiol.* 155, 361–370. doi:10.1016/j.cbpa.2009.11.025

Tipsmark, C. K., Sørensen, K. J., and Madsen, S. S. (2010b). Aquaporin Expression Dynamics in Osmoregulatory Tissues of Atlantic salmon during Smoltification and Seawater Acclimation. *J. Exp. Biol.* 213, 368–379. doi:10.1242/Jeb.034785

Usami, M., Komurasaki, T., Hanada, A., Kinoshita, K., and Ohata, A. (2003). Effect of γ-linolenic Acid or Docosahexaenoic Acid on Tight junction Permeability in Intestinal Monolayer Cells and Their Mechanism by Protein Kinase C Activation And/or Eicosanoid Formation. *Nutrition* 19, 150–156. doi:10.1016/S0899-9007(02)00927-9

Usami, M., Muraki, K., Iwamoto, M., Ohata, A., Matsushita, E., and Miki, A. (2001). Effect of Eicosapentaenoic Acid (EPA) on Tight junction Permeability in Intestinal Monolayer Cells. *Clin. Nutr.* 20, 351–359. doi:10.1054/clnu.2001.0430

Veillette, P. A., Sundell, K., and Specker, J. L. (1995). Cortisol Mediates the Increase in Intestinal Fluid Absorption in Atlantic salmon during Parr-Smolt Transformation. *Gen. Comp. Endocrinol.* 97, 250–258. doi:10.1006/gcen.1995.1024

Veillette, P. a., White, R. J., and Specker, J. L. (1993). Changes in Intestinal Fluid Transport in Atlantic salmon (*Salmo salar* L) during Parr-Smolt Transformation. *Fish. Physiol. Biochem.* 12, 193–202. doi:10.1007/BF00004367

Venkatakrishnan, V., Padra, J. T., Sundh, H., Sundell, K., Jin, C., Langeland, M., et al. (2019). Exploring the Arctic Charr Intestinal Glycome: Evidence of Increased N-Glycolylneuraminic Acid Levels and Changed Host-Pathogen Interactions in Response to Inflammation. *J. Proteome Res.* 18, 1760–1773. doi:10.1021/acs.jproteome.8b00973

Vidakovic, A., Langeland, M., Sundh, H., Sundell, K., Olstorpe, M., Vielma, J., et al. (2015). Evaluation of Growth Performance and Intestinal Barrier Function in Arctic Charr (*Salvelinus alpinus*) Fed Yeast (*Saccharomyces cerevisiae*), Fungi (*Rhizopus Oryzae*) and Blue Mussel (*Mytilus edulis*). *Aquaculture Nutr.* 22, 1343–1360. doi:10.1111/anu.12344

Whittamore, J. M. (2012). Osmoregulation and Epithelial Water Transport: Lessons from the Intestine of marine Teleost Fish. *J. Comp. Physiol. B* 182, 1–39. doi:10.1007/s00360-011-0601-3

Willemsen, L. E. M., Koetsier, M. A., Balvers, M., Beermann, C., Stahl, B., and Van Tol, E. A. F. (2008). Polyunsaturated Fatty Acids Support Epithelial Barrier Integrity and Reduce IL-4 Mediated Permeability *In Vitro*. *Eur. J. Nutr.* 47, 183–191. doi:10.1007/s00394-008-0712-0

Ytrestøyl, T., Aas, T. S., and Åsgård, T. (2015). Utilisation of Feed Resources in Production of Atlantic salmon (*Salmo salar*) in Norway. *Aquaculture* 448, 365–374. doi:10.1016/j.aquaculture.2015.06.023

**Conflict of Interest:** The authors declare that the research was conducted in the absence of any commercial or financial relationships that could be construed as a potential conflict of interest.

**Publisher's Note:** All claims expressed in this article are solely those of the authors and do not necessarily represent those of their affiliated organizations, or those of the publisher, the editors and the reviewers. Any product that may be evaluated in this article, or claim that may be made by its manufacturer, is not guaranteed or endorsed by the publisher.

frontiers | Frontiers in Physiology

ORIGINAL RESEARCH
published: 13 May 2022
doi: 10.3389/fphys.2022.882973

# Transport and Barrier Functions in Rainbow Trout Trunk Skin Are Regulated by Environmental Salinity

*D. Doyle*, B. Carney Almroth, K. Sundell, N. Simopoulou and H. Sundh*

*Department of Biological and Environmental Sciences, University of Gothenburg, Gothenburg, Sweden*

The mechanisms underpinning ionic transport and barrier function have been relatively well characterised in amphibians and fish. In teleost fish, these processes have mostly been characterised in the gill and intestine. In contrast, these processes remain much less clear for the trunk skin of fish. In this study, we measured barrier function and active transport in the trunk skin of the rainbow trout, using the Ussing chamber technique. The effects of epithelial damage, skin region, salinity, and pharmacological inhibition were tested. Skin barrier function decreased significantly after the infliction of a superficial wound through the removal of scales. Wound healing was already underway after 3 h and, after 24 h, there was no significant difference in barrier function towards ions between the wounded and control skin. In relation to salinity, skin permeability decreased drastically following exposure to freshwater, and increased following exposure to seawater. Changes in epithelial permeability were accompanied by salinity-dependent changes in transepithelial potential and short-circuit current. The results of this study support the idea that barrier function in rainbow trout trunk skin is regulated by tight junctions that rapidly respond to changes in salinity. The changes in transepithelial permeability and short circuit current also suggest the presence of an active transport component. Immunostaining and selective inhibition suggest that one active transport component is an apical V-ATPase. However, further research is required to determine the exact role of this transporter in the context of the trunk skin.

**Keywords: ussing chamber, V-ATPase, tight junction (TJ), fish skin, wound healing**

OPEN ACCESS

***Edited by:***
*Marce Herrera,*
*IFAPA Centro Agua del Pino, Spain*

***Reviewed by:***
*Dennis Kolosov,*
*California State University San Marcos, United States*
*Salvatore Blair,*
*Winthrop University, United States*
*Ignasi Sanahuja,*
*University of Barcelona, Spain*

****Correspondence:***
*D. Doyle*
*darragh.doyle@bioenv.gu.se*

***Specialty section:***
*This article was submitted to Aquatic Physiology, a section of the journal Frontiers in Physiology*

***Received:*** *24 February 2022*
***Accepted:*** *29 April 2022*
***Published:*** *13 May 2022*

***Citation:***
*Doyle D, Carney Almroth B, Sundell K, Simopoulou N and Sundh H (2022) Transport and Barrier Functions in Rainbow Trout Trunk Skin Are Regulated by Environmental Salinity. Front. Physiol. 13:882973. doi: 10.3389/fphys.2022.882973*

## INTRODUCTION

The mucosal barriers of fish include the skin, gill and intestine. As these membranes are the first point of contact between the animal and the environment, their integrity is crucial for fish health and welfare (Segner et al., 2012; Rombout et al., 2014). The mucosal barriers are essential to separate the internal environment of the fish from the external environment. In this respect, they allow the fish to osmoregulate by limiting passive ion and fluid diffusion. Further, some mucosal epithelia such as those of the gill, kidney, and intestine are sites of active ionic transport (Loretz, 1995; Marshall, 2002; Takvam et al., 2021). This combination of barrier function and active transport is vital to maintain ion homeostasis, as fish are constantly exposed to osmotic pressures that challenge the internal environment. In addition to facilitating ion homeostasis, the mucosal surfaces provide an important barrier to prevent pathogens from entering the fish and causing infection (Gomez et al., 2013). The contribution of the intestine and gills to ion transport and barrier function have been relatively well

described (Evans et al., 2005; Grosell, 2010; Whittamore, 2012). In comparison, less is known about these processes in the skin.

Fish skin consists of two main layers, an outer epidermis and an inner dermis with scales attached. While both the epidermis and dermis function in concert as a protective barrier for internal organs, muscles, nerves, and blood vessels, the epidermis alone is the layer that constitutes the physical barrier towards ions, pathogens, and toxins within the environment (Rakers et al., 2010). Epidermal barrier function is provided by the epithelial cells (keratocytes), which are connected by a network of intercellular proteins known as tight junctions (TJs). TJs are composed of several transmembrane proteins, most notably claudin and occludin isoforms (Günzel and Fromm, 2012), which collectively regulate permeability and selectivity through the paracellular pathway (Chasiotis et al., 2012; Günzel and Yu, 2013).

The expression of claudin isoforms in fish skin has been shown to vary based on both body region (Gauberg et al., 2017) and environmental salinity (Bagherie-Lachidan et al., 2008; Bagherie-Lachidan et al., 2009). In relation to the latter, certain claudin-10 isoforms are thought to be associated with the formation of cation selective pores in seawater acclimated fish (Bui and Kelly, 2014; Marshall et al., 2018; Chen et al., 2021). In rainbow trout, the mRNA abundance of 10 different claudin isoforms was shown to vary in response to elevated cortisol (Gauberg et al., 2017), which is an important osmoregulatory hormone (Redding et al., 1984). This divergent expression of claudin isoforms likely contributes to differences in the permeability and selectivity of the paracellular pathway in fish skin. Goblet cell density and epidermal thickness have also been shown to vary in rainbow trout skin based following cortisol exposure (Gauberg et al., 2017), providing further evidence that the permeability and selectivity of the skin barrier may be physiologically regulated and may vary depending on body site.

The majority of knowledge related to ion transport and barrier function in fish skin stems from *in vitro* studies of the operculum, cleithrum or jaw skin - collectively referred to as cephalic skin (McCormick, 1994; Marshall and Bellamy, 2010; Glover et al., 2013). In teleost fish, mitochondria rich cells (MRCs) make up a significant proportion of both gill and cephalic skin epithelia (Foskett and Scheffey, 1982). Given the structural similarities between the two epithelia, the cephalic skin is suggested to be functionally similar to the gill, in which barrier and active transport functions have been extensively studied (McCormick, 1994; Glover et al., 2013). As such, it is unlikely that insights gained from studies of the cephalic skin are representative of trunk skin. Historically, the trunk skin has been cited as an impermeable barrier, incapable of electrogenic transport (Fromm, 1968). However, there is now growing evidence to suggest the trunk skin of teleost fish is capable of active ion transport. For example, the sodium-hydrogen antiporter (NHE), vacuolar type ATPase (V-ATPase), and Rhesus (Rh) proteins have all been identified in the trunk skin of rainbow trout (Zimmer et al., 2014). However, it has yet to be determined if these transporters contribute significantly to overall ion homeostasis (Wright and Wood, 2009).

The aim of this study was to assess and characterise the functional organization of the trunk skin barrier of rainbow trout and elucidate potential active transport mechanisms. To achieve this, two separate experiments were carried out. In the first experiment, barrier function and active transport were assessed in fully-intact skin (dermis, epidermis, and scales present) and in superficially wounded skin (scales removed). This allowed for the assessment of the contribution of each of these skin components to barrier function and active transport. Sampling at different time points following wounding also allowed barrier function and active transport to assessed at different points throughout the wound-healing process. In the second experiment, the contribution of the different skin layers to barrier function and active transport was further assessed in fully intact skin (dermis, epidermis, and scales present) and wounded skin (only dermis present). This experiment also measured regional differences in skin function, as well as the response of the skin to environmental variation in the form of salinity change. Finally, the second experiment assessed the effect of pharmacological inhibition on potential sites of active transport in the skin.

# METHODS

## Experimental Fish and Holding Conditions

Rainbow trout (150–200 g) were obtained from Vänneån fish farm and maintained at the Department of Biological and Environmental Sciences, University of Gothenburg. Fish were maintained in 1 $m^3$ concrete tanks supplied with freshwater (10°C) from a recirculating aquaculture system (RAS). For experiment two, a subset of fish was acclimated to SW by exchanging the inlet water from FW to 10°C artificial SW from another RAS so that full strength SW (35 ppt) was reached after approximately 24 h. This subset was maintained in SW for at least 2 weeks prior to commencing the experiment. All fish were maintained on a 12:12 day/night cycle and were fed commercial pellets (Biomar). All experimental procedures were approved by the Swedish Board of Agriculture (ethical permit number: 5.8.18-15096/2018). There were no mortalities reported during the experiment.

## Ussing Chamber Methodology

In both experiments, skin barrier function and active transport were assessed using the Ussing chamber technique (UCC-401; UCC-Laboratories Ltd.) described by Sundell et al. (2003), and using modifications described by Sundell and Sundh (2012). In brief, this method involves the measurement of several electrophysiological parameters from an isolated epithelium, which is simultaneously bathed by two independent solutions (one environmental/apical and one internal/basal). In both experiments, the skin was mounted in the chambers with the epidermis exposed to the environmental/apical chamber half, and the dermis exposed to the internal/basal chamber half. A gas mixture consisting of 99.7% air and 0.3% CO2 provided circulation, oxygenation and pH regulation to both chamber halves. This ensured viability of the excised skin for the

duration of the experiment. The temperature of the chambers was kept at 10°C using a water-cooled mantle.

Alternating adaptive DC voltages (U) were applied to the mounted skin every 5 min using platinum electrodes. The applied voltages generated corresponding currents (I) varying between −30 and 30 μA, which prevented electrical charging of the epithelia. The U/I pairs assessed were fitted to a straight line using the least-square method. The slope of the line represented the transepithelial electrical resistance (TER). The short circuit current (SCC) was calculated where U = 0. A pair of KCl electrodes in a 3 M KCl solution continuously measured the transepithelial potential difference (TEP) across the epithelium *via* a series of agar bridges. The TER mainly reflects the paracellular shunt resistance created across the tight junction proteins between the epithelial cells, while the TEP reflects the net ion distribution across the epithelium as a result of the paracellular and transcellular transfer of ions. Finally, SCC is a measure of the net active ion transport across the epithelium.

## Experiment 1 – Skin Functions in Different Skin Tissue Layers and Healing of a Superficial Wound

FW acclimated rainbow trout ($N$ = 31) were anaesthetised with FW buffered tricaine methanesulfonate (MS-222; 100 mg/L). The skin was superficially wounded by descaling an area (~1.5 $cm^2$) just below the dorsal fin using a scalpel. Fish were then allowed to recover in the concrete tanks before the skin was sampled. To sample the skin, the fish were euthanised in buffered tricaine methanesulfonate (MS-222; 250 mg/L), after which the gill arch was severed. Skin was sampled at the following time points: right after the wound (0 h), 3, 24, and 48 h post wounding. A dorsal-ventral incision was made posterior to the wound site. From here, two longitudinal incisions were made (one above the lateral line and one at the uppermost dorsal region), which extended towards the head. This resulted in a single strip of dorsal flank skin, roughly 3 cm wide, including the wounded area. This strip of skin was carefully separated from the underlying muscle by lifting and peeling with a scalpel. A section of intact skin was then sampled anterior to the wounded area. The excised skin was mounted in the Ussing chambers, with the epidermis facing the environmental side. Four millilitres of chilled Ringer's solution (mmol $L^{-1}$: NaCl 140, KCl 2.5, $CaCl_2$ 1.5, $MgSO_4$*$7H_2O$ 0.8, $NaHCO_3$ 15, $KH_2PO_4$ 1, HEPES 5, D-Glucose 10, L-Glutamine 20) was added to both the apical and basal chamber halves, making the preparation isosmotic i.e. there was no concentration gradient to facilitate passive ion movement. A gas mixture consisting of 99.7% air and 0.3% $CO_2$ provided circulation, oxygenation and pH regulation to ensure viability of the excised skin for the duration of the experiment. The temperature of the chambers was kept at 10°C using a water-cooled mantle. The skin was acclimated for 60 min.

After the acclimation period, Ringer's solution containing $^{14}$C-mannitol (0.04 MBq $ml^{-1}$) was added to the apical chamber half, while the basal side was also replenished with fresh Ringer's solution. $^{14}$C-mannitol was used to assess epithelial permeability to small, uncharged molecules. After 20 min, 50 μl of solution was taken from both the apical and basal chamber halves. Additional 50 μl samples were taken from the basal side after 25, 30, 60, 80, 85 and 90 min. The samples were placed in scintillation vials filled with 4.5 ml UltimaGold (PerkinElmer, MA, United States). Radioactivity was determined in a beta counter (Wallac 1409 DSA Liquid Scintillation Counter; PerkinElmer, MA, United States). The apparent permeability was calculated as:

$$P_{app} = dQ \div dt \times 1\,(A \times Co)$$

Where dQ ÷ dt is the rate of radioactivity of the measured basal side (mol/s), A is the area of the Ussing chamber aperture, and Co (mol/ml) is the concentration of $^{14}$C-mannitol measured from the apical side. TER was also assessed for the duration of experiment 1, to determine the permeability of the skin to ion movement.

## Experiment 2

### Effect of Body Region and Epidermal Loss on Skin Function

In experiment 2, the skin was sampled in the same manner as described in **Section 2.3**. However, to assess the effect of body region on skin function, skin was sampled from eight different locations on the body of each fish i.e. two dorsal and two ventral sections (posterior and anterior) on both the right and left side of each fish. To assess the contribution of the dermis to barrier function and active transport, one dorsal section and one ventral section from both the left and right side of each fish were experimentally damaged. This was achieved by scraping away both the epidermis and scales, leaving only the dermis. The damaged sections were alternated (anterior or posterior) between each fish. This resulted in four intact skin sections, and four damaged skin sections for each individual. The sampled regions are shown in **Figure 1**.

In total, 36 individuals were analysed, which comprised 288 skin sections. Once all of the skin sections were removed and prepared, they were mounted in their respective Ussing chambers as described in **Section 2.3**, with the difference that $^{14}$C-Mannitol was not used in experiment 2. FW Ringer's solution (described in **Section 2.3**) or SW Ringer's solution (mmol $L^{-1}$: NaCl 150, KCl 2.5, $CaCl_2$ 2.5, $MgCl_2$*$6H_2O$ 1, $NaHCO_3$ 7, $NaH_2PO4$*$2H_2O$ 0.7, HEPES 5, D-Glucose 10, L-Glutamine 20) was added to each chamber half depending on acclimation salinity. The skin was then acclimated under isosmotic conditions for 60 min.

### Effect of Salinity on Skin Function

To determine potential long-term and short-term responses to environmental salinity, four different salinity exposures were conducted. To explore barrier function and active transport in long-term acclimated fish, skin sampled from FW acclimated fish was exposed to FW, while skin from SW acclimated fish was exposed to SW. To explore the effect of acute salinity change on barrier function and active transport, skin from FW acclimated fish was exposed to SW, while skin from SW acclimated fish was exposed to FW. Each salinity exposure took place on the apical/epidermis side. To achieve this, the apical Ringer's solution was replaced with 4 ml of either FW or SW after the 60 min acclimation period, while Ringer's solution remained present

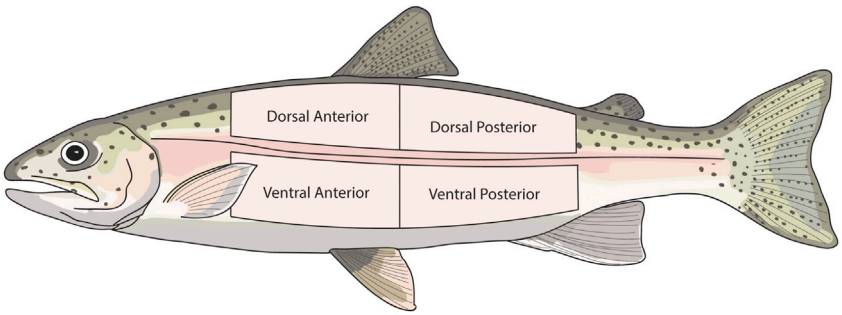


**FIGURE 1 |** Diagram showing the skin regions that were sampled in experiment 2. The same skin regions were sampled from both the right and left side of each fish.

in the basal chamber half. The basal Ringer's solution was refreshed 110 min after commencing the experiment. In the first two series (FW-FW and SW-SW), 12 rainbow trout were analysed. Six individuals were analysed in each of the other series (FW-SW and SW-FW).

### Effect of Pharmacological Inhibition on Skin Function

To characterise potential active transport, N-ethylmaleimide (NEM) was used to test for the presence of V-ATPase. This inhibitor was used as V-ATPase has previously been reported in rainbow trout skin (Zimmer et al., 2014). A stock solution of NEM (100 mM) was prepared using 70% ethanol as vehicle. Forty microliters of this stock solution was added to either the apical or basal chamber half, yielding a 1 mM concentration in the chambers. The chamber half that did not receive the inhibitor was supplied with 40 µl of vehicle only as the control. NEM was added 150 min after commencing the experiment. Once NEM was added, the experiment continued until the electrical parameters reached an approximate asymptote, hereafter referred to as steady state. When steady state was reached, the experiment was terminated.

## Immunohistochemistry

Immunohistochemistry was used to test for the presence of V-ATPase and NKA in the skin. Skin sections were excised from the same regions as experiment 2. The sections were fixed in 4% paraformaldehyde (PFA; 24 h), followed by decalcification in EDTA (0.5M; pH 8; 24 h). The samples were embedded in paraffin and sectioned (5 µm) using a rotary microtome (Shandon Finesse 325, Thermo Fisher Scientific, United States). The sections were attached to aminopropyltriethoxysilane (APES; Sigma A3648) coated slides. The slides were dewaxed using Histoclear and rehydrated *via* a graded ethanol series (100–70%) to distilled water, followed by tris-buffered saline and Tween 20 (TBST; 0.05M, pH 7.6, 2 × 5 min baths). The sections were bathed in a blocking buffer (5% normal goat serum, 5% normal donkey serum, 3% BSA in TBST) at room temperature for 60 min, followed by incubation in a humidity chamber overnight at 4°C with the primary antibody. The V-ATPase primary antibody (GenScript Cat. No. A00938) was diluted 1:1600 in blocking buffer, while the NKA (monoclonal mouse-anti NKA; α5) primary antibody was diluted 1:800. The slides were rinsed in TBST and incubated at room temperature with the secondary antibody. The V-ATPase secondary antibody (donkey anti-rabbit, Jackson ImmunoResearch) was diluted 1:200 in 0.05M TBST, while the NKA antibody (donkey anti-mouse, Jackson ImmunoResearch) was diluted 1:1000 in 0.05 M TBST. The slides were incubated with avidin-biotin-complex substrate (Vectastain ABC kit) for 30 min. Finally, the slides were stained with Vector NovaRed for 8–10 min, after which they were dehydrated *via* a graded ethanol series and mounted in Pertex mounting medium (Histolab Products AB, Sweden). The α5 antibody were developed by D. Fambourgh (John Hopkins University, Baltimore, MD) and was obtained from the Developmental Studies Hybridoma Bank developed under the auspices of the National Institute of Child Health and Human Development (NICHD; www.nichd.nih.gov) and maintained by the University of Iowa, Department of Biology, Iowa City, IA.

## Statistical Analysis

### Experiment 1

Two-way ANOVAs were carried out to test the effect of superficial wounding on both TER and $^{14}$C-mannitol $P_{app}$ (Log-transformed). For these tests, the main effects of wounding (intact/control and wounded) and time were tested. A possible significant interaction between the two was also tested. Tukey's *post hoc* tests were carried out to assess which groups differed significantly.

### Experiment 2

Welch tests were used to test for the effects of body region (dorsal-ventral, anterior-posterior, and right-left side) on TER and TEP under isosmotic conditions. Two-Way ANOVA was used to test for the effect of acclimation salinity and epidermal removal on TER (Log-transformed) and TEP under isosmotic conditions. To test for the effects of salinity, acclimation salinity and treatment salinity were combined into a new variable, hereafter referred to as salinity. This variable had four levels and is represented as "acclimation salinity-treatment salinity" (FW-FW, SW-SW, FW-SW, SW-FW). Welch's ANOVA was used to test for the effect of salinity on TER, TEP, and SCC using the final measurement prior to pharmacological inhibition. *Post-hoc* comparisons were carried out for the ANOVA using Games-Howell tests. Welch tests were also used to test for significant differences

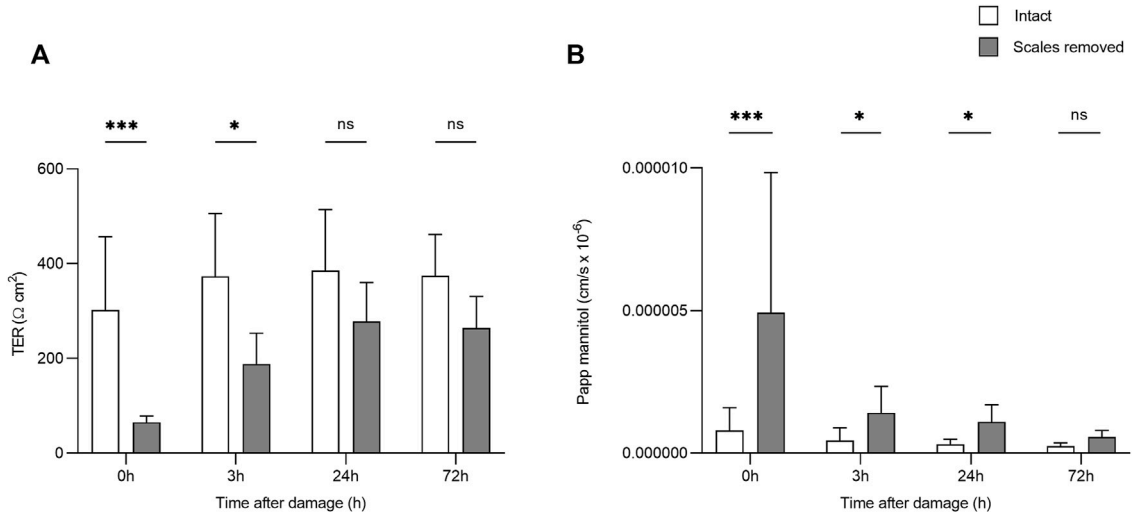


**FIGURE 2 |** Bar chart showing **(A)** transepithelial resistance (TER) and **(B)** $^{14}$C-mannitol $P_{app}$ (Log-transformed) in intact skin, and skin without scales but with intact dermis. Higher TER values indicate greater barrier function/lower transepithelial permeability, while higher $^{14}$C-mannitol $P_{app}$ values indicate greater epithelial permeability. Bars represent mean and whiskers indicate standard deviation. Significant differences based on *post-hoc* Tukey tests are denoted with asterisks (***$p$ < 0.001; *$p$ < 0.05; ns, no significant difference).

in TER, TEP, and SCC for each salinity in response to NEM exposure. Here, the final steady state measurements were used. To visualise how TER, TEP and SCC changed over time, time series were plotted for random samples to show the acute effects of salinity alteration and NEM addition. All analyses were carried out in SPSS version 27 and Graphpad Prism version 9.

# RESULTS

## Experiment 1 - Skin Functions in Different Skin Tissue Layers and Healing of a Superficial Wound

After the creation of a superficial wound, TER varied significantly over time ($F_{3,50}$ = 4.34, $p$ = 0.009, $\eta^2$ = 0.206) and based on damage ($F_{1,50}$ = 38.10, $p$ = <0.0001, $\eta^2$ = 0.432; **Figure 2**). After 24 h, there was no significant difference in TER between the damaged and intact skin. $^{14}$C-mannitol $P_{app}$ also varied significantly over time in the damaged skin ($F_{3,27}$ = 11.076; $p$ = <0.0001; $\eta^2$ = 0.552), with $^{14}$C-mannitol $P_{app}$ being significantly higher in the 0 h group compared to the 3, 24, and 72 h groups. Immediately after wounding (0 h), $^{14}$C-mannitol $P_{app}$ was 83.6% higher in the damaged skin than in the intact skin. This had decreased to 68.7 and 71.7% after 3 and 24 h respectively. After 72 h, the difference had decreased to 56.6%, at which point the damaged and intact skin did not differ significantly. This reduction in permeability indicated the gradual formation of a neo-epidermis i.e. a newly formed epithelium. Significant differences in TER and $^{14}$C-mannitol $P_{app}$ are shown in **Figure 2**.

## Experiment 2

### Contribution of the Dermis to Skin Function and Variation Based on Body Region

There were no significant differences in TER or TEP based on body region (not shown). Under isosmotic conditions, complete epidermis/scale loss resulted in a 96 and 97% decrease in TER in the SW and FW acclimated fish respectively. The intact SW acclimated skin had significantly higher TER than the intact FW acclimated skin ($F_{1,\ 143}$ = 23.87, $p$ = <0.001) The TEP remained close to zero at isosmotic conditions, regardless of epidermal removal/acclimation salinity. However, there was a significant interaction between acclimation salinity and damage ($F_{1,284}$ = 11.53, $p$ = 0.039, $\eta^2$ = 0.039). Subsequent analysis of simple effects showed that intact SW acclimated skin had a small but significantly higher TEP than intact FW acclimated skin ($F_{1,143}$ = 23.87, $p$ = <0.001) and damaged SW skin ($F_{1,143}$ = 15.86, $p$ = <0.001). Significant differences in TER and TEP are shown in **Figure 3**.

The ion content in the water directly affects the conductivity and hetero-osmotic solutions in each half chamber, resulting in passive ion potentials that affect the TEP. Based on the negligible changes in TER in the damaged skin (dermis only) following either FW or SW addition (**Supplementary Figures S1, S2** respectively), the changes observed over time in the intact skin were clearly a physiological response of the epidermis. As the dermis did not appear to be functional in relation to either active transport or barrier function, only intact skin sections i.e. those not experimentally damaged were used for subsequent analyses.

### The Effect of Salinity on Barrier Function and Active Transport

When the apical Ringer's solution was replaced with FW, the electrical parameters changed rapidly within minutes (**Figure 4**).

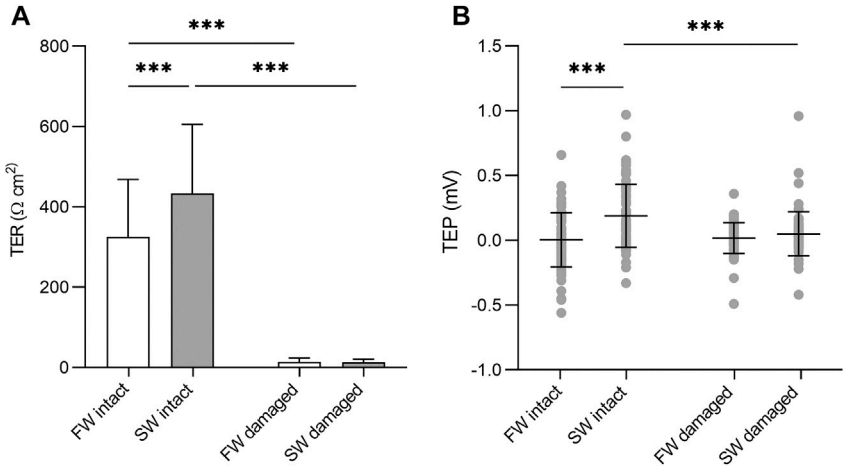


**FIGURE 3 | (A)** Barchart of transepithelial resistance (TER) and **(B)** dotplot of transepithelial potential (TEP) in intact skin and skin without the epidermis. Bars represent mean and whiskers represent SD. Significant differences based on simple effects analysis using one –way ANOVA are denoted with asterisks (***$p < 0.001$).

This was accompanied by a large and rapid change in TEP (−4.2 ± 1.3 mV and −2.9 ± 1.4 mV respectively; basal-side negative) and SCC (3.6 ± 0.7 μA $cm^{-1}$ and 1.9 ± 0.4 μA $cm^{-1}$ respectively). Conversely, when SW was added to the apical chamber the TER instantly decreased, with the TER of the SW-SW and FW-SW groups averaging 301 ± 127 Ω*$cm^2$ and 233 ± 140 Ω*$cm^2$ respectively. This was accompanied by a slight increase in TEP (0.1 ± 0.3 mV and 0.02 ± 0.3 mV respectively; basal-side positive) and SCC (−0.3 ± 0.8 μA $cm^{-1}$ and -0.5 ± 1.1 μA $cm^{-1}$ respectively; **Figure 5**).

The final TER, TEP, and SCC measurements before the addition of NEM were used to carry out separate Welch's ANOVAs to assess the effect of salinity. Altering salinity in the apical chamber was found to significantly effect TER ($F_{3, 140} = 118.40$, $p = < 0.0001$, $\eta^2 = 0.717$), TEP ($F_{3, 140} = 199.47$, $p = < 0.0001$, $\eta^2 = 0.810$) and SCC ($F_{3, 140} = 77.806$, $p = < 0.0001$, $\eta^2 = 0.625$; **Figure 6**). *Post-hoc* Games-Howell tests showed that each level within the factor "salinity" differed significantly from the other for TER and TEP, with the exception of SW-SW and FW-SW. For SCC, each level within the factor "salinity" differed significantly from the other, with the exception of SW-FW and FW-SW.

### Pharmacological Inhibition of Primary Active Transport

The addition of NEM induced a rapid reduction in TER, which was most evident in the FW acclimated fish. In the FW-FW group, this reduction in TER was accompanied by a similarly rapid and negative change in TEP. The effect of NEM addition on TER, TEP, and SCC was statistically tested for each level within the factor salinity (**Figure 7**). The addition of NEM to the apical chamber half significantly reduced TER in the FW-FW ($F_{1,46} = 56.514$; $p = <0.001$, $\eta^2 = 0.551$), SW-FW ($F_{1,22} = 20.734$; $p = <0.001$, $\eta 2 = 0.485$), SW-SW ($F_{1,46} = 43.556$; $p = <0.001$, $\eta^2 = 0.486$) and FW-SW ($F_{1,22} = 13.828$; $p = <0.001$, $\eta^2 = 0.386$) groups. Eta-squared values showed that the addition of NEM had the greatest effect on the FW-FW group, corresponding to a 58% reduction in TER compared to the control. The addition of NEM to the apical chamber half did not affect the TEP of any group, with the exception of FW-FW ($F_{1,46} = 28.744$; $p = <0.001$, $\eta^2 = 0.385$). The addition of NEM also significantly affected SCC for each group: FW-FW ($F_{1,46} = 89.658$; $p = <0.001$, $\eta^2 = 0.661$), SW-FW ($F_{1,22} = 9.742$; $p = 0.005$, $\eta^2 = 0.307$), SW-SW ($F_{1,46} = 9.770$; $p = 0.003$, $\eta^2 = 0.175$), and FW-SW ($F_{1,22} = 7.628$; $p = 0.011$, $\eta^2 = 0.257$).

## Immunohistochemistry

Immunostaining with the V-ATPase antibody showed staining through the epidermis of both the FW and SW acclimated fish (**Figure 8**). The staining was stronger at the apical membrane for both FW and SW acclimated fish. This indicates the presence of V-ATPase in rainbow trout, regardless of acclimation salinity. However, the FW acclimated fish appeared to have stronger staining compared to the SW fish. Immunostaining with the NKA antibody showed no indication of NKA in either FW or SW acclimated fish (not shown), which indicates that MRCs were not present in the trunk skin.

# DISCUSSION

The aim of this study was to assess and characterise the functional organization of the skin barrier of rainbow trout and to elucidate potential active transport mechanisms. To date, most studies into the electrophysiological properties of fish skin have focused on cephalic skin as a proxy for the gill (Glover et al., 2013), while the trunk skin has generally been overlooked as a site of both active transport and passive diffusion. In this study, we provide evidence to support the idea that rainbow trout skin is a dynamic tissue that quickly responds to salinity perturbations and is an active site of ion transport, functionally different from the branchial tissue and cephalic skin. We also confirm that the trunk skin creates a functional neo-

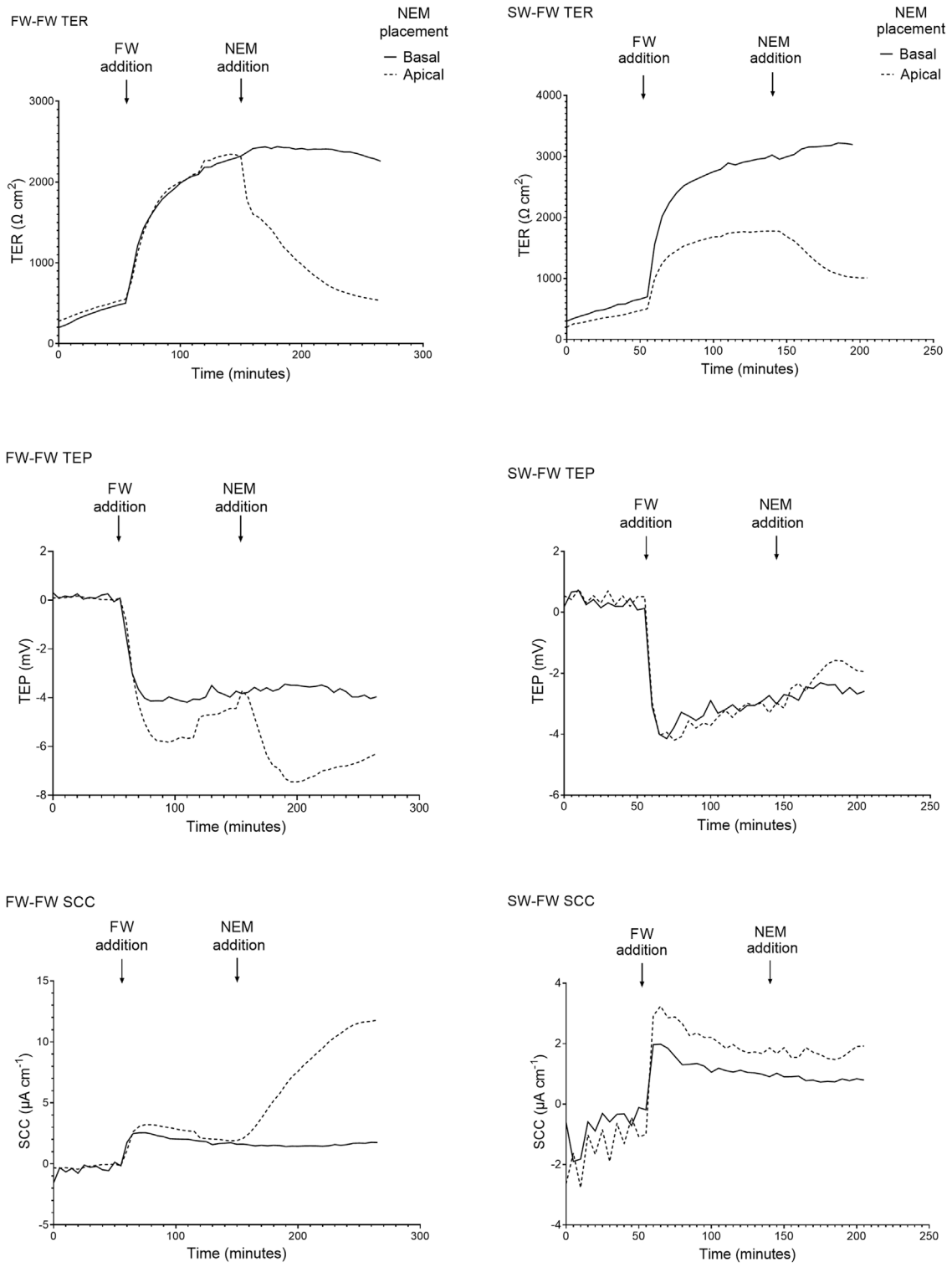


**FIGURE 4 |** Representative traces of the electrical parameters transepithelial resistance (TER), transepithelial potential (TEP), and short circuit current (SCC) time series of fish exposed to FW (FW-FW and SW-FW) in the apical chamber half. A drastic increase in TER can be seen in the FW acclimated fish, accompanied by a reduction in TEP. The response to NEM addition is also shown, with a large reduction in TER and a reduction in TEP and SCC (most evident in the FW acclimated skin).

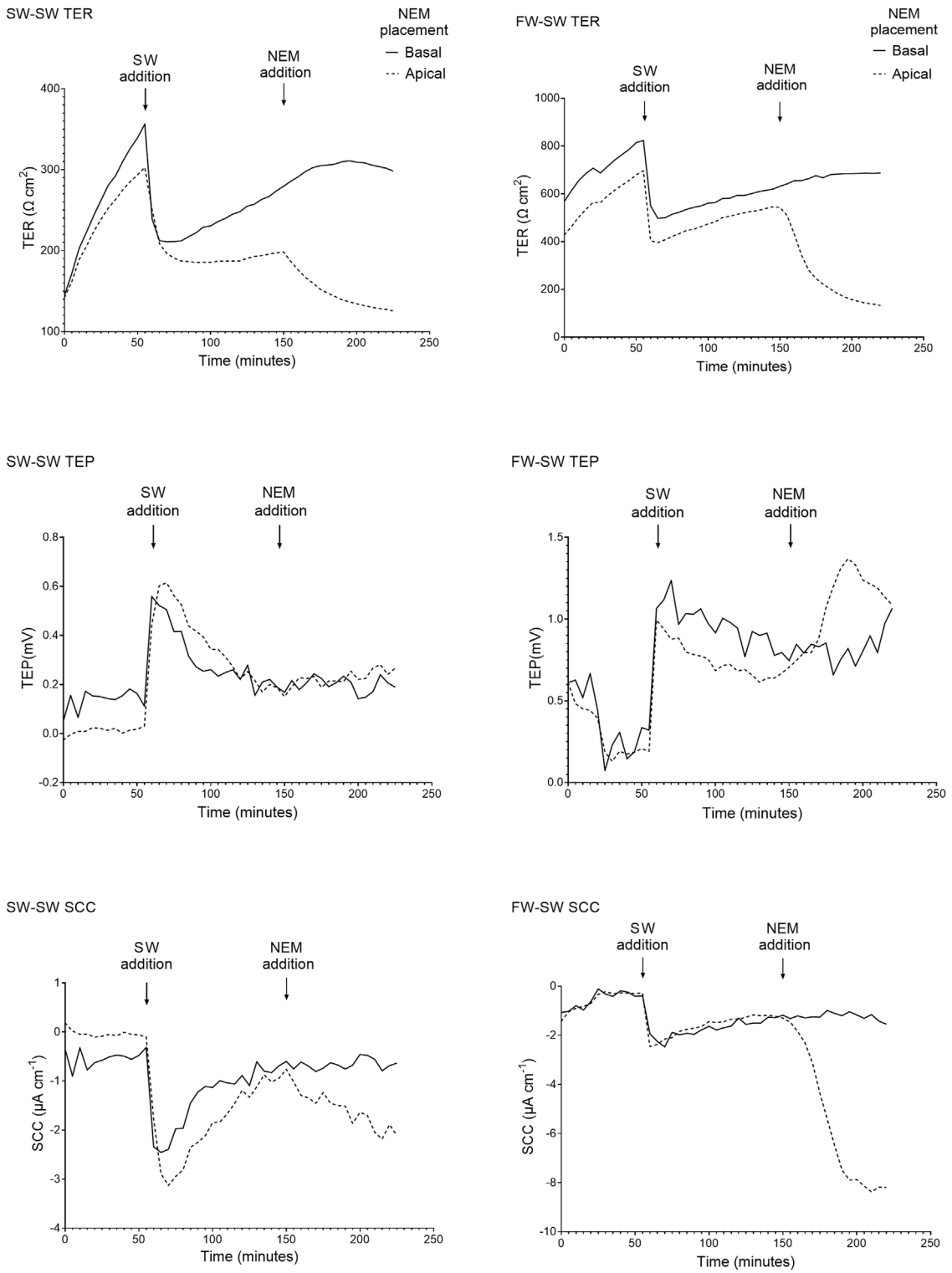


**FIGURE 5 |** Representative traces of the electrical parameters transepithelial resistance (TER), transepithelial potential (TEP), and short circuit current (SCC) time series of fish exposed to SW (SW-SW and FW-SW) in the apical chamber half. A large and acute reduction in TER is shown following SW addition, accompanied by an acute change in TEP (basal-positive). The addition of NEM is also shown, with a reduction in TER and a change in TEP (basal-positive). Again, the changes in TEP and SCC following NEM addition are far more pronounced in the FW acclimated group.

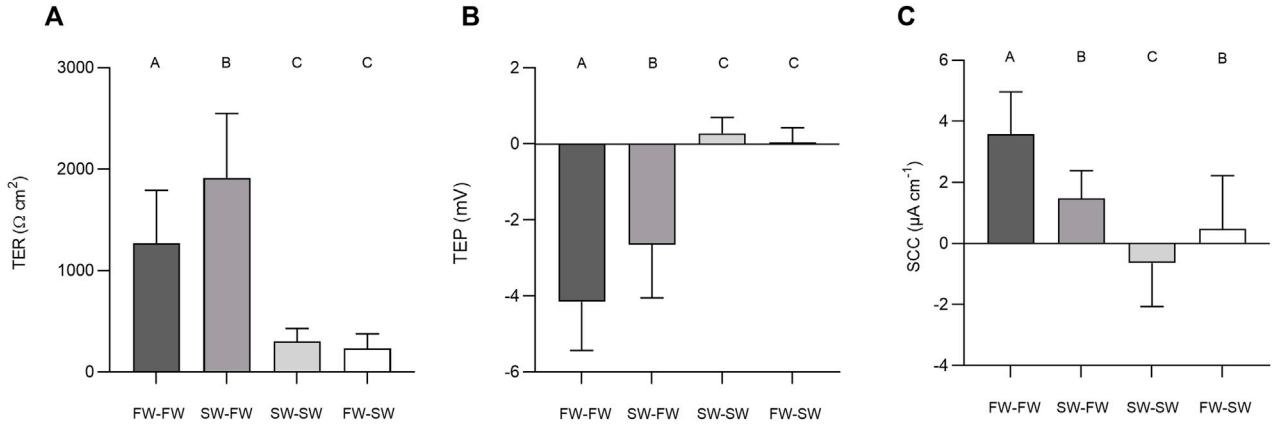


**FIGURE 6 |** Barcharts showing the effect of salinity on **(A)** transepithelial resistance (TER), **(B)** transepithelial potential (TEP), and **(C)** short-circuit current (SCC). Bars represent means and whiskers represent SD. Groups not sharing a letter differ significantly based on the results of Welch's ANOVAs and *post-hoc* Games-Howell tests.

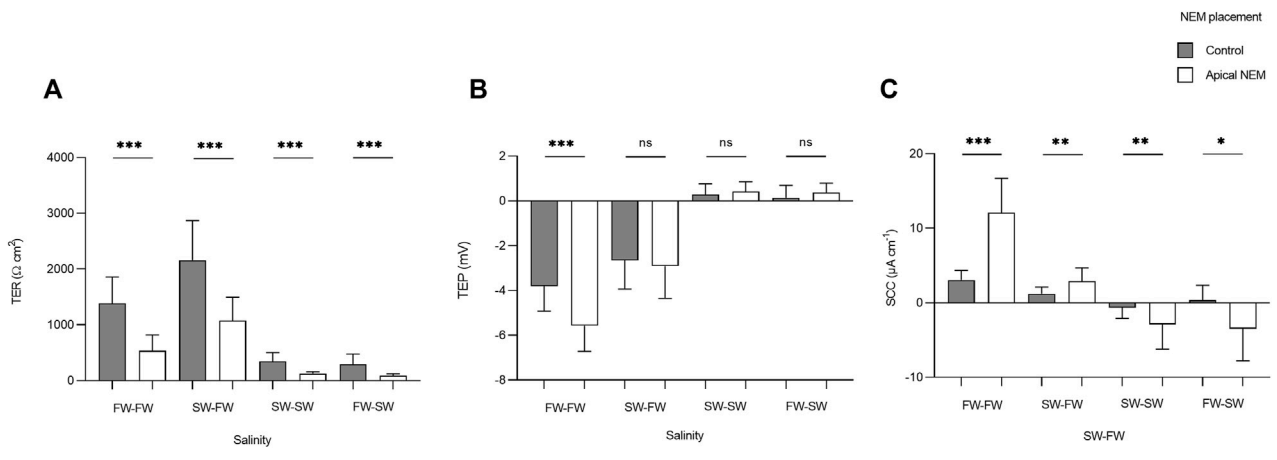


**FIGURE 7 |** Barcharts showing the effect of basal (control) and apical N-ethylmaleimide (NEM) addition on **(A)** transepithelial resistance (TER), **(B)** transepithelial potential (TEP), and **(C)** short-circuit current (SCC) for each salinity. Bars represent means and whiskers represent SD. Significant differences based on Welch tests are denoted with asterisks (***$p < 0.001$; **$p < 0.01$; *$p < 0.05$, ns, no significant difference).

epidermis within hours after wounding. In addition, we provide evidence to show that the epidermis is the main barrier forming component of the skin, while the dermis and scales play a negligible role in this regard.

## Skin Functions in Different Skin Tissue Layers and Healing of a Superficial Wound

The >95% loss of barrier function towards ions (TER) after removal of the epidermis and scales clearly showed that the dermis is not the rate limiting diffusion barrier of the skin. This was further demonstrated by comparing TER in the damaged and intact skin following acute salinity change. After altering salinity in the apical chamber half, the TER of the damaged skin changed only slightly, while the TER of the intact skin changed drastically. Further, the findings that the scales do not contribute significantly to barrier function, indicated as no significant difference between skin with scales and descaled skin with neo-epidermis, shows that the epidermis is the functional diffusion barrier in the skin. The dermis, in contrast to the epidermis, is composed mostly of fibrous connective tissue and is richly vascularised, which would structurally indicate a more leaky tissue layer (Rakers et al., 2010; Elliott, 2011). Thus, the epidermis is the main barrier between the environment and the underlying circulation. As such, any epidermal damage may lead to increased disease susceptibility and osmoregulatory problems that must be counteracted by the fish through energy demanding mechanisms (Sveen et al., 2020), which represents a threat to the health and welfare of the fish. In addition, damage to the

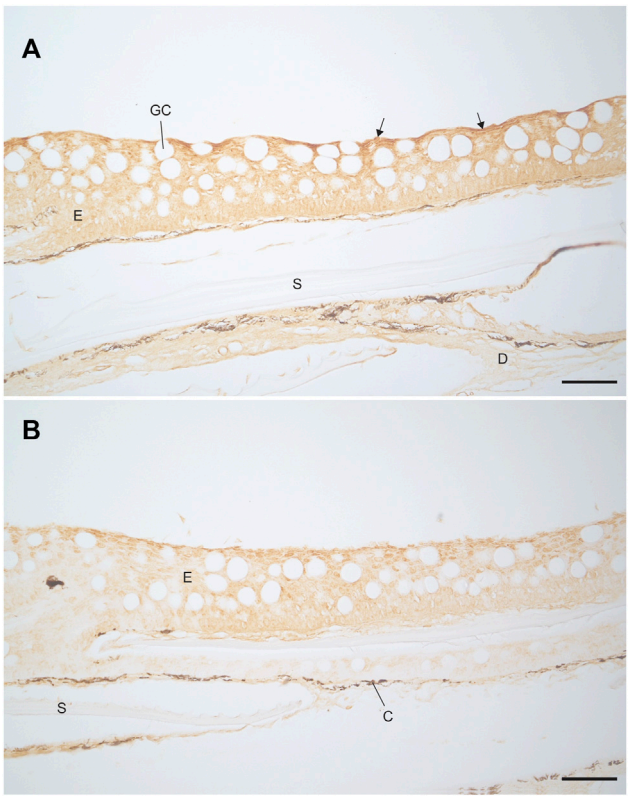


**FIGURE 8 |** Localisation of V-ATPase in the trunk skin of **(A)** FW and **(B)** SW acclimated rainbow trout. Darker staining is visible along the apical epidermal cells of the FW fish (highlighted with arrows) compared to the SW fish. Scale bar = 50 μm. E, epidermis; D, dermis; GC, goblet cell; S, scale pocket; C, chromatophore.

epidermis may hinder the production of mucus, which is the first line of defence against adverse environmental conditions and pathogens (Shepherd, 1994; Benhamed et al., 2014; Kulczykowska, 2019). These results highlight the importance of minimizing skin damage in husbandry conditions.

The wound-healing experiment showed that scale/partial epidermal loss results in an almost complete loss of barrier function. However, significant healing or re-epithelialization appears to occur within 3 h. These results are consistent with histological studies of wound healing in *Salmo salar* (Roubal and Bullock, 1988; Sveen et al., 2019), *Bagarius bagarius* (Mittal and Munshi, 1974) *Cyprinus carpio* (Iger and Abraham, 1990), and *Danio rerio* (Richardson et al., 2013). In wounds where scales and epidermis are lost but the dermis remains, such as those used in the current study, the migration of epithelial cells occurs from the intact epidermis surrounding the wound and stops when the two fronts meet (Quilhac and Sire, 1999). The migration of epithelial cells has been shown to occur rapidly in cichlids and zebrafish, with a rate of 500 μm/h reported for both species (Quilhac and Sire, 1999; Richardson et al., 2016). However, the rate of re-epithelialization in rainbow trout is likely to be slower, given the much lower ambient temperature. This migration of epithelial cells and sealing of the epidermal layer provides a functional barrier while the scales regrow (Richardson et al., 2016; Sveen et al., 2020). In salmonids, scale remodelling begins 14 days post-wound and continues for around 36 days, with the rate of scale regrowth depending on several factors including diet, temperature, and stocking density (Jensen et al., 2015; Sveen et al., 2018). Although re-epithelialization is a fast process, scale loss as a result of husbandry practices will result in acute barrier failure in the short term. For this reason, scale loss should be considered an indication of severely impaired welfare.

Interestingly, the scales themselves do not appear to provide a significant diffusion barrier for ions or molecules. The plausible explanation for this is that the scales are embedded and surrounded by the extracellular matrix of the dermis, which in itself is leaky and clearly does not provide an adequate diffusion barrier to either ions or small inert molecules such as mannitol. In addition, the scale are separated from each other and hence do not constitute a continuous layer of tissue. However, as scales are composed of both a mineralised layer and an overlapping fibrous, mineralized collagen layer, they serve as a protective, armour-like barrier against physical trauma (Elliott, 2011). Thus, even though descaled skin is quickly covered by a neo-epidermis, the wounded area is still very sensitive to physical trauma.

## Regional Differences in Skin Functions and Effect of Salinity

There was no difference in electrical parameters of the trunk skin based on body regions investigated. This is consistent with Zimmer et al. (2014), who found no differences in body region in rainbow trout trunk skin regarding ammonia transport. The lack of regional variation in any electrical parameter is interesting as Gauberg et al. (2017) previously showed differences in claudin expression along the dorsoventral axis of rainbow trout trunk skin. However, claudins are not only present in the TJs, but are also important in normal cell-cell interactions outside of the TJs. In the mammalian skin, claudins are expressed throughout the stratified epithelium of the epidermis, while functional TJs including claudins, occludins and ZO-1 are mainly formed in the cell layer just underneath the keratinized dead layer (Brandner, 2009). Thus, variations in claudin expression may also reflect general cell-cell contact in the stratified epithelium of fish skin.

Acute exposure to FW or SW, rather than long-term salinity acclimation, showed that trunk skin has the ability to respond to salinity changes, with increased TER being observed following FW exposure. This is consistent with responses observed in cephalic skin (Marshall et al., 1992), and cultured rainbow trout gill epithelia (Wood and Pärt, 1998; Wood et al., 2002). While the physiological mechanism behind the acute change in skin permeability in response to salinity is unknown, there are several possibilities. First, the selectivity and permeability of the paracellular pathway in epithelia is determined by the characteristics of the tight junctions (Mills et al., 1977; Bäsler et al., 2016), and in particular by the claudin protein family (Kolosov et al., 2013).

In fish skin, claudin expression has been shown to vary in response to environmental salinity, with the expression of certain claudin-10 isoforms increasing following SW acclimation in several species (Bui and Kelly, 2014). This is consistent with studies of the gill of several teleost species, where SW transfer also increases the expression of claudin-10 isoforms (Tipsmark et al., 2008a, Tipsmark et al., 2008b, Tipsmark et al., 2016; Bossus et al., 2015) and with the opercular skin of *Fundulus heteroclitus* (Marshall et al., 2018; Chen et al., 2021). Certain claudin-10 isoforms are thought to provide the paracellular pathway with cation selective pores, which facilitate ion efflux in SW (Marshall et al., 2018). However, Kolosov et al. (2020) recently demonstrated that claudin-10 is downregulated following SW acclimation in the lamprey, indicating that the contribution of claudins to epithelial barrier function may be species dependent.

Conversely, the decrease in epithelial permeability observed in the current study following exposure to FW may be related to the incorporation of barrier forming claudins into the TJs. Studies into claudin expression in *tetraodon nigroviridis* skin (Bagherie-Lachidan et al., 2008; Bagherie-Lachidan et al., 2009) and intestine (Clelland et al., 2010) suggested that an increase in claudin-3 abundance was associated with reduced permeability, while an increase in claudin-27a abundance following SW acclimation was associated with reduced permeability. In FW *O. mykiss* skin, claudin-30 is the most abundantly expressed isoform, with claudins-28b and -31 also expressed abundantly (Gauberg et al., 2017). Claudin-30 has been functionally characterized in *Salmo salar* where it forms a barrier towards $Na^+$ (Engelund et al., 2012). In addition, claudins-28b and -31 have been shown to increase in abundance following transfer from SW to FW in *Oreochromis mossambicus* (Tipsmark et al., 2016), suggesting a possible role in reducing epithelial permeability. This pattern is consistent with observations in cultured *O. mykiss* gill pavement cells, where claudin-28b abundance is drastically reduced following hyperosmotic stress (Sandbichler et al., 2011).

Another possible explanation to the differences in barrier function between FW and SW could lay in the morphological arrangement of the TJs. The length of TJs can be broadly categorised into shallow or deep, based on the relative depth of the protein strands comprising the TJs (Engelund et al., 2012). Shallow TJs have been reported in the gills of SW acclimated fish (Sardet et al., 1979; Karnaky, 1986). These shallow TJs are much leakier than the deep TJs found in FW acclimated fish (Sardet et al., 1979) and primary gill cell cultures exposed to FW, which also display deep TJs (Wood and Pärt, 1997). Thus, the acute changes in TER observed in the current study in response to salinity changes may be related to a rapid remodelling of the TJs, where the TJ complexes increase and decrease in depth following exposure to FW and SW respectively. Similar changes in TJ structure have been shown to occur rapidly in cultured branchial epithelia after alteration of salinity (Wood et al., 2002; Chasiotis et al., 2012). As such, it is possible that similar morphological changes occur in the skin TJs. The exact mechanisms of TJ remodelling in teleost fish are unclear. However, there is ample evidence from mammalian cells to suggest that the TJs are dynamic and capable of rapidly remodelling in response to changes in external stimuli through phosphorylation and/or endocytosis of TJ proteins (Van Itallie and Anderson, 2006; Shen et al., 2008; Stamatovic et al., 2017). Such responses to external stimuli have been shown to occur over minutes (Gonzalez et al., 2008).

Finally, it is possible that the mucus layer may have contributed to the observed differences in barrier function between FW and SW exposed skin. The mucus provides the first layer of protection to the fish and acts as a direct defence against environmental contaminants. However, there is also evidence to suggest that mucus composition is salinity dependent, with SW acclimated fish having more viscous mucus, which is related to differences in mucus hydration (Roberts and Powell, 2005). The salinity-dependent nature of mucus also appears to hold true for the skin, with Ordóñez-Grande et al. (2020) showing increased mucus exudation in hyperosmotic conditions. In addition, Ordóñez-Grande et al. (2021) suggested a possible role of skin mucus as a layer to trap ions in hyposmotic conditions while the facilitating water retention in hyperosmotic conditions, thus playing an important role in osmoregulation. Further studies are needed to elucidate the role of rainbow trout skin mucins in barrier function during salinity acclimation.

## Evidence for Active Transport in the Trunk Skin

A pronounced basal-negative TEP and corresponding change in SCC quickly developed after the exchanging the isosmotic Ringer's solution with FW to the apical chamber of the FW acclimated group. The parameters stabilized after approximately 30 min at ~ −4mV and ~3.6 $\mu A/cm^2$. The levels were stable for the remainder of the experiment, suggesting the involvement of at least one active transporting component. Similar responses in TEP have been observed in salmonid cephalic skin and gill primary cell cultures (Marshall et al., 1992; Wood and Pärt, 1997; Wood et al., 2002). A negative basal solution can be the result of a net movement of negative ions from the apical to the basal side, or a net movement of positive ions from the basal to apical side. The latter is supported by strong immunoreactivity of V-ATPase in the apical part of the epidermis of FW acclimated fish.

These findings are in agreement with the localization of a V-ATPase in the FW gill pavement cells of rainbow trout (PVCs; Sullivan et al., 1995). In the FW gill, apical H+ extrusion by V-ATPase drives the uptake of Na+ from the environment through a phenamil sensitive Na+ channel (ENaC; Reid et al., 2003). Interestingly, in SW acclimated trout gill, V-ATPase abundance and activity decreases 70–80% compared to FW (Hawkins et al., 2003) and H+ secretion is instead achieved by an apical NHE driven by the inwardly directed Na+ gradient (Evans et al., 2005).

An attempt to elucidate the role of the V-ATPase in trunk skin was made by inhibiting skin V-ATPase using NEM, a highly potent and specific inhibitor (Lin and Randall, 1995). Addition of NEM to the apical but not basal chamber half resulted in changes in TEP and SCC (basal-negative), indicating that V-ATPase may be one component of the active transport in rainbow trout trunk skin. However, the apical addition of NEM also resulted in reduced TER. This suggests that NEM has the capacity to increase paracellular permeability. The ability of NEM to increase TJ permeability has been demonstrated in toad bladder (Marples et al., 1994) and Madin-Darby canine kidney (MDCK) cells

(Kanda et al., 2018). Thus, in addition to inhibiting the apical V-ATPase, NEM also increases ion permeability across the TJs, which may facilitate passive ion diffusion due to the difference in ion composition between the two chamber halves. As NEM contributes to changes in both active transport and passive diffusion across the skin, the observed changes in TEP and SCC following NEM addition cannot be assigned solely to inhibition of the V-ATPase, but is probably also a result of increased paracellular permeability due to disrupted tight junctions.

## CONCLUSIONS

In this study, we assessed the contribution of the different skin layers to barrier function, determined the effect of salinity, and tested for possible active transport mechanisms. The epidermis was found to be the diffusion barrier in the skin, with the scales and dermis playing a negligible role. Epidermal barrier function was mainly determined by environmental salinity, with FW exposure resulting in a strong reduction of epithelial permeability. While the rapid salinity-dependent changes in skin function are likely related to acute changes in TJ structure and function, the exact mechanisms behind the acute changes in epithelial permeability remain unclear. However, the salinity dependent differences in barrier function observed in the current study are consistent with previous studies that have showed varying expression of TJ proteins in the skin of fish. In relation to active transport, further research is required to determine if skin V-ATPase contributes significantly to overall ion homeostasis in rainbow trout, or whether it plays a more specialised role.

## DATA AVAILABILITY STATEMENT

The raw data supporting the conclusions of this article will be made available by the authors, without undue reservation.

## ETHICS STATEMENT

The animal study was reviewed and approved by Swedish Board of Agriculture (ethical permit number: 5.8.18-15096/2018).

## AUTHOR CONTRIBUTIONS

DD, HS, and BC conceived and planned the experiments. DD, HS, and NS carried out the experiments. DD and HS analysed the data and interpreted the results. DD, HS, KS, and BC contributed to the writing of the manuscript. All authors provided feedback on the manuscript and assisted with revisions.

## FUNDING

This work was supported by the Swedish Research Council (FORMAS; grant number: 2018-01201) and the Carl Tryggers Stiftelse (grant number: 19:61).

## ACKNOWLEDGMENTS

The authors thank Niklas Warwas and Ida Hedén for their practical assistance.

## SUPPLEMENTARY MATERIAL

The Supplementary Material for this article can be found online at: https://www.frontiersin.org/articles/10.3389/fphys.2022.882973/full#supplementary-material

## REFERENCES

Bagherie-Lachidan, M., Wright, S. I., and Kelly, S. P. (2008). Claudin-3 Tight Junction Proteins in *Tetraodon nigroviridis*: Cloning, Tissue-specific Expression, and a Role in Hydromineral Balance. *Am. J. Physiol. Regul. Integr. Comp. Physiol.* 294 (5), R1638–R1647. doi:10.1152/ajpregu.00039.2008

Bagherie-Lachidan, M., Wright, S. I., and Kelly, S. P. (2009). Claudin-8 and -27 Tight Junction Proteins in Puffer Fish *Tetraodon nigroviridis* Acclimated to Freshwater and Seawater. *J. Comp. Physiol. B* 179 (4), 419–431. doi:10.1007/s00360-008-0326-0

Bäsler, K., Bergmann, S., Heisig, M., Naegel, A., Zorn-Kruppa, M., and Brandner, J. M. (2016). The Role of Tight Junctions in Skin Barrier Function and Dermal Absorption. *J. Control Release* 242, 105–118. doi:10.1016/j.jconrel.2016.08.007

Benhamed, S., Guardiola, F. A., Mars, M., and Esteban, M. Á. (2014). Pathogen Bacteria Adhesion to Skin Mucus of Fishes. *Vet. Microbiol.* 171 (1-2), 1–12. doi:10.1016/j.vetmic.2014.03.008

Bossus, M. C., Madsen, S. S., and Tipsmark, C. K. (2015). Functional Dynamics of Claudin Expression in Japanese Medaka (*Oryzias latipes*): Response to Environmental Salinity. *Comp. Biochem. Physiology Part A Mol. Integr. Physiology* 187, 74–85. doi:10.1016/j.cbpa.2015.04.017

Brandner, J. M. (2009). Tight Junctions and Tight Junction Proteins in Mammalian Epidermis. *Eur. J. Pharm. Biopharm.* 72 (2), 289–294. doi:10.1016/j.ejpb.2008.08.007

Bui, P., and Kelly, S. P. (2014). Claudin-6, -10d and -10e contribute to seawater acclimation in the euryhaline puffer fish *Tetraodon nigroviridis*. *J. Exp. Biol.* 217 (10), 1758–1767. doi:10.1242/jeb.099200

Chasiotis, H., Kolosov, D., Bui, P., and Kelly, S. P. (2012). Tight Junctions, Tight Junction Proteins and Paracellular Permeability across the Gill Epithelium of Fishes: a Review. *Respir. physiology Neurobiol.* 184 (3), 269–281. doi:10.1016/j.resp.2012.05.020

Chen, C. C., Marshall, W. S., Robertson, G. N., Cozzi, R. R. F., and Kelly, S. P. (2021). Mummichog Gill and Operculum Exhibit Functionally Consistent Claudin-10 Paralog Profiles and Claudin-10c Hypersaline Response. *Biol. Open* 10 (7), bio058868. doi:10.1242/bio.058868

Elliott, D. G. (2011). "THE SKIN | Functional Morphology of the Integumentary System in Fishes," in *Encyclopedia of Fish Physiology*, 476–488. doi:10.1016/b978-0-12-374553-8.00108-8

Engelund, M. B., Yu, A. S., Li, J., Madsen, S. S., Færgeman, N. J., and Tipsmark, C. K. (2012). Functional Characterization and Localization of a Gill-specific Claudin Isoform in Atlantic Salmon. *Am. J. Physiol. Regul. Integr. Comp. Physiol.* 302 (2), R300–R311. doi:10.1152/ajpregu.00286.2011

Evans, D. H., Piermarini, P. M., and Choe, K. P. (2005). The Multifunctional Fish Gill: Dominant Site of Gas Exchange, Osmoregulation, Acid-Base Regulation, and Excretion of Nitrogenous Waste. *Physiol. Rev.* 85 (1), 97–177. doi:10.1152/physrev.00050.2003

Foskett, J. K., and Scheffey, C. (1982). The Chloride Cell: Definitive Identification as the Salt-Secretory Cell in Teleosts. *Science* 215 (4529), 164–166. doi:10.1126/science.7053566

Fromm, P. O. (1968). Some Quantitative Aspects of Ion Regulation in Teleosts. *Comp. Biochem. Physiology* 27, 865–869. doi:10.1016/0010-406x(68)90627-0

Gauberg, J., Kolosov, D., and Kelly, S. P. (2017). Claudin Tight Junction Proteins in Rainbow Trout ( *Oncorhynchus mykiss* ) Skin: Spatial Response to Elevated Cortisol Levels. *General Comp. Endocrinol.* 240, 214–226. doi:10.1016/j.ygcen.2016.10.006

Glover, C. N., Bucking, C., and Wood, C. M. (2013). The Skin of Fish as a Transport Epithelium: a Review. *J. Comp. Physiol. B* 183 (7), 877–891. doi:10.1007/s00360-013-0761-4

Gomez, D., Sunyer, J. O., and Salinas, I. (2013). The Mucosal Immune System of Fish: the Evolution of Tolerating Commensals while Fighting Pathogens. *Fish shellfish Immunol.* 35 (6), 1729–1739. doi:10.1016/j.fsi.2013.09.032

González-Mariscal, L., Tapia, R., and Chamorro, D. (2008). Crosstalk of Tight Junction Components with Signaling Pathways. *Biochimica Biophysica Acta (BBA)-Biomembranes* 1778 (3), 729–756.

Grosell, M. (2010). The Role of the Gastrointestinal Tract in Salt and Water Balance. *Fish. Physiol.* 30, 135–164. doi:10.1016/s1546-5098(10)03004-9

Günzel, D., and Fromm, M. (2012). Claudins and Other Tight Junction Proteins. *Compr. Physiol.* 2 (3), 1819–1852.

Günzel, D., and Yu, A. S. (2013). Claudins and the Modulation of Tight Junction Permeability. *Physiol. Rev.* 93 (2), 525–569.

Iger, Y., and Abraham, M. (1990). The Process of Skin Healing in Experimentally Wounded Carp. *J. Fish. Biol.* 36 (3), 421–437. doi:10.1111/j.1095-8649.1990.tb05622.x

Jensen, L. B., Wahli, T., McGurk, C., Eriksen, T. B., Obach, A., Waagbø, R., et al. (2015). Effect of Temperature and Diet on Wound Healing in Atlantic Salmon (*Salmo salar* L.). *Fish. Physiol. Biochem.* 41 (6), 1527–1543. doi:10.1007/s10695-015-0105-2

Kanda, Y., Yamasaki, Y., Sasaki-Yamaguchi, Y., Ida-Koga, N., Kamisuki, S., Sugawara, F., et al. (2018). TRPA1-dependent Reversible Opening of Tight Junction by Natural Compounds with an α,β-unsaturated Moiety and Capsaicin. *Sci. Rep.* 8 (1), 2251. doi:10.1038/s41598-018-20526-7

Karnaky, K. J., Jr (1986). Structure and Function of the Chloride Cell ofFundulus Heteroclitusand Other Teleosts. *Am. Zool.* 26 (1), 209–224. doi:10.1093/icb/26.1.209

Kolosov, D., Bui, P., Chasiotis, H., and Kelly, S. P. (2013). Claudins in Teleost Fishes. *Tissue Barriers* 1 (3), e25391. doi:10.4161/tisb.25391

Kolosov, D., Bui, P., Wilkie, M. P., and Kelly, S. P. (2020). Claudins of Sea Lamprey ( *Petromyzon marinus* ) - Organ-specific Expression and Transcriptional Responses to Water of Varying Ion Content. *J. Fish. Biol.* 96 (3), 768–781. doi:10.1111/jfb.14274

Kulczykowska, E. (2019). Stress Response System in the Fish Skin-Welfare Measures Revisited. *Front. Physiol.* 10, 72. doi:10.3389/fphys.2019.00072

Lin, H., and Randall, D. (1995).9 Proton Pumps in Fish Gills. *Fish. Physiol.*, 14, 229–255. doi:10.1016/s1546-5098(08)60248-4

Loretz, C. A. (1995).2 Electrophysiology of Ion Transport in Teleost Intestinal Cells. *Fish. Physiol.* 14, 25–56. doi:10.1016/s1546-5098(08)60241-1

Marples, D., Bourguet, J., and Taylor, A. (1994). Activation of the Vasopressin-Sensitive Water Permeability Pathway in the Toad Bladder by N-Ethyl Maleimide. *Exp. Physiol.* 79 (5), 775–795. doi:10.1113/expphysiol.1994.sp003807

Marshall, W. S., Breves, J. P., Doohan, E. M., Tipsmark, C. K., Kelly, S. P., Robertson, G. N., et al. (2018). claudin-10 Isoform Expression and Cation Selectivity Change with Salinity in Salt-Secreting Epithelia of Fundulusheteroclitus. *J. Exp. Biol.* 221 (1), jeb168906. doi:10.1242/jeb.168906

Marshall, W. S., and Bellamy, D. (2010). The 50year Evolution of In Vitro Systems to Reveal Salt Transport Functions of Teleost Fish Gills. *Comp. Biochem. Physiology Part A Mol. Integr. Physiology* 155 (3), 275–280. doi:10.1016/j.cbpa.2009.11.016

Marshall, W. S., Bryson, S. E., and Wood, C. M. 1992. Calcium Transport by Isolated Skin of Rainbow Trout. *J. Exp. Biol.*, 166(1): 297–316.doi:10.1242/jeb.166.1.297

Marshall, W. S. (2002). Na+, Cl? Ca2+ and Zn2+ Transport by Fish Gills: Retrospective Review and Prospective Synthesis. *J. Exp. Zool.* 293 (3), 264–283. doi:10.1002/jez.10127

McCormick, S. D. (1994). Opercular Membranes and Skin. *Anal. Tech.* 3, 231–238. doi:10.1016/b978-0-444-82033-4.50026-x

Mills, J. W., Ernst, S. A., and DiBona, D. R. (1977). Localization of Na+-Pump Sites in Frog Skin. *J. Cell Biol.* 73 (1), 88–110. doi:10.1083/jcb.73.1.88

Mittal, A. K., and Datta Munshi, J. S. (1974). On the Regeneration and Repair of Superficial Wounds in the Skin of Rita Vita (Ham.) (Bagridae, Pisces). *Cells Tissues Organs* 88, 424–442. doi:10.1159/000144250

Ordóñez-Grande, B., Guerreiro, P. M., Sanahuja, I., Fernández-Alacid, L., and Ibarz, A. (2021). Environmental Salinity Modifies Mucus Exudation and Energy Use in European Sea Bass Juveniles. *Animals* 11 (6), 1580.

Ordóñez-Grande, B., Guerreiro, P. M., Sanahuja, I., Fernández-Alacid, L., and Ibarz, A. (2020). Evaluation of an Acute Osmotic Stress in European Sea Bass via Skin Mucus Biomarkers. *Animals* 10 (9), 1546.

Quilhac, A., and Sire, J.-Y. (1999).Spreading, Proliferation, and Differentiation of the Epidermis after Wounding a Cichlid fish,Hemichromis Bimaculatus, *Anat. Rec.*, 254.3, 435–451. doi:10.1002/(sici)1097-0185(19990301)254:3<435::aid-ar15>3.0.co;2-d

Rakers, S., Gebert, M., Uppalapati, S., Meyer, W., Maderson, P., Sell, A. F., et al. (2010). 'Fish Matters': the Relevance of Fish Skin Biology to Investigative Dermatology. *Exp. Dermatol.* 19 (4), 313–324. doi:10.1111/j.1600-0625.2009.01059.x

Redding, J. M., Schreck, C. B., Birks, E. K., and Ewing, R. D. (1984). Cortisol and its Effects on Plasma Thyroid Hormone and Electrolyte Concentrations in Fresh Water and during Seawater Acclimation in Yearling Coho Salmon, *Oncorhynchus kisutch*. *General Comp. Endocrinol.* 56 (1), 146–155. doi:10.1016/0016-6480(84)90071-6

Reid, S. D., Hawkings, G. S., Galvez, F., and Goss, G. G. (2003). Localization and Characterization of Phenamil-Sensitive Na+influx in Isolated Rainbow Trout Gill Epithelial Cells. *J. Exp. Biol.* 206 (3), 551–559. doi:10.1242/jeb.00109

Richardson, R., Metzger, M., Knyphausen, P., Ramezani, T., Slanchev, K., Kraus, C., et al. (2016). Re-epithelialization of Cutaneous Wounds in Adult Zebrafish Combines Mechanisms of Wound Closure in Embryonic and Adult Mammals. *Development* 143 (12), 2077–2088. doi:10.1242/dev.130492

Richardson, R., Slanchev, K., Kraus, C., Knyphausen, P., Eming, S., and Hammerschmidt, M. (2013). Adult Zebrafish as a Model System for Cutaneous Wound-Healing Research. *J. Investigative Dermatology* 133 (6), 1655–1665. doi:10.1038/jid.2013.16

Roberts, S. D., and Powell, M. D. (2005). The Viscosity and Glycoprotein Biochemistry of Salmonid Mucus Varies with Species, Salinity and the Presence of Amoebic Gill Disease. *J. Comp. Physiol. B* 175 (1), 1–11. doi:10.1007/s00360-004-0453-1

Rombout, J. H. W. M., Yang, G., and Kiron, V. (2014). Adaptive Immune Responses at Mucosal Surfaces of Teleost Fish. *Fish Shellfish Immunol.* 40 (2), 634–643. doi:10.1016/j.fsi.2014.08.020

Roubal, F. R., and Bullock, A. M. (1988). The Mechanism of Wound Repair in the Skin of Juvenile Atlantic Salmon, *Salmo salar* L., Following Hydrocortisone Implantation. *J. Fish. Biol.* 32 (4), 545–555. doi:10.1111/j.1095-8649.1988.tb05394.x

Sandbichler, A. M., Egg, M., Schwerte, T., and Pelster, B. (2011). Claudin 28b and F-Actin Are Involved in Rainbow Trout Gill Pavement Cell Tight Junction Remodeling under Osmotic Stress. *J. Exp. Biol.* 214 (9), 1473–1487. doi:10.1242/jeb.050062

Sardet, C., Pisam, M., and Maetz, J. (1979). The Surface Epithelium of Teleostean Fish Gills. Cellular and Junctional Adaptations of the Chloride Cell in Relation to Salt Adaptation. *J. Cell Biol.* 80 (1), 96–117. doi:10.1083/jcb.80.1.96

Segner, H., Sundh, H., Buchmann, K., Douxfils, J., Sundell, K. S., Mathieu, C., et al. (2012). Health of Farmed Fish: its Relation to Fish Welfare and its Utility as Welfare Indicator. *Fish. Physiol. Biochem.* 38 (1), 85–105. doi:10.1007/s10695-011-9517-9

Shen, L., Weber, C. R., and Turner, J. R. (2008). The Tight Junction Protein Complex Undergoes Rapid and Continuous Molecular Remodeling at Steady State. *J. Cell Biol.* 181 (4), 683–695. doi:10.1083/jcb.200711165

Shephard, K. L. (1994). Functions for Fish Mucus. *Rev. Fish. Biol. Fish.* 4 (4), 401–429. doi:10.1007/bf00042888

Stamatovic, S. M., Johnson, A. M., Sladojevic, N., Keep, R. F., and Andjelkovic, A. V. (2017). Endocytosis of Tight Junction Proteins and the Regulation of Degradation and Recycling. *Ann. N.Y. Acad. Sci.* 1397 (1), 54–65. doi:10.1111/nyas.13346

Sullivan, G., Fryer, J., and Perry, S. (1995). Immunolocalization of Proton Pumps (H+-ATPase) in Pavement Cells of Rainbow Trout Gill. *J. Exp. Biol.* 198 (12), 2619–2629. doi:10.1242/jeb.198.12.2619

Sundell, K., Jutfelt, F., Ágústsson, T., Olsen, R.-E., Sandblom, E., Hansen, T., et al. (2003). Intestinal Transport Mechanisms and Plasma Cortisol Levels during Normal and Out-Of-Season Parr-Smolt Transformation of Atlantic Salmon, *Salmo salar*. *Aquaculture* 222, 265–285. doi:10.1016/s0044-8486(03)00127-3

Sundell, K. S., and Sundh, H. (2012). Intestinal Fluid Absorption in Anadromous Salmonids: Importance of Tight Junctions and Aquaporins. *Front. Physiol.* 3 (388), 388. doi:10.3389/fphys.2012.00388

Sundh, H., and Sundell, K. S. (2015). "Environmental Impacts on Fish Mucosa," in *Mucosal Health in Aquaculture* (Academic Press), 171–197. doi:10.1016/b978-0-12-417186-2.00007-8

Sveen, L., Karlsen, C., and Ytteborg, E. (2020). Mechanical Induced Wounds in Fish - a Review on Models and Healing Mechanisms. *Rev. Aquacult.* 12 (4), 2446–2465. doi:10.1111/raq.12443

Sveen, L. R., Timmerhaus, G., Krasnov, A., Takle, H., Handeland, S., and Ytteborg, E. (2019). Wound Healing in Post-smolt Atlantic Salmon (*Salmo salar* L.). *Sci. Rep.* 9 (1), 3565. doi:10.1038/s41598-019-39080-x

Sveen, L. R., Timmerhaus, G., Krasnov, A., Takle, H., Stefansson, S. O., Handeland, S. O., et al. (2018). High Fish Density Delays Wound Healing in Atlantic Salmon (*Salmo salar*). *Sci. Rep.* 8 (1), 16907–16913. doi:10.1038/s41598-018-35002-5

Takvam, M., Wood, C. M., Kryvi, H., and Nilsen, T. O. (2021). Ion Transporters and Osmoregulation in the Kidney of Teleost Fishes as a Function of Salinity. *Front. Physiol.* 12 (513), 664588. doi:10.3389/fphys.2021.664588

Tipsmark, C. K., Baltzegar, D. A., Ozden, O., Grubb, B. J., and Borski, R. J. (2008a). Salinity Regulates Claudin mRNA and Protein Expression in the Teleost Gill. *Am. J. Physiol. Regul. Integr. Comp. Physiol.* 294 (3), R1004–R1014. doi:10.1152/ajpregu.00112.2007

Tipsmark, C. K., Kiilerich, P., Nilsen, T. O., Ebbesson, L. O., Stefansson, S. O., and Madsen, S. S. (2008b). Branchial Expression Patterns of Claudin Isoforms in Atlantic Salmon during Seawater Acclimation and Smoltification. *Am. J. Physiol. Regul. Integr. Comp. Physiol.* 294 (5), R1563–R1574. doi:10.1152/ajpregu.00915.2007

Tipsmark, C. K., Breves, J. P., Rabeneck, D. B., Trubitt, R. T., Lerner, D. T., and Grau, E. G. (2016). Regulation of Gill Claudin Paralogs by Salinity, Cortisol and Prolactin in Mozambique tilapia (*Oreochromis mossambicus*). *Comp. Biochem. Physiology Part A Mol. Integr. Physiology* 199, 78–86. doi:10.1016/j.cbpa.2016.05.014

Tipsmark, C. K., and Madsen, S. S. (2012). Tricellulin, Occludin and Claudin-3 Expression in Salmon Intestine and Kidney during Salinity Adaptation. *Comp. Biochem. Physiology Part A Mol. Integr. Physiology* 162 (4), 378–385. doi:10.1016/j.cbpa.2012.04.020

Van Itallie, C. M., and Anderson, J. M. (2006). Claudins and Epithelial Paracellular Transport. *Annu. Rev. Physiol.* 68, 403–429. doi:10.1146/annurev.physiol.68.040104.131404

Whittamore, J. M. (2012). Osmoregulation and Epithelial Water Transport: Lessons from the Intestine of Marine Teleost Fish. *J. Comp. Physiol. B* 182 (1), 1–39. doi:10.1007/s00360-011-0601-3

Wood, C. M., Kelly, S. P., Zhou, B., Fletcher, M., O'Donnell, M., Eletti, B., et al. (2002). Cultured Gill Epithelia as Models for the Freshwater Fish Gill. *Biochim. Biophys. Acta* 1566 (1-2), 72–83. doi:10.1016/s0005-2736(02)00595-3

Wood, C. M., Gilmour, K. M., and Pärt, P. (1998). Passive and Active Transport Properties of a Gill Model, the Cultured Branchial Epithelium of the Freshwater Rainbow Trout (*Oncorhynchus mykiss*). *Comp. Biochem. Physiology Part A Mol. Integr. Physiology* 119 (1), 87–96. doi:10.1016/s1095-6433(97)00403-0

Wood, C. M., and Pärt, P. (1997). Cultured Branchial Epithelia from Freshwater Fish Gills. *J. Exp. Biol.* 200 (6), 1047–1059. doi:10.1242/jeb.200.6.1047

Wright, P. A., and Wood, C. M. (2009). A New Paradigm for Ammonia Excretion in Aquatic Animals: Role of Rhesus(Rh) Glycoproteins. *J. Exp. Biol.* 212 (15), 2303–2312. doi:10.1242/jeb.023085

Zimmer, A. M., Brauner, C. J., and Wood, C. M. (2014). Ammonia Transport across the Skin of Adult Rainbow Trout (*Oncorhynchus mykiss*) Exposed to High Environmental Ammonia (HEA). *J. Comp. Physiol. B* 184 (1), 77–90. doi:10.1007/s00360-013-0784-x

**Conflict of Interest:** The authors declare that the research was conducted in the absence of any commercial or financial relationships that could be construed as a potential conflict of interest.

**Publisher's Note:** All claims expressed in this article are solely those of the authors and do not necessarily represent those of their affiliated organizations, or those of the publisher, the editors and the reviewers. Any product that may be evaluated in this article, or claim that may be made by its manufacturer, is not guaranteed or endorsed by the publisher.

frontiers | Frontiers in Marine Science

ORIGINAL RESEARCH
published: 14 June 2022
doi: 10.3389/fmars.2022.924110

# The Welfare of Nile Tilapia (*Oreochromis niloticus*, GIFT Strain) Juveniles Cultured in Different Light Spectra

*Mengmeng Yi[1†], Wanting Zhai[1†], Miao Wang[1†], He Wang[1], Zhigang Liu[1], Fengying Gao[1], Xiaoli Ke[1,2], Changbin Song[3], Jianmeng Cao[1,2*] and Maixin Lu[1,2*]*

[1] Key Laboratory of Tropical & Subtropical Fishery Resource Application & Cultivation, Ministry of Agriculture and Rural Affairs, Key Laboratory of Aquatic Animal Immune Technology of Guangdong Province, Pearl River Fisheries Research Institute, Chinese Academy of Fishery Science, Guangzhou, China, [2] Maoming Branch, Guangdong Laboratory for Lingnan Modern Agriculture, Maoming, China, [3] Institute of Semiconductors, Chinese Academy of Science, Beijing, China

OPEN ACCESS

**Edited by:**
Marce Herrera,
IFAPA Centro Agua del Pino, Spain

**Reviewed by:**
Chao Song,
Chinese Academy of Fishery Sciences, China
Ming Jiang,
Chinese Academy of Fishery Sciences, China
Eric M. Hallerman,
Virginia Tech, United States

***Correspondence:**
Jianmeng Cao
caojianmeng@aliyun.com
Maixin Lu
mx-lu@163.com

[†]These authors have contributed equally to this work

**Specialty section:**
This article was submitted to Aquatic Physiology, a section of the journal Frontiers in Marine Science

**Received:** 20 April 2022
**Accepted:** 12 May 2022
**Published:** 14 June 2022

**Citation:**
Yi M, Zhai W, Wang M, Wang H, Liu Z, Gao F, Ke X, Song C, Cao J and Lu M (2022) The Welfare of Nile Tilapia (Oreochromis niloticus, GIFT Strain) Juveniles Cultured in Different Light Spectra. Front. Mar. Sci. 9:924110. doi: 10.3389/fmars.2022.924110

The light spectrum is a vital environmental factor for the culture of fish, and the welfare of farmed fish is a crucial issue in aquaculture. In this study, Nile tilapia (*Oreochromis niloticus*, GIFT strain) juveniles were exposed to full-spectrum (LW), red (LR), yellow (LY), or blue (LB) light. After the 45-day experiment, growth performance, stress responses, and aggressive behaviors were evaluated, and transcriptomic analysis was carried out. The results revealed that LW and LR positively affected growth performance. At the same time, LY and LB had a negative effect. Light spectrum induced stress responses of juvenile fish exposed to LY, under which the total antioxidant capacity (T-AOC) and cortisol (COR) contents were the highest. The activities of α-amylase (AMS), protease (PES), and lipase (LPS) in the digestive tract showed a similar tendency, indicating that the light spectra altered the digestive enzyme activities and then affected growth. Behavioral analyses showed increased chase and bite activities of tilapia juveniles exposed to LW and LY. The affected functions included the nervous system, muscle morphogenesis, and immune system-related regulation. Enriched Kyoto Encyclopedia of Genes and Genomes (KEGG) pathways include the tryptophan metabolism signaling pathway, protein digestion and absorption signaling pathway, Jak-STAT signaling pathway, arachidonic acid metabolism signaling pathway, and alpha-linolenic acid metabolism signaling pathway. Overall, light spectra influenced the welfare of farmed tilapia juveniles in terms of growth, stress, and behavior. Our results suggested that LR should be used in juvenile tilapia culture.

**Keywords: light spectrum, GIFT tilapia juvenile, growth, stress, behavior, welfare, transcriptomics**

## 1 INTRODUCTION

Aquaculture has grown faster than other modes of food production and currently represents 47% of global fish production (FAO, 2018). Nevertheless, farmed fish are subject to an unfavorable environment, such as high stocking densities and lack of control over food and habitat choice. Like other agricultural animals, such as mammals and birds, fish welfare has received considerable

attention in recent decades (Ashley, 2007; Barreto et al., 2022). Fish welfare requires freedom from hunger, discomfort, pain, injury, disease, fear, and distress, as well as the freedom to express normal behavior (Ashley, 2007). Several environmental factors relevant to fish welfare have been recognized (Toni et al., 2017). With advanced breeding technology and facilities, environmental factors, including temperature, dissolved gasses, pH, salinity, nitrogen compounds, and artificial chemical pollutants are maintained within acceptable ranges for cultured fish. Another environment parameter that requires further attention for fish welfare is light.

Fishes have color vision (Cheng and Flamarique, 2004), and light, including the light spectrum, affects the growth, development, maturation, and other physiological processes of fish (Karakatsouli et al., 2010; Qiu et al., 2015; Choi et al., 2019). Providing the ideal light character for farmed aquatic animals may improve animal welfare. Orange and full-spectrum light were beneficial to turbot (*Scophthalmus maximus*) embryo incubation and survival of larvae (Wu et al., 2019). Giant freshwater prawn (*Macrobrachium rosenbergii*) larvae under green or white light expressed the fastest growth and metamorphosis (Wei et al., 2021). Green light kept olive flounder (*Paralichthys olivaceus*) from oxidative stress and strengthened its immunity under high density (Choi et al., 2019). Blue light could protect zebrafish (*Danio rerio*) against Cd toxicity (Yuan et al., 2017). At the same time, the preferred light spectrum of different fish species is varied. Scaled common carp (*Cyprinus carpio*) preferred red and blue light when the fish were reared at low and high stocking density, respectively, while red or blue light was unsuitable for mirror carp (*C. carpio*) (Karakatsouli et al., 2010). Koi carp (*C. carpio*) cultured under blue and green light exhibited better growth performance and improved non-specific immune ability (Bairwa et al., 2017). Nevertheless, blue light was stressful for rainbow trout (*Oncorhynchus mykiss*), and red was stressful for gilthead seabream (*Sparus aurata*) (Karakatsouli et al., 2007).

Animal behavior is flexible in response to the light environment. The red spectrum disturbed endocrine homeostasis and was associated with aggressive behaviors in spotted sea bass (*Lateolabrax maculatus*) culture (Hou et al., 2019). Higher light intensities and ultraviolet light altered virile (*Faxonius virilis*) and rusty (*Faxonius rusticus*) crayfish social interactions (Jackson and Moore, 2019). Collector urchins (*Tripneustes gratilla*) are highly sensitive to and dislike blue LED light, exhibiting the most hiding behavior and expressing a lower level of melanin (Li et al., 2021). Blue and white light could improve sea urchins' (*Strongylocentrotus intermedius*) foraging and feeding abilities (Yang et al., 2020).

Improper lighting conditions may harm growth and stress responses and may negatively affect behavior. Red light disadvantaged giant freshwater prawn larval development (Wei et al., 2021). The red spectrum disturbed endocrine homeostasis associated with stress responses, growth, and behavior and so was unfavorable for spotted sea bass (Hou et al., 2019). It was found that long wavelengths hurt the growth of turbot larvae and induced stress responses (Wu et al., 2020). White and red light strongly affected the behavioral responses of European sea bass (*Dicentrarchus labrax*) larvae (Villamizar et al., 2011b). Sea urchins under blue light spend more time on righting response and foraging, and red light significantly inhibits growth in long-term rearing (Yang et al., 2021).

Tilapias account for 10% of current cultured fish production (FAO, 2018). The GIFT strain of Nile tilapia (*Oreochromis niloticus*) is well known worldwide for its high growth performance and hardiness and accounted for a significant proportion of Nile tilapia production (Khaw et al., 2012). It is necessary to evaluate the welfare of farmed tilapia with increasing public concern over the welfare of farmed fish. The importance of water quality parameters and feeding to the welfare of farmed tilapia has been recognized (Villarroel et al., 2011; Lopez-Luna et al., 2013). However, little is known about the light conditions relevant to juvenile tilapia welfare based on metabolic, behavioral, and physiological indicators (Jin et al., 2019; Toni et al., 2019). Therefore, the growth performance, stress, and behavioral responses of Nile tilapia juveniles cultured under different light spectra were assessed in the current study.

# 2 MATERIALS AND METHODS

## 2.1 Juvenile Tilapia and Experiment Design

The juvenile GIFT tilapias (0.02 ± 0.00 g, 1.09 ± 0.04 cm) used in this research were 15 days post-hatching (dph) before the experiment and were randomly obtained from the same parents. The juveniles were placed into twelve glass tanks (1.0 m in length, 0.5 m in width, 0.5 m in depth, approximately 200 L of water, and 0.3 juveniles per liter). The twelve glass tanks were divided into full-spectrum, red (LR, 625–630 nm), yellow (LY, 590 nm–595 nm), and blue (LB, 450 nm–455 nm) light groups (three tanks per spectrum). Light-emitting diodes provided by Shenzhen Fluence Technology PLC (Shenzhen, China) were placed in the bottom center of the fish tank. Photosynthetic photon flux density (PPFD) of LW, LR, LY, and LB were set at 2.67 ± 0.33, 1.97 ± 0.51, 2.18 ± 0.56, and 2.21 ± 0.13 μmol/$m^2$/s, respectively. The photoperiod was set to 12:12 h according to the natural rhythm, and the light intensity was measured with a Lighting Analyzer (PLA-20, EVERFINE Photo-e-info Co., Ltd., Hangzhou, China). The juvenile GIFT tilapias in all groups were maintained in tanks supplied with a continuous flow of fresh water. The fish tanks were wrapped with shade cloth to avoid ambient light interference. During the 45-day experiment, the juveniles were fed with artemia (*Artemia salina*) to apparent satiation twice a day (09:00 and 17:00), and the water temperature was maintained at 27°C ± 0.5°C. Uneaten artemia was removed 30 min after feeding by flowing water.

The tilapias used in this research were handled according to the guidelines of the Laboratory Animal Ethics Committee of the Pearl River Fisheries Research Institute, Chinese Academy of Fishery Science.

## 2.2 Sampling and Behavior Surveillance

After the 45-day experiment, all but ten juveniles' body weight and length were measured. The digestive tract and liver of ten juveniles

anesthetized by MS-222 were sampled and stored at −80°C. After sampling, a camera (C6TC, EZVIZ, Hangzhou, China) on top of each tank was used to capture and track the movements of the ten remaining juveniles from 10:00 to 16:00. Video recordings were subsequently replayed, and behavior was quantified. Nine videos were selected randomly from the complete video recordings (10 min per video), and the numbers of chase and bite behaviors in each video were measured. Biting was defined as mouth contact with lateral body regions, fin, tail, and eyes of other juveniles, with each time the mouth contacted another fish counting as one bite. Aggressive behavior was labeled as biting and chasings. Another thirty juveniles per tank were freeze-dried using a vacuum freeze dryer (Alpha 1-4/2-4 LD Plus, Martin Christ, Osterode am Harz, Germany) for moisture, crude protein, and lipid content quantification.

## 2.3 Growth Index

Condition factor (CF) and specific growth rate (SGR) were computed, as follows:

$$\mathrm{CF}\left(\mathrm{g}\cdot\mathrm{cm}^{-3}\right)=\frac{W_2}{L^3}\times 100 \qquad \text{(equation 1)}$$

$$\mathrm{SGR}\left(\%\cdot\mathrm{d}^{-1}\right)=\frac{(\ln W_2-\ln W_1)}{T}\times 100 \qquad \text{(equation 2)}$$

where $W_1$ and $W_2$ are the initial and final average body weights (g), respectively. $L$ is the final average body length (cm). $T$ is the number of days of experiment (days).

## 2.4 Biochemical Analysis

The activities of α-amylase (AMS), protease (PES), and lipase (LPS) of the digestive tract, and superoxide dismutase (SOD) of the liver, as well as total antioxidant capacity (T-AOC) and cortisol (COR) in the liver, were measured using detection kits (Nanjing Jiancheng Bioengineering Institute, Nanjing, China). The moisture, crude protein, and crude lipid were quantified by the drying method (Alpha 1-4/2-4 LD Plus, Martin Christ, Germany), Kjeldahl method (Kjeltec 2300, Foss, Hillerød, Denmark), and Soxhlet extraction method (Soxtec 2055, Foss, Denmark), respectively.

## 2.5 Transcriptomic Analysis

### 2.5.1 Total RNA Extraction and Sequencing

The total RNA of ten juveniles per tank was isolated using TRIzol (Invitrogen, Carlsbad, CA, USA). RNA quality was measured using Bioanalyzer 2100 (Agilent, Santa Clara, CA, USA). RNA sequence library construction and sequencing were carried out by LC-Bio (Hangzhou, China), which conducted 2 × 150 bp paired-end sequencing (PE150) on an Illumina Novaseq™ 6000.

### 2.5.2 The Analysis of RNA-seq Reads

After quality control using FastQC v0.10.1 (http://www.bioinformatics.babraham.ac.uk/projects/fastqc), low-quality raw reads and adaptor sequences were removed using Cutadapt-1.9 (https://cutadapt.readthedocs.io/en/stable/) to obtain clean reads. Clean data were mapped to the *O. niloticus* reference genome (Accession GCA_922820385.1) using Hisat v2-2.0.4 (https://daehwankimlab.github.io/hisat2/) and assembled by StringTie v1.3.4d (http://ccb.jhu.edu/software/stringtie/). Then, the transcriptomes were merged to reconstruct a comprehensive transcriptome using Gffcompare v0.9.8 (http://ccb.jhu.edu/software/stringtie/gffcompare.shtml). The expression levels of transcripts were estimated by StringTie and ballgown (http://www.bioconductor.org/packages/release/bioc/html/ballgown.html) and calculated by FPKM. Differentially expressed genes (DEGs) were identified by edgeR (https://bioconductor.org/packages/release/bioc/html/edgeR.html) with Fold Change > 2 and $p < 0.05$ used as indicators for significant differences, followed by an analysis of Gene Ontology (GO) enrichment and Kyoto Encyclopedia of Genes and Genomes (KEGG) enrichment for DEGs.

### 2.5.3 RT-qPCR

RT-qPCR was carried out after screening the KEGG pathways to characterize the genes. A TransScript® One-Step gDNA Removal and cDNA Synthesis SuperMix (TransGen Biotech, Beijing, China) was used for reverse transcription of total RNA. Primers were designed by Primer Premier 5.0 (http://www.premierbiosoft.com/primerdesign/index.html) (**Supplementary Table 1**) and synthesized by Sangon Biotech (Shanghai, China). RT-qPCR was run on the QuantStudio 3&5 Real-Time PCR System (Thermo Fisher, Waltham, MA, USA) using the 2× SG Fast qPCR Master Mix (High Rox, B639273, BBI, ABI, Foster, CA, USA) and a standard RT-qPCR amplification procedure (3 min at 95°C followed by 45 cycles including 5 s at 95°C and 30 s at 60°C).

## 2.6 Statistical Analysis

The data were analyzed by one-way ANOVA after the homogeneity of variance test with SPSS v19.0 and expressed as the mean ± SEM. A significance level of $p < 0.05$ was used.

# 3 RESULTS

## 3.1 Effects of Different Light Spectra on the Growth and Related Enzyme Activities of GIFT Tilapia Juveniles

Different light spectra affected the body weight, length, and SGR of GIFT tilapia juveniles (**Table 1**). The body weight, length, and SGR of GIFT tilapia juveniles under LW and LR were significantly higher than those under LY and LB ($p < 0.05$, **Table 1**). No statistical differences in body weight, length, and SGR between LW and LR and LY and LB were observed ($p > 0.05$, **Table 1**). GIFT tilapia juveniles under LY exhibited a higher CF than those under LR ($p < 0.05$), and both groups showed significantly higher CF than the LW and LB groups ($p < 0.05$). CF of GIFT tilapia juveniles in the LW and LB groups showed no statistical difference ($p > 0.05$, **Table 1**).

The effects of light spectra on the nutritional contents of GIFT tilapia juveniles are shown in **Table 2**. GIFT tilapia juveniles under LY had the highest moisture content ($p < 0.05$), but no

statistical difference existed among those under LW, LR, and LB ($p > 0.05$, **Table 2**). There were no statistical differences in crude protein among the LW, LR, and LB groups ($p > 0.05$), and all showed significantly higher crude protein content than the LY group ($p < 0.05$, **Table 2**). No statistical difference existed in crude lipid between LW and LR and between LY and LB ($p > 0.05$, **Table 2**). Nevertheless, the crude lipid contents of juveniles under LW and LR were higher than those under LY and LB ($p < 0.05$, **Table 2**).

The effects of light spectra on the enzymes associated with digestion are shown in **Figure 1**. The AMS activities of GIFT tilapia juveniles under LR were higher than those under LW, LY, and LB ($p < 0.05$, **Figure 1A**). AMS activities of LW and LY were higher than those of LB ($p < 0.05$, **Figure 1A**), yet no statistical differences in AMS activities existed between the LW and LY groups ($p > 0.05$, **Figure 1A**). The PES activities in the LW group were higher than those in the LR, LY, and LB groups ($p < 0.05$), and significant differences were found between LR and LY, as well as LR and LB ($p < 0.05$, **Figure 1B**). Nevertheless, no statistical differences in PES activities existed between LY and LB ($p > 0.05$, **Figure 1B**). The LPS activities of fish under LY, which did not statistically differ from LW and LR ($p > 0.05$), were higher than those under LB ($p < 0.05$, **Figure 1C**). No statistical differences in LPS activities existed among the LW, LR, and LB groups ($p > 0.05$, **Figure 1C**).

## 3.2 Effects of Different Light Spectra on the Non-Specific Immune Responses and Stress of GIFT Tilapia Juveniles

The influences of light spectra on the immune and stress responses of GIFT tilapia juveniles are shown in **Figure 2**. The SOD activities of juveniles under LB were higher than those under LW, LR, and LY ($p < 0.05$), while no statistical differences existed among LW, LR, and LY ($p > 0.05$, **Figure 2A**). The T-AOC contents of fish under LY were higher than those under LW, LR, and LB ($p < 0.05$, **Figure 2B**). The T-AOC contents of fish under LW did not statistically differ from those under LR ($p > 0.05$) and were higher than fish under LB ($p < 0.05$, **Figure 2B**). No statistical differences in T-AOC contents were found between LR and LB ($p > 0.05$, **Figure 2B**). The COR contents of LY were higher than those under LW, LR, and LB ($p < 0.05$), while no statistical differences in COR contents existed among LW, LR, and LB groups ($p > 0.05$, **Figure 2C**).

## 3.3 Effects of Different Light Spectra on the Behavioral Responses of GIFT Tilapia Juveniles

As shown in **Figure 3**, light spectra significantly influenced the frequency of aggressive behaviors of GIFT tilapia juveniles. Similar effects of different light spectra on GIFT tilapia juveniles' chase and bite behaviors were observed. Fish under LW and LY exhibited significantly more chase and bite behaviors than those under LR and LB ($p < 0.05$), yet no statistical differences in the chase and bite behaviors were found between the LW and LY groups, as well as between the LR and LB groups ($p > 0.05$, **Figures 3A, B**).

## 3.4 Transcriptome Responses of GIFT Tilapia Juveniles to Different Light Spectra

RNA-seq was carried out to investigate the influences of light spectra on the expression of key compounds in GIFT tilapia juveniles. The results showed that 26 (LR vs. LW), 42 (LY vs. LW), and 24 (LB vs. LW) GO terms were upregulated and 12 (LR vs. LW), 6 (LY vs. LW), and 9 (LB vs. LW) GO terms were downregulated (**Supplementary Table 2**). GO pathway enrichment was re-analyzed ($q$-value <0.05, DEGs > 2) to explore the biological processe (BP), cellular component (CC), and molecular function (MF) pathways of DEGs, and there were 7, 21, and 7 GO terms related to BP, CC, and MF of LR vs. LW, LY vs. LW, and LB vs. LW, respectively (**Figure 4**).

The Venn diagram (**Figure 5**) shows that the GO BP terms of LR vs. LW are mainly related to cell growth and apoptosis,

**TABLE 1** | Growth indices of GIFT tilapia juveniles cultured under different light spectra.

| Light spectra | Body weight (g) | Body length (cm) | SGR (%·d$^{-1}$) | CF (g·cm$^{-3}$) |
|---|---|---|---|---|
| LW | 0.44 ± 0.01$^{a}$ | 2.46 ± 0.02$^{a}$ | 7.48 ± 0.16$^{a}$ | 2.98 ± 0.06$^{c}$ |
| LR | 0.43 ± 0.01$^{a}$ | 2.42 ± 0.01$^{a}$ | 7.42 ± 0.06$^{a}$ | 3.05 ± 0.09$^{b}$ |
| LY | 0.39 ± 0.01$^{b}$ | 2.32 ± 0.01$^{b}$ | 7.21 ± 0.04$^{b}$ | 3.13 ± 0.06$^{a}$ |
| LB | 0.39 ± 0.01$^{b}$ | 2.36 ± 0.01$^{b}$ | 7.18 ± 0.09$^{b}$ | 2.95 ± 0.02$^{c}$ |

*Different superscript letters indicate significant differences ($p < 0.05$).*
*LW, full-spectrum light; LR, red light; LY, yellow light; LB, blue light; SGR, specific growth rate; CF, condition factor.*

**TABLE 2** | Effects of different light spectra on the composition of GIFT tilapia juveniles.

| Light spectra | Moisture (%) | Crude protein (%) | Crude lipid (%) |
|---|---|---|---|
| LW | 81.94 ± 0.13$^{b}$ | 13.04 ± 0.09$^{a}$ | 1.22 ± 0.09$^{a}$ |
| LR | 81.67 ± 0.11$^{b}$ | 13.08 ± 0.24$^{a}$ | 1.22 ± 0.06$^{a}$ |
| LY | 84.17 ± 0.26$^{a}$ | 11.06 ± 0.05$^{b}$ | 0.87 ± 0.05$^{b}$ |
| LB | 82.25 ± 0.28$^{b}$ | 13.11 ± 0.19$^{a}$ | 0.89 ± 0.07$^{b}$ |

*Different superscript letters indicate significant differences ($p < 0.05$).*
*LW, full-spectrum light; LR, red light; LY, yellow light; LB, blue light.*

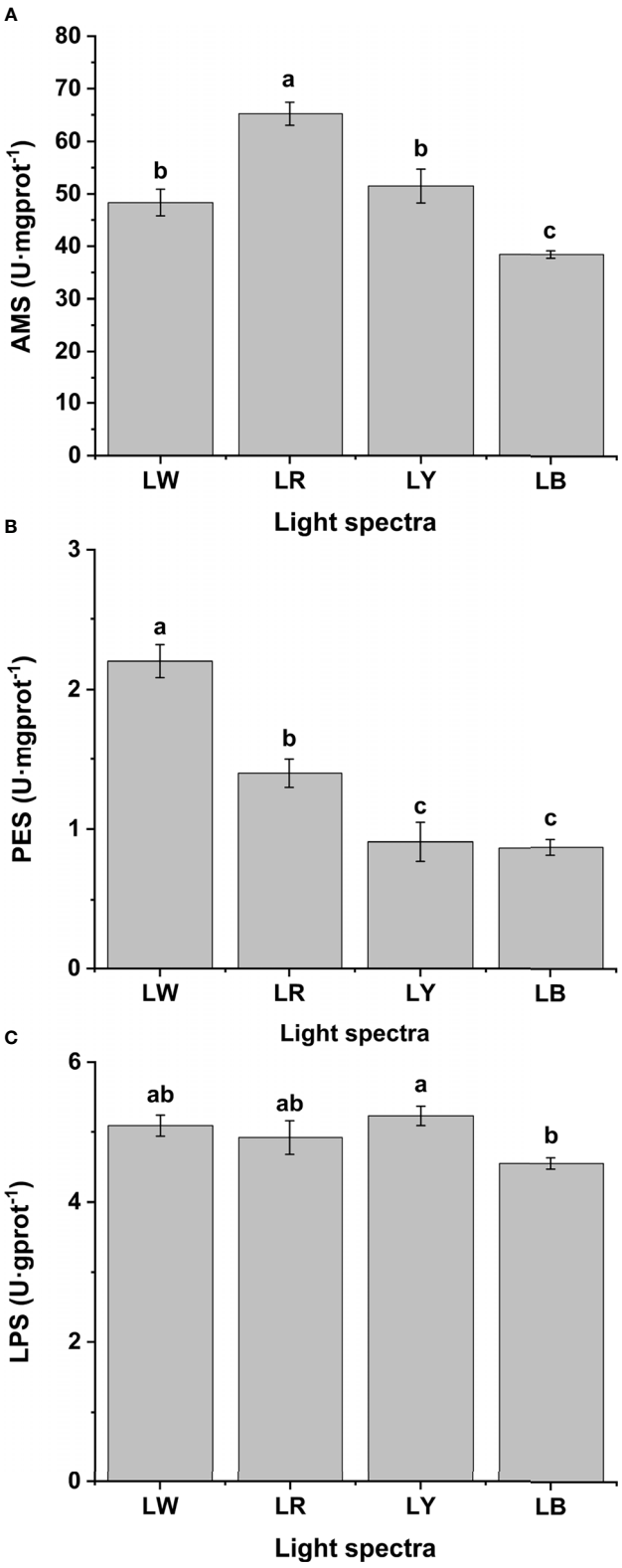


**FIGURE 1** | Related digestive enzyme activities of GIFT tilapia juveniles cultured under different light spectra. **(A)** The α-amylase (AMS) activities of GIFT tilapia juveniles under four light spectra. **(B)** The protease (PES) activities of GIFT tilapia juveniles under four light spectra. **(C)** The lipase (LPS) activities of GIFT tilapia juveniles under four light spectra. Different letters implies statistical differences ($p < 0.05$).

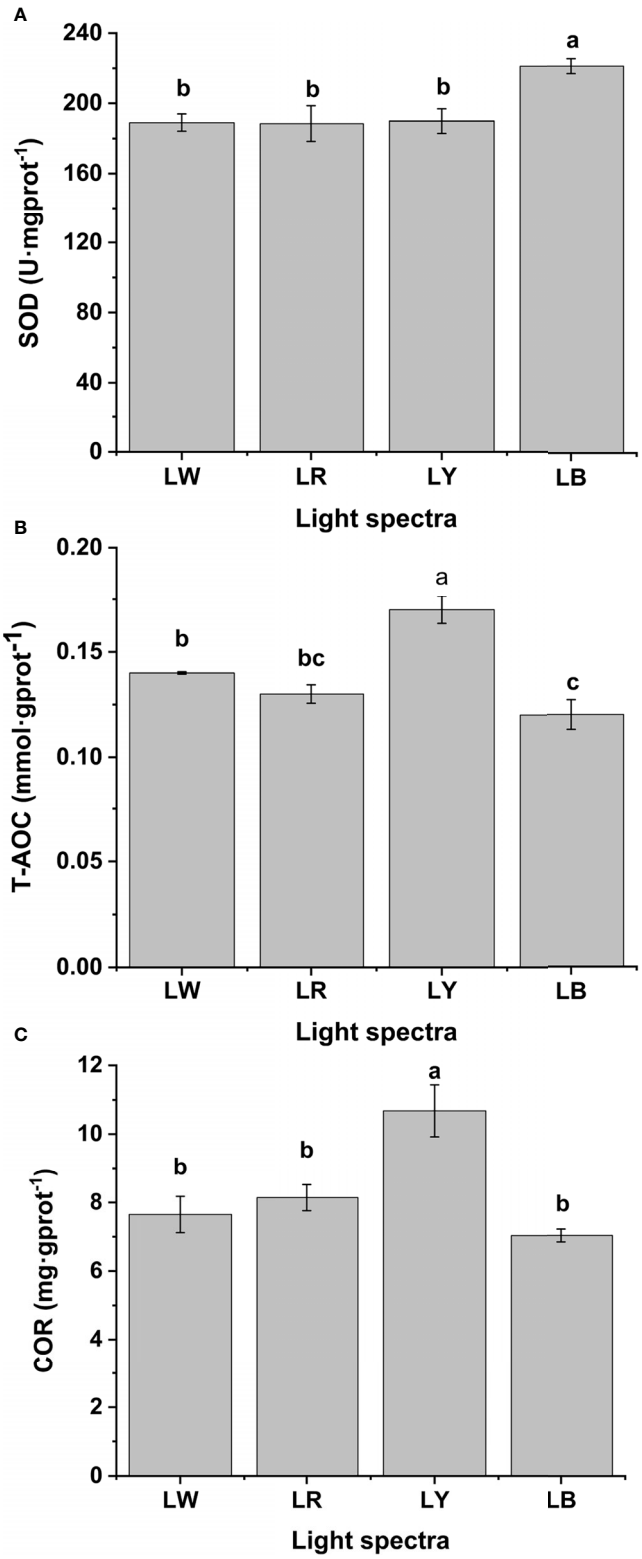


**FIGURE 2** | Related non-specific immune enzyme activities of GIFT tilapia juveniles cultured under different light spectra. **(A)** The superoxide dismutase (SOD) activities of GIFT tilapia juveniles under four light spectra. **(B)** The total antioxidant capacity (T-AOC) content of GIFT tilapia juveniles under four light spectra. **(C)** The cortisol (COR) content of GIFT tilapia juveniles under four light spectra. Different letters implies statistical differences ($p < 0.05$).

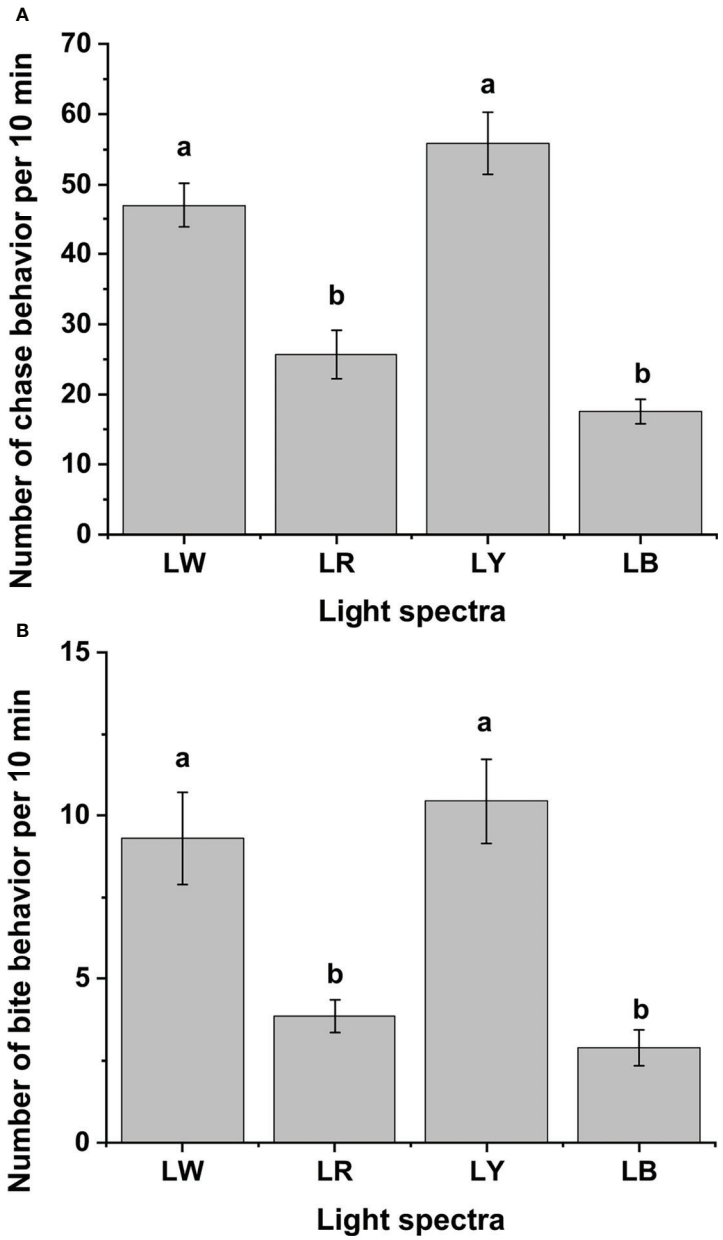


**FIGURE 3** | The aggressive behaviors of GIFT tilapia juveniles under different light spectra. **(A)** The chase behavior number of GIFT tilapia juveniles under different light spectra per 10 min. **(B)** The bite behavior number of GIFT tilapia juveniles under different light spectra per 10 min. Different letters implies statistical differences ($p < 0.05$).

protein localization, DNA damage and repair, energy generation, neurotransmitter transport, sensory perception, immune and stress responses, and proteometabolism. GO BP terms of LY vs. LW are mainly related to immune and stress responses, proteometabolism, protein localization, DNA damage and repair, energy generation, the JAK-STAT cascade, sensory perception, neurodevelopment, osteogenesis, muscle morphogenesis, and the cytokine-mediated signaling pathway. GO BP terms of LB vs. LW are mainly related to immune and stress responses, cell growth and apoptosis, proteometabolism, DNA damage and repair, neurodevelopment, lipid metabolism, glycometabolism, the JAK-STAT cascade, and smoothened signaling pathway.

KEGG results showed that the tryptophan metabolism signaling pathway, protein digestion and absorption signaling pathway, Jak-STAT signaling pathway, arachidonic acid metabolism signaling pathway, and alpha-linolenic acid metabolism signaling pathway were enriched (**Supplementary Table 3**). These signaling pathways play a significant role in teleost fishes' behavior, growth, and immunology. We further verified the expression of three genes (C*yp1a*, *Cyp1b1*, and *Cyp1c1*) of the tryptophan metabolism signaling pathway, two

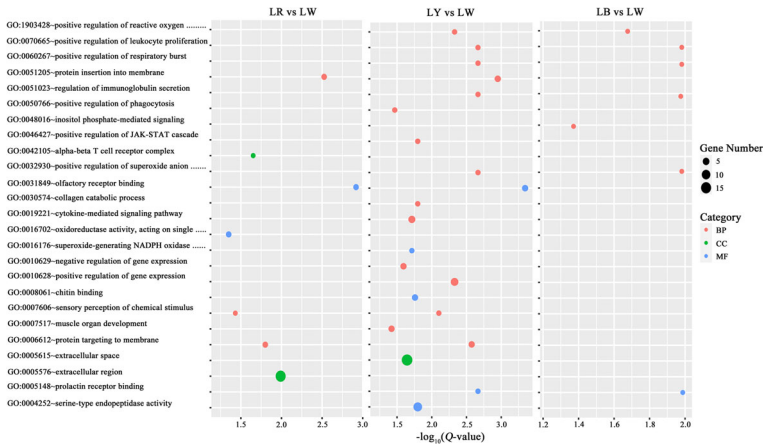


**FIGURE 4** | Enriched GO terms of biological processes (BPs; red), cellular components (CCs; green), and molecular functions (MFs; blue) between treatment groups and LW. The dots' size represents the number of genes involved in a function. GO, Gene Ontology; LW, full-spectrum light.

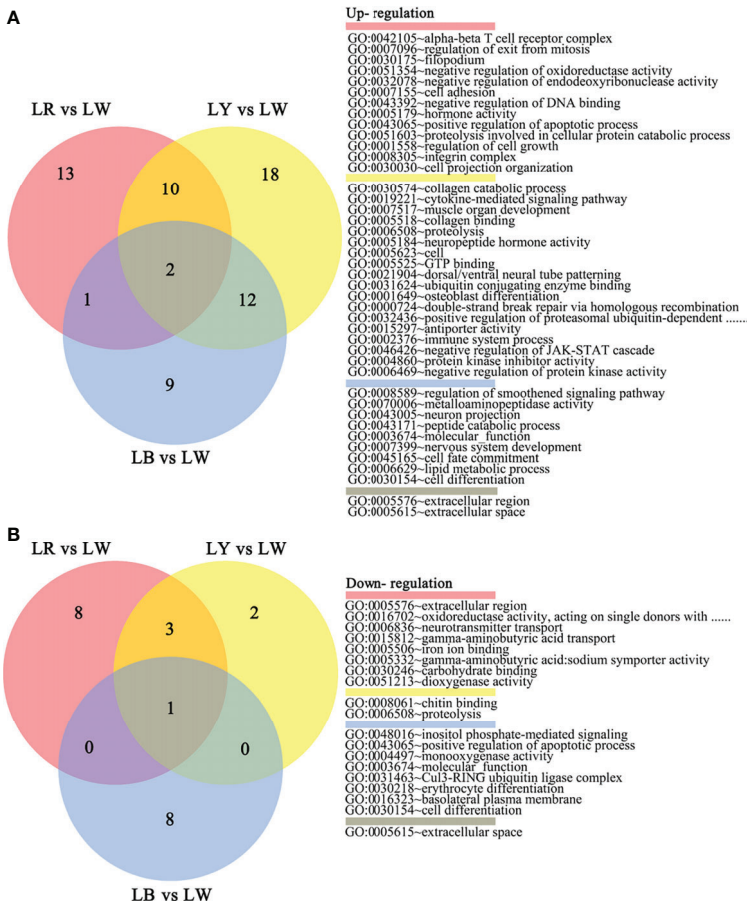


**FIGURE 5** | The number of different GO terms upregulated **(A)** and downregulated **(B)** in each treatment vs. LW of GIFT tilapia juveniles. The DEGs common to different groups were represented as overlapped regions, and those unique to each group were represented as non-overlapped regions. GO, Gene Ontology; LW, full-spectrum light; DEGs, differentially expressed genes.

genes (*Slc7a6* and *Kcnj13*) of the protein digestion and absorption signaling pathway, four genes (*Socs1b*, *Smtla*, *Prl*, and *Gh1*) of the Jak-STAT signaling pathway, three genes (*Cbr1*, *Pla2g1b*, and *Ggt1b*) of the arachidonic acid metabolism signaling pathway, and *Pla2g1b* of the alpha-linolenic acid metabolism signaling pathway by RT-qPCR. A significant positive correlation between RNA-seq and RT-qPCR was shown by a principal component analysis (PCA) ($r$ = 0.569, $p$ < 0.0001; **Figure 6**), supporting the reliability of the RNA-seq data.

## 4 DISCUSSION

Light influences fish through light intensity, spectra, and photoperiod (Karakatsouli et al., 2010; Qiu et al., 2015; Wei et al., 2021). Teleost fishes have different preferred spectral environments and exhibit different responses, including growth performance, stress responses, or behavior (Hou et al., 2019; Jin et al., 2019). The ideal light spectrum for farmed fish should be reflected in production efficiency and animal welfare. Moreover, the welfare of farmed fish should be assessed through several endpoints, such as metabolic, performance, anatomical, behavioral, and physiological indicators (Toni et al., 2019). Unfortunately, relatively few studies have shed light on farmed fishes' welfare under different light spectra. In this study, the growth, stress, and behavioral responses of GIFT tilapia juveniles cultured in different light spectra were assessed.

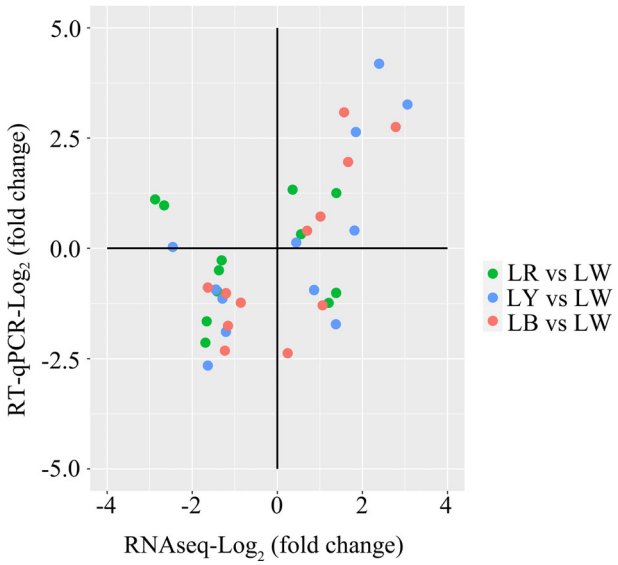


**FIGURE 6** | Correlation between RNA-seq and RT-qPCR determination of gene expression ($r$ = 0.569, $p$ < 0.0001). Green, comparisons between LR and LW (LR vs. LW). Blue, comparisons between LY and LW (LY vs. LW). Red, comparisons between LB and LW (LB vs. LW). LR, red light; LW, full-spectrum light; LY, yellow light; LB, blue light.

More and more evidence indicates that the light spectrum influences the growth of teleost fishes (Bairwa et al., 2017; Wu et al., 2020). Body weight, body length, and SGR are growth parameters commonly used (Du and Turchini, 2021), and crude protein and lipid contents of an organism can be used to measure the compositional status of fish (Shioya et al., 2012). Our results indicated that the light spectrum affected the growth of GIFT tilapia juveniles. GIFT tilapia juveniles showed higher growth performance, measured as body weight, length, SGR, and crude protein and lipid contents under LW and LR. These findings are consistent with results on European sea bass larvae and common carp. The total length of European sea bass larvae was significantly larger when reared under white light (Villamizar et al., 2009). Common carp showed higher body weight, total length, CF, and SGR under red than under white and blue lights (Karakatsouli et al., 2010). Nevertheless, the influence of the light spectrum on fish growth varied with fish species or growth and developmental stage (Karakatsouli et al., 2007; Villamizar et al., 2009; Karakatsouli et al., 2010). Turbot larval growth performance was affected by the light spectrum, and the influence was stage-specific (Wu et al., 2020). Spotted sea bass juveniles had the highest growth performance under blue light, while red seriously hurt their growth (Hou et al., 2019). Blue and green lights accelerated the growth of koi carp (Bairwa et al., 2017). This study with the GIFT strain of Nile tilapia achieved higher body weight and SGR of fish under LW and LR in terms of higher crude protein, crude lipids, and body length. Furthermore, the lower CF of fish under LW and LR may be due to the relatively fast development of body length. Digestive enzymes play an essential role in digesting nutrients, such as starch, fat, and protein of feed (García-Meilán et al., 2016). Absorption capacities are affected by environmental factors such as photoperiod, stocking density, and biotic factors such as species and diet (Espinosa-Chaurand et al., 2017; García-Meilán et al., 2020; Hernández-López et al., 2021; Upadhyay et al., 2022). AMS, PES, and LPS activities of GIFT tilapia juveniles under LW and LR were higher, compared with LY and LB. We explain this as increased digestive enzyme activities inducing GIFT tilapia juveniles' higher crude protein and lipid contents under LW and LR.

Reactive oxygen species (ROS) are easily induced during the oxidative decomposition of organic matter. The antioxidant defense system can scavenge ROS and protect against oxidative stress; T-AOC and SOD are important indicators for evaluating the antioxidant capacity of aquatic animals (Kong et al., 2021). Oxidative stress occurs when there is an imbalance between ROS production and the ability of the antioxidant defense system. Furthermore, COR is an important indicator of stress (Samaras et al., 2021). In this study, SOD activities of GIFT tilapia juveniles under LB, and T-AOC and COR content of fish under LY were the highest. These results indicated that tilapia juveniles reared under LY and LB suffered oxidative stress. Previous studies have reported that the light spectrum could influence the antioxidant defense system of teleost fishes. Green wavelength light could prevent oxidative stress of the olive flounder under high density (Choi et al., 2019). Nevertheless, unsuitable light spectrum

conditions can cause oxidative stress. The SOD activity of zebrafish under blue light-emitting diodes was higher than that under white fluorescent bulbs (Yuan et al., 2017). A higher COR level of snubnose pompano *Trachinotus blochii* (Lacépède, 1801) larvae under yellow light was observed (Mapunda et al., 2021). These results support our interpretation that LY and LB induced oxidative stress in tilapia juveniles.

Individual behavior is the comprehensive reflection of the external environment and internal factors. It has considerable practical significance for understanding the behavioral ecology and improving breeding protocols for fish, so the behavior should be considered when assessing fish welfare (Barreto et al., 2022). The light spectrum is an external environmental factor affecting farmed fish behavior (Li et al., 2021). Lighting conditions strongly affected the behavioral responses of European sea bass larvae (Villamizar et al., 2011b). In this research, GIFT tilapia juveniles under LW and LY exhibited more aggressive chase and bite behaviors than fish under LR and LB, indicating that juvenile fish under LW and LY experienced poor welfare. Previous research also showed that an unsuitable light spectrum induced discomfort or abnormal animal behavior. The red spectrum, disturbing endocrine homeostasis associated with aggressive behaviors, induced stress responses, while blue light was beneficial for spotted sea bass culture (Hou et al., 2019). Exposure to ultraviolet light affected the behavior of virile (*F. virilis*) and rusty (*F. rusticus*) crayfishes, and the duration of time spent fighting and the number of fights significantly increased (Jackson and Moore, 2019). Collector urchins are highly sensitive to and dislike blue LED light, exhibiting the most hiding behavior with a lower level of melanin expression (Li et al., 2021). These results indicate that aquatic animals exhibit different preferred light spectra and that preferred light spectra for different species at different developmental stages should be determined and provided in culture systems. In the wild, Nile tilapia prefers to live in shallow waters and the upper, middle, or near surface of the water during the daytime, where the spectral composition is varied including the long wavelengths (Villamizar et al., 2011a). In the current study, GIFT tilapia juveniles under LR exhibited faster growth performance, fewer stress responses, and more aggressive behaviors as compared with those under LW, LY, and LB. Therefore, red light is the preferred light spectra for GIFT tilapia juveniles.

Results of this study suggested that the light spectrum had growth, stress, and behavioral influences on GIFT tilapia juveniles. Furthermore, the results of previous studies support our findings (Villamizar et al., 2009; Bairwa et al., 2017; Yang et al., 2021). Therefore, RNA-seq was carried out to investigate potential molecular pathways. Results of the GO BP revealed that the component of the nervous system associated with behavior (GO:0006836 neurotransmitter transport and GO:0005332~gamma-aminobutyric acid:sodium symporter activity) was significantly affected by LR, leading to decreased aggression behaviors, such as chase and bite. GIFT tilapia juveniles under LY showed that muscle morphogenesis (GO:0007517 muscle organ development and GO:0021904: dorsal/ventral neural tube patterning) and immune system (GO: 0002376 immune system process) functions associated with the growth and immune responses were significantly affected, resulting in decreased growth performance and more stress. Juvenile fish exposed to blue light showed that nervous system development and lipid metabolic processes changed significantly, resulting in decreased growth performance and aggressive behaviors.

Moreover, we analyzed the potential mechanisms of the spectrum on the growth, stress, and behavior of GIFT tilapia juveniles through the KEGG pathway. Tryptophan (Trp) is a precursor of crucial compounds related to immune and nerve development and social behavior. Disturbance of Trp metabolic pathways, as well as the content of Trp or its derivatives, can induce behavioral and neuropsychiatric disorders (Galley et al., 2021). Studies show that *Cyp1a1* and *Cyp1b1* of this pathway regulated Trp/5-HT metabolism and transport (Galley et al., 2021). Moreover, aberrant metabolism and transport of Trp/5-HT can affect normal neurodevelopment and behavior (Connors et al., 2014; Herculano and Maximo, 2014; Barreiro-Iglesias et al., 2015). In this study, the tryptophan metabolism signaling pathway of GIFT tilapia juveniles under different light spectra was enriched, and the behavior of fish exposed to LR and LB changed significantly as compared with fish under LW.

The JAK-STAT signal pathway is crucial to cellular proliferation, differentiation, and immunomodulation. In medaka (*Oryzias melastigma*), the JAK-STAT signaling pathway regulates hepcidin1 expression, which exerts an important role associated with pathogen infection or inflammation (Wrighting and Andrews, 2006; Cui et al., 2019). In our study, GIFT tilapia juveniles exposed to LY underwent stress, reflected by the increased T-AOC and COR contents. There are reports that long wavelengths of light can induce stress and immune responses in turbot larvae (Wu et al., 2020), which is consistent with our results. Moreover, the transcriptomic analysis revealed that the JAK-STAT signaling pathway associated with immunomodulator was enriched in tilapia juveniles under LY. Thus, we believe that the light spectrum regulated the JAK-STAT signaling pathway, inducing the stress responses of juvenile fish exposed to LY.

The protein digestion and absorption pathway regulate the hydrolysis and transport of proteins, peptides, and amino acids. Metabolism of protein and lipid in the diet directly influences fish growth, such as weight gain, protein content, trypsin, and chymotrypsin specific activities (Ma et al., 2019). Dietary nutrition regulated protein digestion of large yellow croaker (*Larimichthys crocea*) larvae through the transcription of peptide transporter 1, cholecystokinin, and trypsin, and growth performance was influenced (Cai et al., 2015). Choline deficiency impeded the absorption of intestinal amino acids in juvenile grass carp (*Ctenopharyngodon idella*), which might be related to the expression of the corresponding transporters, including SLC7A6 associated with protein digestion and absorption pathway (Yuan et al., 2020). Fatty acids (FAs), especially arachidonic acid and alpha-linolenic acid, are among the most important nutritional factors for successful fish production (Norambuena et al., 2013; Magalhães et al., 2021). Dietary

arachidonic acid could regulate lipid metabolism and accelerate the growth of striped bass (*Morone saxatilis*) juveniles (Araújo et al., 2021). Dietary linoleic acid affected the growth and FA composition of rabbitfish (*Siganus canaliculatus*) (Xie et al., 2018), and both the growth and gonadal development of the juvenile common carp were altered (Ma et al., 2020). The main FA constituents significantly affected pike perch (*Sander lucioperca*) larvae tissue FA content (Lund et al., 2019). In the current research, GIFT tilapia juveniles under LY and LB exhibited poor growth performance. Considering the vital role of these signal pathways on fish growth, we believe that light spectra regulated protein digestion and absorption, arachidonic acid metabolism, and alpha-linolenic acid metabolism pathways, inducing poor growth of juvenile fish exposed to LY and LB.

## 5 CONCLUSIONS

This study confirmed that light spectra significantly affected the welfare of GIFT tilapia juveniles in terms of growth performance, stress responses, and behavior. LW and LR positively affected the growth performance of tilapia juveniles, while LY could induce a stress response in juvenile fish. Moreover, tilapia juveniles exposed to LW and LY exhibited more aggressive behaviors than fish under LR and LB. The transcriptomic analysis demonstrated that different light spectra could regulate signaling pathways associated with the tilapia juveniles' growth, stress, and behavior. In terms of growth performance, stress responses, and behavior, the optimal light spectrum for the welfare of GIFT tilapia juveniles is LR.

## DATA AVAILABILITY STATEMENT

Illumina NovaSeq 6000 were used to generate transcriptomic data. The data are deposited in the NCBI repository, accession number PRJNA833495.

## ETHICS STATEMENT

The animal study was reviewed and approved by Laboratory Animal Ethics Committee Pearl River Fisheries Research Institute, CAFS.

## AUTHOR CONTRIBUTIONS

MY: conceptualization, data curation, formal analysis, investigation, methodology, writing—original draft, and writing—review and editing. WZ: validation and formal analysis. MW: software and visualization. HW: methodology and writing—reviewing and editing. ZL: visualization. FG: data curation. XK: project administration. CS: writing—reviewing and editing. JC: resources. ML: supervision and conceptualization. All authors listed have made a substantial, direct, and intellectual contribution to the work and approved it for publication.

## FUNDING

This work was supported by the National Natural Science Foundation of China [grant number 31902428], China Agriculture Research System of MOF and MARA [grant number CARS-46], Independent Research and Development Projects of Maoming Laboratory [grant number 2021ZZ007], National Natural Science Foundation of China [grant number 31972783], and Guangdong Basic and Applied Basic Research Foundation [grant numbers 2019A1515111046, 2021A1515010852].

## SUPPLEMENTARY MATERIAL

The Supplementary Material for this article can be found online at: https://www.frontiersin.org/articles/10.3389/fmars.2022.924110/full#supplementary-material

## REFERENCES

Araújo, B. C., Rodriguez, M., Honji, R. M., Rombenso, A. N., del Rio-Zaragoza, O. B., Cano, A., et al. (2021). Arachidonic Acid Modulated Lipid Metabolism and Improved Productive Performance of Striped Bass (*Morone Saxatilis*) Juvenile Under Sub- to Optimal Temperatures. *Aquaculture* 530, 735939. doi: 10.1016/j.aquaculture.2020.735939

Ashley, P. J. (2007). Fish Welfare: Current Issues in Aquaculture. *Appl. Anim. Behav. Sci.* 104, 199–235. doi: 10.1016/j.applanim.2006.09.001

Bairwa, M. K., Saharan, N., Rawat, K. D., Tiwari, V. K., and Prasad, K. P. (2017). Effect of Light Spectra on Growth Performance and Immune Response of Koi Carp, *Cyprinus Carpio* (Linnaeus 1758). *Fishery Technol.* 54, 100–106. doi: 10.18805/ijar.v0iof.8452

Barreiro-Iglesias, A., Mysiak, K. S., Scott, A. L., Reimer, M. M., Yang, Y., Becker, C. G., et al. (2015). Serotonin Promotes Development and Regeneration of Spinal Motor Neurons in Zebrafish. *Cell Rep.* 13, 924–932. doi: 10.1016/j.celrep.2015.09.050

Barreto, M. O., Rey Planellas, S., Yang, Y., Phillips, C., and Descovich, K. (2022). Emerging Indicators of Fish Welfare in Aquaculture. *Rev. Aquacul.* 14, 343–361. doi: 10.1111/raq.12601

Cai, Z., Li, W., Mai, K., Xu, W., Zhang, Y., and Ai, Q. (2015). Effects of Dietary Size-Fractionated Fish Hydrolysates on Growth, Activities of Digestive Enzymes and Aminotransferases and Expression of Some Protein Metabolism Related Genes in Large Yellow Croaker (*Larimichthys Crocea*) Larvae. *Aquaculture* 440, 40–47. doi: 10.1016/j.aquaculture.2015.01.026

Cheng, C. L., and Flamarique, I. N. (2004). New Mechanism for Modulating Colour Vision. *Nature* 428, 279–280. doi: 10.1038/428279a

Choi, C. Y., Choi, J. Y., Choi, Y. J., Kim, B. S., and Kim, J. W. (2019). Effects of Green Wavelength Light on Antioxidant and Non-Specific Immune Responses of the Olive Flounder *Paralichthys Olivaceus* Maintained at Different Stocking Densities. *Aquacul. Eng.* 84, 23–28. doi: 10.1016/j.aquaeng.2018.11.004

Connors, K. A., Valenti, T. W., Lawless, K., Sackerman, J., Onaivi, E. S., Brooks, B. W., et al. (2014). Similar Anxiolytic Effects of Agonists Targeting Serotonin 5-$HT_{1A}$ or Cannabinoid CB Receptors on Zebrafish Behavior in Novel Environments. *Aquat. Toxicol.* 151, 105–113. doi: 10.1016/j.aquatox.2013.12.005

Cui, Q., Chen, F. Y., Zhang, M., Peng, H., and Wang, K. J. (2019). Transcriptomic Analysis Revealing Hepcidin Expression in *Oryzias Melastigma* Regulated Through the JAK-STAT Signaling Pathway Upon Exposure to BaP. *Aquat. Toxicol.* 206, 134–141. doi: 10.1016/j.aquatox.2018.11.015

Du, Z. Y., and Turchini, G. M. (2021). Are We Actually Measuring Growth?—An Appeal to Use a More Comprehensive Growth Index System for Advancing Aquaculture Research. *Rev. Aquacul.* 14, 525–527. doi: 10.1111/raq.12604

Espinosa-Chaurand, D., Vega-Villasante, F., Carrillo-Farnés, O., and Nolasco-Soria, H. (2017). Effect of Circadian Rhythm, Photoperiod, and Molt Cycle on Digestive Enzymatic Activity of *Macrobrachium Tenellum* Juveniles. *Aquaculture* 479, 225–232. doi: 10.1016/j.aquaculture.2017.05.029

FAO (2018). *The State of World Fisheries and Aquaculture 2018 - Meeting the Sustainable Development Goals* (Rome).

Galley, J. D., Chen, H. J., Antonson, A. M., and Gur, T. L. (2021). Prenatal Stress-Induced Disruptions in Microbial and Host Tryptophan Metabolism and Transport. *Behav. Brain Res.* 414, 113471. doi: 10.1016/j.bbr.2021.113471

García-Meilán, I., Ordóñez-Grande, B., Machahua, C., Buenestado, S., Fontanillas, R., and Gallardo, M. A. (2016). Effects of Dietary Protein-to-Lipid Ratio on Digestive and Absorptive Processes in Sea Bass Fingerlings. *Aquaculture* 463, 163–173. doi: 10.1016/j.aquaculture.2016.05.039

García-Meilán, I., Ordóñez-Grande, B., Valentín, J. M., Fontanillas, R., and Gallardo, Á. (2020). High Dietary Carbohydrate Inclusion by Both Protein and Lipid Replacement in Gilthead Sea Bream. Changes in Digestive and Absorptive Processes. *Aquaculture* 520, 734977. doi: 10.1016/j.aquaculture.2020.734977

Herculano, A. M., and Maximino, C. (2014). Serotonergic Modulation of Zebrafish Behavior: Towards a Paradox. *Prog. Neuropsychopharmacol. Biol. Psychiatry* 55, 50–66. doi: 10.1016/j.pnpbp.2014.03.008

Hernández-López, I. A., Ibarra-Castro, L., Álvarez-González, C. A., Martínez-Brown, J. M., Maytorena-Verdugo, C. I., and Peña-Marín, E. S. (2021). Characterization of Digestive Enzymes During Early Ontogeny of White Snook (*Centropomus Viridis*). *Aquaculture* 535, 736399. doi: 10.1016/j.aquaculture.2021.736399

Hou, Z. S., Wen, H. S., Li, J. F., He, F., Li, Y., Qi, X., et al. (2019). Effects of Photoperiod and Light Spectrum on Growth Performance, Digestive Enzymes, Hepatic Biochemistry and Peripheral Hormones in Spotted Sea Bass (*Lateolabrax Maculatus*). *Aquaculture* 507, 419–427. doi: 10.1016/j.aquaculture.2019.04.029

Jackson, K. M., and Moore, P. A. (2019). The Intensity and Spectrum of Artificial Light at Night Alters Crayfish Interactions. *Conserv. Physiol.* 8, 131–150. doi: 10.1080/10236244.2019.1663124

Jin, G., Zhao, J., Zhang, Y. D., Liu, G., Liu, D. Z., Zhu, S. M., et al. (2019). Light Spectrum Preference of Nile Tilapia (*Oreochromis Niloticus*) Under Different Hunger Levels. *Int. J. Agric. Biol. Eng.* 12, 51–57. doi: 10.25165/j.ijabe.20191205.4170

Karakatsouli, N., Papoutsoglou, S. E., Pizzonia, G., Tsatsos, G., Tsopelakos, A., Chadio, S., et al. (2007). Effects of Light Spectrum on Growth and Physiological Status of Gilthead Seabream *Sparus Aurata* and Rainbow Trout *Oncorhynchus Mykiss* Reared Under Recirculating System Conditions. *Aquacul. Eng.* 36, 302–309. doi: 10.1016/j.aquaeng.2007.01.005

Karakatsouli, N., Papoutsoglou, E. S., Sotiropoulos, N., Mourtikas, D., Stigen-Martinsen, T., and Papoutsoglou, S. E. (2010). Effects of Light Spectrum, Rearing Density and Light Intensity on Growth Performance of Scaled and Mirror Common Carp *Cyprinus Carpio* Reared Under Recirculating System Conditions. *Aquacul. Eng.* 42, 121–127. doi: 10.1016/j.aquaeng.2010.01.001

Khaw, H. L., Ponzoni, R. W., Hamzah, A., Abu-Bakar, K. R., and Bijma, P. (2012). Genotype by Production Environment Interaction in the GIFT Strain of Nile Tilapia (*Oreochromis Niloticus*). *Aquaculture* 326-329, 53–60. doi: 10.1016/j.aquaculture.2011.11.016

Kong, Y., Li, M., Chu, G., Liu, H., Shan, X., Wang, G., et al. (2021). The Positive Effects of Single or Conjoint Administration of Lactic Acid Bacteria on *Channa Argus*: Digestive Enzyme Activity, Antioxidant Capacity, Intestinal Microbiota and Morphology. *Aquaculture* 531, 735852. doi: 10.1016/j.aquaculture.2020.735852

Li, Y. Y., Su, F. J., Hsieh, Y. J., Huang, T. C., and Wang, Y. S. (2021). Embryo Development and Behavior in Sea Urchin (*Tripneustes Gratilla*) Under Different Light Emitting Diodes Condition. *Front. Mar. Sci.* 8. doi: 10.3389/fmars.2021.684330

Lopez-Luna, J., Ibanez, M. A., and Villarroel, M. (2013). Using Multivariate Analysis of Water Quality in RAS With Nile Tilapia (*Oreochromis Niloticus*) to Model the Evolution of Macronutrients. *Aquacul. Eng.* 54, 22–28. doi: 10.1016/j.aquaeng.2012.10.005

Lund, I., Rodríguez, C., Izquierdo, M. S., El Kertaoui, N., Kestemont, P., Reis, D. B., et al. (2019). Influence of Salinity and Linoleic or α-Linolenic Acid Based Diets on Ontogenetic Development and Metabolism of Unsaturated Fatty Acids in Pike Perch Larvae (*Sander Lucioperca*). *Aquaculture* 500, 550–561. doi: 10.1016/j.aquaculture.2018.10.061

Magalhães, R., Martins, N., Fontinha, F., Moutinho, S., Olsen, R. E., Peres, H., et al. (2021). Effects of Dietary Arachidonic Acid and Docosahexanoic Acid at Different Carbohydrates Levels on Gilthead Sea Bream Growth Performance and Intermediary Metabolism. *Aquaculture* 545, 737233. doi: 10.1016/j.aquaculture.2021.737233

Ma, R., Liu, X., Meng, Y., Wu, J., Zhang, L., Han, B., et al. (2019). Protein Nutrition on Sub-Adult Triploid Rainbow Trout (1): Dietary Requirement and Effect on Anti-Oxidative Capacity, Protein Digestion and Absorption. *Aquaculture* 507, 428–434. doi: 10.1016/j.aquaculture.2019.03.069

Mapunda, J., Mtolera, M. S. P., Yahya, S. A. S., Ngo, V. M., and Golan, M. (2021). Light Colour Affect the Survival Rate, Growth Performance, Cortisol Level, Body Composition, and Digestive Enzymes Activities of Different Snubnose Pompano (*Trachinotus Blochii* (Lacépède 1801) Larval Stages. *Aquacul. Rep.* 21, 100804. doi: 10.1016/j.aqrep.2021.100804

Ma, X., Wang, L., Xie, D., Tian, X., Zhang, Y., Wu, L., et al. (2020). Effect of Dietary Linolenic/Linoleic Acid Ratios on Growth Performance, Ovarian Steroidogenesis, Plasma Sex Steroid Hormone, and Tissue Fatty Acid Accumulation in Juvenile Common Carp, *Cyprinus Carpio*. *Aquacul. Rep.* 18, 100452. doi: 10.1016/j.aqrep.2020.100452

Norambuena, F., Morais, S., Estévez, A., Bell, J. G., Tocher, D. R., Navarro, J. C., et al. (2013). Dietary Modulation of Arachidonic Acid Metabolism in Senegalese Sole (*Solea Senegalensis*) Broodstock Reared in Captivity. *Aquaculture*, 372–375, 80-88. doi: 10.1016/j.aquaculture.2012.10.035

Qiu, D., Xu, S., Song, C., Chi, L., Li, X., Sun, G., et al. (2015). Effects of Spectral Composition, Photoperiod and Light Intensity on the Gonadal Development of Atlantic Salmon *Salmo Salar* in Recirculating Aquaculture Systems (RAS). *Chin. J. Oceanol. Limnol.* 33, 45–56. doi: 10.1007/s00343-015-4011-3

Samaras, A., Dimitroglou, A., Kollias, S., Skouradakis, G., Papadakis, I. E., and Pavlidis, M. (2021). Cortisol Concentration in Scales is a Valid Indicator for the Assessment of Chronic Stress in European Sea Bass, *Dicentrarchus Labrax* L. *Aquaculture* 545, 737257. doi: 10.1016/j.aquaculture.2021.737257

Shioya, I., Takemura, S., Ishizuka, R., and Yamaguchi, T. (2012). Variations in the Proximate Composition of Muscle in Cultured Yellowtail *Seriola Quinqueradiata* at Different Anatomical Portions. *Fish. Sci.* 78, 725–733. doi: 10.1007/s12562-012-0477-5

Toni, M., Angiulli, E., Malavasi, S., Alleva, E., and Cioni, C. (2017). Variation in Environmental Parameters in Research and Aquaculture: Effects on Behaviour, Physiology and Cell Biology of Teleost Fish. *J. Aquacul. Mar. Biol.* 5, 137. doi: 10.15406/jamb.2017.05.00137

Toni, M., Manciocco, A., Angiulli, E., Alleva, E., Cioni, C., and Malavasi, S. (2019). Review: Assessing Fish Welfare in Research and Aquaculture, With a Focus on European Directives. *Animal* 13, 161–170. doi: 10.1017/S1751731118000940

Upadhyay, A., Swain, H. S., Das, B. K., Ramteke, M. H., Kumar, V., Krishna, G., et al. (2022). Stocking Density Matters in Open Water Cage Culture: Influence on Growth, Digestive Enzymes, Haemato-Immuno and Stress Responses of *Puntius Sarana* (Ham 1822). *Aquaculture* 547, 737445. doi: 10.1016/j.aquaculture.2021.737445

Villamizar, N., Blanco-Vives, B., Migaud, H., Davie, A., Carboni, S., and Sánchez-Vázquez, F. J. (2011a). Effects of Light During Early Larval Development of Some Aquacultured Teleosts: A Review. *Aquaculture* 315, 86–94. doi: 10.1016/j.aquaculture.2010.10.036

Villamizar, N., Garcia-Alcazar, A., and Sanchez-Vazquez, F. J. (2009). Effect of Light Spectrum and Photoperiod on the Growth, Development and Survival of European Sea Bass (*Dicentrarchus Labrax*) Larvae. *Aquaculture* 292, 80–86. doi: 10.1016/j.aquaculture.2009.03.045

Villamizar, N., Garcia-Mateos, G., and Sanchez-Vazquez, F. J. (2011b). Behavioral Responses of European Sea Bass (*Dicentrarchus Labrax*) Larvae and *Artemia* Sp Exposed to Constant Light or Darkness vs. Light/Dark Cycles of White, Red or Blue Wavelengths. *Aquaculture* 317, 197–202. doi: 10.1016/j.aquaculture.2011.03.036

Villarroel, M., Alavrino, J. M. R., and Lopez-Luna, J. (2011). Effect of Feeding Frequency and One Day Fasting on Tilapia (*Oreochromis Niloticus*) and Water Quality. *Israeli. J. Aquaculture-Bamidgeh.* 63, 1–6. doi: 10.46989/001c.20600

Wei, J., Tian, L., Wang, Y., Yu, L., and Zhu, X. (2021). Effects of Salinity, Photoperiod, and Light Spectrum on Larval Survival, Growth, and Related

Enzyme Activities in the Giant Freshwater Prawn, *Macrobrachium Rosenbergii*. *Aquaculture* 530, 735794. doi: 10.1016/j.aquaculture.2020.735794

Wrighting, D. M., and Andrews, N. C. (2006). Interleukin-6 Induces Hepcidin Expression Through STAT3. *Blood* 108, 3204–3209. doi: 10.1182/blood-2006-06-027631

Wu, L., Han, M., Song, Z., Xu, S., Li, J., Li, X., et al. (2019). Effects of Different Light Spectra on Embryo Development and the Performance of Newly Hatched Turbot (*Scophthalmus Maximus*) Larvae. *Fish. Shellfish. Immunol.* 90, 328–337. doi: 10.1016/j.fsi.2019.05.007

Wu, L., Wang, Y., Han, M., Song, Z., Song, C., Xu, S., et al. (2020). Growth, Stress and non-Specific Immune Responses of Turbot (*Scophthalmus Maximus*) Larvae Exposed to Different Light Spectra. *Aquaculture* 520, 734950. doi: 10.1016/j.aquaculture.2020.734950

Xie, D., Liu, X., Wang, S., You, C., and Li, Y. (2018). Effects of Dietary LNA/LA Ratios on Growth Performance, Fatty Acid Composition and Expression Levels of Elovl5, Δ4 Fad and Δ6/Δ5 Fad in the Marine Teleost *Siganus Canaliculatus*. *Aquaculture* 484, 309–316. doi: 10.1016/j.aquaculture.2017.08.039

Yang, M. F., Chen, Z. L., Hu, F. Y., Sun, J. N., Ding, J. Y., Chang, Y. Q., et al. (2020). Light Spectra Regulated Foraging and Feeding Behaviors Shed Light on Stock Enhancement of the Sea Urchin *Strongylocentrotus Intermedius*. *Aquacul. Rep.* 18, 100480. doi: 10.1016/j.aqrep.2020.100480

Yang, M. F., Hu, F. Y., Leng, X. F., Chi, X. M., Yin, D. H., Ding, J. Y., et al. (2021). Long-Term Effects of Light Spectra on Fitness Related Behaviors and Growth of the Sea Urchin *Strongylocentrotus Intermedius*. *Aquaculture* 537, 736518. doi: 10.1016/j.aquaculture.2021.736518

Yuan, Z. H., Feng, L., Jiang, W. D., Wu, P., Liu, Y., Jiang, J., et al. (2020). Choline Deficiency Decreased the Growth Performances and Damaged the Amino Acid Absorption Capacity in Juvenile Grass Carp (*Ctenopharyngodon Idella*). *Aquaculture* 518, 734829. doi: 10.1016/j.aquaculture.2019.734829

Yuan, S. S., Lv, Z. M., Zhu, A. Y., Zheng, J. L., and Wu, C. W. (2017). Negative Effect of Chronic Cadmium Exposure on Growth, Histology, Ultrastructure, Antioxidant and Innate Immune Responses in the Liver of Zebrafish: Preventive Role of Blue Light Emitting Diodes. *Ecotoxicol. Environ. Saf.* 139, 18–26. doi: 10.1016/j.ecoenv.2017.01.021

**Conflict of Interest:** The authors declare that the research was conducted in the absence of any commercial or financial relationships that could be construed as a potential conflict of interest.

**Publisher's Note:** All claims expressed in this article are solely those of the authors and do not necessarily represent those of their affiliated organizations, or those of the publisher, the editors and the reviewers. Any product that may be evaluated in this article, or claim that may be made by its manufacturer, is not guaranteed or endorsed by the publisher.

frontiers | Frontiers in Marine Science

TYPE Original Research
PUBLISHED 20 September 2022
DOI 10.3389/fmars.2022.939749



OPEN ACCESS

EDITED BY
Enric Gisbert,
Institute of Agrifood Research and Technology (IRTA), Spain

REVIEWED BY
Marco Antonio Vindas,
Norwegian University of Life Sciences, Norway
Martin Iversen,
Nord University, Norway

*CORRESPONDENCE
Dong Zhang
zdfit63@163.com

SPECIALTY SECTION
This article was submitted to Aquatic Physiology, a section of the journal Frontiers in Marine Science

RECEIVED 09 May 2022
ACCEPTED 29 August 2022
PUBLISHED 20 September 2022

CITATION
Li S, Liu X, Lin T, Zhang D and Zou X (2022) The consistent background color preference highlights the personality in the lined seahorse, *Hippocampus erectus*. *Front. Mar. Sci.* 9:939749. doi: 10.3389/fmars.2022.939749



# The consistent background color preference highlights the personality in the lined seahorse, *Hippocampus erectus*

Siping Li, Xin Liu, Tingting Lin, Dong Zhang* and Xiong Zou

Key Laboratory of Inland Saline-alkaline Aquaculture, Ministry of Agriculture and Rural Affairs, East China Sea Fisheries Research Institute, Chinese Academy of Fishery Sciences, Shanghai, China

Background color in aquaculture has been paid more attention due to the effect on fish growth, survival, health, and reproduction. In the present study, we evaluated the background color preference of the lined seahorse (*Hippocampus erectus*) and its relationship with personality. Preference was assessed over 10 consecutive days through allowing the lined seahorse to freely choose six different colored compartments, i.e., white, red, green, black, yellow, and blue backgrounds. To minimize the spurious preference response, the individual preference index (PI) was applied to calculate the preference intensity of the background colors. Preference reliability was further verified by a binary choice test through the choice for the most preferred or non-preferred color. Preference consistency under stress situation was assessed by a "knock-at-the-door" test as confining the seahorse in a transparent circle after a 30-s air exposure and measuring the proportion of knock toward different colored backgrounds. The personality was conjointly analyzed by new environment test and novel object test. Overall, the lined seahorse showed a general preference for white and blue while avoidance of black and red backgrounds at either unstressed or stressed situations. The shyer the seahorse was, the more preference for white background it displayed. Thus, white and blue background colors are recommended for culturing the lined seahorse. Furthermore, white color preference is a potential indicator in personality study of the lined seahorse.

KEYWORDS

**the lined seahorse, background color, preference, fish personality, welfare condition**

## Introduction

Color patterns in the surroundings can be detected by fish *via* the visual pigments. Fishes use color vision to see prey against a variety of backgrounds and to detect potential mates and predators (Lythgoe and Partridge, 1989; Neumeyer, 1992; Espmark et al., 2000; Losey et al., 2003; Bowmaker et al., 2007). On the other hand, color sources, including

light color and background color, prominently affect fishes' physiological–behavioral processes, such as in relieving stress (Barcellos et al., 2009; Karakatsouli et al., 2010; Maia and Volpato, 2013), food intake (Spence and Smith, 2008; Volpato et al., 2013), growth (Ruchin, 2004; Karakatsouli et al., 2007), survival (Barcellos et al., 2009; Kang and Kim, 2013a), and reproduction (Volpato et al., 2004). Background color has been paid more attention in fish culture, as regards to the growth rate and fish welfare (Karakatsouli et al., 2007; Strand et al., 2007; Kang and Kim, 2013a; Kang and Kim, 2013b). For example, white background was recommended in flounder and the Eurasian perch culture to obtain a better growth rate (Tamazouzt et al., 2000; Takahashi et al., 2007; Sunuma et al., 2009).

The ability to sense the color enables fishes to make a choice for a preferred or avoided color. Similar to motivation for an essential resource in animals (Mason et al., 2001; Asher et al., 2009; Houpt, 2012), animals should have a motivation for choosing a favorable background color in captivity. For example, the rainbow trout (*Oncorhynchus mykiss*) was more motivated to access to blue background—a strongly preferred color (Maia et al., 2017). Generally, preference behaviors are consistent across time and vary among individuals, such as mating preference in the sand goby (*Pomatoschistus minutus*) and the treehoppers (*Enchenopa binotata*) (Lehtonen and Lindstrom, 2006; Fowler-Finn and Rodriguez, 2013). It is probably similar in color preference (Maia et al., 2017).

In human beings, the relationship between color preference and personality has been studied intensively (Birren, 1973; Stimpson and Stimpson, 1979; Nikolaenko and Ostrovskaia, 1989; Fetterman et al., 2015; Tao et al., 2015). Personality is defined as the inter-individual variation in behavior, characterized as stability through time and/or consistency across situations (Réale et al., 2007; Kaiser and Müller, 2021). In another word, color preference could be a personality trait as well if it was consistent across time and situations. It is interesting to know whether there is a relationship between color preference and personality in animals. Animal personality highlights the difference in physiology and behaviors, e.g., bold fishes with high adrenergic axis activity and low hypothalamo–pituitary–interrenal axis activity are more active and more likely to explore novel environments or objects versus shy fish (Sneddon, 2003; Sih et al., 2004; Carere et al., 2005; Thomson et al., 2011). Investigating whether bold–shy personality participates in fishes' color choice would further provide insights into understanding fitness of color preference in fishes.

Seahorses are a valuable traditional Chinese medicine and fascinated aquarium fishes. All 53 recognized seahorse species were listed on Appendix II of the Convention on International Trade in Endangered Species of Wild Fauna and Flora, due to overexploitation of the wild populations to meet growing demands in traditional Chinese medicine and ornamental markets (Vincent, 1996; Lourie et al., 1999). The commercial culture of seahorses has advanced significantly in the past 15 years to meet growing demands. More than 10 seahorse species have been reared successfully in captivity, such as *Hippocampus abdominalis* (Woods 2000; Woods, 2003), *H. comes* (Job et al., 2006), *H. erectus* (Correa et al., 1989; Scarratt, 1995; Lin et al., 2008, 2009; Zhang et al., 2010), *H. kuda* (Job et al., 2002; Lin et al., 2006; Lin et al., 2007), *H. reidi* (Olivotto et al., 2008), *H. subelongatus* (Payne and Rippingale, 2000), *H. guttulatus* (Faleiro et al., 2008; Miquel et al., 2008), and *H. trimaculatus* (Sheng et al., 2006). The lined seahorse (*H. erectus*) has been considered as one of the best seahorse species for large-scale culture due to its good characteristics in growth, eurytherm, and high disease resistance (Zhang et al., 2010; Qin et al., 2016; Qu et al., 2016). Color preference of fishes in aquaculture is paid more attention (Li et al., 2016; Maia et al., 2021; Yang et al., 2021), however, only a few studies in seahorse. For example, the juveniles of the yellow seahorse (*H. kuda*) cultured in darker tank color had higher growth rate (Pawar et al., 2011), and mixed colors (green and orange, and green and red) resulted in higher survival than a single background color in the lined seahorse (Lin et al., 2009). Recently, our work revealed that the survival rate of the larval lined seahorse under blue and gray tanks with light intensity of 200–700 Lux was 72.0% and 49.6%, respectively (Zhang et al., 2020). Although the limited information tells us that background color should be important to culture the lined seahorse, we still do not know which background color should be chosen in practice; actually, gray, black, and white tanks provided by manufacturers are normally used in farms.

The main aim of the present study is to identify background color preference in the lined seahorse under unstressed and stressed situations and to explore the effect of personality on the color preference in the species. The present study would guide the application of background color in seahorse culture practice. Moreover, color preference could be used as a potential indicator in personality study of the lined seahorse. In the present study, we analyzed the color preference of individual adult lined seahorse by preference index (PI). PIs calculation is a history-based method to necessarily represent the consistent preference response over time and can minimize the influence of possible stress or other momentary reaction that may lead to the spurious preference response (Maia and Volpato, 2016; Maia et al., 2021). A binary choice test and a "knock-at-the-door" test were conducted to further complement the preference reliability and consistence, respectively.

# Materials and methods

## Animal culture and experimental conditions

The 3-month-old lined seahorses (*Hippocampus erectus* Perry, 1810) (wet weight, 3.05 ± 1.07 g; height, 9.07 ± 0.94

cm) for the experiment that was conducted in December 2021 were bred at the Qionghai Research Center of the East China Sea Fisheries Research Institute, Hainan, China. The experimental seahorses were kept in a flow-through fiberglass tank (4 × 2 × 1 m) with light gray background. Seawater was sand-filtrated and ultraviolet-sterilized. Salinity, temperature, light intensity, and photoperiod were 32‰, 23°C–25°C, 800–1,000 Lux, and 13-h light:11-h dark (natural photoperiod), respectively. Transparent plastic tube was provided as holdfast. The seahorses were fed twice a day with frozen mysis (*Neomysis awatschensis*) purchased from a harvester/supplier located in Wudi County, Shandong Province, China. A total of 32 seahorses were tested for the background color preference. The seahorses were selected randomly from the holding tank and cultured individually in glass tanks (45 × 45 × 20 cm) a week prior to test. These flow-through glass tanks had the same culture conditions as in the holding tank, and each tank was labeled to mark the individual seahorses. All seahorses were handled in accordance with the IACUC #160413 established by the Chinese Academy of Sciences.

## Background color preference test procedures

Blue, red, yellow, and green are the colors normally provided in fish color preference test (Maia and Volpato, 2016; Maia et al., 2017; de Abreu et al., 2020), and black and white are the most common colors used in seahorse farms. Thus, six colors, i.e., blue, red, yellow, green, white, and black, were tested. The test tank was divided into six equal compartments colored with polyvinyl chloride (PVC) tape of six corresponding colors (Figure 1A). For the color preference test, seahorses were individually transferred daily with a 250-ml beaker into a transparent plastic cylinder of 18 cm in diameter, which was placed in the central of the test tank. After 5 min of acclimation to minimize the possible spurious stress reactions, the seahorse was released from the cylinder to allow the seahorse moving at will. The seahorse's color choices among the six compartments were recorded for 1 h by a monitor (EZVIZ Company, Hanzhou, China) mounted on a custom-built wood frame. All seahorses were active to make a choice between the six colored compartments during the entire one test hour. The test was run for 10 days, including an acclimation phase, i.e., the first 3 days, and a test phase, i.e., the following 7 days. During the test phase, the total time (min) that individual seahorse visited each colored compartment was registered for calculating PI of each color. The entrance was defined as the whole body got inside a colored compartment.

Daily test was conducted in eight test tanks, i.e., eight seahorses were tested each batch, from 8:00 to 14:00 to ensure that the seahorse was in active status. Handling procedures were the same for the two phases. After the daily test, each seahorse was returned to the respective glass tank. All seahorses were fed

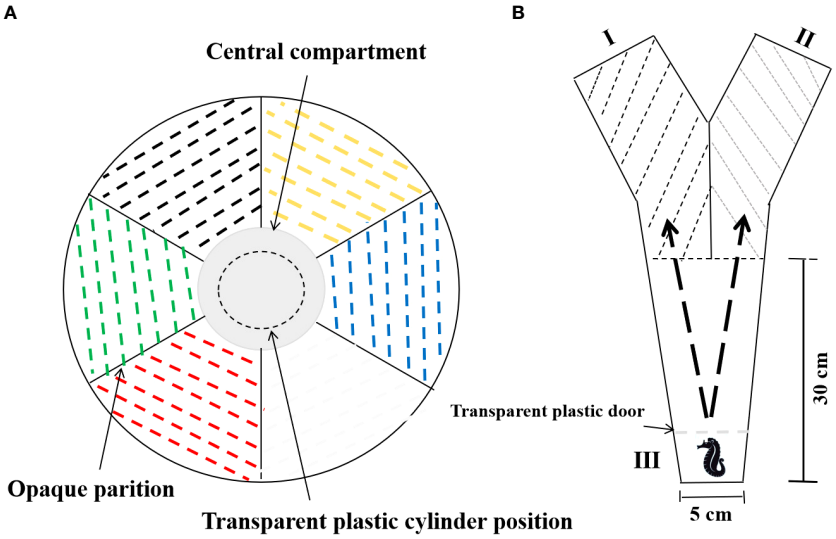


FIGURE 1
Top view of the aquaria for the background color preference test **(A)** and binary choice test **(B)**. **(A)** The colored PVC adhesive tape (white, blue, yellow, black, green, and red) was used to cover the aquaria area, and identical colored foam boards (40 × 35 cm) were used to divide the tank into individual compartments. In the center, the gray color presented the central compartment for seahorse introduction and acclimation. The water column was 25 cm in depth and 100 cm in diameter. **(B)** The test aquarium was in "Y" shape. On the one side, the long route was in "V" shape, covered with black PVC tape (III). On the other side, two choice compartments were covered by blue or red PVC tape to create the most preferred or the most non-preferred option (I or II), respectively. The water column was 15 cm in depth.

at least 2 h before the test to eliminate the feeding effect on behavior. The same seahorse was always tested in the same test tank at the fixed test time (i.e., 8:00–14:00). Moreover, the test tanks were rotated daily to eliminate the possible effects of orientation memory and the light intensity. The temperature in the test tanks was the same as that in the isolation tanks.

## PI calculations

To analyze the preferred or non-preferred color choice and the intensity of the response to colored background, the PI for individual seahorses over the 7 test days was calculated according to Maia and Volpato (2016) with a little modification. As an example, the PI calculation of blue color preference in seahorse 1 is presented in Table 1. First, the time (Rt) that individual seahorse visited blue compartment was registered daily, from D1 to D7 (step 1). Then, the cumulative time (Ct) of seahorse 1 in blue background was calculated over the test days (step 2, e.g., when Dn = 3, $Ct_3 = Rt_1 + Rt_2 + Rt_3$). Considering that the most recent choices might highly impact on the preference, the area above the line built from the XY axes (X axis, test number; Y axis, step 1) was calculated to present the variation over time and more recent choices [step 3, e.g., Dn = 3, $Area_3 = (Ct_3 - Ct_2) \times 5/2$]. The cumulative area above the cumulative frequency line of each colored compartment was calculated (step 4, e.g., Dn = 3, Cumulative $area_3 = Area_1 + Area_2 + Area_3$). Expected area (step 5) was the mean of cumulative areas (step 4) from all the tested color in the respective test number of the seahorse [e.g., when Dn = 3, Expected $area_3$ = (Cumulative $area_3$ of blue + Cumulative $area_3$ of red + Cumulative $area_3$ of white + Cumulative $area_3$ of black + Cumulative $area_3$ of green + Cumulative $area_3$ of yellow)/6]. Variation of cumulative area was the value that the cumulative area minus ExA (step 6 = step 4 – step 5). Finally, the PIs (step 7) were calculated from the cumulative data of step 6 (for example, when Dn = 3, $PI_3 = ExA_1^f + ExA_2^f + ExA_3^f$). Finally, a PI of 1529.15 based on a 7-day test was calculated to present the preference for blue color in seahorse 1. The same procedure was applied to PI calculation of each seahorse for each color as well. The PI value ranges from the negative to positive, of which any positive value was considered as preferred color and negative value as non-preferred color. The value of each PI indicates the intensity of the response, which means that the larger the PI, the stronger the color preference.

## Binary choice test and "knock-at-the-door" test

On the basis of the PIs, we found that the lined seahorse preferred for white and blue and avoided black and red backgrounds. To further confirm the results achieved with PI, a binary choice test and a "knock-at-the-door" test were performed.

On day 11, we applied the binary choice test to clarify the individual seahorses' first chosen background compartment after they moved across the aversive route (Maia et al., 2017). The test aquaria were made in a "Y" shape, constituted of a long route (chamber III) with two exits at the upper end to chamber I and II, respectively (Figure 1B). The chamber III was a "V" shape and covered with black PVC tape to make it as an aversive area to make sure the seahorse would across this section to make a binary choice, which black had been manifested to be the most

TABLE 1 Step-by-step preference index (PI) calculation seahorse 1 and blue color as an example.

| Test Day (Dn) | Step 1 Raw Time (Rt)[a] | Step 2 Cumulative Time (Ct)[b] | Step 3 Area[c] | Step 4 Cumulative Area[d] | Step 5 Expected Area (ExA)[e] | Step 6 Variation of Cumulative Area From the ExA[f] | Step 7 Preference Index (PI)[g] |
|---|---|---|---|---|---|---|---|
| 1 | 0.00 | 0.00 | 0.00 | 0.00 | 3.36 | −3.36 | −3.36 |
| 2 | 0.00 | 0.00 | 0.00 | 0.00 | 3.36 | −3.36 | −6.71 |
| 3 | 30.62 | 30.62 | 76.54 | 76.54 | 25.30 | 51.24 | 44.53 |
| 4 | 37.82 | 68.43 | 132.36 | 208.90 | 58.30 | 150.60 | 195.13 |
| 5 | 45.53 | 113.97 | 204.90 | 413.80 | 100.31 | 313.49 | 508.62 |
| 6 | 31.93 | 145.90 | 175.63 | 589.43 | 149.99 | 439.44 | 948.06 |
| 7 | 28.78 | 174.68 | 187.09 | 776.53 | 195.44 | 581.09 | 1529.15 |

The procedure was independently calculated on the basis of each color choice for each seahorse.
a. Time obtained in each daily test.
b. $\sum_{t3}^{tn}$ Rt.
c. Areas above the cumulative time-line are calculated for each daily test. $Area_n = ((Ct)_n - (Ct)_{n-1})^*(2n - 1)/2$
d. $\sum_{t3}^{tn}$ Area.
e. Mean of cumulative areas from each color in the respective test number and seahorse. The ExA is calculated from data of all tested choice options at tn for seahorse 1.
f. Data from Step 4 to Step 5.
g. Cumulative data of Step 6.
Grey box showed the final PI value.

non-preferred color for the lined seahorse. As the lined seahorse were normally cultured in gray, white, or black tanks, to avoid a learned bias, blue and red were selected as the most preferred and the most non-preferred color, respectively. Thus, chambers I and II were covered by either blue or red PVC tape to create the most preferred or the least preferred option, respectively. A transparent plastic door was set up at the low end of chamber III to create an acclimation area. After 5 min of acclamation, the door was carefully removed, and the seahorse would cross over the black aversive route toward to chamber I or II as assumed. The behavior was recorded for 10 min, and the first chosen compartment was recorded. After the test, seahorses were returned to the respective isolation tanks.

A "knock-at-the-door" test was conducted on day 12. We supposed that the color choice of the stressed (i.e., "knock-at-the-door" test) lined seahorse would be consistent with that at unstressed (i.e., background color preference test) situation. We applied a 30-s air exposure to the lined seahorse, which has been widely used to induce an acute physiological stress response in fishes (Pickering and Pottingger, 1989; Thomson et al., 2011; Skrzynska et al., 2018), and confined the seahorse in the transparent plastic cylinder that was placed in center of the test tank (Figure 1). Behaviors in the cylinder were recorded immediately for 10 min, to allow seahorse fully expressing the response to color under stress. On the basis of preliminary observations (i.e., after a 30-s air exposure, the seahorse repetitively knocked the cylinder wall toward a specific-colored compartment with its snout in an upright posture and attempted to get access), the knock behavior is defined as the seahorse knocks the cylinder wall with its snout toward different colored compartments. Thus, we registered the frequency of the knock toward individual color compartment for further analysis. After the test, seahorses were returned as well.

## Bold–shy personality screening assays

After 3 days of recovery, the bold–shy personality of all the seahorses used for background color preference test was screened by new environment and novel object test according to Freret-Meurer and Alves (2018) and Toms et al. (2011) with a little modification. All seahorses were fasting for 24 h prior to test. The assay was individually conducted in a white polyethylene tank (60 × 45 × 45 cm) with a transparent plastic tube provided as holdfast placed in the middle of the tank for the seahorse, to create a new environment different from the transparent glass tank where seahorse was cultured. Three behaviors of seahorse have been demonstrated (Freret-Meurer and Alves, 2018): a) inspecting the new habitat: seahorses exhibit the behavior of swimming throughout the aquarium; b) protection: grasping the holdfast and still; and c) rest: grasping the holdfast with active movement, such as body or head wiggling. After 5 min of acclimation in a corner of the aquarium restricted by transparent plastic cylinder, the seahorse was released gently. The following behavioral parameters were measured: 1) the total time of swimming and 2) the latency to grasp the holdfast. The behaviors were recorded for 30 min and scored later. About 1 h after the new environment test, when the seahorses were in the rest state, a green plastic plant was introduced in front of the seahorse as a novel object. Then, another 30 min was recorded: 1) the total time of the first protection state; 2) the total time of the protection state; and 3) the latency to change the holdfast. A total of 31 seahorses were individually tested due to missing one. The personality score for individual seahorse was calculated by principal components analysis (PCA).

## Data analysis

The recorded behaviors were analyzed by one person to minimize the observer bias. The data of PI and knock frequency toward individual-colored backgrounds that failed to meet the normality by a Kolmogorov–Smirnov test were analyzed with a non-parametric test (i.e., Kruskal–Wallis test). If the Kruskal–Wallis test result was significant, then a *post hoc* test (Dunn test with Bonferroni adjustment) was applied. A Chi-square test was used to test whether the seahorse chosen the blue or red color as the expected in the binary choice test. A r × c contingency table Chi-square test was applied to test the significant difference between the colored backgrounds in the frequency of seahorses that prefer and do not prefer. If outcome variables were statistically significant, then a *post hoc* test using partitions of Chi-square method with Bonferroni adjustment was followed. Kendall's tau-b correlation analysis was conducted to reveal the correlation between PI and the personality score. To screen the shy–bold continuum behavior, behavior responses from the new environment and novel object trials were standardized and collapsed into the principal component composite score by PCA. The Kaiser–Meyer–Olkin test for sample adequacy was greater than 0.5, and the Bartlett's test of sphericity was significant ($P< 0.05$), indicating that PCA is suitable. The principal component scores were weighted by the contribution rate of each principal component to get the principal component composite score.

# Results

## The colored background preference of the lined seahorse

The final PIs of the lined seahorse that responded to the colored backgrounds over the 7 test days are presented in Figure 2. The PIs were significantly (Kruskal–Wallis test, $P< 0.0001$) different among individual background colors, ranking

in descending order as follows: white (median PI = 900.81), blue (median PI = 385.91), green (median PI = −376.80), yellow (median PI = −518.34), black (median PI = −568.03), and red (median PI = −620.13). *Post hoc* pairwise comparison outcomes are presented in Figure 2. Moreover, all tested seahorses for red background had negative PI value, whereas either preference or non-preference responses for the other colors were found.

Figure 3 shows the results of a r × c contingency table Chi-square test with the number of the seahorse showing preference (positive PIs) or non-preference (negative PIs) compared among colors (Figure 3A) and with the number of the seahorse with most preference or most non-preference compared among colors (Figure 3B), followed by a *post hoc* test with partitions of Chi-square method and Bonferroni adjustment. The results indicate that the two frequencies are significantly ( $\chi^2_5 = 89.949$, $P< 0.0001$, Figure 3A; $\chi^2_5 = 53.826$, $P< 0.0001$, Figure 3B) associated with colors, respectively. *Post hoc* tests for the two analyses indicated that more lined seahorses expressed the preference for white and blue than for red and black, whereas more seahorses disliked the red and black than white and blue ($P< 0.05$, Figures 3A, B).

## Verification of the color preference by binary choice test and "knock-at-the-door" test

The binary choice test shows that significantly more seahorses entered the blue than red (28 versus 4, $\chi^2_1 = 18$, $P< 0.0001$) as the first chosen background compartment after across the long black route (Figure 4A). Generally, when the door opened, the seahorse would swim out of the acclimation area and crossed the black route toward either the blue or red chamber within 2 min and remained in the first chosen compartment. In the "knock-at-the-door" test (Figure 4B), the result shows that the proportion of knock the lined seahorse toward different colored compartments is significantly (Kruskal–Wallis test, $P< 0.0001$) associated with background color. The proportion that the seahorse knocked white background was significantly ($P< 0.05$) higher than the remaining background colors. The lowest frequency was found in red and black backgrounds.

## Bold–shy personality and its relationship with color preference

A total of five behavioral responses were recorded to structure the seahorse personality. Two components were derived (for component 1, Eigenvalue = 2.095; for component 2, Eigenvalue = 1.844), and each explains 41.909% and 36.889% variation, respectively (Table 2A). Thus, we collapsed the behaviors into the first and second component to calculate the principal component score to characterize of individual personality, as component matrix shown in Table 2B. The personality score distribution for individuals as shown in Figure 5 depicted the pronounced continuous variable with range from −1.43 to 3.06. The increasing value represented a stronger protective behavior and neophobia when faced a novel subject and inactive swimming behavior in a new environment, by which shyer seahorses were featured. Furthermore, we analyzed the correlation between personality score obtained from PCA values and PI of each color. The only significantly positive correlation was identified between personality score and the PI of white background (Kendall's tau-b, $P = 0.02$, Table 3), indicating the shyer the seahorse was, the more preference white background color it displayed. The figure showing the actual

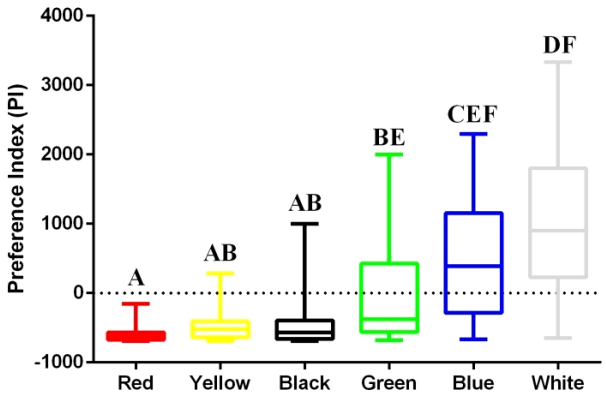


FIGURE 2
The final PIs of the lined seahorse indicating the intensity of preference for each color. Different capital letters indicate the significant differences of preferred options among the colors of red, yellow, black, green, blue, and white (Kruskal–Wallis test, $P< 0.0001$). Preference is showed as positive values and non-preference is showed as negative values. The more positive the value is, higher preference the seahorse is; N = 32.

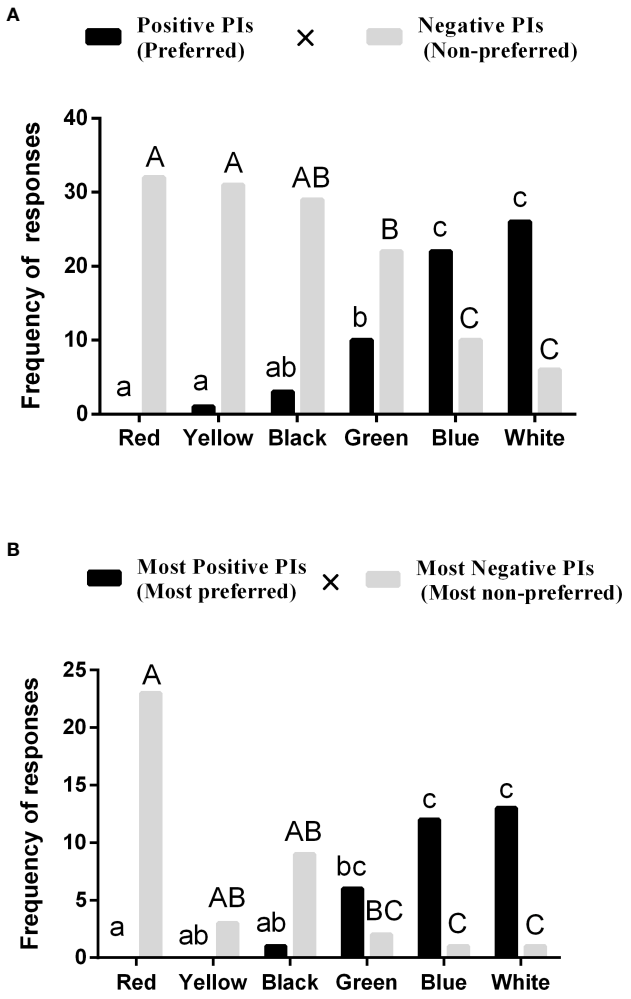


FIGURE 3
Frequency of preference and non-preference **(A)**, and the most preference and most non-preference **(B)** responses of the seahorse to different colors. Different small or capital letters indicate significant differences among the colors in respective pairwise comparisons (N = 32).

data points and the correlation line tendency of PI of white background with personality score is presented in Supplementary Figure 2. No significant correlation was identified for the other background color preference with personality score (Kendall's tau-b, $P > 0.05$).

## Discussion

Color resources in the environment can affect fishes' social, cognitive, and affective responses (de Abreu et al., 2020). Many fish species exhibit specific color preference on account of the distinct evolutionary and ecological history (Egger et al., 2011; Selz et al., 2014). In the present study, we found that the lined seahorse preferred white and blue color backgrounds and avoided red and black ones in captivity, and the color preference was consistent under unstressed and stress situations. More importantly, our pioneering study explored for the first time the relationship between personality trait and color preference in fishes, as shy seahorses showed stronger protection, neophobia, and inactive swimming behavior in contrast to the bold ones. The shyer the seahorse was, the more preference for white background it displayed.

### The preference for white and blue background

It has been reported that inhabiting in the adapted color enables fishes simultaneously to minimize the energy investment

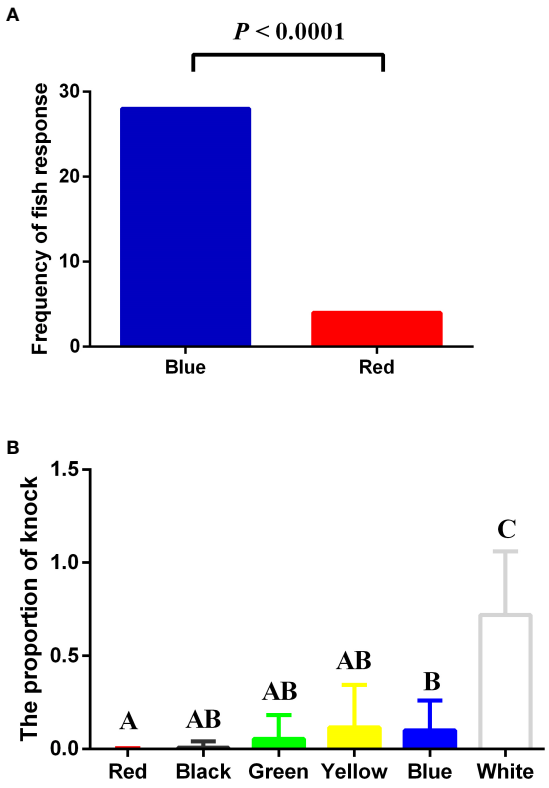


FIGURE 4
Binary choice test **(A)** and "knock-at-the-door" test **(B)** to verify the color preference. **(A)** Frequency of the seahorse entering blue chamber is significantly (Chi-square test, $P < 0.0001$) higher than red chamber. **(B)** The proportion of knock against the cylinder wall toward different colored backgrounds after a 30-s air exposure differs significantly (Kruskal–Wallis test, $P < 0.0001$, *post hoc* test with Dunn test and Bonferroni adjustment, N = 32). Different capital letters indicate significant differences among the colors.

of color adaption to achieve growth and physical conditions and to reduce predator risk (Li et al., 2012; Rodgers et al., 2013). Many fish species have been demonstrated the preference for blue color (Li et al., 2016; Park et al., 2016; Maia et al., 2017; Roy et al., 2019), as blue color improves reproduction (Volpato et al., 2004) and growth (Ruchin, 2004) and reduces stress (Volpato and Barreto, 2001; Karakatsouli et al., 2008; Maia and Volpato, 2013). In the present study, we revealed that the lined seahorse has strong preference for blue background color as well. This may explain why the survival rate of low-quality juveniles of the lined seahorse cultured in blue tank (72.0%) was significantly higher than that in gray (49.6%) ones (Zhang et al., 2020). Seahorses prefer inhabiting shallow waters of marine and estuarine ecosystems where more blue light than green and yellow lights penetrate (Chiang et al., 2011) and grasp coral reefs, sea-grass beds, rocky, and mangrove roots to hide (Lourie et al., 1999),. Thus, it is not surprised that most fish species including the lined seahorse prefer for blue color. Meanwhile, the PIs imply that the lined seahorse mostly preferred white background. This might be related to their experience in early development that also affects the color preference (DePasquale et al., 2016). For example, Li et al. (2016) showed that juvenile turbot (*Scophthalmus maximus*) more frequently occupied the white background than other colored background after a 60-day adaptation to white background. In the present study, the lined seahorse was cultured originally under a light gray background, quite close to white condition. In addition, against white background would make food object more visible, probably accounting for the white background preference (Amiya et al., 2008; Sunuma et al., 2009).

## The non-preference for black and red background

Red color is suggested having some disruptive effect on growth in some fish species (Ruchin, 2004; Karakatsouli et al., 2010). Maia et al. (2021) recommended red shelters should be avoided in juvenile Nile tilapia (*Oreochromis niloticus*) aquaculture. Unanimously, all 32 tested seahorses show a

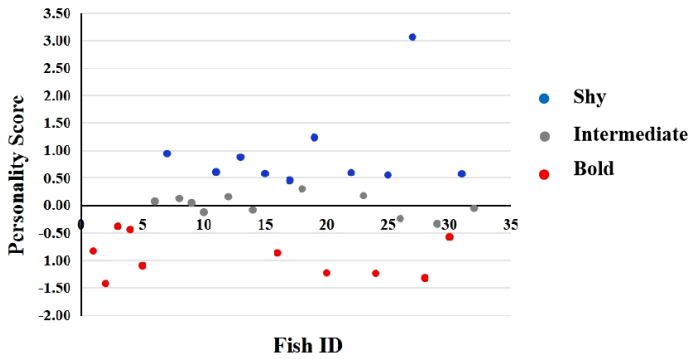


FIGURE 5
The bold–shy axis of the lined seahorse identified on the basis of personality score by the principal components analysis (PCA) (N = 31).

**TABLE 2** Eigen explain (A) and component matrix (B) in terms of behavioral responses of the lined seahorse to assess the bold–shy axis for personality identification.

A

| Axis | Eigenvalues | Percentage % | Cum. Percentage % |
|---|---|---|---|
| 1 | 2.095 | 41.909 | 41.909 |
| 2 | 1.844 | 36.889 | 78.797 |

B

| | PCA 1 Loading | PCA 2 Loading |
|---|---|---|
| The total time of protection | 0.909 | 0.024 |
| The first total time of protection | 0.827 | 0.215 |
| The latency to change holdfast | 0.745 | 0.050 |
| The total time of swimming | −0.124 | 0.951 |
| The latency to grab holdfast | −0.126 | 0.944 |

**TABLE 3** Pairwise correlations between background color preference and personality score.

| Background | | Red | Black | Yellow | Green | Blue | White |
|---|---|---|---|---|---|---|---|
| **Personality Score** | r | −0.123 | −0.103 | −0.216 | 0.018 | −0.115 | 0.285 |
| | *P* | 0.322 | 0.408 | 0.083 | 0.884 | 0.355 | **0.022** |

Data were shown with the Kendall's tau-b and corresponding P values. The only significant (P = 0.022) positive correlation was with bold font detected in white color.

strong non-preference for black and red backgrounds. It is widely accepted that the "behavioral background matching" or "cryptic coloration" strategy is adopted in fishes to best match the habitats with coloration for concealment and avoiding predators (Kjernsmo and Merilaita, 2012; Rodgers et al., 2013; Phillips et al., 2017). Obviously, the hypothesis does not apply to the lined seahorse, because the tested seahorses were the black in body color, and 90.6% of the seahorses showed black color avoidance in the present study. Seahorses, a group of habitat mimicry or crypsis species, can rapidly translate the color that they see in the surroundings and accurately display the color through the skin (Stevens and Merilaita, 2011; Duarte et al., 2019). We inferred that the lined seahorses may adapt themselves to the color in nature or cultured environment,

rather than selecting a habitat that has the similar color as their own body coloration.

Unusually, in 24 days after birth of the yellow seahorse (*H. kuda*), darker background (red, green, blue, and black) rearing had a higher growth than lighter background (yellow and transparent) (Pawar et al., 2011), whereas in pelagic phase longsnout seahorse (*H. reidi*), the tank color did not affect the growth and survival (Hora et al., 2017). Strains should be considered in the color-related behaviors (Vignet et al., 2013). Furthermore, age is demonstrated to affect the color preference in zebrafish (*Danio rerio*). As for larval zebrafish, the preference for light over dark background revealed the "survival" adaptive behavioral strategies (Bai et al., 2016). Nevertheless, adult zebrafish showed the dislike of bright light or white areas to avoid predators (Kysil et al., 2017). It should be mentioned here that background color preference was not biased by colored compartments position in test tank. Individual PI profile over time (Supplementary Figure 1) exhibiting consistent responses further supports the assumption. Interestingly, the PI of green background did not differ significantly from that of either blue or yellow background (Figure 2), which might be related to that green light that is the second highest amount of sunlight in shallow waters of the ocean.

### Bold–shy personality involved in background color preference

The bold–shy axis in personality greatly affects the decision-making, especially in unpredictable environments, that varied greatly among individuals (Freret-Meurer and Alves, 2018). The bold individuals are more active, have courage in exploration, and are willing to take more risks and learn faster versus the shy ones (Sneddon, 2003; Martins et al., 2012). The bold longsnout seahorse readily inspected new habitats and objects, whereas the shy ones were inactivity and had neophobia response to novelties (Freret-Meurer and Alves, 2018). Similarly, the shy lined seahorse presented a stronger protection behavior and neophobia when confronted a novel object and had an inactive swimming behavior in a new environment, in contrast to the bold ones. As the color preference in the lined seahorse was consistent across situations, it is necessary to explore whether color preference could be a personality trait as well. Interestingly, the personality score has significant positive correlation with white color preference, suggesting that the white color preference could be used as an indicator to identify personality in the lined seahorse. However, it should be firmly confirmed whether the preference for blue is correlated with the personality in the future study. Nevertheless, whether background color of culture tank affects the personality, behaviors, physiology, and growth of the lined seahorse is worth further study.

## Conclusion

In general, the lined seahorse displayed intense preference for white and blue background and avoidance of black and red background in either stressed or unstressed situation. Furthermore, the shy seahorses show defensive and neophobia behavior in contrast to the bold ones. A positive correlation that the shyer the individual, the more preference for white coloration suggests that color preference could be used as an indicator to identify bold–shy personality in the lined seahorse. Overall, on the basis of the findings of the present study, white or blue background color is recommended to be the optimal background colors for rearing the lined seahorse.

## Data availability statement

The original contributions presented in the study are included in the article/Supplementary Material. Further inquiries can be directed to the corresponding author.

## Ethics statement

The animal study was reviewed and approved by Chinese Academy of Sciences(IACUC #160413).

## Author contributions

SL designed and conducted the experiment, analyzed the data, and prepared the draft manuscript. XL and TL provided assistance in conducting the experiment; DZ provided suggestions in experiment design and manuscript preparation. XZ helped to remold the test aquaria, cultured, and bred the seahorse for the experiment. All authors finally approved for publication.

## Funding

This work was supported by the Shanghai Sailing Program (21YF1459800) and the Central Public-Interest Scientific Institution Basal Research Fund, Chinese Academy of Fishery Sciences (2020TD53, 2017HYZD0401).

## Acknowledgments

We thank all laboratory members for their constructive suggestions and discussions. We are also grateful to the reviews for their valuable suggestions and modifications.

## Conflict of interest

The authors declare that the research was conducted in the absence of any commercial or financial relationships that could be construed as a potential conflict of interest.

## Publisher's note

All claims expressed in this article are solely those of the authors and do not necessarily represent those of their affiliated organizations, or those of the publisher, the editors and the reviewers. Any product that may be evaluated in this article, or claim that may be made by its manufacturer, is not guaranteed or endorsed by the publisher.

## Supplementary material

The Supplementary Material for this article can be found online at: https://www.frontiersin.org/articles/10.3389/fmars.2022.939749/full#supplementary-material

SUPPLEMENTARY FIGURE 1
Individual profiles of preference (positive PIs) and non-preference (negative PIs) responses of the lined seahorse to different background color conditions (X axis: Test Day; Y axis: Preference Index (PI), N = 32).

SUPPLEMENTARY FIGURE 2
The actual data points and the correlation line tendency of PI of white background (Y axis) with personality score (X axis) (N = 31).

## References

Amiya, N., Amano, M., Yamanome, T., Yamamori, K., and Takahashi, A. (2008). Effects of background color on GnRH and MCH levels in the barfin flounder brain. *Gen. Comp. Endocrinol.* 155, 88–93. doi: 10.1016/j.ygcen.2007.03.007

Asher, L., Kirkden, R. D., and Bateson, M. (2009). An empirical investigation of two assumptions of motivation testing in captive starlings (*Sturnus vulgaris*): do animals have an energy budget to "spend"? and does cost reduce demand? *Appl. Anim. Behav. Sci.* 118, 152–160. doi: 10.1016/j.applanim.2009.02.029

Bai, Y., Liu, H., Huang, B., Wagle, M., and Guo, S. (2016). Identification of environmental stressors and validation of light preference as a measure of anxiety in larval zebrafish. *BMC Neurosci.* 17 (1), 63. doi: 10.1186/s12868-016-0298-z

Barcellos, J. G., Kreutz, L. C., Quevedo, R. M., da Rosa, J. G. S., Koakoski, G., Centenaro, L., et al. (2009). Influence of color background and shelter availability on jundiá (*Rhamdia quelen*) stress response. *Aquaculture* 288, 51–56. doi: 10.1016/j.aquaculture.2008.11.002

Birren, F. (1973). Color preference as a clue to personality. *Art. Psychother.* 1 (1), 13–16. doi: 10.1016/0090-9092(73)90005-7

Bowmaker, J. K., and Loew, E. R. (2007). "Vision in fish," in *The senses: a comprehensive reference*, *1st ed.* Eds. A. Basbaum, A. Kaneko, G. Shepherd and G. Westheimer (Oxford, UK: Elsevier), 53–76.

Carere, C., Drent, P. J., Privitera, L., Koolhaas, J. M., and Groothuis, T. G. G. (2005). Personalities in great tits, *Parus major*: stability and consistency. *Anim. Behav.* 70, 795–805. doi: 10.1016/j.anbehav.2005.01.003

Chiang, J. Y., Chen, Y. C., and Chen, Y. F. (2011). "Underwater image enhancement: using wavelength compensation and image dehazing (WCID)," in *ACIVS 2011, LNCS 6915*. Eds. J. Blanc-Talon, R. P. Kleihorst, W. Philips, D. C. Popescu and P. Scheunders (Dessau, Germany: Springer), 372–383.

Correa, M., Chung, K. S., and Manrique, R. (1989). Cultive experimental. del caballito de mar, *Hippocapus erectus*. *Bol. Inst. Oceanogr. Venez* 28 (1-2), 191–196.

de Abreu, M. S., Giacomini, A. C. V. V., Genario, R., dos Santos, B. E., Marcon, L., Demin, K. A., et al. (2020). The impact of housing environment color on zebrafish anxiety-like behavioral and physiological (cortisol) responses. *Gen. Comp. Endocrinol.* 294, 113499. doi: 10.1016/j.ygcen.2020.113499

DePasquale, C., Neuberger, T., Hirrlinger, A., and Braithwaite, V. A. (2016). The influence of complex and threatening environments in early life on brain size and behavior. *P. R. Soc B-Biol. Sci.* 283, 20152564. doi: 10.1098/rspb.2015.2564

Duarte, M., Gawryszewski, F. M., Ramineli, S., and Bessa, E. (2019). Disruptive coloration and habitat use by seahorses. *Neotrop. Ichthyol* 17 (4), e190064. doi: 10.1590/1982-0224-20190064

Egger, B., Klaefiger, Y., Theis, A., and Salzburger, W. (2011). A sensory bias has triggered the evolution of egg-spots in cichlid fishes. *PloS One* 6, e25601. doi: 10.1371/journal.pone.0025601

Espmark, Y., Amundsen, T., and Rosenqvist, G. (2000). *Animal signals: signalling and signal design in animal communication* (Norway: Tapir Academic Press).

Faleiro, F., Narciso, L., and Vicente, L. (2008). Seahorse behaviour and aquaculture: How to improve *Hippocampus guttulatus* husbandry and reproduction? *Aquaculture* 282 (1-4), 33–40. doi: 10.1016/j.aquaculture.2008.05.038

Fetterman, A. K., Liu, T., and Robinson, M. D. (2015). Extending color psychology to the personality realm: interpersonal hostility varies by red preferences and perceptual biases. *J. Pers.* 83 (1), 106–116. doi: 10.1111/jopy.12087

Fowler-Finn, K. D., and Rodriguez, R. L. (2013). Repeatability of mate preference functions in enchenopa treehoppers (*Hemiptera: Membracidae*). *Anim. Behav.* 85, 493–499. doi: 10.1016/j.anbehav.2012.12.015

Freret-Meurer, N. V., and Alves, M. A. S. (2018). Personality in the longsnout seahorse, *Hippocampus reidi* ginsbur: Are males shyer than females? *Behav. Process* 157, 106–110. doi: 10.1016/j.beproc.2018.09.006.

Hora, M. S. C., Joyeux, J. C., Guabiroba, H. C., and Tsuzuki, M. Y. (2017). Effect of photoperiod and tank colour on growth and survival of pelagic-phase seahorse *Hippocampus reidi*. *Aquac. Res.* 48, 1–8. doi: 10.1111/are.13252

Houpt, K. A. (2012). Motivation for cribbing by horses. *Anim. Welf.* 21, 1–7. doi: 10.7120/096272812799129367

Job, S., Buu, D., and Vincent, A. (2006). Growth and survival of the tiger tail seahorse, *Hippocampus comes*. *J. World Aquacult. Soc.* 37, 322–327. doi: 10.1111/j.1749-7345.2006.00044.x

Job, S. D., Do, H. H., Meeuwigc, J. J., and Hall, H. J. (2002). Culturing the oceanic seahorse, *Hippocampus kuda*. *Aquaculture* 214, 333–341. doi: 10.1016/S0044-8486(02)00063-7

Kaiser, M. I., and Müller, C. (2021). What is an animal personality? *Biol. Philos.* 36, 1. doi: 10.1007/s10539-020-09776-w

Kang, D. Y. , and Kim, H. C. (2013a). Importance of bottom type and background color for growth and blind-side hypermelanosis of the olive flounder, *Paralichthys olivaceus*. aquac. *Eng* 57, 1–8. doi: 10.1016/j.aquaeng.2013.05.001

Kang, D. Y. , and Kim, H. C. (2013b). Influence of density and background color to stress response, appetite, growth, and blind-side hypermelanosis of flounder, *Paralichthys olivaceus*. fish physiol. *Biochem* 39, 221–232. doi: 10.1007/s10695-012-9693-2

Karakatsouli, N., Papoutsoglou, S. E., and Manolessos, G. (2007). Combined effects of rearing density and tank colour on the growth and welfare of juvenile white sea bream *Diplodus sargus* l. in a recirculating water system. *Aquac. Res.* 38, 1152–1160. doi: 10.1111/j.1365-2109.2007.01780.x

Karakatsouli, N., Papoutsoglou, S. E., Panopoulos, G., Papoutsoglou, E. S., Chadio, S., and Kalogiannis, D. (2008). Effects of light spectrum on growth and stress response of rainbow trout *Oncorhynchus mykiss* reared under recirculating system conditions. *Aquacult. Eng.* 38, 36–42. doi: 10.1016/j.aquaeng.2007.10.006

Karakatsouli, N., Papoutsoglou, E. S., Sotiropoulos, N., Mourtikas, D., Stigen-Martinsen, T., and Papoutsoglou, S. E. (2010). Effects of light spectrum, rearing density and light intensity on growth performance of scaled and mirror common carp *Cyprinus carpio* reared under recirculating system conditions. *Aquacult. Eng.* 42 (3), 121–127. doi: 10.1016/j.aquaeng.2010.01.001

Kjernsmo, K., and Merilaita, S. (2012). Background choice as an anti-predator strategy: the roles of background matching and visual complexity in the habitat choice of the least killifish. *Proc. Biol. Sci.* 279 (1745), 4192–4198. doi: 10.1098/rspb.2012.1547

Kysil, E. V., Meshalkina, D. A., Frick, E. E., Echevarria, D. J., Rosemberg, D. B., Maximino, C., et al. (2017). Comparative analyses of zebrafish anxiety-like behavior using conflict-based novelty tests. *Zebrafish* 14 (4), 197–208. doi: 10.1089/zeb.2016.1415

Lehtonen, T. K., and Lindstrom, K. (2006). Repeatability of mating preferences in the sand goby. *Anim. Behav.* 75, 55–61. doi: 10.1016/j.anbehav.2007.04.011

Li, X., Chi, L., Tian, H., Meng, L., Zheng, J., Gao, X., et al. (2016). Color preferences of juvenile turbot (*Scophthalmus maximus*). *Physiol. Behav.* 156, 64–70. doi: 10.1016/j.physbeh.2016.01.007

Li, X., Fan, L., Liu, Z., Ren, X., and Liu, Y. (2012). Preference habit of juvenile turbot for different color backgrounds based on computer vision. *Trans. Chin. Soc Agric. Eng.* 28, 189–193. doi: CNKI:SUN:NYGU.0.2012-10-031

Lin, Q., Gao, Y. L., Sheng, J. Q., Chen, Q. X., Zhang, B., and Lu, J. Y. (2007). The effect of food and the sum of effective temperature on the embryonic development of the seahorse, *Hippocampus kuda* bleeker. *Aquaculture* 262, 481–492. doi: 10.1016/j.aquaculture.2006.11.011

Lin, Q., Lin, J., and Huang, L. (2009). Effects of substrate color, light intensity and temperature on survival and skin color change of juvenile seahorses, *Hippocampus erectus* perr. *Aquaculture* 298, 157–161. doi: 10.1016/j.aquaculture.2009.10.015

Lin, Q., Lin, J., and Zhang, D. (2008). Breeding and juvenile culture of the lined seahorse, *Hippocampus erectus*. *Aquaculture* 277, 287–292. doi: 10.1016/j.aquaculture.2008.02.030

Lin, Q., Lu, J. Y., and Gao, Y. L. (2006). The effect of temperature on gonad, embryonic development and survival rate of juvenile seahorses, *Hippocampus kuda* bleeker. *Aquaculture* 254, 701–713. doi: 10.1016/j.aquaculture.2005.11.005

Losey, G. S., McFarland, W. N., Loew, E. R., Zamzow, J. P., Nelson, P. A., and Marshall, N. J. (2003). Visual biology of Hawaiian boral reef fishes. i. ocular transmission and visual pigments. *Copeia* 2003 (3), 433–454. doi: 10.1643/01-053

Lourie, S. A., Vincent, A. C., and Hall, H. J. (1999). Seahorse: An identification guide to the world's species and their conservation. *Proj. Seahorse London.*, 214.

Lythgoe, J. N., and Partridge, J. C. (1989). Visual pigments and the acquisition of visual information. *J. Exp. Biol.* 146, 1–20. doi: 10.1242/jeb.146.1.1

Maia, C. M., Alves, N. P. C., and Tatemoto, P. (2021). Juvenile Nile tilapia fish avoid red shelters. *J. Appl. Anim. Welf. Sci.* 1, 98–106. doi: 10.1080/10888705.2020.1848567

Maia, C. M., Ferguson, B., Volpato, G. L., and Braithwaite, V. A. (2017). Physical and psychological motivation tests of individual preferences in rainbow trout. *J. Zool.* 302 (2), 108–118. doi: 10.1111/jzo.12438

Maia, C. M., and Volpato, G. L. (2013). Environmental light color affects the stress response of Nile tilapia. *Zoology* 116, 64–66. doi: 10.1016/j.zool.2012.08.001

Maia, C. M., Ferguson Volpato, B. G. L., and Braithwaite, V. A. (2017). Physical and psychological motivation tests of individual preferences in rainbow trout. *Zoology* 302 (2), 108–18. doi: 10.1038/srep28328

Martins, C. I. M., Schaedelin, F. C., Mann, M., Blum, C., Mandl, I., Urban, D., et al. (2012). Exploring novelty: a component trait of behavioural syndromes in a colonial fish. *Behaviour* 149, 215–231. doi: 10.1163/156853912X634430

Mason, G. J., Cooper, J., and Clarebrough, C. (2001). Frustrations of fur-farmed mink. *Nature* 410, 35–36. doi: 10.1038/35065157

Miquel, P., Alexandro, C., Patricia, Q., and Antonio, V. (2008). Establishment and maintenance of threatened long-snouted seahorse, *Hippocampus guttulatus*, broodstock in captivity. *Aquaculture* 283 (1-4), 0–28. doi: 10.1016/j.aquaculture.2008.06.023

Neumeyer, C. (1992). Tetrachromatic color-vision in goldfish-evidence from color mixture experiments. *J. Comp. Physiol. A* 171, 639–649. doi: 10.1007/BF00194111

Nikolaenko, N. N., and Ostrovskaia, M. I. (1989). Color preference as an index of emotional-personality characteristics (research under conditions of transient depression of the right or left hemisphere). *Fiziol. Cheloveka* 15 (4), 11–15.

Olivotto, I., Avella, M. A., Sampaolesi, G., Piccinetti, C. C., Ruiz, P. N., and Carnevali, O. (2008). Breeding and rearing the longsnout seahorse *Hippocampus reidi*: rearing and feeding studies. *Aquaculture* 283, 92–96. doi: 10.1016/j.aquaculture.2008.06.018

Park, J. S., Ryu, J. H., Choi, T. I., Bae, Y. K., Lee, S., Kang, H. J., et al. (2016). Innate color preference of zebrafish and its use in behavioral analyses. *Mol. Cells* 39 (10), 750–755. doi: 10.14348/molcells.2016.0173

Pawar, H. B., Sanaye, S. V., Murugan, A., and Sreepada, R. A. (2011). Effect of background color of tanks on growth and survival of juvenile yellow seahorse, *Hippocampus kuda* (Bleeker 1852), in the pelagic phase. *ISR. J. Aquacult-Bamid* 63, 1–6. doi: 10.3750/AIP2011.41.3.14

Payne, M. F., and Rippingale, R. J. (2000). Rearing West Australian seahorse, *Hippocampus subelongatus*, juveniles on copepod nauplii and enriched *Artemia*. *Aquaculture* 188, 353e361. doi: 10.1016/S0044-8486(00)00349-5

Phillips, G. A. C., How, M. J., Lange, J. E., Marshall, N. J., and Cheney, K. L. (2017). Disruptive colouration in reef fish: does matching the background reduce predation risk? *J. Exp. Biol.* 220 (11), 1962–1974. doi: 10.1242/jeb.151480

Pickering, A. D., and Pottinger, T. G. (1989). Stress responses and disease resistance in salmonid fish-effects of chronic elevation of plasma-cortisol. *Fish Physiol. Biochem.* 7, 253–258. doi: 10.1007/BF00004714

Qin, G., Zhang, Y., Wang, X., and Lin, Q. (2016). Effects of anesthetic disposal on the physiological and behavioral responses of the lined seahorses, *Hippocampus erectus.* J. *World Aquacult. Soc.* 47, 387–395. doi: 10.1111/jwas.12282

Qu, H., Luo, W., and Lin, Q. (2016). Development of SNP markers in lined seahorse (*Hippocampus erectus*) based on transcriptome sequencing. *Conserv. Genet. Resour.* 8, 1–4. doi: 10.1007/s12686-015-0510-y

Réale, D., Reader, S. M., Sol, D., McDougall, P. T., and Dingemanse, N. J. (2007). Integrating animal temperament within ecology and evolution. *Biol. Rev. Camb. Philos. Soc* 82 (2), 291–318. doi: 10.1111/j.1469-185X.2007.00010.x

Rodgers, G. M., Gladman, N. W., Corless, H. F., and Morrell, L. J. (2013). Costs of colour change in fish: food intake and behavioural decisions. *J. Exp. Biol.* 216, 2760–2767. doi: 10.1242/jeb.080879

Roy, T., Suriyampola, P. S., Flores, J., López, M., Hickey, C., Bhat, A., et al. (2019). Color preferences affect learning in zebrafish, *Danio rerio*. sci. *Rep* 9 (1), 14531. doi: 10.1038/s41598-019-51145-5

Ruchin, A. B. (2004). Influence of colored light on growth rate of juveniles of fish. *Fish Physiol. Biochem.* 30 (2), 175–178. doi: 10.1007/s10695-005-1263-4

Scarratt, A. M. (1995). Techniques for raising lined seahorses (*Hippocapus erectus*). *Aquarium Front.* 3, 24–29.

Selz, O. M., Pierotti, M. E. R., Maan, M. E., Schmid, C., and Seehausen, O. (2014). Female preference for male color is necessary and sufficient for assortative mating in 2 cichlid sister species. *Behav. Ecol.* 25, 612–626. doi: 10.1093/beheco/aru024

Sheng, J. Q., Lin, Q., Chen, Q. X., Gao, Y. L., Shen, L., and Lu, J. Y. (2006). Effects of food, temperature and light intensity on the feeding behavior of three-spot juveniles, *Hippocampus trimaculatus* leach. *Aquaculture* 256, 596–607. doi: 10.1016/j.aquaculture.2006.02.026

Sih, A., Bell, A., and Johnson, J. C. (2004). Behavioural syndromes: an ecological and evolutionary overview. *Trends Ecol. Evol.* 19, 372–378. doi: 10.1016/j.tree.2004.04.009

Skrzynska, A. K., Maiorano, E., Bastaroli, M., Naderi, F., Míguez, J. M., Martínez-Rodriguez, G., et al. (2018). Impact of air exposure on vasotocinergic and isotocinergic systems in gilthead Sea bream (*Sparus aurata*): New insights on fish stress response. *Front. Physiol.* 13 (9), 96. doi: 10.3389/fphys.2018.00096

Sneddon, L. U. (2003). The bold and the shy: individual differences in rainbow trout. *J. Fish Biol.* 62, 971–975. doi: 10.1046/j.1095-8649.2003.00084.x

Spence, R., and Smith, C. (2008). Innate and learned colour preference in the zebrafish, *Danio rerio*. *Ethology* 114 (6), 582–588. doi: 10.1111/j.1439-0310.2008.01515.x

Stevens, M., and Merilaita, S. (2011). *Animal camouflage: mechanisms and function* (Cambridge: United Kingdom at the University Press).

Stimpson, D. V., and Stimpson, M. F. (1979). Relation of personality characteristics and color preferences. *Percept. Mot. Skills* 49 (1), 60–62. doi: 10.2466/pms.1979.49.1.60

Strand, A., Alanärä, A., Staffan, F., and Magnhagen, C. (2007). Effects of tank colour and light intensity on feed intake, growth rate and energy expenditure of juvenile Eurasian perch, *Perca fluviatilis* l. *Aquaculture* 272, 312–318. doi: 10.1016/j.aquaculture.2007.08.052

Sunuma, T., Yamanome, T., Amano, M., Takahashi, A., and Yamamori, K. (2009). White background stimulates the food intake of a pleuronectiform fish the

barfin flounder, *Verasper moseri* (Jordan and Gilbert). *Aquacult. Res.* 40, 748–751. doi: 10.1111/j.1365-2109.2009.02179.x

Takahashi, A., Kosugi, T., Kobayashi, Y., Yamanome, T., Schioth, H. B., and Kawauchi, H. (2007). The melanin-concentrating hormone receptor 2 (MCH-R2) mediates the effect of MCH to control body color for background adaptation in the barfin flounder. *Gen. Comp. Endocrinol.* 151, 210–219. doi: 10.1016/j.ygcen.2007.01.011

Tamazouzt, L., Chatain, B., and Fontaine, P. (2000). Tank wall colour and light level affect growth and survival of Eurasian perch larvae (*Perca fluviatilis* l.). *Aquaculture* 182 (1-2), 85–90. doi: 10.1016/S0044-8486(99)00244-6

Tao, B., Xu, S., Pan, X., Gao, Q., and Wang, W. (2015). Personality trait correlates of color preference in schizophrenia. *Transl. Neurosci.* 6 (1), 174–178. doi: 10.1515/tnsci-2015-0018

Thomson, J. S., Watts, P. C., Pottinger, T. G., and Sneddon, L. U. (2011). Physiological and genetic correlates of boldness: characterising the mechanisms of behavioural variation in rainbow trout, *Oncorhynchus mykiss*. horm. *Behav* 59 (1), 67–74. doi: 10.1016/j.yhbeh.2010.10.010

Vignet, C., Bégout, M. L., Péan, S., Lyphout, L., Leguay, D., and Cousin, X. (2013). Systematic screening of behavioral responses in two zebrafish strains. *Zebrafish* 10 (3), 365–375. doi: 10.1089/zeb.2013.0871

Vincent, A. C. J. (1996). *The international trade in seahorse* (Cambridge: TRAFFIC International), 164.

Volpato, G. L., and Barreto, R. E. (2001). Environmental blue light prevents stress in the fish Nile tilapia. *Braz. J. Med. Biol. Res.* 34, 1041–1045. doi: 10.1590/S0100-879X2001000800011

Volpato, G. L., Bovi, T. S., de Freitas, R. H. A., da Silva, D. F., Delicio, H. C., Giaquinto, P. C., et al. (2013). Red light stimulates feeding motivation in fish but does not improve growth. *PloS One* 8, e59134. doi: 10.1371/journal.pone.0059134

Volpato, G. L., Duarte, C. R. A., and Luchiari, A. C. (2004). Environmental color affects Nile tilapia reproduction. *Brazil J. Med. Biol. Res.* 37 (4), 479–483. doi: 10.1590/S0100-879X2004000400004

Woods, C. M. C. (2000). Improving initial survival in cultured seahorse, Hippocampus abdominalis Lesson, 1827 (Teleostei: Syngathidae). *Aquaculture* 190, 377–388. doi: 10.1016/S0044-8486(00)00408-7

Woods, C. M.C. (2003). PGrowth and survival of juvenile seahorse Hippocampus abdominalis reared on live frozen and artificial foods. *Aquaculture* 220, 287–98. doi: 10.1016/S0044-8486(02)00227-2

Yang, T., Kasagi, S., Takahashi, A., and Mizusawa, K. (2021). Effects of background color and feeding status on the expression of genes associated with body color regulation in the goldfish *Carassius auratus*. gen. *Comp. Endocrinol.* 312, 113860. doi: 10.1016/j.ygcen.2021.113860

Zhang, D., Liu, X., Lin, T. T., and Xin, S. M. (2020). A method to improve low-quality juvenile seahorse by background color and light CN111631185A.

Zhang, D., Zhang, Y., Lin, J., and Lin, Q. (2010). Growth and survival of juvenile lined seahorse, *Hippocampus erectus* (Perry), at different stocking densities. *Aquacult. Res.* 42, 9–13. doi: 10.1111/j.1365-2109.2010.02482.x

# Frontiers in Marine Science

**Explores ocean-based solutions for emerging global challenges**

The third most-cited marine and freshwater biology journal, advancing our understanding of marine systems and addressing global challenges including overfishing, pollution, and climate change.

---

## Discover the latest Research Topics

See more →

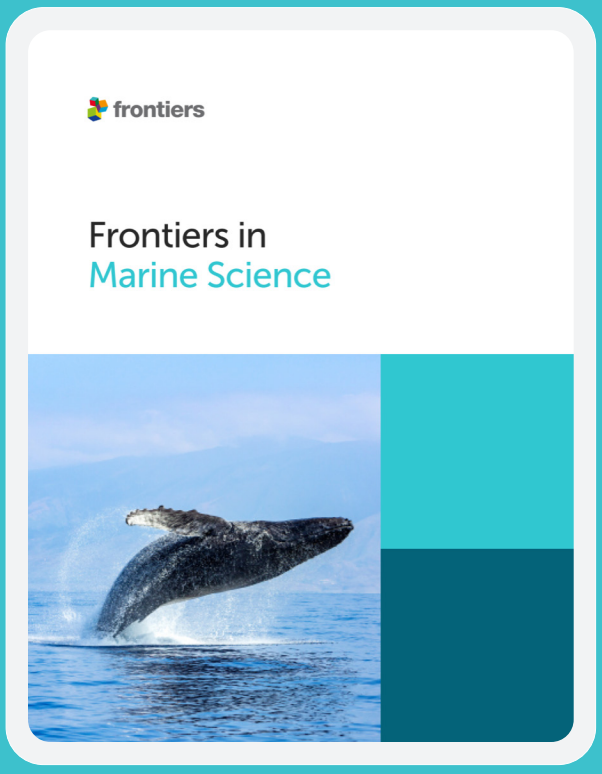


**Frontiers**

Avenue du Tribunal-Fédéral 34
1005 Lausanne, Switzerland
frontiersin.org

**Contact us**

+41 (0)21 510 17 00
frontiersin.org/about/contact